ACTA PHYSICA

ACADEMIAE SCIENTIARUM HUNGARICAE

TOMUS XV. FASCICULUS 1.

AKADÉMIAI KIADÓ, BUDAPEST
1962

ACTA PHYSICA

A MAGYAR TUDOMÁNYOS AKADÉMIA FIZIKAI KÖZLEMÉNYEI

SZERKESZTŐSÉG ÉS KIADÓHIVATAL: BUDAPEST V., ALKOTMÁNY UTCA 21.

Az *Acta Physica* német, angol, francia és orosz nyelven közöl értekezéseket a fizika tárgyköréből.

Az *Acta Physica* változó terjedelmű füzetekben jelenik meg: több füzet alkot egy kötetet.

A közlésre szánt kéziratok a következő címre küldendők:

Acta Physica, Budapest 502, Postafiók 24.

Ugyanerre a címre küldendő minden szerkesztőségi és kiadóhivatali levelezés.

Az *Acta Physica* előfizetési ára kötetenként belföldre 80 forint, külföldre 110 forint Megrendelhető a belföld számára az Akadémiai Kiadónál (Budapest V., Alkotmány utca 21. Bankszámla 05-915-111-46), a külföld számára pedig a „Kultúra" Könyv- és Hírlap Külkereskedelmi Vállalatnál (Budapest I., Fő u. 32. Bankszámla 43-790-057-181 sz.), vagy annak külföldi képviseleteinél és bizományosainál.

Die *Acta Physica* veröffentlichen Abhandlungen aus dem Bereiche der Physik in deutscher, englischer, französischer und russischer Sprache.

Die *Acta Physica* erscheinen in Heften wechselnden Umfanges. Mehrere Hefte bilden einen Band.

Die zur Veröffentlichung bestimmten Manuskripte sind an folgende Adresse zu richten:

Acta Physica, Budapest 502, Postafiók 24.

An die gleiche Anschrift ist auch jede für die Redaktion und den Verlag bestimmte Korrespondenz zu senden.

Abonnementspreis pro Band: 110 forint. Bestellbar bei dem Buch- und Zeitungs-Aussenhandels-Unternehmen »Kultura« (Budapest I., Fő u. 32. Bankkonto Nr. 43-790-057-181) oder bei seinen Auslandsvertretungen und Kommissionären.

ACTA PHYSICA

ACADEMIAE SCIENTIARUM HUNGARICAE

TOMUS XV

AKADÉMIAI KIADÓ, BUDAPEST
1963

ACTA PHYSICA

Tomus XV

INDEX

ON THE ANOMALOUS SPLITTINGS OF THE MULTIPLET Σ STATES IN DIATOMIC MOLECULES I.

By

I. Kovács

DEPARTMENT OF ATOMIC PHYSICS, POLYTECHNICAL UNIVERSITY, BUDAPEST

(Received 20. VII. 1961)

It has been shown that the anomalies observed in the multiplet splitting of the $X^2\Sigma^+$ term of the HgH, the $B^2\Sigma$ term of the YO and the $A^3\Sigma_u^+$ and the $B'^3\Sigma_u^-$ terms of the N_2 molecule are the same character as those observed at the $^7\Sigma$ term of the MnH molecule, the reason in al the five cases being the same: the perturbation of not too far lying Π terms. A satisfactory agreement has been found between the experimental and theoretical results.

As is known, for diatomic molecules in most of the cases the multiplet Σ terms can be described by a simple formula as follows:

$$^{2S+1}F_i(N) = BN(N+1) + DN^2(N+1)^2 + {}^{2S+1}f_i(N), \qquad (1)$$

where $2S+1$ means the multiplicity of the respective Σ term, $i = 1, \ldots 2S+1$ and the individual indices correspond in the usual notation to the states $J = N+S, N+S-1, \ldots, N-S$, where N and J are the rotational quantum numbers in Hund's case b) and a) respectively, B and D are the rotational constants, and in $^{2S+1}f_i\,(N)$ apart from the rotational quantum number occur two constants: ε, the constant of the spin-spin interaction and γ, the constant of the interaction between rotation and spin.

If the perturbation, disregarded in the first approximation, caused partly by the spin-orbit interaction and partly by the terms neglected at the separation of the wave equation is added to the above formula, the influence of other neighbouring terms may also be taken into account. In this respect it has been found that, should these latter terms be lying far enough, in a first approximation the influences of the more distant lying terms alter only the values of the constants B, D, ε and γ in formula (1) without any change taking place in the structure of formula (1). [1, 2, 3, 4].

More detailed investigations have, however, shown that for a few diatomic molecules, such as HgH, YO, N_2, and MnH, the $X^2\Sigma^+$, $B^2\Sigma$, $A^3\Sigma_u^+$, $B'^3\Sigma_u^-$ and $^7\Sigma$ terms, respectively, indicate a considerable deviation from a formula of the structure of (1) [5, 6, 7, 8, 9]. This deviation manifests itself by the fact that the multiplet splittings observed experimentally cannot be harmonized with those calculated on the basis of formulas of type (1). The author of the present paper succeeded in interpreting the above anomaly observed at the $^7\Sigma$ term of the MnH molecule as the perturbation of a $^7\Pi$

term which is lying far enough from the $^7\Sigma$ term to cross the latter but not so far as to render the *variation* of the distance between the two terms with the rotational quantum number negligible compared to the *distance* itself between the two terms [4]. The anomalous behaviour of the $X^2\Sigma^+$ and the $B^2\Sigma$ terms of the HgH and YO molecules, respectively and that of the $A^3\Sigma_u^+$ and $B'^3\Sigma_u^-$ terms of the N_2 molecule will, in the present work, be interpreted in the same way, viz. by the perturbation of the not too far lying Π terms.

$^2\Sigma$ terms

Detailed calculations lead to the result that the $^2\Sigma$ terms for the perturbation of distant lying $^2\Pi$ terms satisfy the following formula:

$$\begin{aligned} F_1'(N) &= \frac{\xi^2}{h\nu} + \left(B_\Sigma + 8\,\frac{\eta^2}{h\nu}\right) N(N+1) + D_\Sigma\, N^2(N+1)^2 + \\ &\quad + \frac{1}{2}\left(\gamma - 8\,\frac{\xi\eta}{h\nu}\right) N \\ F_2'(N) &= \frac{\xi^2}{h\nu} + \left(B_\Sigma + 8\,\frac{\eta^2}{h\nu}\right) N(N+1) + D_\Sigma\, N^2(N+1)^2 - \\ &\quad - \frac{1}{2}\left(\gamma - 8\,\frac{\xi\eta}{h\nu}\right)(N+1)\,, \end{aligned} \tag{2}$$

where ξ is the constant occurring in the matrix elements of the spin-orbit interaction and η is that of the interaction resulting from the terms neglected at the separation of the wave equation (cf. [10, 11]), $h\nu$ being the distance between the $^2\Sigma$ and $^2\Pi$ terms. Formula (2) apart from a constant displacement does not show any difference in structure from (1).

If, on the other hand, the variation of $h\nu$ with the rotational quantum number is not negligible, $h\nu$ has to be replaced by another expression:

$$h\nu(^2\Sigma, ^2\Pi) \approx h\nu + (B_\Sigma - B_\Pi)\, N(N+1)\,, \tag{3}$$

where $h\nu$ represents this time the term difference between the vibrational states, whereas from the point of view of perturbation the two components of the $^2\Pi$ term can be replaced by their arithmetic mean.

Since in (2) the reciprocal values of term distances are given, we expand (3) in a series in powers of the same functions and we obtain

$$\frac{1}{h\nu(^2\Sigma, ^2\Pi)} \sim \frac{1}{h\nu} - \frac{(B_\Sigma - B_\Pi)\, N(N+1)}{(h\nu)^2}\,. \tag{4}$$

Substituting (4) in (2) we have

$$\left.\begin{aligned} F_1'(N) &= \overline{F_1(N)} - \sigma N^2(N+1), \\ F_2'(N) &= \overline{F_2(N)} + \sigma N(N+1)^2, \end{aligned}\right\} \tag{5}$$

where

$$\left.\begin{aligned} \overline{F_1(N)} &= \frac{\xi^2}{h\nu} + \bar{B}N(N+1) + \bar{D}N^2(N+1)^2 + \frac{1}{2}\bar{\gamma}N, \\ \overline{F_2(N)} &= \frac{\xi^2}{h\nu} + \bar{B}N(N+1) + \bar{D}N^2(N+1)^2 - \frac{1}{2}\bar{\gamma}(N+1) \end{aligned}\right\} \tag{6}$$

and

$$\bar{B} = B_\Sigma + 8\frac{\eta^2}{h\nu} - \frac{\xi^2(B_\Sigma - B_\Pi)}{(h\nu)^2}\,;\quad \bar{D} = D_\Sigma - 8\frac{\eta^2(B_\Sigma - B_\Pi)}{(h\nu)^2}\,;$$

$$\bar{\gamma} = \gamma - 8\frac{\xi\eta}{h\nu}\,;\quad \sigma = 4\frac{\xi\eta(B_\Pi - B_\Sigma)}{(h\nu)^2}\,. \tag{7}$$

Since $\overline{F_1(N)}$ and $\overline{F_2(N)}$ apart from a constant displacement are of completely the same structure as the unperturbed terms in (1), the experimental data will furnish the constants $\bar{B}$, $\bar{D}$ and $\bar{\gamma}$ instead of B_Σ, D_Σ and γ. Thus for the experimentalist $\overline{F_1(N)}$ and $\overline{F_2(N)}$ will represent the "unperturbed" term values and deviations from these are to be taken as the perturbations caused by the $^2\Pi$ term.

On the basis of (5) for the doublet splitting of the $^2\Sigma$ term we have

$$\Delta F_{12}' = \Delta\overline{F}_{12} = 2\sigma N(N+1)\left(N+\frac{1}{2}\right), \tag{8}$$

where

$$\Delta\overline{F}_{12} = \bar{\gamma}\left(N+\frac{1}{2}\right). \tag{9}$$

Thus, the difference of the perturbed and unperturbed doublet splittings will be

$$\Delta F_{12}' - \Delta\overline{F}_{12} = -2\sigma N(N+1)\left(N+\frac{1}{2}\right). \tag{10}$$

Figs. 1a, 1b and 1c refer to the vibrational states $v'' = 0, 1, 2$ of the $X^2\Sigma^+$ term of the HgH molecule. The circles represent the deviations between the experimentally observed doublet splittings and the theoretical ones computed with the experimentally determined values $\bar{\gamma} = 2{,}11,\ 1{,}78,\ 1{,}30\ \mathrm{cm}^{-1}$ (cf. [5]), whereas the lines drawn in full represent the expressions on the right side of (10), calculated with the values $\sigma_0 = 4{,}24 \cdot 10^{-4}\,\mathrm{cm}^{-1}$, $\sigma_1 = 5{,}45 \cdot 10^{-4}$

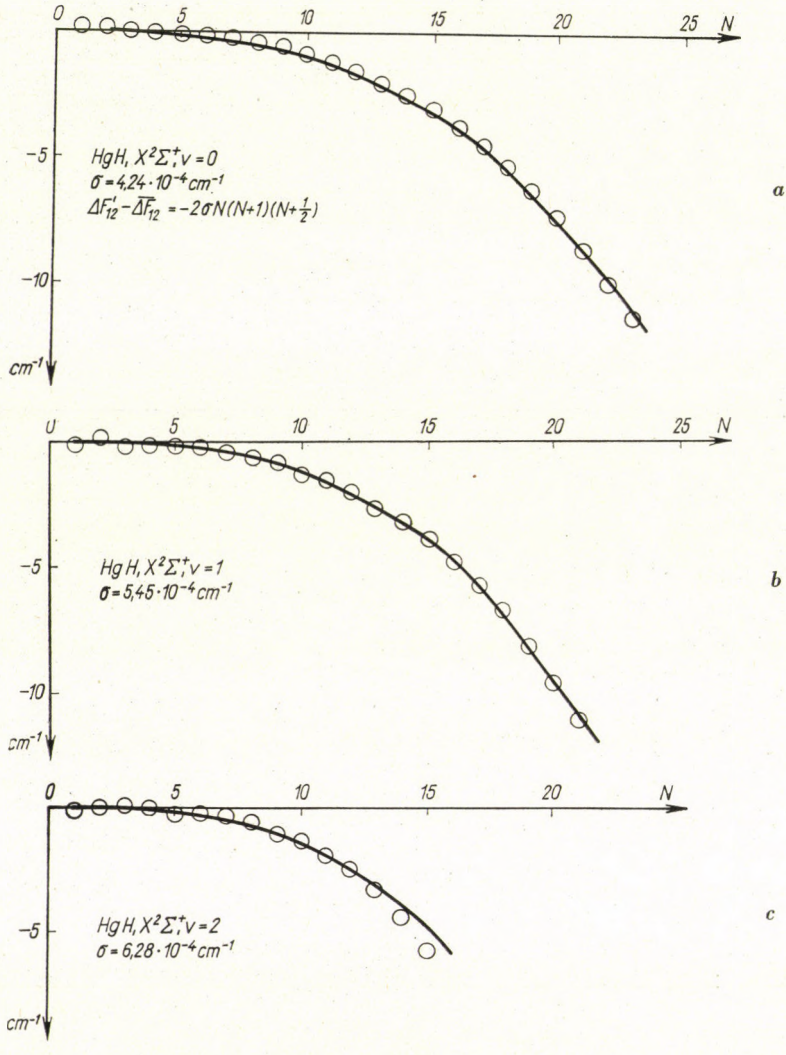

Fig. 1 a, b, c

cm^{-1}, $\sigma_2 = 6{,}28 \cdot 10^{-4}$ cm^{-1}. Experiment and theory have been found to be in good agreement.

If on the basis of (7) the value of σ is calculated theoretically (see [9], formula (40)) by assuming that the perturbation is caused by the $A^2\Pi$ term lying over the $X^2\Sigma^+$ term as high as $h\nu \sim 26\,000$ cm^{-1}, we obtain indeed values of the order of 10^{-4} cm^{-1}. The increase of these values with the growth of the vibrational quantum number is made clear as well, since, as regards the vibrational states lying higher, $h\nu$ decreases gradually and in (7) $(h\nu)^2$ figures as the denominator.

Similarly to the above, Fig. 2 shows the deviation from the expected multipet splitting on the $v' = 0$ vibrational state of the $B^2\Sigma$ term of the YO molecule. Here $\gamma' = 0{,}143\ \mathrm{cm}^{-1}$ (instead of the evidently erroneous $0{,}148\ \mathrm{cm}^{-1}$ in [6]), while $\sigma = -1{,}92 \cdot 10^{-7}\ \mathrm{cm}^{-1}$. Taking into consideration that the

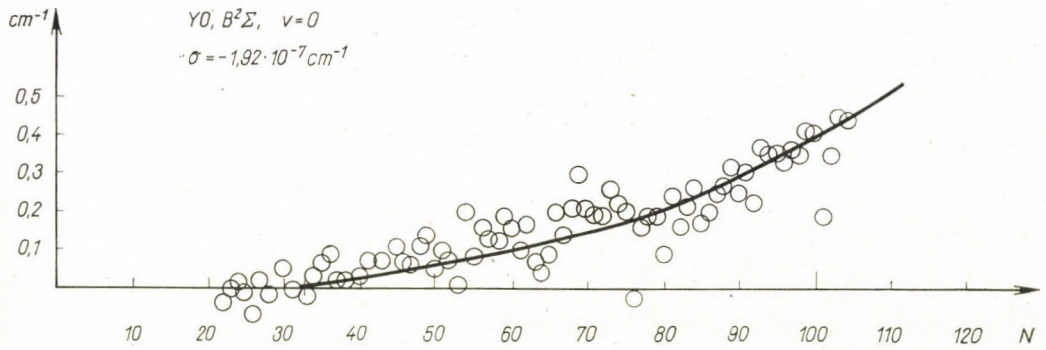

Fig. 2

$A^2\Pi$ term in this molecule is lying about $h\nu \sim 4000\ \mathrm{cm}^{-1}$ from the $B^2\Sigma$ term the theoretically calculated value of σ is indeed of the order of $10^{-7}\ \mathrm{cm}^{-1}$. The agreement between theory and experiment is here also satisfactory.

$^3\Sigma$ terms

For the perturbation of more distant lying $^3\Pi$ terms formula (1) of the $^3\Sigma$ term is in first approximation modified in the following way:

$$F_1'(N) = \frac{2}{3}\frac{\xi^2}{h\nu} + \left(B_\Sigma + 8\frac{\eta^2}{h\nu}\right)N(N+1) + D_\Sigma N^2 (N+1)^2 - \\ - \left(\varepsilon - \frac{\xi^2}{6h\nu}\right)\frac{N}{2N+3} + \left(\gamma - 4\frac{\xi\eta}{h\nu}\right)N,$$

$$F_2'(N) = \frac{2}{3}\frac{\xi^2}{h\nu} + \left(B_\Sigma + 8\frac{\eta^2}{h\nu}\right)N(N+1) + D_\Sigma N^2(N+1)^2 + \\ + \left(\varepsilon - \frac{\xi^2}{6h\nu}\right) - \left(\gamma - 4\frac{\xi\eta}{h\nu}\right), \qquad (11)$$

$$F_3'(N) = \frac{2}{3}\frac{\xi^2}{h\nu} + \left(B_\Sigma + 8\frac{\eta^2}{h\nu}\right)N(N+1) + D_\Sigma N^2(N+1)^2 - \\ - \left(\varepsilon - \frac{\xi^2}{6h\nu}\right)\frac{N+1}{2N-1} - \left(\gamma - 4\frac{\xi\eta}{h\nu}\right)(N+1).$$

In a similar way as in the foregoing calculations we obtain

$$\begin{aligned} F_1'(N) &= \overline{F_1(N)} - [\sigma(N+1) - \tau]\, N(N+1), \\ F_1'(N) &= \overline{F_2(N)}, \\ F_3'(N) &= \overline{F_3(N)} + [\sigma N + \tau]\, N(N+1), \end{aligned} \tag{12}$$

where

$$\begin{aligned} F_1(N) &= \frac{2}{3}\frac{\xi^2}{h\nu} + \bar{B}N(N+1) + \bar{D}N^2(N+1)^2 - \bar{\varepsilon}\frac{N}{2N+3} + \bar{\gamma}N, \\ F_2(N) &= \frac{2}{3}\frac{\xi^2}{h\nu} + \bar{B}N(N+1) + \bar{D}N^2(N+1)^2 + \bar{\varepsilon} - \bar{\gamma}, \\ \overline{F_3(N)} &= \frac{2}{3}\frac{\xi^2}{h\nu} + \bar{B}N(N+1) + DN^2(N+1)^2 - \bar{\varepsilon}\frac{N+1}{2N-1} - \bar{\gamma}(N+1) \end{aligned} \tag{13}$$

and

$$\begin{aligned} \bar{B} &= B_\Sigma + 8\frac{\eta^2}{h\nu} - 4\frac{\xi\eta}{(h\nu)^2}(B_\Sigma - B_\Pi) - \frac{\xi^2(B_\Sigma - B_\Pi)}{2(h\nu)^2}; \\ \bar{D} &= D_\Sigma - 8\frac{\eta^2(B_\Sigma - B_\Pi)}{(h\nu)^2}, \\ \bar{\varepsilon} &= \varepsilon - \frac{\xi^2}{6(h\nu)}; \quad \bar{\gamma} = \gamma - 4\frac{\xi\eta}{h\nu}; \quad \sigma = 4\frac{\xi\eta(B_\Pi - B_\Sigma)}{(h\nu)^2}; \\ \tau &= \frac{\xi^2(B_\Pi - B_\Sigma)}{4(h\nu)^2}. \end{aligned} \tag{14}$$

Similarly to the foregoing now $\overline{F_1(N)}$, $\overline{F_2(N)}$, $\overline{F_3(N)}$ represent the unperturbed term values determined from experimental data. For the difference between the observed and calculated multiplet splitting

$$\begin{aligned} \Delta F_{12}' - \overline{\Delta F_{12}} &= -[\sigma(N+1) - \tau]\, N(N+1), \\ \Delta F_{32}' - \overline{\Delta F_{32}} &= [\sigma N + \tau]\, N(N+1) \end{aligned} \tag{15}$$

is obtained.

In Figs. 3a, 3b, 3c the vibrational states $v = 0$, 1, 2 of the $A^3\Sigma_u^+$ term of the N_2 molecule are shown [7]. The circles represent the deviations between the experimentally observed triplet splitting and the theoretical ones calculated with the values $\bar{\varepsilon}_0 = +0{,}888$ cm^{-1}, $\bar{\varepsilon}_1 = +0{,}884$ cm^{-1}, $\bar{\varepsilon}_2 = +0{,}876$ cm^{-1} and $\bar{\gamma} = +0{,}005$ cm^{-1} (instead of $\varepsilon = -0{,}444$, $-0{,}442$, $-0{,}438$ and $\gamma = -0{,}0020$ in [7]) which have been determined experimentally, whereas the lines drawn in full represent the expressions on the right sides of (15) calcul-

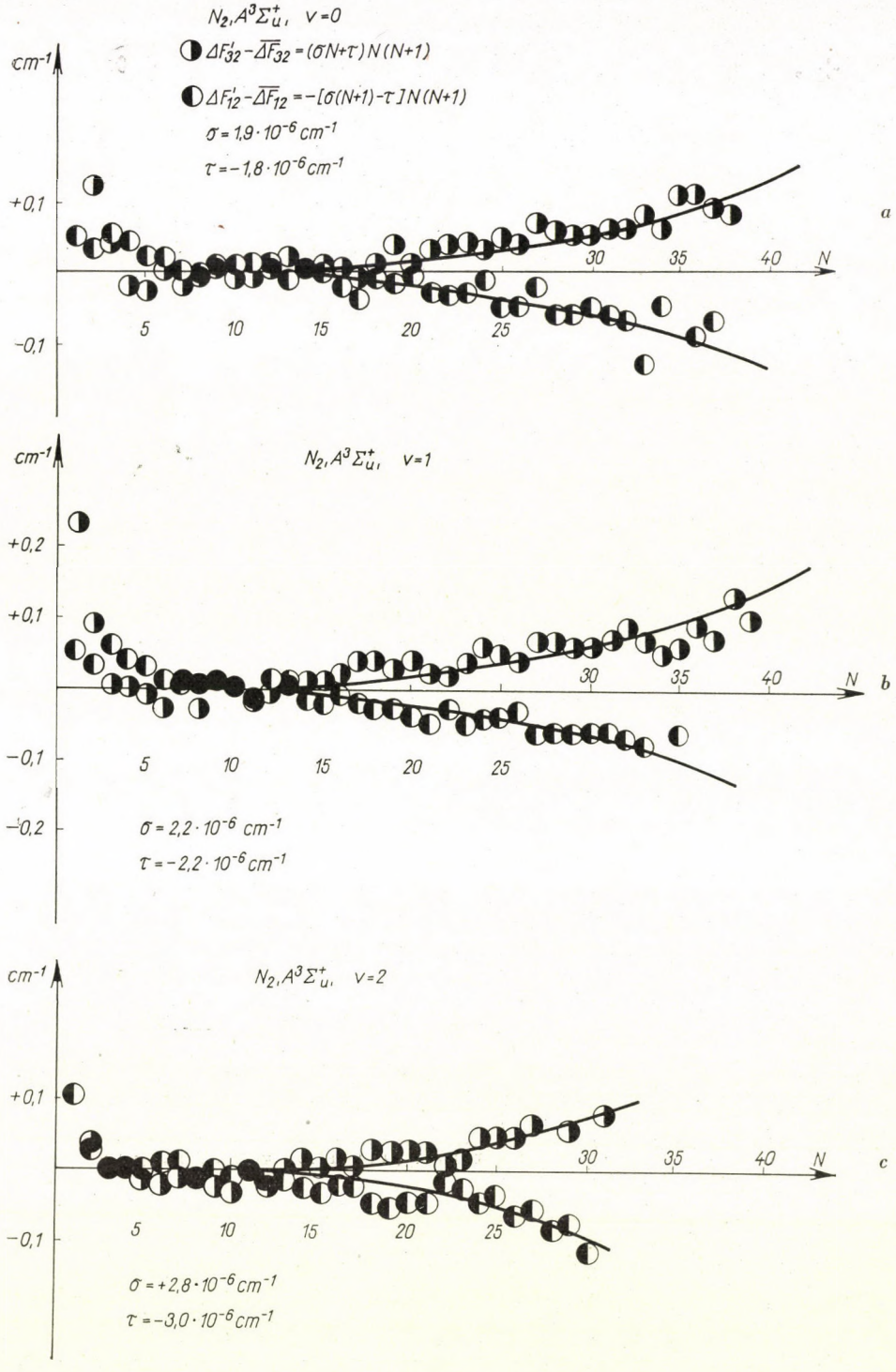
$N_2, A^3\Sigma_u^+$, $v=0$
$\Delta F'_{32} - \overline{\Delta F}_{32} = (\sigma N + \tau) N(N+1)$
$\Delta F'_{12} - \overline{\Delta F}_{12} = -[\sigma(N+1) - \tau] N(N+1)$
$\sigma = 1{,}9 \cdot 10^{-6}\ cm^{-1}$
$\tau = -1{,}8 \cdot 10^{-6}\ cm^{-1}$
cm⁻¹
+0,1
−0,1
5 10 15 20 25 30 35 40 N
a
$N_2, A^3\Sigma_u^+$, $v=1$
cm⁻¹
+0,2
+0,1
−0,1
−0,2
5 10 15 20 25 30 35 40 N
b
$\sigma = 2{,}2 \cdot 10^{-6}\ cm^{-1}$
$\tau = -2{,}2 \cdot 10^{-6}\ cm^{-1}$
$N_2, A^3\Sigma_u^+$, $v=2$
cm⁻¹
+0,1
−0,1
5 10 15 20 25 30 35 40 N
c
$\sigma = +2{,}8 \cdot 10^{-6}\ cm^{-1}$
$\tau = -3{,}0 \cdot 10^{-6}\ cm^{-1}$

Fig. 3 a, b, c

ated with the values $\sigma_0 = +1{,}1 \cdot 10^{-6}$ cm^{-1}, $\tau_0 = -1{,}8 \cdot 10^{-6}$ cm^{-1}, $\sigma_1 = +2{,}2 \cdot 10^{-6}$ cm^{-1}, $\tau_1 = -2{,}2 \cdot 10^{-6}$ cm^{-1}, $\sigma_2 = 2{,}8 \cdot 10^{-6}$ cm^{-1}, $\tau_2 = -3{,}0 \cdot 10^{-6}$ cm^{-1}. Experiment and theory have been found to be in good agreement.

If on the basis of (14) the values of σ and τ are calculated theoretically (see [10] formula (36, (37)) by assuming that the perturbation is caused by the $C^3\Pi_u$ term lying over the $A^3\Sigma_u^+$ term as high as $h\nu \sim 29\,000$ cm^{-1} we obtain values of the order of 10^{-7} cm^{-1}. It is probable that the perturbations of the $B'^3\Sigma_u^-$ and the $a'^1\Sigma_u^-$ states or of the unknown lower state of the

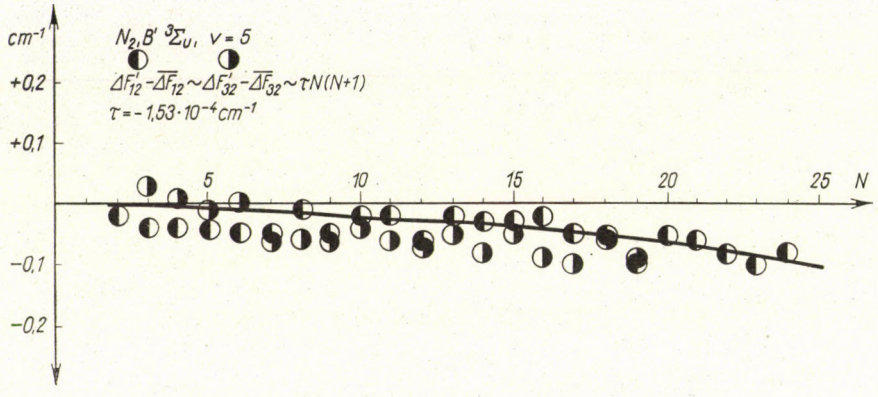

Fig. 4

Kaplan bands play even an important part in the formation of the value of τ (see below). The increase of these values with the growth of the vibrational quantum number is made clear as well, since as regards the vibrational states lying higher, $h\nu$ decreases gradually.

In Fig. 4 the vibrational state $v' = 5$ of the $B'^3\Sigma_u^-$ term of the N_2 molecule is shown. The circles represent the deviations between the experimentally observed triplet splittings and the theoretical ones calculated with the values $\bar{\varepsilon} = 0{,}41$ cm^{-1} $\left(\text{cf. [8], where } \lambda = \frac{3\bar{\varepsilon}}{2}\right)$ and $\bar{\gamma} = -0{,}0033$ cm^{-1} which have been determined experimentally. As can be seen the circles representing the two triplet splittings practically coincide indicating that on the right side of (15) $\sigma \approx 0$, which is possible through (14) if $B_\Sigma = B_\Pi$, but in this case even $\tau \approx 0$ may result. Thus, this interpretation does not appear probable and moreover taking into account the term scheme of the N_2 molecule [12] the nearest $^3\Pi$ term which might cause this perturbation is lying so far, i. e. $h\nu$ is so high, that the theoretical estimations for the value of τ furnish a value of an order of magnitude which is much lower than would follow from the experimental results.

If, by taking into account the spin-orbit interaction, similarly to the foregoing we examine the influence of other terms as well for the perturbations of the $^1\Sigma$, $^1\Pi$, $^5\Sigma$, $^5\Pi$ and $^3\Sigma$ terms we obtain a formula similar to (15) with the only difference that in these the first term does not appear at all, that is $\sigma = 0$, hence the two curves coincide. Thus e. g. for the perturbation of the $^1\Pi$ term

$$\left.\begin{aligned} \Delta F'_{12} - \overline{\Delta F_{12}} &= \tau \frac{N(N+1)^2}{N+\frac{3}{2}} \sim \tau N(N+1), \\ \Delta F'_{32} - \overline{\Delta F_{32}} &= \tau \frac{N^2(N+1)}{N-\frac{1}{2}} \sim \tau N(N+1) \end{aligned}\right\} \tag{16}$$

is obtained, where values of all the constants ($\bar{B}$, $\bar{D}$, $\bar{\varepsilon}$, $\bar{\gamma}$, τ) are to be obtained by substituting $\eta = 0$ in (14) the difference being that the sign of τ this time is the opposite. In this case the two curves coincide, this single curve is shown in Fig. 4, where $\tau = -1{,}53 \cdot 10^{-4}\ \mathrm{cm}^{-1}$. In the term scheme there are singulet terms to be found in the neighbourhood of the $B'^3\Sigma_u^-$ term, out of which the unknown lower state of the Kaplan bands, both from the point of view of distance and symmetry, appears to be a possible cause of this perturbation.

Summing up it can be stated that the anomalous behaviour of the $X^2\Sigma^+$, $B^2\Sigma$, $A^3\Sigma_u^+$, $B'^3\Sigma_u^-$ and $^7\Sigma$ term of the HgH, YO, N_2 and MnH molecule, respectively, is of the same character and in all the five cases it is caused alike by the perturbation of not too distant lying Π terms. These perturbations are brought about by the spin-orbit interaction and by the transmission of the terms neglected at the separation of the wave equation. Since the nearness of other terms is not infrequent, such deviations may occur elsewhere as well, and in all probability they do appear in several other cases, too, apart from those described in the present work.

REFERENCES

1. J. H. Van Vleck, Phys. Rev., **33,** 467, 1929.
2. M. H. Hebb, Phys. Rev., **49,** 610, 1936.
3. A. Budó and I. Kovács, Hung. Act. Phys., **1,** 1, 1948.
4. I. Kovács, Proc. Roy. Ir. Acad., **60,** 15, 1959.
5. E. Hulthén, Zs. F. Phys., **50,** 319, 1928.
6. U. Uhler and A. Akerlind, Ark. f. Fys., **19,** 1, 1961.
7. P. K. Caroll, Proc. Roy. Ir. Acad., **54A,** 369, 1952.
8. P. K. Caroll and H. E. Rubalcava, Proc. Phys. Soc., **76,** 342, 1960.
9. T. E. Nevin, Proc. Roy. Ir. Acad. **48,** 1, 1942; **50,** 123, 1945.
10. I. Kovács, Can. Journ. Phys., **36,** 348, 1958.
11. I. Kovács, Can. Journ. Phys., **36,** 325, 1958.
12. G. Herzberg, Spectra of Diatomic Molecules, Van Nostrand, New York, 1951.

ОБ АНОМАЛЬНОМ РАСЩЕПЛЕНИИ МУЛЬТИПЛЕТНЫХ Σ-СОСТОЯНИЙ В ДВУХАТОМНЫХ МОЛЕКУЛАХ I

И. КОВАЧ

Р е з ю м е

Доказывается, что обнаруженные аномалии в мультиплетном расщеплении термов $X^2\Sigma^+$ молекулы **HgH**, $B^2\Sigma$ молекулы **YO**, $A^3\Sigma_u^+$ и $B'^3\Sigma_u^-$ молекулы N_2 по характеру подобны аномалиям, обнаруженным на $^7\Sigma$ — терме молекулы **MnH**. Показывается далее, что причина во всех этих пяти случаях одна и та же: возмущение Π — термов, не очень далеко лежащих. Экспериментальные и теоретические данные хорошо согласуются.

INVESTIGATION OF AN ARBITRARY SCREW DISLOCATION IN A CYLINDRICAL ELASTIC BODY

By

I. Kovács

INSTITUTE FOR EXPERIMENTAL PHYSICS, ROLAND EÖTVÖS UNIVERSITY, BUDAPEST

(Presented by E. Nagy. — Received 5. VIII. 1961)

A straight screw dislocation situated excentrically within an elastic cylinder was investigated. By applying a conformal transformation such a solution of the stress field is determined, which fulfils the boundary conditions along the surface of the cylinder as well as along the core of the dislocation. With the help of this stress field the dislocation energy as a function of distance from the centre of the cylinder can be obtained. Using this energy expression one arrives at the conclusion that the stress required for the production of a screw dislocation in a perfect elastic cylinder is of the order of $\mu/2\pi$, which is the theoretical critical shear stress for the perfect crystal, as determined by FRENKEL with his simplified model.

Introduction

According to our present knowledge the plastic deformation of crystalline materials takes place by dislocations [1]. Namely, in case of the perfect crystal the value of the critical shear stress at which the slip begins is

$$\sigma_{cr} = \frac{\mu}{2\pi} , \tag{1}$$

where μ is the shear modulus of the material. This estimate is given by FRENKEL [2] on the basis of a simple crystal model. According to experiments, however, the slip will begin at a value of $10^{-4}\ \mu - 10^{-5}\ \mu$. Thus it is evident that we are not dealing with perfect crystals when investigating the plastic deformation, but that we have to suppose some kind of internal irregularities which make the slip in the crystal significantly lighter. Such crystal defects are just the dislocations.

We can distinguish two kinds of dislocations: edge and screw dislocations. With the help of these numerous plastic properties of crystalline materials can be explained. For the theoretical treatment we restrict ourselves first of all to elastic models, which give sufficiently good approximation. The simplest models are the VOLTERRA dislocations [3] (Fig. 1). Here the dislocations are in a central position in an elastic cylinder and they are formed by cutting up the crystal along a plane containing the axis and displacing the cut surfaces with respect to each other. In the case of a perfect cylinder, however, this

displacing gives infinite stresses at the axis of the cylinder, to avoid which we remove a hole with radius r_0 along the axis of the cylinder.

The properties of VOLTERRA dislocations may be easily obtained from the theory of elasticity. To our knowledge, a solution of the more general problem, namely the determination of the stresses produced by these distortions and the elastic energy stored in the solid for screw dislocations not in the centre of the cylinder, has never been attempted. This problem is, however, interesting, because if we know the energy of dislocation as a function of the distance from the axis, then the gradient of this energy gives the force

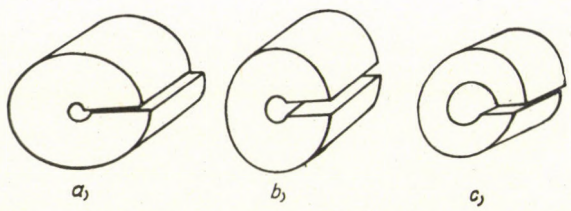

Fig. 1. Volterra dislocations; a, b edge dislocations, c screw dislocation

acting on the dislocation. Calculations have already been carried out for edge dislocations by J. S. KOEHLER [4]. In the following we investigate the general screw dislocations.

The Volterra dislocations in general position

Let us assume a dislocation parallel with the axis of a cylinder with radius R, at a distance x_0. The slip plane of the dislocation goes through the axis of the cylinder (Fig. 2). The displacement (b) along the cut is now only

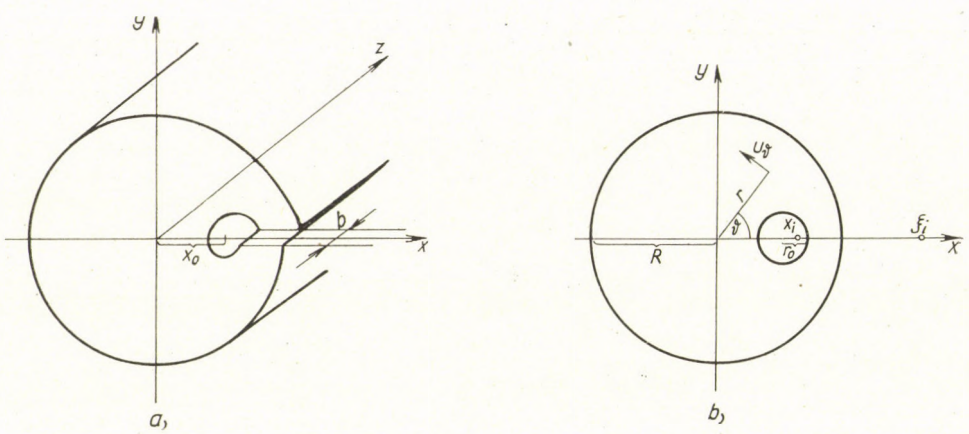

Fig. 2. a) screw dislocation on the distance x_0 from the axis of cylinder
b) coordinate systems in a z = const. plane

in the z-direction, thus all the components of the displacement vector $\boldsymbol{u}(u_x, u_y, u_z)$ except u_z are zero. Because of the axial symmetry we have

$$\frac{\partial}{\partial z} \equiv 0 \,. \tag{2}$$

u_z is determined by the equations of elastic equilibrium ([1] p. 36.), according to this:

$$\Delta u_z = 0 \,, \tag{3}$$

where $\Delta = \frac{\partial^2}{\partial x^2} + \frac{\partial^2}{\partial y^2}$ is the two-dimensional Laplacian operator. Knowing u_z the only stresses differing from zero can be calculated:

$$\sigma_{xz} = \sigma_{zx} = \mu \frac{\partial u_z}{\partial x} \; ; \quad \sigma_{yz} = \sigma_{zy} = \mu \frac{\partial u_z}{\partial y} \,.$$

We have to find such a solution of equ. (3) which fulfils the following condition:

$$-\lim_{y \to +0} u_z + \lim_{y \to -0} u_z = b \,,$$

because u_z is discontinuous at $y = 0$. The suitable solution for centrally situated dislocations [1] is found to be

$$u_{z0} = \frac{b}{2\pi} \operatorname{arc\,tg} \frac{y}{x} \,. \tag{5}$$

In order to solve the general problem we apply such a conformal transformation in the (x, y) plane (Fig. 2b), which transforms two circles with different centres into two concentric circles. As such a transformation does not change the two-dimensional Laplacian equation we can use immediately the central solution for the dislocation in the image plane. From this solution an inverse transformation gives the solution in the general case.

Let us determine the necessary conformal mapping. We introduce the complex variables

$$\bar{z} = x + iy \tag{6}$$

and in the image plane

$$\omega = u + iv \,. \tag{7}$$

It is known that the function

$$\omega = \frac{a \cdot \bar{z} + b}{c \cdot \bar{z} + d}$$

transforms a circle into another circle. In the present case a suitable function is

$$\omega = \frac{\bar{z} - x_i}{\bar{z} - \xi_i}, \tag{8}$$

where x_i, ξ_i are the inverse points of both circles, which are given by

$$x_i \cdot \xi_i = R^2 \tag{9}$$

and

$$(x_i - x_0) \cdot (\xi_i - x_0) = r_0^2 \tag{10}$$

From these we have

$$x_i, \xi_i = \frac{R^2 + x_0^2 - r_0^2 \pm \sqrt{(R^2 + x_0^2 - r_0^2)^2 - 4x_0^2 R^2}}{2x_0}. \tag{11}$$

A simple calculation shows that with such a choice of x_i and ξ_i the function (8) transforms the nonconcentric circles of Fig. 2b into concentric circles with centre in the origin of the (u, v) plane. Thus we can write

$$u_z = \frac{b}{2\pi} \operatorname{arc\,tg} \frac{v}{u}. \tag{12}$$

On the basis of the equs. (6), (7), (8) we find

$$u + iv = \frac{x^2 + y^2 - (x_i + \xi_i)\, x + R^2}{(x - \xi_i)^2 + y^2} + i \frac{(x_i - \xi_i)\, y}{(x - \xi_i)^2 + y^2}. \tag{13}$$

With the use of the Cauchy—Riemann relations

$$\frac{\partial u}{\partial x} = \frac{\partial v}{\partial y}, \quad \frac{\partial u}{\partial y} = -\frac{\partial v}{\partial x},$$

and the equations

$$\Delta u = 0, \qquad \Delta v = 0$$

we have

$$\frac{\partial^2 u_z}{\partial x^2} + \frac{\partial^2 u_z}{\partial y^2} = 0.$$

The function (12) thus satisfies equ. (3). If we substitute the value of v/u, u_z will have the following form:

$$u_z = \frac{b}{2\pi} \operatorname{arc\,tg} \frac{(x_i - \xi_i)\, y}{x^2 + y^2 - (x_i + \xi_i)\, x + R^2}. \tag{14}$$

This solution satisfies the boundary conditions too (Appendix I):

$$x\frac{\partial u_z}{\partial x}+y\frac{\partial u_z}{\partial y}=0\,, \qquad \text{for} \quad x^2+y^2=R^2\,, \tag{15}$$

and

$$(x-x_0)\frac{\partial u_z}{\partial x}+y\frac{\partial u_z}{\partial y}=0\,, \qquad \text{for} \quad (x-x_0)^2+y^2=r_0^2\,. \tag{16}$$

respectively.

A final simple computation shows that if $x_0 \to 0$, then the expression (14) will go over into the central solution

$$u_{z0}=\frac{b}{2\pi}\operatorname{arc\,tg}\frac{y}{x}\,.$$

Further we have to take into consideration that the stresses, derived from the displacement (14), produce a non-zero couple [5] in the point $(x_0, 0)$. This means that our screw dislocation is not yet stable. In order to stabilize the dislocation the couple must be zero, therefore we have to consider the following equations:

$$\frac{\partial^2 u_x}{\partial x^2}+\frac{\partial^2 u_x}{\partial y^2}+\frac{\partial^2 u_x}{\partial z^2}=0\,,\ \frac{\partial^2 u_y}{\partial x^2}+\frac{\partial^2 u_y}{\partial y^2}+\frac{\partial^2 u_y}{\partial z^2}=0\,. \tag{17}$$

In the case of a screw dislocation the volume dilatation is zero, thus

$$\frac{\partial u_i}{\partial i}=0\,, \qquad i=x,y,z\,.$$

The condition of axial symmetry ensures that the stress field does not depend on z. The solutions which satisfy these conditions are

$$u_x=A_0\,yz \quad , \quad u_y=-A_0\,xz\,, \tag{18}$$

where A_0 is a constant. From (18) we have

$$\sigma_{xy}=\mu\left(\frac{\partial u_x}{\partial y}+\frac{\partial u_y}{\partial x}\right)=\mu\,(A_0\,z-A_0\,z)\equiv 0\,,$$

and

$$\sigma'_{xz}=\mu A_0\,y\,,\ \sigma'_{yz}=-\mu A_0\,x\,. \tag{19}$$

The latter stresses do not fulfil yet the boundary conditions. To reach this we have to determine such a solution (u'_z) of equ. (3) that the amount

of stress given by the displacement u_z' and stresses (19) satisfy together the boundary conditions. This means:

$$\text{I.}\ \mu\left(x\frac{\partial u_z'}{\partial x}+y\frac{\partial u_z'}{\partial y}\right)+x\sigma_{xz}'+y\sigma_{yz}'=\mu\left(x\frac{\partial u_z'}{\partial x}+y\frac{\partial u_z'}{\partial y}\right)=0$$

$$\text{for}\quad x^2+y^2=R^2,$$

$$\text{II.}\ \mu\left[(x-x_0)\frac{\partial u_z'}{\partial x}+y\frac{\partial u_z'}{\partial y}\right]+(x-x_0)\sigma_{xz}'+y\sigma_{yz}'=\mu\left(x\frac{\partial u_z'}{\partial x}+y\frac{\partial u_z'}{\partial x}\right)-$$

$$-\mu x_0\frac{\partial u_z'}{\partial x}-\mu x_0 A_0 y=0 \qquad \text{for}\quad (x-x_0)^2+y^2=r_0^2.$$

In polar coordinates we have

$$\frac{\partial u_z'}{\partial x}=\cos\vartheta\frac{\partial u_z'}{\partial r}-\frac{\sin\vartheta}{r}\frac{\partial u_z'}{\partial\vartheta},$$

therefore the boundary conditions are

$$\text{I.}\qquad \frac{\partial u_z'}{\partial r}=0 \qquad \text{for}\quad r=R,$$

$$\text{II.}\ r\frac{\partial u_z'}{\partial r}-x_0\frac{\partial u_z'}{\partial r}\cos\vartheta+x_0\frac{\sin\vartheta}{r}\frac{\partial u_z'}{\partial\vartheta}=0 \qquad \text{for}\quad (x-x_0)^2+y^2=r_0^2.$$

We confine ourselves to an approximative solution of this problem. If x_0 is very small, then the two boundary conditions are identical in a good approximation, and then $u_z'\cong 0$. The case interesting for us is $x_0 \gg r_0$. We may take then $r\cong x_0$ and $\vartheta \ll 1$, or $\cos\vartheta\cong 1$. With these approximations the boundary condition II will be significantly simplified:

$$\frac{\partial u_z'}{\partial\vartheta}=A_0 x_0^2 \qquad \text{for}\quad r\cong x_0 \text{ and } \cos\vartheta\cong 1\ . \tag{20}$$

Further

$$\frac{\partial u_z'}{\partial r}=0 \qquad \text{for}\quad r=R\ . \tag{21}$$

We can satisfy these two conditions by the following solution of equ. (3):

$$u_z'=(A+B\cdot\log r)\,r^2\sin 2\vartheta\ . \tag{22}$$

A simple computation shows that

$$A=\frac{A_0}{2}\,\frac{1+2\log R}{1-2\log\frac{x_0}{R}}\ ;\quad B=-\frac{A_0}{1-2\log\frac{x_0}{R}}$$

and thus

$$u_z' = \frac{A_0}{2} \frac{1 - 2\log\frac{r}{R}}{1 - 2\log\frac{x_0}{R}} r^2 \sin 2\vartheta \,. \tag{23}$$

We will choose the value of A_0 so that the stresses acting in the plane $z = \text{const.}$ produce zero couple in the point $(x_0, 0)$. This ensues if (Appendix II)

$$\int_r \int_\vartheta [(r - x_0 \cos\vartheta)\,\sigma_{\vartheta z}]\, r\,dr\,d\vartheta = \int_r \int_\vartheta (r - x_0\cos\vartheta)\left(\frac{\mu}{r}\frac{\partial \bar{u}_z}{\partial\vartheta} + \mu\frac{\partial u_\vartheta}{\partial z}\right) r\,dr\,d\vartheta = 0, \tag{24}$$

where

$$\bar{u}_z = u_z + u_z' = \frac{b}{2\pi}\operatorname{arc\,tg}\frac{(x_i - \xi_i)\,y}{x^2 + y^2 - (x_i + \xi_i)\,x + R^2} + \\ + \frac{A_0}{2}\frac{1 - 2\log\frac{r}{R}}{1 - 2\log\frac{x_0}{R}} r^2 \sin 2\vartheta \,, \tag{25}$$

and

$$u_\vartheta = A_0\, rz \,. \tag{26}$$

From (24) we have

$$A_0 = -\frac{b}{(R^4 - r_0^4)}\left\{R^2 - r_0^2 + (x_i - x_0)^2 - x_i^2 + x_0 x_i \log\frac{x_i}{R}\right\}. \tag{27}$$

Knowing A_0 we can finally obtain the stresses acting around a screw dislocation in a general position

$$\sigma_{\vartheta z} = \frac{\mu b}{2\pi}\frac{(x_i - \xi_i)[(r^2 + R^2)\cos\vartheta - (x_i + \xi_i)\,r]}{[r^2 + R^2 - (x_i + \xi_i) r\cos\vartheta]^2 + (x_i - \xi_i)^2 r^2 \sin^2\vartheta} + \\ + \mu A_0 \frac{1 - 2\log\frac{r}{R}}{1 - 2\log\frac{x_0}{R}} r\cos 2\vartheta + \mu A_0\, r \,. \tag{28}$$

The energy of a screw dislocation in general position

The energy of a screw dislocation is ([1] p. 38)

$$U = \frac{1}{2}\int_S \sigma_{\vartheta z}\, b\, dr \,, \tag{29}$$

where the integration has to be performed over the surfaces of the cut, or in the present case, at $\vartheta = 0$. From (28)

$$\sigma_{\vartheta z}(\vartheta = 0) = \frac{\mu b}{2\pi} \frac{x_i - \xi_i}{r^2 + R^2 - (x_i + \xi_i) r} + \mu A_0 \frac{1 - 2 \log \frac{r}{R}}{1 - 2 \log \frac{x_0}{R}} r + \mu A_0 r \,. \quad (30)$$

Consider the first term of (30). The determination of the energy derived from this term gives a result valid in the whole interval $-(R - r_0) \leqq x_0 \leqq \leqq (R - r_0)$. According to (29) making use of expressions (9), (10):

$$U_0 = \frac{\mu b^2}{4\pi} \int_{x_0 + r_0}^{R} \frac{x_i - \xi_i}{r^2 + R^2 - (x_i + \xi_i) r} dr =$$

$$= \frac{\mu b^2}{4\pi} \int_{r_0 + x_0}^{R} \left[\frac{1}{r - x_i} - \frac{1}{r - \xi_i} \right] dr = \frac{\mu b^2}{8\pi} \log \frac{R^2 - x_0 x_i}{R^2 - x_0 \xi_i} \,.$$

If we insert the values of x_i and ξ_i we can write

$$U_0 = \frac{\mu b^2}{8\pi} \log \frac{R^2 - x_0^2 + r_0^2 + \sqrt{(R^2 + x_0^2 - r_0^2)^2 - 4 x_0^2 R^2}}{R^2 - x_0^2 + r_0^2 - \sqrt{(R^2 + x_0^2 - r_0^2)^2 - 4 x_0^2 R^2}} \,. \quad (31)$$

If $x_0 = 0$ we obtain $U_0 = \frac{\mu b^2}{4\pi} \log \frac{R}{r_0}$, in agreement with a former result ([1] p. 38.) further if $x_0 = R - r_0$ (there is still no slip thus there is no dislocation) then $U_0 = 0$. The remaining two terms lead to

$$U_1 = \frac{\mu b A_0}{2} \frac{R^2 - (x_0 + r_0)^2 \left[1 - \log \frac{x_0 + r_0}{R} \right]}{1 - 2 \log \frac{x_0}{R}} \quad (32)$$

and

$$U_2 = \frac{\mu b A_0}{2} [R^2 - (x_0 + r_0)^2] \,. \quad (33)$$

The expressions (32), (33) are valid only in the case $x_0 \geqslant r_0$. We shall see, however, that for dislocations which have greater distances from the surface of the cylinder the energy very rapidly reaches practically the total energy. The terms (32), (33) give very little correction also in the vicinity

of the surface, thus their effects are entirely negligible. Therefore we have to study only the term given by (31). A form suitable for calculation results, if the following substitutions are introduced:

$$r_0 = k \cdot b, x_0 = R - n \cdot b - r_0 = R - (n + k)\, b\,,$$

where $n \cdot b$ is the distance of the dislocation from the surface. With these

$$(R^2 + x_0^2 - r_0^2)^2 - 4x_0^2 R^2 = 4R^2 b^2 (n+k)^2 \left[1 - \frac{k^2}{(n+k)^2}\right]\left[1 - \frac{b(n+k)}{R} + \right.$$

$$\left. + \frac{(n+k)^2 - k^2}{4R^2} b^2\right] \cong 4R^2 b^2 (n+k)^2 \left[1 - \frac{k^2}{(n+k)^2}\right], \quad \text{for} \quad n \cdot b \ll R\,,$$

further

$$R^2 - x_0^2 + r_0^2 = 2(n+k) Rb - (n+k)^2 b^2 + k^2 b^2 \cong 2(n+k) Rb, \quad \text{for} \quad n \cdot b \ll R\,.$$

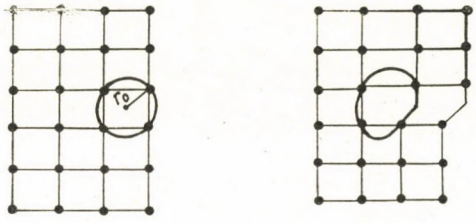

a) *b)*

Fig. 3. a) perfect crystal; *b)* screw dislocation on an interatomic distance from the surface of crystal

Substituting these expressions into (31) we have

$$U_0 = \frac{\mu b^2}{8\pi} \log \frac{n + k + \sqrt{n(n+2k)}}{n + k - \sqrt{n(n+2k)}}\,. \tag{34}$$

It can be seen that the energy of dislocation in this approximation is independent of the radius of the cylinder, while for small n it depends significantly on the radius of the core of the dislocation.

Before proceeding further some assumptions are to be made about r_0. Consider at first a perfect cubic crystal. A simple answer can be obtained by consulting Fig. 3. It seems clear that in this case the only logical choice of

$$r_0 \text{ is } b\sqrt{2}/2, \text{ thus } k = \sqrt{2}/2.$$

For increasing integer values of n the dislocation moves off from the surface of the cylinder by steps of the interatomic distance. If we determine

the change of the dislocation energy for such an elementary slip, then we can determine an average force acting along the path b and resulting in just the same amount of work. It is obvious that this force must be given by the minimum force F leading to slip along an interatomic distance. For such an elementary slip the work done by the external stress per unit length is given by

$$A = \sigma \cdot b^2 = F \cdot b = \Delta U_0 .$$

From this

$$\sigma = \frac{\Delta U_0}{b^2} . \tag{35}$$

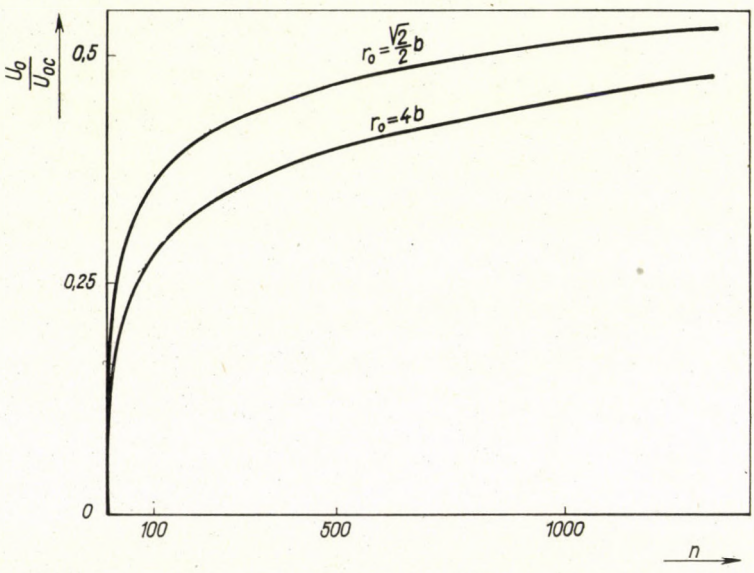

Fig. 4. Energy of a screw dislocation as a function of distance from the surface of cylinder

Figs. 4 and 5 show the energy of a screw dislocation and the stress (35) as a function of distance from the surface in the case of a perfect crystal. On the ordinates of Fig. 4 we have plotted the quotient of the actual and maximum value of dislocation energy. The maximum of the energy is found evidently in the centre. For the computation we used the value $R = 0{,}1$ cm and $b = 2{,}5 \cdot 10^{-8}$ cm. It may be seen that at 1000 interatomic distances from the surface the energy of dislocation rises to more than half of its maximum value. At the same time the force required for the movement of dislocation decreases very rapidly by orders of magnitude. The greatest force required for the slip will be necessary at the first elementary step. Then the

crystal is still perfect, so this force can be regarded as the critical shear stress of the perfect crystal. For this we get from (34) and (35)

$$\sigma_{cr} \cong \frac{3}{4} \frac{\mu}{2\pi} .$$

Thus we have obtained the theoretical shear stress of the perfect crystal on the basis of an elastic model.

With the dislocation moving off from the surface, the force decreases very rapidly, further slip taking place on the influence of very small forces. All this is in perfect agreement with experience. The presence of defects of the type investigated decreases the stress significantly, leading to plastic deformation. At a few thousand interatomic distances from the surface the force

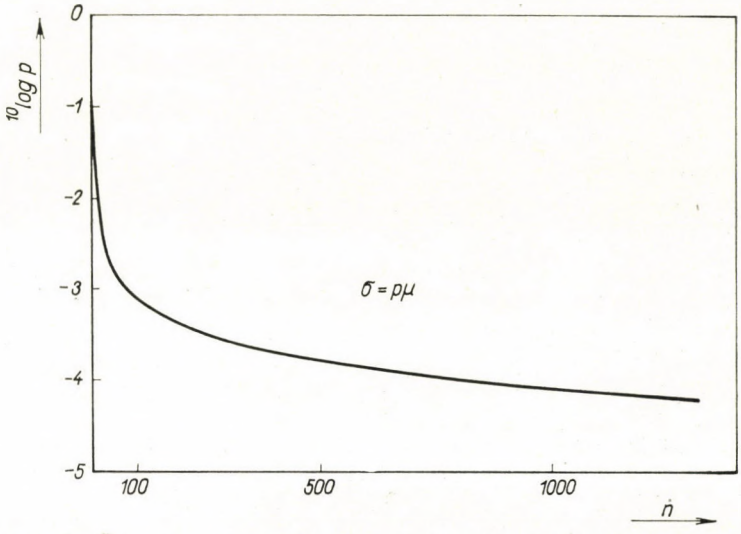

Fig. 5. Force acting on a screw dislocation as a function of distance from the surface of cylinder

derived from the change of the elastic energy of dislocation is practically zero, but the movement of the dislocation is hindered by some frictional force, giving the required stress of 10^{-4} μ—10^{-5} μ for the plastic deformation. This frictional force cannot be studied, however, on hand of this elastic model, because here all the forces acting between the atoms play an important role.

In Fig. 4 we have plotted the energy for a dislocation the core radius of which is $r_0 = 4b$. In this case the curve reaches its maximum a little slower, but the shape of the curve is identical with the former one. The difference between the forces acting on the two kinds of dislocations is very small and cannot be represented in the figure. Larger differences are found only between the forces, which are required for the first step, this value is here $0{,}35 \frac{\mu}{2\pi}$.

This decrease can be understood because in the presence of a core with radius $4b$ the crystal cannot any longer be considered perfect, and, as we have seen, the largest force is necessary for the plastic deformation of the perfect crystal.

Summary

On the basis of an elastic model we show that the stresses required for plastic deformation decrease very significantly in the presence of a dislocation, as well as the commencement of the plastic deformation of a perfect crystal is equivalent to the production of a dislocation. For the production of a dislocation the stress required is of the order of (1).

We can conclude from this result that even if a perfect crystal would exist, nevertheless the slip would not take place simultaneously in the whole slip plane, but the critical shear stress would produce a dislocation first. About a few thousand interatomic distances from the surface this can be moved already by very small forces, leading to the production of a new dislocation, etc. In this fictitious process extremely large slips would arise, which probably would lead to the fracture of the solid. Thus we see that a crystal free from dislocations would behave as a perfectly rigid body suffering fracture under the critical stress. From this we have to conclude that dislocations not only make the plastic deformation easier, but that without this mechanism brittle fracture would set in before a plastic deformation could commence.

Appendix I

By differentiating equ. (12) we have

$$\frac{\partial u_z}{\partial x} = \frac{b}{2\pi} \frac{1}{1+\left(\frac{v}{u}\right)^2} \frac{\partial}{\partial x}\left(\frac{v}{u}\right),$$

and

$$\frac{\partial u_z}{\partial y} = \frac{b}{2\pi} \frac{1}{1+\left(\frac{v}{u}\right)^2} \frac{\partial}{\partial y}\left(\frac{v}{u}\right).$$

With these we can write instead of (15), (16)

$$x \frac{\partial}{\partial x}\left(\frac{v}{u}\right) + y \frac{\partial}{\partial y}\left(\frac{v}{u}\right) = 0, \qquad \text{for} \quad x^2 + y^2 = R^2,$$

and

$$(x - x_0) \frac{\partial}{\partial x}\left(\frac{v}{u}\right) + y \frac{\partial}{\partial y}\left(\frac{v}{u}\right) = 0 \qquad \text{for} \quad (x - x_0)^2 + y^2 = r_0^2.$$

respectively. After differentiating we find

$$\frac{\partial}{\partial x}\left(\frac{v}{u}\right) = -\frac{2x-(x_i+\xi_i)}{(x_i-\xi_i)y}\left(\frac{v}{u}\right),$$

and

$$\frac{\partial}{\partial y}\left(\frac{v}{u}\right) = \frac{x^2-y^2-(x_i+\xi_i)\,r+R^2}{(x_i-\xi_i)\,y^2}\left(\frac{v}{u}\right).$$

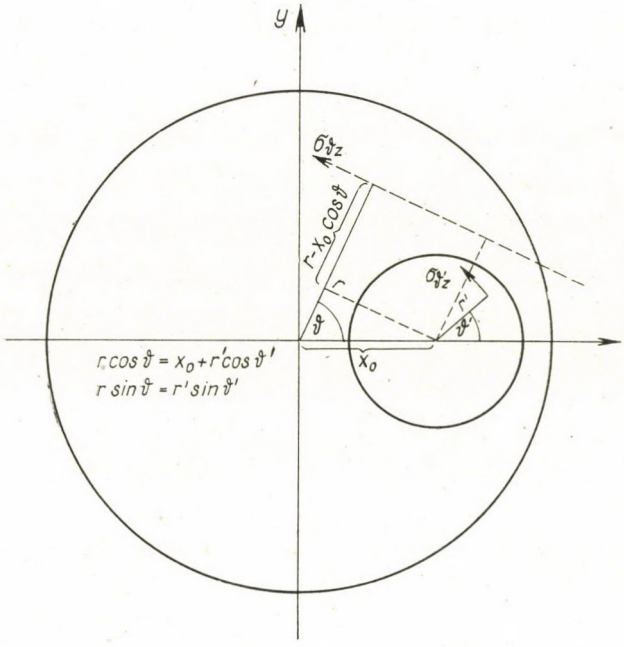

Fig. 6. On the calculation of the couple acting on the point $(x_0, 0)$

Thus we obtain

$$x\frac{\partial}{\partial x}\left(\frac{v}{u}\right)+y\frac{\partial}{\partial y}\left(\frac{\partial}{u}\right) = \frac{R^2-x^2-y^2}{(x_i-\xi_i)\,y}\left(\frac{v}{u}\right)^2 \equiv 0 \quad \text{for } x^2+y^2=R^2,$$

further

$$(x-x_0)\frac{\partial}{\partial x}\left(\frac{v}{u}\right)+y\frac{\partial}{\partial y}\left(\frac{v}{u}\right) = \frac{r_0^2-(x-x_0)^2-y^2}{(x_i-\xi_i)\,y}\left(\frac{v}{u}\right)^2 \equiv 0$$

$$\text{for } (x-x_0)^2+y^2=r_0^2.$$

We applied here (11)

$$x_0\,(x_i+\xi_i) = R^2+x_0^2-r_0^2.$$

Appendix II

It is evident on the basis of Fig. 6 that the couple acting on the point $(x_0, 0)$ is

$$\int_r \int_\vartheta [(r - x_0 \cos\vartheta)\,\sigma_{\vartheta z}]\, r\,d\,r\,d\vartheta = \int_0^R \int_0^{2\pi} (r - x_0 \cos\vartheta)\,\sigma_{\vartheta z}\, r\,d\,r\,d\,\vartheta - \int_0^{r_0} \int_0^{2\pi} (r'\,\sigma_{\vartheta' z})\, r'\,dr'\,d\vartheta' \,. \tag{36}$$

In the first term on the right side we have written

$$\sigma_{\vartheta z} = \sigma^1_{\vartheta z} + \sigma^2_{\vartheta z} + \sigma^3_{\vartheta z} \,,$$

where

$$\sigma^1_{\vartheta z} = \frac{\mu b}{2\pi} \frac{(x_i - \xi_i)\,[(r^2 + R^2)\cos\vartheta - (x_i + \xi_i)\,r]}{[r^2 + R^2 - (x_i + \xi_i)\,r\cos\vartheta]^2 + (x_i - \xi_i)^2\, r^2 \sin^2\vartheta} \,,$$

$$\sigma^2_{\vartheta z} = \mu A_0 \frac{1 - 2\log\dfrac{r}{R}}{1 - 2\log\dfrac{x_0}{R}}\, r\cos 2\vartheta \,,\quad \sigma^3_{\vartheta z} = \mu A_0\, r \,.$$

Let us investigate at first the following integral

$$I_1 = \int_0^R \int_0^{2\pi} (r\sigma^1_{\vartheta z})\, r\,d\,r\,d\,\vartheta \,.$$

An elementary calculation shows that I_1 can be written in the following form:

$$I_1 = \frac{\mu b}{4\pi} \int_0^R \left\{ \frac{r^2 - \xi_i^2}{2\,r\,\xi_i} \int_0^{2\pi} \frac{d\vartheta}{\cos\vartheta - \dfrac{r^2 + \xi_i^2}{2\,r\,\xi_i}} - \frac{r^2 - x_i^2}{2\,r\,x_i} \int_0^{2\pi} \frac{d\vartheta}{\cos\vartheta - \dfrac{r^2 + x_i^2}{2\,r\,x_i}} \right\} r\,dr \,.$$

Because

$$I_a = \int_0^{2\pi} \frac{d\vartheta}{\cos\vartheta - a} = -\frac{2\pi}{\sqrt{a^2 - 1}} \qquad \text{for} \quad a > 1 \,,$$

we can write

$$I_{\xi i} = \frac{4\pi r \xi_i}{r^2 - \xi_i^2}, \quad I_{x_i} = \begin{cases} -\dfrac{4\pi r x_i}{r^2 - x_i^2} & \text{for} \quad r > x_i , \\ \dfrac{4\pi r x_i}{r^2 - x_i^2} & \text{for} \quad r < x_i . \end{cases}$$

With these we have

$$I_1 = \frac{\mu b}{4\pi}\left[\int_0^R 2\pi r dr + \int_{x_i}^R 2\pi r dr - \int_0^{x_i} 2\pi r dr\right] = \frac{\mu b}{2}(R^2 - x_i^2) .$$

After a similar computation we find

$$I_2 = -x_0 \int_0^R \int_0^{2\pi} \sigma_{\vartheta z}^1 \cos\vartheta \, r dr d\vartheta = \frac{\mu b}{2} x_0 x_i \log \frac{x_i}{R} .$$

Further we have

$$I_3 = \int_0^R \int_0^{2\pi} (r - x_0 \cos\vartheta)\, \sigma_{\vartheta z}^2 \, r dr d\vartheta = 0 ,$$

and

$$I_4 = \int_0^R \int_0^{2\pi} (r - x_0 \cos\vartheta)\, \sigma_{\vartheta z}^3 \, r dr d\vartheta = \mu A_0 \pi \frac{R^4}{2} .$$

With these the value of the first term becomes

$$I_1 + I_2 + I_3 + I_4 = \frac{\mu b}{2}\left(R^2 - x_i^2 + x_0 x_i \log \frac{x_i}{R}\right) + \mu A_0 \pi R^4/2 . \qquad (37)$$

The second term on the right side of equ. (36) can be calculated in the following way. Let us consider the expression

$$I_5 = \int_0^{r_0} \int_0^{2\pi} (r' \sigma_{\vartheta' z}^1)\, r' \, dr' \, d\vartheta' ,$$

where

$$\sigma_{\vartheta' z}^1 = \frac{\mu b}{2\pi} \frac{(x_i - \xi_i)\left[(r'^2 + r_0^2)\cos\vartheta' - (x_i + \xi_i - 2x_0) r'\right]}{\left[r'^2 + r_0^2 - (x_i + \xi_i - 2x_0) r' \cos\vartheta'\right]^2 + (x_i - \xi_i)^2 r'^2 \sin^2\vartheta'} .$$

It can be seen that the integral I_5 can be obtained from the integral I_1, if we substitute $(x_i - x_0)$, $\xi_i - x_0)$, r_0 for x_i, ξ_i, R, respectively. On the basis

of this we have

$$I_5 = \frac{\mu b}{2} \{r_0^2 - (x_i - x_0)^2\} . \tag{38}$$

In the calculation of the integral

$$I_6 = \int_0^{r_0} \int_0^{2\pi} (r' \sigma_{\vartheta' z}^2) \, r' \, dr' \, d\vartheta'$$

we confine ourselves to an approximation. From (23) we have

$$u_z'(\vartheta', r') = \frac{A_0}{2} \frac{1 - 2\log \frac{r}{R}}{1 - 2\log \frac{x_0}{R}} (r'^2 \sin 2\vartheta' + 2x_0 r' \sin \vartheta'),$$

where

$$r = \sqrt{r'^2 + x_0^2 + 2x_0 r' \cos \vartheta'} .$$

Because $r' \leqq r_0 \ll x_0$ we can take x_0 instead of r in good approximation, and thus we can write

$$\sigma_{\vartheta' z}^2 = \frac{\mu}{r'} \frac{\partial u_z'(r', \vartheta')}{\partial \vartheta'} \cong \mu A_0 (r' \cos 2\vartheta' + x_0 \sin \vartheta') ,$$

with this we have $I_6 = 0$.

Using the expression

$$u_{\vartheta'} = A_0 \, z \, (r' + x_0 \cos \vartheta') ,$$

the value of the final integral can be obtained too. This is

$$I_7 = \int_0^{r_0} \int_0^{2\pi} (r' \sigma_{\vartheta' z}^3) \, r' \, dr' \, d\vartheta' = \mu A_0 \pi \frac{r_0^4}{2} .$$

With the values from (24) and (36) we find

$$\frac{\mu b}{2} \left[R^2 - x_i^2 + x_0 x_i \log \frac{x_i}{R} \right] + \mu A_0 \pi \frac{R^4}{2} -$$

$$- \frac{\mu b}{2} [r_0^2 - (x_i - x_0)^2] - \mu A_0 \pi \frac{r_0^4}{2} = 0$$

and from this

$$A_0 = - \frac{b}{\pi (R^4 - r_0^4)} \left\{ R^2 - r_0^2 + (x_i - x_0)^2 - x_i^2 + x_0 x_i \log \frac{x_i}{R} \right\} .$$

Acknowledgement

The author wishes to express his sincere thanks to Professor E. NAGY for his interest and the valuable discussions of this work.

REFERENCES

1. A. H. COTTRELL, Dislocations and Plastic Flow in Crystals, Oxford University Press Oxford 1953.
2. J. FRENKEL, Z. Physik, **37**, 572, 1926.
3. V. VOLTERRA, Ann. Ecole Norm. Sup. (3), **24**, 400, 1907.
4. J. S. KOEHLER, Phys. Rev., **60**, 397, 1941.
5. E. H. MANN, Proc. Roy. Soc. A, **199**, 376, 1949.

ИССЛЕДОВАНИЕ ВИНТОВОЙ ДИСЛОКАЦИИ, ЭКСЦЕНТРИЧЕСКИ РАЗМЕЩАЮЩЕЙСЯ В УПРУГОМ ЦИЛИНДРЕ

И. КОВАЧ

Р е з ю м е

Исследовалась винтовая дислокация, эксцентрически размещающейся в упругом цилиндре. Применением конформного преобразования для пространства напряжений можно получить решение, выполняющее граничные условия как по поверхности цилиндра, так и по полости дислокации. Если данное пространство напряжений известно, можно определить энергию дислокации как функцию расстояния от центра цилиндра. На основании полученного таким путем выражения энергии можно сделать вывод по отношению порядка величины напряжения, необходимого для создания винтовой дислокации в упругом цилиндре, не имеющем дефектов: он получается равным $\mu/2\pi$. Данная величина совпадает с теоретическим критическим напряжением сдвига идеального кристалла, определенным Френкелем на основе простой модели кристалла.

A CONTRIBUTION TO THE PROBLEM OF INELASTIC MAGNETIC SCATTERING OF POLARIZED NEUTRONS IN Fe AND Ni

By

L. VALENTA and ŠT. ZAJAC

FACULTY OF TECHNICAL AND NUCLEAR PHYSICS, ČVUT, PRAHA, CZECHOSLOVAKIA

(Presented by A. Kónya. — Received 2. X. 1961)

Magnetic small-angle scattering of slow polarized neutrons is studied in Fe and Ni at 0°K by means of the spin wave theory. The cross section is calculated in dependence on the polarization of incoming and scattered neutrons supposing the spin of the incoming particles to be polarized parallel or antiparallel to the spontaneous magnetization of the crystal. With the constants used in this paper, the value of the limiting angle within which scattering can only take place was about 49′ for Fe and 23′ for Ni.

1. Inelastic magnetic scattering proves to have become an interesting tool for studying the spin waves in ferromagnetics. There is a great number of papers dealing with this problem, nevertheless little attention has been paid to polarization effects till now (see e. g. [1], . . . , [16]). Since the experimental possibilities for studying such effects have increased in the last years, it seems to be interesting to examine the polarization effects in more detail. In this paper we will try to gain more insight into what magnitude of the polarization effects can be expected from the small-angle scattering experiments with slow polarized neutrons.

2. It is known that two mechanisms are important in our problem [17], [18], [3], namely the creation and annihilation of spin waves and phonons. Now, the annihilation of both spin waves and phonons tends to zero if the temperature decreases to 0° K [18], [3]. If we choose the energy of the scattered neutrons so that their wave length is greater than the corresponding Bragg wave length and their velocity is smaller than the velocity of sound in the crystal, phonons cannot be produced.

Hence, taking the neutrons slow enough and limiting our considerations to 0° K we may confine our discussion to the mechanism of excitation of spin waves only. This will be done in this paper, because it simplifies the theoretical approach to the problem and moreover, it has the advantage that the experiments are more "pure" and their interpretation is easier. Recently this effect has been studied experimentally by means of unpolarized neutrons [16].

3. In this paper we will avail ourselves of the paper by AVAKYANTS [2], who discussed the magnetic small-angle scattering of an unpolarized neutron beam on a simple cubic lattice at 0° K. Following AVAKYANTS we will extend his results to include polarization effects and apply the results to iron and nickel. First of all, it is necessary to sketch AVAKYANTS' procedure briefly:

The interaction energy operator is taken in the form

$$V = e\mu_n \sum_k \frac{\alpha_k \times (\mathbf{r} - \mathbf{r}_k)}{|\mathbf{r} - \mathbf{r}_k|^3}, \tag{1}$$

$$\mu_n = \frac{e\hbar}{2Mc} p_n \sigma,$$

where e is the charge of the electron; μ_n is the magnetic moment of the neutron; α_k is the Dirac matrix of the k-th electron whose position vector is $\mathbf{r}_k$; $\mathbf{r}$ is the position vector of the neutron, M its mass; $\hbar$ is Planck's constant; c is the velocity of light in vacuum and $\gamma_n \cong -1{,}91$; finally σ is the Pauli spin matrix for the neutron.

The motion of the neutron before (index 0) and after (index 1) scattering is described by wave functions of the form of a plane wave

$$\varphi_{0,1} = \frac{1}{\sqrt{\Omega}} e^{i/\hbar \mathbf{p}_{0,1} \cdot \mathbf{r}} \chi_{\mu 1,2}(\sigma), \tag{2}$$

where Ω is the volume of the ferromagnetic crystal, $\mathbf{p}_{0,1}$ the momentum of the neutron and $\mu_{1,2} = \pm \frac{1}{2}$ its spin quantum number; χ is the spin wave function of the neutron. The crystal before scattering is supposed to be completely magnetized with spins directed along the z-axis. It can be described by the wave function

$$\Phi_0 = \frac{1}{\sqrt{N!}} \sum_p \varepsilon_p P \psi_1(\mathbf{r}_1) S_{1/2}(s_1) \ldots \psi_N(\mathbf{r}_N) S_{1/2}(s_N), \tag{3}$$

where N is the number of atoms in the crystal, P is the permutation operator, $\varepsilon_p = \pm 1$ (+ for even permutations, — for the odd ones). The atomic wave functions $\psi_k(\mathbf{r}_l)$ for the l-th electron on the k-th atom are supposed to be s-functions identical for all the atoms, the only difference being in the centre of the atoms to which they are attached. $S \pm {}^1/_2(s_l)$ are the corresponding electronic spin wave functions. The one-spin wave state of the crystal can be described after Bloch [19] by

$$\Phi_1 = \frac{1}{\sqrt{N!\,N}} \sum_{l,P} \varepsilon_p e^{i\mathbf{k}\mathbf{R}_l} P \psi_1(\mathbf{r}_1) S_{1/2}(s_1) \ldots$$
$$\ldots \psi_l(\mathbf{r}_l) S_{-1/2}(s_l) \ldots \psi_N(\mathbf{r}_N) S_{1/2}(s_N); \tag{4}$$

here $\mathbf{k}$ is the spin wave vector (see § 4) and l runs over all indices of the atoms in the crystal. AVAKYANTS has shown that introducing the abbreviations

$$\mathbf{q} = \frac{1}{\hbar}(\mathbf{p}_0 - \mathbf{p}_1), \qquad \mathbf{q}_0 = \frac{\mathbf{q}}{|\mathbf{q}|},$$

$$F = \int \psi^* \psi e^{i\mathbf{q}\mathbf{r}}\, d\tau, \qquad r_0 = \frac{e^2}{mc^2},$$

$$\boldsymbol{\sigma}_{01} = \chi^+_{\mu_1}(\sigma)\, \boldsymbol{\sigma} \chi_{\mu_0}(\sigma), \quad \boldsymbol{\sigma}^{(l)}_{01} = S^+_{-1/2}(s)\, \boldsymbol{\sigma}^{(l)}\, S_{1/2}(s),$$

we may write for the matrix element $V_{0\to 1}$

$$V_{0\to 1} = < \varphi_1 \Phi_1 | V | \varphi_0 \Phi_0 > =$$

$$= \frac{\pi r_0 F \gamma_n \hbar^2}{\Omega \sqrt{N}\, M} \sum \left\{ \boldsymbol{\sigma}_{01} \cdot \boldsymbol{\sigma}^{(l)}_{01} - (\boldsymbol{\sigma}_{01} \cdot \mathbf{q}_0)(\boldsymbol{\sigma}^{(l)}_{01} \cdot \mathbf{q}_0) \right\} \cdot e^{i(\mathbf{q}-\mathbf{k})\mathbf{R}_l}; \tag{5}$$

$\mathbf{R}_l$ is the position vector of the l-th atom. Calculating $|V_{0\to 1}|^2$, AVAKYANTS used the usual averaging procedure and obtained the formula for unpolarized beams.

4. Let us proceed now to the discussion of the polarization effects. As may easily be seen, $\boldsymbol{\sigma}^{(l)}_{01}$ is a vector with constant components

$$\boldsymbol{\sigma}^{(l)}_{01} \equiv (1, i, 0).$$

Denoting symbolically the state with the spin component $+\frac{1}{2}\left(-\frac{1}{2}\right)$ by $\uparrow(\downarrow)$, we find $\boldsymbol{\sigma}_{01}$ for the four possible transitions:

Transition	$\boldsymbol{\sigma}_{01}$
$\uparrow \to \uparrow$	$(0, \quad 0, \quad 1)$
$\uparrow \to \downarrow$	$(1, \quad i, \quad 0)$
$\downarrow \to \uparrow$	$(1, \quad -i, \quad 0)$
$\downarrow \to \downarrow$	$(0, \quad 0, \quad -1)$

Hence, we obtain for $|V_{0\to 1}|^2$

$$|V_{0\to 1}|^2 = \frac{1}{N}\left(\frac{\pi r_0 \hbar^2 \gamma_n F}{\Omega M}\right)^2 P \left| \sum_l e^{i(\mathbf{q}-\mathbf{k})\mathbf{R}_l} \right|^2, \tag{7}$$

where, according to (5) and (6), the following value is to be substituted for P:

Transition	P
$\uparrow \to \uparrow$	$q_{0z}^2 (1 - q_{0z}^2)$
$\uparrow \to \downarrow$	$(1 - q_{0z}^2)^2$
$\downarrow \to \uparrow$	$(1 + q_{0z}^2)^2$
$\downarrow \to \downarrow$	$q_{0z}^2 (1 - q_{0z}^2)$.

The corresponding cross section is given by the formula

$$d\sigma = \frac{2\pi}{\hbar} |V_{0\to 1}|^2 \varrho_E \frac{\Omega M}{p_0}, \tag{8}$$

where

$$\varrho_E = \frac{p_1 M \Omega^2}{(2\pi\hbar)^3 (2\pi)^3} d\Omega_{\mathbf{p}_1} d^3\mathbf{k};$$

$d\Omega_{\mathbf{p}_1}$ is the element of the scattering angle of $\mathbf{p}_1$, $d^3\mathbf{k} = dk_x\, dk_y\, dk_z$ and

$$k_i = \frac{2\pi}{Ga} \varkappa_i, \quad (\varkappa_i = 0, 1, \ldots, G-1).$$

G^3 is equal to the number of elementary cells in the crystal, a is the lattice constant of the crystal.

Hence, inserting (7) into (8) we obtain

$$d\sigma = \frac{2\pi}{\hbar} \frac{\Omega M}{p_0} \frac{p_1 M \Omega^2}{(2\pi\hbar)^3 (2\pi)^3} \frac{1}{N} \left(\frac{\pi r_0 \hbar^2 \gamma_n F}{\Omega M} \right)^2 \cdot P \left| \sum e^{i(\mathbf{q}-\mathbf{k})\mathbf{R}_l} \right|^2 d\Omega_{\mathbf{p}_1} d^3 \cdot \mathbf{k}. \tag{9}$$

Now, according to WEINSTOCK [17],

$$\left| \sum_l e^{i(\mathbf{q}-\mathbf{k})\mathbf{R}_l} \right|^2 = \frac{(2\pi)^3}{B} N \sum_{\tau} \delta(\mathbf{q} - \mathbf{k} + 2\pi\boldsymbol{\tau}), \tag{10}$$

where B is the volume per atom and $\boldsymbol{\tau}$ is any reciprocal lattice vector. Because we are dealing with very slow neutrons, whose wave length is greater than $C\frac{\hbar}{a}$ $(C \sim 1)$ we can take only $\boldsymbol{\tau} = 0$ in (10), since the conservation of momentum could not be respected otherwise. For B we have $B = \frac{a^3}{N_j}$, where N_j is the

number of atoms in any elementary cell. Hence, we have

$$\left| \sum_l e^{i(\mathbf{q}-\mathbf{k})\mathbf{R}_l} \right|^2 = \left(\frac{2\pi}{a} \right)^3 N N_j \delta (\mathbf{q} - \mathbf{k}) \tag{11}$$

with $N_j = 2$ resp. 4 for Fe resp. Ni. Inserting (11) into (9), putting $F \cong 1$ and integrating over $\mathbf{k}$, we get

$$d\sigma = \frac{r_0^2 \gamma_n^2 N}{4 p_0} p_1 P d\Omega_{\mathbf{p}_1}. \tag{12}$$

Finally, integration over $d\Omega_{\mathbf{p}_1}$ gives

$$\sigma = \frac{r_0^2 \gamma_n^2 N}{4 p_0} \int p_1 P d\, \Omega_{\mathbf{p}_1}. \tag{13}$$

5. Integrating in (13) we must respect the conservation of energy and momentum where we take Ia^2k^2 for the energy of the spin wave and $\hbar\mathbf{k}$ for its momentum [19], [2]. I is the exchange integral. We get

$$p_1 = p_0 \frac{\cos\vartheta + \sqrt{\cos^2\vartheta + \beta^2 - 1}}{1 + \beta}, \tag{14}$$

where

$$\cos\vartheta = \frac{\mathbf{p}_0 \cdot \mathbf{p}_1}{|\mathbf{p}_0||\mathbf{p}_1|}, \qquad \beta = \frac{\hbar^2}{2MI a^2}.$$

Taking $I = 205\ k$ for Fe [20] and $I = 290\ k$ for Ni [21] (k is the Boltzmann constant) we obtain $\beta_{\mathrm{Fe}} = 1{,}43 \cdot 10^{-2}$ and $\beta_{\mathrm{Ni}} = 6{,}69 \cdot 10^{-3}$. Since $\mathbf{p}_1$ must be real and positive, the inequality

$$\sin\vartheta \leqslant \beta \tag{15}$$

must hold. We see that scattering is possible only within a small angle given by (15). Using the values of β for Fe and Ni we find the value of the limiting angle for both metals. We obtain 49′ for Fe and 23′ for Ni. We see that the scattering cone is extremely narrow. Nevertheless, successful measurements have recently been made on iron [16].

6. For further calculations we use the spherical coordinates for $\mathbf{p}_0$ (p_0, Θ_0, Φ_0) and $\mathbf{p}_1$ (p_1, Θ, Φ). In the following results for $\Theta_0 = 0$ are presented. In this case the following formulae are necessary:

$$p_1 = p_0 \frac{\cos\Theta + \sqrt{\cos^2\Theta + \beta^2 - 1}}{1 + \beta}, \tag{16}$$

$$q_{0z}^2 = \frac{\beta + \sin^2\Theta - \cos\Theta\sqrt{\cos^2\Theta + \beta^2 - 1}}{2\beta}. \tag{17}$$

Using (16) and (17) we obtain from (12) the differential cross section for Fe and Ni in dependence on the polarization of the incoming and outcoming neutrons as shown in Fig. 1 and Fig. 2.

Inserting (16)—(17) into (13) and carrying out the integration Θ within the interval (0, arccos $\sqrt{1-\beta^2}$) we obtain after some rather tedious calculations the total cross section per atom as shown in Table 1.

Table 1

Transition	Fe σ (barns)	Ni σ (barns)
$\uparrow - \uparrow$	$5.86 \cdot 10^{-6}$	$1.27 \cdot 10^{-6}$
$\uparrow - \downarrow$	$3.32 \cdot 10^{-5}$	$7.22 \cdot 10^{-6}$
$\downarrow - \uparrow$	$6.44 \cdot 10^{-5}$	$1.40 \cdot 10^{-5}$
$\downarrow - \downarrow$	$5.86 \cdot 10^{-6}$	$1.27 \cdot 10^{-6}$
unpolarized	$5.47 \cdot 10^{-5}$	$1.19 \cdot 10^{-5}$

Here the formulae for the particular integrals have been expanded into power series in β and higher terms omitted. The detailed calculation of the integrals and their expansion into power series can be found in [22].

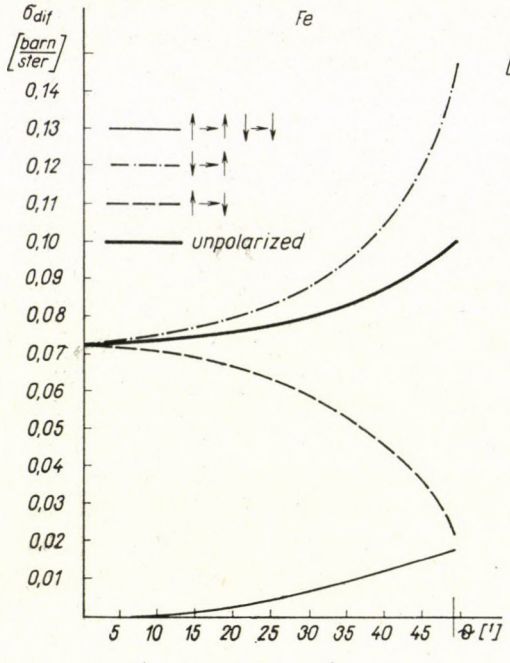

Fig. 1

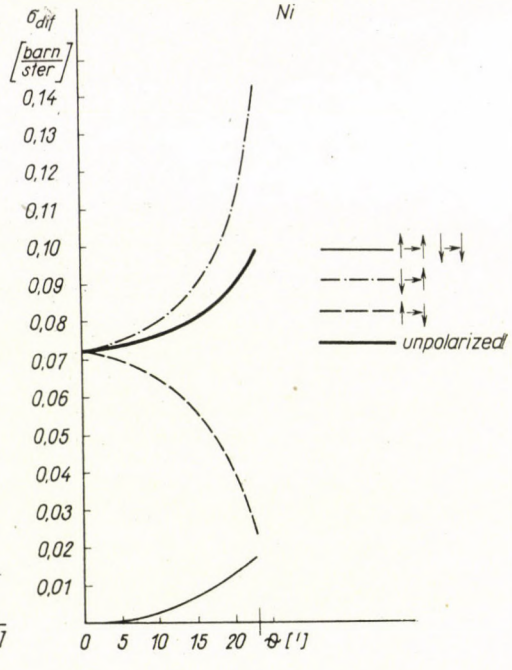

Fig. 2

7. Fig. 1, 2 and Table 1 show clearly a strong dependence of the cross sections on the polarization of the neutrons before and after the scattering process. There is some hope that similar effects may be expected at a temperature higher than 0° K. The small value of the scattering cross section at 0° K is not surprizing, since similar results have been obtained for the unpolarized beams. Moreover, we may expect, on the basis of calculations carried out for unpolarized beams [6] that a fairly great increase of the cross section will set in with increasing temperature. The influence of temperature will be the subject of further calculations.

8. As may be seen from (14), all angles Θ are allowed for $\beta > 1$. Hence, the scattering is no longer limited to small angles as in the case of iron and nickel. The analysis shows that it could appear at materials with a low Curie temperature. A rough estimation shows [22] that it might be so in some of the rare earth metals.

9. Let us briefly summarize our results: The scattering cross sections per atom for the scattering at 0° K were calculated for various initial and final polarizations of the spin of the neutron in the direction of the magnetization of the crystal. A strong dependence of the scattering cross section on the polarization of neutrons before and after scattering has been found. With the constants used in this paper the value of the limiting angle within which scattering can only take place was about 49′ for Fe and 23′ for Ni.

Acknowledgment: Our thanks are due to P. HÁJÍČEK for the checking some of our calculations.

LITERATURE

1. O. HALPERN and M. H. JOHNSON, Phys. Rev., **55,** 898, 1939.
2. G. AVAKYANTS, J. Exp. Theor. Phys., **18,** 444, 1948.
3. R. G. MOORHOUSE, Proc. Phys. Soc. A, **64,** 1097, 1951.
4. W. MARSHALL, Proc. Phys. Socc. A, **67,** 85, 1954.
5. R. D. LOWDE, Proc. Roy. Soc. A, **221,** 1954.
6. R. J. ELLIOTT and R. D. LOWDE, Proc. Roy. Soc. A, **230,** 46, 1955.
7. R. D. LOWDE, Proc. Roy. Soc. A, **235,** 305, 1956.
8. R. J. ELLIOTT, R. D. LOWDE and W. MARSHALL, Proc. Phys. Soc. A, **69,** 939, 1956.
9. L. VAN HOVE, Phys. Rev., **93,** 268, 1954.
10. L. VAN HOVE, Phys. Rev., **95,** 249, 1954.
11. L. VAN HOVE, Phys. Rev., **95,** 1374, 1954.
12. S. V. MALEEV, J. Exp. Theor. Phys., **33,** 1010, 1957.
13. S. V. MALEEV, J. Exp. Theor. Phys., **34,** 1518, 1958.
14. A. W. SÁENZ, Phys. Rev., **119,** 1542, 1960.
15. A. W. SÁENZ, J. Appl. Phys., **31,** 1088, 1960.
16. R. D. LOWDE and N. UMAKANTHA, Phys. Rev. Letters, **4,** 452, 1960.
17. R. WEINSTOCK, Phys. Rev., **65,** 1, 1944.
18. A. AKHIEZER and I. POMERANCHUK, J. Exp. Theor. Phys., **17,** 769, 1947.
19. F. BLOCH, Zs. f. Phys., **61,** 206, 1930.
20. C. KITTEL, Rev. Mod. Phys., **21,** 541, 1949.
21. S. FONER and E. D. THOMPSON, Suppl. J. Appl. Phys., **30,** 229S, 1959.
22. Š. ZAJAC, Diploma Thesis, Faculty of Technical and Nuclear Physics, Praha, 1961 (in Czech).

О НЕЭЛАСТИЧНОМ МАГНИТНОМ РАССЕЯНИИ ПОЛЯРИЗОВАННЫХ НЕЙТРОНОВ В Fe И Ni НА МАЛЫЕ УГЛЫ

Л. ВАЛЕНТА и Ш. ЗАЯЦ

Р е з ю м е

На основе теории спиновых волн изучено неупругое магнитное рассеяние медленных поляризованных нейтронов на малые углы в железе и никеле при 0° К. Эффективное сечение рассчитано в зависимости от поляризации до и после рассеяния нейтронов, предполагая спины ориентированные параллельно или антипараллельно спонтанной намагниченности кристалла. Пользуясь константами, применяемыми в этой работе, для предельного угла, внутри которого возможно рассеяние, получилось значение 49' для железа и 23' для никеля.

DAS STATISTISCHE ATOMMODELL IM IMPULSRAUM. I

Von

A. KÓNYA

FORSCHUNGSGRUPPE FÜR THEORETISCHE PHYSIK DER UNGARISCHEN AKADEMIE DER WISSENSCHAFTEN, BUDAPEST

(Eingegangen: 9. X. 1961)

Es wird hier gezeigt, dass im Rahmen der statistischen Theorie des Atoms die Dichteverteilung $\omega(p)$ der Elektronen in dem dreidimensionalen Impulsraum eine Näherungslösung des Mehrteilchenproblems darstellt, welche der Dichteverteilung $\varrho(r)$ der Elektronen in dem dreidimensionalen Koordinatenraum äquivalent ist. Die beiden Dichtefunktionen sind durch symmetrische Relationen miteinander verknüpft, die in nullter Näherung der quantenmechanischen Transformationstheorie entsprechen.

Die Probleme der Quantenmechanik können in verschiedenen Repräsentationen behandelt werden. Bei den Problemen der Elektronenschalen benutzt man meistens die Koordinaten- und die Impulsrepräsentation. Je nach der gewählten Repräsentation bekommt man die Lösung in der Form der Koordinatenwellenfunktion $\psi(r_1, r_2, \ldots)$ bzw. der Impulswellenfunktion $\chi(p_1, p_2, \ldots)$. Die beiden Wellenfunktionen sind miteinander durch die Fourier-Transformation verknüpft. Kennt man die Funktion ψ, so lässt sich $\varrho(r)$, die Elektronendichte im dreidimensionalen Koordinatenraum, bzw. $D(r) = 4\pi r^2 \varrho(r)$, die radiale Elektronenverteilung im Koordinatenraum definieren, welche letztere mit dr multipliziert die Anzahl der Elektronen in der Kugelschale zwischen den Radien r und $r + dr$ angibt. Ebenso können wir aus der Kenntnis der Funktion χ die Elektronendichte im dreidimensionalen Impulsraum $\omega(p)$, bzw. $\Omega(p) = 4\pi p^2 \omega(p)$, die radiale Elektronenverteilung im Impulsraum ableiten [1], [2], wo $\Omega(p)dp$ die Anzahl der Elektronen mit einem Impulsbetrag zwischen p und $p + dp$ angibt.

Für Atome mit mehreren Elektronen liefert die statistische Theorie des Atoms eine sehr einfache und zu vielen Zwecken nützliche Näherung der Elektronendichte im Koordinatenraum [3]. BURKHARDT hat gezeigt [4], dass man in Rahmen dieser Theorie die radiale Elektronenverteilung im Impulsraum $\Omega(p)$ aus der Kenntnis der Dichte $\varrho(r)$ berechnen kann. KÓNYA [5], bzw. COULSON und MARCH [6], [7] haben später diesbezüglich ausführliche Rechnungen durchgeführt und die gewonnene Impulsverteilung für die Bestimmung der Form und Breite der Compton-Linie angewendet.

Unser Ziel ist es jetzt, die von der statistischen Theorie des Atoms gelieferte Impulsverteilung ausführlich zu untersuchen. Wir wollen zeigen, dass in Rahmen dieser Theorie nicht nur die Elektronendichte $\varrho(r)$, sondern auch

$\omega(p)$ als eine äquivalente Näherungslösung des quantenmechanischen Mehrteilchenproblems zu betrachten ist, welche der Impulsrepräsentation entspricht.

Zu diesem Zwecke werden wir in § 1 die Berechnung von $\omega(p)$ aus $\varrho(r)$ erörtern und Zusammenhänge zwischen den beiden Dichtefunktionen ableiten. Danach beweisen wir in § 2, dass $\omega(p)$ eine äquivalente Näherungslösung des Mehrteilchenproblems ist, aus welcher $\varrho(r)$ sich wieder eindeutig bestimmen lässt und zwar der umgekehrten Aufgabe entsprächend auf eine symmetrische Weise. In § 3 werden wir zeigen, dass die Beschreibung der Elektronenverteilung durch $\omega(p)$ der Impulsrepräsentation der Quantenmechanik entspricht und eine Näherung der quantenmechanischen Resultate vom selben Grade bedeutet wie die Beschreibung im Koordinatenraum.

§ 1

Bei der Ableitung der Grundzusammenhänge der statistischen Theorie des Atoms zerteilt man das Atomvolumen in kleine Volumenelemente dv_r, innerhalb welcher das Potential annähernd konstant ist, wo aber noch genug viele Elektronen sich befinden, die wir statistisch behandeln können. Diese Elektronen in einem Raumelement von der Anzahl $\varrho(r)dv_r$ bilden dann ein vollständig entartetes, freies Fermi-Gas am absoluten Nullpunkt der Temperatur. Der Impulsbetrag der Elektronen ändert sich in jedem Volumenelement von Null bis zu dem maximalen Wert

$$P = (3\pi^2)^{1/3}\hbar\varrho^{1/3}(r). \tag{1}$$

Die Elektronen befinden sich also in einer Kugel vom Radius P um den Anfangspunkt des Impulsraumes.

Wenn wir nun annehmen, dass die Funktion $\varrho(r)$ gegeben ist und sie eine monoton fallende Funktion der Veränderlichen r ist, so können wir für die Dichte $\omega(p)$ eine einfache Formel angeben. Wir bestimmen hier sofort die Anzahl der Elektronen mit einem Impulsbetrag grösser als p, also die Grösse $\int_p^\infty \Omega(p)dp$. Daraus können wir dann $\omega(p)$ einfach erhalten.

Elektronen, die einen Impulsbetrag grösser als p haben, kommen in allen Volumenelementen vor, für welche

$$p \leqq P \tag{2}$$

ist.

Die Elektronen in einem solchen Volumenelement erfüllen also im Koordinatenraum den Rauminhalt dv_r, und im Impulsraum den Rauminhalt $\frac{4\pi}{3}(P^3 - p^3)$. Ihre Anzahl ergibt sich daraus zu

$$\frac{1}{\hbar^3}\,\frac{1}{3\pi^2}(P^3 - p^3)\,dv_r.$$

Die Anzahl aller Elektronen mit einem Impulsbetrag grösser als p erhalten wir durch eine Summation dieser Beiträge, wo wir alle Volumenelemente in Betracht ziehen müssen, die der Relation (2) genügen. Es ist also

$$\int_p^\infty \Omega(p)\,dp = \frac{1}{\hbar^3}\,\frac{4}{3\pi}\int_0^{r(p)} r^2\,(P^3 - p^3)\,dr\,, \tag{3}$$

wo $r(p)$ den Betrag des Radiusvektors bedeutet, für welchen

$$p = P = (3\pi^2)^{1/3}\,\hbar\varrho^{1/3}(r) \tag{4}$$

ist.* Die Funktion $r(p)$ ist also die inverse Funktion von $p = P(r)$.

Aus Gl. (3) können wir sofort sehen, dass $\Omega(p)$ ebenso wie $D(r)$ normiert ist. Wenn wir nämlich den Grenzradius des Atoms im Koordinatenraum mit r_0 bezeichnen, so bekommen wir mit Hilfe von Gl. (1)

$$\int_0^\infty \Omega(p)\,dp = \frac{1}{\hbar^3}\,\frac{4}{3\pi}\int_0^{r_0} r^2P^3\,dr = \int_0^{r_0} D(r)\,dr = N, \tag{5}$$

wo N die Anzahl der Elektronen in dem betrachteten atomaren System bedeutet.

Der physikalische Inhalt der Gl. (3) wird besonders klar, wenn wir diese folgendermassen umformen:

$$\int_p^\infty \Omega(p)\,dp = \int_0^{r(p)} D(r)\,dr - \frac{1}{\hbar^3}\,\frac{4}{9\pi}\,p^3\,r^3(p). \tag{6}$$

Elektronen mit einem grösseren Impulsbetrag als p befinden sich im Koordinatenraum nur innerhalb der Kugel mit dem Radius $r(p)$, wo $r(p)$ durch die Gl. (4) bestimmt ist. Das erste Glied auf der rechten Seite von Gl. (6) gibt die Anzahl aller Elektronen innerhalb dieser Kugel an. Um nur die Anzahl der Elektronen mit einem Impulsbetrag grösser als p zu erhalten, müssen wir diesen Wert um die Anzahl der dort befindlichen, aber kleineren Impuls als p besitzenden Elektronen verkleinern. Diese letzteren erfüllen im Koordinatenraum den Raumteil $\frac{4\pi}{3}\,r^3(p)$ und im Impulsraum den Raumteil $\frac{4\pi}{3}\,p^3$. So erhal-

* Wenn $\varrho(r)$ keine monoton fallende Funktion von r ist, dann haben wir im allgemeinen mehrere $r_i(p)$-Werte. Dementsprechend wird dann auf der rechten Seite der Gl. (3) eine Summe von mehreren Integralen stehen. Die Rechnungen sind in diesem allgemeineren Falle auch ohne Schwierigkeit durchführbar, wir werden aber uns damit hier nicht beschäftigen.

ten wir für ihre Anzahl

$$\frac{1}{\hbar^3}\frac{4}{9\pi}p^3 r^3(p), \tag{7}$$

was genau das zweite Glied auf der rechten Seite der Gl. (6) ist.

Mit Hilfe der Gln. (5) und (6) können wir sofort auch die Anzahl der Elektronen mit einem Impulsbetrag kleiner als p angeben:

$$\int_0^p \Omega(p)\,dp = \int_{r(p)}^{r_0} D(r)\,dr + \frac{1}{\hbar^3}\frac{4}{9\pi}p^3 r^3(p), \tag{8}$$

welche — wie die Gl. (6) — eine einfache, anschauliche Bedeutung hat. Alle Elektronen nämlich, die sich ausserhalb der Kugel mit dem Radius $r(p)$ im Koordinatenraum befinden, haben einen kleineren Impulsbetrag als p. Das erste Glied auf der rechten Seite der Gl. (8) gibt eben die Anzahl dieser Elektronen an. Es kommen aber noch Elektronen mit einem Impulsbetrag kleiner als p auch im Inneren der Kugel mit Radius $r(p)$ vor, ihre Anzahl gibt uns eben der Ausdruck unter (7) an. Darum steht dieser Ausdruck jetzt mit positivem Vorzeichen in Gl. (8).

Die radiale Elektronenverteilung im Impulsraum, $\Omega(p)$, lässt sich aus jeder der Gln. (3), (6) oder (8) berechnen. So folgt z. B. aus Gl. (3)

$$\Omega(p) = -\frac{d}{dp}\int_p^\infty \Omega(p)\,dp = \frac{1}{\hbar^3}\frac{4}{\pi}p^2\int_0^{r(p)} r^2\,dr = \frac{1}{\hbar^3}\frac{4}{3\pi}p^2 r^3(p). \tag{9}$$

Dieser Zusammenhang wurde zum erstenmal von BURKHARDT für die radiale Impulsverteilung angegeben.

Man kann sofort bemerken, dass das zweite Glied auf den rechten Seiten der Gln. (6) und (8) sich einfach mit Hilfe von $\Omega(p)$ ausdrücken lässt. So bekommt man diese Gleichungen in folgenden Formen:

$$\int_p^\infty \Omega(p)\,dp = \int_0^{r(p)} D(r)\,dr - \frac{1}{3}p\Omega(p), \tag{10}$$

$$\int_0^p \Omega(p)\,dp = \int_{r(p)}^{r_0} D(r)\,dr + \frac{1}{3}p\Omega(p). \tag{11}$$

Aus Gl. (9) für $\Omega(p)$ haben wir endlich den einfachen Ausdruck für die Elektronendichte im Impulsraum

$$\omega(p) = \frac{1}{\hbar^3}\frac{1}{3\pi^2}r^3(p). \tag{12}$$

Zusammenfassend kann man also auf Grund der Gln. (4) und (12) folgendes behaupten: Ist die Elektronendichte im Koordinatenraum durch die monoton fallende Funktion $\varrho(r)$ beschrieben, so ist die Elektronendichte im Impulsraum

$$\left.\begin{array}{ll} \text{bei dem Impulswert} & p = (3\pi^2)^{1/3}\hbar\varrho^{1/3}(r) \\ \text{gegeben durch die Formel} & \omega(p) = \dfrac{1}{\hbar^3}\dfrac{1}{3\pi^2}r^3(p)\,. \end{array}\right\} \tag{13}$$

Es ist leicht festzustellen, dass mit der Funktion $\varrho(r)$ auch $\omega(p)$ monoton abnimmt.

§ 2

Wir wenden uns jetzt zu der umgekehrten Aufgabe. Wir wollen annehmen, dass die Elektronendichte im Impulsraum $\omega(p)$ bekannt und eine monoton fallende Funktion ist. Unsere Aufgabe sei es, die Elektronendichte im Koordinatenraum $\varrho(r)$ zu bestimmen.

Formal gewinnt man die Lösung dieser Aufgabe sehr einfach durch die Umkehrung der Ausdrücke unter (13): Die Dichte $\varrho(r)$ ist

$$\left.\begin{array}{ll} \text{bei dem Koordinatenwert} & r = (3\pi^2)^{1/3}\hbar\omega^{1/3}(p) \\ \text{gegeben durch die Formel} & \varrho(r) = \dfrac{1}{\hbar^3}\dfrac{1}{3\pi^2}p^3\,. \end{array}\right\} \tag{14}$$

Wieder sieht man sofort, dass mit der Funktion $\omega(p)$ auch $\varrho(r)$ monoton abnimmt.

Bei dem Vergleich der Gln. (13) und (14) fällt die volle Symmetrie der beiden Transformationen auf. Weiter ist es auch ersichtlich, dass die Anwendung der zwei Transformationen nacheinander die ursprüngliche Funktion reproduziert. Damit haben wir also zwischen den beiden Dichtefunktionen einen wechselseitigen und eindeutigen Zusammenhang gewonnen.

Die grundlegenden Formeln unter (14) kann man auch ohne Benützung der Ergebnisse der Untersuchungen im Koordinatenraum erhalten, durch eine Umkehrung unseres bisherigen Gedankenganges, in dem man die Eigenschaften der Verteilung im Impulsraum zugrunde legt. Das wollen wir nun im folgenden durchführen.

Nehmen wir ein Volumenelement dv_p des Impulsraumes, wo die Elektronendichte $\omega(p)$ ist. In diesem Volumenelement befinden sich also $\omega(p)dv_p$ Elektronen, die alle einen Impulsbetrag p haben. Unsere erste Frage ist: wo befinden sich diese Elektronen im Koordinatenraum?

Ein Elektron mit dem Impulsbetrag p ist in unserem System nur dann gebunden, wenn seine Gesamtenergie dem maximal möglichen Wert der potentiellen Energie höchstens gleich ist:

$$\frac{p^2}{2m} \leq e\,(V - V_0)\,,$$

wo e die Elementarladung, m die Masse des Elektrons, $V = V(r)$ das Potential und $V_0 = V(r_0)$ den Wert des Potentials am Atomrand bedeuten. Daraus folgt also, dass die Elektronen mit dem Impulsbetrag p sich um den Atomkern innerhalb einer Kugel mit dem Radius $r(p)$ befinden, so dass im Inneren der Kugel die obige Ungleichung gültig ist.

Da die ausgewählte Elektronengruppe im Impulsraum den Rauminhalt dv_p, im Koordinatenraum den Rauminhalt $\frac{4\pi}{3} r^3(p)$ ausfüllt, lässt sich die Anzahl der Elektronen in dieser Gruppe in der Form

$$\omega(p)\,dv_p = \frac{1}{\hbar^3}\,\frac{1}{3\pi^2}\,r^3(p)\,dv_p$$

ausdrücken, woraus

$$r(p) = (3\pi^2)^{1/3}\,\hbar\omega^{1/3}(p) \tag{14}$$

folgt. Dieser Ausdruck ist mit der ersten Zeile der Formel (13) identisch.

So sind wir also in der Lage, bei gegebenem $\omega(p)$ zu jedem Impulsbetrag p den Betrag des Radiusvektors $r(p)$ angeben zu können, so dass alle Elektronen mit dem Impulsbetrag p sich im Koordinatenraum im Inneren einer Kugel mit dem Radius $r(p)$ befinden.

Jetzt gehen wir zur Bestimmung der Dichte $\varrho(r)$ über. Wählen wir ein Volumenelement dv_r im Koordinatenraum, welches vom Atomkern aus gemessen eben den durch Gl. (14) bestimmten Abstand $r(p)$ hat. Die Elektronen, die sich in diesem Volumenelement aufhalten, können höchstens den Impulsbetrag p haben, welcher Gl. (14) genügt. Diese Elektronen erfüllen also im Impulsraum die Kugel mit dem Radius p. So ist aber

$$\varrho(r)\,dv_r = \frac{1}{\hbar^3}\,\frac{1}{3\pi^2}\,p^3\,dv_r,$$

woraus

$$\varrho(r) = \frac{1}{\hbar^3}\,\frac{1}{3\pi^2}\,p^3 \tag{15}$$

folgt, was mit der zweiten Zeile der Formel (13) identisch ist.

Ähnlich unserem Gedankengang im § 1 kann man auch integrale Zusammenhänge herleiten, die den Zusammenhängen unter (3), (10) und (11) entsprechen.

Bestimmen wir z. B. mit Hilfe der jetzt bekannten Funktion $\omega(p)$ die Anzahl der Elektronen, welche einen Radiusvektor kleiner als r haben, d. h. die Grösse $\int_0^r D(r)dr$. Im folgenden bezeichnen wir wieder den Impulsbetrag mit p, welcher bei dem angenommenen r-Wert Gl. (14) genügt.

Zu jedem Volumenelement $dv_{p'}$ des Impulsraumes, welches zu einem Impulsbetrag $p' > p$ gehört, ordnet die Gl. (14) wegen des monotonen Abfalls der Funktion $\omega(p)$ einen Radiuswert $r' < r$ zu. Alle Elektronen in diesen Volumenelementen des Impulsraumes gehören also zu der betrachteten Gruppe. Die Anzahl aller dieser Elektronen ist $\int_p^\infty \omega(p')dv_{p'}$.

Bei den Volumenelementen des Impulsraumes, die zu Impulsbeträgen $p' < p$ gehören, ist das Verhältnis der Radiuswerte nach Gl. (14) $r' > r$. Aus einem solchen Volumenelement des Impulsraumes gehören also nicht mehr alle dort befindlichen $\omega(p')dv_{p'}$ Elektronen zu unserer betrachteten Gruppe. Wir müssen nämlich die Elektronen ausser Rechnung lassen, die im Raum-inhalt $\frac{4\pi}{3}(r'^3 - r^3)$ sich ausserhalb der Kugel mit dem Radius $r(p)$ im Koordinatenraum befinden. Die Anzahl der so losgetrennten Elektronen in einem Volumenelement $dv_{p'}$ ist

$$\frac{1}{\hbar^3}\,\frac{1}{3\pi^2}\,(r'^3 - r^3)\,dv_{p'}\,.$$

So gelangen wir zu dem Ausdruck

$$\int_0^r D(r)\,dr = \int_0^\infty \omega(p')\,dv_{p'} - \frac{1}{\hbar^3}\,\frac{1}{3\pi^2}\int_{p'<p} (r'^3 - r^3)\,dv_{p'}\,,$$

woraus wir mit Rücksicht auf Gl. (5) den der Gl. (3) entsprechenden Zusammenhang

$$\int_0^r D(r)\,dr = N - \frac{1}{\hbar^3}\,\frac{4}{3\pi}\int_0^p p'^2(r'^3 - r^3)\,dp' \tag{16}$$

erhalten. Nach einigen Umformungen und mit Hilfe der Gln. (5) und (15) folgt daraus, dass

$$\int_0^r D(r)\,dr = \int_p^\infty \Omega(p')\,dp' + \frac{1}{3}\,rD(r) \tag{17}$$

ist, welche das Analogon zur Gl. (10) ist.

Nochmals auf Gl. (5) zurückgreifend erhalten wir auch die Relation

$$\int_{r}^{r_0} D(r)\,dr = \int_{0}^{p} \Omega(p')\,dp' - \frac{1}{3} rD(r)\,, \tag{18}$$

welche der Gl. (11) entspricht.

Die Gln. (16), (17) und (18) sind natürlich auch mit der Gl. (15) in Übereinstimmung. So folgt z. B. aus Gl. (16) durch eine Differentiation nach r, dass

$$D(r) = \frac{1}{\hbar^3}\frac{4}{\pi} r^2 \int_0^p p'^2\,dp' = 4\pi r^2 \frac{1}{h^3}\frac{1}{3\pi^2} p^3$$

ist, was mit Gl. (15) identisch ist.

§ 3

Nachdem wir die Zusammenhänge der Funktionen $\varrho(r)$ und $\omega(p)$ festgestellt haben, steht vor uns die folgende Frage: welche Beziehung besteht zwischen diesen und den quantenmechanischen Ergebnissen?

Im wesentlichen kann man den Zusammenhang zwischen den beiden Dichtefunktionen $\varrho(r)$ und $\omega(p)$ durch die folgenden zwei Gleichungen ausdrücken:

$$\varrho(r) = \frac{1}{\hbar^3}\frac{1}{3\pi^2} P^3, \tag{19}$$

$$\omega(p) = \frac{1}{\hbar^3}\frac{1}{3\pi^2} r^3. \tag{20}$$

Bei der Bestimmung der Funktion $\omega(p)$ aus $\varrho(r)$ gibt uns die Gl. (19) den Wert der unabhängigen Variablen $p = P$, wo der Wert von $\omega(p)$ nach Gl. (20) zu berechnen ist. Im umgekehrten Falle, bei der Bestimmung von $\varrho(r)$ aus $\omega(p)$, gibt uns die Gl. (20) den Wert der unabhängigen Variablen r, wo der Wert von $\varrho(r)$ nach Gl. (19) zu berechnen ist.

Die Beziehung dieser Resultate zu der Quantenmechanik wurde bezüglich der Gl. (19) schon früher festgestellt. FÉNYES hat nämlich bewiesen [8], dass man den Ausdruck (19) herleiten kann, indem man die Einelektrondichten im Koordinatenraum aus der nullten Näherung der Koordinatenwellenfunktionen der Elektronen nach der WKB-Methode [9] bildet und diese über die vollbesetzten Quantenzustände summiert (bzw. integriert).

Unsere Aufgabe ist also hier, nur einen ähnlichen Beweis für die Gl. (20) zu geben. Dazu verfahren wir folgendermassen. Durch die Fourier-Transformation der — mit Hilfe der WKB-Methode gewonnenen — nullten Näherung der Koordinatenwellenfunktionen stellen wir eine Näherung der Impulswellenfunktionen vom selben Grade her, mit Hilfe deren wir näherungsweise die Einelektronendichten im Impulsraum bilden können. Zum Schluss müssen wir noch diese Einelektronendichten über alle vollbesetzten Quantenzustände summieren (bzw. integrieren).

Nehmen wir an, dass die Schrödinger-Gleichung unseres Einelektronproblems sich z. B. in den Descartes-Koordinaten separieren lässt, dass man also die Lösung in der Form

$$\psi = \psi_x(x)\,\psi_y(y)\,\psi_z(z)$$

schreiben kann.

Nach der WKB-Methode ist die nullte Näherung der Wellenfunktion im Bereich der klassischen Bahn

$$\psi = A \exp\left[\frac{i}{\hbar}\int (p_x dx + p_y dy + p_z dz)\right] = A \exp\left(\frac{i}{\hbar}\int p\, dr\right), \qquad (21)$$

wo p_x, p_y, p_z die Impulskomponente und A den Normierungskoeffizienten bezeichnen.

Die Impulskomponenten sollen noch die folgenden »Quantenbedingungen« erfüllen:

$$\oint p_x\, dx = 2\pi\hbar k_x\,,\quad \oint p_y\, dy = 2\pi\hbar k_y\,,\quad \oint p_z\, dz = 2\pi\hbar k_z,$$

wo k_x, k_y, k_z ganze Zahlen (Quantenzahlen) sind.

Durch die Fourier-Transformation der Näherungswellenfunktion (21) gewinnen wir eine Näherung der Impulswellenfunktion vom selben Grad:

$$\chi = C\int \exp\left(-\frac{i}{\hbar}pr\right)\psi dv_r = C'\int \exp\left[\frac{i}{\hbar}\left(pr - \int p\, dr\right)\right] dv_r\,,$$

wo C der Normierungskoeffizient ist.

Durch elementare Umformungen bekommen wir daraus, wenn wir die Änderung der Funktion exp [. .] in dem Integrationsbereich vernachlässigen.

$$\chi \cong C'' \exp\left(-\frac{i}{\hbar}\int r\, dp\right). \qquad (22)$$

Zu dieser Näherung der Impulswellenfunktion gehören noch die Quantenbedingungen in der Form

$$\oint x\, dp_x = 2\pi\hbar k'_x\,,\quad \oint y\, dp_y = 2\pi\hbar k'_y\,,\quad \oint z\, dp_z = 2\pi\hbar k'_z\,,$$

wo k'_x, k'_y, k'_z wieder ganze Zahlen sind.

Die Gesamtelektronendichte im Impulsraum ist nun durch die Summe

$$\omega(p) = 2 \sum_j \chi_j^*(p)\, \chi_j(p) \tag{23}$$

gegeben, wo j den durch die 3 Quantenzahlen beschriebenen Quantenzustand bezeichnet. Die Summation ist auf alle vollbesetzte Zustände auszudehnen.

Wenn wir uns auf ein kleines Volumen v_p des Impulsraumes beschränken, so wird $C'' = v_p^{-1/2}$, womit aus Gl. (23)

$$\omega(p) = \frac{2}{v_p} \int dn$$

folgt. Die Integralgrösse gibt hier einfach die Anzahl der besetzten Quantenzustände. Es ist also

$$dn = dk_x' \, dk_y' \, dk_z'.$$

Mit Hilfe der Quantenbedingungen — analog zum Verfahren von FÉNYES [8] — ergibt sich folgender Ausdruck für $\omega(p)$:

$$\omega(p) = \frac{2}{v_p} \frac{1}{(2\pi\hbar)^3} v_p \iiint dx\, dy\, dz = \frac{2}{(2\pi\hbar)^3} v_r, \tag{24}$$

wo v_r das Volumen im Koordinatenraum bedeutet, welches durch die Elektronen mit Impulsbetrag p ausgefüllt ist.

Bei gegebenem Impulsbetrag p (d. h. bei gegebener kinetischen Energie) liegen die Zustände mit der kleinstmöglichen Energie im Koordinatenraum im Inneren einer Kugel mit Radius $r(p)$ um den Kern. Das ausgefüllte Volumen im Koordinatenraum ist also

$$v_r = \frac{4\pi}{3} r^3(p),$$

welcher Wert in Gl. (24) eingesetzt zur Gl. (20) führt, was zu beweisen unser Ziel war.

LITERATUR

1. H. A. BETHE and E. E. SALPETER, Hb. d. Phys., Bd. XXXV, S. 122, Springer-Verlag, Berlin—Göttingen—Heidelberg, 1957.
2. W. E. DUNCANSON and C. A. COULSON, Proc. Phys. Soc., **LX,** 175, 1948.
3. P. GOMBÁS, Hb. d. Phys., Bd. XXXVI, Springer-Verlag, Berlin—Göttingen—Heidelberg, 1957.
4. G. BURKHARDT, Ann. d. Phys. (5), **26,** 567, 1936.
5. A. KÓNYA, Hung. Acta Phys., **1,** 12, 1949.
6. C. A. COULSON und N. H. MARCH, Proc. Phys. Soc., **LXIII,** 367, 1950.
7. N. H. MARCH, Advances in Physics, **6,** 1, 1957.
8. I. FÉNYES, Zs. f. Phys., **125,** 336, 1948.
9. Eine kurze Zusammenfassung ist gegeben z. B. in E. U. CONDON und G. H. SHORTLEY, The Theory of Atomic Spectra, S. 339. University Press, Cambridge, 1959.

СТАТИСТИЧЕСКАЯ МОДЕЛЬ АТОМА В ПРОСТРАНСТВЕ ИМПУЛЬСОВ. I

А. КОНЬЯ

Резюме

В настоящей работе показывается, что в рамках статистической теории атома распределение электронов $\omega(p)$ в трехмерном пространстве импульсов составляет приближенное решение проблемы многих тел, эквивалентное распределению плотности электронов $\varrho(r)$ в трехмерном пространстве координат. Между этими двумя распределениями плотности имеются симметрические зависимости, которые в нулевом приближении соответствуют теории преобразования квантовой механики.

THE SPACE-TIME CORRELATION FUNCTION FOR A SYSTEM OF IDENTICAL PARTICLES AT ZERO TEMPERATURE

By

D. KISDI

RESEARCH GROUP FOR THEORETICAL PHYSICS OF THE HUNGARIAN ACADEMY OF SCIENCES, BUDAPEST

(Presented by A. Kónya. — Received 15. III. 1962)

The ground state space-time correlation function is calculated for both of boson and fermion systems by using the BOGOLIUBOV's canonical transformation technique. The method employed is valid for fluids exhibiting quantum degeneracy like He II.

1. Introduction

In the description of slow-neutron scattering by a system of interacting particles the space-time correlation function $G(\mathbf{r}, t)$ introduced by VAN HOVE [1] plays an important role. The calculation of $G(\mathbf{r}, t)$ from first principles is extremely difficult, requiring the knowledge of the solutions of the energy eigenvalue problem

$$H\,|\Phi_A> = E_A\,|\Phi_A>, \tag{1}$$

where H is the Hamiltonian of the scattering system and the eigenstates are labelled by A. Owing to the difficulties involved in the many-body problem $G(\mathbf{r}, t)$ has been calculated for a number of simple models and besides a series of approximation methods has been developed for the determination of $G(\mathbf{r}, t)$. In this paper we are using a new method for the calculation of $G(\mathbf{r}, t)$, which is based on the BOGOLIUBOV's [2] canonical transformation technique and is valid for systems composed of a large number of weakly interacting identical particles at zero temperature, i. e. for such systems in which the quantum degeneracy plays a significant role.

In the following we are employing units in which $\hbar = 1$ and $M = \frac{1}{2}$, where M is the mass of a particle in the system. The space-time correlation function for a large, homogeneous fluid in the quantum state $|\Phi_A>$ is defined by [1, 3]

$$\begin{gathered} G(\mathbf{r}_2 - \mathbf{r}_1, t_2 - t_1) = \varrho_0^{-1} <\Phi_A\,|\,\varrho_{t_1}(\mathbf{r}_1)\,\varrho_{t_2}(\mathbf{r}_2)\,|\,\Phi_A>, \\ \varrho_t(\mathbf{r}) = e^{iHt}\,P(\mathbf{r})\,e^{-iHt}, \end{gathered} \tag{2}$$

where ϱ_0 is the average density of the particles, $\varrho_0 = N/\Omega$ (N: the number of the particles, Ω: the volume of the system; both of them approach infinity

but ϱ_0 remains finite) and $P(\mathbf{r})$ is the density operator. In the configuration space $P(\mathbf{r})$ is given by

$$P(\mathbf{r}) = \sum_{j=1}^{N} \delta(\mathbf{r} - \mathbf{R}_j), \tag{3}$$

where $\mathbf{R}_1, \ldots \mathbf{R}_N$ are the position vectors of the particles. For a large, homogeneous system

$$< \Phi_A | P(\mathbf{r}) | \Phi_A > = \varrho_0 \tag{4}$$

and thus the definition (2) can be rewritten

$$G(\mathbf{r}_2 - \mathbf{r}_1, t_2 - t_1) = \varrho_0 + \varrho_0^{-1} \sum_{\substack{B \\ (B \neq A)}} < \Phi_A | P(\mathbf{r}_1) | \Phi_B > \tag{5}$$
$$< \Phi_B | P(\mathbf{r}_2) | \Phi_A > e^{i(E_B - E_A)(t_2 - t_1)}.$$

On the basis of (5) the calculation of the space-time correlation function is reduced to the determination of the off-diagonal matrix elements of the density operator. These matrix elements of $P(\mathbf{r})$ are determined and $G(r, t)$ is calculated in Secs. 2 and 3, respectively, for systems of identical bosons and fermions.

2. System of interacting bosons

First we consider the problem of a system composed of a large number of weakly interacting bosons. It is convenient to use the method of second quantization. Let $\psi(\mathbf{r})$ be the field operator of the boson field considered, and let it be Fourier-analysed:

$$\psi(\mathbf{r}) = \frac{1}{\sqrt{\Omega}} \sum_{\mathbf{k}} a_{\mathbf{k}} e^{i\mathbf{k}\mathbf{r}}. \tag{6}$$

The annihilation operator $a_{\mathbf{k}}$ and its Hermitian conjugate, the creation operator $a_{\mathbf{k}}^*$ satisfy the commutation rules appropriate for Bose statistics. The Hamiltonian of the system can then be written in the form

$$\begin{aligned} H &= H_0 + H_{\text{int}}, \\ H_0 &= -\int \psi^*(\mathbf{r}) \nabla^2 \psi(\mathbf{r}) \, d^3\mathbf{r} = \sum_{\mathbf{k}} k^2 a_{\mathbf{k}}^* a_{\mathbf{k}}, \\ H_{\text{int}} &= \frac{1}{2} \iint \psi^*(\mathbf{r}_1) \psi^*(\mathbf{r}_2) U(\mathbf{r}_2 - \mathbf{r}_1) \psi(\mathbf{r}_2) \psi(\mathbf{r}_1) \, d^3\mathbf{r}_1 \, d^3\mathbf{r}_2 \\ &= \frac{1}{2} \sum V_{\mathbf{k}} a_{\mathbf{p}-\mathbf{k}}^* a_{\mathbf{q}+\mathbf{k}}^* a_{\mathbf{q}} a_{\mathbf{p}}, \end{aligned} \tag{7}$$

where $U(\mathbf{r})$ is the interaction potential and $V_\mathbf{k}$ is its Fourier transform

$$V_\mathbf{k} = \Omega^{-1} \int U(\mathbf{r})\, e^{i\mathbf{k}\mathbf{r}}\, d^3\mathbf{r}. \tag{8}$$

From the symmetry properties $U(-\mathbf{r}) = U(\mathbf{r})$ it follows

$$V_{-\mathbf{k}} = V_\mathbf{k}. \tag{9}$$

If there were no interaction between the particles, the ground state of the system would be one in which all particles are condensed in the same state $\mathbf{k} = 0$, i. e. the ground state would be characterised by

$$a_\mathbf{k} | \Phi_0 > = 0, \quad \text{for all} \quad \mathbf{k} \neq 0. \tag{10}$$

BOGOLIUBOV [2] showed first that when a weak interaction is present, the ground state of the system is characterised by

$$\alpha_\mathbf{k} | \Phi_0 > = 0, \quad \text{for all} \quad \mathbf{k} \neq 0, \tag{11}$$

where $\alpha_\mathbf{k}$ is the annihilation operator for an elementary excitation defined by

$$\alpha_\mathbf{k} = u_\mathbf{k}\, a_\mathbf{k} - v_\mathbf{k}\, a^*_{-\mathbf{k}} \tag{12}$$

or

$$a_\mathbf{k} = u_\mathbf{k}\, \alpha_\mathbf{k} + v_\mathbf{k}\, \alpha^*_{-\mathbf{k}}, \tag{13}$$

with

$$u_\mathbf{k} = \cosh x_\mathbf{k}, \qquad v_\mathbf{k} = \sinh x_\mathbf{k}, \tag{14}$$

$$\tanh 2x_\mathbf{k} = -\frac{N V_\mathbf{k}}{k^2 + N V_\mathbf{k}}. \tag{15}$$

The state with one elementary excitation of momentum $\mathbf{k}$ is

$$|\Phi_\mathbf{k}> = \alpha^*_\mathbf{k} | \Phi_0 > \tag{16}$$

and the energy of the elementary excitation is given by

$$E_\mathbf{k} = \sqrt{(k^2 + N V_\mathbf{k})^2 - N^2 V_\mathbf{k}^2}. \tag{17}$$

Using (11) together with (12) we can compute the average number of particles in the momentum state $\mathbf{k}$ for the ground state $| \Phi_0 >$. One finds

$$< n_\mathbf{k} > = < \Phi_0 | a^*_\mathbf{k}\, a_\mathbf{k} | \Phi_0 > = v^2_\mathbf{k} \quad \text{for} \quad \mathbf{k} \neq 0. \tag{18}$$

It is important to note that all momentum states have finite occupation numbers as $N \to \infty$, except the state with $\mathbf{k} = 0$, for which the occupation number is proportional to N [4]:

$$< n_0 > = (1 - \nu) N , \tag{19}$$

where

$$\nu = N^{-1} \sum_{\mathbf{k}}{}' v_{\mathbf{k}}^2 = \frac{1}{(2\pi)^3 \varrho_0} \int v_{\mathbf{k}}^2 \, d^3 \mathbf{k} . \tag{20}$$

Here Σ' represents a summation over the $\mathbf{k}$ space with $\mathbf{k} \neq 0$.

Now we turn to the calculation of the space-time correlation function for the ground state of the system. Using the language of second quantization the density operator (3) can be written in the form

$$P(\mathbf{r}) = \psi^*(\mathbf{r}) \, \psi(\mathbf{r}) = \frac{1}{\Omega} \sum_{\mathbf{k},\mathbf{l}} a_{\mathbf{l}}^* \, a_{\mathbf{k}} \, e^{i(\mathbf{k}-\mathbf{l})\mathbf{r}} . \tag{21}$$

By using the relation $N = \Sigma a_{\mathbf{k}}^* a_{\mathbf{k}}$ and writing separately the terms in which $\mathbf{k} = 0$ or $\mathbf{l} = 0$, the density operator becomes

$$P(\mathbf{r}) = \frac{1}{\Omega} \left[N + a_0^* \sum_{\mathbf{k}}{}' a_{\mathbf{k}} \, e^{i\mathbf{k}\mathbf{r}} + a_0 \sum_{\mathbf{k}}{}' a_{\mathbf{k}}^* \, e^{-i\mathbf{k}\mathbf{r}} + \sum_{\mathbf{k} \neq}{}' a_{\mathbf{l}}^* \, a_{\mathbf{k}} \, e^{i(\mathbf{k}-\mathbf{l})\mathbf{r}} \right] . \tag{22}$$

When N is a very large number we may regard the momentum state $\mathbf{k} = 0$ as a more or less infinite reservoir for the production and absorption of particles with higher momenta, which means that we do not insist on the constancy of the total number of particles, and thus we may write

$$a_0 \, | \, \Phi_0 > = a_0^* \, | \, \Phi_0 > = C \, | \, \Phi_0 >, \tag{23}$$

where C is a number

$$C = \sqrt{< n_0 >} = \sqrt{(1 - \nu) N} . \tag{24}$$

Using (22) together with (11), (13) and (23), it is easy to determine the matrix elements $< \Phi_B \, | \, P(\mathbf{r}) \, | \, \Phi_0 >$. The nonvanishing off-diagonal matrix elements fall into two categories:

1. those in which $| \, \Phi_B >$ is a state with one elementary excitation: $| \, \Phi_B > \; = | \, \Phi_{\mathbf{k}} > \equiv a_{\mathbf{k}}^* \, | \, \Phi_0 >$. For such a state

$$< \Phi_{\mathbf{k}} \, | \, P(\mathbf{r}) \, | \, \Phi_0 > = \frac{C}{\Omega} (u_{\mathbf{k}} + v_{\mathbf{k}}) \, e^{-i\mathbf{k}\mathbf{r}} . \tag{25}$$

2. those in which $|\Phi_B>$ is a state with two elementary excitations: $|\Phi_B> = |\Phi_{\mathbf{k},\mathbf{l}}> \equiv a_{\mathbf{k}}^* a_{\mathbf{l}}^* |\Phi_0>$. For such a state

$$<\Phi_{\mathbf{k},\mathbf{l}}|P(\mathbf{r})|\Phi_0> = \frac{1}{\Omega}(u_{\mathbf{k}} v_{\mathbf{l}} + u_{\mathbf{l}} v_{\mathbf{k}}) e^{-i(\mathbf{k}+\mathbf{l})r}. \tag{26}$$

The space-time correlation function (5) for the ground state is then

$$\begin{aligned} &G(\mathbf{r}_2 - \mathbf{r}_1, t_2 - t_1) = \\ &= \varrho_0 + \varrho_0^{-1} \sum_{\mathbf{k}}{}' <\Phi_0|P(\mathbf{r}_1)|\Phi_{\mathbf{k}}><\Phi_{\mathbf{k}}|P(\mathbf{r}_2)|\Phi_0> e^{iE_{\mathbf{k}}(t_2-t_1)} + \\ &+ \frac{1}{2}\varrho_0^{-1} \sum_{\mathbf{k},\mathbf{l}}{}' <\Phi_0|P(\mathbf{r}_1)|\Phi_{\mathbf{k},\mathbf{l}}><\Phi_{\mathbf{k},\mathbf{l}}|P(\mathbf{r}_2)|\Phi_0> e^{i(E_{\mathbf{k}}+E_{\mathbf{l}})(t_2-t_1)}. \end{aligned} \tag{27}$$

The insertion of (25) and (26) into (27) yields

$$\begin{aligned} G(\mathbf{r}, t) = [1 + F(\mathbf{r}, t) - \nu]\, h(\mathbf{r}, t) + \varrho_0 \big\{&[1 + F(\mathbf{r}, t)]^2 + \\ &+ [1 + S(\mathbf{r}, t)]^2 - 1 - 2\nu\,[F(\mathbf{r}, t) + S(\mathbf{r}, t)]\big\}, \end{aligned} \tag{28}$$

where

$$h(\mathbf{r}, t) = \Omega^{-1} \sum_{\mathbf{k}}{}' e^{i(E_{\mathbf{k}}t - \mathbf{kr})} = \frac{1}{(2\pi)^3}\int e^{i(E_{\mathbf{k}}t-\mathbf{kr})}\, d^3\mathbf{k} \tag{29}$$

and

$$\begin{aligned} F(\mathbf{r}, t) &= N^{-1} \sum_{\mathbf{k}}{}' v_{\mathbf{k}}^2\, e^{i(E_{\mathbf{k}}t-\mathbf{kr})} = \frac{1}{(2\pi)^3\varrho_0}\int v_{\mathbf{k}}^2\, e^{i(E_{\mathbf{k}}t-\mathbf{kr})}\, d^3\mathbf{k}, \\ S(\mathbf{r}, t) &= N^{-1} \sum_{\mathbf{k}}{}' u_{\mathbf{k}} v_{\mathbf{k}}\, e^{i(E_{\mathbf{k}}t-\mathbf{kr})} = \frac{1}{(2\pi)^3\varrho_0}\int u_{\mathbf{k}} v_{\mathbf{k}}\, e^{i(E_{\mathbf{k}}t-\mathbf{kr})}\, d^3\mathbf{k}. \end{aligned} \tag{30}$$

For $t = 0$ the space-time correlation function reduces to

$$G(\mathbf{r}, 0) = \delta(\mathbf{r}) + g(\mathbf{r}), \tag{31}$$

where $\delta(\mathbf{r})$ denotes the three-dimensional Dirac delta-function and $g(\mathbf{r})$ is the conventional pair distribution function [1]. From (29) and (30), respectively, it follows $h(\mathbf{r}, 0) = \delta(\mathbf{r})$ and $F(0, 0) = \nu$, and therefore (28) leads to

$$g(\mathbf{r}) = \varrho_0\big\{[1 + f(\mathbf{r})]^2 + [1 + s(\mathbf{r})]^2 - 1 - 2\nu\,[f(\mathbf{r}) + s(\mathbf{r})]\big\}, \tag{32}$$

with

$$\begin{aligned} f(\mathbf{r}) &= \frac{1}{(2\pi)^3\varrho_0}\int v_{\mathbf{k}}^2\, e^{-i\mathbf{kr}}\, d^3\mathbf{k}, \\ s(\mathbf{r}) &= \frac{1}{(2\pi)^3\varrho_0}\int u_{\mathbf{k}} v_{\mathbf{k}}\, e^{-i\mathbf{kr}}\, d^3\mathbf{k}. \end{aligned} \tag{33}$$

The expression (32) is in agreement with the result of LEE, HUANG and YANG [5].

3. System of interacting fermions

Next we consider the problem of a system composed of a large number of weakly interacting fermions having spin $\frac{1}{2}$. For simplicity the interaction potential is taken as spin-independent:* $U = U(\mathbf{r})$, where $\mathbf{r}$ is the relative position vector of two particles. The Hamiltonian for such a system is given by

$$\begin{aligned} H &= H_0 + H_{\text{int}}\,, \\ H_0 &= \sum_{\mathbf{k}\sigma} k^2\, a^*_{\mathbf{k}\sigma}\, a_{\mathbf{k}\sigma}\,, \\ H_{\text{int}} &= \frac{1}{2} \sum V_{\mathbf{k}}\, a^*_{\mathbf{p}_1-\mathbf{k}\sigma_1}\, a^*_{\mathbf{p}_2+\mathbf{k}\sigma_2}\, a_{\mathbf{p}_2\sigma_2}\, a_{\mathbf{p}_1\sigma_1}. \end{aligned} \tag{34}$$

Here σ is the spin index which can take on the values $+\frac{1}{2}$ or $-\frac{1}{2}$. The creation and annihilation operators $a^*_{\mathbf{k}\sigma}$, $a_{\mathbf{k}\sigma}$ satisfy the usual anticommutator relations. The summation in the interaction term is taken over $\mathbf{k}$, $\mathbf{p}_1$, $\mathbf{p}_2$, σ_1 and σ_2. The Fourier transform of the interaction potential $V_{\mathbf{k}}$ is given by (8).

Using the technique which has been developed by BOGOLIUBOV [6] it can be shown that the ground state of the system is characterised by

$$a_{\mathbf{k}\sigma}\,|\,\Phi_0\!> = 0\,, \tag{35}$$

where $a_{\mathbf{k}\sigma}$ is the annihilation operator for an elementary excitation given by

$$\begin{aligned} a_{\mathbf{k}\frac{1}{2}} &= u_{\mathbf{k}}\, a_{\mathbf{k}\frac{1}{2}} - v_{\mathbf{k}}\, a^*_{-\mathbf{k}-\frac{1}{2}}\,, \\ a_{\mathbf{k}-\frac{1}{2}} &= u_{\mathbf{k}}\, a_{\mathbf{k}-\frac{1}{2}} + v_{\mathbf{k}}\, a^*_{-\mathbf{k}\frac{1}{2}}\,, \end{aligned} \tag{36}$$

with

$$u_{\mathbf{k}} = \cos x_{\mathbf{k}}\,,\quad v_{\mathbf{k}} = \sin x_{\mathbf{k}}\,,\quad x_{-\mathbf{k}} = x_{\mathbf{k}}\,. \tag{37}$$

The real number $x_{\mathbf{k}}$ is determined by the following system of nonlinear integral equations

$$\operatorname{tang} 2\,x_{\mathbf{k}} = -\frac{\Delta_{\mathbf{k}}}{\varepsilon_{\mathbf{k}} - \lambda}\,, \tag{38}$$

$$\left.\begin{aligned} \Delta_{\mathbf{k}} &= \frac{1}{2} \sum V_{\mathbf{k}-\mathbf{l}} \sin 2\,x_{\mathbf{l}}\,, \\ \varepsilon_{\mathbf{k}} &= k^2 + \sum_{\mathbf{l}} (2\,V_0 - V_{\mathbf{k}-\mathbf{l}}) \sin^2 x_{\mathbf{l}}\,, \\ \sum_{\mathbf{k}} 2 \sin^2 x_{\mathbf{k}} &= N\,, \end{aligned}\right\} \tag{39}$$

where $V_0 = V_{\mathbf{k}=0}$ and the last equation determines the number λ.

* The generalization to spin-dependent interactions is straightforward.

The state with one elementary excitation of momentum $\mathbf{k}$ and spin index σ is

$$|\Phi_{\mathbf{k}\sigma}> = \alpha^*_{\mathbf{k}\sigma}\,|\Phi_0> \tag{40}$$

and the energy of the elementary excitation is given, independently of σ, by

$$E_{\mathbf{k}} = \sqrt{(\varepsilon_{\mathbf{k}} - \lambda)^2 + \Delta_{\mathbf{k}}^2}. \tag{41}$$

The matrix elements of the density operator

$$P(\mathbf{r}) = \psi^*(\mathbf{r})\,\psi(\mathbf{r}) = \frac{1}{\Omega}\sum_{\mathbf{k},\mathbf{l},\sigma} a^*_{\mathbf{l}\sigma}\,a_{\mathbf{k}\sigma}\,e^{i(\mathbf{k}-\mathbf{l})\mathbf{r}} \tag{42}$$

can be calculated by using the inverses of eqs. (36), which are given by

$$\begin{aligned} a_{\mathbf{k}\frac{1}{2}} &= u_{\mathbf{k}}\,\alpha_{\mathbf{k}\frac{1}{2}} + v_{\mathbf{k}}\,\alpha^*_{-\mathbf{k}-\frac{1}{2}}, \\ a_{\mathbf{k}-\frac{1}{2}} &= u_{\mathbf{k}}\,\alpha_{\mathbf{k}-\frac{1}{2}} - v_{\mathbf{k}}\,\alpha^*_{-\mathbf{k}\frac{1}{2}}. \end{aligned} \tag{43}$$

We find that an off-diagonal matrix element $<\Phi_B\,|\,P(\mathbf{r})\,|\,\Phi_0>$ is non-vanishing only if $|\,\Phi_B>$ corresponds to a state with two elementary excitations of opposite spin

$$|\,\Phi_B> = |\,\Phi_{\mathbf{k}\frac{1}{2},\mathbf{l}-\frac{1}{2}}> \equiv \alpha^*_{\mathbf{k}\frac{1}{2}}\,\alpha^*_{\mathbf{l}-\frac{1}{2}}\,|\,\Phi_0> \tag{44}$$

and we get

$$<\Phi_{\mathbf{k}\frac{1}{2},\mathbf{l}-\frac{1}{2}}\,|\,P(\mathbf{r})\,|\,\Phi_0> = \frac{1}{\Omega}\,(u_{\mathbf{k}}\,v_{\mathbf{l}} + u_{\mathbf{l}}\,v_{\mathbf{k}})\,e^{-i(\mathbf{k}+\mathbf{l})\mathbf{r}}. \tag{45}$$

The space-time correlation function (5) for the ground state is then

$$\begin{aligned} G(\mathbf{r}_2 - \mathbf{r}_1, t_2 - t_1) = \varrho_0 + \varrho_0^{-1}\sum_{\mathbf{k},\mathbf{l}} &<\Phi_0\,|\,P(\mathbf{r}_1)\,|\,\Phi_{\mathbf{k}\frac{1}{2},\,l-\frac{1}{2}}> \\ &<\Phi_{\mathbf{k}\frac{1}{2},\,l-\frac{1}{2}}\,|\,P(\mathbf{r}_2)\,|\,\Phi_0>\,e^{i(E_{\mathbf{k}}+E_{\mathbf{l}})\,(t_2-t_1)} \end{aligned} \tag{46}$$

and the insertion of (45) yields

$$G(\mathbf{r},t) = F(\mathbf{r},t)\,h(\mathbf{r},t) + \varrho_0\left\{1 - \frac{1}{2}\,F^2(\mathbf{r},t) + \frac{1}{2}\,S^2(\mathbf{r},t)\right\}, \tag{47}$$

where

$$h(\mathbf{r},t) = \Omega^{-1}\sum_{\mathbf{k}} e^{i(E_{\mathbf{k}}t - \mathbf{k}\mathbf{r})} = \frac{1}{(2\pi)^3}\int e^{i(E_{\mathbf{k}}t-\mathbf{k}\mathbf{r})}\,d^3\,\mathbf{k} \tag{48}$$

and

$$\begin{aligned} F(\mathbf{r},t) &= 2N^{-1}\sum_{\mathbf{k}} v_{\mathbf{k}}^2\,e^{i(E_{\mathbf{k}}t-\mathbf{k}\mathbf{r})} = \frac{2}{(2\pi)^3\,\varrho_0}\int v_{\mathbf{k}}^2\,e^{i(E_{\mathbf{k}}t-\mathbf{k}\mathbf{r})}\,d^3\,\mathbf{k}, \\ S(\mathbf{r},t) &= 2N^{-1}\sum_{\mathbf{k}} u_{\mathbf{k}}\,v_{\mathbf{k}}\,e^{i(E_{\mathbf{k}}t-\mathbf{k}\mathbf{r})} = \frac{2}{(2\pi)^3\,\varrho_0}\int u_{\mathbf{k}}\,v_{\mathbf{k}}\,e^{i(E_{\mathbf{k}}t-\mathbf{k}\mathbf{r})}\,d^3\,\mathbf{k}. \end{aligned} \tag{49}$$

The pair distribution function $g(\mathbf{r})$ can be obtained from the relation (31). The fact that $h(\mathbf{r}, 0) = \delta(\mathbf{r})$ and $F(0, 0) = 1$ leads to

$$g(\mathbf{r}) = \varrho_0 \left\{ 1 - \frac{1}{2} f^2(\mathbf{r}) + \frac{1}{2} s^2(\mathbf{r}) \right\} \tag{50}$$

with

$$\begin{aligned} f(\mathbf{r}) &= \frac{2}{(2\pi)^3 \varrho_0} \int v_{\mathbf{k}}^2 e^{-i\mathbf{kr}} d^3\mathbf{k}, \\ s(\mathbf{r}) &= \frac{2}{(2\pi)^3 \varrho_0} \int u_{\mathbf{k}} v_{\mathbf{k}} e^{-i\mathbf{kr}} d^3\mathbf{k}. \end{aligned} \tag{51}$$

In the case of an ideal fermion gas there is no interaction between the particles and we have [6]

$$\begin{aligned} u_{\mathbf{k}} &= 0, \quad v_{\mathbf{k}} = 1 \quad \text{if} \quad k < k_F, \\ u_{\mathbf{k}} &= 1, \quad v_{\mathbf{k}} = 0 \quad \text{if} \quad k > k_F, \end{aligned} \tag{52}$$

where k_F is the Fermi momentum $k_F = (3\pi^2 \varrho_0)^{1/3}$. Substituting (52) into (51) we get

$$f(\mathbf{r}) = \frac{3 (\sin k_F r - k_F r \cos k_F r)}{k_F^3 r^3} \quad \text{and} \quad s(\mathbf{r}) = 0 \tag{53}$$

and $g(\mathbf{r})$ takes the well-known form developed first by WIGNER and SEITZ [7].

REFERENCES

1. L. VAN HOVE, Phys. Rev., **95**, 249, 1954.
2. N. N. BOGOLIUBOV, J. Phys. USSR., **9**, 23, 1947.
3. L. VAN HOVE, Physica, **24**, 404, 1958.
4. O. PENROSE and L. ONSAGER, Phys. Rev., **104**, 576, 1956.
5. T. LEE, K. HUANG and C. YANG, Phys. Rev., 106, 1135, 1957.
6. N. N. BOGOLIUBOV, Nuovo Cimento, **7**, 794, 1958.
7. E. WIGNER and F. SEITZ, Phys. Rev., **43**, 804, 1933; **46**, 509, 1934.

ПРОСТРАНСТВЕННО-ВРЕМЕННАЯ ФУНКЦИЯ КОРРЕЛЯЦИИ ДЛЯ СИСТЕМ ТОЖДЕСТВЕННЫХ ЧАСТИЦ ПРИ ТЕМПЕРАТУРЕ АБСОЛЮТНОГО НУЛЯ

Д. КИШДИ

Р е з ю м е

В работе определяется пространственно временная функция корреляции основного состояния для систем бозонов и ферми-частиц при помощи метода канонического преобразования Боголюбова. Примененный метод действителен для жидкостей, у которых квантово-механическое вырождение играет важную роль, например He II.

COMMUNICATIONES BREVES

ON THE REVERSE CHARACTERISTICS OF SILICON DIODES

By

A. LŐRINCZY and G. PATAKI

RESEARCH INSTITUTE FOR TECHNICAL PHYSICS OF THE HUNGARIAN ACADEMY OF SCIENCES, BUDAPEST

(Received 16. V. 1961)

In a previous paper [1] we examined the temperature dependence of the reverse current of germanium junction diodes. The reverse characteristics showed — instead of saturation — a linear voltage dependence. The investigations of J. T. LAW [2], W. T. ERIKSEN et al. [3], A. R. F. PLUMMER [4], H. STATZ and G. A. DE MARS [5] and J. I. CARASSO [6] deal with the linear characteristic. On the basis of the temperature dependence of the characteristics and of the measurement of very small currents (10^{-10} A) on the one hand the gap of germanium, on the other the activation energy of the resistance of the supposed shunting water layer could be determined. This activation energy below 0° C showed a fairly good agreement with that of ice. In our present paper we report our examinations on silicon diodes of the type 1N253. The measuring method and the definition of the saturation current are the same as described in [1]. The functions $I_s(1/T)$ and $R(1/T)$ are to be seen in Fig. 1 plotted in a logarithmic scale. On the basis of Fig. 1 a gap of 0.55 eV is obtained for silicon, which value is just half the expected one. This discrepancy can be interpreted by the assumption that in reality in the silicon diode there is a *p-i-n* junction and not a *p-n* one. (In the layer i the condition $N_d - N_a = 0$ is fulfilled.) Namely, as R. N. HALL pointed out [7], the reverse current is determined by the recombination current of the layer i and not by its diffusion current. In such a case the current-voltage characteristics are given by the relation

$$I = \frac{edn_i}{\tau_i}\left(\exp\frac{eV}{2kT} - 1\right),$$

where d is the thickness of the layer i, τ_i the life time of the carriers, $n_i = (N_c N_v)^{1/2} e^{-\frac{\Delta E}{2kT}}$ is the concentration of the carriers in the intrinsic semiconductor. Assuming that τ_i is but a slowly varying function of the temperature, the difference can be explained by the temperature dependence of n_i.*

* Probably, this is the reason also for a similar discrepancy found by V. I. FISTUL [8].

Taking into consideration the factor 2 in $n_i \Delta E = 1{,}1$ eV appears for the gap of silicon, in good agreement with the corresponding data figuring in the literature. The shunting resistance defined on the basis of the linear part of the characteristic shows a temperature dependence, as it was found in case of germanium. There is a break near 0° C and below 0° C the slope is 7.7 kcal/

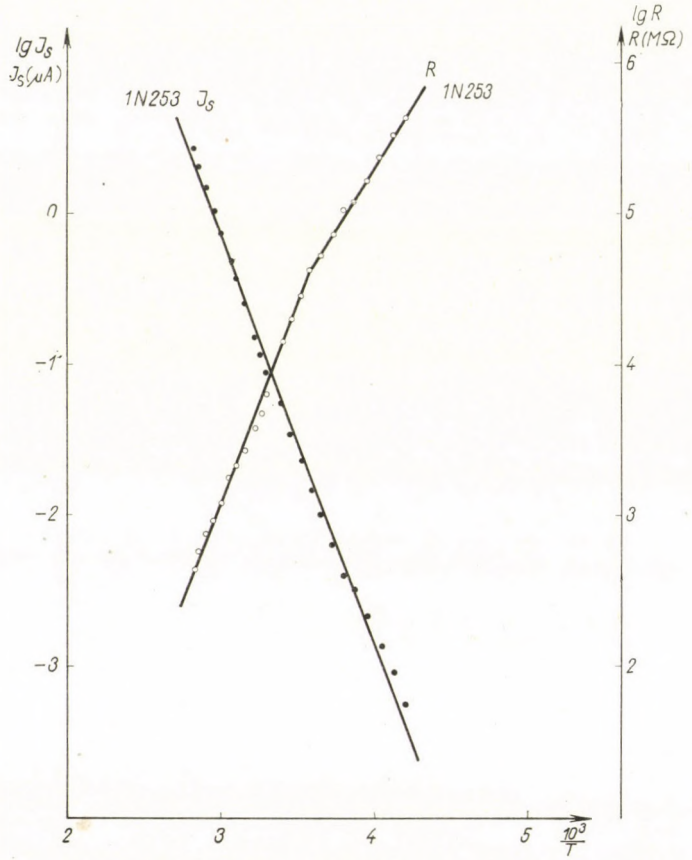

Fig. 1

mol (in case of germanium 9.1 kcal/mol, while the activation energy of ice, according to the measurements of R. C. BRADLEY, is 12.3 kcal/mol).

The facts that by cooling below 0° C the excess current does not disappear and that the shunting resistance shows an activation energy near to that of ice, give reason for the hypothesis suggested first by LAW that the excess current is produced by ionic conduction. Of course, it cannot be assumed that on the surface of germanium pure water is absorbed. The various impurities can considerably influence the temperature dependence of the resistance of the shunting layer. J. I. CARASSO [6] examining the transient pheno-

mena comes to the conclusion that probably the whole excess current is produced by the electrolytic current of the impurity metal ions occurring on the surface. In this case the temperature dependence of the mobility of the metal ions must be taken into account.

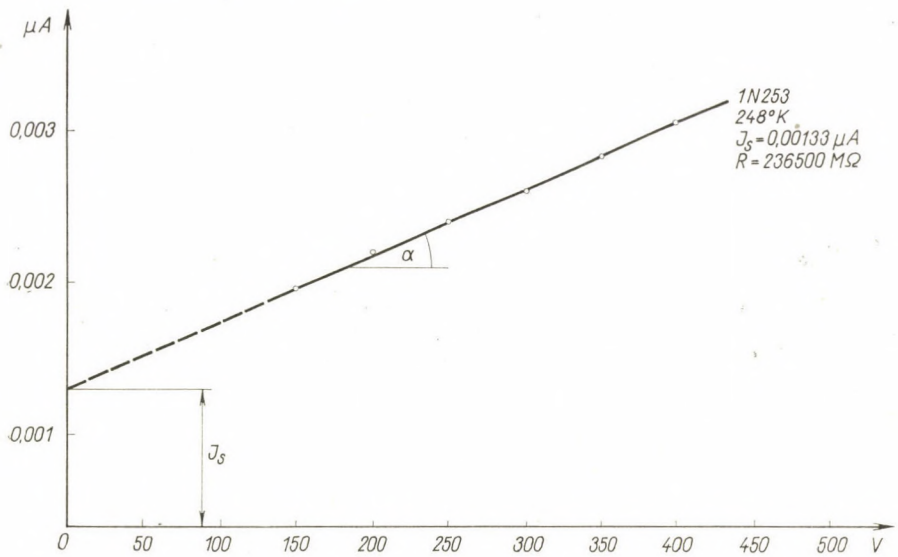

Fig. 2

The examinations were carried out on encapsulated diodes. It seems to be advisable to perform the above-mentioned experiments on grown *p-n*, resp. *p-i-n* junctions.

Finally, the authors wish to express their thanks to Dr. Z. Bodó for his valuable advice and critical remarks.

REFERENCES

1. A. Lőrinczy and G. Pataki, Acta Phys. Hung., **13,** 1, 1961.
2. J. T. Law, Proc. IRE, **42,** 9, 1954.
3. E. T. Eriksen, H. Statz and G. A. de Mars, Journ. of Appl. Phys., **281,** 133, 1957.
4. H. Statz and G. A. de Mars, Phys. Rev., **111,** 169, 1958.
5. A. R. F. Plummer, Proc. Phys. Soc. B **69,** 539, 1956.
6. J. I. Carasso, Proc. IEE, PtB suppl. **17,** 964, 1960.
7. R. N. Hall, Proc. IRE, **40,** 11, 1952.
8. *В. И. Фистуль* и *О. Б. Оржеский,* Ф. Т. Т. 3, 4, 1158, 1961.
9. R. S. Bradley, Trans. Faraday Soc., **53,** 5, 1957.

VIBRATIONAL RELAXATION TIMES FOR GASEOUS HALOGEN MOLECULES

By

D. D. DESHPANDE

PHYSICAL CHEMISTRY LABORATORY, INDIAN INSTITUTE OF TECHNOLOGY, POWAI, BOMBAY-76 (INDIA)

(Received 5. VIII. 1961)

The phenomenon of vibrational relaxation has been observed in a number of gases and vapours through the exhaustive investigations on ultrasonic velocity and absorption. The phenomenon was explained by the HERZFELD—RICE—KNESER theory as due to the delay in the transfer of energy from the external energy of translation to the internal energy of vibration at higher sound frequencies. A number of molecular theories and subsequent modifications utilizing the quantum mechanical treatment [1—3] have been available since then, which try to evaluate the relaxation times and their pressure and temperature dependence. A simple and rapid method to evaluate the relaxation times in gases was suggested in our previous work [4] in which the vibrational relaxation times were evaluated for over 12 molecules. In the present paper, the method has been applied to the halogen molecules and the results have been compared with the experimental data.

Libration of molecules and relaxation

The mechanism of ultrasonic relaxation proposed in our previous communication (loc. cit.) has been based on the assumption of a characteristic frequency of the gas molecules. When the sound frequency approaches this natural frequency of molecules a resonant absorption occurs and the vibrational energy does not contribute to the heat capacity as the molecule becomes "stiffer" at the resonance point, thus giving a rise in the ultrasonic velocity. This natural molecular frequency can be calculated as follows: Consider a single gas molecule. It will be rotating around an axis passing through its centre of gravity. When a sound wave of low frequency is propagated, the rotation of the molecule is unaffected. But at higher frequencies, there are head-on collisions of these rotating molecules due to rapid pressure alterations. This affects the purely rotational motion of molecules and leads to a sort of rotary oscillation of the molecules or the libration of molecules at higher sound frequencies. These rotary oscillations will be characteristic of the

molecules under consideration with definite time constant and may be called the libration frequency of the molecule. This libration frequency can be given by an equation of the type $f_0 = (1/2\pi)(c/I)^{1/2}$, where I is the moment of inertia and c is the couple acting on the molecule to maintain the rotatory oscillations excited by the sound waves of appropriate frequency. To a certain approximation c may be substituted by the interaction energy between a pair of molecules given by LONDON's relationship $E = 0.75 V\alpha^2/r^6$, where V is the ionization potential, α the polarizability and r is the mean molecular separation. Thus the libration frequency (and hence the ultrasonic relaxation frequency, since both are identical at the resonance point) can be evaluated by the relationship $f_0 = (1/2\pi)(0.75 V\alpha^2/r^6 I)^{1/2}$.

Relaxation in halogens

Experimental results are available for relaxation times of halogen molecules from the work of RICHARDSON [5] by the ultrasonic velocity method and of SHIELDS [6] by the absorption method. There is, however, a considerable discrepancy between the data of the two authors and as yet no theoretical values of relaxation times for these molecules are available for comparison.

Using the above relation for f_0 the values of relaxation frequencies have been calculated at 1 atm. pressure for chlorine at 25° C, bromine at 60° C.

Table 1

Molecular constants for halogens

Molecules	V eV	σ °A	$I \times 10^{40}$ gm—cm²	$\alpha \times 10^{24}$ cc.	$r \times 10^{8}$ cm
Chlorine	11.48	3.976	108.0	4.50	5.78 at 20 °C
Bromine	10.55	4.566	342.6	6.43	4.90 at 60 °C
Iodine	9.28	4.982	741.6	18.95	5.60 at 180 °C

Table 2

Relaxation frequencies for halogens

Molecules	Present Work		RICHARDSON		SHIELD	
	Temp. °C	f_0 Kcs	Temp. °C	f_0 Kcs	Temp. °C	f_0 Kcs
Chlorine	25	129.4	17	56	25	39
Bromine	60	167.4	58	130	100	275
Iodine	180	210.7	1808	250	253	2100

and iodine at 180° C. The molecular constants used[6—8] are given in Table 1. The mean distance is assumed to be the same as the mean free path given by the relation $r = 0.707\ kT/\pi\sigma^2 p$. A comparison between the observed and calculated values has been made in Table 2.

Discussion

For chlorine the value of f_0 calculated by ourselves is higher than the values obtained by the two other authors but it just fits the upper part of the S shape dispersion curve given by RICHARDSON (loc. cit.). Bromine and iodine give excellent agreement with the data of RICHARDSON. The agreement obtained is very surprising taking into account the simplicity of the proposed mechanism of relaxation.

SHIELDS (loc. cit.) has rightly pointed out the want of a correlation between the relaxation time and the mass or vibrational spectra of molecule. In the present work the ultrasonic relaxation frequency is found to be related with the moment of inertia and ionisation potential of the molecule.

Since the ultrasonic relaxation is due to the libration of the molecules which are effectively in the ground state as far as the rotational energy level is concerned, an increase in temperature will cause a decrease in the number of such librating molecules. The number of molecules in the ground state will be $N = N_0 \exp(-U/kT)$. The effect of increase in temperature will therefore be to shift the relaxation frequency to a higher value and it should exponentially depend on temperature.

If we use the static value of $r = (v^{1/3} - \sigma)$, where v is the volume per molecule, for molecular separation, the pressure dependence of relaxation can be quantitatively explained. However, it is incorrect to use the static distance for molecular separation as the libration starts after head-on collision. It is, therefore, right to use the mean free path for molecular separation in evaluating libration frequencies.

Conclusion

From LONDON's dispersion energy, the molecular libration frequencies can be calculated, which are found to be identical with ultrasonic relaxation frequencies. This forms a simple and quick method for evaluating vibrational relaxation times for gases. Though the method is not very rigorous, it gives surprisingly excellent agreement with the experimental data and therefore can be utilized for a rapid check of experimental results on new substances if the molecular constants are known.

REFERENCES

1. R. N. SCHWARTZ, Z. L. SLAWSKY and K. F. HERZFELD, J. Chem. Phys., **20**, 1951, 1952.
2. R. N. SCHWARTZ and K. F. HERZFELD, J. Chem. Phys., **22**, 767, 1954.
3. F. I. TANCZOS, J. Chem. Phys., **25**, 439, 1956.
4. S. K. K. JATKAR and D. D. DESHPANDE, Brit., J. App. Phys., **12**, 243, 1961.
5. E. G. RICHARDSON, J. Acoust. Soc. Amer., **31**, 152, 1959.
6. F. D. SHIELDS, J. Acoust. Soc. Amer., **32**, 180, 1960.
7. E. A. MOLEWYN-HUGHES, Physical Chemistry, 1957.
8. J. O. HIRSCHFELDER, C. F. CURTIS and R. B. BIRD, Molecular Theory of Gases and Liquids, 1954.
9. K. WATNABE, J. Chem. Phys., **26**, 542, 1957.

ELECTRICAL RESISTIVITY CHANGE IN SILVER DEFORMED BY TORSION

By

I. Kovács

INSTITUTE FOR EXPERIMENTAL PHYSICS, ROLAND EÖTVÖS UNIVERSITY, BUDAPEST

(Received 31. VIII. 1961)

Introduction

Numerous former investigations deal with the electrical resistivity change of plastically deformed metals [1—5]. In most of them the extra resistivity caused by extension was investigated; VAN BUEREN and JONGENBURGER [4] as well as PRY and HENNIG [5] made combined extension and twisting measurements. All experiments were performed at 78° K or at lower temperatures and except for the results of the combined methods the maximum of the strain was about 40%. According to these measurements the resistivity change depends on the strain in the following way:

$$\Delta\varrho = a \cdot \varepsilon^p , \tag{1}$$

where a is a value between 0,04 and 0,16 $\mu\Omega$ cm, while p lies between 1,3 and 1.5. According to the calculation of VAN BUEREN in the case of single glide the resistivity change expected on the basis of the theory is [6]

$$\Delta\varrho = A \cdot \varepsilon^{5/4} + B \cdot \varepsilon^{3/4}, \tag{2}$$

where A and B are constants depending on the initial defect concentration. The first term on the right-hand side of equ. (2) arises from vacancies and the second from dislocations. For large deformations the glide will be multiple and then the resistivity change is proportional to the square of strain:

$$\Delta\varrho \sim \varepsilon^2 . \tag{3}$$

Thus the previous measurements show that a single glide takes place for small deformations and then the resistivity change caused by dislocations is negligible as compared to the effect caused by vacancies. For large deformations BLEWITT, COLTMAN and REDMAN [7] made measurements for copper single crystals. They have strained the specimens by more than 100%, and at 4.2° K found a quadratic dependence of resistivity on strain in correspondence with (3).

In the present investigation pure torsional strain was applied. The amount of this can be defined as [6]

$$\varepsilon = \frac{3}{2} \Theta \frac{r}{l}, \tag{4}$$

where Θ is the angle of twist and r and l are radius and length of the wire. With this method of deformation $\varepsilon_{\max} = 300—400\%$ can be produced. The measurements were performed at 0° C and the results show that at this temperature the extra resistivity varies with the strain more than linearly for small deformations, but definitely depends on $\varepsilon^{3/4}$ for large deformations ($\varepsilon > 0{,}6$).

Experimental procedure and results

Polycrystalline silver wires annealed at 500° C for two hours, of 99.99% purity, 100 mm long and 1 mm in diameter have been investigated. The apparatus used is shown in Fig. 1. The specimen has been soft-soldered to the heads 1. The disc 2 could move in perpendicular direction, thus the specimen was a little stretched by the springs 3. This stress was about 1 kg/mm². The elongation of the specimen was indicated by the indicator dial 4 (the error is about ± 0.005 mm). The angle of twist is shown by the pointer 5. The elastic effect was eliminated by the free backward motion of the torsion head in a ball bearing when not twisted. The potential leads (V) and current leads (I) were placed as can be seen in the Figure. The entire apparatus was submerged into melting ice, the temperature during one measurement was constant within 0,1° C. The resistivity was determined with a Diesselhorst potentiometer.

The resistivity change and the elongation as a function of strain can be seen in Fig. 2. The specimens can be twisted about 100 times up to fracture, according to (4) this is about $\varepsilon = 400\%$.

To determine the specific resistivity change we have to consider the dimensional changes of the specimen too. The change of cross-section can only be estimated. Let us suppose that the change of the volume is negligible compared to the linear changes, then we can write

$$\Delta V = \Delta(q \cdot l) = l\Delta q + q \cdot \Delta l = 0,$$

from this

$$\left| \frac{\Delta q}{q} \right| = \frac{\Delta l}{l}.$$

With the use of this we have

$$\frac{\Delta \varrho}{\varrho} = \frac{\Delta R}{R} - \frac{2\Delta l}{l}. \tag{5}$$

The maximum elongation of a specimen was about 8 mm, thus for larger twisting the accuracy of elongation measurements may be compared with the accuracy of resistivity measurements. But this is not true for small twisting, thus here significant scattering can be expected. It can also be seen in Fig. 3, which shows the extra specific resistivity calculated on the basis of

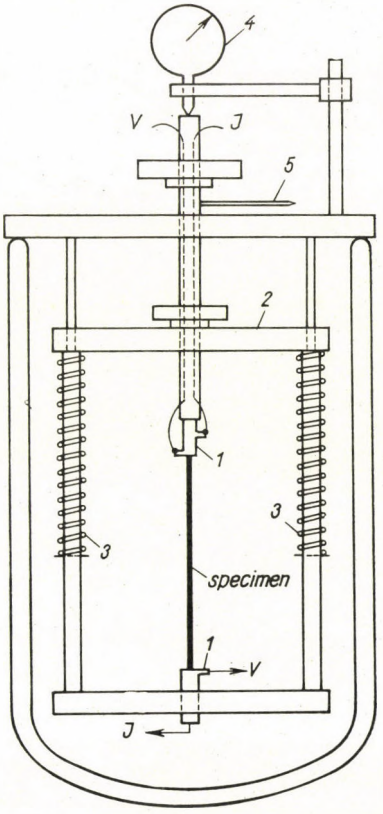

Fig. 1

equ. (5). According to this the extra resistivity varies with an exponent greater than one for strains $\varepsilon < 0{,}5$ in correspondence with former measurements made at low temperatures. But a significant difference appears for $\varepsilon > 0{,}6$. This part of the curve was replotted as a function of $\varepsilon^{3/4}$ (see Fig. 4). The points measured all lie nicely along a straight line. The calculation with the least squares method leads to the following results:

$$\Delta\varrho = 0.046\ \varepsilon^{1.49}\ \mu\Omega\ \text{cm} \qquad \text{for } \varepsilon < 0.5,$$

$$\Delta\varrho = 0.032\ \varepsilon^{3/4}\ \mu\Omega\ \text{cm} \qquad \text{for } \varepsilon > 0.6.$$

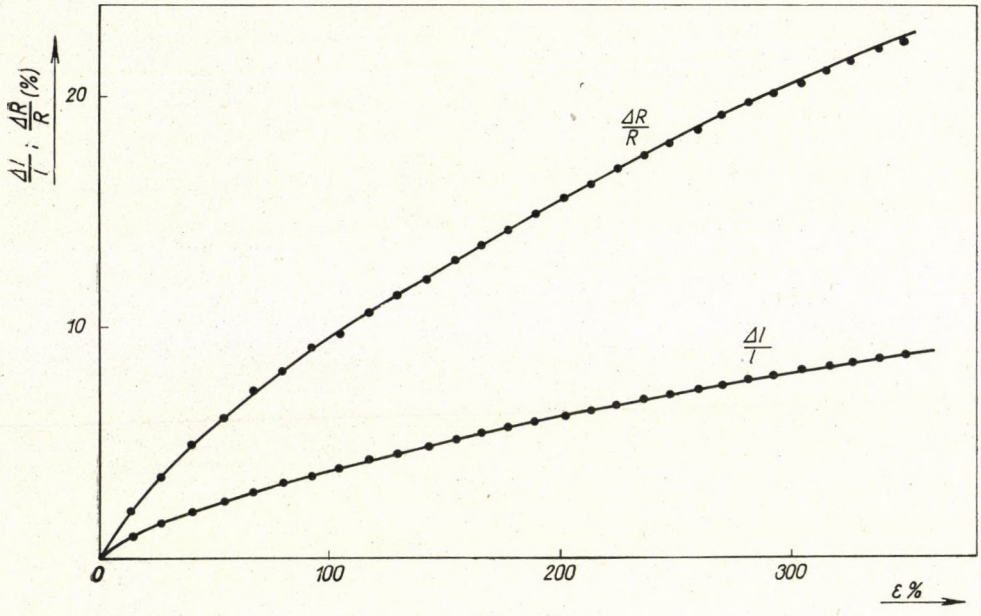
$\frac{\Delta l}{l}$; $\frac{\Delta R}{R}$ (%)
20
10
0
100
200
300
$\frac{\Delta R}{R}$
$\frac{\Delta l}{l}$
ε %

Fig. 2

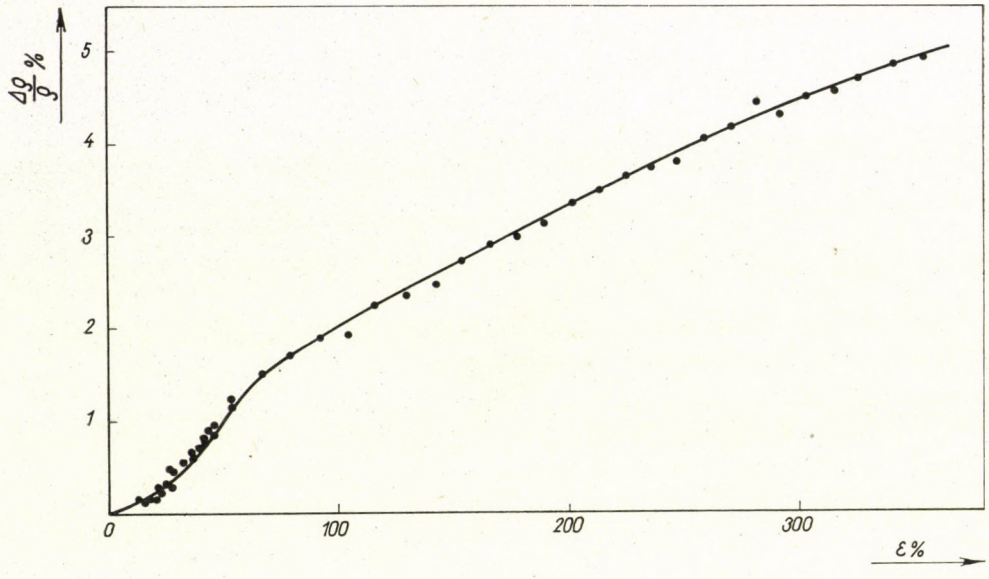
$\frac{\Delta \varrho}{\varrho}$ %
5
4
3
2
1
0
100
200
300
ε %

Fig. 3

These results mean that in polycrystalline silver wires deformed by torsion at 0° C for small deformation the extra resistivity arises first of all from vacancies, while the effect of dislocations is observed only at large deformations. From this it can be concluded that the vacancies very rapidly escape from the material at this temperature if the vacancy concentration exceeds a fixed value.The dependence of extra resistivity on $\varepsilon^{3/4}$ can be compared with the result of BLEWITT and coworkers [7]. They found that the resistivity change

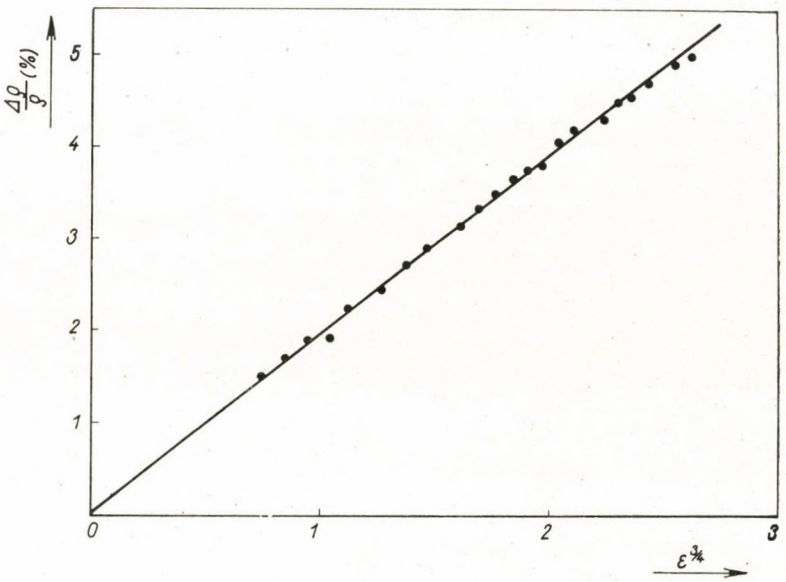

Fig. 4

caused by dislocations is $\Delta\varrho \sim \sigma^2$ (σ is the flow stress) regardless of temperature ($T \leqq 300°$ K). But the relation $\sigma = \sigma(\varepsilon)$ varies with the temperature; approximately there is $\sigma \sim \varepsilon^q$, where $q = 1$ at 4,2° K (then $\Delta\varrho \sim \varepsilon^2$), and q decreases with increasing temperature and is about 0.5 at 300° K. Correct comparison cannot be given, because in the case of single crystals the relation $\sigma = \sigma(\varepsilon)$ depends on the orientation. So it is quite probable that the difference between the present result and the theory leading to equ. (3) is caused by a temperature effect. Further studies will therefore be made in order to investigate the effect of temperature.

Acknowledgements

The author is indebted to Professor ELEMÉR NAGY for his interest and encouragement and valuable discussions during the course of this work. Further he wishes to thank Miss APOLLONIA KOVÁCS for her assistance in the measurements.

REFERENCES

1. M. J. DRUYVESTEYN and J. A. MANINTVELD, Nature, **168,** 868, 1951.
2. J. MOLENAAR and W. H. AARTS, Nature, **166,** 690, 1950.
3. W. H. AARTS and R. K. JARVIS, Acta Met., **2,** 87, 1954.
4. H. G. VAN BUEREN and P. JONGENBURGER, Nature, **175,** 544, 1955.
5. R. N. PRY and R. W. HENNIG, Acta Met., **2,** 318, 1954.
6. H. G. VAN BUEREN, Philips Res. Rep., **12,** 190, 1957.
7. T. H. BLEWITT, R. R. COLTMAN and J. K. REDMAN, Report on Conference on Defects in Crystalline Solids, Bristol, 1954, p. 369. The Physical Society, London, 1955.

DISTANCE TO POTENTIAL MINIMUM OF THE ELECTRONIC SPACE-CHARGE FROM EXTERNALLY HEATED CATHODES IN INERT HIGH-PRESSURE GAS-DISCHARGES

By

T. Z. SZELÉNYI

RESEARCH INSTITUTE FOR TECHNICAL PHYSICS OF THE HUNGARIAN ACADEMY OF SCIENCES, SECTION OF ELECTRON PHYSICS, BUDAPEST

(Received 9. IX. 1961)

In many problems of high-pressure gas discharges from externally heated cathodes the electronic space-charge plays an important part. In contrast to the electron emission in vacuum, where in the last years formulas [1, 2], and a nomogramm [3] have been published by means of which one may calculate the extension and density distribution of the space-charge in high-pressure gases, there are at this time — to our knowledge — no mathematical expressions available for this purpose.

To overcome this difficulty in close analogy to the equation for the case of potential minimum in vacuum, and also to the space-charge equation in high-pressure gases [4], we may set up a differential equation for the one-dimensional case with infinite plane-parallel electrodes on the basis of Poisson's equation

$$\frac{d^2 U}{dx^2} = -\frac{i_s e^{eU/[kT(x)]}}{\varepsilon_0 \bar{K} \left| dU/dx \right|}, \tag{1}$$

where the Boltzmann factor has been inserted on the basis of the equation

$$i = i_s e^{eU_m/[kT(x)]}. \tag{2}$$

In these equations U is the potential at the point x; x is the distance from the cathode; i_s the saturation value of the electronic current density; i the electronic discharge current density which flows without producing ionization between the electrodes; e the electronic charge; k the Boltzmann constant; $T(x)$ the temperature of the gas and also of the electrons at x; ε_0 the dielectric constant; $\bar{K}$ the mean electron mobility in the gas.

Extending a well-known method [5], and taking at first T as a constant we solve eq. (1) by multiplying both sides by $(dU/dx)^2$

$$\left(\frac{dU}{dx}\right)^2 \frac{d^2 U}{dx^2} = -\frac{i_s}{\varepsilon_0 \bar{K}} \left| \frac{dU}{dx} \right| e^{eU/kT}. \tag{3}$$

Then because of the identity

$$\frac{d}{dx}\left(\frac{dU}{dx}\right)^3 = 3\left(\frac{dU}{dx}\right)^2 \frac{d^2U}{dx^2} \tag{4}$$

we are able to integrate eq. (3) between the limits zero and U_m, the potential minimum, which leads for the distance x_m of this to

$$x_m = \left(\frac{kT}{e}\right)^{\frac{2}{3}} \sqrt[3]{\frac{-i_s \varepsilon_0 \bar{K}}{3\, i^2}} \left\{ \frac{3}{2} \ln\left(\sqrt[3]{1 - \frac{i}{i_s}} + \sqrt[3]{\frac{i}{i_s}} \right) + \right.$$
$$\left. + \sqrt{3}\ \mathrm{arctg} \frac{\sqrt{3}\sqrt[3]{i_s - i}}{\sqrt[3]{i_s - i} - 2\sqrt[3]{i}} \right\}. \tag{5}$$

To insert subsequently the temperature variation with distance, we may use on the basis of the data found in ref. [6], the following equation:

$$T(x) = T_0 + (T_c - T_0)\, e^{-\gamma x}. \tag{6}$$

Here T_0 is the temperature of the gas at a relatively great distance from the cathode; T_c is the cathode temperature and γ a constant.

By aid of formula (6) we iterate in a succession of computations to the proper value T_m, taking first in eq. (5) a supposedly correct temperature.

For example in a discharge in argon, specified by the constants: $p = 500$ mm mercury; $T_c = 3000$ °K; $\bar{K} = 1{,}0$ m²/Vs; $i_s = 10^4$ A/m²; $i = 10^{-2}$ A/m²; $\gamma = 6{,}28$ cm^{-1}; $T_0 = 300°$ K, we obtain $x_m = 3{,}5$ mm and $T_m = 535°$ K.

These values are in accordance with the position of the virtual cathode of the discharge, computed on the basis of the mean free path variations, and of the required ionization energy of electrons.

If in eq. (5) i had the value: 0,1 or 1 A/m², then x_m would be diminished to 1,4 or 0,5 mm, respectively. This change of the distance to the potential minimum in direction of the incandescent cathode calls forth the increase of T_m to 1200 and 1920° K. This augmentation transfers in many cases the virtual cathode into a region, where — in consequence of the longer mean free paths — the electrons are able to ionize the gas and so alter completely the character of the discharge. We experienced this change, which occurs reversibly in both directions on augmenting and diminishing the discharge current.

The author would like to thank Professor E. WINTER, member of the Hungarian Academy of Sciences, for suggesting the subject of this paper and for valuable discussions.

REFERENCES

1. W. B. NOTTINGHAM in Handbuch der Physik, Bd. XXI, Springer, Berlin, 1956; p. 43.
2. W. WEIZEL, Lehrbuch der Theoretischen Physik II, Springer, Berlin, 1958, p. 1575.
3. W. B. NOTTINGHAM, The Thermionic Diode as a Heat-to-Electrical-Power Transducer in J. Kaye and J. A. Welsh, Direct Conversion of Heat to Electricity, Wiley, New York, 1960, p. 2—5.
4. J. D. COBINE, Gaseous Conductors, Dover Publications, New York 1958, p. 128.
5. E. KAMKE, Differentialgleichungen I, Akademischer Verlag, Leipzig 1951, p. 113.
6. J. BRÓDY and F. KŐRÖSY, J. of Appl. Phys., **10**, 584, 1939.

INTERPOLATION FORMULAE FOR POSITIVE THOMAS-FERMI IONS

By

T. SZONDY

RESEARCH GROUP FOR THEORETICAL PHYSICS OF THE HUNGARIAN ACADEMY OF SCIENCES, BUDAPEST

(Received 25. X. 1961)

The solution of the THOMAS-FERMI equation $\varphi''(x) = x^{-1/2}\varphi^{3/2}(x)$ can be written in the well-known form $\varphi(x) = \varphi_0(x) + k(x)\eta_0(x)$, $\varphi_0(x)$ and $\eta_0(x)$ being given functions independent of the nuclear charge Z and the number of electrons N. In the case of free positive ions $k(x)$ depends very slightly on x and it is a function of the "degree of ionization" $q = (Z - N)/Z$.[1]

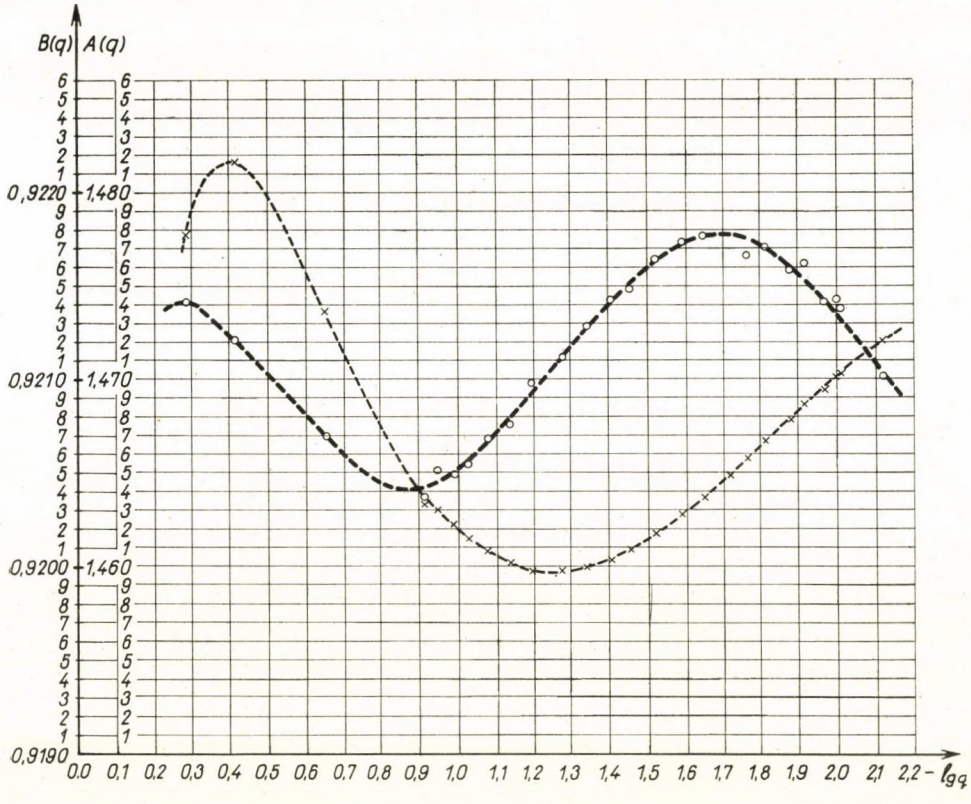

[1] See e. g. P. GOMBÁS, Statistische Behandlung des Atoms. (Hdb. der Phys. Bd. XXXVI. 127. Springer Verlag, Berlin—Göttingen—Heidelberg, 1956.)

The value of the function $k(x = 0, q)$ can be determined in the interval $0{,}5 \gtrsim q \gtrsim 0{,}007$ by the interpolation formula

$$A(q) \equiv 2{,}76 \lg q + 1{,}17\, q - \lg(-k) \approx 1{,}47\,. \tag{1}$$

The boundary radius x_0 of the ion, defined by $\varphi(x_0) = 0$, can be determined in the same interval of q by the interpolation formula

$$B(q) \equiv 0{,}351 \lg q + \lg(x_0 + 7{,}70) \approx 0{,}921\,. \tag{2}$$

The functions $A(q)$ and $B(q)$ given in the Figure[2] depend very slightly on q.

Formulae (1) and (2) are based on the very accurate results presented by S. KOBAYASHI.[3]

[2] In the Figure the circlets and crosses refer to the calculated values of $A(q)$ and $B(q)$, respectively.

[3] S. KOBAYASHI, Jap. Phys. Soc., **14**, 1039, 1959.

DAS KIRCHHOFFSCHE GESETZ IM FALLE STARK ABSORBIERENDER MEDIEN

Von

I. KETSKEMÉTY

INSTITUT FÜR EXPERIMENTALPHYSIK DER UNIVERSITÄT, SZEGED

(Eingegangen 28. X. 1961)

§ 1. PLANCK leitete eine den Emissionskoeffizienten ε_ν und den Absorptionskoeffizienten α_ν enthaltende Form des Kirchhoffschen Gesetzes ab, die durch die Gleichung

$$\frac{\varepsilon_\nu}{\alpha_\nu} = \mathfrak{K}_\nu \tag{1}$$

ausgedrückt werden kann, wobei $\mathfrak{K}_\nu$ die spezifische Strahlungsintensität im nnern des Mediums bedeutet [1]. Bei Herleitung von Gl. (1) wurde von

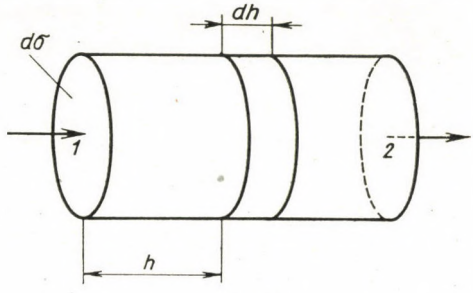

Abb. 1

PLANCK vorausgesetzt, dass das Medium *nicht stark absorbierend*, d. h. das Produkt aus der zu ν gehörigen Wellenlänge λ und dem Absorptionskoeffizienten α_ν klein gegen Eins ist. In der letzteren Zeit versuchte C. v. FRAGSTEIN, Gl. (1) auch für den Fall stark absorbierender Medien herzuleiten [2]. Anschliessend an die kritische Behandlung der FRAGSTEINschen Herleitung wollen wir zeigen, dass die obenerwähnte Forderung von PLANCK, die ursprünglich zur Vermeidung einer komplizierten Berücksichtigung von Beugungserscheinungen diente, als eine *wesentliche Voraussetzung* bezüglich der Gültigkeit von Gl. (1) anzusehen ist.

§ 2. FRAGSTEINS Gedankengang ist der folgende.

Betrachten wir das zylindrische Elementarvolumen dV mit der Basis $d\sigma$ und der Höhe d im Inneren eines stark absorbierenden Mediums (Abb. 1). Im thermodynamischen Gleichgewichte wird die Strahlungsenergie d^6E, die

in Pfeilrichtung, d. h. senkrecht zu $d\sigma$, von dV innerhalb des Frequenzintervalls $(\nu,\ \nu + d\nu)$ in das Raumwinkelelement $d\Omega$ durch die Basisfläche 2 emittiert wird, durch die Gleichung

$$d^6 E = 2\varepsilon_\nu \, d\nu \, d\sigma \, d\Omega \, dt \int_0^d e^{-(d-h)\alpha_\nu} \, dh \tag{I}$$

beschrieben. Die Energie d^6E muss gleich sein demjenigen Bruchteile d^6A der von links (s. Abb. 1) in der gleichen Richtung und im gleichen Raumwinkelelement $d\Omega$ auf die linke Basisfläche 1 des Zylinders fallenden Energie, der in der Zeit dt und im Frequenzintervall $(\nu,\ \nu + d\nu)$ in dV absorbiert wird, d. h. gleich dem Werte

$$d^6 A = 2\,\mathfrak{R}_\nu \, d\nu \, d\sigma \, d\Omega \, dt \, (1 - e^{-\alpha_\nu d}). \tag{II}$$

Aus $d^6E = d^6A$ würde sich Gl. (1) ergeben, wie gross auch α_ν ist. Die obige FRAGSTEINsche Herleitung ist aber für $\alpha_\nu \lambda > 1$ fehlerhaft, obwohl sie formal exakt zu sein scheint. Um dies zu zeigen, wollen wir zunächst auf eine experimentelle Arbeit von S. I. WAWILOW und M. D. GALANIN [3] hinweisen.

§ 3. Von WAWILOW und GALANIN wurde experimentell gezeigt, dass das Lambert-Bouguersche Absorptionsgesetz für Lichtstrahlen, die im Innern eines stark absorbierenden Mediums entstehen, nicht gültig sein kann. Die erwähnten Autoren fanden nämlich, dass die spektrale Intensitätsverteilung des von dünnen Schichten nicht schwach absorbierender Lösungen emittierten Fluoreszenzlichtes bei Verminderung der Schichtdicke eine Änderung aufweist, die nicht gedeutet werden kann, wenn das Lambert-Bouguersche Gesetz — ebenso wie bei Gl. (I) und (II) — hinsichtlich der Absorption des von dem strahlenden Medium emittierten Lichtes als gültig angenommen wird. (Die WAWILOW-GALANINschen Versuchsergebnisse scheinen infolge der starken Fluoreszenzlöschung, d. h. der kleinen Ausbeute, durch eine »spektrale Wirkung« der Sekundärfluoreszenz [4] nicht merklich beeinflusst, also zuverlässig zu sein.) Nach WAWILOW und GALANIN werden die im Inneren eines stark absorbierenden Mediums emittierten Strahlen *viel stärker* als die von aussen eindringenden Strahlen gleicher Frequenz absorbiert. (Somit kann man nicht dieselben Fluoreszenzcharakteristiken den Volumelementen der Oberfläche fluoreszierender Medien wie denen im Inneren der Medien zuordnen, wenn $\alpha_\nu \lambda > 1$ besteht.)

§ 4. Auch vom theoretischen Gesichtspunkt aus kann man die Gültigkeit von Gl. (1) bei stark absorbierenden Medien bezweifeln; es ist vielmehr fraglich, ob sich die drei Grössen ε_ν, α_ν, $\mathfrak{R}_\nu$ im Falle $\alpha_\nu \lambda > 1$ widerspruchslos definieren lassen.

Nehmen wir nämlich an, dass die Gl. (1) auch für $\alpha_\nu \lambda' > 1$ besteht; λ' soll die Wellenlänge im Medium bezeichnen. Mit dem Einsetzen $v\mathfrak{U}_\nu/8\pi$-

statt $\mathfrak{K}_\nu$ in Gl. (1), d. h. mit der Einführung der räumlichen spektralen Energiedichte u_ν und der Lichtgeschwindigkeit v im Medium, ergibt sich

$$\frac{v}{8\pi} u_\nu a_\nu = \varepsilon_\nu \tag{2}$$

oder wegen $\frac{v}{\nu} = \lambda'$

$$\nu a \lambda' u_\nu \, d\nu \, dt = 8\pi \varepsilon_\nu \, d\nu \, dt. \tag{3}$$

Die rechte bzw. linke Seite dieser Gleichung ist offenbar gleich der zu $d\nu$ gehörigen Strahlungsenergie, die in der Volumeneinheit, in dem Zeitabschnitt dt emittiert bzw. absorbiert wird. Aus Gl. (3) folgt, dass für den Quotienten aus der Zahl der in der Raum-, Zeit- und Frequenzintervalleinheit absorbierten Lichtquanten und der spektralen Lichtquantendichte $n_\nu \left(= \frac{u_\nu}{h\nu}\right)$ die Beziehung

$$\frac{\left(\frac{dn_\nu}{dt}\right)_{abs}}{n_\nu} = \frac{\frac{\nu a_\nu \lambda' u_\nu}{h\nu}}{\frac{u_\nu}{h\nu}} = \nu a_\nu \lambda' \tag{4}$$

besteht, d h., dass sämtliche Photonen der Frequenz ν nur eine mittlere Lebensdauer $\Delta t = \frac{1}{\nu a_\nu \lambda'}$ besitzen. Ist nun $a_\nu \lambda' \gg 1$, so soll $\Delta t \ll \frac{1}{\nu}$ sein, und hieraus folgt wegen $\Delta\nu \Delta t \approx 1$, dass die Unbestimmtheit $\Delta\nu$ der Frequenz der Lichtquanten $h\nu$ viel grösser als ν selbst ist. Diese Diskrepanz lässt sich unseres Erachtens nur dadurch eliminieren, dass man u_ν im Spektralgebiete, wo $a_\nu \lambda < 1$ nicht besteht, als gleich Null annimmt. Anders gesagt, kann die Form (1) des Kirchhoffschen Gesetzes bei starker Absorption nicht angewendet werden. Dagegen ist die das Absorptions- und Emissions*vermögen* enthaltende, ursprüngliche Form des Kirchhoffschen Gesetzes — wie man dies leicht einsieht — auch für stark absorbierende Medien gültig.

Auch an dieser Stelle sei Herrn Prof. Dr. A. Budó aufrichtiger Dank für die wertvollen Konsultationen ausgesprochen.

LITERATUR

1. M. Planck, Vorlesungen über die Theorie der Wärmestrahlung, J. A. Barth, Leipzig, 1921.
2. C. V. Fragstein, Optik, **18**, 264, 1961.
3. *С. И. Вавилов, М. Д. Галанин,* ДАН СССР, **67**, 811, 1949; *С. И. Вавилов,* Микроструктура света, Изд. АН СССР, Москва, 1950.
4. A. Budó und I. Ketskeméty, J. Chem. Phys., **25**, 595, 1956; Acta Phys. Hung., **7**, 207, 1957.

RECENSIONES

ENGEL—THIELHEIM: Kernenergie-Technik

Einführung in die Physik und Technik der Kernenergie-Erzeugung, Verlag Moderne Industrie, München, 300 Seiten, 99 Abb., 360 Tabellen, Leinen, DM 36.—

Das Ziel der Verfasser ist es, über die physikalischen, technischen und ökonomischen Fragen der Atomreaktoren einen Überblick zu geben, der die allgemeinen Kenntnisse eines durchschnittlichen Ingenieurs zu bereichern geeignet ist, und dabei auch für den gebildeten, doch nicht fachmännischen Leser eine nützliche Lektüre bildet.

Das Buch ist im wesentlichen in vier Abschnitte zu teilen. Das erste Kapitel behandelt auf ungefähr 100 Seiten die physikalischen und technischen Grundlagen des Themas. Nach Einführung in die wichtigsten kernphysikalischen Begriffe erläutern die Verfasser die Entstehungsbedingungen der sich selbst erhaltenden Spaltungskettenreaktionen. Diese Erläuterung wird von zahlreichen Tabellen und Graphikons begleitet, die die grundlegenden Angaben über die Reaktionsphysik enthalten. Nach einer kurzen Bekanntmachung mit der Steuerung und Regelung der Reaktoren behandelt das Buch die Kühlung derselben, sowie Fragen in Verbindung mit dem Schutz gegen Strahlungen. Am Ende des Kapitels besprechen die Verfasser die Herstellung von Brennstoffen für Reaktoren und die Prinzipien der Kernstrahlungsmessungen.

Im zweiten Kapitel behandelt das Buch die verschiedenen Reaktorentypen. Auf ungefähr 60 Seiten liest man über heterogene Wasserreaktoren, homogene Reaktoren, organisch gekühlte, gasgekühlte, graphitmoderierte, flüssigmetallgekühlte Reaktoren, sowie Flüssigmetall-Brennstoff-Reaktoren und schnelle Reaktoren. Abschliessend befassen sich die Autoren mit den Problemen der Schnellreaktoren und führen deren bekannteste Typen vor.

Im dritten Kapitel untersuchen die Verfasser die Wirtschaftlichkeit der Kernreaktoren. Aus Daten über den Energiebedarf der wichtigsten Gebiete der Erde ziehen sie Schlüsse auf den Zeitpunkt, zu dem die Kernenergieerzeugung wirtschaftlich betrieben werden kann. Ein verhältnismässig ausführlicher Teil dieses Kapitels befasst sich mit dem Schiffsantrieb durch Reaktoren.

Das letzte Kapitel des Werkes untersucht die Möglichkeiten der praktischen Anwendung der thermonuklearen Energie, und gibt eine Übersicht über den gegenwertigen Stand der wissenschaftlichen Forschung.

Das Buch behandelt fast alle wichtigen Gebiete der friedlichen Anwendung der Kernenergie und eben dieses umfassende Bestreben der Verfasser macht es schon von vorneherein unmöglich auf entsprechendem wissenschaftlichem Niveau ausführliche Informationen über die behandelten Fragen zu geben. Das Buch muss also als ein volkstümlich-wissenschaftliches Werk angesprochen werden, da weder die Behandlungsart, noch die aus dem Buch zu schöpfenden Kenntnisse dem Fachmann Neues sagen können. Immerhin wird das Interesse an diesem Buch durch die vielen Abbildungen, die der schnellen Referenz und dem leichten Verständnis dienlich sind, beträchtlich gehoben.

Die Autoren haben der Darlegung der sowjetischen Fachliteratur sichtbar keinen grossen Raum gewidmet; besonders auffallend ist dies hinsichtlich der die Reaktorphysik und die thermonuklearen Reaktionen behandelnden Kapitel.

L. PÁL

Halbleiterprobleme

in Referaten des Halbleiterausschusses auf Tagungen des Verbandes Deutscher Physikalischer Gesellschaften. Bad Pyrmont 1959. Band V. Herausgegeben von Prof. Dr. Fritz Sauter, Köln. Mit 132 Abbildungen. Friedr. Vieweg und Sohn, Braunschweig, 1960.

Das Buch enthält acht Aufsätze von verschiedenen Autoren und eine kurze Berichtigung zum Referat von J. TELTOW aus dem III. Band der Serie »Halbleiterprobleme«. Die einzelnen Referate sind der Reihe nach folgende:

1. J. JAUMANN, *Neuere Ergebnisse der Ultrarotspektroskopie von festen Körpern* (mit 41 Abbildungen).

Das Absorptionspektrum des festen Körpers kommt durch drei Effekte zustande:

1. Erregung von Gitterschwingungen,
2. Stromwärme erzeugt von den freien Ladungsträgern und
3. innerer lichtelektrischer Effekt vom kurzwelligen Ultrarot bis ins Ultraviolett.

Die Absorptionsbandenkante ist der charakteristischeste Teil des Spektrums. Der ihr entsprechende Quantensprung ist der grösste im beobachtbaren Spektrum. Weiterhin gehören der Kante noch sehr viele energieärmere Quantenübergänge an. Das Referat befasst sich überwiegend mit den Vorgängen in der Nähe der Bandenkanten des Ge und Si. Diese Vorgänge sind:

1. Gitterschwingungen im fernen Ultrarot (in Emission und Absorption),
2. Exzitonenspektren (in Absorption),
3. Elektronenspektren von Fremdatomen und Störstellen (nur in Emission) sowie
4. »Diamagnetische Resonanzspektren« freier Ladungsträger im Magnetfeld (in Absorption).

Die experimentell erhaltenen Ergebnisse sind durch zahlreiche schöne Abbildungen veranschaulicht, die hier nur zum Teil erwähnt werden können. So z. B. Bändermodelle von Ge und Si; effektive Masse von Elektronen des Ge bei 4° K; Absorptionsband von Ag und Au und der Unterschied zwischen den Absorptionsbändern des Ge bzw. des Si und ihre Temperaturabhängigkeit; das Absorptionsband des Ge im Magnetfeld und dessen Deutung; experimentell einwandfreie Darstellung und Deutung der Exzitonenniveaus. In Unterkapiteln wird auf die Fälle hingewiesen, in denen FERMI-Statistik verwendet werden muss (Indiumantimonid, Indiumarsenid).

Auf dem Gebiete der Spektren der freien Ladungsträger wird das Absorptionsspektrum von p-Ge bei verschiedenen Trägerkonzentrationen, das Absorptionspektrum von Te und die Elektronenbänder im Trägerspektrum des n-Si behandelt.

Die Besprechung der Absorptionspektren von Fremdatomen enthält den Fall von B in Si, wo ein wasserstoffähnliches Spektrum in Absorption erhalten wurde, und weiter den von As in Ge und die Oszillation im magnetischen Felde. Es folgt die Verteilung des lichtelektrischen Stromes im Spektrum des golddotierten Ge und eisendotierten Si. Interessant ist fernerhin die Tabelle über die Ionisierungsspannungen von gelösten Fremdatomen in Ge. Weiter folgen die Absorptionsspektren der Gitterschwingungen von Ge- bzw. Si-Kristallen und ihre theoretische Deutung. Nach optischer Anregung oder Trägerinjektion stellt sich das thermische Gleichgewicht durch Strahlung her. Lehrreich sind schliesslich auch die Abbildungen zur Rekombinationsstrahlung von Si und Ge sowie zu den thermischen Emissionsspektren von Ge im Vergleich mit der »schwarzen« Strahlung.

2. O. G. FOLBERTH, *Überblick über einige physikalisch-chemische Eigenschaften der $A^{III}B^{V}$-Verbindungen unter besonderer Berücksichtigung der Zustandsdiagramme* (mit 10 Abbildungen).

Die $A^{III}B^{V}$-Verbindungen sind neben den Halbleiterwerkstoffen und dem Ge und Si die bedeutendsten Grundstoffe der modernen Technologie der Halbleiter. Diese Verbindungen können in folgende Gruppen eingeteilt werden:

Gruppe I. Verbindungen mit geringem Dampfdruck am Schmelzpunkt: InSb, GaSb, AlSb.

Gruppe II. Verbindungen mit erheblichem Dampfdruck am Schmelzpunkt: InAs, GaAs, InP, GaP.

Gruppe III. Verbindungen mit hohem Schmelzpunkt und hohem Dampfdruck am Schmelzpunkt: AlAs, AlP, BAs, BP, InN, GaN, AlN, BN.

Nach den Zustandsdiagrammen der I. Gruppe werden die technologisch wichtigen Daten der einzelnen Glieder nur kurz bekanntgegeben, da die Behandlung dieser Gruppe der beim Ge und Si üblichen Verfahren ähnlich ist.

Bei der II. Gruppe sind die Herstellungsverfahren der Verbindungen, die Methoden zum Umschmelzen und Kristallzüchten beschrieben. Danach werden für jedes Glied die bezüglichen Zustandsdiagramme und zahlreiche kennzeichnende technologische Angaben mitgeteilt.

Die Glieder der III. Gruppe sind am wenigsten erforscht, daher werden hier keine Zustandsdiagramme vorgelegt; dagegen werden bei den einzelnen Verbindungen, wenn auch nur ganz kurz, wichtige Angaben über Behandlung und Eigenschaften mitgeteilt. Sehr wertvoll ist die Tabelle am Ende des Referates, in der die charakteristischesten technischen Daten der ganzen $A^{III}B^{V}$-Verbindungsgruppe zusammengefasst sind. (Unter dem Titel »Literatur« werden 130 Literaturstellen aufgereiht.)

3. H. KRÖMER, *Negative effektive Massen in Halbleitern* (mit 5 Abbildungen).

Der Referent gibt zuerst die Begriffe der effektiven und der gerichteten effektiven Masse und die tensoriellen Begriffe der longitudinalen und transversalen Massen an. Dann wird die Lagerung der negativen Massen im Valenzband von Ge in verschiedenen kristallographischen Richtungen (100), (110), (111) mitgeteilt. Durch Resonanzmessungen gelang es mit Hilfe des Zyklotrons an Ge-Kristallen die Existenz negativer Massen $m = -0{,}22\, m_0$ (wo m_0 die Masse des freien Elektrons bedeutet) im Einklang mit der Theorie experimentell nachzuweisen. Es wird auf die praktischen Anwendungsmöglichkeiten der negativen Masse hingewiesen, wie z. B. Mikrowellengenerator und -verstärker (14 Literaturstellen).

4. O. MADELUNG, *Das Verhalten von Halbleitern in hohen Magnetfeldern* (mit 22 Abbildungen).

In anschaulicher Weise wird zuerst die LANDAUsche Theorie der Halbleiter in starken Magnetfeldern besprochen. In starken Magnetfeldern krümmen sich nämlich die Elektronenbahnen kreisförmig, wodurch sich die Bewegung periodisch gestaltet und diese muss gemäss der Quantenmechanik gequantelt werden. Es werden die Folgen der abgeleiteten Gleichungen besprochen. Solche Folgen sind z. B. die Änderung des Bändermodells, die Aufspaltung der Therme im Magnetfeld und damit die Änderung der Zustandsdichte.

Die Verteilung der Ladungsträger verändert sich im Magnetfeld, wodurch auch die elektrische Leitfähigkeit geändert wird. Im folgenden Unterkapitel wird die Theorie der galvanomagnetischen Effekte in starken Magnetfeldern angegeben. Die longitudinalen und transversalen Widerstandsänderungen im Einklang mit der Theorie werden in Abbildungen wiedergegeben. Die Ergebnisse von Messungen magneto-optischer Effekte sind nach der Besprechung der Theorie, in den Abbildungen 11—22, durch Graphikonen zusammengefasst. Auf Grund der Theorie werden diese experimentellen Befunde kritisch behandelt. Die Vorteile und Ergebnisse der Magnetoabsorptionsmessungen für die Bestimmung von Halbleiterparametern werden in 5 Punkten zusammengefasst. (Zum Referat gehören 88 Literaturstellen).

5. H. SCHMIDT, *Einfluss von Bandstruktur und Elektron-Gitter-Wechselwirkung auf die Lichtabsorption in Halbleitern* (mit 7 Abbildungen).

Dieses Referat behandelt von einem einheitlichem Gesichtspunkt aus die Theorie der Halbleiter Ge, In und InSb. Bei der Fülle des Stoffes beschränkt sich der Autor nur auf zwei Fälle der Lichtabsorption, u. z. auf die sogenannten direkten Übergänge, Sprung des Elektrons oder Loches zwischen zwei Bändern, der bei hohen Frequenzen den Hauptanteil der Absorption liefert. Die andere Gruppen bilden die sogenannten indirekten Übergänge mit Beteiligung des Gitters. Sprung eines Elektrons (Loches) innerhalb eines Bandes oder zwischen zwei Bändern, wobei noch ein Schallquant der Gitter-schwingungen am Prozess teilnimmt. Der ganze Stoff wird in drei Aufsätze geteilt:

A) Im Aufsatz »Bandstruktur in Halbleitern« liest man über die Einteilchennäherung, Symmetrien des InSb- und Ge-Gitters, Wellenfunktionen bei $k = 0$ ohne Spin, Feinstruktur des Valenzbandes in Ge, kugelsymmetrische Näherung für das Valenzband in Ge und die Gesamtheit der bekannten Energiebänder in Ge, Si, InSb mit Abbildungen.

B) Im Abschnitt über Elektron-Gitter-Wechselwirkung werden nach Umgrenzung der allgemeinen Ansätze die Wechselwirkung zwischen Löchern und Gitter in Ge, die Leitfähigkeit von p-Ge und die Elektron-Gitter-Wechselwirkung in Ge, Si, InSb besprochen.

C) Schliesslich behandelt der Referent im letzten Aufsatz die allgemeine Theorie der Absorption durch direkte Übergänge; die Lichtabsorption in p-Ge durch direkte Übergänge von Valenz- ins Leitungsband und die Lichtabsorption an freien Ladungen. Auf die experimentellen Arbeiten wird nur hingewiesen (Das Referat berücksichtigt 43 Literaturstellen.)

6. D. GEIST, *Der Maser* (Bericht mit 19 Abbildungen).

Die Bezeichnung Maser ist aus den Anfangsbuchstaben des Satzes »Microwave amplification by stimulated emission of radiation« gebildet, und es wäre angeraten, diese Bezeichnung auch im Ungarischen beizubehalten.

Der Maser kann als Verstärker von 300 MHz bis hinauf zu 20 000 MHz auftreten, während Transistoren von Tonfrequenz bis hinauf zu 250 MHz reichen. Sie werden also vom Maser in dieser Hinsicht weit übertroffen. Er zeichnet sich in praktischer Hin-

sicht durch extrem geringes Rauschen aus. Die Wirkungsweise des Masers wird am Beispiel des Ammoniakmoleküls erläutert. Ausser dem Ammoniak werden auch andere zur Maserherstellung geeignete Stoffe beschrieben, wie Alkalidampf, paramagnetische Salze, z. B. Gadolinium — und Chromsalze samt ihrer Herstellung und Wirkungsweise. Es gehören hierher neutronenbestrahltes Quarz und phosphordotiertes Si. Die Arbeit macht uns weiterhin mit der Arbeitsweise von Zwei- und Drei-Niveau-Masern sowie mit den theoretischen Bedingungen der Hochfrequenzstabilität der Drei-Niveau-Masern bekannt. Im Kapitel über die Maser-Schaltungen sind in einer grossen Tabelle die technischen Daten der verschiedenen Anwendungsmöglichkeiten zusammengefasst. Am Schluss wird die Theorie und Messung des Maser-Rauschens erläutert. (Der Referent gibt 173 Literaturstellen an.) Abschliessend folgt eine kurze Diskussionsbemerkung von KRÖMER,

7. H. ZÜCKLER, *Nachtrag zum Referat : Siliziumkarbid, Eigenschaften und Anwendung als Material für spannungsabhängige Widerstände* (Halbleiterprobleme Bd. III, S. 207—229) mit 2 Abbildungen).

Auf dem Gebiete der Herstellung von SiC sind infolge Benützung von Ar-, H_2-, CO- und N_2-Schutzatmosphären hervorragende Ergebnisse erzielt worden. Die Bestimmung der optischen Konstanten geschah durch Absorptionsmessungen.

Die an Kristallen auftretenden flächenhaften Elektrolumineszenzerscheinungen lassen sich als Rekombinationsstrahlung der über die p-n-Grenze injizierten Ladungsträger verstehen. Das Punktleuchten entsteht, wenn die p-n-Schicht an Stellen hoher Störstellendichte zusammenbricht (Stossionisation).

Die Ergebnisse von Leitfähigkeitsmessungen an Einkristallen (Hallkonstante, spez. Leitfähigkeit und Beweglichkeit) werden in 6 Abbildungen mitgeteilt und Kontaktwiderstandsmessungen für Spezialfälle durch Zahlenangaben wiedergegeben (Die Arbeit gibt 62 Literaturstellen an.)

8. K. HAUFFE und W. SCHOTTKY, *Deckschichtbildung auf Metallen* (mit 26 Abbildungen).

Das Referat umfasst beinahe die Hälfte des V. Bandes. Die am Ende gegebene Aufreihung der 148 Bezeichnungsschlüssel erfordert 6 Seiten, was auf die Fülle und Vielfältigkeit des Stoffes hinweist.

Die Problemstellung kann am kürzesten mit den Worten der Autoren gekennzeichnet werden: »In der vorliegenden Darstellung wird der Versuch unternommen, die gegenwärtige Kenntnis über den Mechanismus der Deckschichtbildung auf Metallen in einem zusammenfassenden Bericht niederzulegen. Bringt man Metalle und Legierungen in Berührung mit gasförmigen, flüssigen oder festen chemischen Agenzien, und sind die thermodynamischen Voraussetzungen für einen Reaktionsablauf gegeben, so beobachtet man eine mehr oder minder rasche Reaktion mit dem Metall, deren Mechanismus und Geschwindigkeit von den jeweiligen Versuchsbedingungen abhängen«.

Das Referat verteilt sich auf drei grössere Kapitel. Das erste Kapitel behandelt die Transportvorgänge in binären Verbindungen mit Eigenstörstellen, die Verallgemeinernng der Transporttheorie und die Tracerdiffusion.

Im zweiten Kapitel berichten die Referenten über die stromlose Deckschichtbildung in Gasen bei Quasineutralität und lokalem Störstellengleichgewicht, über das damit verbundene allgemeine Wachstumsgesetz sowie wichtige Sonderfälle, über Verallgemeinerung bei innerem Gitterumbau, mehrphasige Deckschichten, Messung des Schichtwachstums, Beobachtungsergebnisse und über Prüfung der Theorie.

Im dritten Abschnitt folgt schliesslich die Besprechung der vorangehenden Vorgänge in Spezialfällen wie z. B. divergenzfreier Störstellentransport, Oberflächen- und Raumladungseffekte, Raumladungsrandschichten im elektrochemischen Gleichgewicht mit der Gasphase, Chemisorption, ambipolare Diffusion, allgemeine Grundgleichungen in Deckschichten ohne Quasineutralität, Spezialisierungen: grosse Ionenbeweglichkeit und elektronischer Tunneleffekt in sehr dünnen Deckschichten, Keimbildungsprozesse im Anfangsstadium des Wachstums sehr dünner Deckschichten, Deckschichtbildung auf Metallen in Elektrolytlösungen. (Das Referat berücksichtigt 138 Literaturstellen.)

9. J. TELTOW, *Berichtigung zum Referat : Assoziation und Wechselwirkung von Störstellen in Ionenkristallen und Halbleitern* (Halbleiterprobleme Bd. III, 1956, S. 26 ff.). Es werden fünf Stellen mit den verbesserten Texten angegeben.

Der Band enthält abschliessend die Inhaltsübersicht über die früheren vier Bände.

Z. GYULAI

GEORG V. BÉKÉSY: Experiments in Hearing

Translated and edited by E. G. Wever. McGraw-Hill Book Co., New York, etc. 1960. 745 pages

The book in question can reckon on particular interest in this country. This is due not only to the personality of the author, but also to the Nobel-Prize he was awarded lately. The McGraw-Hill Publishing Company have issued in their Series »Psychology« the most important works of BÉKÉSY in English. All are scientific publications which have appeared in periodicals, part of them being translations from the original German.

BÉKÉSY has not written any books — apart from a smaller summary chapter in the Handbook of Experimental Psychology — but his literary activity is all the same very impressive. Making an estimation on the basis of the reviewed book, the bibliography of BÉKÉSY's articles must contain at least 83 pages, in reality a somewhat greater number was printed. The issued bulky volume although not containing all publications of BÉKÉSY succeeds through systematization, arrangement and contraction of the articles as well as by omitting some parts in presenting his whole life-work in the form of a book. It represents at the same time an appreciation of the scientist who has just celebrated his 60th birthday.

BÉKÉSY is an intuitive researcher, an excellent experimentist and a man of clear reasoning. The results, obtained by his precision preparative techniques, which have been mentioned repeatedly with great admiration, represent the most important phases of up-to-date biophysics. His Hungarian friends and his former collaborators know him as a versatile researcher. He found always, even under adverse circumstances, an adequate and practicable solution, he himself designed his experimental instruments and moreover also made his characteristic illustrations. His activity falls — it may be said — completely in the field of acoustics, where he proved to be many-sided. The acoustic plans of the first studios of the Hungarian Broadcasting Station are also connected with his name, as well as the construction of a new audiometer named after him. As professor he lectured at the University of Budapest in the years 1941—46 on practical and physiological physics.

From the 83 publications of the book 45 contain researches made in the Post-Office Research Institute of Budapest and about 32 report on work done in the Psycho-acoustic Laboratory of Harvard University.

The editor does not follow the chronological order when compiling the subject matter, but he arranges the substance of the individual articles — as far as possible — logically in groups. In this manner e. g. a very instructive experimental technical part (Chapters 3 and 4) results, which has been collected from the substance of 14 papers.

The whole matter is divided into four parts. The first part constitutes an introduction to the reading of the other parts. Besides the afore-mentioned experimental technical chapters it deals with the problems of hearing researches and with the anatomy of the ear.

The second part collects — well-ordered — the substance of work on the conduction of hearing. In this part of 100 pages are published the results referring to the physics of the middle ear (Chapter 5) and bone conduction (Chapter 6).

The following part comprising 200 pages bears the title "Psychology of Hearing". This is the most heterogeneous part of the book, though it can count, no doubt, on the most universal interest. The papers dealing with the perception of hearing, as well as with the determination threshold of hearing (Chapter 7), further those on the perception of direction and distance (Chapter 8) and on the distortion and inertia of the ear (Chapter 9) are contained in this part, and here can also be found the room acoustics (Chapter 10), consisting of the subject of 3 papers.

Finally, the fourth part contains the results of the most interesting and the most profound work of BÉKÉSY. These are publications dealing with the mechanics of the inner ear. The whole part comes to 300 pages, of which the earlier papers, treating of the vibrations of the cochlea, occupy 2 chapters (Chapters 11 and 12, 130 pages). The classical papers of the first period of work of BÉKÉSY can here be read in English translation. The following chapter leads already to a new period of research (frequency analysis and law of contrast). The (last) Chapter 14 sums up the latest papers of BÉKÉSY on the electrophysiology of the cochlea (80 pages).

Besides the bibliography referred to above, the works mentioned in the papers of BÉKÉSY are also enumerated at the end of the book. It may not be superfluous to publish some addenda to the bibliography, thus making the collection more complete.

01. Folyadékok diffúziós állandójának mérése (Measurement of the diffusion constant of fluids). Szt. István Akadémia felolvasásai, I, 10, 1925 (dissertation).

02. Über ein Verfahren um, für Diffusionsmessungen, zwei Flüssigkeiten übereinander zu schichten. Phys. Zeits., 28., 812—814, 1927.

ad 19. Published also in Russian: Uspekhi Fizich. Nauk 15, 756—772, 1935.

ad 24. Unaltered reprint: Akust. Zeits., 1, 128—134, 1936.

ad 25. The correct title: Über die photoelektrische Fourier-Analyse eines gegebenen Kurvenzuges.

ad 25*a*. Sur la réverberation optimum des petites salles. Revue d'Acoustique, 5, 145—182, 1936. — Kis zenetermek optimális akusztikai viszonyairól (On the optimum acoustical conditions of small rooms). Magyar Posta Műszaki Közlemények, 11, 135—163, 1937.

ad 27. To be precise: an answer without title to the letter of W. LOTTERMOSER entlitled "Bemerkungen zu den subjektiven, harmonischen Teiltönen nach G. von BÉKÉSY"

ad 36. Appeared: Schriften zur Sing- und Sprechkultur Bd. I, München und Berlin, 1940, pp. 110—113.

ad 37*a*. A vibrációs érzés szerepe a technikában (The role of the sensation of vibrations in the technics). Magyar Posta Műszaki Közlemények, 15, 9—20, 1941.

ad 41. Page numbers: 67—75. Published also: Arch. für Sprach- und Stimmphysiol., 5, 117—124, 1941.

ad 71. Page numbers: 448—468.

Reverting again to the subject matter collected in the present volume, we may state that it is a properly selected and compiled collection, which can be read as if it were indeed a book. Professor ERNEST GLEN WEVER deserves high appreciation for the first rate solution of the very hard literary task, taking care also of the translation. The book has an exemplary finish and shows excellent typographical taste — routine matters as regards the publishers. Its price is fairly high, which evidently has to be ascribed to the necessity of obtaining so many permissions for reprinting.

T. TARNÓCZY

Absorption Spectra in the Ultraviolet and Visible Region

Edited by L. LÁNG, Publishing House of the Hungarian Academy of Sciences, Budapest

The introductory volume and the first volume of the compilation issued by the Publishing House of the Hungarian Academy of Sciences in 1959 has been discussed in Volume VII of the Hungarian Journal of Physics (Magyar Fizikai Folyóirat, p. 400, 1959). In the meantime the second edition of the introductory volume and the first volume have appeared (March, 1961) and the first edition of the second volume (July, 1961). We must consider it as fortunate that after a good start a new volume has been added to this useful series, as for those working in the field of chemical structure research, every new volume in the international literature brings a great help, owing to the vast number of organic compounds. The necessity and indispensability of handbooks of this kind for those dealing with absorption spectroscopy is demonstrated by the fact that recently the following comprehensive works amply supplied with tables have been published:

H. M. HERSHENSON: Ultraviolet and Visible Absorption Spectra, Index for 1930—1954. Academic Press Inc. 1956, Volume II. Index for 1955—1957; Academic Press Inc. 1961.

M. J. KAMLET: Organic Electronic Spectral Data, Volume I. 1946—1952. Interscience Publishers Inc. 1960.

H. E. UNGNADE: Organic Electronic Spectral Data, Volume II. 1953—1955, Interscience Publishers Inc. 1960.

As another feature of interest it may be added that the series edited by the Publishing House of the Hungarian Academy of Sciences has been taken over without change by the Academic Press Inc., to be issued in cooperation with the right of distribution in North and South America. These facts prove that it was right to start the edition of this series and that it is desirable to continue it.

In the second volume the aim expressed in the preface begins to take shape, namely emphasis on the importance of the international character of the series. This volume already includes spectra taken by Polish authors. It is to be hoped that in the future more and more research workers from abroad will submit their works for publication in this series.

In the second volume similarly to the method followed in the first the spectra of further substances (289) are published with continuous numbering (171—349). The measurement data given were obtained in various solvents and often in media of varying pH and the figures contain the log ε curves computed from the measurement records. The table of contents annexed to the volume

lists all the material mentioned in the book, according to both name and molecular formula. The index mentions also the names and place of work of the authors, giving the reference numbers of the spectra prepared by each author. The index summarizes the bibliographic data of the articles in which the spectra in question were published, or those which are in any relation with the material.

The series can be considered to be of great value to spectroscopic research and in view of this one might have expected the publishers to pay greater attention to the binding of the various volumes. The structure keeping the pages loosely in the otherwise tasteful black clothcover does not seem to stand up to much use. This, naturally, does not diminish the intrinsic value of the volume but in our opinion the rich material would have deserved greater care to avoid such minor faults.

The publication of further volumes is awaited with great interest; it is hoped that they will bring new success to Hungarian spectroscopists in the international field of research.

I. Kovács*

* Department of Atomic Physics, Polytechnical University, Budapest.

Printed in Hungary

A kiadásért felel az Akadémiai Kiadó igazgatója — Műszaki szerkesztő: Farkas Sándor
A kézirat nyomdába érkezett: 1962. VIII. 23. — Terjedelem: 7,50 (A/5) ív, 24 ábra

62.55877 Akadémiai Nyomda, Budapest — Felelős vezető: Bernát György

The *Acta Physica* publish papers on physics, in English, German, French and Russian.
The *Acta Physica* appear in parts of varying size, making up volumes.
Manuscripts should be addressed to:

Acta Physica, Budapest 502, Postafiók 24.

Correspondence with the editors and publishers should be sent to the same address.
The rate of subscription to the *Acta Physica* is 110 forints a volume. Orders may be placed with "Kultura" Foreign Trade Company for Books and Newspapers (Budapest I., Fő u. 32. Account No. 43-790-057-181) or with representatives abroad.

Les *Acta Physica* paraissent en français, allemand, anglais et russe et publient des travaux du domaine de la physique.
Les *Acta Physica* sont publiés sous forme de fascicules qui seront réunis en volumes.
On est prié d'envoyer les manuscrits destinés à la rédaction à l'adresse suivante:

Acta Physica, Budapest 502, Postafiók 24.

Toute correspondance doit être envoyée à cette même adresse.
Le prix de l'abonnement est de 110 forints par volume.
On peut s'abonner à l'Entreprise du Commerce Extérieur de Livres et Journaux «Kultura» (Budapest I., Fő u. 32. — Compte-courant No. 43-790-057-181) ou à l'étranger chez tous les représentants ou dépositaires.

«*Acta Physica*» публикуют трактаты из области физических наук на русском немецком, английском и французском языках.
«*Acta Physica*» выходят отдельными выпусками разного объема. Несколько выпусков составляют один том.
Предназначенные для публикации рукописи следует направлять по адресу:

Acta Physica, Budapest 502, Postafiók 24.

По этому же адресу направлять всякую корреспонденцию для редакции и администрации.
Подписная цена «*Acta Physica*» — 110 форинтов за том. Заказы принимает предприятие по внешней торговле книг и газет «*Kultura*» (Budapest I., Fő u. 32. Текущий чет: № 43-790-057-181) или его заграничные представительства и уполномоченные.

22,— Ft

INDEX

COMMUNICATIONES BREVES

RECENSIONES

Acta Phys. Hung. Tom. XV. Fasc. 1. Budapest, 30. XI. 1962.

ACTA PHYSICA

ACADEMIAE SCIENTIARUM HUNGARICAE

TOMUS XV. FASCICULUS 2.

AKADÉMIAI KIADÓ, BUDAPEST
1962

ACTA PHYSICA

A MAGYAR TUDOMÁNYOS AKADÉMIA FIZIKAI KÖZLEMÉNYEI

SZERKESZTŐSÉG ÉS KIADÓHIVATAL: BUDAPEST V., ALKOTMÁNY UTCA 21.

Az *Acta Physica* német, angol, francia és orosz nyelven közöl értekezéseket a fizika tárgyköréből.

Az *Acta Physica* változó terjedelmű füzetekben jelenik meg: több füzet alkot egy kötetet.

A közlésre szánt kéziratok a következő címre küldendők:

Acta Physica, Budapest 502, Postafiók 24.

Ugyanerre a címre küldendő minden szerkesztőségi és kiadóhivatali levelezés.

Az *Acta Physica* előfizetési ára kötetenként belföldre 80 forint, külföldre 110 forint. Megrendelhető a belföld számára az Akadémiai Kiadónál (Budapest V., Alkotmány utca 21. Bankszámla 05-915-111-46), a külföld számára pedig a „Kultúra" Könyv- és Hírlap Külkereskedelmi Vállalatnál (Budapest I., Fő u. 32. Bankszámla 43-790-057-181 sz.), vagy annak külföldi képviseleteinél és bizományosainál.

Die *Acta Physica* veröffentlichen Abhandlungen aus dem Bereiche der Physik in deutscher, englischer, französischer und russischer Sprache.

Die *Acta Physica* erscheinen in Heften wechselnden Umfanges. Mehrere Hefte bilden einen Band.

Die zur Veröffentlichung bestimmten Manuskripte sind an folgende Adresse zu richten:

Acta Physica, Budapest 502, Postafiók 24.

An die gleiche Anschrift ist auch jede für die Redaktion und den Verlag bestimmte Korrespondenz zu senden.

Abonnementspreis pro Band: 110 forint. Bestellbar bei dem Buch- und Zeitungs-Aussenhandels-Unternehmen »Kultura« (Budapest I., Fő u. 32. Bankkonto Nr. 43-790-057-181) oder bei seinen Auslandsvertretungen und Kommissionären.

ANISOTROPE STRUKTUR SCHRÄG AUFGEDAMPFTER ALUMINIUMSCHICHTEN

Von

E. F. PÓCZA

FORSCHUNGSINSTITUT FÜR TECHNISCHE PHYSIK DER UNGARISCHEN AKADÉMIE DER WISSENSCHAFTEN, BUDAPEST

(Vorgelegt von Z. Gyulai. — Eingegangen 23. I. 1961)

Die mit in einem Winkelbereich von 5°—90° schräg aufgedampften dünnen halbdurchsichtigen Aluminiumschichten durchgeführten optischen Elektronendiffraktions- und Elektronenmikroskopischen Untersuchungen haben das anisotrope Verhalten der Schichten gezeigt. Ursache der Anisotropie ist, dass in der Struktur der Schichten die einzelnen Kristalle mit ihrer Längsrichtung in senkrechter Richtung zur Einfallsfläche der Bedampfung wachsen, ohne dass aber in solchen dünnen Schichten noch eine kristallstrukturell ausgezeichnete Orientation auftreten würde. Wenn wir das Kristallaggregat als zweidimensional betrachten, lässt sich ein geeigneter Ordnungsgrad einführen. Unter Verwendung der Statistik der auf den elektronenmikroskopischen Aufnahmen befindlichen Kristalle wurde der Ordnungsgrad von bei verschiedenem Einfallwinkel bedampften Schichten gemessen. Dieser wurde mit befriedigender Annäherung dem die optische Anisotropie der Kristallaggregate kennzeichnenden Polarisationsgrad gleich gefunden. Aus den Statistiken über die Abmessungen wurde die Erklärung der anisotropen Struktur des Aggregates an Hand der Berechnung der Wachstumsbedingungen der einzelnen Kristallkörnchen gegeben und festgestellt, dass möglicherweise die Ausgestaltung der anisotropen Struktur des ganzen Aggregates durch die Anisotropie des Wachstums der einzelnen Kristalle verursacht wird.

Übersicht über die Literatur

Die im Vakuum aufgedampften, weniger als einige hundert Å dicken halbdurchsichtigen Metallschichten finden heute bereits in zahlreichen Gebieten der Technik und der Wissenschaft praktische Anwendung. Obwohl bei der Herstellung solcher Schichten der Dampfstrahl bei Bedampfung fast in jedem Falle senkrecht auf die Oberfläche des Substrates auffällt, so spielt doch unter den kontraststeigernden Methoden der elektronenmikroskopischen Untersuchungen oft die schräge Bedamfpung der Präparate mit einem Schwermetalldampf, der kleinkörnige Kristalle ergibt, wie z. B.: Gold, Palladium, Platin, Uran, eine Rolle.

Die auf diese Weise hergestellten Schichten weisen vielfach eine leicht erkennbare optische Anisotropie auf und bei polarisiertem Licht hängt ihre Absorption von der Lage der Polarisationsebene zu der bei der Bedampfung ausgezeichneten Einfallsebene ab. Diese Erscheinung wurde zuerst von KUNDT [1] bei Kathodenzerstäubung beobachtet. Die hier ebenfalls aus den schräg auf die Metalloberfläche fallenden Atomstrahlen entstehende zusammenhängende Metallschicht zeigt auch im Falle des senkrecht einfallenden polarisierten Lichtes die Abhängigkeit der Durchlässigkeit vom Azimut und

dies ergibt einen dem Dichroismus ähnlichen Effekt. BRAUN [2] nimmt als Erklärung der Erscheinung eine fadenartige Ausbildung der Struktur der aufgedampften Schichten an und erklärt damit, dass die in der Schichtenstruktur entstehenden länglichen Kristalle die polarisierten elektromagnetischen Wellen nur dann durchlassen, wenn die Schwingungsrichtung des elektrischen Vektors der Wellen senkrecht zur Richtung der Fäden ist, d. h. wenn diese längliche Fadenstruktur einen Hertz-Effekt verursacht. Die Voraussetzung dafür ist, dass die Fadenentfernungen in die Grössenordnung der Kristallabmessungen fallen, also im Vergleich zur Wellenlänge klein sind. Ist dies nicht der Fall, so kommt der von DU BOIS und RUBENS [3] beobachtete Effekt zur Geltung; sind nämlich die Abmessungen der Längsfäden (Kristalle) grösser als die Wellenlänge des benützten Lichtes, so ist die Richtung der grösseren Durchlässigkeit diejenige, in welcher die Schwingungsrichtung parallel zu der Richtung der Fäden verläuft. Die Richtigkeit der Annahme von BRAUN wurde durch Untersuchungen von KÖNIG und HELWIG [4] nachgewiesen. Ihre elektronenmikroskopischen Untersuchungen zeigten, dass die in schräg aufgedampfte Schichten eingeordneten Kristalle annähernd eine Netzstruktur aufweisen, und als Wirkung dieser Struktur kann die entstehende optische Anisotropie als ein Hertz-Effekt erklärt werden. Bei der qualitativen Diskussion der Strukturen wird darauf verwiesen, dass in der die optische Anoistropie verursachenden Struktur die Kristallkerne nicht orientiert, jedoch hinsichtlich ihrer Form gewissermassen geordnet sind, und die Ursache dieser Ordnung der schattenwerfenden Wirkung der Kristallkerne zugeschrieben werden kann. REIMER [5] führte mit Au, Ag, Cu, Mn-Schichten parallel optische und elektronenmikroskopische Untersuchungen durch. Nach seinen Beobachtungen haben die aufgedampften Metallschichten im sichtbaren Spektrum für das senkrecht zur Einfallsebene der Bedampfung polarisierte Licht eine grössere Durchlässigkeit als für das mit der Einfallsebene parallel polarisierte. Bei den untersuchten Stoffen zeigte der Polarisationsgrad eine starke Wellenlängenabhängigkeit. Die elektronenmikroskopischen Untersuchungen wiesen in den untersuchten Schichten eine fadenförmige Anordnung der länglichen Kristallaggregate auf und lieferten den Beweis dafür, dass die Erscheinung ein Hertz-Effekt ist. Bei einzelnen in Toluol getauchten Silberschichten konnte auch nachgewiesen werden, dass im Falle richtig gewählter Kristallabmessungen auch der DU BOIS-Effekt erzeugt werden kann, und dass die Bestimmung des kritischen Inversionspunktes möglich ist. Die Untersuchungen von REIMER bieten wegen der starken Wellenlängenabhängigkeit des Polarisationsgrades keine Möglichkeit, durch eine vereinfachende Annahme zu einem quantitativen Zusammenhang zwischen der Struktur und dem für die entstehende Anisotropie charakteristischen Polarisationsgrad zu gelangen. Es bedarf eingehenderer Untersuchungen, um auch die Ursachen der Entstehung solcher Schichtstrukturen aufzuklären.

Die optische Anisotropie aufweisenden Metalle haben im allgemeinen einen hohen Schmelzpunkt. Nach den Untersuchungen von EVANS und WILMAN [6] ergeben solche Metalle im Falle schräger Aufdampfung, über einer Schichtdicke von einigen hundert Å, eine sehr charakteristische, in Richtung der Aufdampfung beugende — laut den jüngsten Untersuchungen von RUMS und BAKLAGINA [7] genau mit der Richtung der Aufdampfung zusammenfallende — einachsige (Typ II) Textur. Die Frage liegt auf der Hand, ob nicht auch der für das optisch nachweisbare anisotrope Verhalten verantwortliche Effekt mit dieser Eigenschaft im Zusammenhange stehe. Die Ergänzung der morphologischen Untersuchungen durch Elektronendiffraktionsuntersuchungen bezweckt, gerade diese Frage zu klären. Obwohl nach den zur Verfügung stehenden Literaturangaben [8, 9] und nach unseren Erfahrungen bei diesen Metallen eine ausgezeichnete Orientation im Bereich einer Schichtdicke von weniger als hundert Å nicht zu erwarten ist, erscheint es doch der Mühe wert, dies mit einer empfindlicheren Methode nachzuprüfen, weil eine solche Textur in geringem Masse eventuell bereits unmittelbar im Ausgangsstadium der Entstehung der Schichten auftritt.

Für die beschriebenen Zielsetzungen wurde als Versuchsmaterial Aluminium gewählt. Dieses Metall zeigt im Falle einer schrägen Aufdampfung ein aussergewöhnliches Verhalten, da es trotz seines niedrigen Schmelzpunktes einen schrägwinkligen einachsigen Texturtypus darstellt, wie es sonst nur Metalle mit hohem Schmelzpunkte sind. Aluminium ist als das zur Herstellung von Spiegeln und halbdurchlässigen Schichten verwendete Material schon wegen seiner Verbreitung in der Industrie interessant. Es zeigt im Falle von kleinen Aufdampfungswinkeln sehr gut den Lichtpolarisationseffekt, in der Literatur sind jedoch im Hinblick darauf durchgeführte quantitative Untersuchungen nicht zu finden [10].

Herstellung von Aluminiumschichten

Bei der Herstellung der Schichten wurde die übliche Anordnung verwandt (Abb. 1). Das 99.995-prozentig reine Aluminium wurde von einem Wolframfaden (W) abgedampft. Das nötige Vakuum, in dem der gesamte Gasdruck unter 10^{-5} Torr war, wurde durch eine Quecksilberdiffusionspumpe, die mit einer Gefriervorrichtung mit flüssiger Luft versehen war, erzeugt. Bis zum Absaugen der bei der Aufdampfung freigewordenen Gase waren die als Präparatbehälter dienenden, auch die Mikrogitter tragenden und mit einer Formvar-Haut versehenen Mikroskopobjektträger (D) durch einen von aussen beweglichen Deckel (F) vom Dampfstrahl abgedeckt. Die Abdeckung wurde bei $2 \cdot 10^{-5}$ Torr abgenommen und die Präparate hergestellt. Der Aufdampfungswinkel (α) wurde zwischen 5° und 90°, die Menge des verdampften

Materials, vom Aufdampfungswinkel abhängig, zwischen 5 mg und 100 mg variiert. Die Entfernung des Präparates vom Wolframfaden variierte zwischen 10—20 cm, die Aufdampfung erfolgte im allgemeinen aus einer Entfernung von 14 cm. Die verdampfte Menge konnte aus der Aufdampfungsgeschwindigkeit, d. h. auf Grund der Messung der zur Aufdampfung nötigen Zeit bestimmt werden. Die Menge des hineingebrachten Materials wurde so bemessen, dass diese auch im Falle des kleinsten gewählten Winkels die pro Oberflächeneinheit benötigte Materialmenge auch dann noch zu decken fähig war, wenn

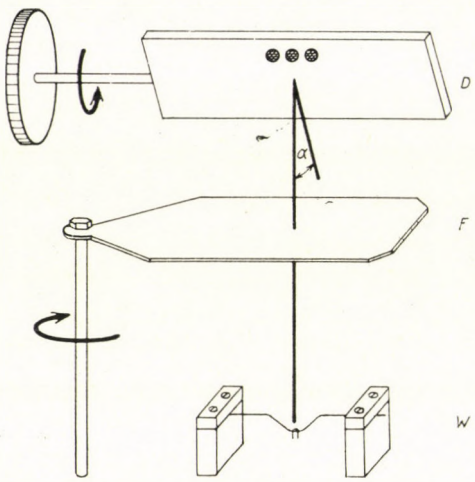

Abb. 1. Schema der Herstellung der Schichten

das Präparat für die Zeitdauer (etwa 15 sec) des Absaugens der beim Schmelzen des Materials freiwerdenden Gase abgedeckt wurde. Die Gleichmässigkeit der Abdampfung vom Wolframfaden wurde wie folgt nachgeprüft: bei genau bemessenem Glühstrom wurde in verschiedenen Mengen aufgetragenes Material verdampft. Nach den Beobachtungen erwies sich die Verdampfungsgeschwindigkeit (die pro Sekunde verdampfte Materialmenge) im verwendeten Gebiet innerhalb von 10% unverändert und war nur von der Temperatur abhängig (Tab. I).

Bei reproduzierbarer Dampfstrahlintensität war die Feststellung der Schichtdicke durch Berechnung möglich, eine weitere Methode zur Messung der Schichtdicke war durch Absorptionsmessungen gegeben, ausserdem konnte die bei gleichen Bedingungen durch mehrmaliges Aufdampfen hergestellte Schicht von mehrfacher Dicke nach dem TOLANSZKYschen Verfahren [11] gemessen werden. Die drei Methoden ermöglichten die Bestimmung der Schichtdicke mit einem relativen Fehler von weniger als 15%. Diese befriedigende Übereinstimmung ermöglichte die Durchführung der Schichtdickenbestimmung durch eine einfache Absorptionsmessung bei zwei Wellenlängen (5360 Å, 7700 Å).

Tabelle I

Beziehung zwischen den Parametern der Aufdampfung

Heizstrom	Die Menge des eingeführten Materials	Bedampfungszeit	Bedampfungs-geschwindigkeit
Ampère	mg	sec	mg/sec
30	31,3	61	0,51
30	15,0	28	0,53
30	14,5	26	0,56
28	14,0	35	0,40
28	14,0	41	0,34
28	15,0	42	0,36
28	15,0	37	0,40
28	10,0	26	0,38
28	10,0	27	0,37
28	20,0	57	0,35

Messung des Polarisationsgrades

An unter definierten Bedingungen hergestellten Schichten wurden mit Hilfe eines in unserem Laboratorium gebauten Polarisationsmikroskops und eines Lichtintensitätsmessers, Typ Magnephot II, Transmissionsmessungen in den vier Maximum- und Minimumpositionen des drehbaren Objekttisches durchgeführt und der Polarisationsgrad der Schicht aus dem Mittelwert der fast gleichen Intensitäten der Parallelpositionen berechnet. Diese Methode lieferte zugleich eine Kontrolle, da im Falle einer unrichtigen Zentrierung, einer Verletzung oder sonstiger Asymmetrie die zwischen den Intensitäten der zwei parallelen Maximum-Minimumpositionen auftauchende wesentliche Differenz sofort auf eine Unstimmigkeit aufmerksam machte, die dann durch entsprechende Einstellung des Kreuztisches beseitigt werden konnte. Die Abweichung der Maximum-Minimumpositionen von der senkrechten, bzw. parallelen Lage ermöglichte ebenfalls die empfindliche Registrierung der Asymmetrie der Einstellung. Die vor der Lichtquelle angebrachten Schmalband-Interferenzfilter ermöglichten auch die Messung und Absorptionskontrolle in den verschiedenen Spektralgebieten. Die Messungen wurden im allgemeinen im 7700 Å Bereich durchgeführt. Von der geringen elliptischen Polarisation des durchgelassenen Lichtes wurde wegen deren Geringfügigkeit abgesehen.

Die Wellenlängenabhängigkeit des Polarisationsgrades im sichtbaren Licht wurde mit einem aus einem Monochromator in unserem Laboratorium hergestellten Spektrophotometer nachgeprüft. Die Messungen an einigen Präparaten überzeugten uns, dass bei den Aluminiumschichten im Bereich

zwischen 4000—8000 Å der Polarisationsgrad nur eine geringfügige Wellenlängenabhängigkeit aufweist, und im Grossteil der Präparate den in der oben beschriebenen Bestimmung des Polarisationsgrades auftretenden Messfehler nicht bedeutend überschreitet. Die im vollen Spektralbereich gemessenen

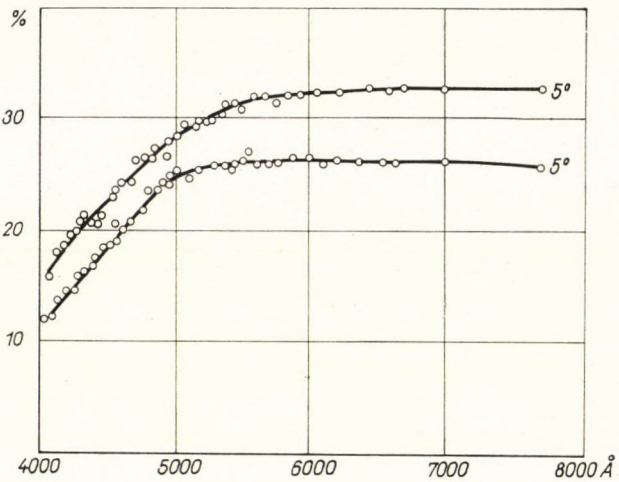

Abb. 2/a Wellenlängenabhängigkeit des Polarisationsgrades

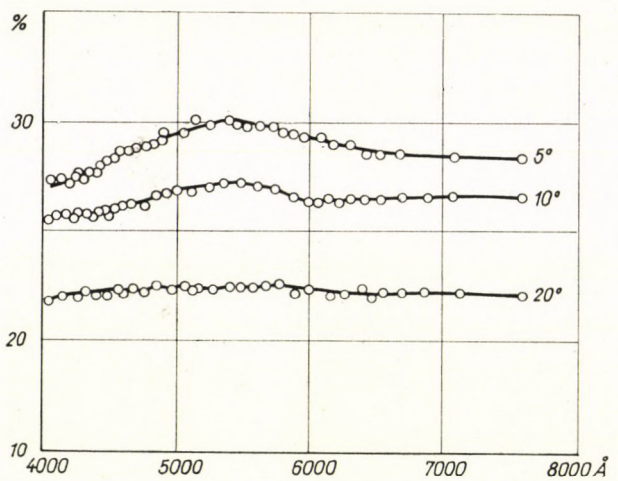

Abb. 2/b Wellenlängenabhängigkeit des Polarisationsgrades

Werte einiger solcher Schichten sind in Abb. 2/*a* dargestellt. Die Präparate wurden eben wegen dieser geringen Wellenlängenabhängigkeit gewählt, da bei solchen Präparaten zu erwarten ist, dass ein eindeutiger Zusammenhang zwischen der Struktur und dem auftretenden Polarisationseffekt aufgefunden werden kann. Obzwar sich bei einem Teil der Präparate (Abb. 2/*b*) auch eine

stärkere Wellenlängenabhängigkeit zeigte und der Ablauf den Messungen von REIMER [5] für Silberschichten ähnlich war, wurden keine Präparate gefunden, bei denen die von REIMER bei Silber nachgewiesene Gitterinversion beobachtet werden konnte. In einigen Fällen verringert sich der Polarisationsgrad mit der

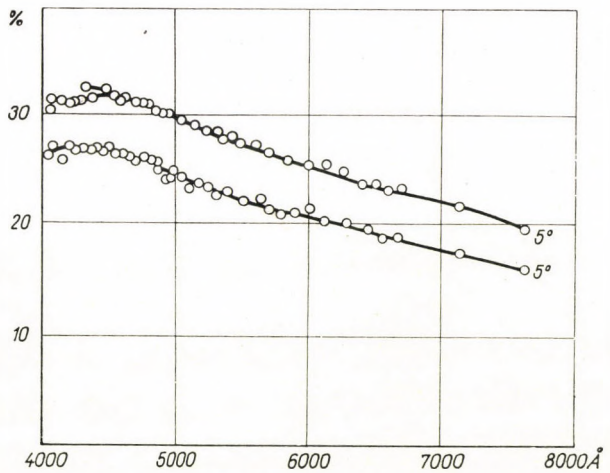

Abb. 2/c. Wellenlängenabhängigkeit des Polarisationsgrades

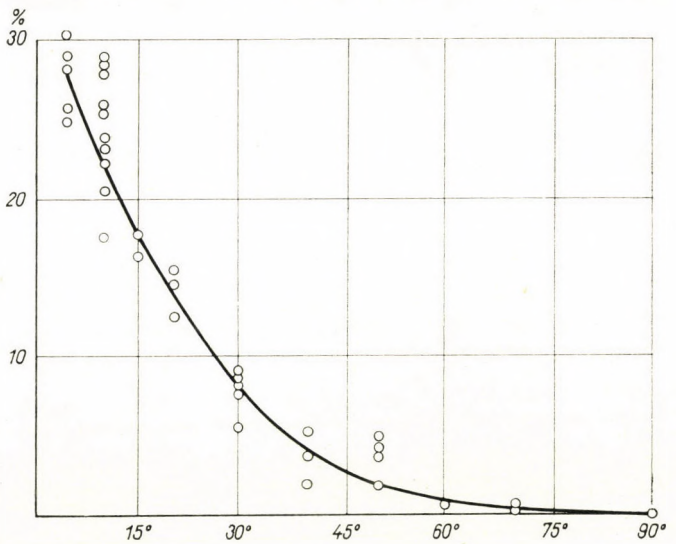

Abb. 3. Abhängigkeit des Polarisationsgrades vom Aufdampfungswinkel der Schichten

Vergrösserung der Wellenlänge (Abb. 2/c). Diese Inhomogenität der Präparate ist in den bei der Aufdampfung unvermeidlichen Unterschieden zu suchen, und deren Klärung bildet den Gegenstand weiterer Untersuchungen. Vorliegender Aufsatz berichtet über Untersuchungen, die an homogenen und dadurch

Wellenlängenabhängigkeit kaum aufweisenden Präparaten durchgeführt wurden.

Die unter einem kleinen Einfallswinkel schräg aufgedampften Aluminiumschichten zeigen einen starken Polarisationseffekt. Abb. 3 stellt die Messergebnisse von bei verschiedenen Einfallswinkeln aufgedampften Schichten dar. Der Polarisationsgrad verringert sich stark von den kleinen Winkeln (flacher Einfall) zu den grossen Winkeln hin (steiler Einfall), ein geringer Effekt war jedoch auch noch im Falle eines Winkels von 70° zu beobachten. Die Messungen des Polarisationsgrades an den in den Bereich von 40—80 Å fallenden Schichten wurden in einem gemeinsamen Diagramm angegeben. Die verhältnismässig grosse Streuung in einem so kleinen Bereich gab keine Möglichkeit zur Feststellung einer eindeutigen Dickenabhängigkeit. Die ausgezogene Linie stellt eine volle Messreihe der Schichtdicke um 70 Å dar. Die relative Streuung der gemeinsam hergestellten Schichten war klein, die zwischen den verschiedenen Messreihen bestehende Streuung stammt wahrscheinlich von den schwer zu kontrollierenden Vakuumverhältnissen her. Im Falle kleinerer Winkel kann die grössere Streuung auch durch die mit dem Glühfadenwechsel in kleinem Masse variierende Geometrie erklärt werden.

Elektronendiffraktionsuntersuchungen

An Aluminiumschichten durchgeführte Elektronendiffraktionsuntersuchungen haben bewiesen, das bei den unter einem Winkel von 5—90° aufgedampften Schichten in dem untersuchten Schichtdickenbereich von 30—150 Å keine ausgezeichnete Orientation auftritt. Von den Schichten wurden Transmissionsaufnahmen gemacht, wobei das Elektronenbündel unter einem Winkel von 0°, 30° und 45° einfiel. Die von diesen Elektronogrammen erhaltenen Intensitätsverteilungen wiesen weder visuell noch nach Auswertung der Ringe auf photometrischem Wege auf eine ausgezeichnete Orientation hin. Abb. 4/*a* stellt eine unter einem Winkel von 30° gemachte Aufnahme von einer unter einem Winkel von 10° aufgedampften Schicht und die Photometrierkurve eines für die Untersuchung solcher Intensitätsverteilungen geeigneten Kreisdiagrammes dar. Das Photometer tastet den Ring mit dem kleinen leuchtenden Fleck in der Weise ab, dass bei der im Kreise gedrehten Aufnahme der Tisch auch eine Oszillationsbewegung durchführt und der in Abb. 4/*b* eingezeichnete Weg häufig nacheinander über das Ringmaximum führt. Wäre die Intensität entlang des Ringes wegen einer ausgezeichneten Orientation nicht gleichmässig, so sollte an der Hüllkurve der häufigen Maximalwerte die symmetrisch ungleichmässige Intensitätsverteilung bemerkbar sein.

Unser Elektronenmikroskop ermöglichte, auch Elektronendiffraktionsaufnahmen von einem ausgewählten Gebiet des Präparates zu machen,

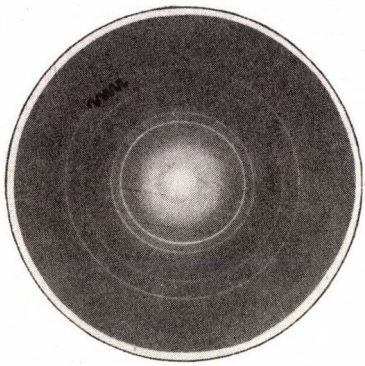

Abb. 4/a. Elektronendiffraktionsaufnahme eines unter 10° aufgedampften Präparates von einer Schichtdicke von 70 Å mit einem zu der Normalen des Präparates um 30° geneigten Elektronenbündel. Die Strecke der Fotometrierung ist eingezeichnet

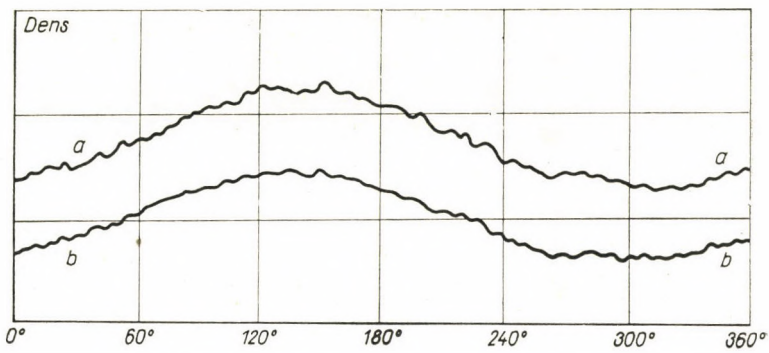

Abb. 4/b. Die aufgenommene Fotometerkurve

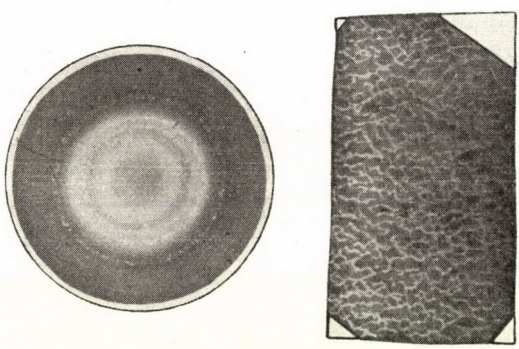

Abb. 5. Kleinfeld-Elektronenbeugungsdiagramm einer unter 20° aufgedampften 70 Å dicken Schicht

dadurch, dass durch das vor der Projektionslinse angebrachte Diaphragma nur jene Bündel durchgelassen werden, die von diesem bestimmten Gebiet kommen. Mit diesen Bündeln wurde dann das Elektronenbeugungsdiagramm des Präparates hergestellt. Auf den so hergestellten Aufnahmen machen sich entlang der den Debye—Scherrer Ringen entsprechenden Kreise bereits die den einzelnen Kristallkörnchen entsprechenden Einkristallflecke, übereinander gelagert, bemerkbar. Auf den in dieser Weise hergestellten Aufnahmen hätte sich eine schräge Texturachse auffallend bemerkbar machen müssen. Eine Asymmetrie solcher Natur machte sich auch auf diesen Aufnahmen nicht bemerkbar, die statistische Unordnung der von den einzelnen Kristalliten entstammenden Flecken ist offensichtlich (Abb. 5).

Als Ergebnis der Elektronendiffraktionsuntersuchungen kann daher festgestellt werden, dass die kristallographischen Achsen der im Kristallaggregat angeordneten Kristalliten im Raum statistisch ungeordnet liegen, und dass bei den untersuchten Schichtdicken keine ausgezeichnete Orientation auftritt.

Elektronenmikroskopische Untersuchungen

Auf den mit einem Formvar-Film bedeckten Objektträger wurde bei Herstellung der aufgedampften Schichten in jedem Falle auch das mit einem Formvar-Film bedeckte Mikrogitter gelegt, sodass von der gegebenen Probe ein für die Untersuchung im Elektronenmikroskop geeignetes Präparat leicht abgetrennt werden konnte. Von diesen Präparaten wurden die elektronenmikroskopischen Aufnahmen mit einem Elektronenmikroskop Typ »Hitachi«, mit einem Auflösungsvermögen von 8 Å, gemacht. Die unmittelbare Vergrösserung war im allgemeinen 50 000-fach, in einzelnen Fällen 100 000-fach. Auf den Elektronenmikroskopaufnahmen konnten vom Aufdampfungswinkel abhängig Kristallaggregate verschiedener Abmessungen und Anordnungen beobachtet werden. Auf die Bilder wurde in der Weise eingestellt, dass an denselben kleine Verunreinigungen geeigneter Grösse ausgesucht wurden, deren Schatten die Bedampfungsrichtung gut nachwies. Bei den unter einem kleinen Winkel aufgedampften Schichten war die Bedampfungsrichtung nicht nur wegen der Richtung der Schatten, sondern auch wegen der Anordnung der Kristalle nach ihrer Längsrichtung, bereits mit einem Blick, in guter Annäherung zu erkennen. In Abb. 6 ist die Elektronenmikroskopaufnahme eines unter einem Winkel von 10° aufgedampften Aluminiumpräparates von einer Schichtdicke von etwa 70 Å dargestellt. Um zu beweisen, dass eine auffallende ausgezeichnete Anordnung auftritt, wurden zwei Kopien der Aufnahme nebeneinander gestellt. In Lage *a)* verläuft die Aufdampfungsrichtung von links nach rechts, in Lage *b)* von oben nach unten. Bei einer Schichtdicke von

70 Å wurde für Aufdampfungswinkel zwischen 5—90° auch die statistische Auswertung der Elektronenmikroskopaufnahmen durchgeführt. Auf je einer Aufnahme wurden 500—1000 Kristalle gefunden. Die bei einer unmittelbaren 50 000-fachen Vergrösserung aufgenommenen Bilder wurden im allgemeinen noch durch eine sechsfache optische Vergrösserung vergrössert. An den sich mit ihrer Längsachse in verschiedenen Richtungen anordnenden Kristallen, die im allgemeinen eine längliche Form hatten, wurde die Richtung der Längs-

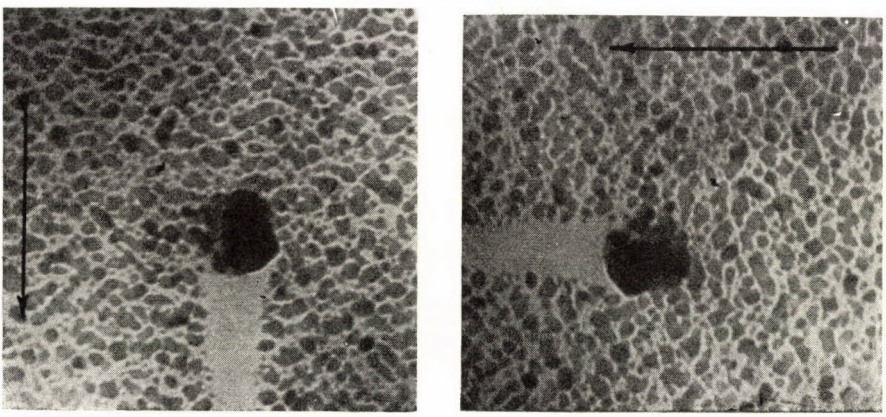

Abb. 6. Elektronenmikroskopische Aufnahme einer unter 10° aufgedampften 70 Å dicken Aluminiumschicht. Der Pfeil am Rand der Aufnahme weist auf die Richtung der Bedampfung hin, ihre Länge beträgt 2000 Å. Etwa 50 000-fache Vergrösserung

achse bezeichnet, sodann wurde in Intervallen von je 10° die Richtungsverteilung der Kristalle, d. h. der Prozentsatz der sich zu einer Richtung parallel anordnenden Kristalle bestimmt. Jeder Kristall wurde proportional seiner Längenabmessung berücksichtigt. In Abb. 7 sind die so erhaltenen Hystogramme für die verschiedenen Aufdampfungswinkel dargestellt. Der äusserste in das Diagramm eingezeichnete Kreis entspricht 16%. Die erhaltenen Hystogramme beweisen, dass sich die Kristallkörnchen mittlerer Abmessungen mit ihrer Längsachse senkrecht zur Aufdampfungsrichtung anordnen. Diese Anordnung ist umso ausgeprägter, je flacher der Einfallswinkel des Dampfstrahles bei der Bedampfung ist.

Ordnungsgrad des Kristallkonglomerats

Zum quantitativen Vergleich der Hystogramme ist es zweckmässig, den Ordnungsgrad des Kristallaggregats zu definieren. Stellt man sich die einzelnen Kristallkörnchen als dünne Stäbchen vor, deren Richtung und Länge

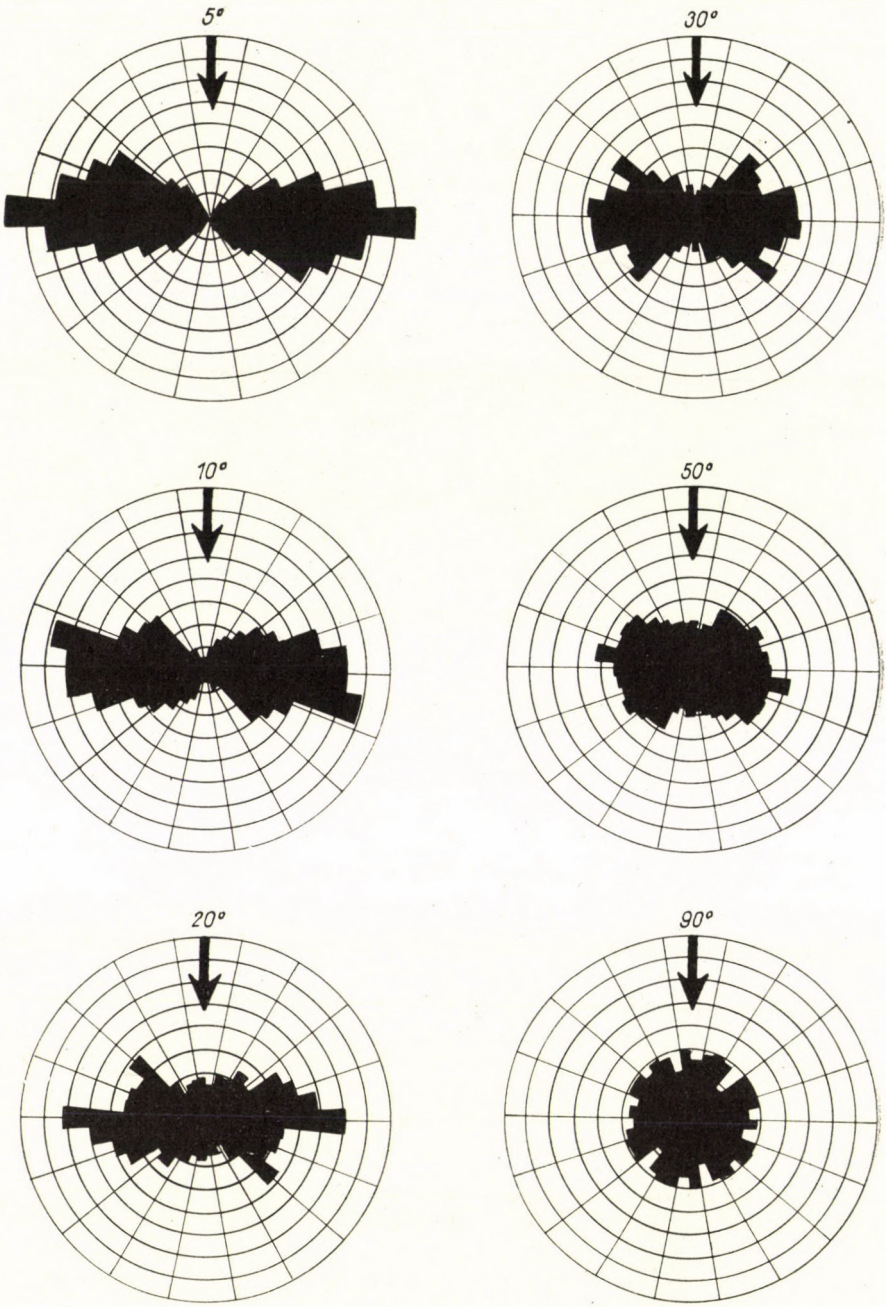

Abb. 7. Richtungsverteilung von Längsachsen der Kristalle

der Längsachse der Kristallkörnchen entspricht, so soll dem Kristallaggregat eine Zahl zugeordnet werden, deren Wert ± 1 ist, wenn alle Stäbchen parallel zueinander liegen und 0, wenn sämtliche Stäbchen nach Richtung und Grösse ungeordnet sind. Eine diesen Voraussetzungen entsprechende Masszahl kann durch das folgende Verfahren ermittelt werden: Die Längsachse des Teilchens von einer Länge h_i schliesse mit einer willkürlichen, als Bezugsachse gewählten X-Achse eines Koordinatensystems X, Y einen Winkel φ_i ein. Dann sei der Einstellungsgrad der Linienstrecke in Bezug auf diese Achse die Grösse R_i, die sofort in einer leicht verallgemeinbaren Form definiert werden soll:

$$R_i = \frac{h_i \cos^2 \varphi_i - h_i \sin^2 \varphi_i}{h_i} = \frac{h_i \cos 2\varphi_i}{h_i} .$$

Für ein Linienstreckenkonglomerat, das aus mehreren Linienstrecken (Stäbchen) — deren Richtungswinkel φ_i und Gesamtlänge h_i ist — besteht, ist der Einstellungsgrad R_0 bezogen auf die durch $\varphi = 0$ ausgezeichnete X-Achse

$$R_0 = \frac{\Sigma h_i \cos 2\varphi_i}{\Sigma h_i} .$$

Ist für eine grosse Zahl von Linienstrecken in dem gewählten Koordinatensystem die Verteilungsfunktion $h = h(\varphi)$ bekannt, die gleich durch die Bedingung $\int_0^{2\pi} h(\varphi)\, d\varphi = 0$ normiert gegeben sei, so ist

$$R_0 = \int_0^{2\pi} h(\varphi) \cos 2\varphi \, d\varphi .$$

Diese gleichwohl von der Verteilung und der Achse abhängige Grösse kann durch eine nur für die Verteilung charakteristische, als Masszahl des Ordnungsgrades geeignete Grösse ersetzt werden: nämlich durch den Maximalwert der Einstellungsgrade bezogen auf die verschiedenen Achsen (R_ψ) mit Richtungswinkel ψ (s. Abb. 8).

Diese Bedingung zeichnet die Achse $\psi = \psi_0$ dadurch aus, dass der Einstellungsgrad in dieser Richtung einen Maximalwert und in dazu senkrechter Richtung einen Minimalwert aufnimmt. Setzt man die in der Abb. 8 angegebenen Werte ein, so erhält man wegen der Periodizität von $h(\varphi)$ und der cos-Funktionen

$$R_\psi = \int_0^{2\pi} h(\varphi) \cos 2(\varphi - \psi)\, d\varphi .$$

ψ_0 und R_{ψ_0} können aus der Bedingung

$$\left(\frac{dR_\psi}{d\psi}\right)_{\psi_0} = 0$$

berechnet werden.

Der dazugehörige Wert des Einstellungsgrades — Ordnungsgrad genannt —

$$R = R_{\psi_0} = \int_0^{2\pi} h(\varphi) \cos 2\left[\varphi - \operatorname{arc\,tg}\left(\int_0^{2\pi} h(\varphi) \sin 2\varphi \, d\varphi \Big/ \int_0^{2\pi} h(\varphi) \cos 2\varphi \, d\varphi\right)\right]$$

ist nun nur für die Verteilung kennzeichnend.

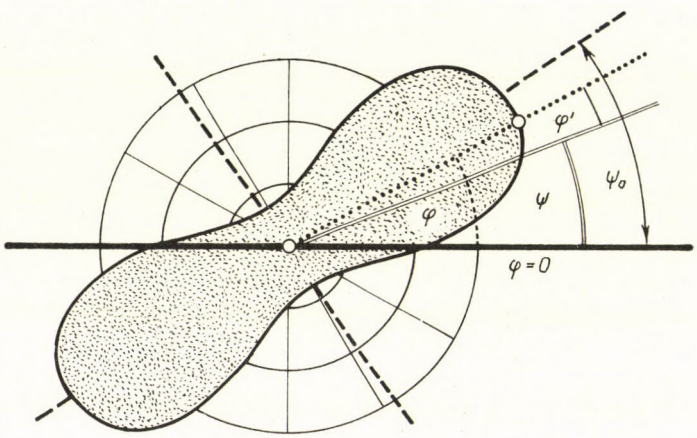

Abb. 8. Feststellung des Ordnungsgrades eines durch gegebene Verteilungsfunktion gekennzeichneten Aggregates

Bei Auswertung der Hystogramme muss noch ein Gesichtspunkt berücksichtigt werden. Bei der Deutung der physikalischen Eigenschaften solcher Kristallaggregate können die Kristallkörnchen offensichtlich nicht durch eine gerade Strecke charakterisiert werden, da doch ihre Ausdehnung in andere Richtungen auch nicht gleichgültig ist. Dementsprechend kann die Definition des Ordnungsgrades weiter verallgemeinert werden. Als Ordnungsgrad des aus zweidimensionalen Kristallen bestehenden Konglomerates nimmt man den Ordnungsgrad eines Konglomerates aus eindimensionalen Kristallen, deren Länge teils mit den Längs-, teils mit den Querdimensionen der ursprünglichen Kristalle übereinstimmt.

Im einfachsten Falle, wenn die Annahme von Teilchen gleicher Form, bzw. gleichen Verhältnisses a/b von Längen und Querausdehnungen begründet ist, vermindert sich der Ordnungsgrad, abhängig von dem Verhältnis a/b, wegen der Ausdehnung der Kristalle in zwei Richtungen — im Verhältnis $(a/b - 1)/(a/b + 1)$, wie dies leicht nachweisbar ist. Zur quantitativen Auswertung der Hystogramme ist auch im Hinblick auf die Bestimmung dieses

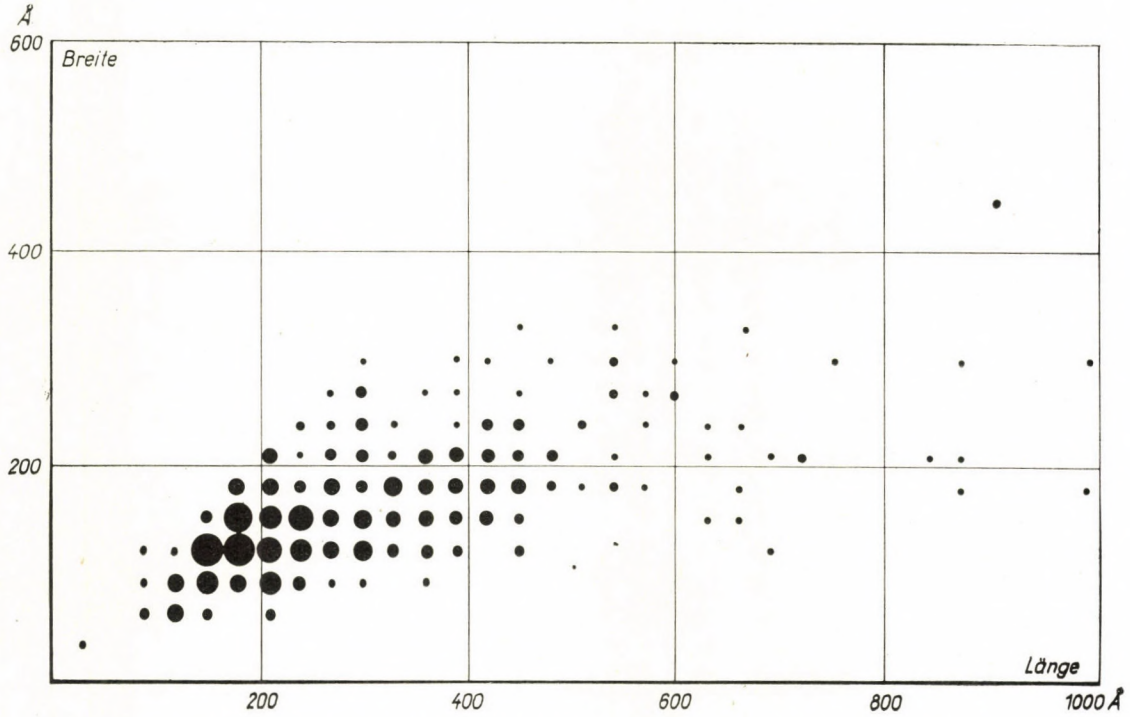

Abb. 9. Massverteilung der Kristalle einer unter 10° aufgedampften 70 Å dicken Schicht

Ausdehnungsverhältnisses die statistische Untersuchung der Kristallausdehnungen notwendig.

Statistik der Kristallausdehnungen

An den sich auf den elektronenmikroskopischen Aufnahmen befindlichen 500—1000 Kristallkörnchen wurden Messungen durchgeführt und eine Statistik aufgestellt. Abb. 9 stellt eine vollständige Verteilung dar. Die Fläche der aufgetragenen Punkte ist der Zahl der Kristalle der gegebenen Abmessungen

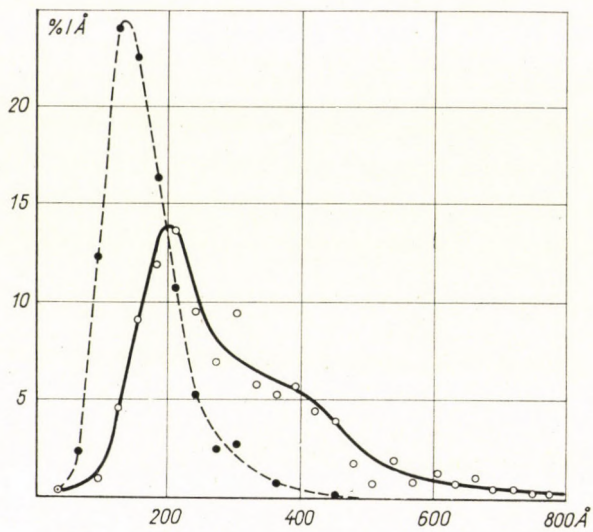

Abb. 10. Längs- und Querverteilungsfunktion

proportional. In Abb. 10 sind getrennt auch die Verteilungen bezüglich der Längenausdehnung und der darauf senkrechten Querausdehnungen dargestellt. Die angegebene Statistik gibt die Daten einer unter einem Aufdampfungswinkel von 10° hergestellten Schicht an. Die Verteilungen der Kristalle in Bezug auf Längs- und Querdimension sind beide einer nichtsymmetrischen Glockenkurve ähnlich. Der Mittelwert weicht bei der Verteilung bezüglich der Längenausdehnung wesentlich vom wahrscheinlichsten Wert ab. Die Momente der Verteilung μ_n sind in Tab. II angegeben. Laut Angaben der Tabelle liegt die Verteilung nicht sehr weit von der logarithmischen Normalverteilung. Berechnet man mit Hilfe des Mittelwertes der Quotienten der aufeinanderfolgenden Momente den Mittelwert der logarithmischen Streuung (σ) und den logarithmischen Mittelwert (X_g) gemäss dem Zusammenhang [12] der logarithmischen Normalverteilung

$$\log \mu_n = \log X_g + \frac{1}{2} n \log^2 \sigma,$$

Tabelle II

Daten der Verteilungsfunktionen

$\mu_n = \frac{\Sigma x_i^n N_i}{N}$	μ_1	μ_2	μ_3	μ_4	μ_n/μ_{n-1}	σ_{mitt}	X_g
Länge Å	302,1	333,0	357,0	376,2	1,101 1,082 1,055	1,481	285,6
Breite Å	166,2	173,7	181,5	188,1	1,047 1,047 1,036	1,333	159,5

so sind diese um 5% bzw. 4% niedriger als der dem ersten Moment entsprechende einfache Mittelwert. Das Verhältnis der Abmessungen, als Quotient der logarithmischen Mittelwerte, ist gleich 1,79. Der Quotient der durch einfache Mittelwertbildung bestimmbaren Durchschnittsabmessungen ist gleich 1,83. Der Durchschnittswert der Ausdehnungsverhältnisse (1,89) stimmt hiermit und auch mit dem Wert 1,98 gut überein; der letztere Wert wurde für dasselbe Präparat in der Weise bestimmt, dass die Statistik nur für jene Kristalle aufgestellt wurde, deren Längsrichtung mit der Aufdampfungsrichtung einen Winkel von $\pm 15°$ einschloss. Es kann festgestellt werden, dass die Längenausdehnung der Kristalle annähernd doppelt so gross ist wie die Querausdehnung.

Zusammenhang des Ordnungsgrades und des Polarisationsgrades

Wird sowohl die Verteilung der Abmessungen sowie die Anordnung der Kristalle berücksichtigt, so kann der Ordnungsgrad für ein Kristallaggregat, das praktisch als in einer Fläche angeordnet angenommen werden kann, mit Hilfe der obigen Überlegungen berechnet werden. Die Integralwerte wurden aus den für Intervalle von je 10° aufgenommenen Treppenfunktionen durch Summierung berechnet (Tab. III R_∞). Die Abmessungen der Kristalle wurden

Tabelle III

Zusammenhang zwischen Ordnungsgrad und Bedampfungswinkel

Bedampfungswinkel	5°	10°	20°	30°	50°	90°
R_∞ %	63,9	46,2	30,3	28,8	13,8	1,3
R_2 %	21,3	15,4	10,1	9,6	4,6	0,4

— gemäss ihrem Durchschnittsverhältnis — mit $a/b = 2$ in die Rechnungen eingesetzt. Für die Verteilungen der in Abb. 5 aufgetragenen Hystogramme ergeben sich nach dieser Rechnung als Ordnungsgrade die in Tab. III angegebenen Werte R_2. Der Lichtstreueffekt des als zweidimensional anzusehenden Kristallaggregates, bzw. die Entstehung der Polarisation kann so gedeutet werden, als wären diese kleine für Licht undurchlässige Streuteilchen. Unter Anwendung des BABINET-Prinzips [13] kann das Aggregat der Kristalle — die undurchsichtigen Teilchen als Spalten ähnlicher Form angenommen — als ein der Form des Kristalls entsprechender Spalt angesehen werden. Das Aggregat,

Tabelle IV

Zusammenhang zwischen Polarisationsgrad und Ordnungsgrad

Präparat	Gemessener Polarisationsgrad %	Berechneter Ordnungsgrad %
Al 5°	23,8	21,3
Al 10°	16,4	15,4
Al 20° A	12,6	11,1
Al 20° B	14,6	10,1
Al 20° C	13,0	9,3
Al 30° A	8,5	9,7
Al 30° B	8,8	9,6
Al 50°	2,6	4,6
Al 90°	0,5	0,4

das einem Spalt entspricht, dessen Länge um eine Grössenordnung kleiner ist als die auffallende Wellenlänge, polarisiert das darauffallende natürliche Licht. Nehmen wir an, dass ein kleiner Kristall als ein unendlich dünner Spalt, von derselben Länge wie der Kristall in dieser Richtung, angesehen werden kann. Dann lässt er aus dem auf ihn fallenden natürlichen Licht polarisiertes Licht durch, dessen Intensität mit der Längsdimension des Kristalls proportional ist. Wird das zweidimensionale Kristallkörnchen durch zwei in Längs- bzw. Querabmessungen gleiche aufeinander senkrechte dünne Spalte angenähert, so ist das durchgelassene Licht teilweise polarisiert, und sein Polarisationsgrad kann aus dem Verhältnis a/b der Abmessungen durch den Zusammenhang $(a/b - 1)/(a/b + 1)$ berechnet werden. Ist die Verteilung des sich in verschiedenen Richtungen anordnenden, verschieden langen Spaltaggregates seiner Richtung nach bekannt, so kann die Streuung des Kristallaggregats als Summe der Intensität der polarisierten Streuungen der einzelnen Elemente berechnet werden, undzwar wie leicht einzusehen ist, durch eine Rechnung, die der bei der Einführung des Ordnungsgrades des Kristallaggregats durchge-

führten analog ist. Hieraus kann sofort die Folgerung gezogen werden, dass der oben definierte Ordnungsgrad des bei den besagten Einschränkungen in einer Fläche angeordneten Kristallaggregats mit dem Polarisationsgrad des entstehenden polarisierten Lichtes bei genügend grosser Wellenlänge übereinstimmen muss. In Tab. IV ist der Ordnungsgrad einiger Schichten und deren bei einer Wellenlänge von 7700 Å gemessener Polarisationsgrad verglichen. Mit Rücksicht darauf, dass ja die Verhältnisse bei den Schichten endlicher Dicke bei der Berechnung nur annähernd in Betracht gezogen wurden, ist die Übereinstimmung zwischen den gemessenen und berechneten Angaben überraschend gut.

Folgerungen aus der Statistik der Kristallausdehnungen auf die bei der Aufdampfung auftretenden Vorgänge

Aus der in Abb. 9 dargestellten Statistik kann die Abhängigkeit der Querabmessung der Kristalle von der Länge des Kristalls bestimmt werden (Abb. 11., *a*, *b*).

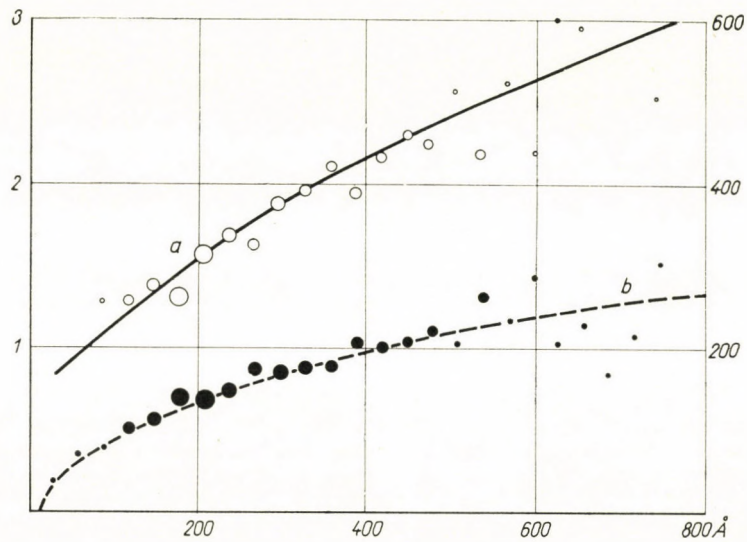

Abb. 11.a. Abhängigkeit des Dimensionverhältnisses der Kristalle von der Länge
b. Abhängigkeit der durchschnittlichen Breite der Kristalle von der Länge

An der Abbildung ist die Fläche der Messpunkte proportional der Zahl der Kristalle der gegebenen Abmessungen. Bei der Darstellung wurde die Mittelwertbildung für die Ausdehnung in der Querrichtung durchgeführt. Es kann festgestellt werden, dass im Bereich, in welches die Kristallkörnchen durchschnittlicher Abmessungen fallen, das Ausdehnungsverhältnis annähernd 2 ist. Die kürzeren Kristalle sind runder, die Längeren schlanker als diesem Verhältnis entspricht.

Das Anwachsen der Kristallkörnchen schräg aufgedampfter Schichten steht laut unserer vorhergehenden Feststellungen nicht mit der in dünnen Schichten auftretenden kristallstrukturell ausgezeichneten Orientation im Zusammenhang. Trotzdem wachsen die Kristalle — wie aus den elektronenmikroskopischen Aufnahmen geschlossen werden kann — senkrecht zur Richtung der Aufdampfung in länglicher Form, und auch als Ergebnis der statistischen Auswertung kann festgestellt werden, dass die vom kristallstrukturellen Standpunkt ungeordneten Körnchen doch bezüglich ihrer geometrischen Form ausgezeichnet sind. Aus dem Obigen folgt für das Wachstum ein Mechanismus, laut welchem die sich formenden Kristallkerne senkrecht zur Aufdampfungsrichtung schneller wachsen als in Richtung der Aufdampfung. Ein ganz

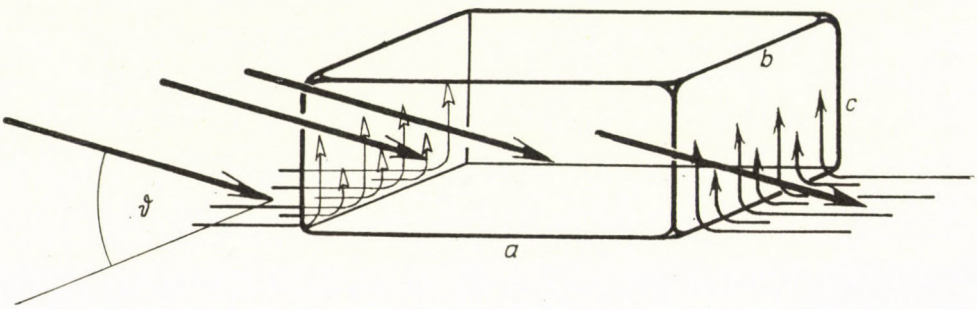

Abb. 12. Mechanismus des Wachstums der Kristalle

schematischer Mechanismus des Wachstums kann für ein in einer Fläche angeordnetes Kristallaggregat, in guter Übereinstimmung mit den Versuchsergebnissen, wie folgt angegeben werden: In einer Schicht gegebener Schichtdicke können die sich formenden kleinen Kristalle durch kleine Rechtecke konstanter Dicke angenähert werden, deren eine Seite (b) fast parallel zur Richtung der Aufdampfung verläuft. Ihre andere Seite (a) liegt annähernd senkrecht zur Richtung der Aufdampfung. Das auf die Fläche (ac) einfallende Bündel erreicht die Fläche unter einem Winkel von $90° - \vartheta$ und nimmt das Material zum Anwachsen auf (Abb. 12). Dagegen kann das Anwachsen des Kristalls in seitlicher Richtung nicht unmittelbar durch das Strahlenbündel verursacht werden, da aus dem unmittelbaren Bündel kein Material auf die Fläche (bc) fällt. Die Fläche (bc) sammelt das zu ihrem eigenen Wachstum nötige Material aus ihrer Umgebung durch Migration und strömt das für das Wachstum nötige Material auf einer Strecke von der Länge der Kante (b) — quasi wie von einer negativen Quelle — proportional zum Quadrat der Länge (b) auf die Fläche (bc) aus.

Ist die Intensität des Dampfstrahles $\Delta V/\Delta t$ — gemessen z. B. durch das Materialvolumen, das durch die auf den Dampfstrahl senkrechte Flächen-

einheit in der Zeiteinheit durchgeht, — so erreicht pro Sekunde und pro Flächeneinheit die Substratfläche ein Dampfstrahlvolumen von $\Delta V/\Delta t \sin\vartheta$ und die Fläche (ac), die dem Dampfstrahl gegenüber liegt, ein Volumen von $\Delta V/\Delta t \cos\vartheta$. Die Wachstumsgeschwindigkeit der Kantenlängen $\Delta a/\Delta t$ bzw. $\Delta b/\Delta t$ kann aus der auf die Flächen (bc) bzw. (ac) pro Sekunde gelagerten Schichtdicke gerechnet werden.

Angenommen, dass auf der Fläche (ac) das Reflexionsvermögen des Dampfstrahles (r) ist, dann ist die Wachstumgeschwindigkeit der Kante (b)

$$\frac{\Delta b}{\Delta t} = r \frac{\Delta V}{\Delta t} \cos\vartheta.$$

Durch die die einander gegenüberliegenden zwei Flächen (bc) erreichende Materialmenge wächst die Kante (a) in beiden Richtungen mit der Geschwindigkeit:

$$\frac{\Delta a}{\Delta t} = 2 \frac{\varkappa b^2}{bc} \frac{\Delta V}{\Delta t} \sin\vartheta,$$

wo der Proportionalitätsfaktor $\varkappa$ auch die für die Migration charakteristische Konstante enthält. Aus dem Grenzwert der Quotienten beider Wachstumsgeschwindigkeiten ergibt sich für den Zusammenhang zwischen der Breite und der Länge die Differentialgleichung:

$$\frac{db}{da} = \left(\frac{rc}{2\varkappa \operatorname{tg}\vartheta}\right) b^{-1} = Kb^{-1}.$$

Betrachtet man das Flächenproblem ($c = \text{const}$), so ist die Lösung

$$b = K\sqrt{a - k_0},$$

bzw. es ergibt sich für das Verhältnis der Abmessungen

$$\frac{a}{b} = \frac{1}{K} \frac{\sqrt{a}}{\sqrt{1 - k_0/a}}.$$

In Abb. 12 wurden für die dort angegebenen Daten die mit diesem Zusammenhange berechneten Kurven eingetragen. Aus der sich an die (von der Statistik herrührenden) Messpunkte mit dem kleinsten Fehler anschmiegenden Kurve ergab sich

$$K = 9{,}56 \text{ Å}^{-1} \quad \text{und} \quad k_0 = 15 \text{ Å}.$$

Der Mechanismus des Wachstums ist für das Wachstum in zwei Richtungen nicht derselbe. Grundsätzliche Ursache der Abweichung ist, dass der schräg

einfallende Dampfstrahl nur die ihm gegenüberliegende Fläche erreicht, nicht aber die beiden seitlichen Flächen. Auch vom angegebenen Mechanismus unabhängig ergibt sich bei einer derartigen geometrischen Anordnung auf jeden Fall eine Asymmetrie beim Wachstum in zwei Richtungen, und damit kann vielleicht der ungefähre Wert von 2 für das durchschnittliche Verhältnis

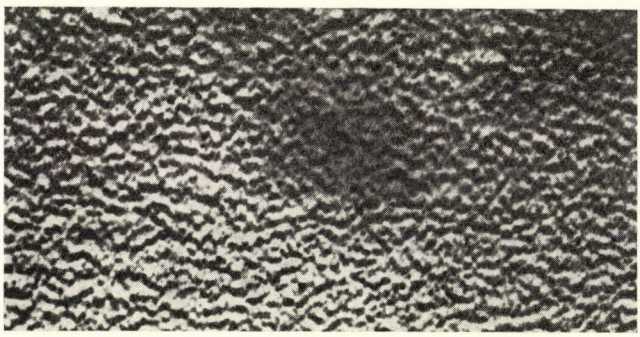

Abb. 13. Aufnahme einer auf eine schräge Glasplatte mit Sedimentierung aufgetragenen Schicht. Vergrösserung 5-fach

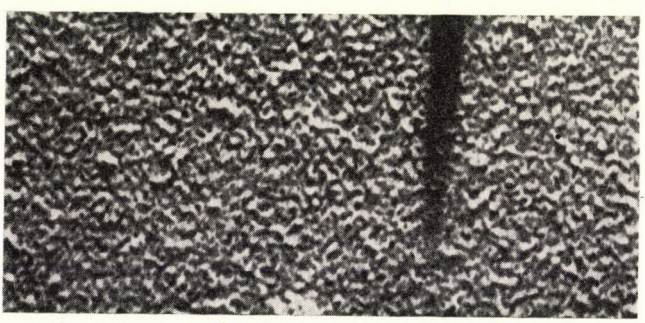

Abb. 14. Elektronenmikroskopische Aufnahme einer Aluminiumschicht. Vergrösserung 220 000-fach

der Abmessungen qualitativ erklärt werden. Bei der Schrägaufdampfung werfen nämlich die sich nach Einfallen des Dampfstrahles formenden Kristallkerne in Richtung der Aufdampfung einen Schatten an der Rückfläche der Kristalle, sodass hierher Material weder durch Migration noch direkt gelangt. Es besteht daher auch im Falle gleichmässiger Materialaufnahme ein Unterschied zwischen dem Wachstum der Kristalle nach vorne und nach den Seiten, haben ja die Kristalle nur eine Richtung nach vorne und zwei seitliche Richtungen. Der bei den Kristallen durchschnittlicher Abmessungen gefundene Wert des Verhältnisses der Ausdehnungen der Kristalle von ungefähr 2, kann als Wirkung der qualitativ erklärten Asymmetrie verstanden werden. Um

zu beweisen, dass solche aus rein geometrischen Verhältnissen stammende asymmetrische Wachstumsbedingungen die auf den elektronenmikroskopischen Aufnahmen beobachtete Kristallformverteilung und Schichtstruktur verursachen können, wurde ein qualitativer Versuch durchgeführt. Auf eine von der Vertikalen um 20° geneigte Glasplatte wurde eine auf dem Funkenerosionswege hergestellte Messingkörnchen von etwa 1 μ Durchmesser enthaltende Suspension sedimentiert. Vergleicht man die Aufnahme der sich formenden Schichtstruktur (Abb. 13) mit der elektronenmikroskopischen Aufnahme (Abb. 14) einer unter 20° aufgedampften Aluminiumschicht, so bekommt man einen vollkommen gleichen Eindruck, und es ist danach wahrscheinlich, dass beim Entstehen der anisotropen Struktur beider Schichten solche geometrische Schattenwurfeffekte eine wesentliche Rolle spielen.

Bei der Herstellung der elektronenmikroskopischen Aufnahmen hat Herr Ingenieur JÁNOS TREMMEL, bei der Verfertigung der Statistiken haben meine Mitarbeiterinnen Frl. ILDIKÓ KOLESZÁR und Frl. ZSUZSANNA ŐSAPAI mitgewirkt, wofür ihnen herzlich gedankt sei.

LITERATUR

1. A. KUNDT, Wied. Ann., **27,** 59, 1886.
2. F. BRAUN, Ann. d. Phys., **16,** 1, 1905.
3. G. DU BOIS und H. RUBENS, Wied. Ann., **49,** 593, 1893.
4. H. KÖNIG und G. HELWIG, Optik, **6,** 11, 1950.
5. L. REIMER, Optik, **14,** 83, 1957.
6. P. EVANS und H. WILMAN, Acta Cryst., **5,** 731, 1952.
7. M. A. RUMS und G. BAKLAGINA, Zs. Techn. Fisiki, **26,** 1498, 1956.
8. W. G. BURGERS und C. J. DIPPEL, Physica, **1,** 549, 1934.
9. D. O. SMITH, J. Appl. Phys., **30,** 264, 1959.
10. D. O. SMITH, M. S. COHEN und G. P. WEISS, J. Appl. Phys., **31,** 1755, 1960.
11. S. TOLANSKY, Phil. Mag., **35,** 120, 1944.
12. G. U. YULE und M. G. KENDALL, An Introduction to the Theory of Statistics, London, 1950.
13. GRIMSEHL, Lehrbuch d. Phys., Bd. 3., Leipzig, 1955. S. 71.

АНИЗОТРОПИЧЕСКАЯ СТРУКТУРА КОСО НАПАРЕННЫХ АЛЮМИНИЕВЫХ СЛОЕВ

Й. ПОЦА

Резюме

Оптические, электроннодифракционные и электронномикроскопические исследования, проведенные на тонких полупрозрачных алюминиевых слоях, косо напаренных в интервале углов от 5° до 90°, показали, что они имеют анизотропический характер. Причиной анизотропии является рост некоторых небольших кристаллов в структуре слоев в направлении их длины перпендикулярно к плоскости падения при напылении. Он происходит, однако, без появления в таких тонких слоях какой-нибудь ориентации, отличной с точки зрения структуры кристалла. Вводится мера степени упорядоченности,

подходящая для характеристики упорядоченности по формам таких агрегатов, которые можно рассматривать, как двухмерные друзы. Применением статистики кристаллов, находящихся на электронно-микроскопических съемках, измерялась степень упорядоченности испаренных при разных углах падения слоев. Результат измерения оказался равным со степенью поляризации, характерной для оптической анизотропии друза. Исходя из статистики дается объяснение анизотропической структуры друзов с одновременным вычислением условий роста кристаллов. Установлено, что сформирование анизотропической структуры всего друза обусловливается анизотропическим характером роста отдельных кристаллов.

ZEITABHÄNGIGE DÄMPFUNGSERSCHEINUNGEN AN NICKEL BEI ZIMMERTEMPERATUR*

Von

I. GAÁL

I. LEHRSTUHL FÜR EXPERIMENTALPHYSIK, ROLAND EÖTVÖS UNIVERSITÄT, BUDAPEST**

(Vorgelegt von E. Nagy. — Eingegangen: 26. V. 1961)

Mit einem Torsionspendel nach KE wurde die zeitabhängige Änderung der amplitudenabhängigen Dämpfung an statisch und dynamisch im nicht-plastischen Gebiet deformiertem Nickel bei Zimmertemperatur untersucht. Es war unser Ziel, uns einen allgemeinen Überblick über die Wirkung der mit den Dämpfungsmessmethoden untrennbar zusammenhängenden Deformationen auf die Dämpfung zu verschaffen. Die Messergebnisse lassen sich dadurch erklären, dass sich die Konzentration der um die Versetzungen angehäuften atomaren Fehlstellen unter der Wirkung elastischer Deformationen ändert.[1]

Einleitung

Als ein sehr wertvolles Hilfsmittel zum Studium der Gitterfehlstellen haben sich Messungen der inelastischen Eigenschaften erwiesen. Ihre besondere Bedeutung liegt darin, dass sie einerseits auch bei höheren Temperaturen auf die Fehlordnung sehr empfindlich sind, und andererseits mit ihrer Hilfe auch die den Fehlstellen eigenen Bewegungen und ihre Wechselwirkungen untersucht werden können. Die experimentell und theoretisch am einfachsten zu behandelnden inelastischen Erscheinungen sind die Dämpfung der Deformationsschwingung und die Abhängigkeit der elastischen Modulen von der Frequenz der Messchwingung. Bei den Dämpfungsmessungen kann man bei geeigneter Wahl der Frequenz, der Temperatur und verschiedener Vorbehandlungen der Probe die einzelnen Typen der Fehlstellen und ihre verschiedenen Wechselwirkungen voneinander getrennt untersuchen.[2]

Wenn wir Dämpfungsmessungen bei der Untersuchung einer durch irgendeine Vorbehandlung zustande gebrachten Fehlordnung durchführen oder die Theorien der Dämpfungserscheinungen mit den Messergebnissen vergleichen wollen, so ist es unbedingt notwendig die Wirkung der Messchwingungen und anderer mit der Messmethode untrennbar zusammenhängender Deformationen auf die Fehlordnung zu kennen. Deshalb ist es wünschenswert, sich einen

* Auszug aus der Diplomarbeit; Roland Eötvös Universität, Budapest.

** Neue Adresse: Forschungsinstitut für Technische Physik der Ungarischen Akademie der Wissenschaften, Budapest.

[1] Die um die Versetzungen angehäuften atomaren Fehlstellen werden im folgenden die Cottrellatmosphäre der Versetzung genannt werden.

[2] Über die Dämpfungserscheinungen befindet sich eine umfangsreiche Zusammenfassung in [1].

allgemeinen Überblick über die Wirkung elastischer Deformationen auf die Fehlordnung zu verschaffen.

Die ersten Untersuchungen über die Wirkung elastischer Deformationen auf die Dämpfung stammen von READ [2, 3], der bei einer Frequenz von 10 kHz die Wirkung der statischen Kompression, die Änderung der Dämpfung während der Schwingung bei ein und derselben Amplitude und den Einfluss der Schwingung mit einer grössten Amplitude auf die bei den kleineren Amplituden gemessene Dämpfung untersuchte. Die Abhängigkeit der Dämpfung von den früheren Schwingungsamplituden wurde auch schon bei den Niederfrequenzen beobachtet [4, 5]. Vor kurzem haben CHAMBERS und SMOLUCHOWSKI [6] experimentell gezeigt, das sich eine Reihe der durch die Messschwingungen zustandegekommenen Dämpfungsänderungen als die Veränderung der Konzentration der Cottrell-atmosphäre beschreiben lässt.

Experimentelles

Zu unseren Untersuchungen benutzten wir ein Torsionspendel nach KE [7]. Als Torsionsfaden, das heisst als Probekörper, wurden bei 750° C im Vakuum vier Stunden lang geglühte und nachher mit einer Geschwindigkeit von 1° C/sec abgekühlte, polykristalline Feinnickelfäden[3] verwendet, die einen Durchmesser von 1 mm hatten und 600 mm lang waren. Das Gewicht des Pendelkörpers war 310 pond, und wir erregten nur solche Schwingungen, deren Deformationsamplituden[4] kleiner als $15 \cdot 10^{-6}$ waren. Dementsprechend war die *an einer beliebigen Ebene* des Fadens angreifende makroskopische äussere Spannung immer kleiner als 520 pond/mm². Da die kritische Gleitspannung in der aktiven Gleitebene der Nickeleinkristalle bei Zimmertemperatur nach [8] 580 pond/mm² beträgt, dürfen wir voraussetzen, dass unter unseren Messbedingungen nur wenige neue Versetzungen zustande kommen können.[5]

Das Abklingen der freien Schwingungen des Pendels wurde mit der POGGENDORFschen visuellen Methode beobachtet. Um die »mittlere Dämpfung« gemäss

$$Q^{-1}(A) = \frac{\log 2}{\pi} N^{-1}\left(A, \frac{1}{2} A\right) \tag{1}$$

[3] Johnson-Matthew high purity nickel.

[4] Die Schwingungs- oder Deformationsamplitude einer Deformationsschwingung des Torsionsfadens ist der Wert der $\varepsilon_{\varphi z}$-Komponente des in Zylinderkoordinaten aufgeschriebenen Deformationstensors in der »Rinde« des Fadens im Moment, wo die kinetische Energie der Schwingung Null ist. In der quasistatischen Näherung ist $\varepsilon_{\varphi z} = \frac{1}{2} \frac{\varphi_l(t)}{l} R$. (Hierbei sind φ_l die »Winkelamplitude« der Schwingung, l die Länge und R der Radius des Fadens.)

[5] Obwohl vor kurzem an Kupfer und Aluminiumeinkristallen auch dreimal so kleine kritische Gleitspannungen gemessen wurden als in [8] angegeben sind, zeigt sich unsere Voraussetzung doch als befriedigend, weil die kritische Gleitspannung in den polykristallinen Körpern 20 *oder* 30 mal grösser ist als in den entsprechenden Einkristallen [14].

ausrechnen zu können, zählten wir die Anzahl der Schwingungen während der Zeit, in der die Schwingungsamplitude auf die Hälfte ihres ursprünglichen Wertes sank.

Die mittlere Dämpfung

Integriert man die aus der Bewegungsgleichung stammende Energiegleichung nach der Zeit über eine Periode der Schwingung des Probestücks, so erhält man, da *freie* äussere Kräfte fehlen, das folgende Resultat:

$$\int_{t_0}^{t_0+T} \int_{V} \sigma_{ik}(x_s, t)\, \dot{\varepsilon}_{ik}(x_s, t)\, dV\, dt = 0. \tag{2}$$

Hierbei ist das Volumenintegral über den Probekörper ausgedehnt, und die Periode ist dadurch definiert, dass am Anfang ($t = t_0$) und am Ende ($t = t_0 + T$) der Periode die kinetische Energie des Probekörpers gleich Null ist.

Der Deformationstensor (ε_{ik}) lässt sich ebenso wie der Spannungstensor (σ_{ik}) in einen idealelastischen und einen inelastischen Anteil spalten. Der idealelastische Deformationstensor (ε^e_{ik}) stellt den Deformationszustand des Idealgitters in harmonischer Näherung dar, und der inelastische Tensor (ε^i_{ik}) entspricht dem Beitrag der eigentlichen Gitterfehlstellen und des anharmonischen Teiles der Gitterschwingungen[6] zur Gesamtdeformation. Die Bedeutung der Aufteilung des Spannungstensors ($\sigma_{ik} = \sigma^e_{ik} + \sigma^i_{ik}$) ist völlig analog der des Deformationstensors. Das adiabatische HOOKEsche Gesetz drückt den Zusammenhang zwischen den idealelastischen Teilen der Deformations- und Spannungstensoren aus.

Dieser Aufteilung nach lässt sich die Gl. (2) in die folgende Form schreiben:

$$\int_{t_0}^{t_0+T} \int_{V} \sigma^e_{ik}(x_s, t)\, \frac{\partial \varepsilon^e_{ik}(x_s, t)}{\partial t}\, dV\, dt = -\int_{t_0}^{t_0+T} \int_{V} \left[\sigma^i_{ik}(x_s, t)\, \frac{\partial \varepsilon^e_{ik}(x_s, t)}{\partial t} + \right.$$
$$\left. + \sigma_{ik}(x_s, t)\, \frac{\partial \varepsilon^i_{ik}(x_s, t)}{\partial t} \right] dV\, dt. \tag{3}$$

Dementsprechend ist die Abnahme der adiabatischen elastischen Energie während einer Periode der Schwingung

$$\frac{1}{2} \int_{V} \sigma^e_{ik}(x_s, t_0 + T)\, \varepsilon^e_{ik}(x_s, t_0 + T)\, dV - \frac{1}{2} \int_{V} \sigma^e_{ik}(x_s, t_0)\, \varepsilon^e_{ik}(x_s, t_0)\, dV =$$
$$= -\int_{t_0}^{t_0+T} \int_{V} \left[\sigma^i_{ik}(x_s, t)\, \frac{\partial \varepsilon^e_{ik}(x_s, t)}{\partial t} + \sigma_{ik}(x_s, t)\, \frac{\partial \varepsilon^i_{ik}(x_s, t)}{\partial t} \right] dV\, dt. \tag{4}$$

[6] Vgl.: Thermische Unelastizität, Wärmeleitung und Wärmeausdehnung. (z. B.: in [15]).

Definieren wir die Dämpfung der Probe auf die folgende Weise:

$$\Delta^{\text{Probe}} = \frac{\text{in einer Periode dissipierte adiabatische elastische Energie}}{2\pi\text{. adiabatische elastische Energie der Probe}},$$

so ergibt sich aus der Gl. (4), dass einerseits

$$\Delta^{\text{Probe}} = \frac{\frac{1}{2}\int_{\dot{V}} \sigma^e_{ik}(x_s, t_0)\,\varepsilon^e_{ik}(x_s, t_0)\,dV - \frac{1}{2}\int_{\dot{V}} \sigma^e_{ik}(x_s, t_0 + T)\,\varepsilon^e_{ik}(x_s, t_0 + T)\,dV}{2\pi\frac{1}{2}\int_{\dot{V}} \sigma^e_{ik}(x_s, t_0)\,\varepsilon^e_{ik}(x_s, t_0)\,dV} \tag{5}$$

und andererseits

$$\Delta^{\text{Probe}} = \frac{\int_{t_0}^{t_0+T}\int_{\dot{V}}\left[\sigma^i_{ik}\cdot\frac{\partial\varepsilon^e_{ik}}{\partial t} + \sigma_{ik}\cdot\frac{\partial\varepsilon^i_{ik}}{\partial t}\right]dV\,dt}{2\pi\cdot\frac{1}{2}\int_{\dot{V}}\sigma^e_{ik}\cdot\frac{\sigma\varepsilon^e_{ik}}{\partial t}\,dV} \tag{6}$$

ist.

Aus (5) bekommt man für den schwingenden Torsionsfaden:

$$\Delta^{\text{Pendel}}(\varepsilon^e_{z\varphi}, t_0) = \frac{\mu^e_{AD}\left(\varepsilon^e_{z\varphi}(R, t_0)\right)^2 - \mu^e_{AD}\left(\varepsilon^e_{z\varphi}(R, t_0 + T)\right)^2}{2\pi\,\mu^e_{AD}\left(\varepsilon_{z\varphi}(R, t_0)\right)^2}. \tag{7}$$

Hierbei sind $\varepsilon^e_{z\varphi}(R, t_0)$ der idealelastische Anteil der Schwingungsamplitude und μ^e_{AD} der adiabatische, elastische Torsionsmodul. Weil $|\varepsilon_{z\varphi}(R, t_0) - \varepsilon_{z\varphi}(R, t_0 + T)| \ll 1$ und $\varepsilon^e_{z\varphi} = a\varepsilon^i_{z\varphi}$ mit einem $a \ll 1$ ist, lässt sich die Gl. (7) auch so schreiben:

$$-\frac{d\log(S)}{dt} = \pi\cdot\frac{\Delta^{\text{Pendel}}(S, t)}{T(S, t)}, \tag{8}$$

wobei wir die Schwingungsamplitude, $\varepsilon_{z\varphi}(R, t_0) = \varepsilon^e_{z\varphi}(R, t_0) + \varepsilon^i_{z\varphi}(R, t_0)$ mit S bezeichnet haben.

Endlich erhält man aus (8) für die mittlere Dämpfung bei der Schwingungsamplitude A:

$$Q^{-1}(A) = \frac{\log 2}{\int_{A/2}^{A}\left(S\cdot\Delta^{\text{Pendel}}(S, t(S))\right)^{-1}ds}. \tag{9}$$

Messergebnisse

Die ersten Messungen bezogen sich auf die Wirkung der statischen elastischen Deformation, welche im Torsionsfaden durch Belastung mit dem Pendelkörper zustande kommt. Abb. 1 zeigt die Dämpfung des Pendels[7], als Funktion der nach der Belastung des Fadens abgelaufenen Zeit in dem Fall von aufeinander folgenden Entlastungen und Wiederbelastungen. Die Dämpfung erreicht mit der Zeit einen stationären Wert. Die zur Einstellung des stationären Wertes erforderliche Zeit war nach allen drei Belastungen

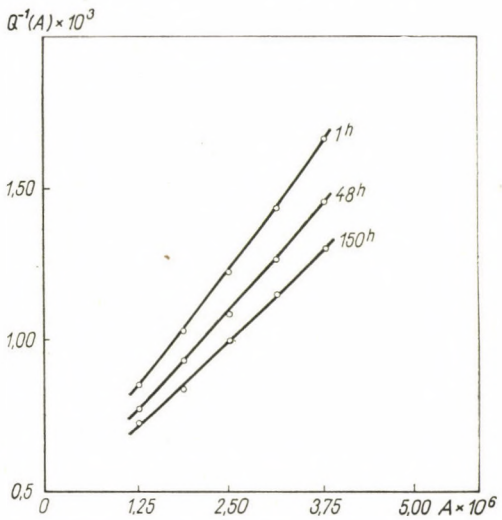

Abb. 1a. Die amplitudenabhängige Änderung der Pendeldämpfung nach der Belastung des Torsionsfadens mit dem Pendelkörper.
(Neben den Kurven ist die nach der Belastung abgelaufene Zeit vermerkt.)

annähernd 150 Stunden: und während 300 Stunden konnte man keine ausserhalb des Messfehlers liegende Änderung des stationären Wertes feststellen. Mit Hilfe milder, dem Stativ des Pendels gegebener Stösse wurden solche kleine transiente Biegungen erregt, die ähnlich den Biegungen sind, die bei der Belastung und Entlastung des Fadens unvermeidlich auftreten. Die so zustandegekommenen Biegungen verursachten eine Änderung des sich schon eingestellten stationären Wertes der Dämpfung, die in 2—5 Stunden völlig abklang. Dementsprechend lässt sich die Dämpfungsänderung nach der Belastung des Fadens im Wesentlichen durch die in der Anfangsphase der statischen Dehnung auftretenden Vorgänge erklären.

[7] Die Dämpfung eines Pendels in der Luft besteht aus zwei Anteilen; aus der viskosen Dämpfung der Luft und aus der durch die Fehlordnung der Probe bestimmten, sogenannten inneren Dämpfung. In [16] wurde an Hand von vielseitigen Experimenten festgestellt, dass unter unseren Messbedingungen die Dämpfung der Luft amplitudenunabhängig ist.

Die Wirkung der Messschwingungen als dynamische Deformationen wurde im nach der statischen Belastung erreichten stationären Zustand untersucht. Es wurde mit [5] übereinstimmend festgestellt, dass bei derselben Temperatur und bei derselben Frequenz an derselben Probe die (mittlere) Dämpfung eine eindeutige Funktion der momentanen Schwingungsamplitude und der Anfangsamplitude der Messschwingung ist, sofern eine bestimmte Zeit zwischen den auf einanderfolgenden Anregungen der Messschwingungen abgewartet wurde. Die nötige »Wartezeit« hängt von der Anfangsamplitude der vorherigen Schwingungen stark ab. Der Einfluss der Temperatur auf die Wartezeit wurde nicht untersucht.

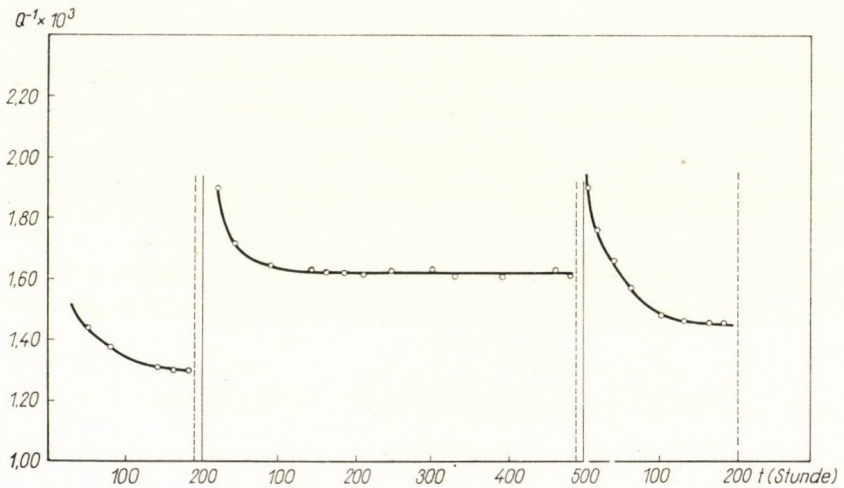

Abb. 1b. Die Änderung der zur Amplitude $3{,}75 \cdot 10^{-6}$ gehörigen Dämpfung bei aufeinanderfolgenden Belastungen und Entlastungen. Die Zeitpunkte der Belastungen sind durch ausgezogene Linien bezeichnet, während die Zeitpunkte der Entlastungen durch punktierte Linien dargestellt sind. Daten der aufeinanderfolgenden Messungen sind die folgenden: $T_1 = 3{,}06$ sec und $\vartheta_1 = 17°$ C; $T_2 = 1{,}7$ sec und $\vartheta_2 = 19°$ C und $T_3 = 3{,}03$ sec und $\vartheta_3 = 20{,}5°$ C.

Nach dem Abklingen einer Schwingung, deren Anfangsamplitude $11{,}25 \cdot 10^{-6}$ war, sanken die zu einer beliebigen Amplitude gehörigen Dämpfungswerte, die während des Abklingens der mit der Anfangsamplitude von $5 \cdot 10^{-6}$ angeregten Schwingungen gemessen wurden, allmählich. 5 Stunden nach der Anregung der Schwingung mit einer Anfangsamplitude von $11{,}25 \cdot 10^{-6}$ änderten sich die bei den Anregungen von Schwingungen mit Anfangsamplituden von $5 \cdot 10^{-6}$ gemessenen Dämpfungswerte nicht mehr, sofern die Wartezeit zwischen den Kontrollmessungen mehr als 1 Stunde betrug. Diese letzteren Dämpfungswerte waren natürlich dieselben, welche bei den Schwingungen, die mit einer Anfangsamplitude von $5 \cdot 10^{-6}$ angeregt worden waren unabhängig von den früheren Schwingungszuständen auftraten, sofern mit

der Messung eine hinreichende Zeit nach der letzten Anregung gewartet wurde (vgl. Abb. 2).

Endlich wurde die Frequenzabhängigkeit der amplitudenabhängigen Dämpfung untersucht. Die Messungen wurden an demselben Faden durchgeführt, und das Gewicht des Pendelkörpers war bei den beiden Frequenzen dasselbe, nur wurde sein Trägheitsmoment entsprechend verändert. Zuerst wurde die mittlere Dämpfung bei $T_1 = 3{,}06$ sec und $\vartheta_1 = 17°$ C, dann bei

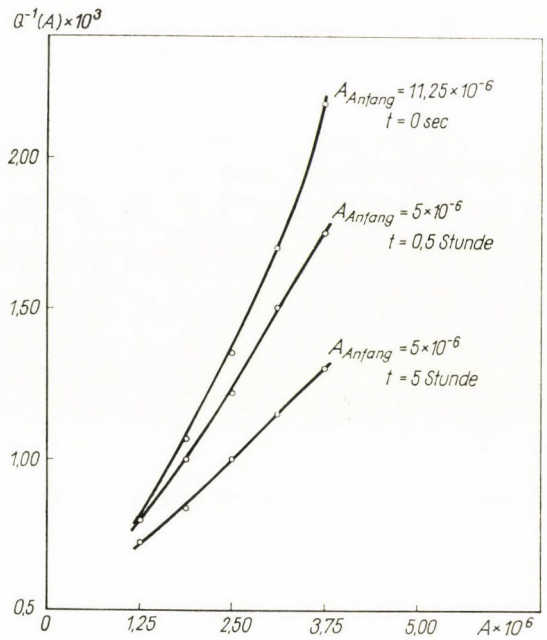

Abb. 2. Die Abhängigkeit der mittleren Dämpfung von der Anfangsamplitude und von der Wartezeit.

(Neben den Kurven ist die Anfangsamplitude der Messschwingung und die nach der Anregung der Schwingung mit der Anfangsamplitude von $11{,}25 \cdot 10^{-6}$ abgelaufene Zeit vermerkt.)

$T_2 = 1{,}7$ sec und $\vartheta_2 = 19°$ C und zum Schluss wieder bei $T_3 = 3{,}03$ sec und $\vartheta_3 = 20{,}5°$ C gemessen. Die Anfangsamplitude war immer $6{,}25 \cdot 10^{-6}$ und nach allen Veränderungen der Frequenz wurde die Einstellung des stationären Zustands abgewartet (vgl. Abb. 3).

In Abb. 4 ist die Dämpfung in dem stationären Zustand bei $T_1 = 3{,}06$ sec und $\vartheta_1 = 17°$ C als Funktion der Schwingungsamplitude dargestellt. Die Anfangsamplitude war $6{,}25 \cdot 10^{-6}$.

Diskussion

Unter der Voraussetzung, dass der amplitudenabhängige Anteil der Dämpfung ausschliesslich von der durch GRANATO und LÜCKE vorgeschlagenen

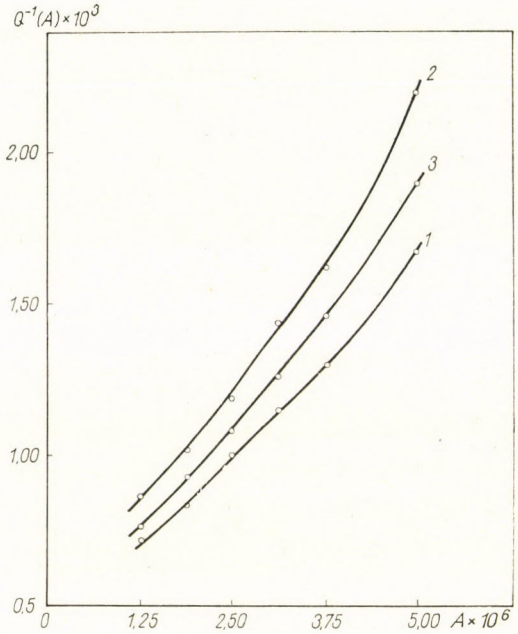

Abb. 3. Die Frequenzabhängigkeit der mittleren Dämpfung im stationären Zustand. (Die Nummern bezeichnen die aufeinanderfolgenden Messungen.)

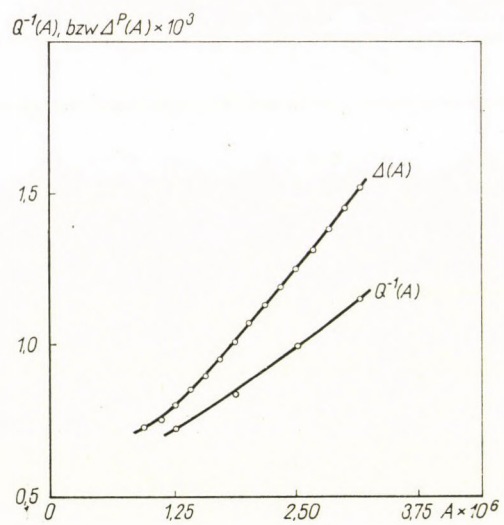

Abb. 4. Die Dämpfung und die mittlere Dämpfung als Funktion der Schwingungsamplitude.

Wechselwirkung zwischen dem Versetzungsnetzwerk und der Cottrellatmosphäre stammt [9], erhalten wir nach [9] und [5] für die Dämpfung des Pendels den folgenden Ausdruck[8]

$$\Delta^{\text{Pendel}}(S) = \Delta^0(\omega, \vartheta) - \frac{4}{S^4}\int_0^S K\Gamma^3 \varepsilon\, Ei\left(-\frac{\Gamma}{\varepsilon}\right) d\varepsilon. \tag{10}$$

Hierbei sind $\Delta^0(\omega, \vartheta)$ der amplitudenunabhängige Anteil der Dämpfung und S die Schwingungsamplitude. K hängt nur von den Daten des Versetzungsnetzwerkes ab, und Γ ist *bei ein und demselben* Versetzungsnetzwerk eine lineare Funktion der »mittleren« Konzentration der Cottrellatmosphäre, also eine eindeutige Funktion der Konfiguration der um die Versetzungen angehäuften atomaren Fehlstellen. Zum Schluss sei noch bemerkt, dass bei der Ableitung des Ausdrucks (10) vorausgesetzt war, dass während der Schwingung der Versetzungsstrecken einerseits neue Versetzungen nicht entstehen können und andererseits die Konfiguration der Cottrellatmosphäre unverändert bleibt. Dementsprechend beschreibt die Gleichung (10) die Dämpfung als eine eindeutige Funktion der momentanen Schwingungsamplitude (S), der Frequenz (ω) und der Temperatur (ϑ).

Da die Dämpfung unter unseren Messumständen stark von der Anfangsamplitude der Messchwingung und der Wartezeit zwischen den aufeinanderfolgenden Messungen abhängt, müssen wir mindestens eine der bisherigen Voraussetzungen ablehnen.

Bei der Revision der Voraussetzungen können wir gleich bemerken, dass sich die Konfiguration der Cottrellatmosphäre während der Schwingung der Versetzungsstrecken verändert, weil *einerseits das Spannungsfeld* einer schwingenden Versetzungsstrecke und dementsprechend *die Wechselwirkungsenergie* zwischen ihr und einer atomaren Fehlstelle und infolgedessen *die Gleichgewichtskonfiguration* der Cottrellatmosphäre *von der Schwingungsamplitude* der Versetzungsstrecken *abhängt*, und weil *andererseits die Beweglichkeit* der Zwischengitteratome und der Leerstellen auch bei Zimmertemperatur *gross genug ist*, um die Konfiguration der Cottrellatmosphäre in der Richtung des momentanen Gleichgewichts während der »Messung« merklich zu verschieben.

Um die Verhältnisse modellmässig zu veranschaulichen, schreiben wir den zeitlichen Mittelwert der Wechselwirkungsenergie zwischen einer harmo-

[8] In der Arbeit [9] ist die Dämpfung für homogene und harmonisch deformierte Proben angegeben, und dort wurde die Funktion $Ei(-x) = \int_{-\infty}^{-x} \frac{e^s}{s} ds$ in eine Potenzreihe entwickelt. Das Glied $\iint \sigma_{ik}^i \dot{\varepsilon}_{ik}^e \, dV dt$ wurde neben $\iint \sigma_{ik} \dot{\varepsilon}_{ik}^i \, dV dt$ in der Gl. (6) vernachlässigt, weil nach [17] $\frac{\mu_{AD}(A) - \mu_{AD}(0)}{\mu(0)} \sim \Delta(A)$ ist.

nisch, mit einer Amplitude ξ_0 schwingenden Stufenversetzung[9] und einer ruhenden atomaren Fehlstelle auf:

$$u_{\xi_0}(x, y, z) = \frac{1}{\pi} \int_{-1}^{+1} \frac{Ay}{(x - \xi_0 u)^2 + y^2} \cdot \frac{1}{\sqrt{1 - u^2}} du. \tag{11a}$$

Dementsprechend ist die Gleichgewichtskonzentration der Cottrellatmosphäre um die schwingende Stufenversetzung:

$$C_{\xi_0}(x, y, z) = C_0 \exp\left[- \frac{U_{\xi_0}(x, y. z)}{k\vartheta} \right], \tag{11b}$$

also ist C_{ξ_0} von der Schwingungsfrequenz unabhängig und nimmt mit zunehmender Schwingungsamplitude — z. B. in der Lage $(0, \delta, z)$ gemäss $\exp(-(\delta^2 + \xi_0^2)^{-1})$ — ab. Obwohl spannungsinduzierte Platzwechselvorgänge in der Nähe der schwingenden Versetzungen in der Einstellung der Gleichgewichtskonzentration eine wesentliche Rolle spielen, weisen wir doch darauf hin, dass die Leerstellen bzw. die Zwischengitteratome während 10 Minuten vgl. Tab. I) bei Zimmertemperatur (in einem spannungsfreien Kristallbereich) durch die BROWNsche Bewegung 2 bzw. $4 \cdot 10^4$ Gitterabstände zurücklegen,[10] was mit der »Ausdehnung« der Cottrellatmosphäre vereinbar ist (vgl. [20]) und infolgedessen bemerkenswerte Konfigurationsänderungen in der Cottrellatmosphäre bei Zimmertemperatur zustande kommen können.

Entsprechend diesen Erwägungen werden wir die Messergebnisse unter den Annahmen diskutieren, dass

1. der amplitudenabhängige Anteil der Dämpfung ausschliesslich von der durch GRANATO und LÜCKE vorgeschlagenen Wechselwirkung zwischen dem Versetzungsnetzwerk und der Cottrellatmosphäre stammt,

2. neue Versetzungen unter den gegebenen Messbedingungen nicht entstehen können,

3. die Konfiguration der Cottrellatmosphäre sich so »langsam« ändert, dass die Gleichung (10) gültig bleibt und die Veränderung der Cottrellatmosphäre sich nur in der Änderung des Parameters Γ widerspiegelt.

Obwohl die Gleichgewichtskonzentration der Cottrellatmosphäre mit abnehmender Amplitude zunimmt (vgl. Gl. (11b)), nimmt die Konzentration

[9] Die Gleichgewichtslage der Stufenversetzung ist in der Z-Achse und sie schwingt in der X-Richtung.

[10] Der Diffusionskoeffizient der Leerstellen wurde nach der Formel $D = a^2 \cdot \nu \cdot \exp/S/k/ \cdot \exp/-H/k\vartheta/$ berechnet [11]. Die eingesetzten Zahlenwerte waren die folgenden: Gitterabstand, $a = 3{,}5$ Å; Aktivierungsentropie für die Wanderung der Leerstellen (BOLTZMANN-Konstante, $S/k = 2$ [11]; $\nu = 5 \cdot 10^{12}$ sec^{-1} (ist etwa gleich der DEBYE-Frequenz, vgl. [22]); Aktivierungsenthalpie für die Wanderung der Leerstellen = 0,98 eV [10] und Messtemperatur $\vartheta = 300°$ K.

Das Verhalten der Zwischengitteratome ist hier und im folgenden durch das Beispiel der Wasserstoffverunreinigungen veranschaulicht. Der Diffusionskoeffizient des Wasserstoffes in Nickel wurde gemäss der Formel $D = D_0 \exp(-Q/k\vartheta)$ aus den Daten $D_0 = 2 \cdot 10^{-3}$ cm^2 sec^{-1} und 8,7 kcal/gAt extrapoliert, die bei 650° C bestimmt wurden [12].

der Cottrellatmosphäre während des Abklingens der Schwingung doch allmählich ab, weil die Platzwechselvorgänge die Gleichgewichtskonzentration während der Abklingungszeit der freien Schwingung auch bei den niedrigsten messbaren Amplituden noch nicht einstellen können. Die Konzentrationsabnahme hängt stark davon ab, wie lange die Schwingung bei den verschiedenen Amplituden gedauert hat (vgl. Gl. (28)). Dementsprechend hängt die Dämpfung auch von der Anfangsamplitude und von der Wartezeit ab, da die Dämpfungswerte nur dann reproduzierbar sind, wenn die Messchwingung von demselben Anfangszustand in derselben Weise ausgeht, also wenn einerseits die Wartezeit zwischen den aufeinanderfolgenden Messungen gross genug ist, sodass die Gleichgewichtskonfiguration um das ruhende Versetzungsnetzwerk sich wieder einstellen kann, und wenn andererseits die Schwingungen immer mit derselben Anfangsamplitude angeregt werden. Geht die Schwingung nämlich von denselben Anfangszuständen aber mit verschiedenen Anfangsamplituden aus, so werden sich die zu einer beliebigen Amplitude gehörenden Dämpfungswerte nicht reproduzieren, da die Schwingung in den verschiedenen Fällen bei den verschiedenen Amplituden verschiedene Zeit gedauert hat.

Die allmähliche Abnahme des Parameters Γ während des Abklingens zeigt unmittelbar, dass die mittlere Konzentration der Cottrellatmosphäre während der Schwingung tatsächlich abnimmt. Die zu den verschiedenen Amplituden gehörigen Γ-Werte wurden aus der Gleichung

$$\Delta^{\text{Pendel}} + \frac{S}{4}\frac{\partial \Delta^{\text{Pendel}}}{\partial S} = \Delta^0(\omega, \vartheta) - K\frac{\Gamma^3}{S^2} Ei\left(-\frac{\Gamma}{S}\right) \qquad (12)$$

berechnet. (Die Gleichung (12) wurde aus der Gleichung (10) durch partielle Ableitung nach S erhalten.) Die Resultate der Auswertung der in der Abb.4 dargestellten Messergebnisse ist in der Tab. I zusammengefasst. Die starke

Tabelle I

$S \times 10^6$	$\Gamma \times 10^6$	$K \times 10^{-3}$	$\Delta^0 \times 10^3$	$\left[\Delta^0 - K\Gamma^3/s^2\, Ei\left(-\frac{\Gamma}{s}\right)\right] \times 10^3$	$\left[\Delta^P + \frac{S}{4}\frac{\partial \Delta^P}{\partial S}\right] \times 10^3$	$\frac{\Gamma(S^2)}{\Delta(S_1)}$	$t(S_2) - t(S_1)$ (sec)	$\frac{\Gamma(S)}{S}$
3,125	10,00	1,12	0,68	1,84	1,87			3,2
						0,875	175	
2,500	8,75	1,12	0,68	1,52	1,49			3,5
						0,860	240	
1,875	7,50	1,12	0,68	1,19	1,19			4,0
						0,835	925	
1,250	6,25	1,12	0,68	0,88	0,90			5,0

Abnahme des Parameters Γ ist nicht überraschend, weil die mittlere Konzentration der Cottrellatmosphäre auf die Konfiguration der Fehlstellen sehr empfindlich ist.

Da die Abnahme der Cottrellatmosphärenkonzentration nach unseren Voraussetzungen durch die Schwingung verursacht ist, hat man nach dem Abklingen einer Schwingung die Zunahme der Cottrellatmosphäre zu beobachten. Diese Zunahme zeigt sich sehr prägnant in der Abnahme der Dämpfung, sofern die Anfangsamplitude der Schwingung, die für die Beobachtung der allmählichen Zunahme der Cottrellatmosphäre benutzt wird, wesentlich kleiner als die Anfangsamplitude der Schwingung ist, die den zu beobachtenden Effekt zustande gebracht hat (Abb. 2). Die Abnahme der Dämpfung lässt sich als Zunahme der Cottrellatmosphärenkonzentration interpretieren, weil die mittlere Dämpfung

$$Q^{-1}(A) = \log 2 \left[\int_{\frac{1}{2}A}^{A} \left\{ S \left(\Delta^0(\omega, \vartheta) + \frac{4}{S^4} \int_0^S \varepsilon K \Gamma^3 Ei\left(-\frac{\Gamma}{\varepsilon}\right) d\varepsilon \right) \right\}^{-1} ds \right]^{-1} \tag{13}$$

bei $\Gamma \geq 2{,}22$, konstantem $\Delta^0(\omega, \vartheta)$, K und A eine monoton abnehmende Funktion des Parameters Γ ist. (Auch bei den vorgekommenen niedrigsten Dämpfungswerten war nach der Tab. I $\Gamma > 3$.)

Die Abnahme der Dämpfung nach statischer Deformation lässt sich folgenderweise erklären. Im Moment der Belastung bauchen sich die in den Gleitebenen liegenden Versetzungsstrecken sprunghaft aus [13], und die Anhäufung der atomaren Fehlstellen um die neue Lage der Versetzungen verursacht eine allmähliche Abnahme der Dämpfung bis zur Einstellung des »Gleichgewichtes«.

Im folgenden werden wir die zur Anhäufung der »neuen« Cottrellatmosphäre erforderliche Zeit abschätzen, um zeigen zu können, dass das beobachtete »Gleichgewicht« der Einstellung der Gleichgewichtskonfiguration der Zwischengitteratome und der Leerstellen um die neue Lage der Versetzungen entspricht.

Da das Ausbauchen der Versetzungsstrecken unter unseren Messbedingungen gross genug ist[11] um die spannungsinduzierte Kopplung zwischen den ausgebauchten Versetzungsstrecken und den in ihren ursprünglichen Lagen zurückgebliebenen atomaren Fehlstellen aufzuheben, lässt sich der Einstellungsvorgang der Gleichgewichtskonzentration als die Überlagerung zweier verschiedener Vorgänge behandeln. Diese zwei Vorgänge sind das Verschwinden der Anhäufung der atomaren Fehlstellen, die um die ursprüngliche Lage der Versetzungen die Cottrellatmosphäre gebildet haben, und die allmähliche

[11] Nach den Daten [18] liegt die Amplitude des Ausbauchens bei den Spannungen von 400 pond in der Grössenordnung von 10^3 Gitterabständen.

Zunahme der Konzentration der Fehlstellen um die neue Lage der Versetzungen bis zur Einstellung des Gleichgewichtszustandes. Dementsprechend wird die Konzentration der verschiedenartigen atomaren Fehlstellen in der »neuen« bzw. in der »alten« Cottrellatmosphäre — $C_n^1(x_s, t)$, $C_n^2(x_s, t)$, ..., $C_n^i(x_s, t)$ bzw. $C_a^1(x_s, t)$, $C_a^2(x_s, t)$, ..., $C_a^i(x_s, t)$ — durch die folgenden Gleichungen und Anfangsbedingungen gegeben:[12]

$$\Delta c_a^i = \frac{1}{D^i} \frac{\partial c_a^i}{\partial t}, \tag{14}$$

$$C_a^i(x_S. 0) = C_{a0}^i(x_S), \tag{15}$$

$$\Delta C_n^i + \operatorname{grad} C_n^i \operatorname{grad} U^i = \frac{1}{D^i} \frac{\partial c_n^i}{\partial t}, \tag{16}$$

$$C_n^i(x_S, 0) = C_0^i. \tag{17}$$

Hierbei sind $U(x_s)$ die Wechselwirkungsenergie zwischen dem Versetzungsnetzwerk und den in der Lage $\{x_s\}$ liegenden atomaren Fehlstellen, C_{a0}^1, C_{a0}^2, ..., C_{a0}^i die Teilkonzentrationen der durch das sprunghafte Ausbauchen zerstörten unbekannten alten Cottrellatmosphäre im Zeitpunkt Null, C_0^1, C_0^2, ..., C_0^i die mittleren Teilkonzentrationen der verschiedenartigen atomaren Fehlstellen in der Probe und D^1, D^2, ..., D^i ihre Diffusionskoeffizienten. Da C_{a0}^i und U^i unbekannt sind, müssen wir uns mit groben Näherungen begnügen.

Die Lösung der Gl. (14) und (16) unter den Annahmen, dass

$$\frac{U^i}{k\vartheta} = \frac{1}{k\vartheta}\left\{U^i(x_{10}, x_{20}) + \frac{\partial U^i}{\partial x_1}(x_1 - x_{10}) + \frac{\partial U^i}{\partial x_2}(x_2 - x_{20}) =\right.$$

$$= \begin{cases} -a^i + b^i X_1 + b^i X_2 \text{ wenn } X_1 \geqq 0, X_2 \geqq 0 \text{ und } X_1 + X_2 < \dfrac{a^i}{b^i} \text{ ist}, \\ -a^i + b^i X_1 - b^i X_2 \text{ wenn } X_1 \geqq 0, X_2 \leqq 0 \text{ und } -X_1 + X_2 > -\dfrac{a^i}{b^i} \text{ ist}, \\ -a^i + b^i X_1 + b^i X_2 \text{ wenn } X_1 \leqq 0, X_2 \geqq 0 \text{ und } -X_1 + X_2 < \dfrac{a^i}{b^i} \text{ ist}, \\ -a^i - b^i X_1 - b^i X_2 \text{ wenn } X_1 \leqq 0, X_2 \leqq 0 \text{ und } X_1 + X_2 > -\dfrac{a^i}{b^i} \text{ ist}, \end{cases} \tag{18}$$

[12] Der obere Index i unterscheidet immer die zu den verschiedenartigen atomaren Fehlstellen gehörenden Grössen.

und

$$C_{a0}^{i}(x_s) = C_0^i \exp\left(-\frac{U^i}{k\vartheta}\right), \tag{19}$$

wird die folgende z. B. im Bereich $X_1 \geqq 0$, $X_2 \geqq 0$ und $X_1 + X_2 < \frac{a^i}{b^i}$:

$$C_a^i(x_s, t) = C_0^i - \frac{C_0^i}{\pi} \int_D^B \int_F^E e^{-(u^2+v^2)}\, du\, dv + \\ + \frac{C_0^i}{\pi} \exp\left(a^i b^i X_1 - b^i X_2 + b^i \sqrt{Dt}\right) \int_{D+2C}^{B+2C} \int_{F+2C}^{E+2C} e^{-(u^2+v^2)}\, du\, dv \tag{20}$$

$$C_n^i(x_s, t) = C_0^i \exp\left(a^i - b^i X_1 - b^i X_2\right) + \frac{C_0^i}{\pi} \int_{D-C}^{B-C} \int_{F-C}^{E-C} e^{-(u^2+v^2)}\, du\, dv - \\ - \frac{C_0^i}{\pi} \exp\left(a^i - b^i X_1 - b^i X_2\right) \int_{D+C}^{B+C} \int_{F+C}^{E+C} e^{-(u^2+v^2)}\, du\, dv, \tag{21}$$

wobei:

$$B = \frac{\frac{a^i}{b^i} - x_1}{\sqrt{4D^i t}}; \quad C = \frac{b^i \sqrt{D^i t}}{2}; \quad D = \frac{-X_1}{\sqrt{4D^i t}};$$

$$E = \frac{\frac{a^i}{b^i} - X_1 - X_2}{\sqrt{4D^i t}}; \quad F = \frac{-X_2}{\sqrt{4D^i t}}$$

sind.

Die Bedeutung dieser Näherung liegt darin, dass sie zeigt, dass wenn sich die Ausdehnung der Cottrellatmosphäre, $\frac{a^i}{b^i}$, bei beliebig gewählten t_e^i und t_v^i aus den Gl.[13]

$$\max \frac{C_n^i(x_s, t_e^i)}{C_n^i(x_s, \infty)} = 0.99, \tag{22a}$$

$$\max \frac{C_a^i(x_s, t_v^i)}{C_a^i(x_s, 0)} = 0.10 \tag{22b}$$

[13] Da wir auf das Verschwinden der Cottrellatmosphäre des deformierten Versetzungsnetzwerkes während der Entlastung aus der Reproduzierbarkeit der Einstellungszeit des stationären Zustandes bei den Wiederbelastungen schliessen und weil sie auf die kleinen Mengen der zurückgebliebenen Anhäufungen nicht zu empfindlich ist, müssen wir in (22a) und in (22b) verschiedene Einstellungsgenauigkeiten fordern.

zu weniger als einige Gitterabstände ergibt, die in (22) vorgeschriebenen Konzentrationsänderungen auch bei den tatsächlichen U^i und C^i_{a0} während t^i_e und t^i_v natürlich nicht eintreten können.

Die Einstellung des stationären Zustandes der Dämpfung erforderte 150 Stunden nach der Belastung des Fadens. Nach (22a) ist die dieser Zeitdauer entsprechende Ausdehnung der aus Leerstellen gebildeten Cottrellatmosphäre 100 Gitterabstände. Die in derselben Weise berechnete Ausdehnung der aus Wasserstoffatomen bzw. aus Kupferatomen gebildeten Cottrellatmosphäre ist $3{,}3 \cdot 10^6$ bzw. $7{,}3 \cdot 10^{-2}$ Gitterabstände.[14] Dementsprechend stellte sich die Gleichgewichtskonfiguration der Wasserstoffatome um das Versetzungsnetzwerk schon während eines Bruchteiles der 150 Stunden »vollständig« ein. Die beobachtete Einstellungszeit wurde durch die Beweglichkeit der Leerstellen bestimmt. Die Beobachtungszeit war jedoch zu kurz, um merkliche Bewegung der Kupferatome beobachten zu können.[15]

Weil die Einstellungszeit bei allen Wiederbelastungen fast dieselbe war, darf man voraussetzen, dass die Cottrellatmosphäre, die sich im deformierten Zustand angehäuft hatte, während der 10 Stunden der Entlastung wieder »fast völlig« verschwindet. Aus der Gl. (22b) ergibt sich, dass $\frac{a^i}{b^i}$ (10 Stunden) für die Leerstellen 60 Gitterabstände ist, was den obigen Daten der Ausdehnung der Leerstellen-Cottrellatmosphäre entspricht, wenn wir nicht ausser acht lassen, dass die Cottrellatmosphäre des Versetzungsnetzwerkes bei der Entlastung des Fadens durch die sprunghafte Bewegung der Versetzungsstrecken zerstört wird, was bei der Ableitung der Gl. (21) und (22b) vernachlässigt wurde.

Zum Schluss diskutieren wir die Frequenzabhängigkeit der Dämpfung. Wir bemerken, dass unter unseren Messbedingungen selbst der amplitudenabhängige Anteil der Dämpfung frequenzabhängig war. Wenn der amplitudenabhängige Anteil der Dämpfung frequenzunabhängig wäre, so dürfte man statt

$$Q_2^{-1}(A) - Q_3^{-1}(A) = \frac{Q_3^{-1}(A)}{\Delta_3^P(A^*)} \left(\Delta_2^{\text{Pendel}}(A^*) - \Delta_3^{\text{Pendel}}(A^*)\right) \qquad \left(\frac{A}{2} \leq A^* \leq A\right) \tag{23}$$

[14] Die Aktivierungsenergie der Cottrellatmosphäre wurde in allen drei Fällen als 0,15 eV angenommen [20]. Der Diffusionskoeffizient der Kupferatome wurde aus den Daten $D_0 = 10^{-3}$ cm^{2}sec^{-1} und $Q = 35$ kcal/gAt berechnet. ([12], vgl. Fussnote 10).

[15] Dementsprechend kann man bei geeigneter Wahl der Temperatur, der Belastung und der Beobachtungszeit eine aus beliebigartigen atomaren Fehlstellen gebildete Cottrellatmosphäre um die Versetzungen herstellen.

schreiben:

$$Q_2^{-1}(A) - Q_3^{-1}(A) \ll \frac{Q_3^{-1}(A)}{Q_3^{-1}\left(\frac{A}{2}\right)} [\Delta_2^0 - \Delta_3^0], \tag{24}$$

und infolgedessen wäre nach den Daten der Abb. 3

$$\Delta_2^0 - \Delta_3^0 \gg 0{,}17 \cdot 10^{-3}. \tag{25}$$

Die Ungleichung (25) widerspricht aber der folgenden Ungleichung:

$$\Delta_2^0 - \Delta_3^0 < Q_2^{-1}(A) - \Delta_3^0 \sim Q_2^{-1}(A) - \Delta_1^0, \tag{26}$$

weil nach Tab. I und Abb. 3

$$\Delta_2^0 - \Delta_3^0 < 0{,}16 \cdot 10^{-3} \tag{27}$$

ist.[16]

Entsprechend der Voraussetzung der allmählichen Abnahme der Cottrellatmosphärenkonzentration während des Abklingens müssen wir versuchen die Frequenzabhängigkeit der amplitudenabhängigen Dämpfung dadurch zu erklären, dass die Abnahmegeschwindigkeit der mittleren Konzentration der Cottrellatmosphäre bei den verschiedenen Frequenzen verschieden ist. Nun setzen wir voraus, dass die Konfigurationsänderung der Cottrellatmosphäre während der Schwingung mit spannungsinduzierter Diffusion unter dem Einfluss einer frequenzunabhängigen Wechselwirkungsenergie zwischen dem Versetzungsnetzwerk und den atomaren Fehlstellen stattfindet. Diese Voraussetzung ist darauf gegründet, dass unter unseren Messumständen die Geschwindigkeit der Versetzungen (die 10^{-7} m/sec war; vgl. [18]) um 10 Grössenordnungen kleiner war als die Schallgeschwindigkeit in Nickel ($5 \cdot 10^3$ m/sec). Dementsprechend lässt sich die quasistatische Berechnung des Spannungsfeldes der schwingenden Versetzungsstrecken (vgl. Gl. (11a)) als eine gute Näherung betrachten.

Wenn während des Abklingens der Schwingung von der Amplitude A auf die Amplitude B in den Zeitpunkten $t_0 = 0,\ t_1, \ldots, t_k, \ldots, t_n = t$ die Amplituden $A = A_0, \ldots, A_k, \ldots, A_n = B$ sind, und zu diesen Schwingungsamplituden die Wechselwirkungsenergien $U_0, U_1, \ldots, U_k, \ldots, U_n$ gehören, so wird die Konfiguration der Cottrellatmosphäre in der Zeit t

$$C^i_{A\to B}(x_s, t) = \lim_{n\to\infty} C^i_n(x_s, t_0, t_1, \ldots, t_k, \ldots, t_n), \tag{28}$$

wobei C^i_n durch die Rekursionsformel

[16] Der amplitudenunabhängige Anteil der Dämpfung ändert sich nach dem Gesetz:

$$O^{-1}(\omega, \vartheta)(\omega \Delta\tau (1 + \omega^2 \tau_0^2 \exp(-Q/k\vartheta)^2 + \omega^2 \Delta\tau^2)^{-1/2},$$

wo Q in der Grössenordnung der Aktivierungsenergien der Diffusion liegt [21].

$$C_0^i = \text{Gleichgewichtskonzentration im Zeitpunkt Null,}$$

$$C_1^i = C_0^i + D^i (\Delta C_0^i + \operatorname{grad} U_0^i \operatorname{grad} C_0^i)(t_1 - t_0),$$

$$\cdots$$

$$C_{k+1}^i = C_k^i + D^i (\Delta C_k^i + \operatorname{grad} U_k^i \operatorname{grad} C_k^i)(t_{k+1} - t_k),$$

$$\cdots$$

$$C_n^i = C_{n+1}^i + D^i (\Delta C_{n+1}^i + \operatorname{grad} U_{n+1}^i \operatorname{grad} C_{n-1}^i)(t_n - t_{n-1})$$

gegeben sind (vgl. Gln. (14) und (16)). Weil einerseits $t_k - t_{k-1}$ bei $T_3 = 3{,}03$ sec immer grösser als bei $T_2 = 1{,}7$ sec war,[17] und weil andererseits $C_{02}^i \geqq C_{03}^i$ und $D_{03}^i > D_{02}^i$ waren,[18] ist nach der Gl. (13) $\Delta_2^{\text{Pendel}}(A^*) < \Delta_3^{\text{Pendel}}(A^*)$, und infolgedessen dürfen wir statt (23) wieder die Ungleichung (24) schreiben, woraus sich der schon bekannte Widerspruch ergibt.

Dieser Widerspruch weist darauf hin, dass entweder die Wechselwirkungsenergie von der Frequenz abhängt, oder die Wirkung der durch die nicht plastischen Deformationen zustande gebrachten Versetzungen nicht vernachlässigt werden darf (vgl. [14]). Da bei der Ableitung der Gl. (10) die durch die Cottrellatmosphäre dissipierte kinetische Energie der zurücklaufenden Versetzungsstrecken ausser acht gelassen war [9], so können wir zwischen diesen zwei Möglichkeiten nur nach neueren Erwägungen einen Unterschied machen. Bemerken wir aber, dass wenn man eine geschwindigkeitsabhängige Wechselwirkung voraussetzt, welche von der Geschwindigkeit der Versetzungsbewegung so abhängt, dass bei den grösseren Geschwindigkeiten auch die dissipierte Energie grösser ist, so ist nicht nur die Möglichkeit der Erklärung der Frequenzabhängigkeit gegeben, sondern damit kann vielleicht auch erklärt werden, warum man bei den mit den grösseren Anfangsamplituden angeregten Schwingungen bedeutend grössere Dämpfungswerte misst als bei den Schwingungen, die eine kleinere Anfangsamplitude haben.

Schlussfolgerungen

1. Die amplitudenabhängige Dämpfung ist eine eindeutige Funktion der Anfangsamplitude, der momentanen Schwingungsamplitude, der Frequenz und der Temperatur, sofern zwischen den aufeinanderfolgenden Messungen eine hinreichende Zeit abgewartet wird.

[17] Es sind nämlich $Q_2^{-1} > Q_3^{-1}$ und $T_2^{-1} < T_3^{-1}$.

[18] Die Temperaturabhängigkeit dieser Grössen ist die folgende:

$$D^i = D_0^i \exp(-Q^i/k\vartheta) \text{ und } C_0^i = C_{00}^i \exp(+Q^i/k\vartheta).$$

Vor den Anregungen wurde immer die Einstellung der Gleichgewichtskonzentration um das ruhende Versetzungsnetzwerk abgewartet.

2. Die durch die statischen und dynamischen Deformationen verursachten Dämpfungsänderungen lassen sich als spannungsinduzierte Bewegungen der atomaren Fehlstellen um das Versetzungsnetzwerk beschreiben.

3. Auch der amplitudenabhängige Anteil der Dämpfung ist frequenzabhängig.

4. Eine Ursache der oft gefundenen Widersprüche zwischen den Erwartungen der Theorie von GRANATO und LÜCKE bezüglich des amplitudenabhängigen Anteils der Dämpfung und den Messergebnissen [19] kann in den spannungsinduzierten Konzentrationsänderungen der Cottrellatmosphäre und in der Entstehung neuer Versetzungen vermutet werden.

Herrn Prof. Dr. E. NAGY danke ich herzlich für die Anregung zu dieser Arbeit und für sein ständiges Interesse.

LITERATUR

1. H. G. VAN BUEREN, Imperfections in Crystals, North-Holland Publishing Co., Amsterdam 1960; S. 348—397.
2. W. T. READ, Phys. Rev., **58**, 371, 1940.
3. W. T. READ, Trans. AIME., **143**, 30, 1941.
4. S. WEINIG und E. S. MACHLIN, J. Appl. Phys., **27**, 734, 1956.
5. E. BODE, Z. f. Naturforsch., **14a**, 762, 1959.
6. R. H. CHAMBERS und R. SMOLUCHOWSKI, Phys. Rev., **117**, 725, 1960.
7. T. S. KE, Phys. Rev., **71**, 533, 1947.
8. H. G. VAN BUEREN, op. cit. S. 141.
9. A. GRANATO und K. LÜCKE, J. Appl. Phys., **27**, 538, 789, 1956.
10. J. F. NICHOLAS, Phil. Mag., **46**, 87, 1955.
11. A. SEEGER, Handbuch der Physik, Springer-Verlag, Berlin-Göttingen-Heidelberg, 1955. Bd. VII/1 S. 420, 425.
12. W. SEIT, Diffusion in Metallen, Springer-Verlag, Berlin-Göttingen-Heidelberg, 1955. S. 61.
13. J. FRIEDEL, Phil. Mag., **44**, 437, 1953.
14. A. R. ROSENFIELD und B. L. AVERBACH, Acta Met., **8**, 624, 1960.
15. M. PÄSLER, Z. f. Phys., **72**, 357, 1944.
16. I. GAÁL, Diplomarbeit; Roland Eötvös Universität, Budapest, (unveröffentlicht).
17. A. S. NOWICK, Phys. Rev., **80**, 249, 1950.
18. A. GRANATO und K. LÜCKE, Dislocations and Mechanical Properties of Crystals, Wiley and Sons, New-York, 1956, S. 456.
19. D. H. NIBLETT und J. WILKS, Proc. Phys. Soc., **73**, 95, 1959; R. S. BARNES, N. H. HANCOCK und E. C. H. SILK, Phil. Mag., **3**, 519, 1958; H. L. CASWELL, J. Appl. Phys., **29**, 1210, 1958.
20. H. G. VAN BUEREN, op. cit. S. 194.
21. A. S. NOWICK, Progr. Met. Phys., **4**, 1, 1953.
22. H. G. VAN BUEREN, op. cit. S. 18.

ЗАВИСЯЩИЕ ОТ ВРЕМЕНИ ЯВЛЕНИЯ ИСПАРЕНИЯ НА НИККЕЛЕ ПРИ КОМНАТНОЙ ТЕМПЕРАТУРЕ

И. ГАЛ

Р е з ю м е

При помощи крутильного маятника по *Ke* исследуется изменение зависящего от амплитуды испарения, которое является функцией времени, на никкеле, деформированном статически и динамически в непластичной области, при комнатной температуре. Цель данной работы — дать общий обзор влияния деформаций на испарение, находящихся в неразрывной зависимости с измерительными методами испарения. Результаты измерения объясняются тем, что концентрация мест дефектов в атоме, накопленных вокруг дислокаций, изменяется под действием упругих деформаций.

RELATIVISTIC EQUATION OF MOTION FOR A CHARGED PARTICLE WITH SPIN AND MAGNETIC MOMENT

I. TRANSLATIONAL EQUATION OF MOTION

By

I. F. FARKAS

INSTITUTE FOR THEORETICAL PHYSICS, ROLAND EÖTVÖS UNIVERSITY, BUDAPEST

(Presented by K. Novobátzky. — Received 20. VIII. 1961)

Starting from the modified form of the energy-momentum tensor, the translational equation of motion is determined by using INFELD's method. The four-potential is expanded in terms of the powers of 1/c. The self-force acting on the particle is calculated. The divergent terms in the equations of motion are eliminated by the method of compensating auxiliary field. It is shown that similar results are obtained if field equations of higher order are used. The variation of the rest mass caused by the self-force is also given.

§. 1. Introduction

In recent years the problems of the equations of motion have been studied by a number of authors. Their aim was to investigate the equations of motion for particle models which approach really existing elementary particles as closely as possible. These investigations can be divided into two groups. 1. The reaction of the proper field is calculated on the basis of a rather simple model, and 2. in the case of more complicated models the equations are determined regarding the particle as a test particle. In the case of the simplest model, that of a charged point particle, the radiation reaction was given by DIRAC [1]. Here the divergent terms, that appear in the equations of motion, can be incorporated into the mass. A model which approaches real elementary particles better has been proposed by BHABHA [2]. Later BHABHA and CORBEN [3] improved DIRAC's original method for the derivation of the equations of motion. PRYCE [4] has shown that the method for the elimination of the divergent term proposed by DIRAC is equivalent with the modification of the energy-momentum tensor by adding a term

$$T'_{\alpha\beta} = T_{\alpha\beta} - \partial_\mu K_{\alpha\beta\mu},$$

where $K_{\alpha\beta\mu}$ depends only on the coordinates of the particles and is antisymmetric in the indices α, β. The aim of the further investigations was to ensure the finiteness of the self-energy. In addition to the aforementioned authors ELIEZER [5] and GUPTA [6] also succeeded in obtaining a finite value for the self-energy by applying advanced potentials. This procedure has, however,

two important shortcomings: its rather formal character and the fact that the physical meaning of the advanced potential is not clear enough to be used without criticism.

Many authors derive the equations of motion from a variational principle. In this way important results have been obtained by FRENKEL [7] and HORVÁTH [8]. In the derivation of the correct equations of motion there is another problem to be solved: namely the interaction between charge and external field is known from LORENTZ's work, the interaction between magnetic moment and field has yet to be clarified. Many authors have treated this problem, e. g. BHABHA and CORBEN [3] and MARX [9]. The clarification of the interaction between magnetic moment and field is of paramount importance because this strongly influences the structure of the equations of motion.

We should like to recall one of BHABHA's remarks, according to which the appearance of the divergent terms is caused by the energy-momentum tensor used, which does not describe the singular field of the particles conveniently. This energy-momentum tensor has been modified by MARX [9] and this modified form will be used in our calculations.

§ 2. The derivation of the equations of motion from linear field equations

It is a well-known fact that one cannot deduce the equations of motion from linear field equations. Therefore we use the method proposed by INFELD [10] for their derivation, the essence of which is the following. Introducing into the linear field equations the weak gravitational field created by the particle and its field the field equations cease to be linear and one can deduce the equations of motion from these nonlinear field equations without any other hypothesis. Finally we take the equations of motion in the limit when $g_{\alpha\beta}$ tends to $\delta_{\alpha\beta}$ and the gravitational constant $\varkappa$ tends to zero.

In the calculation we make use of the gravitational and the linear field equations. It follows from the gravitational equations that the complete energy-momentum tensor of the system is divergence-free:

$$\nabla_\beta T^{\alpha\beta} = 0, \tag{1}$$

which ensures the conservation of a four-vector. Now if we integrate eq. (1) over a domain V, which includes the particle, we obtain the equations of motion:

$$\frac{dt}{d\tau} \int \Delta_\beta T^{\alpha\beta} \, dv = 0, \tag{2}$$

which depend only on the positon of the particle. (Here τ denotes the proper time.) Let us take the aforementioned limit, when $g_{\alpha\beta} \to \delta_{\alpha\beta}$ and $\varkappa \to 0$, then the eq. (2) obtains the following form:

$$\frac{dt}{d\tau} \int \partial_\beta T_{\alpha\beta} \, dv = 0. \tag{3}$$

(Greek indices run from 1 to 4, Roman indices from 1 to 3, further $x = ict = ix_0$ and $\partial_\alpha \equiv \frac{\partial}{\partial x_\beta}$).

The complete energy-monemtum tensor consists of two parts: the kinematic energy-momentum tensor $t_{\alpha\beta}$ of the particle and the energy-momentum tensor $E_{\alpha\beta}$ of the electromagnetic field, the latter describes the interaction of the particle and the external field. Therefore

$$T_{\alpha\beta} = t_{\alpha\beta} + E_{\alpha\beta}. \tag{4}$$

Using eq. (4) we write eq. (3) in the form

$$\frac{dt}{d\tau} \int \partial_\beta t_{\alpha\beta} \, dv = - \frac{dt}{d\tau} \int \partial_\beta E_{\alpha\beta} \, dv. \tag{5}$$

In a well-known manner we describe the spin of the particle by a second-order antisymmetric tensor. In the rest system

$$S_{23} = \sigma_x, \quad S_{31} = \sigma_y, \quad S_{12} = \sigma_z, \tag{6}$$

where $\sigma(\sigma_x, \sigma_y, \sigma_z)$ denotes the spin vector of the particle.

As experimental facts suggest a very close connection exists between the spin and the magnetic moment of the particle in the rest system. Therefore, if we wish to proceed in accordance with a model, in which the particle has magnetic moment in the rest system only, we have to require that at the time τ the elements $S_{\alpha 4}$ of the tensor $S_{\alpha\beta}$ vanish in the reference system moving together with the particle. This condition has the covariant form

$$_{\alpha\beta} n_{\beta} S = 0, \tag{7}$$

where u_α denotes the four-velocity of the particle.

§ 3. The kinematic energy-momentum tensor

The mechanical behaviour of the particle is described by the kinematic energy-momentum tensor. Its explicit form is necessary when solving the

equations of motion (5). On the basis of the results obtained by HÖNL [11] and NAGY [12] we write it in the form:

$$t_{\alpha\beta} = \int (m_{\alpha\beta} + m_{\alpha\beta\gamma}\,\partial_\gamma)\,\delta(4)\,d\tau. \tag{8}$$

The tensors $m_{\alpha\beta}$ and $m_{\alpha\beta\gamma}$ are symmetric in the indices α, β. The function δ (4) represents the four-dimensional δ-function of DIRAC

$$\begin{aligned}\delta(4) = \delta(x_1 - \xi_1)\,\delta(x_2 - \xi_2)\,\delta(x_3 - \xi_3)\,\delta\left(\frac{x_4}{ic} - \frac{\xi_4}{ic}\right) = \\ = \delta(3)\,\delta\left(\frac{x_4}{ic} - \frac{\xi_4}{ic}\right).\end{aligned} \tag{9}$$

The $\xi_\nu(\tau)$ denotes the world line.

The tensors $m_{\alpha\beta}$ and $m_{\alpha\beta\gamma}$ are given by NAGY in the form:

$$m_{\alpha\beta} = m_0\,u_\alpha\,u_\beta - \frac{1}{2\,c^2}\,(\dot{S}_{\alpha\nu}\,u_\nu\,u_\beta + \dot{S}_{\beta\nu}\,u_\nu\,u_\alpha)\,,$$

$$m_{\alpha\beta\gamma} = -\frac{1}{2}\,(S_{\gamma\alpha}\,u_\beta + S_{\gamma\beta}\,u_\alpha). \tag{10}$$

With this choice $t_{\alpha\beta}$ fulfils the usual physical conditions. Substituting (10) into (8) and performing the prescribed integration which is very simple because of the δ-functions, the kinematic energy-momentum tensor has the form:

$$\begin{aligned}t_{\alpha\beta} = m_{\alpha\beta}\,\delta(3)\,\frac{d\tau}{dt} + m_{\alpha\beta k}\,\partial_k\,\delta(3)\,\frac{d\tau}{dt} \\ - \frac{1}{ic}\,m_{\alpha\beta 4}\,u_k\,\partial_k\,\delta\,(3)\left(\frac{d\tau}{dt}\right)^2 + \\ + \frac{1}{ic}\,\frac{d}{d\tau}\left(m_{\alpha\beta 4}\,\frac{d\tau}{dt}\right)\frac{d\tau}{dt}\,\delta(3),\end{aligned} \tag{11}$$

where $\delta(3) = \delta(x_1 - \xi_1)\,\ldots\,\delta(x_3 - \xi_3)$. The detailed examination of the eq. (11) shows that the kinematic energy-momentum tensor of the particle describes a point-like pole-dipole system. If we wish to build up a particle model which takes also the spin into account, the simplest way of its realisation is to use a pole-dipole system. We note that in the case of a particle having higher moments, one has to start with an energy-momentum tensor that contains derivatives of higher order.

§ 4. The equation of motion of a particle with charge and magnetic moment

For the derivation of the equation of motion it is necessary to give the electromagnetic properties of the particle. The electric charge of the particle is characterized by the scalar quantity e, the magnetic moment by the vector $\mathfrak{m}(m_x, m_y, m_z)$. The components of the magnetic moment can be associated with the spatial elements of an antisymmetric tensor in the following sense

$$P_{23} = m_x, \quad P_{31} = m_y, \quad P_{12} = m_z.$$

The elements $P_{\alpha 4}$ of the tensor $P_{\alpha\beta}$ can be represented by another vector $\mathfrak{p}(p_x, p_y, p_z)$. It is clear that the vector $\mathfrak{p}$ describes the electric moment of the particle. As we wish to compare the electromagnetic properties of the par-ticle with those of real elementary particles, we require that the electric moment vanish in the rest system of the particle. In other words if the particle is at rest, the vector $\mathfrak{p} = \left[\frac{\mathfrak{v}}{c}, \mathfrak{m}\right]$ has to vanish. This condition can easily be written in the covariant form

$$P_{\alpha\beta} u_\beta = 0. \tag{12}$$

(FRENKEL's condition [7]).

In order to facilitate the calculations we follow MARX and introduce an antisymmetric tensor $M_{\alpha\beta}$ with the prescription

$$M_{\alpha\beta} = P_{\alpha\beta} + \frac{1}{c^2}(u_\varrho P_{\alpha\varrho} u_\beta - u_\varrho P_{\beta\varrho} u_\alpha), \tag{13}$$

where the tensor $P_{\alpha\beta}$ is antisymmetric in the indices α, β and its elements are equal to the components of the vectors $\mathfrak{m}$ and $\mathfrak{p}$, respectively. It is easy to see that (12) is satisfied by the choice of $M_{\alpha\beta}$. Let us suppose further that the tensors which describe the behaviour of the spin and the magnetic moment of the particle are related by

$$M_{\alpha\beta} = g S_{\alpha\beta}, \tag{14}$$

where the constant g is characteristic of the particle.

The fields, both the external one and that caused by the particle, are described by Maxwell's equations which we write in the form

$$\partial_\alpha F_{\beta\varrho} + \partial_\beta F_{\varrho\alpha} + \partial_\varrho F_{\alpha\beta} = 0, \tag{15a}$$

$$\partial_\beta F_{\alpha\beta} = 4\pi(S_\alpha + \partial_\beta \mu_{\alpha\beta}), \tag{15b}$$

where $F_{\alpha\beta}$ denotes the electromagnetic field tensor, S_α is the four-current density, which, in the case of a point particle, takes the form

$$S_\alpha = \frac{e}{c}\int u_\alpha \delta(4)\, d\tau, \tag{16}$$

and $\partial_\beta \mu_{\alpha\beta}$ is the polarized current density arising from the electric and magnetic moment. This is defined by

$$\mu_{\alpha\beta} = \int M_{\alpha\beta}\delta(4)\, d\tau. \tag{17}$$

The tensor field described by Maxwell's equations (15a) and (15b) has a vanishing rotation. This makes possible to represent the tensor field by a four-vector field. The four-vector field (the four-potentials) which we introduce in this way, is related to the field tensor by

$$F_{\alpha\beta} = \partial_\alpha A_\beta - \partial_\beta A_\alpha. \tag{18}$$

The eq. (15a) is automatically satisfied by this choice of $F_{\alpha\beta}$. As the eq. (18) does not specify a unique A_α, we prescribe Lorentz's condition:

$$\partial_\alpha A_\alpha = 0. \tag{19}$$

Substituting (18) into (15b) and making use of (19) we obtain the differential equation

$$\Box A_\alpha = -4\pi (S_\alpha + \partial_\beta \mu_{\alpha\beta}), \tag{20}$$

which determines the four-potentials. On the right-hand side of the equation of motion (5) we have to substitute the energy-momentum tensor $E_{\alpha\beta}$ by the one which describes the interaction between the external field and the particle. In its formulation we have to take into account the fact that the particle has also a magnetic moment. Having this in mind one obtains the energy-momentum tensor $E_{\alpha\beta}$ as a result of the variation of the Lagrangian:

$$E_{\alpha\beta} = \frac{1}{4\pi}\left[F_{\alpha\varrho}F_{\beta\varrho} - \frac{\delta_{\alpha\beta}}{4}F_{\varrho\sigma}F_{\varrho\sigma}\right] - \frac{1}{c^2}\left[u_\alpha \mu_{\beta\sigma} + u_\beta \mu_{\alpha\sigma}\right]F_\sigma. \tag{21}$$

Here we have used the concise notation:

$$F_\sigma = F_{\sigma\varrho}u_\varrho. \tag{22}$$

Our next task is to subtract the divergence of the energy-momentum tensor defined by (21). It follows from a simple calculation that

$$\partial_\beta E_{\alpha\beta} = - F_{\alpha\sigma} S_\sigma - \frac{1}{2} \mu_{\sigma\lambda} \partial_\alpha F_{\sigma\lambda} - \\ - \partial_\lambda [F_{\alpha\sigma} \mu_{\sigma\lambda} + \frac{1}{c^2} (u_\alpha \mu_{\lambda\sigma} + u_\lambda \mu_{\alpha\sigma}) F_\sigma]. \tag{23}$$

The four-potentials defined by (18) can be divided into two parts in the following way:

$$A_\alpha = A^e_\alpha + A^S_\alpha, \tag{24}$$

where A^e_α denotes the four-potentials of the external electromagnetic field and A^S_α gives the contribution of the particle. As we mentioned before, the field of the particle is singular in the place of the particle, but the external field is not. It is very important to stress this if we wish to calculate the right-hand side of (5). Therefore it will be useful to write the divergence of the energy-momentum tensor $E_{\alpha\beta}$ as a sum of terms some of which are singular and some nonsingular in the place of the particle. This can be done easily with the help of (24). Namely, if we substitute (24) into (18), the field tensor is obtained in the form:

$$F_{\alpha\beta} = F^e_{\alpha\beta} + F^S_{\alpha\beta}, \tag{25}$$

and we get the desired decomposition by substituting (25) into (23):

$$\partial_\beta E_{\alpha\beta} = - F^e_{\alpha\sigma} S_\sigma - \frac{1}{2} \mu_{\sigma\lambda} \partial_\alpha F^e_{\sigma\lambda} - \partial_\lambda \Big| F^e_{\alpha\sigma} \mu_{\sigma\lambda} + \\ + \frac{1}{c^2} (u_\alpha \mu_{\lambda\sigma} + u_\lambda \mu_{\alpha\sigma}) F^e_\sigma \Big| - F^s_{\alpha\sigma} S_\sigma - \frac{1}{2} \mu_{\sigma\lambda} \partial_\alpha F^S_{\sigma\lambda} - \tag{26}$$

$$- \partial_\lambda \Big| F^S_{\alpha\sigma} \mu_{\lambda\sigma} + \frac{1}{c^2} (u_\alpha \mu_{\lambda\sigma} + u_\lambda \mu_{\alpha\sigma}) F^S_\sigma \Big|.$$

As $F^e_{\alpha\beta}$ is not singular at the points of the world line of the particle, the integration can be carried out easily. The result is

$$\frac{d}{d\tau} \left(m_0 u_\alpha - \frac{1}{c^2} \dot{S}_{\alpha\varrho} u_\varrho \right) = \frac{e}{c} F^e_{\alpha\varrho} u_\varrho + \frac{1}{2} M_{\sigma\varrho} \partial_\alpha F^e_{\sigma\varrho} - \\ - \frac{1}{c^2} F^e_{\alpha\varrho} \dot{M}_{\varrho\lambda} w_\lambda - \frac{1}{c^4} \dot{M}_{\sigma\lambda} u_\alpha u_\sigma F^e_\lambda + \tag{27}$$

$$+ \frac{1}{c^2} \frac{d}{d\tau} (M_{\alpha\sigma} F^e_\sigma) + F^S_\alpha.$$

In (27) F_α^S denotes the force by which the particle acts on itself. Since we will be interested in it, we write it in detail:

$$F_\alpha^S = \frac{dt}{d\tau}\int\Big\{F_{\alpha\sigma}^S S_\sigma + \frac{1}{2}\mu_{\sigma\lambda}\partial_\alpha F_\lambda^S + \\ + \partial_\lambda\Big[F_{\alpha\sigma}^S\mu_{\sigma\lambda} + \frac{1}{c^2}(u_\alpha\mu_{\lambda\sigma} + u_\lambda\mu_{\alpha\sigma})F_\sigma^S\Big]\Big\}dv\,. \tag{28}$$

The evaluation of F_α^S is not simple because the field quantities $F_{\alpha\beta}^S$ are singular in the place of the particle and — since a point particle model is used — the quantities S_α, $\mu_{\alpha\beta}$ give nonvanishing contributions only in a small vicinity of the particle. Therefore it seems to be advantageous to expand $F_{\alpha\beta}^S$ in a series near the singularity. Then the integration can be carried out easily. In the following we expand the four-potential A_α^S instead of $F_{\alpha\beta}^S$, because this seems to be more advantageous.

§ 5. The expansion of the four-potential

In order to calculate the integral defined by (28), we have to expand the quantities $F_{\alpha\beta}^S$ and A_α^S in series. We follow the method of INFELD and PLEBANSKI [14], which is briefly the following: we expand in power series the Green's function of the equation, which determines the potentials A_α^S, according to increasing powers of $\frac{1}{c}$. The four-potential will be given by its well-known integral representation.

We have thus to consider the equation

$$\Box G = -\delta(4) = -\delta^4(x_\nu - x'_\nu)\,, \tag{29}$$

where $\Box$ is the "function" of x_ν, x'_ν denotes the coordinates of the source. We are seeking the power series in $\frac{1}{c}$ of the function $G(x_\nu, x'_\nu)$ in the following form:

$$G(x_\nu, x'_\nu) = \frac{1}{c}\sum_{n=0}^{\infty} a_{2n}\frac{1}{c^{2n}} + \frac{1}{c}\sum_{n=0}^{\infty} a_{2n+1}\frac{1}{c^{2n+1}}\,. \tag{30}$$

Denote by $G^{\text{even}}(x_\nu, x'_\nu)$ the part of the Green's function that contains the even powers of $\frac{1}{c}$, and by $G^{\text{odd}}(x_\nu, x'_\nu)$ that containing odd powers of $\frac{1}{c}$ only. There-

fore

$$G^{\text{even}} = \frac{1}{c} \sum_{n=0}^{\infty} a_{2n} \frac{1}{c^{2n}}, \tag{31a}$$

$$G^{\text{odd}} = \frac{1}{c} \sum_{n=0}^{\infty} a_{2n+1} \frac{1}{c^{2n+1}}. \tag{31b}$$

Substituting the power series (31a) into (29) a differential equation is obtained for a_{2n}, which is solved by means of successive approximation. Finally G^{even} can be expressed by the power series

$$G^{\text{even}} = \frac{1}{4\pi cr} \sum_{n=0}^{\infty} \frac{r^{2n}}{2n!} \delta^{(2n)}(t - t') \frac{1}{c^{2n}}, \tag{32}$$

where $r = \left| x'_k - x_k \right|$ and

$$\delta^{(2n)}(t - t') = \frac{\partial^{2n}}{\partial t^{2n}} \delta(t - t'). \tag{33}$$

We note that in the literature this part of the Green's function is denoted usually:

$$G^{\text{even}} = \overline{D}. \tag{34}$$

In a similar manner the part of the Green's function which contains the odd powers of $\frac{1}{c}$ can be represented by the series:

$$G^{\text{odd}} = \frac{1}{2\pi rc} \sum_{n=0}^{\infty} \frac{r^{2n+1}}{\frac{1}{c^{2n+1}}(2n+1)!} \delta^{(2n+1)}(t - t'). \tag{35}$$

In the literature the usual notation is

$$G^{\text{odd}} = D. \tag{36}$$

With the help of the functions $\overline{D}$ and D one can construct the retarded Green's function in the following form:

$$D^{\text{ret}} = \overline{D} = \frac{1}{2} D = \frac{1}{4\pi c r} \sum_{n=0}^{\infty} \frac{(-1)^n}{c^n n!} r^n \delta^{(n)}(t - t'). \tag{37}$$

Making use of the retarded Green's function we are now able to calculate the retarded four-potential with the well-known integral representation:

$$A_\alpha^{S,\text{ret}} = 4\pi c \int_{-\infty}^{+\infty} dt' \int_{-\infty}^{+\infty} d^3 x' \, D^{\text{ret}}(x_k - x'_k, t - t') \varrho_\alpha(x'_k, t'), \tag{38}$$

where $\varrho(x'_k, t')$ is the complete current density vector. In our case

$$\delta_\alpha(x'_k, t') = S_\alpha(x'_k, t) + \partial'_\beta \mu_{\alpha\beta}(x'_k, t'), \tag{39}$$

where the notation $\partial'_\beta \equiv \dfrac{\partial}{\partial x'_\beta}$ is used. If we substitute (37) into (38) and perform the integration with respect to t', we obtain

$$A_\alpha^{S,\mathrm{ret}} = \sum_{n=0}^{\infty} \frac{(-1)^n}{c^4\, n!}\, \partial_t^n \int r^{n-1}\, \varrho_\alpha(x'_k\, t')\, d^3 x'. \tag{40}$$

Let us calculate the integral in (39) making use of (39):

$$\begin{aligned} &\int r^{n-1}(S_\alpha + \partial'_k \mu_{\alpha k} + \partial_4 \mu_{\alpha 4})\, d^3 x' = \\ &= \frac{e}{c}\, \frac{d\xi_\alpha}{dt}\, r^{n-1} + \partial_\beta M^*_{\alpha\beta}\, r^{n-1}, \end{aligned} \tag{41}$$

where

$$u_\alpha \frac{d\tau}{dt} = \frac{d\xi_\alpha}{dt} \equiv v_\alpha, \qquad M^*_{\alpha\beta} = M_{\alpha\beta} \frac{d\tau}{dt}. \tag{42}$$

In the integration we took into account the definitions (16) and (17), and the well-known properties of the δ-function. Comparing the expressions (40) and (41), we obtain the retarded four-potential in the form:

$$A_\alpha^{S,\mathrm{ret}} = \sum_{n=0}^{\infty} \frac{(-1)^n}{c^n\, n!}\, \partial_t^n \left(\frac{e}{c}\, v_\alpha\, r^{n-1} + \partial_\beta M^*_{\alpha\beta}\, r^{n-1} \right). \tag{43}$$

With this four-potential one can calculate the field tensor $F_{\alpha\beta}$ on the basis of eq. (18). With this in mind we can start with the evaluation of the self-force given by (28).

The only thing still remaining to be shown is that the four-potential $A_\beta^{S,\mathrm{ret}}$ given by (43) satisfies the Lorentz condition. This can be seen easily in the following way:

$$\partial_\alpha A_\alpha^{S,\mathrm{ret}} = \sum_{n=0}^{\infty} \frac{(-1)^n}{c^n\, n!} \left[\partial_t^n \left(\frac{e}{c}\, \partial_\alpha (v_\alpha\, r^{n-1}) + \partial_\alpha (\partial_\beta M^*_{\alpha\beta}\, r^{n-1}) \right) \right]. \tag{43a}$$

The second term in the sum vanishes because $M^*_{\alpha\beta}$ is antisymmetrical in the indices α and β, therefore only the first term has to be investigated. Let us

write it down in detail:

$$\partial_\alpha A_\alpha^{S,\mathrm{ret}} = \sum_{n=0}^{\infty} \frac{(-1)^n}{c^n\, n!}\, \partial_t^n \frac{e}{c} (r^{n-1}\, \partial_\alpha v_\alpha + v_\alpha \partial_\alpha r^{n-1}). \tag{43b}$$

Since v_α depends only on t, only the term with $\alpha = 4$ remains, therefore:

$$\partial_\alpha A_\alpha^{S,\mathrm{ret}} = \sum_{n=0}^{\infty} \frac{(-1)^n}{c^n n!}\, \partial_t^n \frac{e}{c} (r^{n-1}\, \partial_4 v_4 + v_k \partial_k r^{n-1} + v_4 \partial_4 r^{n-1}). \tag{43c}$$

On the other hand $v_4 = ic$, and so

$$\partial_\alpha A_\alpha^{S,\mathrm{ret}} = \sum_{n=0}^{\infty} \frac{(-1)^n}{c^n\, n!} \frac{e}{c} (v_k (n-1)\, r^{n-3} z_k - (n-1)\, r^{n-3} v_k z_k) = 0, \tag{43d}$$

where $z_k = x_k - \xi_k$. Therefore we infer that the four-potential given by (43) satisfies (19).

§ 6. The evaluation of the self-force

In this § we give the explicit form of the self-force. In order to do this we evaluate the integral, giving the self-force F_α^S in the rest system. Naturally, the final result will be expressed in covariant form.

Eq. (28), taking into account (16) and (17), gives the following equation for the self-force:

$$\begin{aligned} F_\alpha^S = \frac{dt}{d\tau} \int \left(F_{\alpha\sigma}^S \frac{e}{c} u_\sigma \delta(3) + \frac{1}{2} M_{\sigma\lambda}^* \delta(3)\, \partial_\alpha F_{\sigma\lambda} \right) dv + \\ + \frac{dt}{d\tau} \int \partial_k \left[F_{\alpha\sigma}^S M_{\sigma k}^* \delta(3) + \frac{1}{c^2} (u_\alpha M_{k\sigma}^* + u_k M_{\alpha\sigma}^*) F_\sigma^S \right] \delta(3)\, dv + \\ + \frac{dt}{d\tau} \int \partial_4 \left[F_{\alpha\sigma}^S M_{\sigma 4}^* \delta(3) + \frac{1}{c^2} (u_\lambda M_{4\sigma}^* + u_4 M_{\alpha\sigma}^*) F_\sigma^S \right] \delta(3)\, bv. \end{aligned} \tag{44}$$

The second term on the right-hand side of (44) can be transformed with the help of Gauss's theorem into a surface integral. If the surface tends to infinity, then the value of the integral depends on the values that the $\delta(3)$ function and the field tensor $F_{\alpha\beta}^S$ take in inifinity. The δ-function vanishes everywhere except at the location of its singularity, and the functions $F_{\alpha\beta}^S$ tend to zero if the surface tends to infinity. Therefore this integral vanishes.

Now let us write the eq. (44) in the rest system:

$$F_\alpha^S = \int \left(ie\, F_{\alpha 4}^S \delta(3) + \frac{1}{2} M_{ik}^* \partial_\alpha F_{ik}^s \delta(3) \right) dv +$$
$$+ \int \left(-\frac{i}{c} \dot{M}_{k4}^* F_{\alpha k}^S + \frac{i}{c} \delta_{\alpha 4} \dot{M}_{4i}^* F_{i4}^S + \frac{i}{c} \dot{M}_{\alpha i}^* F_{i4}^S + \right. \tag{45}$$
$$\left. + \frac{i}{c} M_{\alpha k}^* \dot{F}_{k4}^S + \frac{1}{c^2} M_{\alpha i}^* F_{ik}^S \dot{v}_k \right) \delta(3)\, dv.$$

The self-force can be decomposed into spatial and time-like parts. The spatial components are

$$F_l^S = \int \left(ie\, F_{l4}^S + \frac{1}{2} M_{ik}^* \partial_l F_{ik}^S - \frac{i}{c} \dot{M}_{k4}^* F_{l4}^S \right) \delta(3)\, dv +$$
$$+ \int \left(\frac{i}{c} \dot{M}_{li}^* F_{i4}^S + \frac{i}{c} M_{lk}^* \dot{F}_{k4}^S + \frac{1}{c^2} M_{li}^* F_{ik}^S \dot{v}_k \right) \delta(3)\, dv, \tag{46a}$$

and the time-like component is

$$F_4^S = \frac{1}{2} \int \left(M_{ik}^* \partial_4 F_{ik}^S + \frac{i}{c} \dot{M}_{4i}^* F_{i4}^S \right) \delta(3)\, dv. \tag{46b}$$

From now on we omit the notations "ret" and "proper" because of the accumulation of the indices. The evaluation will proceed in the following way. Substituting the series (43) of $A_\alpha^{S,\,\mathrm{ret}}$ into (46a) and (46b), and carrying out the prescribed operations one arrives at the final form of the self-force i. e. the term proportional to $\frac{1}{c^0}$, that proportional to $\frac{1}{c}$, etc. of the power series of the four-potential are determined. In each step we thus calculate the contribution to the self-force and obtain the approximations $\underset{0}{F_\alpha^S}$, $\underset{1}{F_\alpha^S}$, $\underset{2}{F_\alpha^S}$, ... one after the other. (Naturally, ordered according to the increasing powers of $\frac{1}{c}$.) The great number of terms that appear in each step of the approximation involves, however, uncertainty in the evaluation, therefore a more concise and shorter procedure will be followed.

Carrying out the differentiations with respect to the spatial coordinates and considering an arbitrary term of the self-force F_α^S, we obtain terms of the following type:

$$\partial_t^n r^n,\ \partial_t^n r^{n-1}, \ldots,\ \partial_t^n r^{n-7}, \tag{47}$$

or putting it in a more concise form:

$$\partial_t^n r^{n-\varrho}, \tag{48}$$

where $\varrho = 0, 1, 2, 3, 4, 5, 6, 7$. After having carried out the differentiations with respect to the time, we get

$$\begin{aligned}
\partial_t^n r^{n-\varrho} = {} & A_n (-1)^n r^{n-\varrho-2n+n} v_n e_n v_{n-1} e_{n-1} \ldots v_1 e_1 + \\
& + A_{n-1} (-1)^{n-1} r^{n-\varrho-2(n-1)+n-1} \big(v_{n-1} e_{n-1} \ldots \partial_t (v_1 z_1) + \ldots + \\
& + \partial_t (v_{n-1} z_{n-1} \ldots v_1 z_1)\big) + \\
& + A_{n-2} (-1)^{n-2} r^{n-\varrho-2(n-2)+n-2} (v_{n-2} e_{n-2} \ldots \partial_t^2 (v_1 z_1) + \ldots + \\
& + v_{n-2} e_{n-2} \ldots \partial_t \big(v_2 z_2 \partial_t (v_1 z_1)\big) + \ldots + \\
& + \partial_t^2 \big(v_{n-2} z_{n-2} \ldots (v_1 z_1)\big) + \ldots + \\
& + A_i (-1)^i r^{n-\varrho-2i+l} \big(v_i e_i \ldots \partial_t^{n-i} (v_1 z_1) + \ldots + \\
& + v_i e_i \ldots \partial_t^{k1} (v_i z_i \ldots \partial_t^{k2} (v_m z_m \ldots \partial_t^{k3} (v_s z_s \ldots \partial_t^{kp} (v_1 z_1))))\big) + \\
& + A_1 (-1) r^{n-\varrho-2+l} \partial_t^{n-1} (v_1 z_1).
\end{aligned} \tag{49}$$

Here the following notations have been used: $A_n, A_{n-1}, \ldots, A_1$ denote the constants due to the differentiations with respect to the time, their indices refer to the number of differentiations performed on $r^{n-\varrho}$; z_i denotes the vector $x_i - \xi_i$, while $e_i = \dfrac{x_i - \xi_i}{|x_i - \xi_i|}$. Because of the accumulation of the indices we have introduced the simplification that the indices occurring twice imply summation and at the same time indicate the number of the differentiations, e. g.:

$$v_{n-1} e_{n-1} = v_{n-1_1} e_{n-1_1} + v_{n-1_2} e_{n-1_2} + v_{n-1_3} e_{n-1_3}, \tag{50}$$

further instead of the vectors $r^{n-\varrho}$ which occur after the differentiations of z_i we use the unit vectors built of them, if they themselves are not differentiated with respect to t. We note that

$$\sum_{S=0}^{p} k_S = n - i, \tag{51}$$

and l gives the number of the unit vectors. In order to determine the nonvanishing terms in the expression of the self-force we go over to the polar coordinate form of the $\delta(3)$-function

$$\begin{aligned}
& \int_{-\infty}^{+\infty}\int\int f(x_k, t)\, \delta(x_1 - \xi_1) \ldots \delta(x_3 - \xi_3)\, dx_1\, dx_2\, dx_3 = \\
& \qquad = \frac{1}{4\pi} \int_0^{\infty} \int_0^{4\pi} f(r, \Omega, t)\, \delta(r)\, dr\, d\Omega,
\end{aligned} \tag{52}$$

where $f(r, \Omega, t)$ represents any one of the terms of the type $M^*_{\alpha\beta} F^S_{\beta\varrho}$ which appear in the equation of the self-force, and Ω is the solid angle.

In connection with the integration of the unit vectors appearing after the differentiation with respect to time and their spatial coordinates, we note the following. It is easy to demonstrate the validity of the following statement: If $e_i e_j \ldots e_k$ is a product of n unit vector components, and n is odd, the integral vanishes; and in the case of even n:

$$\frac{1}{4\pi}\int_0^{4\pi} e_i e_k \, d\Omega = \frac{1}{3}\delta_{ik},$$

$$\frac{1}{4\pi}\int_0^{4\pi} e_i e_k e_l e_S \, d\Omega = \frac{1}{3\cdot 5}(\delta_{ik}\delta_{lS} + \delta_{il}\delta_{kS} + \delta_{iS}\delta_{kl}),$$

$$\begin{aligned}\frac{1}{4\pi}\int_0^{4\pi} e_i e_k e_l e_m e_n e_S \, d\Omega = \frac{1}{3\cdot 5\cdot 7}[&\delta_{ik}(\delta_{lm}\delta_{nS}+\delta_{ln}\delta_{mS}+\delta_{lS}\delta_{mn})+\\ &+\delta_{il}(\delta_{km}\delta_{nS}+\delta_{kn}\delta_{mS}\delta_{mn})+\ldots+\\ &+\delta_{iS}(\delta_{kl}\delta_{mn}+\delta_{km}\delta_{ln}+\delta_{kn}\delta_{em})],\end{aligned} \tag{53}$$

where δ_{ik} is the Kronecker symbol.

Now we are ready to calculate the self-force making use of the results of eqs. (49), (52), and (53).

First of all we have to investigate, for what n the different terms in (47) give a nonvanishing contribution. These terms can be found with the help of (49). As it was mentioned before, the evaluation is carried through in the reference system S^0, which is a rest system at the time τ. This system is characterized by the fact that the spatial components of the velocity four-vector u_α vanish. Therefore in the eq. (49) only those terms remain in which the second, third, and higher derivatives of the velocity with respect to time are involved as factors. The eq. (49) shows that the first nonvanishing term occurs if $n = 2i$. On the other hand we have to take into account the properties (53) of the products of the unit vector components, and the fact that the $\delta(3)$ function is used to give the position of the particle in the argument of the integrand. Therefore the powers of the function $r^j = |x_n - \xi_k|^j$ with positive exponents give zero except for the case $j = 0$.

In the following we give the detailed evaluation of the self-force, where the contributing terms are selected by the principles stated above. Naturally, we have to take into account also FRENKEL's condition (12) and the constancy

of the length of the velocity four-vector in the following way:

$$
\begin{aligned}
&M_{\alpha\beta}\, u_\beta = 0,\\
&\dot{M}_{\alpha\beta}\, u_\beta + M_{\alpha\beta}\, \dot{u}_\beta = 0,\\
&\ddot{M}_{\alpha\beta}\, u_\beta + 2\dot{M}_{\alpha\beta}\, \dot{u}_\beta + M_{\alpha\beta}\, \ddot{u}_\beta = 0,\\
&\dddot{M}_{\alpha\beta}\, u_\beta + 3\ddot{M}_{\alpha\beta}\, \dot{u}_\beta + 3\dot{M}_{\alpha\beta}\, \ddot{u}_\beta + M_{\alpha\beta}\, \dddot{u}_\beta = 0,\\
&M^{(4)}_{\alpha\beta}\, u_\beta + 4\dddot{M}_{\alpha\beta}\, \dot{u}_\beta + 6\ddot{M}_{\alpha\beta}\, \ddot{u}_\beta + 4\dot{M}_{\alpha\beta}\, \dddot{u}_\beta + M_{\alpha\beta}\, u^{(4)}_\beta = 0,
\end{aligned}
\tag{54}
$$

and

$$
\begin{aligned}
&u_\alpha\, u_\alpha = -c^2,\\
&\dot{u}_\alpha\, u_\alpha = 0,\\
&\ddot{u}_\alpha\, u_\alpha + \dot{u}_\alpha\, \dot{u}_\alpha = 0,\\
&\dddot{u}_\alpha\, u_\alpha + 3\ddot{u}_\alpha\, \dot{u}_\alpha = 0,\\
&u^{(4)}_\alpha\, u_\alpha + 4\dddot{u}_\alpha\, \dot{u}_\alpha + 3\ddot{u}_\alpha\, \ddot{u}_\alpha = 0.
\end{aligned}
\tag{55}
$$

As the evaluation is carried out in the rest system S^0, the nonvanishing terms have to be written in a covariant form. For this purpose we require the various derivatives of the expressions $\varkappa = (1 - \frac{v^2}{c^2})^{-1/2}$, $\varkappa^{-1}$, the velocity four-vector u_α and the $M^*_{\alpha\beta}$ with respect to the proper time. In the order of this enumeration, in the rest system these are given by

$$
\begin{aligned}
&\frac{d}{dt}\left(1 - \frac{v^2}{c^2}\right)^{-\frac{1}{2}} = 0,\\
&\frac{d^2}{dt^2}\left(1 - \frac{v^2}{c^2}\right)^{-\frac{1}{2}} = \frac{1}{c^2}\,(\dot{v}_S\, \dot{v}_S),\\
&\frac{d^3}{dt^3}\left(1 - \frac{v^2}{c^2}\right)^{-\frac{1}{2}} = \frac{3}{c^2}\,(\ddot{v}_S\, \dot{v}_S),\\
&\frac{d^4}{dt^4}\left(1 - \frac{v^2}{c^2}\right)^{-\frac{1}{2}} = \frac{1}{c^2}\left[4(\dddot{v}_S\, \dot{v}_S) + 3(\ddot{v}_S\, \ddot{v}_S) + \frac{9}{c^2}\,(\dot{v}_S\, \dot{v}_S)^2\right].
\end{aligned}
\tag{56}
$$

$$
\begin{aligned}
&\frac{d}{dt}\left(1 - \frac{v^2}{c^2}\right)^{\frac{1}{2}} = 0,\\
&\frac{d^2}{dt^2}\left(1 - \frac{v^2}{c^2}\right)^{\frac{1}{2}} = -\frac{1}{c^2}\,(\dot{v}_S\, \dot{v}_S),\\
&\frac{d^3}{dt^3}\left(1 - \frac{v^2}{c^2}\right)^{\frac{1}{2}} = -\frac{3}{c^2}\,(\ddot{v}_S\, \dot{v}_S),\\
&\frac{d^4}{dt^4}\left(1 - \frac{x^2}{c^2}\right)^{\frac{1}{2}} = -\frac{1}{c^2}\left[4(\dddot{v}_S\, \dot{v}_S) + 3(\ddot{v}_S\, \ddot{v}_S) + \frac{3}{c^2}\,(\dot{v}_S\, \dot{v}_S)^2\right].
\end{aligned}
\tag{57}
$$

The derivatives of the velocity four-vector in the rest system are:

$$
\begin{aligned}
&u_\alpha\,(0,\,ic),\\
&\dot{u}_\alpha\,(v_k\,0),\\
&\ddot{u}_\alpha\left(\ddot{v}_k,\ \frac{i}{c}\,(\dot{v}_S\,\dot{v}_S)\right),\\
&\dddot{u}_\alpha\left(\dddot{v}_k+\frac{4}{c^2}\,\dot{v}_k\,(\dot{v}_S\,\dot{v}_S),\quad \frac{3i}{c}\,(\ddot{v}_S\,\dot{v}_S)\right),\\
&u_\alpha^{(4)}\left(v_k^{(4)}+\frac{10}{c^2}\,\ddot{v}_k\,(\dot{v}_S\,\dot{v}_S)+\frac{15}{c^2}\,\dot{v}_k\,(\ddot{v}_S\,\dot{v}_S)\,\frac{i}{c}\left[4(\dddot{v}_S\,\dot{v}_S)+\right.\right.\\
&\qquad\left.\left.+\,3(\ddot{v}_S\,\ddot{v}_S)+\frac{13}{c^2}\,(\dot{v}_S\,\dot{v}_S)^2\right]\right).
\end{aligned}
\tag{58}
$$

Making use of eq. (57), the derivatives of the tensor $M^*_{\alpha\beta}$ with respect to the proper time can be written in the rest system in the form:

$$
\begin{aligned}
&\frac{d}{dt}\,M^*_{\alpha\beta}=\dot{M}_{\alpha\beta},\\
&\frac{d^2}{dt^2}\,M^*_{\alpha\beta}=\ddot{M}_{\alpha\beta}-\frac{1}{c^2}\,M_{\alpha\beta}\,(\dot{v}_S\,\dot{v}_S),\\
&\frac{d^3}{dt^2}\,M^*_{\alpha\beta}=\dddot{M}_{\alpha\beta}-\frac{3}{c^2}\,\dot{M}_{\alpha\beta}\,(\dot{v}_S\,\dot{v}_S)-\frac{3}{c^2}\,M_{\alpha\beta}\,(\ddot{v}_S\,\dot{v}_S),\\
&\frac{d^4}{dt^4}\,M^*_{\alpha\beta}=M^{(4)}_{\alpha\beta}-\frac{6}{c^2}\,\ddot{M}_{\alpha\beta}(\dot{v}_S\,\dot{v}_S)-\frac{12}{c^2}\,\dot{M}_{\alpha\beta}\,(\ddot{v}_S\,\dot{v}_S)\\
&\qquad-\frac{1}{c^2}\,M_{\alpha\beta}\left[4(\dddot{v}_S\,\dot{v}_S)+3(\ddot{v}_S\,\ddot{v}_S)+\frac{3}{c^2}\,(\dot{v}_S\,\dot{v}_S)^2\right].
\end{aligned}
\tag{59}
$$

These equations have the covariant form:

$$
\begin{aligned}
&\dot{M}_{\alpha\beta},\\
&\ddot{M}_{\alpha\beta}-\frac{1}{c^2}\,M_{\alpha\beta}\,(\dot{u}_\nu\,\dot{u}_\nu),\\
&\dddot{M}_{\alpha\beta}-\frac{3}{c^2}\,\dot{M}_{\alpha\beta}\,(\dot{u}_\nu\,\dot{u}_\nu)-\frac{3}{c^2}\,M_{\alpha\beta}\,(\ddot{u}_\nu\,\dot{u}_\nu),\\
&M^{(4)}_{\alpha\beta}-\frac{6}{c^2}\,\ddot{M}_{\alpha\beta}\,(\dot{u}_\nu\,u_\nu)-\frac{3}{c^2}\,\dot{M}_{\alpha\beta}\,(\ddot{u}_\nu\,\dot{u}_\nu)-\\
&\qquad-\frac{1}{c^2}\,M_{\alpha\beta}\left(4(\dddot{u}_\nu\,\dot{u}_\nu)+3(\ddot{u}_\nu\,\ddot{u}_\nu)-\frac{10}{b^2}\,(\dot{u}_\nu\,\dot{u}_\nu)^2\right).
\end{aligned}
\tag{60}
$$

On the right-hand side of the equations the dots denote differentiations with respect to the proper time. We require further that

$$M_{\alpha\beta} M_{\alpha\beta} = b^2, \tag{61}$$

where b^2 is a constant. Differentiating the eq. (61) with respect to the proper time, we obtain the following relations:

$$\begin{aligned} &M_{\alpha\beta} \dot{M}_{\alpha\beta} = b_1^2 = 0, \\ &\ddot{M}_{\alpha\beta} M_{\alpha\beta} + \dot{M}_{\alpha\beta} \dot{M}_{\alpha\beta} = b_2^2 + b_3^2 = 0, \\ &\dddot{M}_{\alpha\beta} M_{\alpha\beta} + 3\ddot{M}_{\alpha\beta} \dot{M}_{\alpha\beta} = b_4^2 + 3b_5^2 = 0, \\ &M^{(4)}_{\alpha\beta} M_{\alpha\beta} + 4\dddot{M}_{\alpha\beta} \dot{M}_{\alpha\beta} + 3\ddot{M}_{\alpha\beta} \ddot{M}_{\alpha\beta} = b_6^2 + 4b_7^2 + 3b_8^2 = 0. \end{aligned} \tag{61a}$$

Considering the integral giving the self-force, we see that the terms which appear in it are of the type:

$$\partial_t^n r^n, \ldots, \partial_t^n r^{n-7}. \tag{62}$$

We should like to know, which of these terms give a nonvanishing contribution if we take into account that the diameter of the particle is zero. It follows that terms, multiplied by r^l give zero, if $l > 0$.

Consider the term $\partial_t^n r^{n-7}$. As it was mentioned already, we obtain a nonzero contribution if $n = 2i$, where i is the number of the differentiations performed on r^{n-7}. In this case we have

$$r^{n-7-2i+i} = r^{i-7}.$$

We see that while $i = 0, 1, 2, 3, 4, 5, 6, 7$, n may take the values $n = 0, 2$' 4, 6, 8, 10, 12, 14. Consider now the case, when $i < n - i \equiv t$ i. e. $t = i + k^*$' where $k^* > 0$. This means that we envisage the term of the type:

$$A_i (-1)^i r^{n-7-2i+l} [\partial_t^{n-i} (v_i z_i \ldots v_1 z_1) + \ldots + v_i z_i \ldots \partial_t^{n-i} (v_1 z_1]. \tag{63}$$

Let us decompose the differentiation in the following way:

$$\partial_t^{n-i} = \partial_t^i \partial_t^{K*}. \tag{64}$$

We see that a term of the type (63) does not vanish in the rest system if all the v_i-s are differentiated at least once with respect to time. Eq. (64) shows that this condition can be satisfied easily, moreover "superfluous" differentiations remain. These will be used either for the differentiations of v_i-s,

or for the differentiations of the z_i-s. It can be seen that the index l gives the number of the unit vectors in the exponent of r, and its value depends on whether we differentiate v_i or z_i. Therefore the exponent of r takes the form:

$$n - 7 - 2i + l = k^* + l - 7\,,$$

because $n = 2i + k^*$. In this case the following possibilities occur:

$$\begin{array}{llll} k^* = 1 & l = 1, 2, 3, 4, 5, 6 & l = i & n = 3, 5, 7, 9, 11, 13, \\ k^* = 2 & l = 0, 1, 2, 3, 4, 5 & l = i & n = 4, 6, 8, 10, 12, \\ k^* = 3 & l = 0, 1, 2, 3, 4 & l = i & n = 5, 7, 9, 11, \\ & & l = i - 1 & n = 4, 6, 8, 10, 12, 14, \\ & & l = i - 1 & n = 5, 7, 9, 11, 13, \end{array}$$

$$\begin{array}{llll} k^* = 4 & l = 0, 1, 2, 3 & l = i & n = 6, 8, 10 \\ & & l = i - 2 & n = 8, 10, 12, 14, \\ k^* = 5 & l = 0, 1, 2 & l = 1 & n = 7, 9 \\ & & l = i - 2 & n = 9, 11, 13, \\ k^* = 6 & l = 0, 1 & l = i & n = 8 \\ & & l = i - 2 & n = 10, 12 \\ k^* = 7 & l = 0 & & \\ & & l = i - 2 & n = 11 \end{array} \qquad \begin{array}{l} l = i - 1 \;\; n = 6,8,10,11, \\ \\ l = i - 1 \;\; n = 7, 9, 11, \\ \\ l = i - 1 \;\; n = 8, 10, \\ l = i - 3 \;\; n = 12, 14 \\ l = i - 1 \;\; n = 9 \\ l = i - 3 \;\; n = 13. \end{array} \quad (65)$$

From the definition of the vector z_i follows that its derivatives with respect to time t are

$$\dot{z}_i = -v_i, \quad \ddot{z}_i = -\dot{v}_i, \ldots \tag{66}$$

On the basis of completely analogous considerations we obtain the other terms too.

Now we are able to give the nonvanishing terms of the self-force. Its spatial part was given by (46a). Let us consider it in detail:

$$\begin{aligned} F_l^S = & ie \int F_{l4}^S \delta(3)\, dv + \frac{1}{2} M_{ik} \int \partial_l F_{ik}^S \delta(3)\, dv + \\ & - \frac{i}{c} \dot{M}_{k4} \int F_{lk}^S \delta(3)\, dv + \frac{i}{c} \dot{M}_{lk} \int F_{k4}^S \delta(3)\, dv + \\ & + \frac{i}{c} M_{lk} \int \dot{F}_{k4}^S \delta(3)\, dv + \frac{1}{c^2} M_{li} \dot{v}_k \int F_{ik}^S \delta(3)\, dv, \end{aligned} \tag{67}$$

The fourth component of the self-force from (46b) is:

$$F_4^S = -\frac{i}{2c} M_{ik} \int \dot{F}_{ik}^S \delta(3)\, dv - \frac{i}{c} \dot{M}_{k4} \int F_{k4}^S \delta(3)\, dv. \tag{68}$$

Note that not all the terms of the self-force need be calculated. It can be seen that the calculation of the first term in (67) makes the evaluation of the fourth term of (67) and of the second term of (68) superfluous. In the same way it is sufficient to determine the third term in (67), because knowing this the sixth term can be written down easily. Therefore, we have to calculate only the first, second, third and fifth term of (67) and the first term of (68). The first term is

$$B_\alpha = ie \int F_{\alpha 4}\, \delta(3)\, dv. \tag{69}$$

It can be seen that the fourth component of B_α is zero. Substituting the four-potential given by (43) into (69), we obtain

$$\begin{aligned} B_l = ie \sum_{n=0}^{\infty} \frac{(-1)^n}{c^n\, n!} \int \Big[& \partial_t^n \left(ie \partial_l r^{n-1} + M_{4k}^* \partial_k \partial_l r^{n-1} \right) - \\ & - \frac{1}{ic} \partial_t^{n+1} \left(\frac{e}{c} v_l r^{n-1} + M_{lk}^* \partial_k r^{n-1} + \right. \\ & \left. + \frac{1}{ic} \dot{M}_{l4}^* r^{n-1} - \frac{1}{ic} M_{l4}^* v_i \partial_i r^{n-1} \right) \Big] \delta(3)\, dv. \end{aligned} \tag{70}$$

Performing now the prescribed spatial differentiations, we obtain only terms of the type appearing also in (47), therefore their value can be determined by the method described above. The result of the lengthy but elementary calculation is:

$$\begin{aligned} B_l = {} & e_2 \left(-\frac{2}{3c^2 r} \dot{v}_l + \frac{2}{3c^3} \ddot{v}_l \right) + ie \left(\frac{1}{3c^2 r} \ddot{M}_{4l}^* - \right. \\ & \left. - \frac{1}{3c^3} \dddot{M}_{4l}^* \right) - e \left(-\frac{1}{3c^3 r} M_{lk} \ddot{v}_k - \frac{1}{c^3 r} \dot{M}_{lk} \dot{v}_k + \right. \\ & + \frac{1}{3c^4} M_{lk} \dddot{v}_k + \frac{4}{3c^4} \dot{M}_{lk} \ddot{v}_k + \frac{2}{c^4} \ddot{M}_{lk}^* \dot{v}_K + \\ & \left. + \frac{1}{c^6} M_{lk} \dot{v}_k (\dot{v}_S \dot{v}_S) \right) + \\ & + e \left(\frac{i}{c^2 r} \ddot{M}_{l4}^* + \frac{1}{ic^3} \dddot{M}_{l4}^* + \frac{5}{c^6} M_{lk} \dot{v}_k (\dot{v}_S \dot{v}_S) \right). \end{aligned} \tag{71}$$

The covariant form of (71) is:

$$B_\alpha = e^2\left(-\frac{2}{3c^2 r}\dot{u}_\alpha + \frac{2}{3c^3}\left(\ddot{u}_\alpha - \frac{1}{c^2}u_\alpha(\dot{u}_\nu \dot{u}_\nu)\right)\right) -$$
$$- \frac{7}{c^6} M_{\alpha\varrho}\dot{u}_\varrho(\dot{u}_\nu \dot{u}_\nu) + \frac{2e}{3c^3 r}\ddot{M}_{\alpha\varrho}u_\varrho - \frac{2e}{3c^4}\dddot{M}_{\alpha\varrho}u_\varrho +$$
$$+ \frac{e}{3c^3 r}M_{\alpha\varrho}\ddot{u}_\varrho - \frac{e}{3c^4}M_{\alpha\varrho}\dddot{u}_\varrho + \frac{e}{c^3 r}\dot{M}_{\alpha\varrho}\dot{u}_\varrho - \tag{72}$$
$$- \frac{4e}{3c^4}\dot{M}_{\alpha\varrho}\ddot{u}_\varrho - \frac{4e}{3c^6}u_\alpha u_\nu \dot{M}_{\nu\varrho}\ddot{u}_\varrho -$$
$$- \frac{2e}{c^4}\ddot{M}_{\alpha\varrho}\dot{u}_\varrho - \frac{2e}{c^6}u_\alpha u_\nu \ddot{M}_{\nu\varrho}\dot{u}_\varrho,$$

where the dot means differentiation with respect to the proper time. In the equation (72) we have taken into account the relations (54) and (60). We see, that if the particle has only charge, we obtain the known result.

The other terms of the self-force can also be determined in a similar way, new problems do not arise anywhere. The terms will be denoted by the letters of the alphabet:

$$C_\alpha = \frac{e}{3c^3 r}M_{\alpha\beta}\ddot{u}_\beta - \frac{e}{3c^4}M_{\sigma\beta}\dddot{u}_\beta + \frac{e}{3c^6}M_{\alpha\beta}\dot{u}_\beta(\dot{u}_\nu \dot{u}_\nu) +$$
$$+ \frac{2e}{3c^6}\dot{M}_{\nu\varrho}u_\nu \ddot{u}_\varrho u_\alpha + \frac{u_\alpha}{c^6 r}\left[\frac{21}{10}M_{\varrho\nu}\dot{u}_\nu \ddot{M}_{\varrho\omega}u_\omega +\right.$$
$$\left. + \frac{19}{30}M_{\varrho\nu}u_\nu \dot{M}_{\varrho\beta}\dot{u}_\beta - \frac{41}{15}M_{\beta\varrho}M_{\beta\varrho}(\ddot{u}_\nu \dot{u}_\nu)\right] +$$
$$+ \frac{u_\alpha}{c^5}\left[-\frac{7}{3c^4}M_{\varrho\nu}\dot{u}_\nu M_{\varrho\beta}\dot{u}_\beta(\dot{u}_\nu \dot{u}_\nu) + \frac{19}{15c^2}M_{\varrho\nu}M_{\varrho\nu}(\dddot{u}_\nu \dot{u}_\nu) -\right.$$
$$- \frac{7}{3c^2}\dot{M}_{\varrho\nu}u_\nu M_{\varrho\beta}\dddot{u}_\beta - \frac{1}{3c^2}\ddot{M}_{\beta\varrho}M_{\beta\varrho}(\dot{u}_\nu \dot{u}_\nu) -$$
$$- \frac{4}{c^2}\ddot{M}_{\varrho\nu}u_\nu M_{\varrho\beta}\ddot{u}_\beta - \frac{6}{c^2}M_{\varrho\beta}\dot{u}_\beta \ddot{M}_{\varrho\nu}\dot{u}_\nu -$$
$$\left. - \frac{214}{35c^4}M_{\varrho\nu}M_{\varrho\nu}(\dot{u}_\nu \dot{u}_\nu)^2 + \frac{1}{3c^2}M_{\varrho\nu}M_{\varrho\nu}(\ddot{u}_\nu \ddot{u}_\nu) - \frac{1}{3}M^{(4)}_{\beta\varrho}M_{\beta\varrho}\right] +$$
$$+ \frac{\dot{u}_\alpha}{rc^4}\left[\frac{1141}{40c^2}M_{\varrho\nu}M_{\varrho\nu}(\dot{u}_\nu \dot{u}_\nu) - \frac{691}{280c^2}M_{\beta\nu}\dot{u}_\nu M_{\beta\varrho}\dot{u}_\varrho -\right.$$

$$-\frac{13}{15}\ddot{M}_{\varrho\nu}M_{\varrho\nu}\Big]+\frac{\dot{u}_\alpha}{c^5}\Big[-\frac{4}{3c^2}M_{\varrho\nu}\dot{u}_\nu M_{\varrho\beta}\ddot{u}_\beta-$$

$$-\frac{6}{c^2}M_{\varrho\nu}\dot{u}_\nu\dot{M}_{\varrho\beta}\dot{u}_\beta+\frac{6}{5c^2}M_{\varrho\nu}M_{\varrho\nu}(\ddot{u}_\nu\dot{u}_\nu)-$$

$$-\frac{1}{15}\dddot{M}_{\varrho\nu}M_{\varrho\nu}+\frac{2}{c^2}\dot{M}_{\varrho\nu}u_\nu\ddot{M}_{\varrho\beta}u_\beta-\frac{4}{c^2}M_{\varrho\nu}\dot{u}_\nu\ddot{M}_{\varrho\beta}u_3\Big]+$$

$$+\frac{\ddot{u}_\alpha}{c^5}\Big[\frac{2}{3c^2}M_{\varrho\nu}\dot{u}_\nu M_{\varrho\beta}\dot{u}_\beta+\frac{1}{3c^2}M_{\varrho\nu}M_{\varrho\nu}(\dot{u}_\nu\dot{u}_\nu)- \tag{73}$$

$$-\frac{2}{3}\ddot{M}_{\varrho\nu}M_{\varrho\nu}\Big]+\frac{\dddot{u}_\alpha}{c^4r}\frac{1}{15}M_{\varrho\nu}M_{\varrho\nu}-\frac{u_\alpha^4}{15c^5}M_{\varrho\nu}M_{\varrho\nu}-$$

$$-\frac{2}{15c^4r}M_{\alpha\beta}M_{\beta\varrho}\dddot{u}_\varrho-\frac{4}{15c^4r}\dot{M}_{\alpha\beta}M_{\beta\varrho}\ddot{u}_\varrho-$$

$$-\frac{13}{15c^4r}M_{\alpha\beta}\ddot{M}_{\beta\varrho}\dot{u}_\varrho-\frac{3299}{60c^6r}M_{\alpha\beta}M_{\beta\varrho}\dot{u}_\varrho(\dot{u}_\nu\dot{u}_\nu)-$$

$$-\frac{1}{2c^4r}M_{\alpha\beta}\dddot{M}_{\beta\varrho}u_\varrho+\frac{2}{15c^5}M_{\alpha\varrho}M_{\varrho\beta}u_\beta^{(4)}+$$

$$+\frac{1}{3c^5}\dot{M}_{\alpha\beta}M_{\beta\varrho}\dddot{u}_\varrho+\frac{2}{c^5}\ddot{M}_{\alpha\beta}M_{\beta\varrho}\ddot{u}_\varrho+\frac{2}{3c^5}\dddot{M}_{\alpha\beta}M_{\beta\varrho}\dot{u}+$$

$$+\frac{5}{12c^5}M_{\alpha\beta}\dot{M}_{\beta\varrho}\dddot{u}_\varrho+\frac{2}{3c^5}M_{\alpha\beta}\ddot{M}_{\beta\varrho}\ddot{u}_\varrho+$$

$$+\frac{2}{3c^5}M_{\alpha\beta}\dddot{M}_{\beta\varrho}\dot{u}_\varrho+\frac{1}{3c^5}M_{\alpha\varrho}M_{\varrho\nu}^{(4)}u_\nu-\frac{4}{c^7}M_{\alpha\beta}M_{\beta\varrho}\ddot{u}_\varrho(\dot{u}_\nu\dot{u}_\nu)-$$

$$-\frac{11}{4c^7}M_{\alpha\beta}M_{\beta\varrho}\dot{u}_\varrho(\ddot{u}_\nu\dot{u}_\nu)-\frac{10}{3c^7}\dot{M}_{\alpha\beta}M_{\beta\varrho}\dot{u}_\varrho(\dot{u}_\nu\dot{u}_\nu)-$$

$$-\frac{11}{3c^7}M_{\alpha\beta}\dot{M}_{\beta\varrho}\dot{u}_\varrho(\dot{u}_\nu\dot{u})-\frac{1}{3c^7}M_{\alpha\beta}\ddot{M}_{\beta\varrho}u_\varrho(\dot{u}_\nu\dot{u}_\nu)+$$

$$+\frac{12u_\alpha}{c^9}M_{\varrho\nu}\dot{u}_\nu\dot{M}_{\varrho\beta}\dot{u}_\beta(\dot{u}_\nu\dot{u}_\nu+\frac{13}{15c^6r}\dot{u}_\alpha M_{\varrho\nu}M_{\varrho\nu}(\dot{u}_\nu\dot{u}_\nu).$$

$$D_\alpha=-\frac{2e}{3c^3r}\dot{M}_{\alpha\varrho}\dot{u}_\varrho+\frac{2e}{3c^4}\dot{M}_{\alpha\varrho}\ddot{u}_\varrho-\frac{2e}{3c^6}\dot{M}_{\alpha\varrho}u_\varrho(\dot{u}_\nu\dot{u})-$$

$$-\frac{e}{3c^6}u_\alpha u_\nu\dot{M}_{\nu\varrho}\ddot{u}_\varrho-\frac{1}{3c^4}\dot{M}_{\alpha\varrho}M_{\varrho\beta}\ddot{u}_\beta-$$

$$- \frac{1}{3c^4 r} \dot{M}_{\alpha\beta} \dot{M}_{\beta\varrho} \dot{u}_\varrho + \frac{2}{3c^5} \left[\dot{M}_{\alpha\beta} \dot{M}_{\beta\varrho} \ddot{u}_\varrho + \right.$$

$$\left. + \frac{1}{c^2} \dot{M}_{\alpha\lambda} u_\lambda \dot{M}_{\beta\varrho} \ddot{u}_\varrho u_\beta \right] + \frac{1}{3c^5} \dot{M}_{\alpha\beta} M_{\beta\varrho} \dddot{u}_\varrho + \tag{74}$$

$$+ \frac{u_\alpha}{c^6 r} \left[\frac{1}{3} M_{\varrho\beta} \dot{u}_\beta \dot{M}_{\varrho\nu} \dot{u}_\nu - \frac{1}{3} M_{\varrho\nu} \dot{u}_\nu \dot{M}_{\varrho\beta} u_\eta \right] +$$

$$+ \left[\frac{2}{3} M_{\varrho\nu} \dot{u}_\nu \dot{M}_{\varrho\beta} \ddot{u}_\beta + M_{\varrho\nu} \dot{u}_\nu M_{\varrho\beta} \dddot{u}_\beta \right] \frac{u_\alpha}{c^7} .$$

$$E_\alpha = - \frac{11}{3c^7} \dot{M}_{\alpha\beta} M_{\beta\varrho} \dot{u}_\varrho (\dot{u}_\nu \dot{u}_\nu) - \frac{71}{8 \cdot 15 c^6 r} M_{\alpha\beta} M_{\beta\varrho} \dot{u}_\varrho (\dot{u}_\nu \dot{u}_\nu) +$$

$$+ \frac{1}{3c^7} M_{\alpha\beta} \ddot{M}_{\beta\varrho} u_\varrho (\dot{u}_\nu \dot{u}_\nu) - \frac{1}{3c^7} M_{\alpha\beta} M_{\beta\varrho} \ddot{u}_\varrho (\dot{u}_\nu \dot{u}_\nu) -$$

$$- \frac{13}{3c^7} M_{\alpha\beta} \dot{M}_{\beta\varrho} \dot{u}_\varrho (\dot{u}_\nu \dot{u}_\nu) + \frac{2}{c^7} M_{\alpha\beta} \ddot{M}_{\varrho\nu} u_\nu \dot{u}_\varrho \dot{u}_\beta +$$

$$+ \frac{1}{3c^4 r} M_{\alpha\beta} M_{\beta\varrho} \dddot{u}_\nu + \frac{4}{3c^4 r} M_{\alpha\beta} \dot{M}_{\beta\varrho} \ddot{u}_\varrho - \tag{75}$$

$$- \frac{1}{3c^5} M_{\alpha\beta} M_{\beta\varrho} u_\varrho^{(4)} - \frac{5}{3c^5} M_{\alpha\beta} \dot{M}_{\beta\varrho} \dddot{u}_\varrho +$$

$$+ \frac{3}{c^4 r} M_{\alpha\beta} \ddot{M}_{\beta\varrho} \dot{u}_\varrho - \frac{10}{3c^5} M_{\alpha\beta} \ddot{M}_{\beta\varrho} \ddot{u}_\varrho -$$

$$- \frac{10}{3c^5} M_{\alpha\beta} \dddot{M}_{\beta\varrho} \dot{u}_\varrho + \frac{2}{3c^4 r} M_{\alpha\beta} \dddot{M}_{\beta\varrho} u_\varrho - \frac{2}{3c^5} M_{\alpha\beta} M^{(4)}_{\beta\varrho} u_\varrho .$$

$$G_\alpha = \frac{2}{c^7} \dot{M}_{\varrho\nu} u_\nu M_{\varrho\beta} \dot{u}_\beta \ddot{u}_\alpha - \frac{2}{3c^7} M_{\alpha\beta} \dot{M}_{\varrho\nu} \dot{u}_\beta u_\nu \ddot{u}_\varrho +$$

$$+ \frac{1}{3c^4 r} \ddot{M}_{\alpha\beta} M_{\beta\varrho} \dot{u}_\varrho - \frac{1}{rc^4} \ddot{M}_{\alpha\beta} M_{\beta\varrho} \dot{u}_\varrho + \frac{2}{3c^5} \dddot{M}_{\alpha\beta} M_{\beta\varrho} \dot{u} +$$

$$+ \frac{4}{3c^7} M_{\alpha\beta} M_{\beta\varrho} \dot{u}_\varrho (\ddot{u}_\nu \dot{u}_\nu) - \frac{2}{3c^7} M_{\alpha\beta} M_{\varrho\nu} \dot{u}_\beta \dot{u}_\nu \ddot{u}_\varrho -$$

$$- \frac{2}{c^7} \dot{M}_{\alpha\beta} M_{\beta\varrho} \dot{u}_\varrho (\dot{u}_\nu \dot{u}_\nu) + \frac{u_\alpha}{c^9} \left(- 2 \dot{M}_{\varrho\nu} u_\nu \dot{M}_{\varrho\nu} u_\nu + \right.$$

$$\left. + 3 M_{\varrho\nu} \dot{u}_\nu \dot{M}_{\varrho\beta} u_\beta \right) (\dot{u}_\nu \dot{u}_\nu) + \frac{\dot{u}_\alpha}{c^7} \left(\frac{4}{3} M_{\varrho\nu} \dot{u}_\nu N_{\varrho\beta} \ddot{u}_\beta + \right. \tag{76}$$

$$+ 2M_{\varrho\nu}\dot{u}_\nu \dot{M}_{\varrho\beta}\dot{u}_\beta\Big) - \frac{1}{3c^6 r}\dot{u}_\alpha M_{\varrho\nu}\dot{u}_\nu M_{\varrho\iota}\dot{u}_\iota -$$

$$- \frac{5}{6c^7} M_{\varrho\nu}\dot{u}_\iota \ddot{M}_{\varrho\beta}u_\beta u_\alpha + \frac{1}{5c^6 r} M_{\alpha\beta}M_{\beta\varrho}\dot{u}_\varrho(\dot{u}_\nu \dot{u}_\nu) +$$

$$+ \frac{7}{6c^6 r} u_\alpha M_{\varrho\nu}\dot{u}_\nu \ddot{M}_{\varrho\beta}u_\beta.$$

$$H_\alpha = -\frac{2}{3c^7} M_{\alpha\alpha}M_{\varrho\nu}\dot{u}_\beta \dot{u}_\varrho \ddot{u}_\nu - \frac{1}{3c^4 r} M_{\alpha\beta}\ddot{M}_{\beta\varrho}\dot{u}_\varrho -$$

$$- \frac{1}{rc^4} M_{\alpha\beta}\ddot{M}_{\beta\varrho}\dot{u}_\varrho + \frac{2}{3c^5} M_{\alpha\beta}\dddot{M}_{\beta\varrho}\dot{u}_\varrho -$$

$$- \frac{1}{c^7} M_{\alpha\beta}\ddot{M}_{\varrho\nu}\dot{u}_\beta u_\nu \dot{u}_\varrho - \frac{1}{c^7} M_{\alpha\beta}\ddot{M}_{\nu\varrho}u_\varrho \dot{u}_\beta \dot{u}_\nu + \tag{77}$$

$$+ \frac{11}{30c^6 r} M_{\alpha\beta}M_{\beta\varrho}\dot{u}_\varrho(\dot{u}_\nu \dot{u}_\nu) - \frac{4}{3c^7} M_{\alpha\beta}M_{\beta\varrho}\dot{u}_\varrho(\ddot{u}_\nu \dot{u}_\nu) +$$

$$+ \frac{1}{c^7} M_{\alpha\beta}\dot{M}_{\beta\varrho}\dot{u}_\varrho(\dot{u}_\nu \dot{u}_\nu) + \frac{2}{c^7} M_{\alpha\beta}\ddot{M}_{\beta\varrho}u_\varrho(\dot{u}_\nu \dot{u}_\nu).$$

Our aim was to determine the effect of the self-force on the particle. The results are contained in the relations (73), (74), (75), (76) and (77). It is a remarkable fact that in the equations the divergent terms tend to infinity in the same order, and the order of the derivatives occurring is not higher than four. The possibilities of the elimination of the divergent terms will be discussed in the next paragraph.

§ 7. The elimination of the divergence of the electromagnetic mass

In the preceding chapter we have calculated the effect of the proper field on the particle. In the expression of the self-force divergent terms occur. We see that these are built up from the products of $M_{\alpha\beta}, \ldots, M^{(4)}_{\alpha\beta}$ and $u_a, \ldots, u^{(4)}_\alpha$. Now our task is to eliminate these divergencies on the basis of some convenient principles, and so to ensure that the electromagnetic mass is of finite value.

One can infer at once that all the divergent terms can be incorporated into the mass by means of the classical mass renormalization. This follows from the fact that the polarized current density four-vector is not proportional to the four-velocity and so the self-force has also components which are not parallel to the acceleration four-vector.

It is a well-known fact that the infinite value of the self-energy of a point particle is due to definition, it has no physical reason. Therefore there are different possible ways to eliminate the divergent self-energy of the point particle. For instance we can use the method proposed by PAULI and VILLARS [15] for the elimination of the divergencies in quantum electrodynamics. The main feature of this regularization theory is that it applies such regularized Green's functions with which the commutators do not become singular. It was this method by means of which WENTZEL and DIRAC obtained the equation of motion of a point particle. The main shortcoming of this method lies in its formal character and it breaks down when it is applied to the self-energy problem in the case of the scalar field. The theory of the compensating auxiliary field has more physical meaning and approaches reality better than the former. This method ensures the finite value of the self-energy by means of the introduction of an auxiliary field. A further possibility for the elimination of the divergencies is offered by the application of field equations of higher order.

The divergencies, which occur in the equation of motion will be eliminated here by means of the compensating field method. Later it will be shown that the result would be identical with that obtained if higher order field equations were applied. It should be noted that all the methods enumerated give identical results in the classical theory.

Denote by $f_{\mu\nu}$ the field tensor and by a_μ the four-potential of the compensating field. The $f_{\mu\nu}$ and a_μ be related as usual:

$$f_{\mu\nu} = \partial_\mu a_\nu - \partial_\nu a_\mu. \tag{78}$$

We have to choose $f_{\mu\nu}$ and a_μ so as to ensure that they act on the particle and cannot be radiated in the form of free waves. With a view to this the four-potential of the compensating field is chosen in the form:

$$a_\mu = \frac{1}{2}(A_\mu^{\text{ret}} + A_\mu^{\text{adv}}). \tag{79}$$

We note that we have chosen the retarded solution from among the A_μ^{ret} functions which satisfy (20) because only this one has a physical meaning. Now because of (79) the potential A_μ^{adv} has to be considered as that of a really existing physical field if we accept the method of the compensating field as a possible way for the determination of the real equation of motion. With these considerations the modified field of the particle becomes:

$$A_\mu^s = A_\mu^{\text{ret}} - a_\mu = \frac{1}{2}(A_\mu^{\text{ret}} - A_\mu^{\text{adv}}). \tag{80}$$

After this introduction we investigate whether in our case the application of only one compensating auxiliary field will be sufficient to ensure the finiteness of the electromagnetic mass. For this purpose we have to expand a_μ into a series. This has been done already for the even function given by (32), namely

$$G^{\text{even}} = \frac{1}{2}(G^{\text{ret}} + G^{\text{adv}}). \tag{81}$$

Now we can write a_μ in the form:

$$a_\mu = \sum_{n=0}^{\infty}{}' \frac{1}{2n!\, c^{2n}} \partial_t^{2n} \int r^{2n-1} \varrho_\mu (x'_k, t)\, d^3 x', \tag{82}$$

where the vector ϱ_μ is defined by (39). Making use of the relations (41) and (42) we can transform (82) into the form

$$a_\mu = \sum_{n=0}^{\infty}{}' \frac{1}{2n!\, c^{2n}} \partial_t^{2n} \left(\frac{e}{c} V_\mu r^{2n-1} + \partial_\beta M^*_{\mu\beta} r^{2n-1} \right). \tag{83}$$

Substituting (43) and (83) into (80) it can be seen at once that only the odd powers of $\frac{1}{c}$ remain. A detailed examination shows that the terms which diverge as "$\frac{1}{r}$" are always proportional to the even powers of $\frac{1}{c}$. This statement will be modified if the term which we have to evaluate has originally been multiplied by some power of $\frac{1}{c}$ in the eqs. (46a) and (46b). However, the divergent terms cancel each other even in this case.

Now we show that the same result is obtained if we use field equations of higher order. The simplest generalization, which satisfies also the symmetry conditions, has been proposed by BOPP [17] and PODOLSKY [18]. Their method is the following. The relation between the field tensor $F_{\alpha\beta}$ and the four-potential A_α is maintained, the Lorentz condition is to be satisfied, but instead of (20) an equation of the fourth order is used:

$$\left(1 - \frac{1}{K_0^2} \Box\right) \Box A_\alpha = -4\pi \varrho'_\alpha. \tag{84}$$

(If $K_0^2 = 0$, we obtain d'Alembert's equation again and in this case $\varrho'_\alpha \equiv \varrho_\alpha$.) The solution of the eq. (84) can be reduced to two functions, which, in their turn, satisfy second order equations. Thus we have:

$$\begin{aligned} \Box A'_\alpha &= -4\pi\varrho'_\alpha, \\ (\Box - K_0^2) A''_\alpha &= -4\pi\varrho'_\alpha, \end{aligned} \tag{85}$$

and

$$A_\alpha = A'_\alpha - A''_\alpha. \tag{86}$$

Note that if $K_0^2 = 0$, or in other words, if we consider a field of zero rest mass, then the results obtained on the basis of the field equations of higher order are identical with those obtained by the method of the compensating field

$$A''_\alpha \equiv a_\alpha. \tag{87}$$

With the help of a compensating auxiliary field we succeeded in eliminating the longitudinal electromagnetic mass. With this the final form of the translational equation of motion can now be given

$$\begin{aligned} B_\alpha = {} & \frac{2e^2}{3c^3}\left(\ddot{u}_\alpha - \frac{1}{c^2} u_\alpha (\dot{u}_\nu \dot{u}_\iota)\right) - \frac{7e}{c^6} M_{\alpha\varrho} \dot{u}_\varrho (\dot{u}_\nu \dot{u}_\nu) - \\ & - \frac{2e}{3c^4} \dddot{M}_{\alpha\varrho} u_\varrho - \frac{e}{3c^4} M_{\alpha\varrho} \dddot{u}_\varrho - \\ & - \frac{4e}{3c^4} \dot{M}_{\alpha\varrho} \ddot{u}_\varrho - \frac{4e}{3c^6} u_\alpha u_\nu \dot{M}_{\nu\varrho} \ddot{u}_\varrho - \\ & - \frac{2e}{c^4} \ddot{M}_{\alpha\varrho} \dot{u}_\varrho - \frac{2e}{c^6} u_\alpha u_\nu \ddot{M}_{\nu\varrho} \dot{u}_\varrho. \end{aligned} \tag{88}$$

$$\begin{aligned} C_\alpha = {} & - \frac{e}{3c^4} M_{\alpha\varrho} \dddot{u}_\varrho + \frac{e}{3c^6} M_{\alpha\beta} \dot{u}_\beta (\dot{u}_\nu \dot{u}_\nu) + \frac{2e}{3c^6} \dot{M}_{\iota\varrho} u_\varrho \ddot{u}_\varrho u_\alpha + \\ & + \frac{u_\alpha}{c^5}\left[- \frac{7}{3c^4} M_{\varrho\nu} \dot{u}_\nu M_{\varrho\beta} \dot{u}_\beta (\dot{u}_\nu \dot{u}_\nu) + \right. \\ & + \frac{19}{15\, c^2} M_{\varrho\varrho} M_{\varrho\nu} (\ddot{u}_\nu \dot{u}_\nu) - \frac{7}{3c^2} \dot{M}_{\varrho\nu} u_\nu M_{\varrho\beta} \ddot{u}_\beta - \\ & - \frac{1}{3c^2} \ddot{M}_{\varrho\beta} M_{\varrho\beta} (\dot{u}_\nu \dot{u}_\iota) - \frac{4}{c^2} \ddot{M}_{\varrho\nu} u_\nu M_{\varrho\beta} \ddot{u}_\beta - \\ & - \frac{6}{c^2} M_{\varrho\beta} \dot{u}_\beta \ddot{M}_{\varrho\nu} \dot{u}_\nu - \frac{214}{35\, c^4} M_{\varrho\nu} M_{\varrho\nu} (\dot{u}_\iota \dot{u}_\nu)^2 + \\ & \left. + \frac{1}{3c^2} M_{\varrho\nu} M_{\varrho\nu} (\ddot{u}_\nu \ddot{u}_\nu) - \frac{1}{3} M^{(4)}_{\beta\varrho} M_{\beta\varrho}\right] + \\ & + \frac{\dot{u}_\alpha}{c^5}\left[- \frac{4}{3c^2} M_{\varrho\nu} \dot{u}_\nu M_{\varrho\beta} \ddot{u}_\beta - \frac{6}{c^3} M_{\varrho\nu} \dot{u}_\nu \dot{M}_{\varrho\beta} \dot{u}_\beta + \right. \end{aligned}$$

$$+\frac{6}{5c^2}M_{\varrho\nu}M_{\varrho\nu}(\ddot{u}_\nu\dot{u}_\nu)-\frac{1}{15}\dddot{M}_{\varrho\nu}M_{\varrho\nu}+$$

$$+\frac{2}{c^2}\dot{M}_{\varrho\nu}u_\nu\ddot{M}_{\varrho\beta}u_\beta-\frac{4}{c^2}M_{\varrho\nu}\dot{u}_\nu\ddot{M}_{\varrho\beta}u_\beta\Big]+$$

$$+\frac{\ddot{u}_\alpha}{c^5}\Big[\frac{2}{3c^2}M_{\varrho\nu}\dot{u}_\nu M_{\varrho\beta}\dot{u}_\beta+\frac{1}{3c^2}M_{\varrho\nu}M_{\varrho\nu}(\dot{u}_\nu\dot{u}_\nu)- \tag{89}$$

$$-\frac{2}{3}\ddot{M}_{\varrho\nu}M_{\varrho\nu}\Big]-\frac{u_\alpha^{(4)}}{15\,c^5}M_{\varrho\nu}M_{\varrho\nu}+$$

$$+\frac{2}{15\,c^5}M_{\alpha\varrho}M_{\varrho\beta}u_\beta^{(4)}+\frac{1}{3c^5}\dot{M}_{\alpha\beta}M_{\beta\varrho}\dddot{u}_\varrho+$$

$$+\frac{2}{c^5}\ddot{M}_{\alpha\beta}M_{\beta\varrho}\ddot{u}_\varrho+\frac{2}{3c^5}\dddot{M}_{\alpha\beta}M_{\beta\varrho}\dot{u}_\varrho+$$

$$+\frac{5}{12\,c^5}M_{\alpha\beta}\dot{M}_{\beta\varrho}\dddot{u}_\varrho+\frac{2}{3c^5}M_{\alpha\beta}\ddot{M}_{\beta\varrho}\ddot{u}_\varrho+$$

$$+\frac{2}{3c^5}M_{\alpha\beta}\dddot{M}_{\beta\varrho}\dot{u}_\varrho+\frac{1}{3c^5}M_{\alpha\varrho}M_{\varrho\nu}^{(4)}u_\nu-$$

$$-\frac{4}{c^7}M_{\alpha\beta}M_{\beta\varrho}\ddot{u}_\varrho(\dot{u}_\nu\dot{u}_\nu)-\frac{11}{4c^7}M_{\alpha\beta}M_{\beta\varrho}\dot{u}_\varrho(\ddot{u}_\nu\dot{u}_\nu)-$$

$$-\frac{10}{3c^7}\dot{M}_{\alpha\beta}M_{\beta\varrho}\dot{u}_\varrho(\dot{u}_\nu\dot{u}_\nu)-\frac{11}{3c^7}M_{\alpha\beta}\dot{M}_{\beta\varrho}\dot{u}_\varrho(\dot{u}_\nu\dot{u}_\nu)-$$

$$-\frac{1}{3c^7}M_{\alpha\beta}\ddot{M}_{\beta\varrho}u_\varrho\,(\dot{u}_\nu\dot{u}_\nu)+$$

$$+\frac{12}{c^9}M_{\varrho\nu}\dot{M}_{\varrho\beta}u_\nu\dot{u}_\beta(\dot{u}_\nu\dot{u}_\nu)u_\alpha.$$

$$D_\alpha=-\frac{2e}{3c^4}\dot{M}_{\alpha\varrho}\ddot{u}_\varrho-\frac{2e}{3c^6}M_{\alpha\varrho}\dot{u}_\varrho(\dot{u}_\nu\dot{u}_\nu)-$$

$$-\frac{e}{3c^6}u_\alpha u_\nu\dot{M}_{\nu\varrho}\ddot{u}_3-\frac{1}{3c^4}\dot{M}_{\alpha\varrho}M_{\varrho\beta}\ddot{u}_\beta- \tag{90}$$

$$-\frac{2}{3c^5}\Big[\dot{M}_{\alpha\beta}\dot{M}_{\beta\varrho}\ddot{u}_\varrho+\frac{1}{c^2}\dot{M}_{\alpha\lambda}u_\lambda\dot{M}_{\beta\varrho}\ddot{u}_\varrho u_\beta\Big]+$$

$$+\frac{1}{3c^5}\dot{M}_{\alpha\beta}M_{\beta\varrho}\dddot{u}_\varrho.$$

$$E_\alpha=-\frac{11}{3c^7}\dot{M}_{\alpha\beta}M_{\beta\varrho}\dot{u}_\varrho(\dot{u}_\nu\dot{u}_\nu)+\frac{1}{3c^7}M_{\alpha\beta}\ddot{M}_{\beta\varrho}u_\varrho(\dot{u}_\nu\dot{u}_\nu)-$$

$$
\begin{aligned}
&- \frac{1}{3c^7} M_{\alpha\beta} M_{\beta\varrho} \ddot{u}_\varrho (\dot{u}_\nu \dot{u}_\nu) - \\
&- \frac{13}{3c^7} M_{\alpha\beta} \dot{M}_{\beta\varrho} \dot{u}_\varrho (\dot{u}_\nu \dot{u}_\nu) + \frac{2}{c^7} M_{\alpha\beta} \ddot{M}_{\varrho\nu} u_\nu \dot{u}_\varrho \dot{u}_\beta - \\
&- \frac{1}{3c^5} M_{\alpha\beta} M_{\beta\varrho} u_\varrho^{(4)} - \frac{5}{3c^5} M_{\alpha\beta} \dot{M}_{\beta\varrho} \dddot{u}_\varrho - \\
&- \frac{10}{3c^5} M_{\alpha\beta} \ddot{M}_{\beta\varrho} \ddot{u}_\varrho - \frac{10}{3c^5} M_{\alpha\beta} \dddot{M}_{\beta\varrho} \dot{u}_\varrho - \\
&- \frac{2}{3c^5} M_{\alpha\beta} M_{\beta\varrho}^{(4)} u_\varrho .
\end{aligned} \tag{91}
$$

$$
\begin{aligned}
G_\alpha = &\frac{2}{c^7} \dot{M}_{\varrho\nu} u_\nu M_{\varrho\beta} \dot{u}_\beta \ddot{u}_\alpha - \frac{2}{3c^7} M_{\alpha\beta} \dot{M}_{\varrho\nu} \dot{u}_\beta u_\nu \ddot{u}_\varrho + \\
&+ \frac{2}{3c^5} \ddot{M}_{\alpha\beta} M_{\beta\varrho} \dot{u}_\varrho + \frac{4}{3c^7} M_{\alpha\beta} M_{\beta\varrho} \dot{u}_\varrho (\ddot{u}_\nu \dot{u}) - \\
&- \frac{2}{3c^7} M_{\alpha\beta} M_{\varrho\nu} \dot{u}_\beta \dot{u}_\nu \ddot{u}_\varrho - \frac{2}{c^7} \dot{M}_{\alpha\beta} M_{\beta\varrho} \dot{u}_\varrho (\dot{u}_\nu \dot{u}) + \\
&+ \frac{u_\alpha}{c^9} (- 2\dot{M}_{\varrho\nu} u_\nu \dot{M}_{\varrho\nu} u_\nu + 3 M_{\varrho\nu} \dot{u}_\nu M_{\varrho\beta} u_\beta) (\dot{u}_\nu \dot{u}_\nu) + \\
&+ \frac{\dot{u}_\alpha}{c^7} \left(\frac{4}{3} M_{\varrho\nu} \dot{u}_\nu M_{\varrho\beta} \ddot{u}_\beta + 2 M_{\varrho\nu} \dot{u}_\nu \dot{M}_{\varrho\beta} \dot{u}_\beta \right) - \\
&- \frac{5}{6c^7} M_{\varrho\nu} \dot{u}_\nu \ddot{M}_{\varrho\beta} u_\beta \, u_\alpha .
\end{aligned} \tag{92}
$$

$$
\begin{aligned}
H_\alpha = &- \frac{2}{3c^7} M_{\alpha\beta} M_{\varrho\nu} \dot{u}_\beta \dot{u}_\varrho \ddot{u}_\nu + \frac{2}{3c^5} M_{\alpha\beta} \ddot{M}_{\beta\varrho} \dot{u}_\varrho - \\
&- \frac{1}{c^7} M_{\alpha\beta} \ddot{M}_{\varrho\nu} \dot{u}_\beta u_\nu \dot{u}_\varrho - \frac{1}{c^7} M_{\alpha\beta} \ddot{M}_{\nu\varrho} u_\varrho \dot{u}_\beta \dot{u}_\nu - \\
&- \frac{4}{3c^7} M_{\alpha\beta} M_{\beta\varrho} \dot{u}_\varrho (\ddot{u}_\nu \dot{u}_\nu) + \frac{1}{c^7} M_{\alpha\beta} \dot{M}_{\beta\varrho} \dot{u}_\varrho (\dot{u}_\nu \dot{u}_\nu) + \\
&+ \frac{2}{c^7} M_{\alpha\beta} \ddot{M}_{\beta\varrho} u_\varrho (\dot{u}_\nu \dot{u}_\nu) .
\end{aligned} \tag{93}
$$

The four-work of the self-force given by (38) is not zero, and therefore it influences the rest mass, too. In the following we give the variation of the

rest mass caused by the effect of the self-force:

$$\dot{m}_0 = -\frac{1}{c^2}(u_\alpha F^e_\alpha + u_\alpha F^S_\alpha), \tag{94}$$

where F^e_α denotes the external force acting on the particle, while F^S_α is the self-force.

Substitute (27) for the first term, (88)...(92) for the second term of (94), then

$$\begin{aligned}
\dot{m}_0 = -\frac{1}{c^2}\Bigg[& \frac{1}{2}\frac{d}{d\tau}(M_{\alpha\beta}F^e_{\alpha\beta}) - \frac{1}{2}\dot{M}_{\alpha\beta}\Bigg(F^e_{\alpha\beta} - \\
& - \frac{1}{c^2}(u_\alpha F^e_\beta - u_\beta F^e_\alpha)\Bigg) + \frac{19}{15\,c^5} M_{\alpha\beta}M_{\alpha\beta}(\ddot{\ddot{u}}_\nu \dot{u}_\nu) + \\
& + \frac{5}{3c^5}\dot{M}_{\alpha\beta}u_\beta M_{\alpha\varrho}\ddot{\ddot{u}}_\varrho + \frac{1}{3c^5}\ddot{M}_{\alpha\beta}M_{\alpha\beta}(\dot{u}_\nu \dot{u}_\nu) + \\
& + \frac{2}{c^5}\ddot{M}_{\alpha\beta}M_{\alpha\varrho}u_\beta \ddot{u}_\varrho - \frac{6}{c^5}M_{\alpha\beta}\dot{u}_\beta \ddot{M}_{\alpha\varrho}\dot{u}_\varrho + \\
& + \frac{214}{25\,c^7}M_{\alpha\beta}M_{\alpha\beta}(\dot{u}_\nu \dot{u}_\nu)^2 + \frac{1}{3c^3}M^{(4)}_{\alpha\beta}M_{\alpha\beta} - \\
& - \frac{1}{3c^5}M_{\alpha\beta}M_{\alpha\beta}(\ddot{u}_\nu \ddot{u}_\nu) + \frac{3}{c^7}M_{\alpha\beta}\dot{u}_\beta M_{\alpha\beta}\dot{u}_\varrho(\dot{u}_\nu \dot{u}_\nu) + \\
& + \frac{u_\alpha \ddot{u}_\alpha}{c^5}\Bigg[\frac{2}{3c^3}M_{\alpha\beta}\dot{u}_\beta M_{\alpha\varrho}\dot{u}_\varrho + \\
& + \frac{1}{3c^2}M_{\alpha\beta}M_{\alpha\beta}(\dot{u}_\nu \dot{u}_\nu) - \frac{2}{3}\ddot{M}_{\alpha\beta}M_{\alpha\beta}\Bigg] - \\
& - \frac{u_\alpha u^{(4)}_\alpha}{15\,c^5}M_{\alpha\beta}M_{\alpha\beta} + \frac{e}{3c^4}\dot{M}_{\nu\varrho}\ddot{u}_\varrho - \\
& - \frac{2}{3c^5}\dot{M}_{\alpha\beta}u_\beta \dot{M}_{\alpha\varrho}\ddot{u}_\varrho + \frac{2}{c^7}u_\varrho \dot{M}_{\alpha\varrho}M_{\alpha\beta}\dot{u}_\beta u_\alpha \ddot{u}_\alpha - \\
& - \frac{4}{c^7}M_{\alpha\beta}\dot{u}_\beta M_{\alpha\varrho}\dot{u}_\varrho(\dot{u}_\nu \dot{u}_\nu) - \frac{12}{c^7}M_{\alpha\varrho}\dot{u}_\varrho \dot{M}_{\alpha\beta}u_\beta(\dot{u}_\nu \dot{u}_\nu)\Bigg]
\end{aligned}$$

is obtained.

REFERENCES

1. P. A. M. Dirac, Proc. Roy, Soc. A., **167**, 148, 1938.
2. H. J. Bhabha, Proc. Ind. Acad. Sci. A, **XI,** 247, 1940.
3. H. J. Bhabha and H. C. Corben, Proc. Roy. Soc. A, **178,** 273, 1941.
4. M. Pryce, Proc. Roy. Soc. A, **168,** 389, 1938.
5. C. J. Eliezer, Rev. Mod. Phys., **19,** 147, 1947.
6. S. N. Gupta, Proc. Phys. Soc. A, **64,** 50, 1951.
7. J. I. Frenkel, Z. f. Phys., **37**, 243, 1926.
8. J. Horváth, MTA III. O. Közl., **5**, 411, 1955.
9. G. Marx, Acta Phys. Hung., **11,** 67, 1952.
10. L. Infeld, Bull. Acad. Polon. Sci. Cl. III. **3**, 213, 1955.
11. H. Hönl, Ergebn. exakt. Naturw., **26,** 291, 1952.
12. K. Nagy, Acta Phys. Hung., **8,** 325, 1957.
13. K. Nagy, Magy. Fiz. Folyóirat, **V,** 311, 1957.
14. L. Infeld and J. Plebanski, Acta Phys. Pol., **XV,** 207, 1956.
15. W. Pauli and F. Villars, Rev. Mod. Phys., **21,** 434, 1949.
16. *A. A. Соколов,* ЖЭТФ, **18**, 280, 1948.
17. F. Bopp, Ann. Phys., **38,** 345, 1940.
18. B. Podolsky, Phys. Rev., **62,** 68, 1941.
19. D. Ivanenko and A. Szokolov, Klasszikus térelmélet, Akadémiai Kiadó, Budapest, 1955.
20. G. Marx, Bull. Acad. Polon. Sci. Cl. III. **II,** 219, 1954.
21. K. Nagy, Bull. Acad. Polon. Sci. Cl. III. **IV,** 341, 1956.

РЕЛЯТИВИСТИЧЕСКОЕ УРАВНЕНИЕ ДВИЖЕНИЯ ДЛЯ ЗАРЯЖЕННЫХ ЧАСТИЦ СО СПИНОМ И МАГНИТНЫМ МОМЕНТОМ

I. Трансляционное уравнение движения

И. Ф. ФАРКАШ

Р е з ю м е

Исходя из модифицированной формы тензора энергии-импульса при помощи метода Инфельда определяется трансляционное уравнение движения. Четырёхмерный потенциал разлагается в степенной ряд по степеням $1/c$. Вычисляется самодействие частиц. Расходящиеся члены в уравнении движения исключаются методом компенсационного вспомогательного поля. Показывается, что подобные результаты получаются и при применении высшего порядка уравнений поля.

RELATIVISTIC EQUATION OF MOTION FOR A CHARGED PARTICLE WITH SPIN AND MAGNETIC MOMENT

II. EQUATION OF MOTION OF SPIN

By

I. F. FARKAS

INSTITUTE FOR THEORETICAL PHYSICS, ROLAND EÖTVÖS UNIVERSITY, BUDAPEST

(Presented by K. Novobátzky. — Received 20. VIII. 1961)

The equation of motion of spin is determined from the modified energy-momentum tensor by the method of INFELD. With the aid of the four-potential the momentum due to the self-field of the particle is calculated. The divergent terms of the equation could be eliminated by the use of a compensating auxiliary field.

Introduction

The particle in the rest-system was characterized in addition to its electrical charge and mechanical mass by its mechanical dipole moment and by its magnetic moment, strongly connected with the former. It is necessary, therefore, to give in addition to the translational equation of motion the equation of motion for the mechanical dipole moment and magnetic moment too.

We have seen that the translational equation of motion can be determined by the elimination of the divergence of the energy-momentum tensor, with the help of a conservation law. This ensured the conservation of the whole fourmomentum of the system. Similarly, we want to derive the equation of motion for the spin from a law of conservation.

Let us introduce therefore the following tensor of rank three:

$$\Theta_{\alpha\beta\gamma} = x_\alpha T_{\beta\gamma} - x_\beta T_{\alpha\gamma}, \tag{1}$$

where x_α is the coordinate of a point of the space, $T_{\alpha\beta}$ the total energy-momentum tensor of the system. $\Theta_{\alpha\beta\gamma}$ can be immediately seen to be antisymmetrical in the first two indices. Determining the divergence of the tensor defined by eq. (1):

$$\partial_\gamma \Theta_{\alpha\beta\gamma} = \delta_{\alpha\gamma} T_{\beta\gamma} - \delta_{\beta\gamma} T_{\alpha\gamma} + x_\alpha \partial_\gamma T_{\beta\gamma} - x_\beta \partial_\beta T_{\alpha\gamma} = 0, \tag{2}$$

where we have taken into account that the tensor is divergence-free. The disappearance of the divergence of the tensor $\Theta_{\alpha\beta\gamma}$, defined by eq. (1), is connected with the conservation of a tensor of rank two. We have to integrate eq. (2) over a three-dimensional region v, containing the particle in its interior. Let us further assume that the quantities of which $T_{\alpha\beta}$ is constructed disappear

on the boundary of the region. Accordingly:

$$\dot{N}_{\alpha\beta} = \frac{dt}{d\tau} \int \partial_\gamma \Theta_{\alpha\beta\gamma}\, dv = 0. \tag{3}$$

As the three-dimensional divergence is equal to zero, the relation (3) takes the following form:

$$\begin{aligned} \dot{N}_{\alpha\beta} &= \frac{dt}{d\tau}\, \partial_4 \int \Theta_{\alpha\beta 4}\, dv = 0, \\ N_{\alpha\beta} &= -N_{\beta\alpha} = \text{const.} \end{aligned} \tag{4}$$

The detailed investigation of $N_{\alpha\beta}$ shows that its spacelike part is equal to the total momentum and its timelike part gives the centre of mass of the system. The energy-momentum tensor of the system can be divided into two characteristic parts:

$$T_{\alpha\beta} = t_{\alpha\beta} + E_{\alpha\beta}, \tag{5}$$

where $t_{\alpha\beta}$ is the kinematic energy-momentum tensor defined by HÖNL [1] and NAGY [2] by the following equation:

$$t_{\alpha\beta} = m_{\alpha\beta}\, \delta(3) \frac{d\tau}{dt} + m_{\alpha\beta k}\, \partial_k \delta(3) \frac{d\tau}{dt} - \frac{1}{ic}\, m_{\alpha\beta 4}\, u_k\, \partial_k\, \delta(3) \left(\frac{d\tau}{dt}\right)^2 + \\ + \frac{1}{ic}\, \frac{d}{dt} \left(m_{\alpha\beta 4} \frac{d\tau}{dt}\right) \delta(3),$$

where

$$\begin{aligned} m_{\alpha\beta} &= m_0\, u_\alpha\, u_\beta - \frac{1}{2c^2} (\dot{S}_{\alpha\nu}\, u_\nu\, u_\beta + \dot{S}_{\beta\nu}\, u_\nu\, u_\alpha), \\ m_{\alpha\beta\gamma} &= -\frac{1}{2} (S_{\gamma\alpha}\, u_\beta + S_{\gamma\beta}\, u_\alpha). \end{aligned} \tag{7}$$

It may be mentioned that $S_{\alpha\beta}$ is an antisymmetrical tensor, which describes the spin of the particle in the following way:

$$S_{23} = \sigma_x, \qquad S_{31} = \sigma_y, \qquad S_{12} = \sigma_z, \tag{8}$$

here $\sigma(\sigma_x, \sigma_y, \sigma_z)$ denotes the spin vector. We have assumed further that in the rest-system the elements $S_{\alpha 4}$ of the tensor $S_{\alpha\beta}$ are equal to zero. This condition may be written in a covariant form:

$$S_{\alpha\beta}\, u_\beta = 0, \tag{9}$$

where u_β gives the four-velocity of the particle. $E_{\alpha\beta}$ is the energy-momentum tensor of the electromagnetic field which was determined by MARX [4] for particles with magnetic moment. In such a case the energy-momentum tensor of the electromagnetic field is:

$$E_{\alpha\beta} = \frac{1}{4\pi}\left[F_{\alpha\varrho}F_{\beta\varrho} - \frac{\delta_{\alpha\beta}}{4}F_{\varrho\sigma}F_{\varrho\sigma}\right] - \frac{1}{c^2}(u_\alpha \mu_{\beta\sigma} + u_\beta \mu_{\alpha\sigma})F_\sigma, \qquad (10)$$

where $F_{\alpha\beta}$ is the electromagnetic field tensor and F_σ means the following abbreviation:

$$F_\sigma = F_{\sigma\varrho}u_\varrho. \qquad (11)$$

Now we have to give the total current density four-vector:

$$\varrho_\alpha = S_\alpha + \partial_\beta \mu_{\alpha\beta}, \qquad (12)$$

where

$$S_\alpha = \frac{e}{c}\int u_\alpha \delta(4)\, d\tau, \qquad \mu_{\alpha\beta} = \int M_{\alpha\beta}\delta(4)\, d\tau \qquad (13)$$

(τ denotes the proper time). In eq. (13) e means the total charge and the antisymmetric tensor $M_{\alpha\beta}$ gives the magnetic moment and electric moment of the particle as follows:

$$M_{23} = m_x, \quad M_{31} = m_y, \quad M_{12} = m_z,$$

where $\mathfrak{M}(m_x, m_y, m_z)$ denotes the magnetic momentum vector of the particle, $\xi_\beta(\tau)$ are the coordinates of the world line, and $\delta(4)$ is the four-dimensional Dirac δ-function

$$\delta(x_1 - \xi_1)\cdot\delta(x_2 - \xi_2)\cdot\delta(x_3 - \xi_3)\cdot\delta\left(\frac{x_4}{ic} - \frac{\xi_4}{ic}\right).$$

Let us assume further that in the rest system the particle has no electric momentum just as actual elementary particles do not have any. This condition may be written in a covariant form:

$$M_{\alpha\beta}u_\beta = 0. \qquad (15)$$

Substituting expression (5) into (4) we obtain:

$$\frac{1}{2c}\frac{d}{d\tau}\int (x_\alpha t_{\beta 4} - x_\beta t_{\alpha 4})\, dv = -\frac{1}{ic}\frac{d}{d\tau}\int (x_\alpha E_{\beta 4} - x_\beta E_{\alpha 4})\, dv. \qquad (16)$$

The paper of NAGY referred to above described the left and right-hand side of (16) taking into account an external field only. In our case it is modified

because we want to take into account also the effect of the self-field of the particle. In this case eq. (16) reads:

$$\dot{S}_{\alpha\beta} + \frac{1}{c^2}(\dot{S}_{\alpha\nu} u_\nu u_\beta - \dot{S}_{\alpha\nu} u_\nu u_\alpha) =$$

$$= F_{\alpha\sigma} M_{\sigma\beta} - F_{\beta\sigma} M_{\sigma\alpha} + \frac{1}{c^2}(u_\alpha M_{\beta\sigma} - u_\beta M_{\alpha\sigma}) F_\sigma - \tag{17}$$

$$- \frac{1}{ic} \frac{d}{d\tau} \int (x_\alpha E^s_{\beta 4} - x_\beta E^s_{\alpha 4})\, dv - \xi_\alpha F^s_\beta + \xi_\beta F^s_\alpha .$$

As the integral on the right side of (17) includes the effect of the self-field, our task is now to determine this integral.

The effect of the self-field

To determine the integral in expression (17), its form given by (3) is used:

$$I_{\alpha\beta} = - \frac{dt}{d\tau} \int \partial_\gamma (x_\alpha E^s_{\beta\gamma} - x_\beta F^s_{\alpha\gamma})\, dv =$$

$$= - \frac{dt}{d\tau} \int (E^s_{\beta\alpha} - E^s_{\alpha\beta} + x_\alpha \partial_\gamma E^s_{\beta\gamma} - x_\beta \partial_\gamma E^s_{\alpha\gamma})\, dv. \tag{18}$$

As $E_{\alpha\beta}$ is symmetrical the first two terms of the integrand cancel each other. The divergence of the energy-momentum tensor $E_{\alpha\beta}$ is:

$$\partial_\beta E_{\alpha\beta} = - F_{\alpha\sigma} S_\sigma - \frac{1}{2} \mu_{\sigma\lambda} \partial_\alpha F_{\sigma\lambda} -$$

$$- \partial_\lambda \left[F_{\alpha\sigma} \mu_{\sigma\lambda} + \frac{1}{c^2}(u_\alpha \mu_{\lambda\sigma} + u_\lambda \mu_{\alpha\sigma}) F_\sigma \right]. \tag{19}$$

Substituting this into (18), we get the following relation:

$$I_{\alpha\beta} = \frac{dt}{d\tau} \int \left\{ x_\alpha \left[F^s_{\beta\sigma} s_\sigma + \frac{1}{2} \mu_{\sigma\lambda} \partial_\beta F^s_{\sigma\lambda} + \right.\right.$$

$$\left. + \partial_\lambda \left(F^s_{\beta\sigma} \mu_{\sigma\lambda} + \frac{1}{c^2}(u_\beta \mu_{\lambda\sigma} + u_\lambda \mu_{\beta\sigma}) F^s_\sigma \right) \right] -$$

$$- x_\beta \left[F^s_{\alpha\sigma} s_\sigma + \frac{1}{2} \mu_{\sigma\lambda} \partial_\alpha F^s_{\sigma\lambda} + \right. \tag{20}$$

$$\left.\left. + \partial_\lambda \left(F^s_{\alpha\sigma} \mu_{\sigma\lambda} + \frac{1}{c^2}(u_\alpha \mu_{\lambda\sigma} + u_\lambda \mu_{\alpha\sigma}) F^s_\sigma \right) \right] \right\} dv.$$

Let us modify further the third and sixth term of the integrand:

$$x_\alpha \partial_\lambda \left(F^s_{\beta\sigma}\, \mu_{\sigma\lambda} + \frac{1}{c^2} (u_\beta\, \mu_{\lambda\sigma} + u_\lambda\, \mu_{\beta\sigma})\, F^s_\sigma \right) =$$

$$= \partial_\lambda x_\alpha \left(F^s_{\beta\sigma}\, \mu_{\sigma\lambda} + \frac{1}{c^2} (u_\beta\, \mu_{\lambda\sigma} + u_\lambda\, \mu_{\beta\sigma})\, F^s_\sigma \right) - \tag{21}$$

$$- \left(F^s_{\beta\sigma}\, \mu_{\sigma\alpha} + \frac{1}{c^2} (u_\beta\, \mu_{\alpha\sigma} + u_\alpha\, \mu_{\beta\sigma})\, F^s_\sigma \right).$$

Introducing the decomposition (21) into integral (20) and neglecting the three- dimensional divergence, we obtain:

$$I_{\alpha\beta} = \frac{dt}{d\tau} \int x_\alpha \left(F^s_{\beta\sigma} S_\sigma + \frac{1}{2} \mu_{\sigma\lambda} \partial_\beta F^s_{\sigma\lambda} \right) dv +$$

$$+ \frac{dt}{d\tau} \int \partial_4 \left(x_\alpha \left(F^s_{\beta\sigma}\, \mu_{\sigma 4} + \frac{1}{c^2} (u_\beta\, \mu_{4\sigma} + u_4\, \mu_{\beta\sigma})\, F^s_\sigma \right) \right) dv - \tag{22}$$

$$- \frac{dt}{d\tau} \int \left(F^s_{\beta\sigma}\, \mu_{\sigma\alpha} + \frac{1}{c^2} (u_\beta\, \mu_{\alpha\sigma} + u_\alpha\, \mu_{\beta\sigma}) \right) F^s_\sigma\, dv + [\alpha \rightleftarrows \beta].$$

As we want to determine integral (22) for a pole-dipole point particle, in the case when the values of S_σ and $\mu_{\sigma\lambda}$ differ from zero in the neighbourhood of the particle only, it is suitable to refer $I_{\alpha\beta}$ to the point of the particle. Then eq. (22) has the following form:

$$I_{\alpha\beta} = \frac{dt}{d\tau} \int (x_\alpha - \xi_\alpha) \left(F^s_{\beta\sigma}\, s_\sigma + \frac{1}{2} \mu_{\sigma\lambda} \partial_\beta F^s_{\sigma\lambda} + \partial_4 \left(F^s_{\beta\sigma}\, \mu_{\sigma 4} + \right. \right.$$

$$\left. + \frac{1}{c^2} (u_\beta\, \mu_{4\sigma} + u_4\, \mu_{\beta\sigma})\, F_\sigma \right) \Big) dv - \frac{dt}{d\tau} \xi_\alpha \int \Big[F^s_{\beta\sigma}\, s_\sigma +$$

$$+ \frac{1}{2} \mu_{\sigma\lambda} \partial_\beta F^s_{\sigma\lambda}{}' + \partial_4 \left(F^s_{\beta\sigma}\, \mu_{\sigma 4} + \frac{1}{c^2} (u_\beta\, \mu_{4\sigma} + u_4\, \mu_{\beta\sigma})\, F_\sigma \right) \Big] dv + \tag{23}$$

$$+ \frac{dt}{d\tau} \partial_4 \int x_\alpha \left[F^4_{\beta\sigma}\, u_{\sigma 4} + \frac{1}{c^2} (u_\beta\, \mu_{4\sigma} + u_4\, \mu_{\beta\sigma})\, F_\sigma \right] dv -$$

$$- \frac{dt}{d\tau} \int \left[F^s_{\beta\sigma}\, \mu_{\sigma\alpha} + \frac{1}{c^2} (u_\beta\, \mu_{\alpha\sigma} + u_\alpha\, \mu_{\beta\sigma})\, F_\sigma \right] dv + [\alpha \rightleftarrows \beta].$$

Using the form of the self-force given above:

$$\int \Big[F_{\alpha\sigma}\, s_\sigma + \frac{1}{2} \mu_{\sigma\varrho} \partial_\alpha F^s_{\sigma\varrho} + \partial_4 \Big(F_{\alpha\beta}\, \mu_{\sigma 4} + \frac{1}{c^2} (u_\beta\, \mu_{4\sigma} +$$

$$+ u_4\, \mu_{\beta\sigma})\, F_\sigma \Big) \Big] dv = \int f^s_\alpha\, \delta(3)\, dv = F^s_\alpha \tag{24}$$

$I_{\alpha\beta}$ takes the following form:

$$I_{\alpha\beta} = \frac{dt}{d\tau}\int (x_\alpha - \xi_\alpha) f^s_\beta \delta(3)\, dv - \xi_\alpha F_\beta + \frac{dt}{d\tau}\int \partial_4 x_\alpha \left[\left(F^s_{\beta\sigma} M^*_{\sigma 4} + \right.\right.$$

$$+ \frac{1}{c^2}(u_\beta M^*_{4\sigma} + u_4 M^*_{\beta\sigma}) F^s_\sigma \left.\right) \delta(3)\Big] dv - \tag{25}$$

$$- \frac{dt}{d\tau}\int F^s_{\beta\sigma} M^*_{\sigma\alpha}\delta(3)\, dv + [\alpha \rightleftarrows \beta].$$

The integrals giving $I_{\alpha\beta}$ in relation (25) will be determined in a coordinate system moving with the particle. In this system $I_{\alpha\beta}$ may be decomposed to spacelike and timelike components. The spacelike component is:

$$I_{ej} = \int (x_e - \xi_e) f^s_i \delta(3)\, dv - \int (x_j - \xi_j) f^s_e \delta(3)\, dv + \xi_e F^s_j - \\ - \xi_j F^s_e + M^*_{ij}\int F_{ei}\delta(3)\, dv - M^*_{ie}\int F_{ji}\delta(3)\, dv \tag{26a}$$

and the time-like components are:

$$I_{4j} = (x_4 - \xi_4)\int f^s_j \delta(3)\, dv - \int (x_j - \xi_j) f^s_4 \delta(3)\, dv + \xi_4 F^s_j - \xi_j F^s_4, \tag{26b}$$

and

$$I_{e4} = \int (x_e - \xi_e) f^s_4 \delta(3)\, dv - (x_4 - \xi_4) F^s_e + \xi_e F^s_4 - \xi_4 F^s_e. \tag{26c}$$

The first term of (26b) and the third term of (26c) are equal to zero. In eq. (26a) we have to determine the first integral only, because the others have already been calculated by the author [5] for the determination of the translational equation of motion. The first term on the right-hand side of (26a) can be determined in the same way as in the determination of the translational equation of motion. The details of the calculation are, therefore, omitted here. We are now able to give the equation of motion of the spin:

$$\dot S_{\alpha\beta} + \frac{1}{c_2}(\dot S_{\alpha\nu} u_\nu u_\beta - \dot S_{\beta\nu} u_\nu u_\alpha) = F_{\alpha\sigma} M_{\sigma\beta} - F_{\beta\sigma} M_{\sigma\alpha} +$$

$$+ \frac{1}{c^2}(u_\alpha M_{\beta\sigma} - u_\beta M_{\alpha\sigma}) F_\sigma - \frac{e}{3cr}\left(\dot M_{\alpha\beta} + \right.$$

$$\left. + \frac{1}{c^2} u_\alpha u_\nu \dot M_{\nu\beta} + \frac{1}{c^2} u_\beta u_\nu \dot M_{\alpha\nu}\right) - \frac{19}{140\, c^4 r} M_{\alpha\varrho} M_{\varrho\beta}(\dot u_\nu \dot u_\nu) -$$

$$- \frac{3}{140\, c^4 r} M_{\alpha\varrho} M_{\varrho\nu} \dot u_\nu u_\beta + \frac{8}{35\, c^4 r} M_{\beta\varrho} M_{\varrho\nu} \dot u_\nu \dot u_\alpha -$$

$$-\frac{1}{6c^2 r}\left[\left(\ddot{M}_{\alpha\varrho}-\frac{1}{c^2}M_{\alpha\varrho}(\dot{u}_\nu\dot{u}_\nu)+\frac{1}{c^2}u_\alpha u_\nu\ddot{M}_{\nu\varrho}\right)M_{\varrho\beta}+\right.$$

$$\left.+M_{\alpha\varrho}\left(\ddot{M}_{\varrho\beta}-\frac{1}{c^2}M_{\varrho\beta}(\dot{u}_\nu\dot{u}_\nu)+\frac{1}{c^2}u_\beta u_\nu\ddot{M}_{\varrho\nu}\right)\right]-$$

$$-\frac{1}{5c^4 r}(M_{\alpha\varrho}\dot{M}_{\varrho\nu}u_\nu\dot{u}_\beta+M_{\beta\varrho}\dot{M}_{\varrho\nu}u_\nu\dot{u}_\alpha)-$$

$$-\frac{u_\alpha}{10\,c^4 r}\left(M_{\varrho\nu}M_{\varrho\nu}\left(\ddot{u}_\beta-\frac{1}{c^2}u_\beta(\dot{u}_\nu\dot{u}_\nu)\right)+2M_{\nu\beta}M_{\nu\varrho}\ddot{u}\right)+$$

$$+\frac{u_\alpha}{3c^4 r}M_{\nu\beta}M_{\nu\varrho}\ddot{u}_\varrho+\frac{u_\alpha}{6c^4 r}M_{\varrho\nu}M_{\varrho\nu}\left(\ddot{u}_\beta-\right.$$

$$\left.-\frac{1}{c^2}u_\beta(\dot{u}_\nu\dot{u}_\nu)\right)+\frac{u_\alpha}{2c^4 r}M_{\varrho\nu}\dot{M}_{\varrho\nu}\dot{u}_\beta-\frac{e}{6c^3 r}u_\alpha M_{\beta\varrho}\dot{u}_\varrho-$$

$$-\frac{1}{3c^4 r}u_\alpha u_\nu\dot{M}_{\iota\varrho}M_{\varrho\beta}+\frac{e}{3cr}\left(\left(\dot{M}_{\alpha\beta}+\frac{1}{c^2}u_\alpha u_\nu\dot{M}_{\nu\beta}+\right.\right.$$

$$\left.+\frac{1}{c^2}u_\beta u_\nu\dot{M}_{\alpha\nu}\right)-\frac{e}{3c^3 r}u_\alpha u_\nu\dot{M}_{\nu\beta}-\frac{1}{3c^2 r}\left(\left(\dot{M}_{\alpha\varrho}+\right.\right.$$

$$\left.+\frac{1}{c^2}u_\alpha u_\nu\dot{M}_{\nu\varrho}\right)\left(\dot{M}_{\varrho\beta}+\frac{1}{c^2}u_\beta u_\mu\dot{M}_{\varrho\mu}\right)+\frac{1}{c^2}\dot{M}_{\alpha\nu}u_\nu\dot{M}_{\varrho\beta}u_\varrho\Big)+$$

$$+\frac{1}{3c^4 r}u_\alpha u_\nu\dot{M}_{\nu\varrho}\left(\dot{M}_{\varrho\beta}+\frac{1}{c^2}u_\beta u_\mu\dot{M}_{\varrho\mu}\right)+$$

$$+\frac{3}{10\,c^4 r}(M_{\alpha\varrho}\dot{M}_{\varrho\nu}u_\nu\dot{u}_\beta+M_{\alpha\nu}M_{\beta\varrho}\dot{u}_\nu u_\varrho)+$$

$$+\frac{1}{2c^4 r}M_{\alpha\varrho}\dot{u}_\varrho\dot{M}_{\varrho\nu}u_\nu-\frac{1}{2c^4 r}\dot{M}_{\alpha\varrho}M_{\varrho\nu}u_\nu\dot{u}_\beta+$$

$$+\frac{1}{2c^4 r}(M_{\alpha\varrho}M_{\varrho\beta}(\dot{u}_\nu\dot{u}_\nu)+M_{\alpha\varrho}M_{\varrho\nu}\dot{u}_\nu\dot{u}_\beta)+$$

$$+\frac{1}{3c^2 r}M_{\alpha\varrho}\left(\ddot{M}_{\varrho\beta}-\frac{1}{c^2}(\dot{u}_\nu\dot{u}_\nu)+\frac{1}{c^2}u_\beta u_\nu\ddot{M}_{\varrho\nu}\right)+$$

$$+\frac{1}{3c^4 r}M_{\alpha\varrho}\dot{M}_{\varrho\nu}u_\nu\dot{u}_\beta+\frac{2}{3c^4 r}M_{\alpha\varrho}\dot{M}_{\varrho\nu}u_\nu\dot{u}_\beta-$$

$$-\frac{1}{5c^4 r}M_{\alpha\varrho}\dot{M}_{\varrho\nu}u_\nu\dot{u}_\beta-\frac{1}{10\,c^4 r}M_{\beta\varrho}\dot{M}_{\varrho\nu}u_\nu\dot{u}_\alpha+$$

$$+\frac{1}{6c^4 r}M_{\beta\varrho}\dot{M}_{\varrho\nu}u_\nu\dot{u}_\alpha+\frac{1}{3c^4 r}M_{\alpha\varrho}\dot{M}_{\varrho\nu}u_\nu\dot{u}_\beta+$$

$$+\frac{1}{3c^4 r} u_\alpha u_\nu \dot{M}_{\nu\varrho}\left(\dot{M}_{\varrho\beta} - \frac{1}{c^2} u_\beta u_\mu \dot{M}_{\varrho\mu}\right) - \frac{1}{5c^4 r} M_{\alpha\varrho} M_{\varrho\nu} \dot{u}_\nu \dot{u}_\beta -$$

$$- \frac{4}{15\, c^4 r} M_{\alpha\varrho} M_{\beta\varrho} \dot{u}_\varrho u_\nu - \frac{1}{15\, c^4 r} M_{\alpha\beta} M_{\varrho\beta} (\dot{u}_\nu \dot{u}_\nu) -$$

$$- \frac{1}{3c^4 r} M_{\alpha\varrho} M_{\varrho\nu} \dot{u}_\nu \dot{u}_\beta - \frac{1}{3c^4 r} M_{\alpha\varrho} \dot{M}_{\varrho\nu} u_\nu \dot{u}_\beta +$$

$$+\frac{1}{c^2} u_\alpha M^*_{\beta\sigma} u_\nu \int F_{\varrho\nu}\, \delta(3)\, dv + M^*_{\varrho\beta} \int F_{\alpha\varrho}\, \delta(3)\, dv + [\alpha \rightleftarrows \beta].$$

Our first remark is that the equation of motion for the spin also contains many divergent terms, if we take into account also the effect of the self-field. Every divergent term is multiplied by the reciprocal of the diameter of the particle. Now we face the same problem as in the case of the determination of the translational equation of motion, namely we have somehow to renormalize the divergent terms. The difficulty is greater in this case as the divergent terms are multiform. Therefore, we have to introduce again a compensating auxiliary field with the aid of which the divergent terms can be eliminated. This auxiliary field is the same as the one used to renormalize the translational equation of motion. Namely, if we compare the translational equation of motion with the equation of motion of spin, it can be seen that they are closely related. The structural uniformity of the equations is also proved by the fact that in relation (27) no higher derivative with respect to the proper time than the fourth is included. Eliminating thus the divergencies in the same way as in the translational equation of motion, the final form of the equation of motion of spin is:

$$\dot{S}_{\alpha\beta} + \frac{1}{c^2}(\dot{S}_{\alpha\nu} u_\nu u_\beta - \dot{S}_{\beta\nu} u_\nu u_\alpha) = F^e_{\alpha\sigma} M_{\sigma\beta} - F^e_{\beta\sigma} M_{\sigma\alpha} +$$

$$+\frac{1}{c^2}(u_\alpha M_{\beta\sigma} - u_\beta M_{\alpha\sigma}) F^e_\sigma + M^*_{\varrho\beta} \int F^{\mathrm{inv}}_{e\varrho}\, \delta(3)\, dv - \tag{28}$$

$$- M^*_{\varrho\alpha} \int F^{\mathrm{inv}}_{j\varrho}\, \delta(3)\, dv.$$

Discussion

The relativistic invariant form of the self-force, acting on a pole-dipole point particle has been given. Considering that many publications are concerned with the same problem, it seems to be useful to compare our results with the previous ones.

It was mentioned above that BHABHA [6] and BHABHA and CORBEN [7] have carried out calculations to determine the self-force acting on the pole-

dipole point particle. In the calculations such an energy-momentum tensor was used for the electromagnetic field, which is valid in vacuum. If the particle has an independent magnetic moment, not deducible from the charge, the interaction with the electromagnetic field cannot be described with this energy-momentum tensor only. We have used, therefore, in our calculations the energy-momentum tensor modified by MARX [4] by which, we think, this kind of electromagnetic field is described better. To describe the mechanical behaviour of our particle we have applied the tensor $t_{\alpha\beta}$ according to NAGY [2]. As the energy-momentum tensor applied here is extended in comparison with BHABHA and CORBEN's, it could be presumed that terms of other kind would appear in the expression of self-force too. It is remarkable — and we want to lay special emphasis on this — that although our energy-momentum tensor is different from the usual, and our method of calculation is also different, the final structure of the self-force is the same as that of the expression given by BHABHA and CORBEN. Terms of other type appear neither in the terms B_α, C_α and G_α given by the translational equation of motion (these terms are due to that part of our energy-momentum tensor which agrees with the usual tensor) nor in terms D_α, E_α and H_α, which are the consequence of the completion of the energy-momentum tensor. Thus in the expresion of the self-force in our work as well as in BHABHA and CORBEN's no higher than the fourth derivative of quantities is included, further the term containing e. g. $\ddot{u}_\alpha$ does not appear. In the two cases the terms of the same type only differ in their coefficients.

However, there exists a great difference between the divergent terms of the self-force, determined by the two methods. In the power series used by us all divergent terms approach infinity in the same order, and because in our case the divergent terms could not be written in the form of a complete differential, of necessity we had to use another method to eliminate the divergencies. The difference in the coefficients is partly due to this, and partly to the use of the modified energy-momentum tensor.

All we have said also applies to the equation of motion of spin. Apart from the constant coefficients, this equation involves terms of the same type as BHABHA and CORBEN's equation. It may be mentioned that it contained at first some terms which did not appear in the expression for the translational equation of motion. These terms were divergent and disappeared with the elimination of divergencies. So the use of the same method to eliminate the divergencies, namely the method of introducing an auxiliary field, seems to be justified.

Our calculations have shown further that the rest mass depends on the self-force too, in the way given in relation (95) of the translational equation of motion.

Thanks are due to Dr. K. NAGY and Dr. G. MARX for valuable advice and continuous interest.

REFERENCES

1. K. Hönl, Ergebn, exact. Naturw., **26**, 291, 1951.
2. K. Nagy, Acta Phys. Hung., **7**, 325, 1957.
3. K. Nagy, Magy. Fiz. Folyóirat, **V**, 311, 1957.
4. G. Marx, Acta Phys. Hung., **2**, 67, 1952.
5. I. F. Farkas, Acta Phys. Hung. **15**, 131, 1962.
6. H. J. Bhabha, Proc. Ind. Acad. Sci. A, **XI**, 247, 1940.
7. H. J. Bhabha—H. C. Corben, Proc. Roy. Soc. A, **178**, 273, 1941.

РЕЛЯТИВИСТИЧЕСКОЕ УРАВНЕНИЕ ДВИЖЕНИЯ ДЛЯ ЗАРЯЖЕННЫХ ЧАСТИЦ СО СПИНОМ И МАГНИТНЫМ МОМЕНТОМ

II. Уравнение движения спина

И. Ф. ФАРКАШ

Р е з ю м е

Уравнение движения спина определялось из модифицированного тензора энергии-импульса применением метода Инфельда. При помощи четырехмерного потенциала вычисляется импульс, появляющийся вследствие собственного поля частицы. Расходящиеся члены уравнения могут быть исключены методом компенсационного вспомогательного поля.

ELECTRONIC POLARIZABILITIES OF THE FREE NEUTRAL ATOM

By

T. TIETZ

UNIVERSITY ŁÓDŹ, DEPARTMENT OF THEORETICAL PHYSICS, ŁÓDŹ, POLAND

(Presented by A. Kónya. — Received 16. X. 1961)

Taking into consideration the statistical method and LATTER's potential we have obtained analytical formulae for the total induced quadrupole moment, the field at the nucleus produced by the change of density corresponding to the change of momentum and the change of the electric field gradient at the nucleus produced by an external charge. Four tables are presented by the help of which we can calculate the above mentioned quantities for any neutral atom.

RABI has pointed out that the hyperfine splitting due to the nuclear quadrupole moment includes the effect of an electric quadrupole moment induced in the electron shells. In order to obtain an estimate of the moment induced in a core we consider the THOMAS—FERMI model and adopt the potential due to LATTER [1]. For the electrons of maximum energy $E = 0$ the momentum p is given for the LATTER potential according to statistical considerations [2]:

$$\frac{p^2}{2m} = \frac{Ze^2\varphi(x)}{r} + \frac{e^2 Q(3\cos^2\Theta - 1)}{4r^3} \quad \text{for} \quad Z\varphi(x) \geqslant 1, \tag{1}$$

and for $Z\varphi(x) < 1$ the momentum p is zero since LATTER's potential vanishes. In eq. (1) $\varphi(x)$ is the THOMAS—FERMI function [3] of the free neutral atom at a point in the electron cloud, r is the length of the vector from the nucleus to this point and x is related to r as follows [4]

$$r = (0.88534\, a_H/Z^{1/3})\, x = \mu x\,, \tag{2}$$

where a_H is the first Bohr radius of the hydrogen atom. In eq. (1) Θ is the angle between the X-axis and the radius vector of length r from the nucleus to an electron in the core, and Q is the nuclear quadrupole moment. Z in eqs. (1) and (2) is the atomic number of the atom considered. The density ϱ of electrons in the statistical theory of the atom is given by $8\pi p^3/3h^3$. If p_0 is the maximum momentum for $Q = 0$ and Δp is the change of momentum associated with the term containing Q in eq. (1) we have

$$(p_0\, \Delta p)/m = e^2 Q(3\cos^2\Theta - 1)/4r^3. \tag{3}$$

Denoting by $\Delta\varrho$ the density due to the second term of eq. (1) we have

$$\Delta\varrho = 8\pi p_0^2 \, \Delta p/h^3 . \tag{4}$$

Taking into consideration eqs. (1), (3) and (4) we obtain

$$\Delta\varrho = \pi(2me^2/h^2 r^2)^{3/2} (Z\varphi/r)^{1/2} Q(3\cos^2\Theta - 1). \tag{5}$$

The potential due to $\Delta\varrho$ is that of a total induced quadrupole moment Q_{ind}.

$$\begin{aligned} Q_{\text{ind}} &= 2\pi \int_0^{\pi} \int_0^{r_0} r^4 (3\cos^2\Theta - 1) \, \Delta\varrho \sin\Theta d\Theta dr = \\ &= (16\pi^2/5) (2me^2/h^2)^{3/2} QZ^{1/3} \int_0^{r_0} (\varphi r)^{1/2} dr, \end{aligned} \tag{6}$$

where r_0 appearing in the upper limit of the integral in the last formula according to LATTER's potential is given by $Z\varphi(r_0/\mu) = Z\varphi(x_0) = 1$ and μ is given by eq. (2). Changing the variable x according to eq. (2) we obtain for Q_{ind} the following expression

$$\begin{aligned} Q_{\text{ind}} &= [2(1.7707)^{2/3}/5\pi] \, Q \int_0^{x_0} [x\varphi(x)]^{1/2} dx = \\ &= (3/10) Q \int_0^{x_0} [x\varphi(x)]^{1/2} dx = (3/10) Q \, I(0, x_0), \end{aligned} \tag{7}$$

where x_0 is given by $Z\varphi(x_0) = 1$. The last formula for Q_{ind} has been obtained by STERNHEIMER [5] with the difference that in the upper limit of the integral in eq. (7) stands ∞ instead of x_0. As the integral of eq. (7) in case of integration from zero to infinity diverges, STERNHEIMER concludes that the THOMAS—FERMI model is inadequate for the calculation of the total induced quadrupole moment Q_{ind}. This conclusion of STERNHEIMER is correct only for the statistical potential of the free neutral atom originally introduced by THOMAS and FERMI, but it is not for the statistical potential of the free neutral atom given by LATTER, as it is shown in eq. (7).

In Table I we have listed the values of x_0 as functions of the atomic number Z.

Using the numerical values of KOBYASHI [6] and TAIMA we have calculated numerically the integral $I(0, x_0)$ given in eq. (7) as a function of x_0. Table II gives some numerical values of $I(0, x_0)$ from $x_0 = 0.42$ to $x = 14.5$.

Table I

The x_0-values as functions of the atomic number Z

Z	2	3	4	5	6	7	8	9	10
x_0	0,7566	1,3977	1,9422	2,4019	2,8464	3,2356	3,5943	3,9281	4,2420
Z	11	12	13	14	15	16	17	18	19
x_0	4,5363	4,8156	5,0817	5,3359	5,5792	5,8130	6,0384	6,2558	6,4659
Z	20	21	22	23	24	25	26	27	28
x_0	6,6695	6,8669	7,0587	7,2452	7,4267	7,6035	7,7764	7,5455	8,1100
Z	29	30	31	32	33	34	35	36	37
x_0	8,2713	8,4342	8,5824	8,7355	8,8841	9,0332	9,1734	9,3141	9,4525
Z	38	39	40	41	42	43	44	45	46
x_0	9,5884	9,7223	9,8542	9.9837	10,1132	10,2374	10,3641	10,4840	10,6059
Z	47	48	49	50	51	52	53	54	55
x_0	10,7238	10,8420	10,9572	10,0725	11,1849	11,2961	11,4070	11,5146	11,6237
Z	56	57	58	59	60	61	62	63	64
x_0	11,7289	11,8352	11,9392	12,0414	12,1443	12,2438	12,3441	12,4432	12,5406
Z	65	66	67	68	69	70	71	72	73
x_0	12,6382	12,7329	12.8293	12,9232	13,0154	13.9049	13,1998	13,2905	13,3810
Z	74	75	76	77	78	79	80	81	82
x_0	13,4690	13,5582	13,6461	13,7319	13 8187	13,9049	13,9884	14,0735	14,1576
Z	83	84	85	86	87	88	89	90	91
x_0	14,2394	14,3224	14,4048	14,4843	14,5656	14,6452	14,7248	14,8028	14,8814
Z	92								
x_0	14,9581								

Table II

$I\ (0,\ x_0)$ as a function of x_0

x_0	0,42	0,54	0,66	0,78	0,90	1,20	1,50
$I(0, x_0)$	0,13174	0,19757	0,26716	0,34008	0,41721	0,61563	0,81951
x_0	1.80	2,10	2,40	2,70	3,00	3,30	3,60
$I(0, x_0)$	1,02703	1,23603	1,44507	1,65322	1.85982	2,06451	2,26681
x_0	3,90	4,50	5,10	5,70	6,30	6,90	7,50
$I(0, x_0)$	2,46654	2,85820	3,23853	3,60774	3,96641	4,31443	4,65193
x_0	8,10	8,7	9,3	10.0	11,50	13,00	14,50
$I(0, x_0)$	4,97967	5,29818	5,60770	5,90910	6,64513	7,31622	7,94992

Table I and II allow us to calculate the numerical value of $I(0, x_0)$ for a given atomic number Z. Using the LATTER potential we can calculate in the same manner as Q_{ind} the following quantities: the field at the nucleus E_{ind} produced by the change of density $\Delta\varrho$ corresponding to Δp as well as the change of the electronic field gradient at the nucleus produced by the

external charge $\left(\frac{\partial Ex}{\partial x}\right)$. If we assume that an external charge $+e$ is placed at $X = R$ then we obtain for $E_{\text{ind}, R}(0)$ and $\left(\frac{\partial Ex}{\partial x}\right)$ the following formulas

$$E_{\text{ind},R}(0) = (e/2R^2) \int_0^{x_0} [x\varphi(x)]^{1/2}\, dx = (e/2R^2)\, I(0, x_0) \tag{8}$$

as well as

$$\Delta\left(\frac{\partial Ex}{\partial x}\right) = \frac{6e}{10R^3} \int_0^{x_0} [x\varphi\ (x)]^{1/2}\, dx = \frac{6e}{10R^3} I(0, x_0), \tag{9}$$

where $I(0, x_0)$ is given by eq. (6) and its numerical values are given in Table II. As it is shown in formulae (7), (8) and (9) the introduction of LATTER's potential enables us to calculate the quantities Q_{ind}, $E_{\text{ind}, R}(0)$ and $\Delta\left(\frac{\partial Ex}{\partial x}\right)$ in the statistical theory of the atom. In Table III we present some numerical values for the total induced quadrupole moment Q_{ind} of several elements, as well as the values for the total corrected quadrupole moment Q_{corr}. For the quadrupole moment Q we have adopted the same values as STERNHEIMER. Our values for Q_{corr} are compared with the theoretical values obtained for Q_{corr} by STERNHEIMER, who proceeded in a way different from ours.

Table III

Effect of the induced quadrupole moment

Element	Z	$Q/10^{-24}$ cm^2	$Q_{\text{corr}}/10^{-24}$ cm^2	
			STERNHEIMER	Our values
Lu	71	5,9	8,0	9,62
Eu	63	1,2	4,2	4,79
Al	13	0,156	0,177	1,13

Table III shows that LATTER's potential gives sensible results for Q_{corr} and allows us to calculate the quantities given by eqs. (7), (8) and (9) in a very simple manner. It is known that the calculation of these quantities with great accuracy is possible only by the methods of quantum mechanics, but this procedure is rather complicated. The only quantity calculated by STERNHEIMER [7] quantum-mechanically is $E_{\text{ind}}(0)$ for helium and helium like ions, for which he used the LÖWDIN approximate wave functions. In order to calculate $E_{\text{ind}}(0)$ for atoms which contain more than two electrons he has adopted

the THOMAS—FERMI—DIRAC model and has calculated $E_{ind}(0)$ numerically for $Z = 18$ and $Z = 57$ using different slopes at $x = 0$, i. e. for various radii of neutral atoms. His results [8] contained in Table IV of his paper [9] are compared with ours for $I(0, x_0)/2$ in Table IV of the present paper.

Table IV

A comparison of our values $(R^2/e)\, E_{ind}, x(0)$ with the corresponding STERNHEIMER values for $(R^2/e)\ E_{ind},\ x(0)$ obtained from the Thomas-Fermi-Dirac model for different slopes at $x = 0$.

Z	STERNHEIMER		Our values	
	x_0	$(R^2/e)\ E_{ind}\ x(0)$	x^0	$(R^2/e)E_{ind}\ x\ (0)$
18	7,25	2,98		
18	6,66	2,73	6,2558	1,96
18	5,46	2,22		
57	9,66	3,50	11,8352	3,36
57	3,81	1,47		

In the THOMAS—FERMI—DIRAC model the solutions with a less negative slope at $x = 0$ pass through a minimum at large x and correspond to neutral atoms, they are cut off at the value x_0. In our case x_0 is given by $Z\varphi(x_0) = 0$. The best values for $(R^2/e)\ E_{ind}$, $x(0)$ are the lowest ones. For $Z = 18$ our value is better than STERNHEIMER's and for $Z = 57$ STERNHEIMER's value is better than ours.

STERNHEIMER has pointed out that his results for $I(0, x_0)/2$ are the better the lower they are, i. e. the best value for $Z = 18$ is $2{,}22(x_0' = 5{,}46)$ and for $Z = 57$ it is $1{,}47(x_0' = 3{,}81)$. Table IV shows that our value for $I(0, x_0)/2$ for $Z = 18$ is better than STERNHEIMER's value and $I(0, x_0)/2$ for $Z = 57$ is worse than his. Our formulas for Q_{ind}, $E_{ind}(0)$ and $\triangle\left(\frac{\partial Ex}{\partial x}\right)$ given by eq. (7), (8) and (9) show that it is possible to calculate these by the help of LATTER's potential in a simple manner. Owing to the accuracy of the experimental values and the lack of theoretical values it is difficult to estimate the accuracy of the formulas (7), (8) and (9). It seems that the values obtained from these formulas will be larger than the experimental ones, but they will not differ essentially from the values obtained by the THOMAS—FERMI—DIRAC method. Undoubtedly, quantum mechanics would give better results but the corresponding data for atoms with more than two electrons are not given in the literature.

REFERENCES

1. R. LATTER, Phys. Rev., **99**, 510, 1955.
2. H. STERNHEIMER, Phys. Rev, **102**, 80, 1950.
3. P. GOMBÁS, Die statistische Theorie des Atoms und ihre Anwendungen, Vienna, Springer Verlag, 1949.
4. See ref. [3].
5. R. M. STERNHEIMER, Phys. Rev., **96**, 951, 1954.
6. Table of the exact values of the T—F function, Kagawa University, Kagawa, Japan (1956).
7. See ref. [5].
8. STERNHEIMER denotes the one half of the integral $I(0, x_0)$ by $E_{\text{ind}}(0)$ and x_0', by x_0.
9. See ref. [5].

ЭЛЕКТРОННАЯ ПОЛЯРИЗУЕМОСТЬ СВОБОДНЫХ НЕЙТРАЛЬНЫХ АТОМОВ

Т. ТИТЦ

Р е з ю м е

В данной работе, применяя статистический метод и потенциал Лэтера, выводится аналитическая формула для плотностью индуцированного квадрупольного момента, для поля ядра, созданного изменением плотности, соответствующей изменению импульса и градиента электрического поля ядра, созданного внешним зарядом. Имеется несколько таблиц, с помощью которых возможно вычисление упомянутых выше величин в случае нейтрального атома.

DERIVATION OF ORTHOGONAL MANY-ELECTRON GROUP ORBITALS AND THE EFFECT OF SMALL EXTERNAL PERTURBATION ON A SYSTEM CONSISTING OF LOOSELY COUPLED ELECTRON GROUPS

By

E. KAPUY

RESEARCH GROUP FOR THEORETICAL PHYSICS OF THE HUNGARIAN ACADEMY OF SCIENCES, BUDAPEST

(Presented by A. Kónya. — Received 30. X. 1961)

A set of equations for deriving orthogonal many-electron group orbitals is deduced. This approach can be utilized to define an exact measure for the localizability of the electron groups in a system. It is shown that an N-electron model operator $\mathscr{H}$ can be introduced the eigenfunctions of which are antisymmetrized products of the many-electron group orbitals. Taking $H-\mathscr{H}$ as perturbation the first order correction vanishes and the second order correction is just the dispersion interaction between the separated groups. Taking an external electric or magnetic field as perturbation the corrections up to second order are additive by groups, i. e., they are the sum of the contributions of the separated electron groups.

Most of the N-electron systems (except homogeneous electron gas) consist of M regions ($N > M \geqslant 2$) of higher density, which are separated by lower density domains. Thus it is reasonable to assume that the total wave function of the system can be taken to a good approximation as an antisymmetrized product of strongly orthogonal antisymmetric many-electron group orbitals

$$\Psi = \sqrt{\frac{N_1!\, N_2! \ldots N_M!}{N!}} \sum_P (-1)^p \psi_1(1, 2, \ldots N_1)$$

$$\times \psi_2(N_1 + 1, \ldots N_1 + N_2) \ldots \psi_M(N - N_M + 1, \ldots N).$$

Here, P means those permutations which interchange the electrons between group orbitals. p is the parity of the permutations.

(Delocalized π-electron cloud must be regarded as *one* group, of course.)

As has been proved [1, 2, 3], for M antisymmetric many-electron group orbitals $\psi_I(1, 2, \ldots, N_I)$ mutually orthogonal in the strong sense there exists a complete set of one-electron functions u_ν which can be partitioned into M subsets

$$u_{11}, u_{12}, u_{13}, \ldots; \ldots u_{I1}, u_{I2}, u_{I3}, \ldots; \ldots u_{M1}, u_{M2}, u_{M3}, \ldots$$

such that each of the $\psi_I(1, 2, \ldots, N_I)$'s can be expanded in terms of u_{I1}, u_{I2}, u_{I3}, ... only

$$\psi_I = \sum_{i_1 < i_2 < \ldots i_{NI}} a^I_{i_1 < i_2 < \ldots i_{NI}} (N_I!)^{-\frac{1}{2}} \det[u_{Ii_1}, u_{Ii_2}, \ldots u_{Ii_{N_I}}].$$

Consequently the full Hilbert space of the set u_ν will be decomposed into M mutually perpendicular subspaces 1, 2, ... M, and each of the $\psi_I(1, 2, \ldots N_I)$'s are localized to the corresponding subspace.

In the beginning we assume that the set u_ν and its decomposition into M subsets are known. Let us introduce the following projection operators

$$q^I(1|1') = \sum_i u_{Ii}(1)\, u_{Ii}^*(1'),$$

$$Q^I = q^I(1|1')\, q^I(2|2') \ldots q^I(N_I|N_I'), \quad (I = 1, 2, \ldots M).$$

When the sum of the subsets comprises the complete set

$$\sum_{I=1}^{M} q^I(1|1') = \delta(1|1').$$

Varying the $\psi_I(1, 2, \ldots N_I)$'s in the energy expression [3, 4, 5, 6]

$$E = H(0) + \sum_I \int \psi_I^*(1,2,\ldots N_I) \left[N_I H(1) + \binom{N_I}{2} \frac{1}{r_{12}} \right] \psi_I(1,2,\ldots N_I) \times d(1)\, d(2) \ldots d(N_I)$$

$$+ \sum_{\substack{IJ \\ J \neq I}} \frac{N_I N_J}{2} \int d(1) d(2) \ldots d(N_I) d(\varkappa)\, d(\lambda) \ldots d(\omega)\, \frac{1 - P_{1\varkappa}}{r_{1\varkappa}}\, \psi_J^*(\varkappa', \lambda, \ldots \omega) \times \psi_J(\varkappa, \lambda, \ldots \omega)\, \psi_I^*(1, 2, \ldots N_I)\, \psi_I(1, 2, \ldots N_I) \tag{1}$$

and taking into account that they are constrained to be normalized and localized to the corresponding subspace, we obtain the following set of equations

$$Q^I H^I \psi_I(1, 2, \ldots N_I) = E^I \psi_I(1, 2, \ldots N_I), \quad (I = 1, 2, \ldots M), \tag{2}$$

$$H^I = \left\{ \sum_{\alpha=1}^{N_I} H(\alpha) + \sum_{1=\alpha<\beta}^{N_I} \frac{1}{r_{\alpha\beta}} + \sum_{J \neq I} N_J \sum_{\alpha=1}^{N_I} \int d(\varkappa)\, d(\lambda) \ldots d(\omega) \times \frac{1 - P_{\alpha\varkappa}}{r_{\alpha\varkappa}}\, \psi_J^*(\varkappa', \lambda, \ldots \omega)\, \psi_J(\varkappa, \lambda, \ldots \omega) \right\}.$$

The antisymmetric solutions $\psi_{I0}(1, 2, \ldots N_I)$ $(I = 1, 2, \ldots M)$ of eqs. (2) belonging to the lowest values $E^{I0}(I = 1, 2, \ldots M)$ correspond to the ground state of the system. Keeping the operators H^I and Q^I fixed, each of eqs. (2) has further antisymmetric solutions $\psi_{I1}, \psi_{I2}, \psi_{I3}, \ldots$ with Lagrangian multi-

pliers $E^{I1}, E^{I2}, E^{I3}, \ldots$. The group orbitals $\psi_{I\varkappa}(1, 2, \ldots N_I)$ $(I = 1, 2, \ldots M;$ $\varkappa = 0, 1, 2, \ldots)$ have the following properties

$$\int \psi^*_{I\varkappa}(1, 2,\ldots N_I)\, \psi_{I\varkappa}(1, 2,\ldots N_I)\, \boldsymbol{d}(1)\, \boldsymbol{d}(2)\ldots \boldsymbol{d}(N_I) = 1, \tag{3}$$

$$\int \psi^*_{I\varkappa}(1, 2,\ldots N_I)\, \psi_{I\lambda}(1, 2,\ldots N_I)\, \boldsymbol{d}(1)\, \boldsymbol{d}(2)\ldots \boldsymbol{d}(N_I) = 0, \quad \varkappa \neq \lambda \tag{4}$$

$$\int \psi^*_{J\varkappa}(1, 2,\ldots N_J)\, \psi_{I\lambda}(1, 2',\ldots N'_I)\, d(1) = 0, \qquad J \neq I. \tag{5}$$

The best ground state energy given by this approach lies between the best energy obtained by the Hartree—Fock method and the exact non-relativistic ground state energy of the system. It may be close to the latter when the electron groups of the real system are strongly localized to different regions of the space. This fact can be utilized to define an exact measure for the localizability of the electron groups in the system. The strongly localized group orbitals may be chemically invariant for changes of distant parts of the molecule and can be used as building units to construct the total electronic wave functions of some molecules without any calculation [7].

To obtain approximate group orbitals orthogonal in the strong sense, we choose a finite set of orthonormalized one-electron spin-orbitals w_ν $(\nu =$ $= 1, 2, \ldots n)$ and divide it up intuitively into M subsets w_{Ii} $(I = 1, 2, \ldots M;$ $i = 1, 2, \ldots n_I \geqslant N_I)$ such that each of the w_ν's occurs in *one* of the subsets only [3, 6, 8]. The approximate group orbitals $\varphi_I(1, 2, \ldots N_I)$ $(I = 1, 2, \ldots M)$ constructed from the individual subsets

$$\varphi_I = \sum_{i_1<i_2<\ldots i_{N_I}} c^I_{i_1<i_2<\ldots i_{N_I}} (N_I!)^{-\frac{1}{2}} \det\left[w_{Ii_1}, w_{Ii_2},\ldots w_{Ii_{N_I}}\right] \tag{6}$$

will then be substituted into the energy expression (1). Variation of the coefficients c^I, taking into account that the functions $\varphi_I(1, 2, \ldots N_I)$ have to be normalized, leads to a set of M eigenvalue equations of the following type

$$\widetilde{\mathbf{H}}^I\, \mathbf{c}^I = \widetilde{\mathbf{E}}^I\, \mathbf{c}^I, \quad (I = 1, 2,\ldots M), \tag{7}$$

which can be solved by iteration for the lowest roots $\widetilde{\mathbf{E}}^{I0}$ $(I = 1, 2, \ldots M)$ and the corresponding coefficients $\mathbf{c}^{I0}$ $(I = 1, 2, \ldots M)$. These quantities belong to the ground state of the system. Keeping the ground state coefficients $\mathbf{c}^{I0}$ in the operators $\widetilde{\mathbf{H}}^I$ fixed we can determine the roots $\widetilde{\mathbf{E}}^{I\varkappa}$ and the coefficients $\mathbf{c}^{I\varkappa}$ $(\varkappa = 1, 2, \ldots \binom{n_I}{N_I};\ I = 1, 2, \ldots M)$ belonging to the excited states of the corresponding electron groups. Even this relatively simple procedure seems to be a very promising one [9].

Of course, the results strongly depend on the choice and the decomposition of the basic set w_ν. It would be probably a good starting point if we knew the exclusive orbitals and some oscillator orbitals of the system which have

been defined by FOSTER and BOYS [10]. However, we can subject the basic set w_{Ii} decomposed intuitively to an arbitrary unitary transformation

$$v_{Ii} = \sum_{Jj} V_{Ii,Jj} w_{Jj},$$

which has to be determined as to give the best total energy for the ground state. Replacing the w's by the v's in the formula for the approximate group orbitals (6) and varying the matrix elements $V_{Ii,Jj}$ in the energy expression (1) we obtain a set of equations for the $V_{Ii,Jj}$'s which has to be solved with eqs. (7) simultaneously. In this way we can determine the best decomposition of the basic set into M subsets of given dimension, and the best approximate group orbitals for the ground state

$$\varphi_{I0} = \sum_{i_1<i_2<\ldots i_{N_I}} c^I_{i_1<i_2<\ldots i_{N_I}} (\mathrm{N}_I!)^{-\frac{1}{2}} \det[v_{Ii_1}, v_{Ii_2}, \ldots v_{Ii_{N_I}}].$$

The latter are solutions of the set of equations

$$\tilde{Q}^I \tilde{H}^I \varphi_{I0}(1, 2, \ldots N_I) = \tilde{E}^{I0} \varphi_{I0}(1, 2, \ldots N_I), \quad (I = 1, 2, \ldots M), \tag{8}$$

where

$$\tilde{H}^I = \Big\{ \sum_{\alpha=1}^{N_I} H(\alpha) + \sum_{1=\alpha<\beta}^{N_I} \frac{1}{r_{\alpha\beta}} + \sum_{J\neq I} N_J \sum_{\alpha=1}^{N_I} \int d(\varkappa)\, d(\lambda) \ldots d(\omega) \times \frac{1 - P_{\alpha\varkappa}}{r_{\alpha\varkappa}} \varphi^*_{I0}(\varkappa', \lambda, \ldots\omega)\, \varphi_{I0}(\varkappa, \lambda, ,, .\omega) \Big\},$$

$$\tilde{q}^I(1|1') = \sum_{i=1}^{n_I} v_{Ii}(1)\, v^*_{Ii}(1'),$$

$$\tilde{Q}^I = \tilde{q}^I(1|1')\, \tilde{q}^I(2|2') \ldots \tilde{q}^I(N_I|N'_I).$$

Keeping the operators $\tilde{H}^I$ and $\tilde{Q}^I$ fixed each of the eqs. (8) has further antisymmetric solutions (of finite number: $\binom{n_I}{N_I}$) $\varphi_{I1}, \varphi_{I2}, \varphi_{I3}, \ldots$ with Lagrangian multipliers $\tilde{E}^{I1}, \tilde{E}^{I2}, \tilde{E}^{I3}, \ldots$ which have also the properties (3), (4) and (5). Increasing suitably the basic set w_ν, we can obtain better approximate group orbitals. To improve convergence we can define "almost" orthogonal group orbitals $\tilde{\psi}_I$ exactly as in case of two-electron orbitals [11].

The "almost" orthogonal group orbitals are the "best" orbitals which are normalized and orthogonal to all one-electron basis functions v_{Jj} of all the other subspaces. Alternatively we can add to the approximate group orbitals $\varphi_I(1, 2, \ldots N_I)$ such antisymmetric functions $f_I(1, 2, \ldots N_I)$ which are

1. flexible enough to take into account the remaining part of the intra-group correlation (containing many variational parameters and the inter-electronic coordinates explicitly),

2. orthogonal to all one-electron basis functions v_{Jj} of all the other subspaces and to its own approximate group orbital φ_I.

The variational parameters have to be determined by using the energy expression

$$\mathscr{E} = \int \tilde{\Psi} H \tilde{\Psi} \, d\tau,$$

where

$$\tilde{\Psi} \sim \sum_P (-1)^p \{\varphi_1 ... \varphi_I ... \varphi_M + \sum_{I=1}^{M} \varphi_1 ... \varphi_{I-1} f_I \varphi_{I+1} ... \varphi_M\}.$$

The following considerations equally hold for the exact case as well as for the approximate one. Observing that the operators $Q^I H^I$ and $Q^I H^I Q^I$ have the same eigenvalues and eigenfunctions we construct the following N electron model operator

$$\mathscr{H} = \sum_P P \left\{ \sum_{I=1}^{M} Q^I H^I (N_1 + ... N_{I-1} + 1, N_1 + \right.$$

$$\left. + ... N_{I-1} + 2, ... N_1 + ... N_I) Q^I \right\} - \sum_{\substack{IJ \\ J \neq I}} I^{IJ}_{00,00} + H(0),$$

where

$$I^{IJ}_{\alpha\beta,\gamma\delta} = \frac{N_I N_J}{2} \int d(1) \, d(2) ... d(N_I) \, d(\varkappa) \, d(\lambda) ... d(\omega) \, \frac{1 - P_{1\varkappa}}{r_{1\varkappa}}$$

$$\times \psi_{J\gamma}{}^*(\varkappa', \lambda, ... \omega) \, \psi_{J\delta}(\varkappa, \lambda, ... \omega) \, \psi_{I\alpha}(1', 2, ... N_I) \, \psi_{I\beta}(1, 2, ... N_I).$$

Here, P means those permutations which permute the electrons between the group orbitals. $\mathscr{H}$ is symmetric in the space-spin variables of the electrons. One can easily show that a wave function of the following type

$$\Psi_{\mu,\nu,...\varrho} = \sqrt{\frac{N_1! \, N_2! ... N_M!}{N!}} \sum_P (-1)^p P \, \psi_{1\mu}(1, 2, ... N_1)$$

$$\times \psi_{2\nu}(N_1 + 1, N_1 + 2, ... N_1 + N_2) ... \psi_{M\varrho}(N - N_M + 1, ... N)$$

is exact eigenfunction of it and belongs to the eigenvalue

$$E_{\mu,\nu,...\varrho} = E^{1\mu} + E^{2\nu} + ... E^{M\varrho} - \sum_{\substack{IJ \\ J \neq I}} I^{IJ}_{00,00} + H(0).$$

Particularly, $\Psi_{0,0,\ldots 0}$ and $E_{0,0,\ldots 0}$ are eigenfunction and eigenvalue of the ground state, respectively. If we take $H - \mathscr{H}$ as a perturbation and carry out a perturbation calculation (the ground state is assumed to be non-degenerate) we observe that the first order correction vanishes (as usual in self-consistent theories) and the second order correction will be

$$\sum_{\substack{IJ \\ J \neq I}} \sum_{\substack{\mu>0 \\ \nu>0}} \frac{4|I^{IJ}_{0\mu,0\nu}|^2}{E^{I0} + E^{J0} - E^{I\mu} - E^{J\nu}} .$$

The latter is just the well-known dispersion interaction. It is a part of the intergroup correlation energies which, apart from the Fermi correlations, are neglected in the zeroth order approximation of this approach.

We assume now that the system is subject to a small external perturbation of the following form (e. g. external electric or magnetic field)

$$\mathscr{V} = \sum_{\alpha=1}^{N} v(\alpha).$$

Taking $\mathscr{V}$ as a perturbation we have up to second order

$$E_{0,0,\ldots 0} + \sum_{I=1}^{M} N_I v^I_{0,0} + \sum_{I=1}^{M} \sum_{\mu>0} \frac{N_I^2 |v^I_{0,\mu}|^2}{E^{I0} - E^{I\mu}} ,$$

$$v^I_{\alpha,\beta} = \int \psi^*_{I\alpha}(1,2,\ldots N_I)\, v\,(1)\, \psi_{I\beta}(1,2,\ldots N_I)\, d(1)\, d(2) \ldots d(N_I),$$

i.e., in this approximation the correction is expressed as a sum of contributions of the separate electron groups. Consequently, in this approach the electric polarizability and the diamagnetic susceptibility (including high-frequency paramagnetism) are exactly additive. Thus in case of systems for which the above approach is valid, it is justified to calculate the electric polarizability and the diamagnetic susceptibility etc. by groups separately. In practice this can be done by a variational method similar to that of GUY and TILLIEU [12].

Note added in proof. (4th August, 1962.) T. L. ALLEN and H. SHULL have based the bond energy concept on the virial theorem. (J. Chem. Phys., **35**, 1644, 1961.) This generalized bond energy concept can be applied to the zeroth order energy of our approach.

REFERENCES

1. T. Arai, J. Chem. Phys., **33**, 95, 1960.
2. P.-O. Löwdin, J. Chem. Phys., **35**, 78, 1961.
3. E. Kapuy, Acta Phys. Hung., **13**, 345, 1961.
4. R. G. Parr, F. O. Ellison and P. G. Lykos, J. Chem. Phys. **24**, 1106, 1956.
5. R. McWeeny, Proc. Roy. Soc., A **253**, 242, 1959.
6. R. McWeeny, Rev. Mod. Phys., **32**, 335, 1960.
7. S. F. Boys, Rev. Mod. Phys., **32**, 296, 1960.
8. P. G. Lykos and R. G. Parr, J. Chem. Phys., **24**, 1166, 1956.
9. R. McWeeny and K. A. Ohno, Proc. Roy. Soc., A **255**, 367, 1960.
10. J. M. Foster and S. F. Boys, Rev. Mod. Phys., **32**, 300, 1960.
11. E. Kapuy, Acta Phys. Hung., **13**, 461, 1961.
12. J. Tillieu and G. Guy, Comptes Rendus, **239**, 1203, 1283, 1954; ibid., **240**, 1402, 1955; ibid., **241**, 382, 1955; ibid., **242**, 1279, 1956.

ПРОИЗВОДСТВО ОРТОГОНАЛЬНЫХ МНОГОЭЛЕКТРОННЫХ ГРУППОВЫХ ОРБИТ И ИССЛЕДОВАНИЕ ВОЗДЕЙСТВИЯ НЕБОЛЬШОГО ВНЕШНЕГО ВОЗМУЩЕНИЯ НА СИСТЕМУ, СОСТОЯЩУЮ ИЗ СЛАБО СВЯЗАННЫХ ЭЛЕКТРОННЫХ ГРУПП

Э. КАПУИ

Р е з ю м е

Для производства ортогональных электронных орбит выводится система уравнений. Данное приближение может быть использовано для определения точной меры локализуемости электронных групп системы. Показывается, что возможно выводить N — электронный модельный оператор $\mathscr{H}$, «собственными функциями» которого являются антисимметризированные произведения многоэлектронных групповых орбит. Принимая $H - \mathscr{H}$ за возмущение, поправка первого порядка исчезает, в то время как поправка второго порядка отвечает дисперсионному взаимодействию между различными группами. Если возмущением считать внешние электрическое или магнитное поля, то поправки до второго порядка аддитивны по группам, то-есть они представляют собой суммы добавок отдельных электронных групп.

THE TIME DISTRIBUTION OF THE GAMMA RADIATION EMITTED IN THE FISSION OF U^{235}

By

S. Dési, A. Lajtai and L. Nagy

CENTRAL RESEARCH INSTITUTE OF PHYSICS, BUDAPEST

(Presented by L. Pál. — Received 2. IV. 1962)

Using a time-to-pulse-height converter of high resolving power, the time distribution of the gamma rays emitted with the thermal fission of U^{235} has been determined up to a few nanoseconds. The time distribution of the gamma radiation was found to be varying with the gamma energies, that is, the time delays with respect to the event of fission were observed to increase with decreasing gamma energies.

Introduction

The energy spectrum in the range of 20 to 250 keV of the gamma radiation from U^{235} fission has been investigated by Skliarevskii et al. [1] by means of an experimental set-up which enabled them, on the basis of geometrical considerations, to obtain some information on the lifetime of the excited states of the fission fragments emitting gamma rays. The values were estimated to be in the range from 0,5 to 2,5 nanoseconds.

In the present measurements the time distribution of the gamma radiation from thermal neutron induced fission of U^{235} has been investigated in the gamma energy range above 25 keV, employing the scintillation method for detecting gamma rays and fission fragments.

Experimental apparatus

The schematic diagram of the experimental equipment is shown in Fig. 1. An uranium layer was exposed to a beam of thermal neutrons from the horizontal reactor channel. The event of fission was observed by a scintillation detector mounted directly on the layer. The gamma detector, on the other hand, was placed at a distance of 20 cm from the layer in a position normal to the neutron beam. The time delay between the pulses from the two detectors was converted by means of a time-to-pulse-height converter into a pulse proportional in amplitude to the time delay, which was analysed by a 128-channel kick sorter.

The layer consisted of an electrolytically deposited mixture of uranium oxides, 2 mg/cm^2 thick, enriched to 35% U^{235} on thin aluminium backing.

The fission fragments were detected by a 18 μ thick plastic scintillation foil [2]. Foils of such thickness are hardly sensitive to gamma rays and to fast neutrons. The light pulses from the scintillator were passed to the multiplier with the aid of a plexiglass light guide 10 cm long, 25 mm in diameter, and in

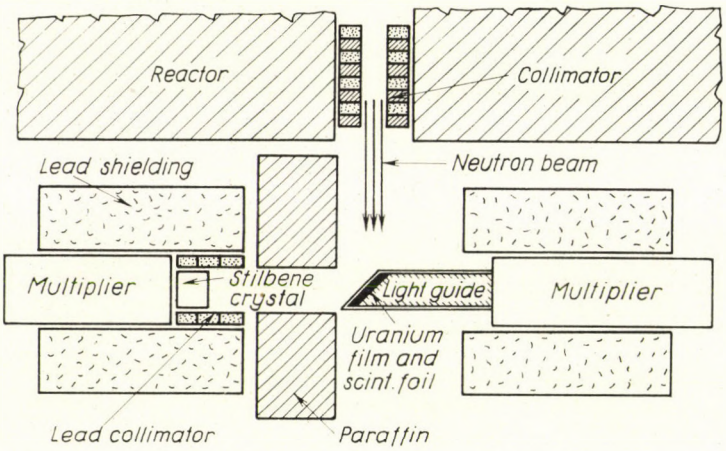

Fig. 1. Experimental arrangement

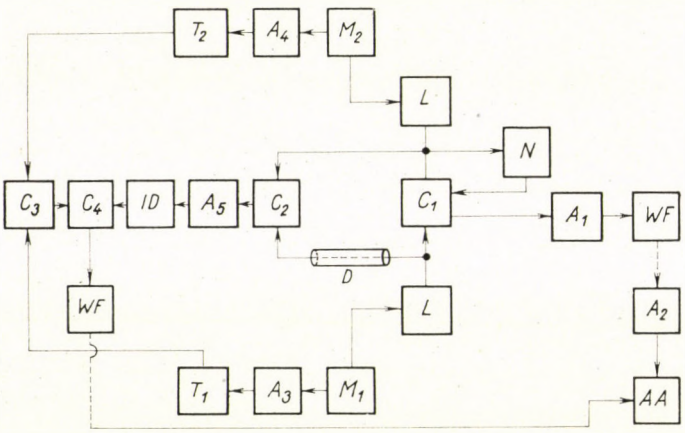

Fig. 2. Block diagram of the apparatus

this way the multiplier was not in the beam of the reactor channel. The gamma detector was a 30×20 mm stilbene crystal. The multipliers were both of 6810 A type. To reduce the time spread only the central areas of 25, resp. 30 mm diameter of the photocathodes were used.

The pulses from the multiplier anodes were put in the time-to-pulse-height converter operating in the nanosecond delay range. The working

principle of this device being identical with that of GARG [3], only the modifications introduced will be dealt with in the following. The block diagram of the apparatus is shown in Fig. 2. Limiter circuits (L) with D3a pentodes have been employed between the phototubes and the converter (C_1) consisting of a 6BN6 tube. Since the plate current pulses of the 6810-A multiplier obtained for the plastic scintillator were of a duration of about 15 nanoseconds, i. e. longer than the intervals to be measured, the pulses from the fission detector were fed to the limiter without their passing through a stretching cathode follower. This had the advantage that the disturbing effect due to the piling-up of low amplitude pulses from the high intensity radiations of gammas and fast neutrons, to which the fission detector and the light guide were exposed, was much less observed than in the case when pulse stretching was applied. The number of background pulses being considerably lower on the gamma detector side, there a pulse shaper was used. The pulses delivered by the limiter were of a width of 8 nanoseconds, thus the time interval analysed was of about the same length.

Pulses arriving in g_3 of the 6BN6 tube not accompanied by pulses in g_1, produced signals at the anode the amplitudes of which, due to the short interval analyzed, were similar to those of coincidence pulses. Since these pulses would have caused a considerable shift in the base level of the amplifying system, a neutralizing stage (N) had been inserted between the third grid and the anode of the converter tube, driven by the limiter. The output pulses from the plate circuit of N, of opposite phase but nearly alike in shape to the input pulses, were fed to the anode of the 6BN6 tube across a trimmer capacitor. This variable trimmer capacitor could be adjusted so that the two pulses passed to the anode of the 6BN6 tube through the inter-electrode capacity and the neutralizing stage were approximately of the same amplitude, thus they neutralized each other. Since this neutralization did not induce a conducting current in the plate circuit of the 6BN6 tube, its effect was merely capacitive and did not affect the amplitudes of the conducting (coincidence) pulses produced by the integration of the conducting current at the RC element of the plate circuit.

The output pulses from the converter, being only of the order of 10 mV, had to be amplified to the value of a few volts by the preamplifier (A_1) and passed through a white follower (WF) to the amplifier (A_2), which amplified the pulses to the level required by the pulse height analyser.

The number of chance events was reduced by a second converter (C_2) of the same construction as the first one, with the difference that a cable of known delay (D) had been introduced in one of its channels, while the other channel received the pulses at the same time as C_1. The signals from C_2 through amplifier (A_5) were fed to a discriminator (ID) which gated the slow coincidence circuit (C_4) only when pulses from M_2 were preceded by those of M_1.

The amplitude i. e. energy sensitivity of the apparatus could be adjusted by the pulses of side channels which were passed through amplifying stages of variable gain (A_3, A_4, resp.) to fast pulse shaping triggers (T_1, T_2, resp.) operating with secondary emission tubes. The output pulses of the quasi-fast coincidence unit C_3, coupled to the triggers, entered the second channel of the slow coincidence unit C_4, which delivered the gating pulses for the pulse height analyser.

Calibration

In the calibration process both detectors were stilbene crystals placed at equal distances from a Na^{22} source. An additional cable of known delay

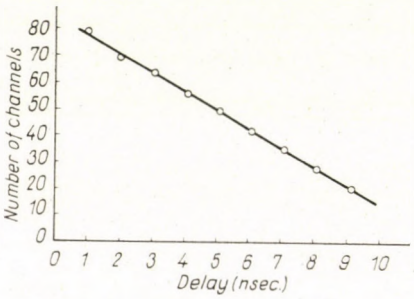

Fig. 3. Time delay vs pulse height calibration curve of the converter

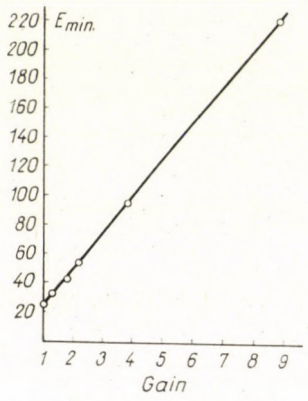

Fig. 4. Threshold energy vs gain calibration curve

was inserted between the detector M_2 and the converter. The number of the channel corresponding to the peak of the resolution curve was determined. The observed positions of the peaks for various lengths of delay are shown in Fig. 3 as the time delay vs pulse height calibration curve of the converter. The channel width was 1.4×10^{-10} sec, the measurable time interval was found to be about 8 nanoseconds.

The threshold energy of the gamma radiation to be measured was determined by the amplification factor of A_4 and by the fixed bias of the trigger T_2 in the side channel of M_2. At a given amplification of A_4 the voltage of M_2 applied in the measurements was decreased to the threshold voltage which had been found just sufficient to make the pulses of a γ-source of known energy trigger T_2. The threshold energy of the gamma radiation was calculated by the ratio of the amplification of the two voltages of the multiplier, taking

into account the energy of the γ-source. The calibration curve is shown in Fig. 4, where the threshold energy vs amplification of A_4 is plotted. Almost the same data were obtained in the checking measurement by means of an X-ray apparatus.

Results

The experimental set-up described above was used to investigate the time distribution of the gamma radiation from fission fragments for various threshold energies. The time distribution curves are shown in Fig. 5 together with the time resolution curves obtained for Na^{22} gamma radiation at the same threshold energies. It is apparent that while the time resolution curves for the Na^{22} gammas are symmetrical, the time distribution curves for the fission fragment gamma rays are asymmetrical. With increasing threshold energies, however, the asymmetry decreases and finally vanishes at the level of 95 keV, where the distribution curve almost coincides with that obtained for Na^{22}. (The lower value of the Na^{22} resolution curve at the half-width is due to the fact that the time spread of the Na^{22} gamma rays of about 500 keV is smaller than that of gamma rays from fission fragments, generally of lower energies. This higher time spread at lower threshold energies is apparent also when the Na^{22} curves in Fig. 5 are compared.) In order to illustrate this growing tendency towards asymmetry in the distribution curves as the threshold energies become lower, we have shown in Fig. 6 the whole set of distribution curves plotted for various threshold energies.

It is to be noted that the distribution as well as the resolution curves do not tend to constant values, but increase anew after having reached their minimum values. This may be due to the fact that the neutralizing stage did not fully compensate the single pulses passing through the inter-electrode capacity. Furthermore, the gamma detector being sensitive to fast neutrons as well, the fission neutrons also must have contributed to the number of counts in this range of delay.

The above results were checked by inserting lead plates of successively increasing thickness (1,3 and 5 mm) in front of the gamma detector. With increasing absorber thickness, the fission gamma rays became increasingly harder. The time distribution curves for the fission gamma rays passing through the absorbers are shown in Fig. 7. For this measurement the lowest threshold energy was chosen. It is seen from the figure that the tendency towards asymmetry in the distribution curves decreases with increasing absorber thickness. Since the distribution curves for lead absorbers of 3 and 5 mm thickness are almost identical, only the curve for 5 mm absorber thickness is shown.

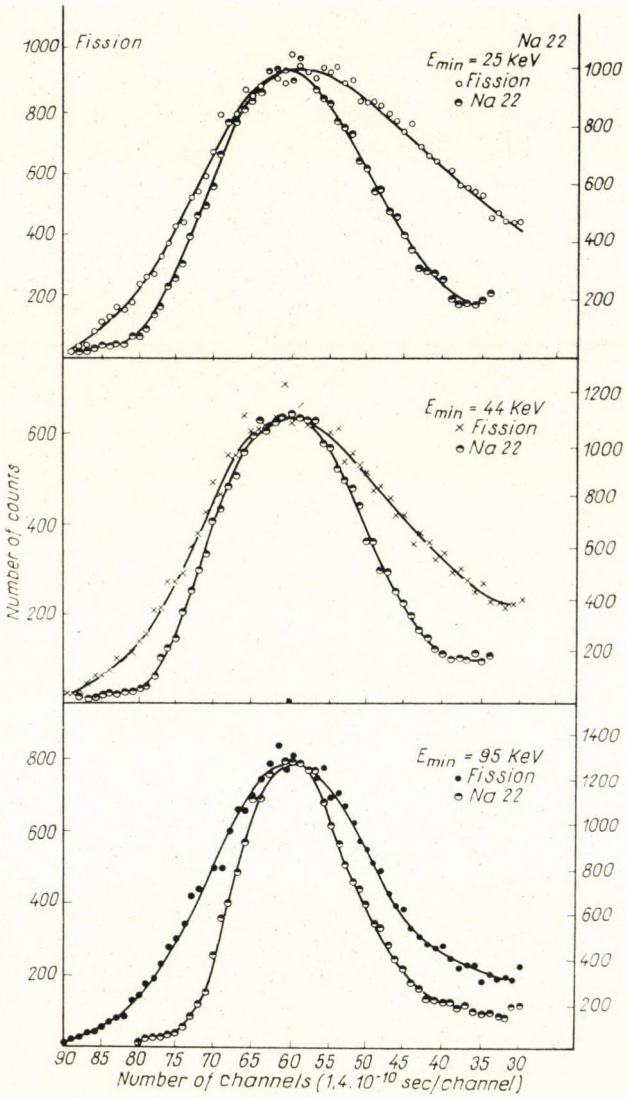

Fig. 5. Time distribution curves of the fission gamma radiation and time resolution curve of the Na^{22} gamma radiation plotted for various threshold energies

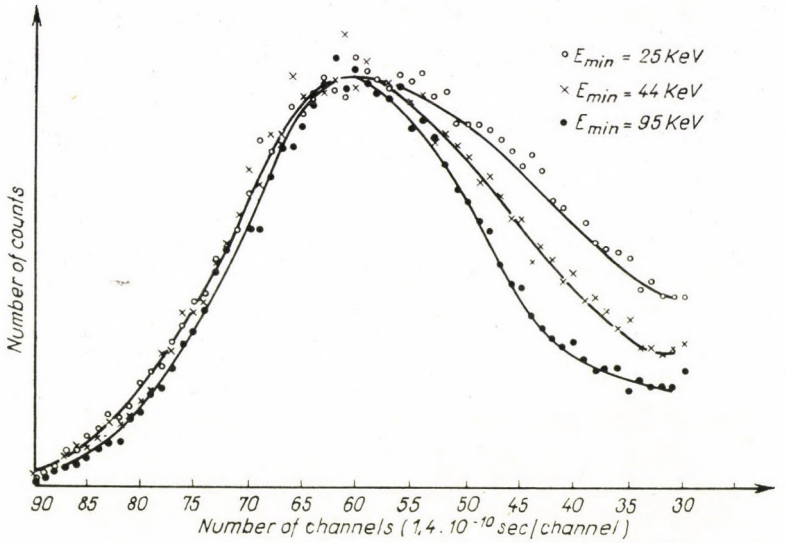

Fig. 6. Time distribution of fission gamma rays for various threshold energies

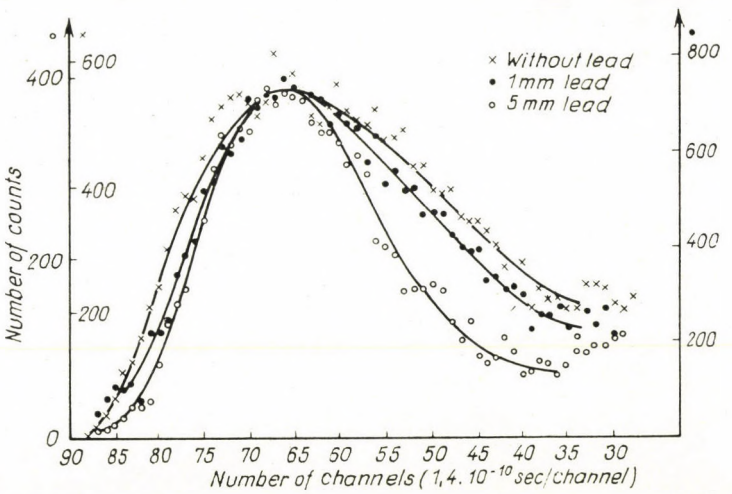

Fig. 7. Time distribution curves of fission gamma radiation for lead absorbers of various thicknesses

As a qualitative statement it can be inferred from the measurements that the gamma rays of 25 to 100 keV in energy are emitted by fission fragments with lifetimes in the range from 10^{-10} to 10^{-9} sec decreasing with increasing energies.

REFERENCES

1. *В. В. Скляревский, Д. Е. Фоменко, Е. П. Степанов,* ЖЭТФ, **32**, 256, 1957.
2. *В. М. Горбачев, М. И. Казаринова,* ПТЭ, № 4, 20, 1957.
3. J. B. Garg, Nucl. Instr. and Meth., **6**, 72, 1960.

РАСПРЕДЕЛЕНИЕ ПО ВРЕМЕНИ ГАММА-ИЗЛУЧЕНИЯ ПРИ ДЕЛЕНИИ U^{235}

Ш. ДЕШИ, А. ЛАЙТАИ и Л. НАДЬ

Р е з ю м е

Измерялось распределение по времени гамма-излучения до нескольких мксек., образующегося при делении U^{235}, т.е. испускающегося из осколков деления с помощью конвертера амплитуда время с большой разрешающей способностью. Распределение по времени гамма-излучения изменялось в зависимости от энергии излучения, а именно, в случае малых энергий получалось большее время запаздывания по отношению к моменту деления.

COMMUNICATIO BREVIS

EINE NEUE FORM DES NICHT-KLASSISCHEN ABSTOSSUNGSPOTENTIALS ZUR ERSETZUNG DES PAULISCHEN BESETZUNGSVERBOTES IM FALLE ZYLINDERSYMMETRISCHER ELEKTRONENVERTEILUNG

Von

T. SZONDY

FORSCHUNGSGRUPPE FÜR THEORETISCHE PHYSIK DER UNGARISCHEN AKADEMIE DER WISSENSCHAFTEN, BUDAPEST

(Eingegangen: 1. XI. 1961)

Auf Grund der statistischen Theorie atomarer Systeme kann ein Abstossungspotential abgeleitet werden, welches die Bildpunkte der Elektronen aus den schon besetzten Phasenraum-Zellen ausstösst, und damit für die annähernde Erfüllung des Paulischen Besetzungsverbotes auch dann sorgt, wenn die Faktoreigenfunktionen der Elektronen in einer Hartreeschen Variationsfunktion nicht orthogonalisiert sind [1]. In dieser Arbeit wird das Abstossungspotential für zylindersymmetrische Systeme abgeleitet. Diese Symmetrieeigenschaft kommt häufig vor, und das Potential hat in diesem Fall eine besonders einfache Form.

Betrachten wir ein System mit der als zylindersymmetrisch vorausgesetzten Elektronendichte ϱ, welche aus den Teildichten ϱ_m der Elektronen mit der magnetischen Quantenzahl m ($m = 0, \pm 1, \ldots$) zusammengesetzt ist [2]. Die Symmetrieachse des Systems sei gleichzeitig die z-Achse eines Zylinderkoordinatensystems, und der Impuls der Elektronen sei in die orthogonalen Komponenten p_R, p_z und p_φ zerlegt (Abb. 1).

Zu den Elektronen in einem kleinen herausgegriffenen Volumenelement dv (Abb. 1) gehört im Impulsraum eine Impulskugel mit dem Radius $P = 3^{1/3}\,\pi^{2/3}\,\hbar\,\varrho^{1/3}$. Wir nehmen an, dass die Bildpunkte derjenigen Elektronen, welche sich in dv befinden und deren magnetische Quantenzahl m ist, im Impulsraum in einem Kugelschnitt enthalten sind, welcher aus der Impulskugel durch die Flächen $Rp_\varphi = (m \pm {}^1/_2)\,\hbar$ herausgeschnitten ist (Abb. 2).

Ein neues Elektron kann infolge des Paulischen Besetzungsverbotes im Volumenelement dv nur dann untergebracht werden, wenn sein Bildpunkt in eine noch nicht besetzte, also ausserhalb der Impulskugel liegende Impulszelle fällt. Dasselbe Ergebnis erhält man aber [1], wenn man annimmt, dass das neue Elektron unter der Wirkung eines nicht-klassischen Abstossungspotentials steht, für welches $\frac{1}{2\mu} P^2$ eine gut annähernde untere Grenze gibt (μ bezeichnet die Elektronenmasse). Dieses Abstossungspotential muss man zu den elektrostatischen Potentialen addieren. Es ist zweckmässig, P^2 durch

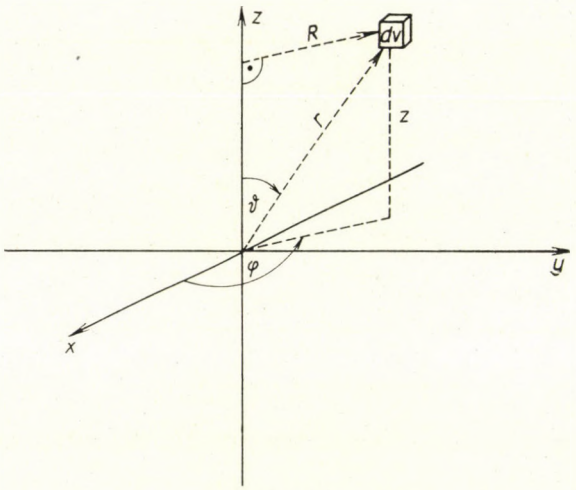

Abb. 1

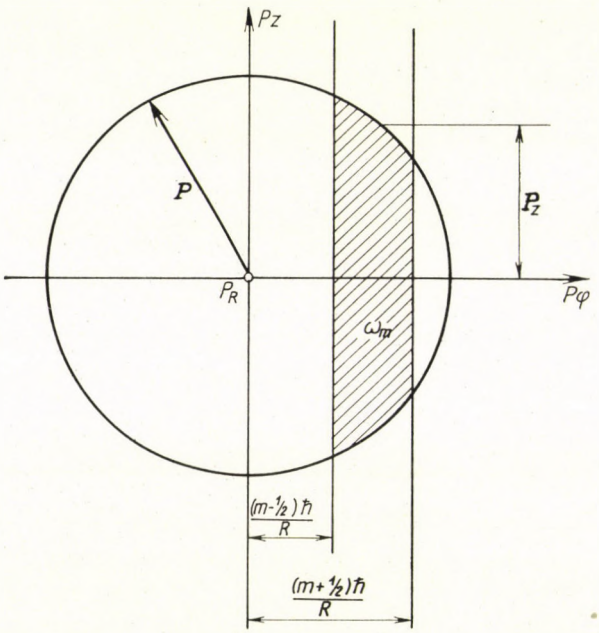

Abb. 2

ϱ_m auszudrücken, wobei m wieder die magnetische Quantenzahl des Elektrons bedeutet.

Es bezeichne $P_z = P_z(p_\varphi)$ den zu einem gegebenen p_φ-Wert gehörenden Maximalwert von p_z (siehe Abb. 2). Aus dem Zusammenhang: Elektronendichte im Phasenraum $= \dfrac{1}{4\pi^3\hbar^3} = 2/h^3$ folgt für das Volumen des Kugelschnitts

ω_m (siehe Abb. 2): $\omega_m = 4\pi^3 \hbar^3 \varrho_m$. Ebenfalls aus der Abbildung folgt $\omega_m = \hbar R^{-1} \pi \overline{P_z^2}$, wo mit $\overline{P_z^2}$ der Mittelwert der zu ω_m gehörenden P_z^2-Werte bezeichnet wurde. Wir haben also:

$$\overline{P_z^2} = 4\pi^2 \hbar^2 R \varrho_m . \tag{1}$$

Der Mittelwert der zu ω_m gehörenden p_φ^2-Werte ist

$$\frac{\int_{(m-1/2)\hbar R^{-1}}^{(m+1/2)\hbar R^{-1}} p_\varphi^2 \, dp_\varphi}{\int_{(m-1/2)\hbar R^{-1}}^{(m+1/2)\hbar R^{-1}} dp_\varphi} = \frac{\hbar^2 (m^2 + 1/12)}{R^2} . \tag{2}$$

Wir haben also für das Abstossungspotential, welches auf ein Elektron mit der magnetischen Quantenzahl m wirkt, den Näherungsausdruck

$$H_m \equiv \frac{1|}{2\mu} P^2 \approx \frac{1}{2\mu} (\overline{P_z^2} + \overline{P_\varphi^2}) = \frac{\hbar^2}{\mu} \left[2\pi^2 \varrho_m R + \frac{m^2 + 1/12}{2R^2} \right] . \tag{3}$$

In der unmittelbaren Nähe der z-Achse wird das Abstossungspotential durch diesen Ausdruck überschätzt, da die Integrationsgrenzen in der Gl. (2) ausserhalb der Impulskugel liegen. Dieser Fehler ist nur im Falle $m = 0$ von Bedeutung. Da das Abstossungspotential in allen praktisch wichtigen Fällen von den inneren, mindestens teilweise abgeschlossenen Schalen der Atomrümpfe stammt, welche auch bei einer Molekülbildung in guter Näherung unverändert bleiben, und da das Abstossungspotential in der besprochenen Näherung nur von der Verteilung der inneren Schalen abhängt, genügt es, den Fehler nur für den Fall freier Atome zu korrigieren.

Im Falle von p, d. . .-Zuständen kann man zur Beseitigung des Fehlers davon Gebrauch machen, dass man aus den zu derselben Nebenquantenzahl aber verschiedenen magnetischen Quantenzahlen gehörenden Wellenfunktionen physikalisch gleichwertige Linearkombinationen bilden kann. Das Verfahren kann man am einfachsten durch ein Beispiel erklären. Nehmen wir an, dass wir das auf ein p_z-Elektron wirkende Abstossungspotential berechnen wollen. Man berechnet dann zunächst das auf ein p_x (oder ein p_y)-Elektron wirkende Potential. Das auf ein p_z-Elektron wirkende Abstossungspotential erhält man daraus infolge von Symmetriegründen durch eine Drehung der Koordinatenachsen um 90°.

Im Falle von s-Zuständen kann man von der Kenntnis Gebrauch machen, dass die genaue Form des Abstossungspotentials kugelsymmetrisch sein muss. Der Kern liege im Nullpunkt des Koordinatensystems. In den in der xy-Ebene liegenden, vom Kern ausgehenden Richtungen (siehe Abb. 1) lautet der Ausdruck (3)

$$H_0 = \frac{\hbar^2}{\mu} \left[2\pi^2 \varrho_0 r + \frac{1}{24r} \right] , \tag{4}$$

wo mit r die in der Abb. 1 dargestellte Polarkoordinate bezeichnet wurde. Die in der Nähe der z-Achse liegende »fehlerhafte Zone« verlässt man aber am schnellsten in einer zur z-Achse senkrechten Richtung. Infolge der Kugelsymmetrie kann man dann den Ausdruck (4) auch in allen anderen Richtungen als gültig annehmen, womit ein überwiegender Teil des Fehlers beseitigt ist.

Selbstverständlich kann man den vor dem Abstossungspotential stehenden Proportionalitätsfaktor auch aus empirischen Daten bestimmen [3], wodurch die Näherung verbessert werden kann.

Um eine Abschätzung der Genauigkeit des neuen Abstossungspotentials zu erhalten, wurde es in das statistische Atommodell, in welchem die Elektronen nach der Hauptquantenzahl gruppiert sind [4], eingebaut und die Energie bzw. die Elektronendichte des Argon-Atoms berechnet. Die erhaltenen Werte für den Variationsparameter bzw. die Energie stimmen mit den von GOMBÁS und LADÁNYI berechneten Werten ausserordentlich gut überein, die Unterschiede sind kleiner als 1,2%.

LITERATUR

1. P. GOMBÁS, Statistische Behandlung des Atoms, Hdb. der Phys. Bd. XXXVI, Ziff. 20. S. 168—71, Springer Verlag, Berlin-Göttingen-Heidelberg, 1956.
2. Vgl. A. KÓNYA, Acta Phys. Hung., **13**, 219, 1961.
3. H. HELLMANN, Einführung in die Quantenchemie, Deuticke Verlag, Leipzig-Wien, 1937.
4. P. GOMBÁS und K. LADÁNYI, Acta Phys. Hung., **5**, 313, 1955; **7**, 263, 1957.

RECENSIO

Theoretical Physics in the Twentieth Century A Memorial Volume to Wolfgang Pauli

edited by M. Fierz and V. F. Weisskopf, Interscience Publishers, Inc. New York 1., N. Y.

Had not unexpected death carried him away, PAULI would have been 60 years old on the 25th April 1960. Originally the editors wanted to celebrate this birthday by publishing "Theoretical Physics in the Twentieth Century". It was a difficult task to compile a volume worthily reflecting the role played by PAULI in the birth and development of modern physics. The difficulty lies in PAULI's scientific character, rather unique in our age.

Nobody has watched with a more passionate inquisitiveness the manifestations of the secrets of the universe, and at the same time, nobody has taken natural science more seriously than he. He looked upon nature with the enthusiasm of GOETHE and with the reverence of NEWTON. He believed with a staunch faith in its comprehensiveness, yet one significant step in the recognition of reality became a deep experience to him. His conception so receptive of physical reality, never led to cheap mystification or obscure announcements. On the contrary, his works are characterised by a modest competence and his respect felt for nature manifests itself in a scientific responsibility of the highest degree. V. F. WEISSKOPF called him the living conscience of physics. When looking through his oeuvre one cannot overemphasize that inspiration with which his vigourous mind and exacting demands — always leading to clarification and ordering of thoughts — filled not only his students in Hamburg and Zurich, but through scientific symposia and his extensive correspondence much wider circles as well.

As we learn from the forword, the editors — contrary to the ordinary practice (of collecting original eassys from the friends and pupils of PAULI) — originally planned a collection of articles comprising the present state of physics in all fields, where PAULI has contributed to the solution of problems. It soon became clear, that the realisation of this plan would simply have meant the writing of a complete modern handbook of physics, as there is practically no field of physics where the thoughts of PAULI have not left their mark. Thereafter the book assumed its final shape in which we can find articles of two kinds, first those summarizing the development achieved in the fields nearest to PAULI's interest; then report-like recollections of the establishment of the PAULI principle, dealing in general with the "romantic" period that saw the formation of the fundamental conceptions of quantum-mechanics.

The first group includes nine essays. The article of G. VENTZEL elaborates the history of the quantum theory of fields till 1947. F. VILLARS' article deals with the methods devised in the following years, to overcome the difficulties presented by divergence first of all with the method of regularisation; furthermore with the non-local theories and their connection with indefinite metrics. The essay of R. JOST "The Pauli principle and the Lorentz group" is devoted to the problems of the fundamental relations between the spin and statistics. It contains a detailed discussion of the TCP-thesis comprising also the recent researches of LEHMANN—SYMANZIK—ZIMMERMANN and WIGHTMAN, respectively into the theory of fields. The relations between spin and statistics are treated also from another aspect, in the work of V. BARGMAN, written about PAULI's general attitude towards the special and general theory of relativity. PAULI holds a special opinion as regards the theory of solid bodies. He did not like this branch of physics, which instead of mathematical severity and logically closed order abounds in uncertain models and uncontrollable mathematical hypotheses. Nevertheless, it is hardly necessary to emphasize the significance of his work done in this field, for instance the role of the PAULI principle in the band theory, or the treatment of spin according to PAULI in the phenomena of magnetic resonance. The short remarks of H. B. G. CASIMIR on

this subject are followed by the article of R. E. PEYERLS dealing with the same problem. PAULI introduced the hypothesis of the neutrino for the explanation of the anomalies observed in β-decay in 1931 (in a year when among the elementary particles only the early recognised electron and proton were known), because the law of conservation of energy etc. connected with the basic principles of relativistic physics was a living reality to him. C. S. WU presents a complete description of the exciting history and present state of neutrino physics.

Two articles in this book revive the spirit of PAULI in a form, which is to some extent independent, the chapter entitled "Statistical Mechanics" by M. FIERZ and L. B. LANDAU's article on "Fundamental Problems". From the first we learn that PAULI lectured for long years on statistical mechanics and especially liked to explain its train of thoughts abounding in hidden refinements to his pupils. That is what makes this article topical in the volume. L. B. LANDAU recalls the memory of Pauli's brave and critical attitude in his "funeral address" on the present form of field theories using ψ-operators and Hamiltonians.

All these articles, written in a serious tone and a clear style serve the purpose well, setting up a memorial in honour of a man who detested everything superficial and negligent.

The articles of R. KRONIG, W. HEISENBERG and B. L. VAN DER WAERDEN give a historical review of the heroic age of quantum theory. From these we should like to mention in particular the last one which, tracing clearly and instructively the birth of the exclusion principle and of the spin theory, dislcoses with an impressive completeness the intuitive strength and the highly responsible self-discipline of PAULI.

To the volume, which ends with an extensive bibliography, N. BOHR has written an introduction in warm words.

F. KÁROLYHÁZY

Printed in Hungary

A kiadásért felel az Akadémiai Kiadó igazgatója — Műszaki szerkesztő: Farkas Sándor

A kézirat nyomdába érkezett: 1962. IX. 10. — Terjedelem: 9,75 (A/5) ív, 28 ábra

62.55946 Akadémiai Nyomda, Budapest — Felelős vezető: Bernát György

The *Acta Physica* publish papers on physics, in English, German, French and Russian.
The *Acta Physica* appear in parts of varying size, making up volumes.
Manuscripts should be addressed to:

Acta Physica, Budapest 502, Postafiók 24.

Correspondence with the editors and publishers should be sent to the same address.
The rate of subscription to the *Acta Physica* is 110 forints a volume. Orders may be placed with "Kultura" Foreign Trade Company for Books and Newspapers (Budapest I., Fő u. 32. Account No. 43-790-057-181) or with representatives abroad.

Les *Acta Physica* paraissent en français, allemand, anglais et russe et publient des travaux du domaine de la physique.
Les *Acta Physica* sont publiés sous forme de fascicules qui seront réunis en volumes.
On est prié d'envoyer les manuscrits destinés à la rédaction à l'adresse suivante:

Acta Physica, Budapest 502, Postafiók 24.

Toute correspondance doit être envoyée à cette même adresse.
Le prix de l'abonnement est de 110 forints par volume.
On peut s'abonner à l'Entreprise du Commerce Extérieur de Livres et Journaux «Kultura» (Budapest I., Fő u. 32. — Compte-courant No. 43-790-057-181) ou à l'étranger chez tous les représentants ou dépositaires.

«*Acta Physica*» публикуют трактаты из области физических наук на русском, немецком, английском и французском языках.
«*Acta Physica*» выходят отдельными выпусками разного объема. Несколько выпусков составляют один том.
Предназначенные для публикации рукописи следует направлять по адресу:

Acta Physica, Budapest 502, Postafiók 24.

По этому же адресу направлять всякую корреспонденцию для редакции и администрации.
Подписная цена «*Acta Physica*» — 110 форинтов за том. Заказы принимает предприятие по внешней торговле книг и газет «*Kultura*» (Budapest I., Fő u. 32. Текущий чет: № 43-790-057-181) или его заграничные представительства и уполномоченные.

27,— Ft

INDEX

ACTA PHYSICA

ACADEMIAE SCIENTIARUM HUNGARICAE

TOMUS XV. FASCICULUS 3.

AKADÉMIAI KIADÓ, BUDAPEST
1963

ACTA PHYS. HUNG.

ACTA PHYSICA

A MAGYAR TUDOMÁNYOS AKADÉMIA FIZIKAI KÖZLEMÉNYEI

SZERKESZTŐSÉG ÉS KIADÓHIVATAL: BUDAPEST V., ALKOTMÁNY UTCA 21.

Az *Acta Physica* német, angol, francia és orosz nyelven közöl értekezéseket a fizika tárgyköréből.

Az *Acta Physica* változó terjedelmű füzetekben jelenik meg: több füzet alkot egy kötetet.

A közlésre szánt kéziratok a következő címre küldendők:

Acta Physica, Budapest 502, Postafiók 24.

Ugyanerre a címre küldendő minden szerkesztőségi és kiadóhivatali levelezés.

Az *Acta Physica* előfizetési ára kötetenként belföldre 80 forint, külföldre 110 forint. Megrendelhető a belföld számára az Akadémiai Kiadónál (Budapest V., Alkotmány utca 21. Bankszámla 05-915-111-46), a külföld számára pedig a „Kultúra" Könyv- és Hírlap Külkereskedelmi Vállalatnál (Budapest I., Fő u. 32. Bankszámla 43-790-057-181 sz.), vagy annak külföldi képviseleteinél és bizományosainál.

Die *Acta Physica* veröffentlichen Abhandlungen aus dem Bereiche der Physik in deutscher, englischer, französischer und russischer Sprache.

Die *Acta Physica* erscheinen in Heften wechselnden Umfanges. Mehrere Hefte bilden einen Band.

Die zur Veröffentlichung bestimmten Manuskripte sind an folgende Adresse zu richten:

Acta Physica, Budapest 502, Postafiók 24.

An die gleiche Anschrift ist auch jede für die Redaktion und den Verlag bestimmte Korrespondenz zu senden.

Abonnementspreis pro Band: 110 forint. Bestellbar bei dem Buch- und Zeitungs-Aussenhandels-Unternehmen »Kultúra« (Budapest I., Fő u. 32. Bankkonto Nr. 43-790-057-181) oder bei seinen Auslandsvertretungen und Kommissionären.

$N-\Theta$ SCATTERING DISPERSION RELATION IN THE LEE MODEL WITH DIPOLE GHOST

By

K. L. NAGY

INSTITUTE OF THEORETICAL PHYSICS, ROLAND EÖTVÖS UNIVERSITY, BUDAPEST

(Presented by K. F. Novobátzky — Received: 28. VIII. 1961)

The $N-\Theta$ scattering dispersion is examined in the LEE model in the dipole ghost case. The dipole ghost produces a second order pole in the relation.

1. Dispersion relations are regarded as appropriate tools (at least we hope they are) when we wish to decide whether in a theory the usual basic principles are fulfilled or not. Since in almost all theories, treated by means of a Hamiltonian formalism, ghost states emerge, the question naturally arises: what is the influence of ghosts, or indefinite metric, on the form of the dispersion relations. Since, however, a theory with an indefinite metric possesses a probabilistical interpretation if it contains only a multipole type of ghost, it is mainly this case in which we are interested. The form, or the modification of the dispersion relations in a relativistic, causal theory with dipole ghosts was calculated earlier [1]. The aim of this paper is to check the relations in the extremely simple case of the LEE model, which thus may give a better insight into the problem.

Dispersion relation methods in the LEE model were applied already by GOLDBERGER and TREIMAN [2], DE CELLES and FELDMAN [3] and by AMADO [4] to several problems, but in each paper the existence of ghosts was excluded by an appropriate cut-off. In this paper the denotations concerning the LEE model are the same as in [5] or [6], those of the dispersion relations follow closely the notations of [2].

2. The LEE model starts from the Hamiltonian

$$H = -m_v \int \psi_v^* \psi_v \, \mathrm{d}p + \int \omega(k)\, a^*(k)\, a(k)\, \mathrm{d}k - \\ - \frac{g_0}{\sqrt{4\pi}} \int \frac{1}{\sqrt{2\omega}} \delta(p-q-k) \left\{ \psi_N^*(q)\, \psi_v(r)\, a^*(k) - \psi_v^*(p)\, \psi_N(q)\, a(k) \right\} \cdot dp\, dq\, dk \tag{1}$$

allowing only the transitions $V \rightleftarrows N + \Theta$, g_0 is the bare coupling constant, which is imaginary, $\omega = (k^2 + \mu^2)^{1/2}$. The commutation relations have the usual form, except for ψ_v, for which

$$\{\psi_v(p), \psi_v^*(p')\} = -\delta(p-p') \tag{2}$$

is prescribed which gives rise to an indefinite metric. The real vacuum $|0>$ and N particle states $|N>$ are the corresponding bare states, the real V particle state (and the scattering eigenstates) have to be determined from

$$(H - E)\,|E> = 0\,, \tag{3}$$

where because of the conservation theorems $|E>$ has the form

$$|E> = \left(-c\psi_v^* + \psi_N^* \int \varphi(k)\, a^*(k)\, dk\right)|0>. \tag{4}$$

In the dipole ghost case beside the real V particle state a dipole ghost state $|D>$ satisfying the equation

$$(H - E)\,|D> = |E> \tag{5}$$

is also needed for completing the state vector space. $|D>$ obviously has also the form

$$|D> = \left(-d\psi_v^* + \psi_N^* \int \Phi(k)\, a^*(k)\, dk\right)|0>. \tag{6}$$

All the results of the model are characterized by a function

$$h(z) = a + bz + z^2\, G(z)\,, \tag{7}$$

where

$$a = -\frac{m_v}{g_0^2} + \int \frac{k^2\, dk}{2\omega^2}\,,\quad b = \frac{1}{g_0^2} + \int \frac{k^2\, dk}{2\omega^3}\,,\quad G(z) = \int \frac{k^2\, dk}{2\omega^3\,(\omega - z)}\,. \tag{8}$$

a and b are finite parameters. Choosing their values appropriately, one can set up the dipole ghost case. The energy eignevalue of the real V particle state can be determined from the zero of $h(z)$, i. e.

$$h(E) = 0\,, \qquad E \neq \omega\,.$$

In the dipole ghost case $E < 0$ and $h'(E) = 0$. The renormalized coupling constant is

$$g^2 = \frac{2\,h''(E)}{3\,(h'''(E))^2}\,. \tag{9}$$

Furthermore

$$\begin{aligned} &<E|E> = |cg_0|^2\, h'(E) = 0\,,\ <E|D> = \frac{|cg_0|^2}{2}\, h''(E) > 0\,, \\ &<D|D> = |cg_0|^2 \left\{\frac{1}{6}\, h'''(E) + \frac{1}{2}\left(\frac{d}{c} + \frac{d^*}{c^*}\right) h''(E)\right\}. \end{aligned} \tag{10}$$

Choosing c and d appropriately we prescribe

$$< D \mid D > = 0 . \tag{11}$$

In this case, the projection operator, projecting the state vectors into the subspace $\mid E >$, $\mid D >$ is

$$P = \frac{\mid E >< D \mid}{< D \mid E >} + \frac{\mid D >< E \mid}{< E \mid D >} , \tag{12}$$

and finally from the SCHRÖDINGER equation and from (3) and (5) we obtain

$$e^{-iHt} \mid E > = e^{-iEt} \mid E >, \; e^{-iHt} \mid D > = e^{-iEt} (\mid D > - it \mid E >) \tag{13}$$

3. We start now to study the $N - \Theta$ scattering dispersion relation. The S-matrix element is [2]:

$$\begin{aligned} S\omega\omega' = < N\Theta_\omega \quad \text{out} \quad \mid N\Theta_{\omega'} \; in > = \delta(k - k') + \\ + 2\pi i \, \delta(\omega - \omega') \frac{1}{2\omega (2\pi)^3} \mathfrak{M}(\omega) , \end{aligned} \tag{14}$$

where

$$\mathfrak{M}(\omega) = i \int_{-\infty}^{+\infty} dt \, \Theta(-t) \, e^{-i\omega t} < N \mid [j, j^*(t)] \mid N > , \tag{15}$$

$$j = \frac{g_0}{\sqrt{4\pi}} \psi_N^* \, \psi_v , \; j^*(t) = e^{iHt} \frac{- g_0}{\sqrt{4\pi}} \psi_v^* \psi_N \, e^{-iHt} . \tag{16}$$

Because of TITCHMARSH's theorem we have the dispersion relation

$$\mathfrak{M}(\omega) = \frac{1}{\pi} \int_{-\infty}^{+\infty} \frac{d\omega' \, Im \, \mathfrak{M}(\omega')}{\omega' - \omega - i\varepsilon} . \tag{17}$$

Using the formulae of the previous section we obtain

$$< N \mid j P j^*(t) \mid N > = e^{iEt} \left(- \frac{g^2}{4\pi} + \frac{it}{2\pi h''(E)} \right), \tag{18}$$

thus from (15)

$$\begin{aligned} Im \, \mathfrak{M}(\omega) = - \frac{g^2}{4} \delta(\omega - E) - (h''(E))^{-1} \delta'(\omega - E) + \\ + \frac{1}{4\pi} (\omega^2 - \mu^2)^{1/2} \mid \mathfrak{M}(\omega) \mid^2 \Theta(\omega - \mu) . \end{aligned} \tag{19}$$

This is in complete agreement with our general result for a relativistic field theory. Note that the coefficient of the δ-function is again the renormalized coupling constant, that of the δ'-function another parameter characteristic of the model. Therefore if one wants to decide whether in a theory there is a dipole ghost by comparing dispersion formulae with the experimental results one has to seek for second order poles in the dispersion relations.

REFERENCES

1. K. L. NAGY, Acta Phys. Hung., **14,** 15, 1962.
2. M. L. GOLDBERGER and S. B. TREIMAN, Phys. Rev., **113,** 1663, 1959.
3. P. DE CELLES and G. FELDMAN, Nuclear Phys., **14,** 517, 1959/60.
4. R. D. AMADO, Phys. Rev., **122,** 696, 1961.
5. W. HEISENBERG, Nuclear Phys., **4,** 532, 1957.
6. K. L. NAGY, Nuovo Cimento Suppl., **17,** 92, 1960.

ДИСПЕРСИОННОЕ СООТНОШЕНИЕ $N-\Theta$ РАССЕЯНИЯ В МОДЕЛИ ЛИ С ДИПОЛЬНЫМ ПРИЗРАКОМ

К. Л. НАДЬ

Резюме

Исследуется дисперсионное соотношение $N-\Theta$ рассеяния в модели Ли в случае дипольного призрака. Полюс второго порядка в соотношении обусловливается дипольным призраком.

HIGH INTENSITY NEUTRON DIFFRACTOMETER

By

P. Szabó, E. Krén and J. Gordon

DEPARTMENT OF SOLID STATE PHYSICS, CENTRAL RESEARCH INSTITUTE OF PHYSICS, BUDAPEST

(Presented by L. Pál — Received 13. IX. 1961)

Design and characteristics of a high intensity neutron diffractometer are described. The suitability of the method of single crystal growing and orientation worked out by the authors is proved by single crystal measurements. Diffraction measurements on crystals of known structure and properties, and comparison between measured and calculated intensities, as well as angles of reflection give a favourable account of the intensity, resolving power and accuracy to be obtained with the equipment described.

1. Introduction

A neutron diffractometer has been built in the Department of Solid State Physics, Central Research Institute of Physics, Budapest. The research work which is being done here is concerned with structural disorder phenomena in solids.

The materials involved are chiefly polycrystalline. The study of structural disorder in polycrystalline materials often requires the measurement of exceedingly weak neutron scattering or of small changes in this. Therefore the problem of getting sufficient intensity* is here still harder than it is generally in the case of the neutron diffraction of polycrystalline materials. Our aim was to build a diffractometer suitable for such experiments.

Neutron diffractometers built only for experiments with single crystals may be of a comparatively small size, occasionally not larger than some commercial X-ray diffractometers [1]. Investigation of polycrystalline materials, on the other hand, requires generally much larger equipment. Principally there are two types of arrangement of these large diffractometers, represented best by those of Wollan and Shull and Bacon, Smith and Whitehead, respectively [2].

The advantage of the Bacon type lies in that it can be used in a simple manner also as neutron spectrometer. In the Wollan and Shull type, on the other hand, it is easier to provide good radiation shielding. This is indispens-

* Intensity is used throughout this work in the sense: number of neutrons flying *through the whole cross section* of the monochromatic beam in unit time.

able not only from the health point of view but also for lowering sufficiently the background intensity, which otherwise reduces the accuracy of the diffraction measurement.

In accordance with our aims we have had to consider this latter circumstance as decisive regarding the choice of type. Thus our neutron diffractometer follows the arrangement of WOLLAN and SHULL.

In our efforts to ensure great intensity we were able to solve some problems arising in the construction of diffractometers. These results have been published elsewhere, their application to the design of our diffractometer will be dealt with here following the description of the equipment. Finally an account is given of our measurements to check the physical characteristics of our apparatus.

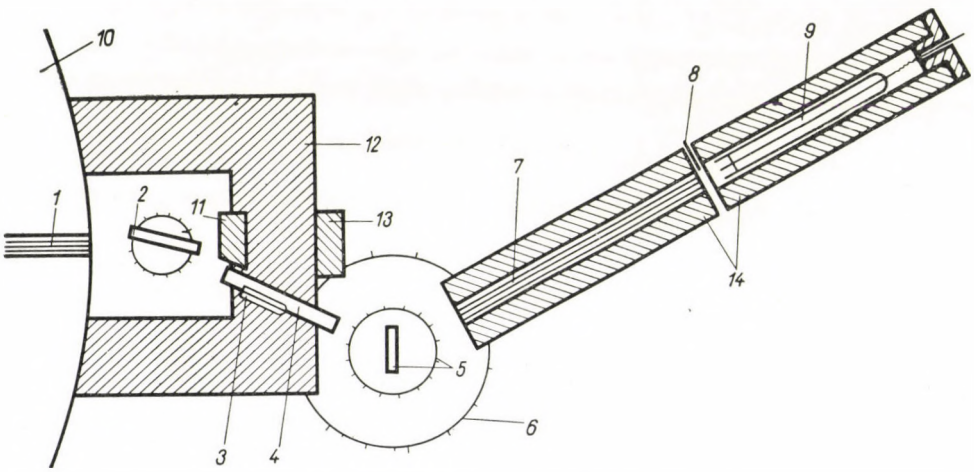

Fig. 1a. Arrangement of the diffractometer
*1*primary collimator, *2* monochromator, *3* monitor counter ,*4* exit tube, *5* sample on goniometer head, *6* angular scale of the detector, *7* secondary collimator, *8* Cd shutter, *9* detector, *10* reactor shielding *11*, *12*, *13* and *14* shieldings

2. Equipment

The design of our arrangement and a photograph of it are shown in Figs. 1*a* and 1*b*.

One of the horizontal channels of the VVRS type reactor of our Institute was used. The channel had a diameter of 10 cm and a length of 250 cm.

A SOLLER type collimator [3] was placed into the channel, at its outlet. This type of collimator allows a large beam cross section with small angular divergence. We were using two different cross sections: 5 cm wide, 4 cm high, and 4 cm wide, 3 cm high, as well as two different angular divergences: 20′

and 10′. The dividing plates were made of steel and were 0.5 and 0.3 mm thick. Their length and number will be discussed in Section 3.

The monochromating single crystal was located in front of this primary collimator, at a distance of about 30 cm from it. It was lying on a goniometer head on which it could be adjusted. Its angular position around a vertical axis could be read on a scale divided in minutes of arc.

The (111) reflection of lead proved to be the most suitable for our purposes [2]. The lead crystal used was 5 cm high, 20 cm long and about 2 cm

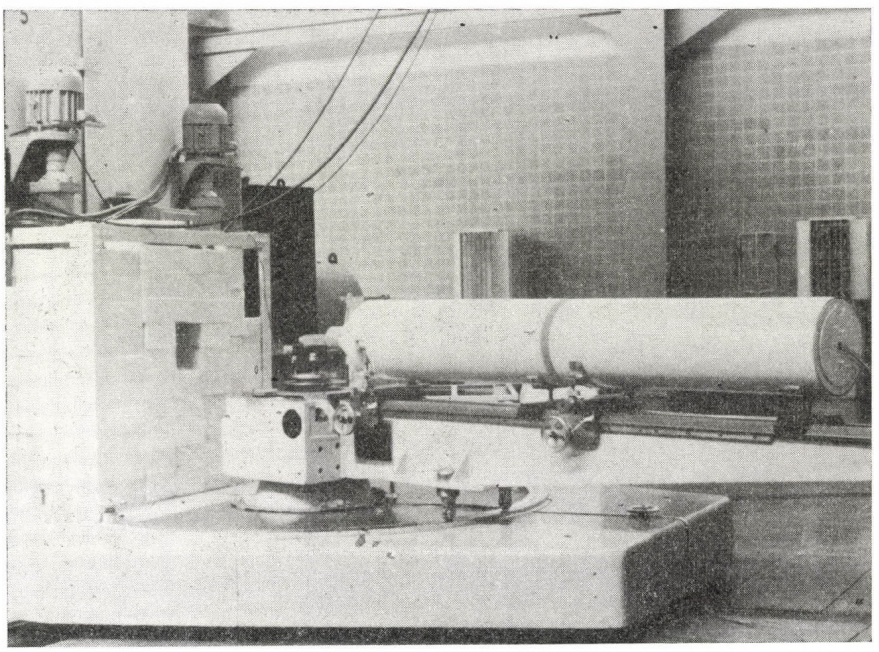

Fig. 1b. Photograph of the diffractometer

thick. It had a "FANKUCHEN cut" [4] at 3.5 degrees to the reflecting plane in order to diminish the cross section of the monochromatic beam without appreciable loss of intensity. Preparation and orientation of large lead crystals are discussed in Section 3.

The monochromator was surrounded by a 50 cm thick boron paraffin shield to absorb the undiffracted neutrons. In addition to this there was a 10 cm thick layer of B_4C inside and a beam stopper containing lead outside the paraffin shield, in front of the beam port. The dial of the monochromator could be inspected across the shield by a periscope.

The monochromatic beam of neutrons, reflected by the monochromating crystal, was allowed to pass through a horizontal exit tube in the shield. This tube had a rectangular cross section 5 cm high and 3.5 cm wide. Its walls were

made of 2 cm thick B_4C and paraffin and were not touched by the monochromatic beam.

One wall of this tube contained a cavity where a monitor counter was placed. The counts of the detector were related to the counts of the monitor to eliminate the effect of the fluctuations of the reactor power.

The subsequent parts of the diffractometer (sample, secondary collimator and detector) were placed on a large goniometer and could be moved on two horizontal rails, both at right angles to the axis of the reactor channel. The axis of the goniometer was at a distance of about 120 cm from the reactor wall.

The sample could be adjusted on a goniometer head and its position could be read on a scale with 2′ marks with reference to the angular position of the detector.

Using such wide beams it is necessary to have also a secondary collimator of SOLLER type in front of the detector to ensure sufficient resolving power in the diffraction measurements. The collimator used was about 120 cm long, 4 cm high, 5 cm wide and of the same angular divergence as the primary one. Its dividing plates were like those of the primary collimator. It could be rotated around its horizontal axis to make its plates parallel to the plates of the primary collimator to an accuracy of 0.5′.

The detector was a special end-window type proportional counter (see Section 3) filled at a pressure of 700 Hgmm with BF_3 enriched in B^{10} to 82%. Its diameter was 6 cm, its length 50 cm.

Detector and secondary collimator had 1.5 cm thick B_4C and 10 cm thick boron paraffin shields. Between secondary collimator and detector there was a shutter containing a Cd plate. The Cd plate could be moved by remote control in front of the end-window of the detector for measurements of the true background counting rates.

Detector and secondary collimator together with their shields weighed about 200 kgs. They were placed upon and adjusted on a large arm of 200 cm length which could be rotated around the axis of the goniometer. Its angular position could be read on a scale with 0.01° division.

The rotations of detector and sample could be coupled in such a manner that the ratio of their angular velocities was 2 : 1. This could be achieved with an accuracy of about $^1/_2$′ by means of steel tapes wrapped around ground steel drums. The range of rotation of the detector was 220°. As the monochromatic beam was inclined by about 22° to the axis of the channel (see section 4), the detector could be rotated at one side up to 132° from the monochromatic beam, i.e. the highest accessible angle of reflection ϑ was 66°.

In addition to the direct visual reading of any of the three angular positions, a mechanical counter system was provided for remote reading in units of 0.01°. Detector, sample and monochromator could be rotated by electromotors. The rotations could be made either continuous or through prescribed

multiples of 0.01°, with the help of a present circuit and mechanical counter. In this manner remote operation and control was possible.

The counting system of the detector and of the monitor was a conventional one and impulses are ruled out by this system.

3. Special features

We investigated the problem of intensity transmitted through SOLLER collimators [5]. According to the result of our considerations there is an optimum in their length, respectively in the number of dividing plates, if their height and total width, the dimensions of the reactor channel and the allowed angular divergence are given. We built collimators with approximately these optimum dimensions. The ratio I_{opt} of the intensity transmitted directly through these optimum collimators to the number of neutrons emerging in unit time and *unit solid angle* through 1 cm^2 of the inlet cross section of the reactor channel is shown in Table 1 along with the principal dimensions of the collimators.

Table 1

Data of the optimum collimators
(All linear dimensions are in cm.)

No.	Total cross section		Horizontal angular divergence	Thickness of dividing plates	Number of collimating channels	$I_{opt.}$
	height	width				
1	4	5	20′	0,05	10	$3{,}47 \cdot 10^{-3}$
2	4	5	10′	0,03	20	$1{,}69 \cdot 10^{-3}$
3	3	4	20′	0,03	18	$2{,}05 \cdot 10^{-3}$
4	3	4	10′	0,03	22	$9{,}5 \cdot 10^{-4}$

We chose a very simple stationary furnace method [6] for the growing of large monochromator crystals, making use of a special X-ray goniometer and following a simple procedure [7] for checking the single crystal character of our large crystals and for orienting them and performing the "FANKUCHEN cut". The crystal chosen as monochromator in this way should not have contained orientation differences greater than $^1/_2$°. While this result, arrived at on the basis of X-ray meausrements, referred only to a thin surface layer of the crystal, it will be proved in Section 4a by neutron diffraction measurements to hold for its whole volume. The measurements of the mosaic spread of the monochromating crystal will be reported also in Section 4a.

We built proportional BF_3 counters of a design [8] differing from that generally used in such work [9]. This improved construction leads to a greater sensitivity, in fact very near to 100% for a thermal neutron beam travelling parallel to the axis of the counter tube [8, 10].

4. Measurements

Our task was to choose the wave length in such a manner that the intensity was largest while the beam contained the least amount of contamination from other wave lengths. Furthermore we had to select a monochromating crystal of suitable mosaic spread (i.e. the half-value breadth β of the angular distribution of the mosaic blocks) so as to obtain the desired resolving power. Finally we made some measurements on polycrystalline materials characteristic of the performance of our equipment.

We used collimator No. 1 (Table 1) for the measurements. It was sufficient to open 3 collimating channels out of the total of 10. Even this intensity was too high for the single crystal measurements. We therefore put a Cd slit of 5 mm high and 35 mm wide opening in front of the detector. For the experiments with polycrystalline materials this slit was not used.

The axis of the monochromator and of the detector as well as the dividing plates of the primary and secondary collimator were adjusted to be approximately vertical and to be parallel to each other with an accuracy of 15′. According to elementary considerations this is already appropriate for all the collimators of Table 1.

a) *Single crystal measurements*

An important requirement of the monochromating single crystal is that its mosaic spread should be approximately equal to the horizontal angular divergence of the primary beam. We choose the monochromating crystal on the basis of an estimate of the mosaic spread from the monochromator rocking curve. The detector was placed to receive neutrons reflected from the monochromator at about 22° to the primary beam. (This corresponds roughly to the maximum of the Maxwell distribution of the thermal neutrons.) After adjustment of the crystal, the intensity (counting rate) was measured as a function of the angular position of the monochromator around its vertical axis. A plot of the number of counts versus counter setting (rocking curve) for the crystal finally chosen is shown in Fig. 2. The half-value breadth of this rocking curve is 0.30°. β can then be computed [11] in a rough approximation from the equation

$$0{,}30 = \sqrt{\frac{\alpha^2 + 2\beta^2}{2}} \,. \tag{1}$$

α was 0.33° and thus $\beta = 0.19°$. Therefore the above crystal is suitable for both our collimators (either 10′ or 20′ angular divergence). The curve shows the intensity at 0.5° out of the maximum of the rocking curve to be less

then 1 per cent of the maximum intensity. This compares favourably with the value of 3 per cent at 2° out of the maximum given by WOLLAN and SHULL [2].

Moreover, nearly the whole of this diffuse radiation occurs also if the Cd shutter mentioned in Section 2 is inserted. Thus it may be regarded as background and can be eliminated from the diffraction measurements by use of the Cd shutter.

So as to check the effect of the "FANKUCHEN cut" of the monochromating crystal on the width of the beam Cd-backed films placed before and behind

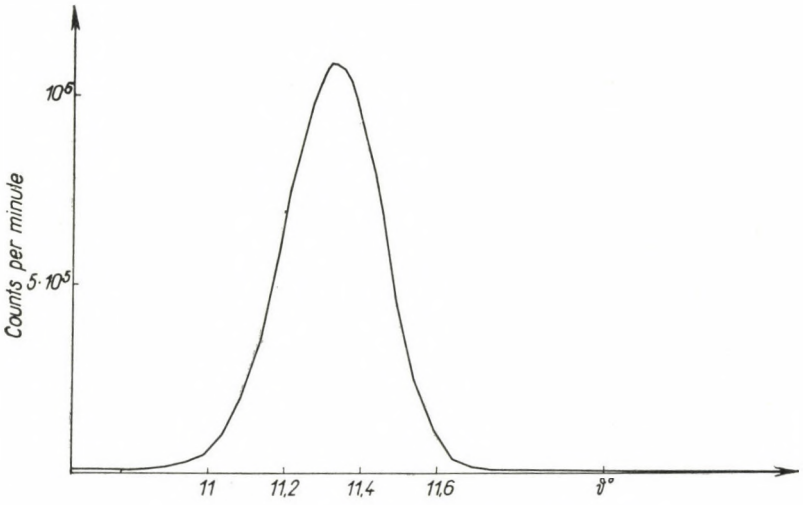

Fig. 2. Rocking curve of the monochromator

the crystal were exposed and showed the beam to become narrower by a factor of about 2 when reflected. This corresponds to what is to be expected from the angle of the "FANKUCHEN cut" (Section 2).

We compared the intensity of the reflected beam with the intensity of the second-order contamination of wave length $\lambda/2$ contained in it with the view of choosing the final position of the monochromating crystal, i.e. the principal wave length λ of the monochromatized beam. This was done by analysing the reflected beam with the help of a second single crystal placed on the goniometer head for samples.

In view of subsequent measurements we used the (111) reflection of lead for the analysis. The analysing crystal had been arranged in the so-called transmission position, otherwise its dimensions would have had to be inconveniently large. The length of this crystal was accordingly 5 cm. Its height was also 5 cm, adjusted to the height of the beam. Its thickness was chosen 1 cm, to give maximum intensity.

We measured the parallel (111) rocking curve of the analysing crystal with optimum thickness. Ti is shown for one position of the monochromating crystal in Fig. 3. This curve contains two peaks. The large one corresponds to the principal wave length λ of the monochromatized beam and the small one to the second-order contamination of wave length $\lambda/2$. The ratio of the latter to the whole intensity is given by the ratio of the areas of the two peaks and is found to be less than 0.010. (WOLLAN and SHULL [2] obtained 0.016 for this). The curve shows furthermore that wave lengths outside these peaks are virtually nonexistent in the monochromatized beam.

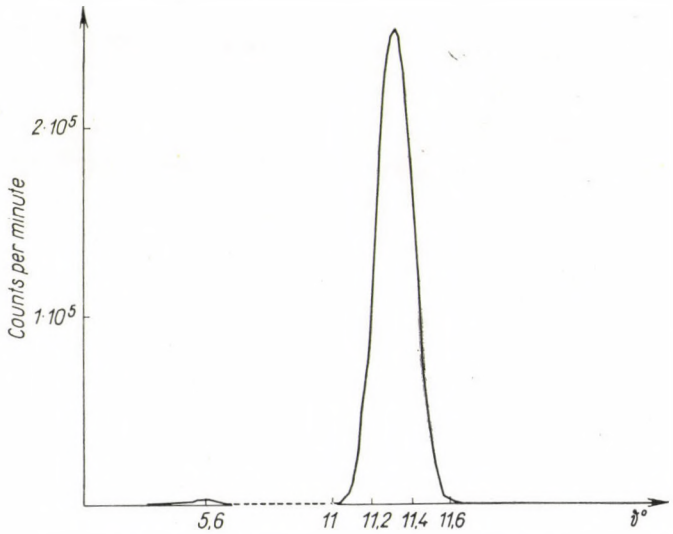

Fig. 3. Rocking curve of analysing crystal

Since the spectral composition of the monochromatized beam was found to be satisfactory we chose this position of the monochromator as the final one. The principal wave length reflected from it was $\lambda = 1.12$ Å, computed from the angle of reflection ϑ_{111}. For the determination of the value of ϑ_{111} it was necessary to know the zero position of the counter. This had been known at first only approximately (see above). It could now be determined as the position of the counter at the maximum of the large peak of Fig. 3.

The analysing crystal was prepared carefully in the same manner as that used as monochromator. We may thus suppose that their mosaic structures are virtually equal. The breadth of the parallel rocking curve (0.20°, see Fig. 3) is then in close connection with the mosaic spread of these crystals. If we suppose the angular distribution of mosaic blocks to be a Gaussian function of

half-value breadth β, the theory of the double crystal spectrometer [12] shows that

$$\beta = \frac{0{,}22^\circ}{1{,}4} = 0{,}16^\circ$$

in reasonably good accord with the value obtained from the single crystal rocking curve, Fig. 2.

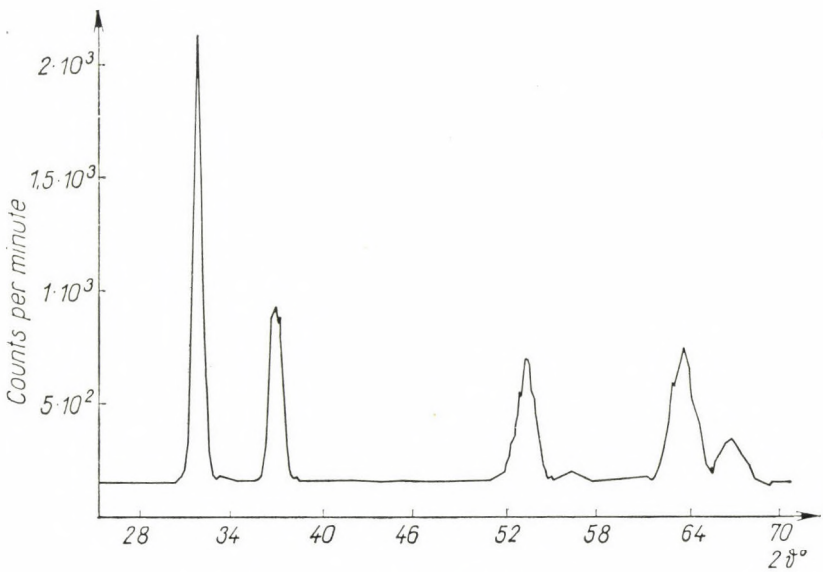

Fig. 4. Powder diffraction pattern of Ni

b) *Measurements with polycrystals*

We measured the reflections of polycrystalline Ni for comparison with calculated data. The first five reflections are shown in Fig. 4, where the counting rate is given as function of the counter angle 2ϑ.

The number of counts at different settings and the number of points constituting a Debye—Scherrer peak was chosen to fulfil the requirement that the statistical accuracy of the integrated peak should be better than 5 per cent with a probability of 97%, assuming Poisson statistics.

We used samples similar in form and dimensions to our analysing crystal. The crystalline powders were contained in vanadium boxes. The vanadium walls were 0.3 mm thick.

The angles of reflection may be determined simply as the angles at the maxima in Fig. 4, they could be measured with an accuracy of about 0.05°. Comparison of the measured values with those calculated shows agreement within 0.05°. (See Table 2.)

The breadth of the Debye—Scherrer lines and its dependence on 2ϑ in Fig. 4 also corresponds to what may be expected on the ground of collimator divergence and mosaic spread of the monochromating crystal.

Comparison of our line breadths, intensities and background (40—50 counts per minute, not shown in the figures) with those found in the literature gives a favourable account of the performance of our equipment. It should be remembered that the intensity could be increased (if a sufficient quantity of the material is available) by opening further collimating channels of the collimator.

When comparing the measured with the calculated intensity ratios, in the latter the attenuation of incident and diffracted beam and the temperature factor have to be taken into account.

Beam attenuation was determined for the Ni sample from the transmission of the monochromatic beam. The *effective* linear absorption coefficient $\mu_{\text{eff.}}$ turned out to be 0.415 cm^{-1} and with this value the beam attenuation in the diffraction measurements could be computed.

The temperature factor as given by the well-known Debye—Waller formula was used, the value of the characteristic temperature being based on specific heat data.

Table 2

Measured and calculated values
of the angle of reflection ϑ and of the ratio $R = I_{hkl}/I_{111}$ for Ni powder

hkl	111	200	220	311	222
$\vartheta_{\text{meas.}}$	15,90	18,50	26,65	31,80	33,35
$\vartheta_{\text{calc.}}$	15,93	18,50	26,67	31,76	33,36
$R_{\text{meas.}}$	1	0,53	0,51	0,68	0,24
$R_{\text{calc.}}$	1	0,56	0,56	0,81	0,25

Table 2 shows measured and calculated values of the ratio of the intensity I_{hkl} of the reflection (*hkl*) to the intensity I_{111} of the reflection (111). The agreement is very good.

Similar measurements made on polycrystalline NaCl have shown the same general features.

5. Summary

We have designed and built a high intensity neutron diffractometer with appropriate resolving power. Our measurements (Section 4) show this aim to have been achieved.

The single crystal measurements show also that by our method of crystal growing [6] and orientation [7] we were able to prepare suitable monochromating crystals.

The intensity may be further increased by using a greater number of collimating channels of our collimator.

The resolving power can be improved, if necessary, by using collimators of smaller angular divergence. Collimators of 10′ horizontal angular divergence were already built for this purpose.

The equipment can be used, of course, for work with small single crystals, soo. In this case a correspondingly smaller number of collimating channels thould be opened.

Acknowledgements

It is a pleasure to express our sincere gratitude to Dr. L. PÁL for his constant interest and advice. We are indebted to O. PETRIK for the mechanical and optical design and to F. SZLÁVIK for the design of the angular counting system.

REFERENCES

1. R. PEPINSKY, B. C. FRAZER and M. L. MCKEOWN, Rev. Sci. Instr., **25,** 699, 1954; G. E. BACON and R. F. DYER, J. Sci. Instr., **32,** 256, 1955.
2. E. W. WOLLAN and C. G. SHULL, Phys. Rev., **73,** 830, 1948; G. E. BACON, J. A. G. SMITH and C. D. WHITEHEAD, J. Sci. Instr., **27,** 330, 1950.
3. W. SOLLER, Phys. Rev., **24,** 158, 1924.
4. I. FANKUCHEN, Nature, **139,** 193, 1937.
5. P. SZABÓ, Nucl. Instr. and Methods, **5,** 184, 1959; **6,** 183, 1960.
6. E. KRÉN and P. SZABÓ, Hung. J. Phys., **9,** 161, 1961. (in Hungarian).
7. P. SZABÓ and E. KRÉN, Pribori i Technika Experimenta, no. 2, 1961, page 76.
8. J. GORDON and P. SZABÓ, Hung. J. Phys., **8,** 211, 1960 (in Hungarian).
9. I. L. FOWLER and P. R. TUNNICLIFFE, Rev. Sci. Isntr., **21,** 734, 1950.
10. J. GORDON and P. SZABÓ, Acta Phys. Hung., **12,** 333, 1960.
11. V. L. SAILOR, H. L. FOOTE, JR., H. H. LANDON and R. E. WOOD, Rev. Sci. Instr., **27,** 26, 1956.
12. E. g. R. W. JAMES, The Optical Principles of the Diffraction of X-Rays (Bell and Sons Ltd., 1954), p. 318.

НЕЙТРОННЫЙ ДИФРАКТОМЕТР С ВЫСОКОЙ ИНТЕНСИВНОСТЬЮ

П. САБО, Е. КРЕН и Й. ГОРДОН

Резюме

Даётся отчёт о конструкции и физических параметрах установки для дифракции нейтронов с высокой интенсивностью. Оказалось, на основе измерений, проведенных нами на монокристалле, что наш метод является пригодным для выращивания и ориентации монокристалла. Дифракционные измерения, проведенные на монокристаллах с известной структурой, сопоставление измеренных и рассчитанных углов отражения и интенсивностей дают представление об интенсивности, разрешающей способности и точности, осуществляемые нашей установкой.

INVESTIGATIONS OF THE VACUUM NEED OF β-SPECTROSCOPES*

By

Z. BŐDY** and D. BERÉNYI

INSTITUTE OF NUCLEAR RESEARCH OF THE HUNGARIAN ACADEMY OF SCIENCES (ATOMKI), DEBRECEN

(Presented by A. Szalay. — Received 16. IX. 1961)

The vacuum dependence of transmission and resolving power for β-spectroscopes was theoretically investigated. For the vacuum dependence of both transmission and resolving power analytic formulae were obtained. These were in good agreement with experimental data obtained by a β-spectrometer of the toroid-sector type.

1. Introduction

It is well known that an apparatus in which a stream of microparticles passes through a given space has to fulfil certain vacuum-technical requirements as the apparatus does not operate independently of the pressure present in that particular space. Namely, at higher pressures, the number of collisions between the particles and the molecules of the gas (air) present in the given space increases. Because of such collisions, the particles may lose energy and may be compelled to change their initial directions. Thus e.g. a beam of particles with parallel trajectories becomes diffuse after passing through the gas-filled space, that is the beam widens.

In β-spectroscopes, the microparticles involved are electrons, which may be scattered on the molecules of the gases of which the air is composed. In case of electrons scattered on atoms and molecules, the cross-section is some orders of magnitude smaller than in case of atom-atom or molecule-molecule scattering [1]. Intensity relations vary through scattering, and the transmission as well as the resolving power deteriorate.

Although the problem of the optimal vacuum always arises whenever β-spectroscopes are designed, yet hardly any investigations have been reported on this subject in the literature. One of the data comes from LAWSON and TYLER [2], who observed that the intensity of a beam of 165 keV electrons reduced to half in their spectrometer at a pressure of 27 mm Hg. Furthermore, in recent years, PORTER et al. investigated the intensity as a function of pressure for several electron lines of lower energy[3] in a magnetic lens β-spectrometer.

* This report is based on investigations carried out at ATOMKI during the physicists' summer practice.

** Present address: Institute for Experimental Physics, Debrecen.

Nevertheless, they did not inquire into the change of resolving power, neither did they deal with the interpretation of the phenomenon. Therefore it seemed worth-while to test how the transmission and resolving power vary as functions of the vacuum in case of different electron energies, when the mean free path of electrons in the spectrometer also is taken into consideration.

Our computations were in fact *estimations*, designed — first of all — to decide on the vacuum value to be maintained in a spectroscope of given resolving power and transmission, in order that practically no effect of the "vacuum" might be observed. (This effect derives from the interaction between the electrons and the molecules of residual gas). Our computations were supplemented by measurements made with a β-spectrometer of toroid-sector type [4—5] and were carried out for several internal conversion lines of different energies and for a continuous β-spectrum, respectively, at various pressures (10^{-3} mm Hg—20 mm Hg).

2. Rough estimate of the vacuum dependence of transmission

The transmission of β-spectroscopes is usually defined as the ratio of the number of monoenergetic particles entering the detector to that leaving the source. It is obvious that in addition to the geometrical factors of the apparatus, the transmission is a function of the pressure, too. Therefore, if the part of the transmission dependent on geometrical and other factors is denoted by T_0, and the part dependent on the vacuum value by P, the effective transmission may be expressed by

$$T = P \cdot T_0 \,, \tag{1}$$

where $0 < P < 1$.

It can be seen that the case of $P = 1$, i.e. $T = T_0$, will take place when "absolute vacuum" is assumed. Evidently P is the probability for the non-scattering of an arbitrary electron passing from the source to the detector. More precisely, the above-defined P is equivalent to the probability of non-scattering only if all the scattered electrons are supposed "to be lost to us", in other words, not to contribute to the transmission. Thus, at any rate, we obtain a rough under-estimate which means that the transmission and resolving power do not essentially deteriorate even at a vacuum value worse than that determined by the above supposition (see also Chapter 4). The facts, however, are as follows: The atom-electron scattering cross-section, elastic or inelastic, is the largest for the small angles subtended by the initial direction. Because of this and on account of the finite width of the detector, a significant number of scattered electrons may also fall within the effective surface of the detector, consequently

$$P < P_t < 1 \,, \tag{2}$$

where P_t is the effective P-value.

Now P and P_t must be calculated. For this purpose, the following conditions are suggested as simplifications:

1. We suppose the air to consist of pure nitrogen, partly because the proportion of nitrogen in air is by far the biggest and partly because the other relatively significant component, i.e. oxygen, behaves like nitrogen from the view-point of the scattering pattern, their atomic numbers (Z) differing by one only.

2. For the sake of simplicity, our calculations were made for a β-spectroscope of semicircular focusing, a condition closely approximated by our β-spectrometer of the toroid-sector type, the calculations giving information also on the vacuum requirements of other types of spectroscopes, particularly those with a transversal magnetic field.

Let us consider a beam of N electrons passing through a gas-filled space. While traversing a path of length ds, the number of electrons scattered from the beam is

$$dN = -N\sigma_0 \cdot n_g \, ds, \tag{3}$$

where σ_0 is the total cross-section (elastic + inelastic) for atom-electron scattering, n_g is the density of gas in particles/cm^3. In our case $n_g = 7.1 \cdot 10^{16} p$ (pressure in mm Hg). The solution of (3) is given by

$$N = N_0 \, e^{-\sigma_0 n_g s}, \tag{4}$$

where N_0 is the initial intensity of the beam (when $s = 0$). The assumption of single scattering is reasonable if N/N_0 does not differ much from unity.

Taking into consideration that $\dfrac{N}{N_0}$ is the probability of non-scattering, we have

$$P = \frac{N}{N_0} = e^{-7{,}1 \cdot 10^{16} \sigma_0 s p} \tag{5}$$

and from (2) and (5)

$$e^{-7{,}1 \cdot 10^{16} \sigma_0 s p} < P_t < 1. \tag{6}$$

Zero index at σ_0 points to the fact that the lower limit in the integration over the solid angle was $\vartheta = 0$. In other words, an electron scattered through an angle, however small, is regarded as scattered out of the "line", that is, it reduces the transmission.

The rather rough estimate obtained in this manner, however, is a definite under-estimate, since choosing the vacuum value accordingly, a requirement higher than the effective vacuum need will be met. On the other hand, in this case we can be sure that no distortion of the spectrum will take place because of the residual air.

Naturally σ is energy-dependent. At higher relativistic energies, however, σ_0 is independent of energy in good approximation; for nitrogen we have [6]

$$\sigma_0 \sim 1.6 \cdot 10^{-18} \text{ cm}^2 ,$$

while in a lower relativistic case, we may calculate σ_0-values on the basis of reference [6].

Thus e.g. from such calculations at a pressure of 10^{-2} mm Hg, if $s = 100$ cm, the inequality $0.975 < P_t < 1$ will be obtained for the high relativistic energies.

3. More accurate computations of the vacuum dependence of transmission and resolving power

Let us consider two electron groups of energies E_1 and E_2 (that is of corresponding momenta), which can just be separated by the spectroscope in question E_1 and E_2 are near values.

The resolving power, as it is well known, is given by the relation

$$\frac{\Delta I}{I} = \frac{\Delta (H\varrho)}{H\varrho} \quad \text{(mostly expressed in percentage)}, \tag{7}$$

where I is the momentum of the particles (proportional to $H\varrho$), H is the magnetic field strength, and ϱ is the radius of the curvature of the path of the electron.

$\Delta(H\varrho)$ is the half-width of the intensity distribution function of the "lines" (appearing at the position of the focus when electrons of a given energy are examined) which belongs to energies E_1 and E_2, respectively. In a less precise way (7) interprets the fact that when two Gaussian-like functions are superimposed, the individual functions can be distinguished from each other only if their maxima are at least a half-width distant from each other. (Considering that the energies are approximately identical, the half-widths are practically the same.)

Subsequently, our computations were made according to the following considerations. First, we determined the point where the particle, scattered at an arbitrary place of its trajectory and through an arbitrary angle, falls on the plane of the detector. Then we ascertained the probability density functions of the parameters (the place and conic angle of scattering and their functional relations) which determine the coordinates of the points, where the electrons fall on the plane of the detector. Then the distribution of these points was computed.

Let us take Fig. 1. Perpendicular to the plane of the Figure, a homogeneous magnetic field is present. The electrons leaving the source at point A reach the detector or the photographic plate at point B when a β-spectroscope of semicircular focusing is used. If an electron undergoes scattering at point C, i.e. is deflected from the initial path by an angle ϑ' (measured in the plane of the Figure), so that it passes to a new orbit, it will not reach the detector at point B any more, but at a certain distance z from it. Of course, by scattering not only a change of direction may occur, but also a loss of energy. The latter,

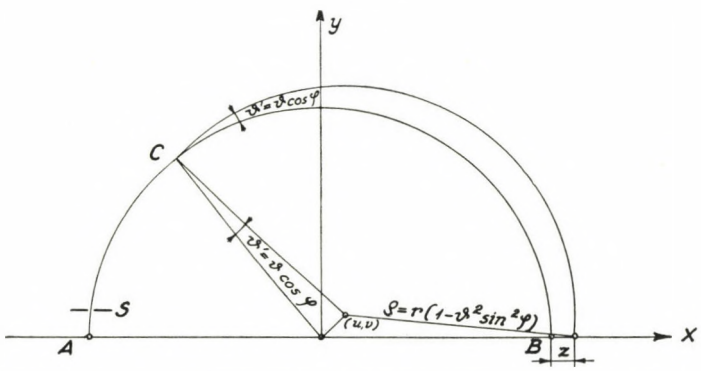

Fig. 1. Scattering of the electron on a nitrogen molecule in a semicircular focusing β-spectroscope

however, is negligible when relativistic energies are concerned. In the case of inelastic scattering, the average loss of energy for nitrogen is 80 eV, while in the case of elastic scattering it is even less.

According to the simple calculations given in Appendix 1, z is related to the conic angle ϑ and the azimuth φ (measured from the medial plane of the spectroscope) of the scattering, as well as to the coordinates of the scattering point in the following way:

$$z = y \cdot \vartheta \cos \varphi - r \vartheta^2 \sin^2 \varphi. \tag{8}$$

It is to be noted, however, that slit S (Fig. 1) is of a finite width, and so the electrons move in a beam of finite width and not along a single path. The beam becomes focused by the effect of the magnetic field, that is, it contracts to the smallest — but finite — width, after having travelled along a semicircle. The electrons do not arrive at individual points of this finite interval with equal probability, but present a probability distribution called "window curve" (Fig. 2).*

* In the Figure the trajectories ending in the different points x, near axis x were considered parallel for the sake of simplicity. For the further considerations, however, this condition is not essential.

Therefore scattering may not be undergone only by electrons moving on the path which ends in point 0 corresponding to the maximum of the line, but also by the electrons travelling along a path which leads to an arbitrary point x of the line (x being the distance from the point belonging to the maximum of the line). Distribution z for point x will be given also by (8), only displaced by x; namely, the electron arriving originally at point x (if not scattered) will fall on the plane in the neighbourhood of x, at distance z from x, owing to the

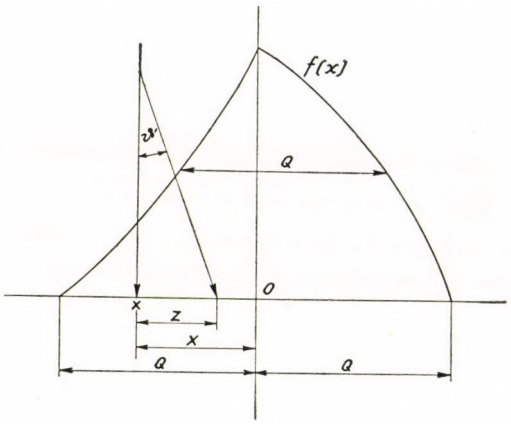

Fig. 2. Window curve in the semicircular focusing spectroscope and schematization of the effect of scattering on a nitrogen molecule

scattering. The arrivals at different points x are not equally probable. The probability of arrival is characterized by the window curve (normalized to unity).

If we want to get information on the deterioration of the resolving power that is the change of the window curve, we must know the distribution of all the scattered electrons, in other words the distribution of the electrons which originally travelled on a path ending in any point x, but which underwent scattering. This distribution can be determined if both x and z are taken to be probability variables, and the density functions belonging to their convolution are considered. It is to be noted that here the majority of the electrons is supposed to have already been scattered. Thus the distribution of scattered electrons will really yield the new window curve.

The probability density function belonging to the probability variable x is given by the aforementioned window curve, and it may approximately be considered a Gaussian curve:*

$$f(x) = \frac{1}{\sqrt{2\pi x^2}} e^{-\frac{x^2}{2x}} . \tag{9}$$

* In this way our calculations become more general as they are thus not restricted to a spectroscope of the semicircular focusing type.

As it is obvious from (8), the density functions of y, $\cos\varphi$, $\sin^2\varphi\,\vartheta\,\vartheta^2$ must be known for the determination of the density function of z, which also will be a Gaussian curve according to the considerations detailed in Appendix 2:

$$g(z) = \frac{1}{\sqrt{2\pi\overline{z^2}}}\, e^{-\frac{z^2}{2\overline{z^2}}}. \tag{10}$$

If the wanted probability variable is denoted by ξ, according to [9], its distribution also will be Gaussian and the mean square will be

$$\overline{\xi^2} = \overline{x^2} + \overline{z^2}, \tag{11}$$

while its density function expressed in a suitable form is given by

$$h(\xi) = \frac{1}{r\sqrt{2\pi\left(\frac{\overline{x^2}}{r^2} + \frac{\overline{z^2}}{r^2}\right)}}\, e^{-\frac{\xi^2}{2r^2\left(\frac{\overline{x^2}}{r^2} + \frac{\overline{z^2}}{r^2}\right)}}, \tag{12}$$

where

$$\frac{\overline{x^2}}{r^2} = \frac{Q^2}{8\ln 2}\,\frac{1}{r^2} = \frac{\eta_0^2}{8\ln 2}, \tag{13}$$

$$\frac{\overline{z^2}}{r^2} \approx 2{,}44\cdot\lambda^4\cdot 10^{-7}\, ps, \tag{14}$$

are calculated on the basis of the density functions of x and z (see Appendix 2). Here Q is the half-width of the original window curve; η_0 is the original resolving power (without scattering), λ is the Broglie wave length of the electron in 10^{-2} Å; p is the pressure in mm Hg and s the average length of the path in cm traversed by the electron from source to detector.

The distribution after scattering (really the window curve after scattering) as shown by (12) will distinctly differ from the original scatter-free distribution (original window curve), when $\overline{z^2}$ is large enough as compared with $\overline{x^2}$. If the half-width of the new lines is denoted by Q_s, then on the basis of (12)

$$Q_s^2 = 8\ln 2\,(\overline{x^2} + \overline{z^2}) \tag{15}$$

and thus from (13), (14) and (15), the deteriorated resolving power will be

$$\eta_s^2 = \frac{Q_s^2}{r^2} = 8\ln 2\left(\frac{\eta_0^2}{8\ln 2} + \frac{\overline{z^2}}{r^2}\right), \tag{16}$$

while the relative deterioration of the resolving power becomes

$$P_r = \frac{\eta_0}{\eta_s} = \frac{\eta_0}{\sqrt{\eta_0^2 + 8\ln 2\,\frac{\overline{z^2}}{r^2}}} = \frac{\eta_0}{\sqrt{\eta_0^2 + 1{,}35\cdot 10^{-6}\,\lambda^4 ps}}, \tag{17}$$

that is P_r varies between 1 and 0. It is 1 if the resolution has not deteriorated at all, and 0 when the line has become imperceptible and has dissolved into the background owing to the scattering.

In the same way, the change of transmission can also be given if we take the maximum of the lines for the measure of transmission. These maxima are obtained by putting x and ξ equal to 0 in (19) and (12), respectively. In this case, the relative deterioration of transmission (as compared with P_t) defined in point 2. will be

$$P_t = \frac{T_s}{T_0} = \frac{\dfrac{1}{r\sqrt{2\pi\left(\dfrac{\overline{x^2}}{r^2} + \dfrac{\overline{z^2}}{r^2}\right)}}}{\dfrac{1}{\sqrt{2\pi\overline{x^2}}}} = \frac{\eta_0}{\sqrt{\eta_0^2 + 1{,}35 \cdot 10^{-6}\,\lambda^4\, p \cdot s}}, \qquad (18)$$

where T_0 is the transmission without scattering, and T_s that with scattering. Then, if the transmission does not deteriorate, P_t is equal to 1; and when the line has become imperceptible and dissolved into the background, $P_t = 0$. As it can be seen, the resolving power and transmission deteriorate in quite the same way, according to our calculations, when the vacuum worsens.

4. Experimental results and comparison with the calculations

Investigations were carried out on the vacuum dependence of transmission and resolving power by means of a magnetic β-spectrometer of the toroid-sector type [4, 5] mentioned in the introduction.

The resolving power of the spectrometer was $\sim 6\%$, the average length of electron path between source and detector was 50 cm. The detector was a scintillation counter, with a scintillator disc 12 mm in diameter.

Measurements were carried through as follows: At 14 vacuum values from 10^{-3} to 20 mm Hg, the 624, 329 and 92 keV internal conversion lines of Cs^{137}, Au^{198} and Ce^{144}, respectively, were taken. Such a series of curves for Cs^{137} is represented in Fig. 3. The asymmetrical position of certain curves (as e.g. in case of the 4 mm Hg one in Fig. 3) is due to the inertness of the vacuum gauge. Furthermore, the influence of the different vacuum values on the continuous β-spectrum of Co^{60} was also investigated with the above spectrometer.

The evaluation of the above measurements for conversion lines reveals how the resolving power and transmission vary at different energies as function of the vacuum, and thus comparison with theoretical computations becomes possible. By transmission here simply the maximum of the line is meant. On the other hand, the photograph of the continuous β-spectrum to be seen in

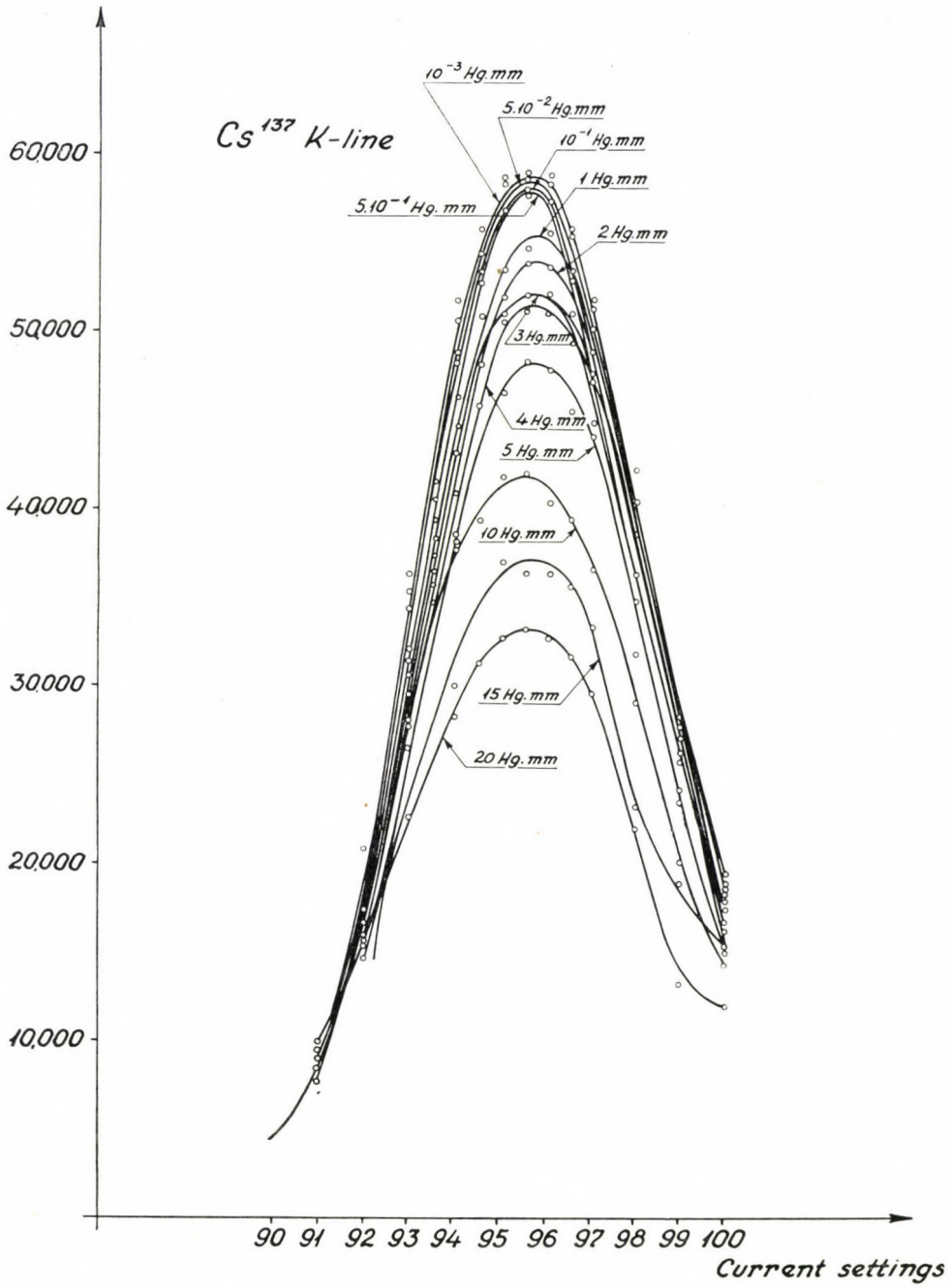

Fig. 3. Internal conversion line of the 624 keV Cs^{137} measured by a β-spectrometer of the toroid-sector type and taken at different vacuum values

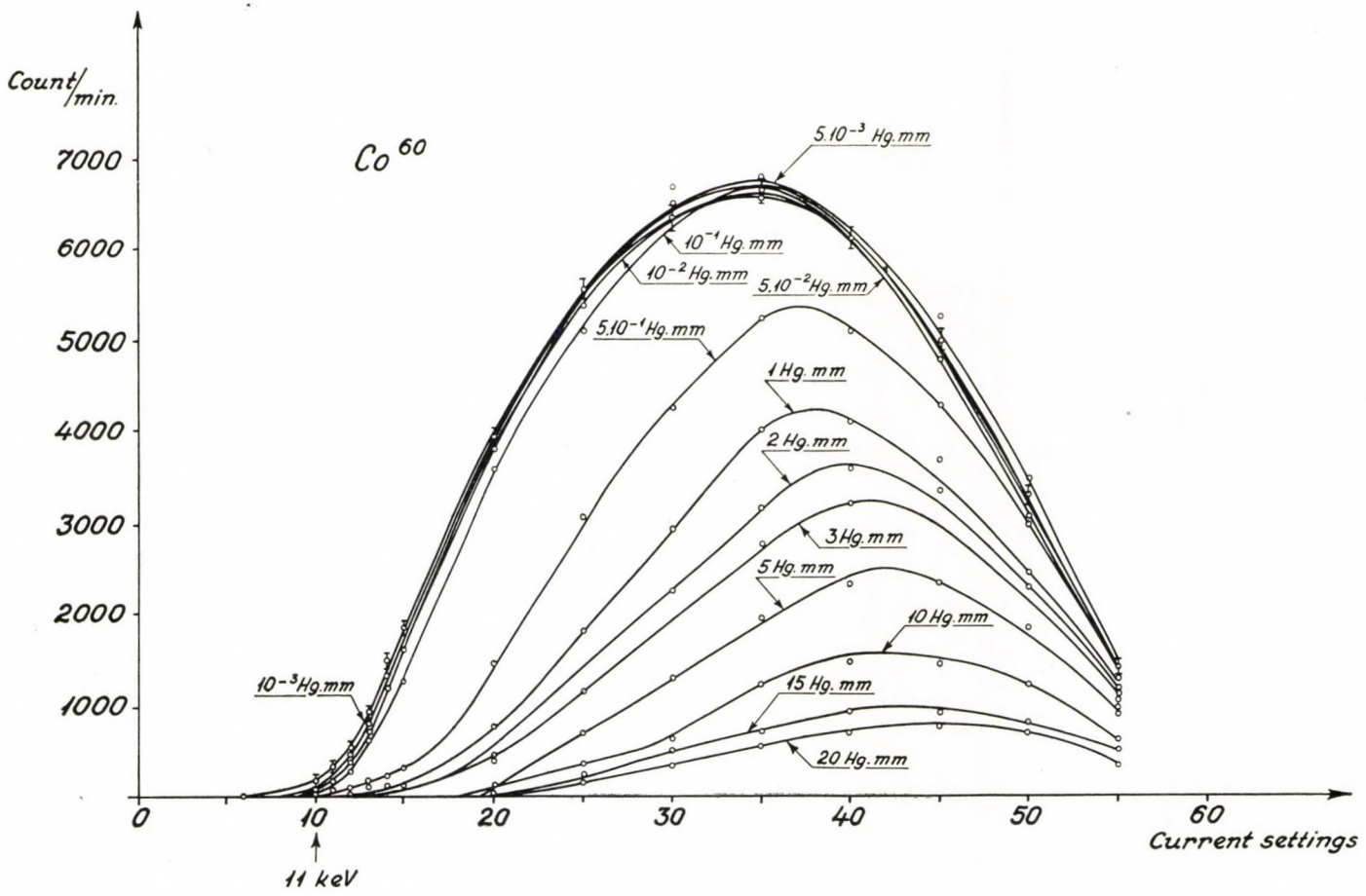

Fig. 4. Continuous beta-spectrum of Co^{60} at different vacuum values

Fig. 4 discloses the vacuum value at which already noticeable deviation is shown by the low energy portion of the continuous spectrum. From the Figure it is seen, that in the case of a vacuum better than $5 \cdot 10^{-2}$ mm Hg the vacuum has no noticeable effect even on the electrons of the smallest energy measurable by our spectrometer under the given conditions; i.e. in our case, the maintenance of a vacuum of $5 \cdot 10^{-2}$ mm Hg seems to be perfectly sufficient.

Fig. 5 illustrates the comparison of our calculations and measurements for the transmission. The dotted lines show the rough estimates given in point 2. It can be seen that they represent an overestimation of one and a half or two orders of magnitude. The fact is that every experimental point lies above them. The continuously drawn curves correspond to the more accurate calculations given in Part 3. The conversion lines for the 92 keV electrons of Ce^{144} and 329 keV electrons of Au^{198} are superimposed on an intensive, continuous β-spectrum. This may result in the apparent deviations owing to scattering out of and into the line, as well as to difficulties of evaluation.

Fig. 6 sums up the experimental and theoretical results for the resolving power. According to the calculations, the theoretical curves are identical for transmission and resolving power. It is to be noted that the experimental points both for Figs. 5 and 6 were obtained by taking as η_0 and T_0 those values η and T which had been evaluated from the shape of the experimental line measured at a pressure 10^{-3} mm Hg.

The Figures, especially Fig. 5 reveal that while e.g. at $3 \cdot 10^{-1}$ mm Hg only 10 per cent of the 624 keV electrons are such that have not scattered at all (dotted curve), at the same time the transmission has scarcely deteriorated (1—2%), which may be due to the majority of electrons having undergone scattering through a small angle. Electrons that have undergone scattering through such a small angle reach the detector despite the scattering, and thus the transmission does not change. In other words, under the above conditions, the majority of electrons have already been scattered, but there are few of them where the scattering angle is larger than a certain angle $\vartheta_{\min}$. This $\vartheta_{\min}$ depends on parameters of the instrument; first of all, on the size of the detector. Thus, the continuously drawn theoretical curve may be regarded as one that shows the proportion of electrons having taken part in the scattering in which they deviated from the original path by an angle larger than $\vartheta_{\min}$. Furthermore, the Figure also reveals that the range of multiple scattering begins at 10^{-1} mm Hg.

Fig. 7 gives — so to speak — a more direct check-up of our assumptions and of the calculations based on these. According to formulae (17) and (18), the relative deterioration of transmission and resolving power as function of the vacuum is expressed by the same function. If this holds good, by forming quotient P_t/P_r from the experimental data and by expressing it as function of the vacuum, we are to obtain a straight line $P_t/P_r = 1$. As it can be seen,

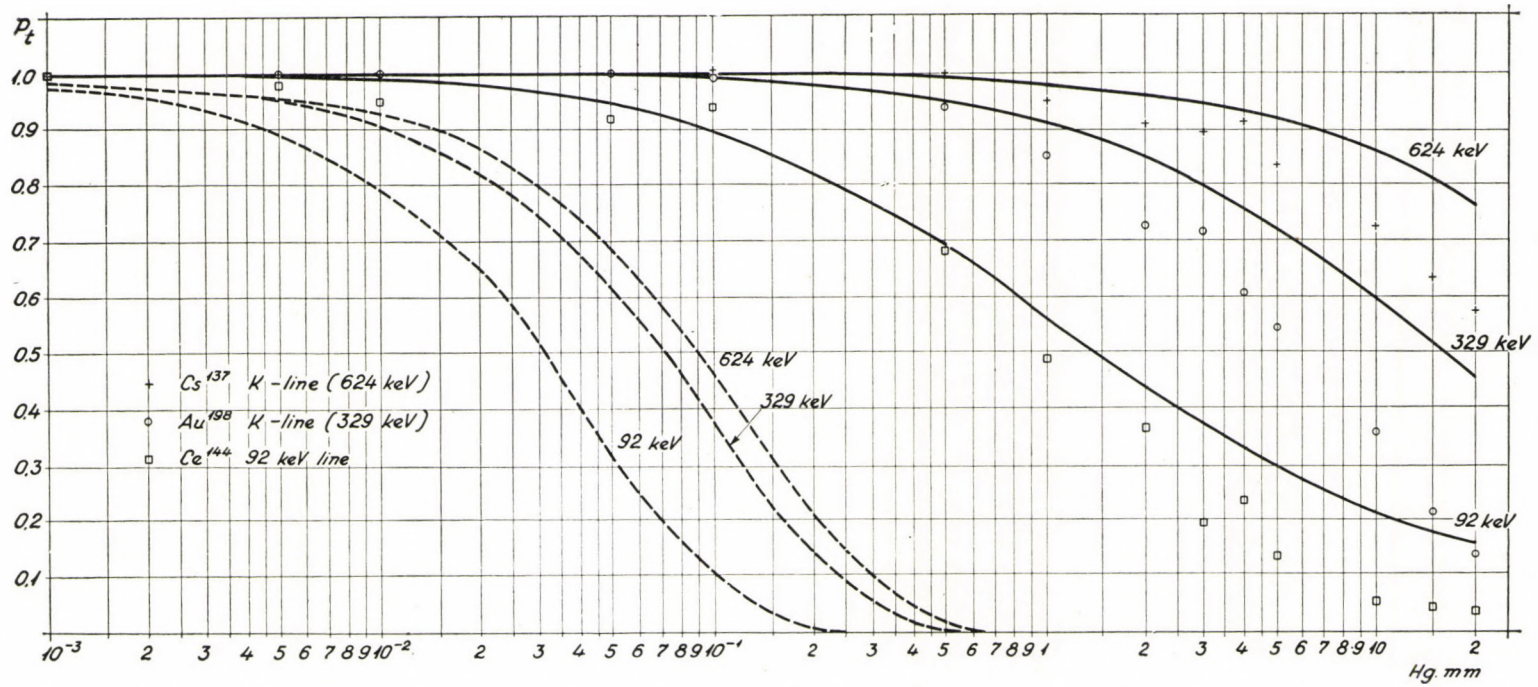

Fig. 5. Relative deterioration of the transmission (P_t) as function of the vacuum for electrons of different energies. The dotted curves correspond to theoretical computations, assuming that electrons once scattered have already scattered out of the beam, while the continuous curve represents the better theoretical estimate

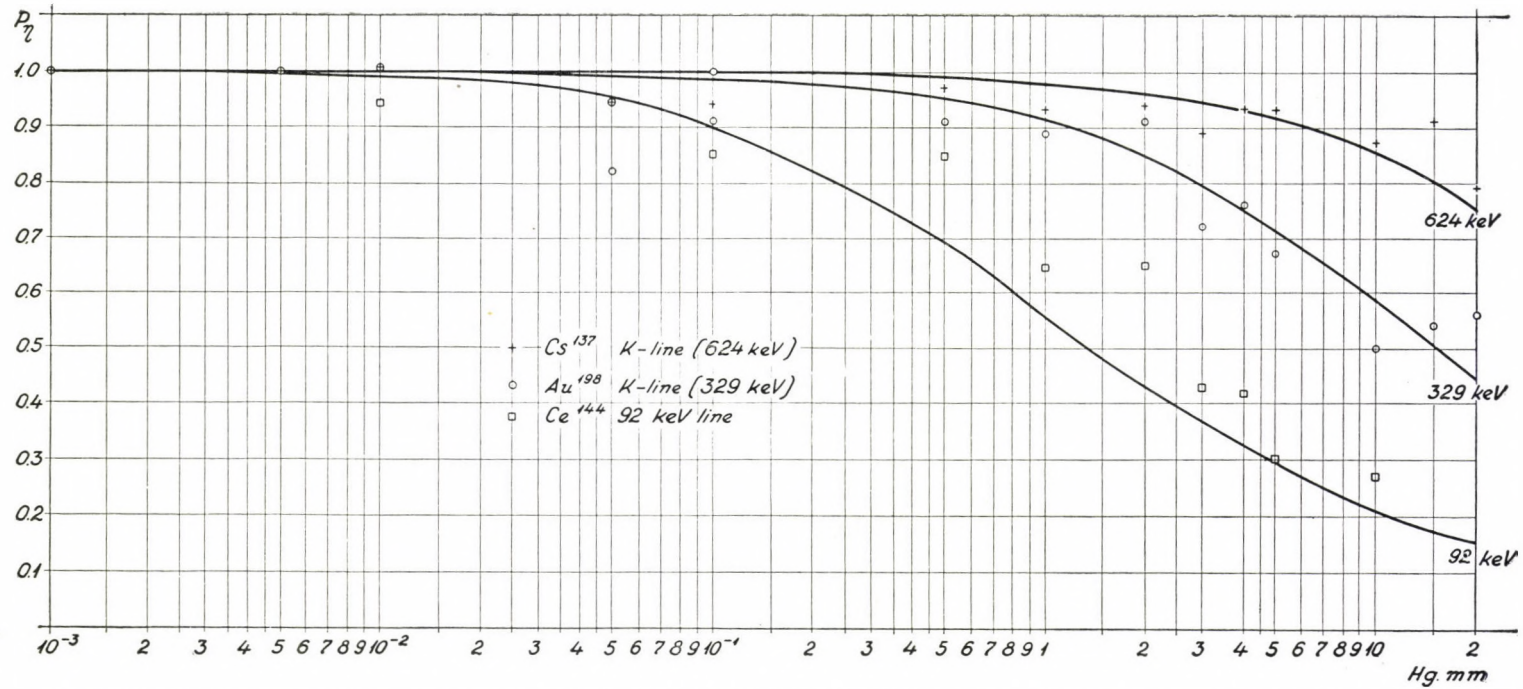

Fig. 6. Relative deterioration of the resolving power (P_η) as function of the vacuum for electrons of different energies. The continuous curves are results of the theoretical estimate

the data although deviating by quite large errors from the straight line, particularly at worse vacuum values, fluctuate around unity inside an order of magnitude.

Thanks are due, first of all, to Prof. A. SZALAY for providing excellent working conditions and to Prof. B. GYIRES for his valuable help with the mathematical calculations. Acknowledgement is due also to Dr. Cs. UJHELYI for preparing the sources as well as to B. GYARMATHY and GY. MESZÉNA for reviewing the manuscript and making helpful suggestions.

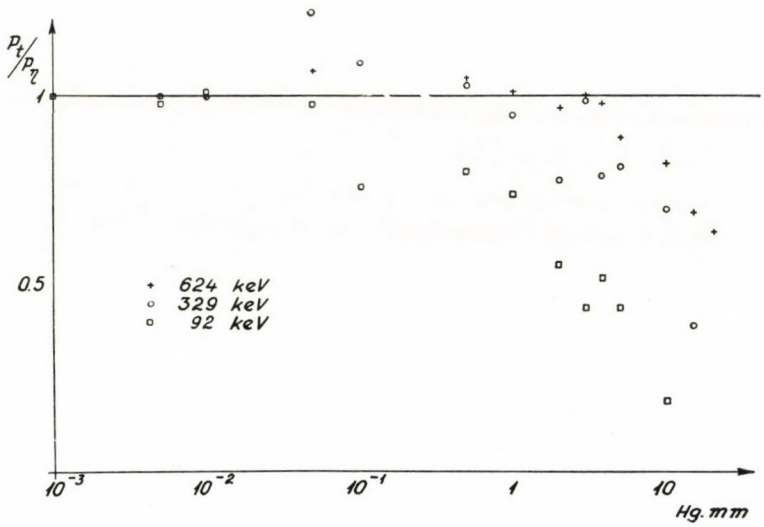

Fig. 7. The measure of reliability of our theoretical estimates. The values obtained from measurements do not differ in order of magnitude from the values expected on the basis of the computations

Appendix 1

Expressions of z in terms of the scattering parameters

Let the equation of orbit before scattering be

$$x^2 + y^2 = r^2\,, \tag{19}$$

after scattering

$$(x - u)^2 + (y - v)^2 = \varrho^2\,. \tag{20}$$

As indicated by Fig. 1

$$\vartheta'_r \approx \sqrt{u^2 + v^2} \tag{21}$$

and

$$z = \sqrt{\varrho^2 - v^2} - r + u\,. \tag{22}$$

To determine ϑ' and ϱ the following should be considered: ϑ' is in fact the projection of the scattering cone angle to the plane perpendicular to the magnetic field. r is the radius of curvature measured in this plane (before scattering) which is determined by the electron velocity component lying in this plane at a constant magnetic field. After scattering, if it did not occur in the above-mentioned plane, the velocity component in the plane will change and so will radius r. The radius thus changed is ϱ.

Let us consider Fig. 8. The particle originally travelled along path $\overline{OB}$. After scattering into cone angle ϑ, its path is represented by section $\overline{OA}$. Triangle $\overline{OAB}$ does not lie in the plane of the Figure. It makes angle φ with the Figure and with triangle $\overline{OCB}$ of its plane. C is the projection of A at angle φ.

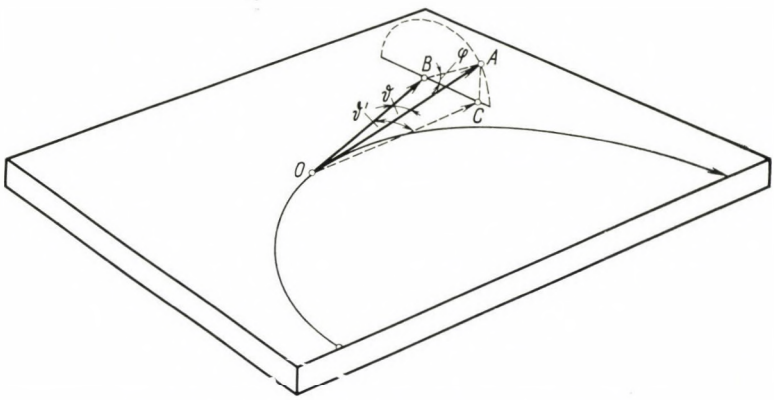

Fig. 8. The cone angle of scattering and its projection

The length of $\overline{OB}$ (not its direction !) can be chosen so that

$$\frac{\overline{BA}}{\overline{OB}} = \tan\vartheta\,, \qquad \frac{\overline{CB}}{\overline{OB}} = \tan\vartheta'\,,$$

$$\frac{\overline{BC}}{\overline{BA}} = \cos\varphi\,,$$

from which

$$\tan\vartheta' = \cos\varphi\,\tan\vartheta\,.$$

For small angles

$$\vartheta' \approx \vartheta\cos\varphi\,. \tag{23}$$

Now let us find $\overline{OC}$, that is the velocity component measured in the plane of the Fig. after scattering.

According to Fig. 8

$$(\overline{OC})^2 = (\overline{OB})^2 + (\overline{BC})^2 ,$$

$$\overline{OB} = \overline{OA} \cdot \cos\vartheta ,$$

$$\overline{BC} = \overline{BA} \cdot \cos\varphi ,$$

$$\overline{BA} = \overline{OA} \cdot \sin\vartheta ,$$

from which

$$(\overline{OA})^2 (\cos^2\vartheta + \cos^2\varphi \cdot \sin^2\vartheta) = (\overline{OC})^2 .$$

$\overline{OA}$ is the total velocity proportional to radius r preceding the scattering, $\overline{OC}$ being proportional to radius ϱ following the scattering having the same factor of proportion.

$$\varrho = \sqrt{r^2 (\cos^2\vartheta + \cos^2\varphi \cdot \sin^2\vartheta)} = r\sqrt{\cos^2\vartheta + \sin^2\vartheta - \sin^2\varphi \cdot \sin^2\vartheta} =$$

$$= r\sqrt{1 - \sin^2\varphi \cdot \sin^2\vartheta} .$$

If ϑ is small

$$\varrho \simeq r\sqrt{1 - \vartheta^2 \sin^2\varphi} . \tag{24}$$

On the basis of equations (19)—(24)

$$z = y\,\vartheta \cos\varphi - r\,\vartheta^2 \sin^2\varphi , \tag{25}$$

i.e. if y is not too small, the higher powers of ϑ are negligible.

Appendix 2

The density functions of probability variables z and x as well as the mean squares

The calculation of the density function of z from (25) is a rather intricate task, as the two members of the sum on the right are not independent of each other. However, as ϑ is a value far below unity (in radian) both for single and multiple scattering, it may be expressed by

$$z = y\,\vartheta \cdot \cos\varphi . \tag{26}$$

The points of scattering along the circumference of the circle show a uniform distribution. Then using the transformation $y = r\frac{y}{r}$ in (26), the density function of $\frac{y}{r}$ will be

$$f_1\left(\frac{y}{r}\right) = \frac{1}{\pi\sqrt{1 - \left(\frac{y}{r}\right)^2}} , \quad \left(-1 < \frac{y}{r} < +1\right). \tag{27}$$

Let us use the approach that instead of y we take its mean value for (27)

$$M(y) = M\left(\frac{y}{r}\right) = \frac{2}{\pi} r \,. \tag{28}$$

Thus

$$z = \frac{2}{\pi} r \vartheta \cos \varphi \,.$$

From the graph of transmission vs. pressure it can be seen that where transmission is reduced by $\sim 10\%$, the probability of nonscattering computed in the previous chapter does not differ much from zero. This means that multiple scattering occurs at such pressures.

The amount $\vartheta \cos \varphi$ gives the projection of ϑ to an arbitrary plane which is, in our case, perpendicular to the direction of the magnetic field. If $\vartheta \cos \varphi = \alpha$, then the density function of α in the case of multiple scattering [1, 7] is

$$f(\alpha)\, \mathrm{d}\alpha = \frac{1}{\sqrt{2\pi\bar{\alpha}^2}} e^{-\frac{\alpha^2}{2\bar{\alpha}^2}} d\alpha \tag{30}$$

and

$$f(z) = \frac{1}{\frac{2}{\pi} r} \cdot f\left(\frac{\alpha}{\frac{2r}{\pi}}\right) = \frac{1}{\sqrt{2\pi\bar{z}^2}} e^{-\frac{z^2}{2\bar{z}^2}} , \tag{31}$$

where

$$\bar{z}^2 = \bar{\alpha}^2 \left(\frac{2}{\pi}\right)^2 r^2 \quad \text{and} \quad \frac{1}{2}\overline{\vartheta^2} = \bar{\alpha}^2 \tag{32}$$

and

$$\bar{\vartheta}^2 = \int_0^{0,1} \vartheta^2 P(\vartheta)\, d\vartheta \,, \ (\text{cf. } [1, 7]).$$

According to [8]

$$P(\vartheta)\, d\vartheta = K \left[\frac{Z+1}{(\vartheta^2 + \vartheta_0^2)^2} + \frac{2\,\vartheta_0^2}{\vartheta^2 (\vartheta^2 + \vartheta_0^2)^2} \right] \vartheta \, d\vartheta \,, \tag{33}$$

$$\vartheta_0 = \frac{\lambda^2 \cdot 6 \cdot Z}{\Theta} \,, \quad K = \frac{\lambda^4 \cdot Z \cdot 8\pi}{a_H^2} n_g \cdot s \,, \quad \Theta = 4\pi \int_0^{\infty} r^2 \varrho(r)\, r^2\, dr \,,$$

where

Z is the atomic number of the scattering atoms,

λ is the wave length of the scattered electrons divided by 2π,

a_H is the first Bohr radius of the hydrogen atom,

n_g is the density of the scattering medium in particles/cm^3,

$\varrho(r)$ denotes the radial electron density in the atom of the scattering medium.

s denotes the path (in cm) travelled by the electrons in the space filled with the scattering medium. Otherwise as in [6]

$$\Theta_{\text{nitrogen}} = 15.6\, a_H^2 .$$

Integral (32) for energies of ~ 0.5 MeV becomes

$$\overline{\vartheta^2} \approx 42\, K = 1.17 \cdot 10^{-6}\, \lambda^4 \cdot ps\,, \tag{34}$$

(λ in 10^{-2} Å; p in mmHg; s in cm).

In (34), factor 42 also is energy-dependent to a slight degree (logarithmically). In more accurate calculations, it also has to be considered, if an energy substantially different from 0.5 MeV is concerned.

Finally we give the value of $\frac{\overline{z}^2}{r^2}$ more accurately calculated for three energies:

$$8 \ln 2 \cdot \frac{\overline{z}^2}{r^2} = 2.55 \cdot 10^{-6} \cdot p \cdot s \qquad (624 \text{ keV}),$$

$$8 \ln 2 \cdot \frac{\overline{z}^2}{r^2} = 1.55 \cdot 10^{-5} . p \cdot s \qquad (329 \text{ keV}),$$

$$8 \ln 2 \cdot \frac{\overline{z}^2}{r^2} = 1.44 \cdot 10^{-4} \cdot p \cdot s \qquad (\ 80 \text{ keV}).$$

(p in mm Hg, s in cm)

$\overline{x^2}$ is the mean square and Q the experimental half-width. Their relation is

$$\overline{x}^2 = \frac{Q}{8 \ln 2} . \tag{35}$$

This relation is simply obtained by the lines being approximated by Gaussian curves.

REFERENCES

1. N. F. Mott and H. S. W. Massey, The Theory of Atomic Collisions, 2nd ed. Clarendon Press, Oxford, 1950.
2. J. L. Lawson and A. W. Tyler, Rev. Sci. Instr., **11,** 6, 1939.
3. M. S. Freedman, F. T. Porter, F. Wagner, Jr. and P. P. Day, Phys. Rev., **108,** 836, 1957.
4. *Ш. Салаи* и *Д. Берени*, Изв. А. Н. СССР. Сер. Физ. **22,** 887, 1958.
5. A. Szalay and D. Berényi, Acta Phys. Hung., **10,** 39, 1959.
6. M. J. Moravcsik, Phys. Rev., **100,** 1009, 1955.
7. L. V. Grosev and I. Sz. Sapiro, Nuclear Spectroscopy. Publ. House of the Hung. Acad. of Sci. (in Hungarian).
8. F. Lenz, Z. Naturforsch., **9***a*, 185, 1954.
9. A. Rényi, Theory of Probability, Text-book Publishers, Budapest, 1954, pp. 210—225, (in Hungarian).

ИССЛЕДОВАНИЕ ВАКУУМНОЙ ПОТРЕБНОСТИ БЕТА-СПЕКТРОМЕТРОВ

З. Бэди и Д. Верени

Резюме

Теоретически исследуется вакуумная зависимость трансмиссионной и разрешающей сил для бета-спектрометров. Выводятся аналитические формулы для вакуумной зависимости трансмиссионной и разрешающей сил. Результаты хорошо согласуются с экспериментальными данными, полученными бета-спектрометром тороидально-секторного типа.

ABSORPTION OF NEUTRINOS IN THE COULOMB FIELD OF THE NUCLEI

By

M. ELKISHEN*

INSTITUTE FOR THEORETICAL PHYSICS, ROLAND EÖTVÖS UNIVERSITY, BUDAPEST

(Presented by K. F. Novobátzky — Received 14. II. 1962)

The cross sections of high energy neutrinos are calculated for the absorption in the Coulomb-field of atomic nuclei, giving another neutrino and two charged leptons. The cases of the local Fermi interaction and the case of the indirect weak interaction (transmitted by a boson field with heavy quanta) are discussed separately. The probability of the emission of a real heavy boson is also determined.

One of the most important problems of the weak interaction is the question: are the terms of the weak current coupled to each other directly (i.e. is the Fermi-type four fermion interaction local) or is the coupling transmitted by a boson field with heavy quanta [1]? The answer to this problem may be expected only from high energy experiments because at low energies (e.g. in the case of spontaneous decays) the detection of any non-locality is impossible. The most important absorbers for high energy neutrinos are the nuclei, but here the possible weak nonlocality is made unobservable by the strong nonlocality coming from the pionic form factors of the nucleons [2]. The only possibility for finding the nonlocality of the weak current interaction is to consider the lepton-lepton coupling: e.g. the $(e\nu)(\mu\eta)$ interactions. The

$$\nu + e \rightarrow \mu + \eta \tag{1}$$

reaction, however, is very far beyond present observational possibilities, because of the very high energy threshold [3]. Therefore we shall now discuss the absorption of high energy neutrinos in the Coulomb field of atomic nuclei, going through the $(e\nu)(\mu\eta)$ coupling:**

$$\begin{aligned} \nu + \text{nucleus} &\rightarrow \eta + \mu^- + e^+ + \text{nucleus} , \\ \nu + \text{nucleus} &\rightarrow \eta + \mu^+ + e^- + \text{nucleus} . \end{aligned} \tag{2}$$

* Permanent address: Cairo University, Department of Physics, Cairo, UAR

** If the interaction is transmitted between the weak currents by a charged heavy boson, the probability of the decay $\mu \rightarrow e + \gamma$ turns out to be rather high, contradicted by the experimental facts. The probability of this unobserved decay type will be, however, zero, if the neutrinos connected with the muons in the weak current (ν) and those connected with the electrons (η) are different particles [4].

We shall discuss the reaction (2) first by the Fermi interaction, then by the hypothesis of the intermediate boson field.

Our Feynmann diagrams using local Fermi interaction will be as follows:

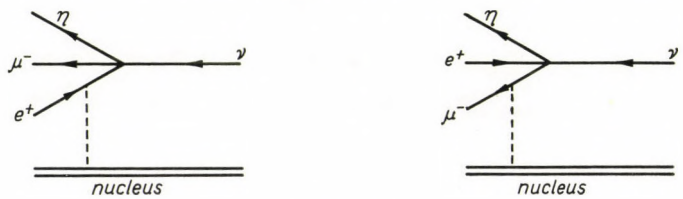

Fig. 1

Assuming the existence of an intermediate boson field transmitting the interaction between the weak currents, the diagrams will be different:

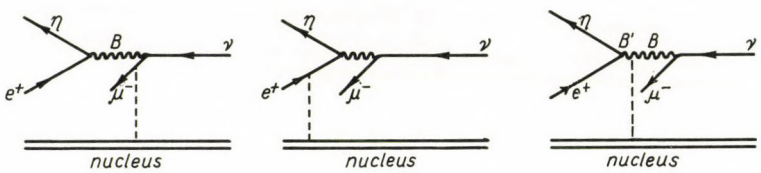

Fig. 2

Our S-matrix elements for Figs. 1 and 2 will be [5]

$$S_1 = \frac{ife}{\hbar V^2}\left\{\iiint \bar{u}_\mu \gamma_\alpha \frac{1+\gamma_5}{2} \bar{u}_\eta \gamma_\alpha \cdot \frac{1+\gamma_5}{2} iS_c(k'_e)\gamma_\beta A_\beta v_e \times \right.$$
$$\times \delta(k_\nu - k_\mu - k_\eta - k'_e)\,\delta(k'_e - k_e + k_\gamma)\,dk'_e\,dk_\gamma + \iint \bar{u}_\eta \gamma_\alpha \frac{1+\gamma_5}{2} v_e \times \tag{3}$$
$$\left. \times \bar{u}_\mu \gamma_\alpha \frac{1+\gamma_5}{2} iS_c(k'_\mu)\gamma_\beta A_\beta u_\nu \delta(k_\nu - k'_\mu - k_\eta - k_e)\,\delta(k'_\mu - k_\mu + k_\gamma)\,dk'_\mu\,dk_\gamma \right\}.$$

$$S_2 = \frac{eg^2(2\pi)^{12}}{\hbar V}\left\{\iiint \bar{u}_\eta \gamma_\alpha \frac{1+\gamma_5}{2} u_\nu v_e \Delta_c(k_B)\,\bar{u}_\mu \gamma_\beta A_\beta(k_\gamma)\, S_c(k'_\mu) \times \right.$$
$$\times \gamma_\alpha \frac{1+\gamma_5}{2} u_\nu \delta(k_B - k_\eta - k_e)\,\delta(k'_\mu - k_\mu + k_\gamma)\,dk_\gamma\,dk_B\,dk'_\mu + \bar{u}_\eta \gamma_\alpha \frac{1+\gamma_5}{2} \times$$
$$\times S_c(k'_e)\gamma_\beta A_\beta(k_\gamma)\, v_e \Delta_c(k_B)\,\bar{u}_\mu \gamma_\alpha \frac{1+\gamma_5}{2} u_\nu \delta(k_B - k_\eta - k'_e)\,\delta(k_\nu - k_B - k_\mu) \times \tag{4}$$
$$\times \delta(k'_e - k_e + k_\gamma)\,dk_\gamma\,dk_B\,dk'_e + \bar{u}_\eta \gamma_\alpha \frac{1+\gamma_5}{2} v_e\,\bar{u}_\mu \gamma_\alpha \frac{1+\gamma_5}{2} u_\nu (\varphi_\alpha^+ \partial_\beta \varphi_\alpha -$$
$$- \partial_\beta \varphi_\alpha^+ \varphi_\alpha) A_\beta(k_\gamma)\,\delta(k_B - k_\eta - k_e)\,\delta(k'_B - k_B + k_\gamma) \times$$
$$\left. \times \delta(k_\nu - k_\mu - k'_B)\,dk_\gamma\,dk'_B\,dk_B \right\}.$$

The external field is assumed to be the Coulomb field of a nucleus of charge Z.

$$A_\mu = n_\mu A\,, \qquad A = \frac{Ze}{4\pi r}\,, \qquad n_\mu^2 = -1\,. \tag{5}$$

The Fourier transform of the Coulomb potential A is given by the following equation:

$$A_\beta(\varkappa) = n_\beta \frac{Ze}{4\pi r} = n_\beta \int A(k_\gamma)\,\delta(k_\gamma^0)\,e^{ik_\gamma \varkappa}\,d^4 k_\gamma\,, \tag{6}$$

where

$$A(k_\gamma) = \frac{Ze}{\mathbf{k}_\gamma^2}\,. \tag{7}$$

One can prove, that S_2 is exactly the same as S_1, if the momentum transfer of the boson is small compared to its mass μ and if the coupling constant is

$$g^2 = f\mu^2 \sqrt{8}\,. \tag{8}$$

So it is sufficient only to calculate the S-matrix element for the case of the intermediate vector boson field, from which one can easily obtain that of the local Fermi interaction by putting the mass of the intermediate boson $\mu = \infty$.

The cross-section can be calculated from S_2 in the usual way and our cross-section will be:

$$\sigma = \frac{Z^2\,\sigma_0}{(137)^2} \iiint \frac{L\delta(k_\eta^0 + k_\mu^0 + k_e^0 - k_\nu^0)}{|\mathbf{k}_\eta + \mathbf{k}_\mu + \mathbf{k}_e - \mathbf{k}_\nu|^4}\,d^3 k_\eta\,d^3 k_\mu\,d^3 k_e\,. \tag{9}$$

We have evaluated the expression L in (9) in the general case [6], but it contains very many terms, so we quote the results by taking zero angle reactions only.

Since

$$d^3 k_\eta = \mathbf{k}_\eta^2\,dk_\eta\,d\Omega_\eta\,, \quad d^2 k_\mu = \mathbf{k}_\mu^2\,dk_\mu\,d\Omega_\mu$$

and

$$d^3 k_e = \mathbf{k}_e^2\,dk_e d\Omega_e\,. \tag{10}$$

Integrating in (9) over the delta function:

$$\sigma = \frac{Z^2\,\sigma_0}{(137)^2} \int F(E,\, E_\mu,\, E_e)\,dE_\mu\,dE_e\,d\Omega_\eta\,d\Omega_e\,d\Omega_\mu\,. \tag{11}$$

Here

$$\sigma_0 = \frac{f^2 M^2}{2\pi\hbar^2 c^2}\,[cm^2],\ k_\nu = EM\,,\ k^{0\mu} = E_\mu M \quad \text{and} \quad k_e^0 = E_e M\,, \tag{12}$$

where M is the nucleon mass. We take it as unit energy.

The differential cross-section for zero angles equals

$$d\sigma = \frac{Z^2 \sigma_0}{(137)^2} F(E, E_\mu, E_e)\, dE_\mu\, dE_e\, d\Omega_\eta\, d\Omega_e\, d\Omega_\mu, \tag{13}$$

where

$$F(E, E_\mu, E_e) = \frac{8M^2 c^4 \hbar^2 \beta_e \beta_\mu (E - E_\mu - E_e)^2 E_e^2 E_\mu^2}{2\pi |E_\mu (1-\beta_\mu) + E_e (1-\beta_e)|^4} \times$$

$$\times \left| \frac{1}{[m_\mu^2 - m_e^2 + 2M^2 E_e (E_e + E_\mu)(1-\beta_e)]^2 \left[1 + \frac{m_e^2 + 2M^2 E_e (E - E_\mu - E_e)(1-\beta_e)}{\mu^2}\right]^2} \right| \times$$

$$\times \Big\{ 1{,}5\, M^2 E_e^2 (1 - 3\beta_e - \beta_\mu + 3\beta_e \beta_\mu - 3\beta_e^2 \beta_\mu + 3\beta_e^2 + \beta_e^2 \beta_\mu - \beta_e^3) +$$

$$+ m_\mu^2 (1 + \beta_\mu - \beta_e - \beta_e \beta_\mu) - 2m_\mu^2 \frac{E_e}{E_\mu} (1 - 2\beta_e + \beta_e^2) \Big\} +$$

$$+ \frac{1}{[m_e^2 - m_\mu^2 + 2M^2 E_\mu (E_e + E_\mu)(1-\beta_\mu)]^2 \left[1 + \frac{-m_\mu^2 + 2M^2 E_\mu E (1-\beta_\mu)}{\mu^2}\right]^2} \times$$

$$\times \Big\{ 0{,}5\, M^2 E_\mu (E_\mu + E_e)(1-\beta_\mu)^2 (1+\beta_e) + M^2 E_\mu^2 (1 - 3{,}5\beta_\mu - 1{,}5\beta_e +$$

$$+ 4\beta_\mu^2 - 1{,}5\beta_\mu^3 + 4\beta_\mu \beta_e - 3{,}5\beta_\mu^2 \beta_e + \beta_\mu^3 \beta_e) - 2m_e \frac{E_\mu}{E_e} (1 - 2\beta_\mu + \beta_\mu^2) +$$

$$+ m_e^2 (1 - \beta_\mu + \beta_e - \beta_e \beta_\mu) \Big\} +$$

$$+ \frac{1}{[m_\mu^2 - m_e^2 + 2M^2 E_e (E_e + E_\mu)(1-\beta_e)] \left[1 + \frac{m_e^2 + 2M^2 E_e (E - E_e - E_\mu)(1-\beta_e)}{\mu^2}\right]} \times$$

$$\times \frac{1}{[m_e^2 - m_\mu^2 + 2M^2 E_\mu (E_e + E_\mu)(1-\beta_\mu)] \left[1 + \frac{-m_\mu^2 + 2M^2 E_\mu E (1-\beta_\mu)}{\mu^2}\right]} \times$$

$$\times \Big\{ 2M^2 [(E_e + E_\mu)^2 - \beta_\mu E_\mu (E_e + E_\mu) - E_e (E_e + E_\mu)] (1-\beta_e)(1-\beta_\mu) -$$

$$- 2M^2 E_e (E_e + E_\mu)(1-\beta_e)^2 - M^2 E_e E_\mu (3 - 6\beta_e - 10\beta_\mu + 18\beta_\mu \beta_e -$$

$$- 8\beta_\mu \beta_e^2 + 3\beta_e^2 + 5\beta_\mu^2 - 8\beta_\mu^2 \beta_e + 3\beta_e^2 \beta_\mu^2) - m_e^2 \frac{E_e + E_\mu}{E_e} (1 - \beta_\mu) +$$

$$+ m_e^2(+4-3\beta_\mu-3\beta_e+2\beta_e\beta_\mu)-m_\mu^2(+2+2\beta_\mu-2\beta_e-2\beta_e\beta_\mu) - 1{,}5\,\frac{m_e^2 m_\mu^2}{M^2 E_e\cdot E_\mu}\Bigg\} +$$

$$+ \frac{4M^2(E-E_\mu)^2(1-\beta_e)(1-\beta_\mu)}{[\mu^2+m_e^2+2M^2E_e(E-E_e-E_\mu)(1-\beta_e)]^2\left[1+\dfrac{-m_\mu^2+2M^2E_\mu E(1-\beta_\mu)}{\mu^2}\right]^2} +$$

$$+ \frac{2M(E_\mu-E)}{[m_\mu^2-m_e^2+2M^2E_e(E_e+E_\mu)(1-\beta_e)][\mu^2-m_\mu^2+2M^2E_\mu E(1-\beta_\mu)]}\times$$

$$\times\left\{\frac{3ME_e(\beta_e-1)[(\beta_e-1)-(\beta_\mu\beta_e-1)+(\beta_\mu-1)]+2\dfrac{m_\mu^2}{ME_\mu}(\beta_e-1)}{\left[1+\dfrac{m_e^2+2M^2E_e(E-E_e-E_\mu)(1-\beta_e')}{\mu^2}\right]^2}\right\} +$$

$$+ \frac{2}{[m_e^2-m_\mu^2+2M^2E_\mu(E_e+E_\mu)(1-\beta_\mu)][\mu^2+m_e^2+2M^2E_e(E-E_e-E_\mu)(1-\beta_e)]}\times$$

$$\times\frac{2M(E-E_\mu)}{\left[1+\dfrac{-m_\mu^2+2M^2E_\mu E(1-\beta_\mu)}{\mu^2}\right]^2}\Big\{(E_e+E_\mu)(1-\beta_e)(1-\beta_\mu)+ME_\mu(\beta_\mu-1)\times$$

$$\times[2(\beta_e-1)-(\beta_e\beta_\mu-1)+(\beta_\mu-1)-2\beta_\mu(\beta_e-1)]-2\frac{m_e^2}{ME_e}(1-\beta_\mu)\Big\}\Bigg|\,. \qquad (14)$$

By putting the mass of the intermediate boson $\mu = \infty$, one can get $F_\infty(E, E_\mu, E_e)$ valid for local Fermi interaction:

$$F_\infty(E,E_\mu,E_e) = \frac{8M^2c^4\hbar^2\beta_e\beta_\mu(E-E_\mu-E_e)E_e^2E_\mu^2}{2\pi|E_\mu(1-\beta_\mu)+E_e(1-\beta_e)|^4}\times$$

$$\times\Bigg|\frac{1}{[m_\mu^2-m_e^2+2M^2E_e(E_e+E_\mu)(1-\beta_e)]^2}\Big\{1{,}5M^2E_e^2(1-3\beta_e-\beta_\mu+3\beta_e\beta_\mu -$$

$$-3\beta_e^2\beta_\mu+3\beta_e^2+\beta_e^3\beta_\mu-\beta_e^3)+m_\mu^2(1+\beta_\mu-\beta_e-\beta_e\beta_\mu)-2m_\mu^2\frac{E_e}{E_\mu}(1-\beta_e)^2\Big\}+$$

$$+\frac{1}{[m_e^2-m_\mu^2+2M^2E_\mu(E_e+E_\mu)(1-\beta_\mu)]^2}\Big\{0{,}5M^2E_\mu(E_\mu+E_e)(1-\beta_\mu)^2(1+\beta_e)+$$

$$+M^2E_\mu^2(1-3{,}5\beta_\mu-1{,}5\beta_e+4\beta_\mu^2-1{,}5\beta_\mu^3+4\beta_\mu\beta_e-3{,}5\beta_\mu^2\beta_e+\beta_\mu^3\beta_e) -$$

$$-2m_e^2\frac{E_\mu}{E_e}(1-\beta_\mu)^2+m_e^2(1-\beta_\mu)(1+\beta_e)\Big\}+$$

$$+\frac{1}{[m_\mu^2-m_e^2+2M^2E_e(E_e+E_\mu)(1-\beta_e)][m_e^2-m_\mu^2+2M^2E_\mu(E_e+E_\mu)(1-\beta_\mu)]}\times$$

$$\times\Big\{2M^2[(E_e+E_\mu)^2-\beta_\mu E_\mu(E_e+E_\mu)-E_e(E_e+E_\mu)](1-\beta_e)(1-\beta_\mu)-$$

$$-2M^2E_e(E_e+E_\mu)(1-\beta_e)^2+M^2E_eE_\mu(+3-6\beta_e-10\beta_\mu+18\beta_\mu\beta_e-$$

$$-8\beta_\mu\beta_e^2+3\beta_e^2+5\beta_\mu^2-8\beta_\mu^2\beta_e+3\beta_e^2\beta_\mu^2)-$$

$$-m_e^2\frac{E_e+E_\mu}{E_e}(1-\beta_\mu)+m_e^2(4-3\beta_\mu-3\beta_e+2\beta_e\beta_\mu)-$$

$$-2m_\mu^2(1+\beta_\mu)(1-\beta_e)-1{,}5\frac{m_e^2m_\mu^2}{M^2E_eE_\mu}\Big\}\Big|. \tag{15}$$

Here

$$\beta_e=\frac{|\mathbf{k}_e|}{k_e^0}, \qquad \beta_\mu=\frac{v_\mu}{c}=\frac{|\mathbf{k}_\mu|}{k_\mu^0} \tag{16}$$

and

$$-(k_e, k_\nu)=k_e^0k_\nu(1-\beta_e). \tag{17}$$

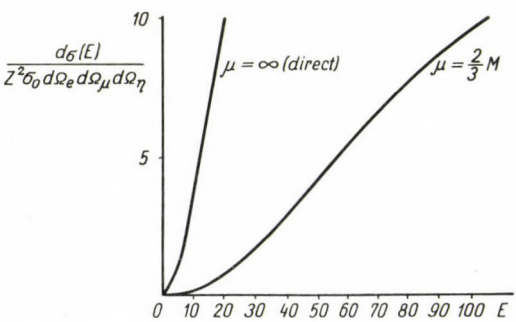

Fig. 3

Fig. 3 shows the energy dependence of the differential cross-section for the two cases (Fermi interaction and assumption of the intermediate boson) for the special energy distribution between the final particles:

$$E_\eta : E_\mu : E_e = 4 : 3 : 3, \tag{18}$$

i.e. $F(E, 0.3E, 0.3E)$. It can be seen from the diagrams that the differential cross-section obtained by using local Fermi interaction increases quickly as the energy of the incident neutrino tends to infinity. In the case of the intermediate boson hypothesis it increases slowly and tends to a finite value as the energy of the incident neutrino tends to infinity. This finite value depends on the mass of the intermediate boson.

From equation (14) and (15) one can find the energy dependence of the cross-section also for other energy distributions:

Firstly, by putting $E_\mu \simeq \frac{m_\mu}{M}$ and $E_e \simeq \frac{m_e}{M}$, β_e and β_μ will be approximately equal to zero. In this case all the kinetic energy is taken away by the emitted neutrino. In this case one gets:

$$\begin{aligned} F\left(E, \frac{m_e}{M}, \frac{m_\mu}{M}\right) &= \text{const, for } E \to \infty, \\ F_\infty\left(E, \frac{m_e}{M}, \frac{m_\mu}{M}\right) &= \infty, \qquad \text{for } E \to \infty. \end{aligned} \tag{19}$$

Secondly, by putting $E_\eta \simeq 0$ and $E_\mu = m\mu/M$ all the kinetic energy was assumed to be taken by the electron. One finds:

$$\begin{aligned} F\left(E, E - \frac{m_\mu}{M}, \frac{m_\mu}{M}\right) &= 0, \quad \text{for} \quad E \to \infty, \\ F_\infty\left(E, E - \frac{m_\mu}{M}, \frac{m_\mu}{M}\right) &= \infty, \text{ for } E \to \infty. \end{aligned} \tag{20}$$

Thirdly, for the case when $E_\eta \cong 0$ and $E_e \simeq \frac{m_e}{M}$ and all the kinetic energy is taken away by the muon, it was found that $F(E, E, 0) = \infty$ and $F_\infty(E, E. 0) = \infty$, when $E \to \infty$.

In equations (14) and (15), by neglecting the mass of the electron with respect to its energy (i.e. taking $\beta_e = 1$) we get a very simple equation:

$$\begin{aligned} F(E, E_\mu, E_e) = {} & \frac{8M^2 c^4 \hbar^2 \beta_\mu (E - E_\mu - E_e)^2 E_e^2 E_\mu^2}{2\pi |E_\mu (1 - \beta_\mu)|^4} \times \\ & \times \frac{M^2 E_\mu (E_\mu + E_e)(1-\beta_\mu)^2 + 0{,}5 M^2 E_\mu^2 (-1 + \beta_\mu + \beta_\mu^2 - \beta_\mu^3)}{\left[-m_\mu^2 + 2M^2 E_\mu (E_e + E_\mu)(1-\beta_\mu)\right]^2 \left[1 + \frac{-m_\mu^2 + 2ME_\mu E(1-\beta_\mu)}{\mu^2}\right]^2} \end{aligned} \tag{21}$$

and

$$\begin{aligned} F_\infty(E, E_\mu, E_e) = {} & \frac{8M^2 c^4 \hbar^2 \beta_\mu (E - E_\mu - E_e)^2 E_e^2 E_\mu^2}{2\pi |E_\mu (1 - \beta_\mu)|^4} \times \\ & \times \frac{M^2 E_\mu (E_\mu + E_e)(1-\beta_\mu)^2 + 0{,}5 M^2 E_\mu^2 (-1 + \beta_\mu + \beta_\mu^2 - \beta_\mu^3)}{\left[-m_\mu^2 + 2M^2 E_\mu (E_e + E_\mu)(1-\beta_\mu)\right]^2}. \end{aligned} \tag{22}$$

This calculation was done by considering that the field of the nucleus is a pure $1/r$ Coulomb field. This is true only if we have a point charge. As we know the

nucleus is surrounded by electrons and this necessitates some important alterations (screening of the Coulomb field due to the electron charge distribution). We intend to get a rough estimation for the influence of this screening on our previous results. So instead of taking the Coulomb field as equ. (5) we take it:

$$A = -\frac{Ze}{4\pi r} e^{-r/r_0}, \tag{23}$$

from which one can obtain instead of (7)

$$A(k_\gamma) = \frac{Ze}{\mathbf{k}_\gamma^2 + 1/r_0^2}, \tag{24}$$

where r_0 is the screening parameter and its value is

$$r_0 = \frac{137}{Z^{1/3} m_e} = Z^{1/3} \cdot 0{,}529 \cdot 10^{-8} \text{ cm}. \tag{25}$$

One would expect, therefore, that the screening of the Coulomb field by the outer electrons would lead to a decrease in the cross-section. From equation (24) we can see the following: if the momentum transfer to the recoil nucleus is large, the value $1/r_0^2$ can be neglected. $\omega, r, t \ll \mathbf{k}_\gamma^2$ and equ. (24) takes the form

$$A(k_\gamma) = \frac{Ze}{\mathbf{k}_\gamma^2}. \tag{26}$$

For small momentum transfer to the recoil nucleus one can neglect $\mathbf{k}_\gamma^2 \omega \cdot r$ to $1/r_0^2$ and equ. (24) will be

$$A(k_\gamma) = r_0^2 Ze. \tag{27}$$

It follows that this screening effect prevents the cross-section from tending to infinity in the case of zero momentum transfer.

So taking the screening effect into consideration one obtains instead of equ. (14)

$$F_{sc}(E, E_\mu, E_e) = \frac{[E_\mu(1-\beta_\mu) + E_e(1-\beta_e)]^4 F(E, E_\mu, E_e)}{\left\{[E_\mu(1-\beta_\mu) + E_e(1-\beta_e)]^2 + \frac{1}{r_0^2}\right\}^2}. \tag{28}$$

It can be seen that the difference between (28) and (14) is that instead of putting the numerator $[E_\mu(1-\beta_\mu)+E_e(1-\beta_e)]^4$ we put:

$$\left\{[E_\mu(1-\beta_\mu) + E_e(1-\beta_e)]^2 + \frac{1}{r_0^2}\right\}^2.$$

The relation between F_{sc} and F will be

$$F_{sc}(E, E_\mu, E_e) = \frac{F(E, E_\mu, E_e)}{\left[1 + \frac{1}{r_0^2 [E_\mu (1-\beta_\mu) + E_e (1-\beta_e)]^2}\right]^2} . \tag{29}$$

Substituting r_0 with its value one gets

$$F_{sc}(E, E_\mu, E_e) = \frac{F(E, E_\mu, E_e)}{\left[1 + \frac{\frac{Z^{2/3}}{(137)^2}}{\left\{\frac{m_\mu}{m_e}\sqrt{\frac{1-\beta_\mu}{1+\beta_\mu}} + \sqrt{\frac{1-\beta_e}{1+\beta_e}}\right\}^2}\right]^2} , \tag{30}$$

where F_{sc} means taking the screening effect into consideration. From (30) it can be seen that for relativistic electron velocities the term $E_e(1-\beta_e)$ will be negligible, and the whole expression will depend only on the energy of the outgoing muon and our equation will be:

$$F_{sc} = \frac{F}{\left[1 + \frac{Z^{2/3}}{(137)^2 \frac{m_\mu^2}{m_e^2} \frac{(1-\beta_\mu)}{(1+\beta_\mu)}}\right]^2} . \tag{31}$$

We will now evaluate the factor in front of $F(E, E_\mu, E_e)$. For different energies

E_μ (KeV)	0	10	10^2	10^3	10^5	10^6
$\frac{F_{sc}}{F}$	0,9997	0,992	0,98	0,943	0,82	0,12

This table was taken for $Z = 64$. So as one can see the Coulomb screening effect is important only for very high energies.

In this second part of our paper the absorption of high energy neutrinos in a field of nucleus giving a real boson and a charged lepton will be discussed.

$$\nu + \text{nucleus} \rightarrow \text{nucleus} + \mu^- + B^+ ,$$
$$\eta + \text{nucleus} \rightarrow \text{nucleus} + e^- + B^+ .$$

One can also get the other reaction:

$$\bar{\nu} + \text{nucleus} \rightarrow \text{nucleus} + \mu^+ + B^- ,$$
$$\bar{\eta} + \text{nucleus} \rightarrow \text{nucleus} + e^+ + B^- .$$

This boson is assumed to be coupled to the weak current directly. It will not live for a long time and decays e.g. to μ^+ or e^+ and neutrino like:

$$B^+ \to \mu^+ + \nu\,, \qquad B^+ \to e^+ + \eta\,. \tag{32}$$

The Feynmann diagrams for reaction (32) will be:

Fig. 4

It can be seen that the S-matrix for Fig. 4 is:

$$S = \frac{eg\,(2\pi)\,i}{V^{3/2}\sqrt{2\omega}\,\hbar}\left[\iint \bar{u}_\mu\,\gamma_\alpha\,A_\alpha\,S_c(k'_\mu)\,\gamma_\beta\,e_\beta\,\frac{1+\gamma_5}{2}\,u_\nu\,\delta(k_\nu - k_B - k'_\mu)\times\right.$$

$$\times\,\delta(k'_\mu - k_\mu + k_\gamma)\,dk'_\mu\,dk_\gamma + \tag{33}$$

$$\left.+\iint \bar{u}_\mu\,\gamma_\alpha\,e_\alpha\,\frac{1+\gamma_5}{2}\,u_\eta\,\Delta_c(k'_B)\,e_\beta\,A_\beta\,\delta(k_\gamma - k_\mu - k'_B)\,\delta(k'_B - k_B + k_\gamma)\,dk'_B\,dk_\gamma\right],$$

where e_β is the polarization vector of the boson. We have calculated the cross section for the S-matrix element, but it contains a lot of terms [6]. We quote again only the zero angle results. The cross-section will be:

$$\sigma = Z^2\,\sigma_B \int G(E, E_B)\,dE_B\,d\Omega_B\,d\Omega_\mu\,, \tag{34}$$

where

$$\sigma_B = \frac{e^2}{\hbar c}\,l_0^2 = 0{,}34\cdot 10^{-37}\ \mathrm{cm}\,,$$

$$E_B = \frac{k_B^0\,\hbar c}{Mc^2}\,, \qquad E = \frac{k_\gamma\,\hbar c}{Mc^2}\,, \tag{35}$$

and

$$l_0 = \sqrt{\frac{f}{\hbar c}} = \frac{g}{8^{1/4}\,\mu} = 0{,}8\cdot 10^{-16}\ \mathrm{cm}\,. \tag{36}$$

Our cross-section for the two different cases of polarization is:

$$\sigma = Z^2\,\sigma_B \int G_{\parallel,\perp}(E, E_\beta)\,dE_\beta\,d\Omega_B\,d\Omega_\mu\,. \tag{37}$$

So

$$G_{\parallel}(E, E_B) = \frac{\sqrt{8}\, c^2 \pi \mu^2}{(\mu^2 + \beta_B^2 M^2 E_B^2)^{1/2}} \frac{\beta_\mu \beta_B M E_B^2 (E - E_B)^2}{|E_\mu (1 - \beta_\mu) + E_B (1 - \beta_B)|^4}$$

$$\left| \frac{1}{[m_\mu^2 - \mu^2 + 2M^2 E E_B (1 - \beta_B)^2} \left\{ M^2 E_B^2 (1 + \beta_B \beta_\mu)(1 - \beta_B) - \mu^2 \frac{1 + \beta_\mu}{2} + \right.\right.$$

$$+ m_\mu^2 \frac{E_B}{E - E_B} (\beta_B - 1) + m_\mu^2 \frac{\beta_\mu + 1}{2} + \frac{2M^2 E^2 (1 - \beta_B)(1 + \beta_\mu) + m_\mu^2 (\beta_\mu + \beta_B)}{1 + \beta_B} +$$

$$\left. + \frac{-2M^2 E^2 E_B (1 - \beta_B)(1 + \beta_\mu)(1 + \beta_B) + \mu^2 (\beta_\mu + \beta_B) + 2m_\mu^2 \dfrac{E}{E - E_B} (1 - \beta_B)}{1 + \beta_B} \right\} +$$

$$+ \frac{4M^2 E_B^2 \left(\dfrac{\beta_\mu - \beta_B}{1 + \beta_B} + \dfrac{1 - \beta_\mu}{2} \right)}{\mu^2 - m_\mu^2 + 2M^2 E (E - E_B)(1 - \beta_\mu)]^2} + \tag{38}$$

$$+ \frac{- M E_B (1 - \beta_B)(1 - \beta_\mu) + \dfrac{m_\mu^2}{M (E - E_B)}}{[m_\mu^2 - \mu^2 + 2M^2 E E_B (1 - \beta_B)][\mu^2 - m_\mu + 2M^2 E (E - E_B)(1 - \beta_\mu)]}$$

$$\left\{ \frac{2ME (1 - \beta_B)(1 + \beta_\mu) - 2M E_B \beta_\mu (1 - \beta_B^2) - m_\mu^2 \dfrac{\beta_B}{M (E - E_B)}}{1 + \beta_B} \right\},$$

$$G_{\perp}(E, E_B) = \frac{\sqrt{8}\, c^2 \pi \mu^2}{(\mu^2 + \beta_B^2 M^2 E_B^2)^{1/2}} \frac{\beta_\mu \beta_B M E_B^2 (E - E_B)^2}{|E_\mu (1 - \beta_\mu) + E_B (1 - \beta_B)|^4} \tag{39}$$

$$\left| + \frac{2M^2 E_B^2 (1 + \beta_B \beta_\mu)(1 - \beta_B) - \mu^2 (1 + \beta_\mu) + 2m_\mu^2 \dfrac{E_B}{E - E_B} (\beta_B - 1) + m_\mu^2 (1 + \beta_\mu)}{2 [m_\mu^2 - \mu^2 + 2M^2 E E_B (1 - \beta_B)]^2} + \right.$$

$$+ \frac{2M^2 E_B^2 (1 - \beta_\mu)}{[\mu^2 - m_\mu^2 + 2M^2 E (E - E_B)(1 - \beta_\mu)]^2} +$$

$$\left. + \frac{2M E_B \left\{ M E_B (\beta_B - 1)(1 - \beta_\mu) + \dfrac{m_\mu^2}{M (E - E_B)} \right.}{[m_\mu^2 - \mu^2 + 2M^2 E E_B (1 - \beta_B)][\mu^2 - m_\mu^2 + 2M^2 E (E - E_B)(1 - \beta_\mu)]} \right| .$$

The differential cross-section obtained from equation (40) is greater than that of (41). Both cross-sections tend to infinity when the energy of the incident neutrino tends to infinity.

Taking the screening effect of the Coulomb field into consideration equations (38) and (39) take the form

$$G_{\parallel sc}(E, E_B) = \frac{1}{\left\{1 + \frac{1}{\nu_0^2 [E_\mu (1-\beta_\mu) + E_B (1-\beta_B)]}\right\}^2} G_{\parallel}(E, E_B) \qquad (40)$$

and

$$G_{\perp sc}(E, E_B) = \frac{1}{\left\{1 + \frac{1}{\nu_0^2 [E_\mu (1-\beta_\mu) + E_B (1-\beta_B)]}\right\}^2} G_{\perp}(E, E_B). \qquad (41)$$

REFERENCES

1. H. YUKAWA, Proc. Phys. Math. Soc. Japan, **17,** 48, 1935; Y. TANIKAWA and S. WATANABE, Phys. Rev., **113,** 1344, 1959; J. SCHWINGER, Ann. of Phys., **2,** 407, 1957.
2. N. GABIBO and R. GATTO, Nuovo Cimento, **15,** 304, 1960; T. D. LEE and C. N. YANG, Phys. Rev. Lett., **4,** 307, 1960.; G. MARX and M. ELKISHEN, Acta Phys. Hung., **3,** 257, 1960.
3. On High Energy Neutrino Physics, J. I. N. R. preprint Dubna 1960.
4. J. KAWAKAMI, Progr. Theor. Phys., **19,** 459, 1958; J. SCHWINGER, Ann. of Phys., **2,** 407, 1957.
5. R. P. FEYNMANN and M. GELL-MANN, Phys. Rev., **109,** 19, 1958.
6. M. ELKISHEN, Absorption of high energy neutrinos. Thesis, Roland Eötvös University Budapest, 1961.

АБСОРПЦИЯ НЕЙТРИНО В КУЛОНОВСКОМ ПОЛЕ ЯДРА

М. ЭЛКИШЕН

Р е з ю м е

Вычисляется сечение нейтрино высоких энергий для абсорпции в кулоновском поле ядра атома, результирующей другое нейтрино и два заряженных лептона. Отдельно обсуждаются случаи локального Ферми-взаимодействия и случай слабого косвенного взаимодействия (переданного полем бозонов с тяжёлыми квантами). Кроме этого определяется и вероятность эмиссии реального тяжёлого бозона.

ÜBER DAS AUFTRETEN VON ELEKTROLUMINESZENZ IN ZINKSULFID-EINKRISTALLEN DURCH EINWANDERUNG VON KUPFER*

Von

H. HARTMANN und G. SCHULTZ

PHYSIKALISCH-TECHNISCHES INSTITUT DER DEUTSCHEN AKADEMIE DER WISSENSCHAFTEN ZU BERLIN, BEREICH LUMINESZENZFORSCHUNG, LIEBENWALDE, DDR

(Vorgelegt von G. Szigeti. — Umgearbeitet eingegangen am 20. X. 1962)

Werden leuchtfähige Zinksulfid-Einkristalle durch nachträgliche Diffusionsversuche mit einer relativ hohen Kupferkonzentration dotiert, so tritt gleichzeitig mit der durch UV-Strahlung anregbaren blauen Fluoreszenz blaue Elektrolumineszenz auf. Die Ergebnisse der Cu-Einwanderungen werden qualitativ beschrieben. Dabei ist unter 300-facher Vergösserung ein über das gesamte Kristallvolumen gleichmässig verteiltes Leuchten zu beobachten, welches nur an den senkrecht zur optischen Achse verlaufenden Streifen oder an anderen mechanischen Baufehlern einen verstärkten Austritt erfährt.

Es wird über einige qualitative Untersuchungen an elektrolumineszierenden ZnS-Einkristallen berichtet. Vorausgeschickt sei, dass diese Versuche vorläufig noch nicht zur Klärung des Anregungsmechanismus der Elektrolumineszenz durchgeführt wurden. Sie dienten als Zusatz mit anderen bereits publizierten Ergebnissen [1, 2] der Weiterführung der Zentrenforschung an ZnS : Cu-Leuchtstoffen.

Die zur Untersuchung verwendeten Einkristalle wurden aus der Dampfphase in einem zweiteiligen Ofen gezüchtet, dessen Temperatur in der Sublimationszone 1300 °C betrug. In der Mitte des Ofenkörpers hatte der Temperaturgradient einen flachen Verlauf von etwa 10 °C/cm. Die Dauer der Züchtung betrug mehrere Tage, und die Versuche konnten sowohl in einer strömenden H_2S—HCl-Gasatmosphäre als auch bei verschiedenen Zusammensetzungen des Trägergases in abgeschmolzenen Ampullen durchgeführt werden. Bei jedem Versuch bildeten sich morphologisch unterschiedliche Kristalle, deren Erscheinungsformen ebenfalls an anderer Stelle beschrieben sind [1].

Für die vorliegenden Experimente wurden zunächst nur die hexagonalen Prismen gewählt, welche hinsichtlich der Polytypie meist stark fehlgeordnet waren. Bereits während der Züchtung konnten bei einem Aktivatorzusatz von 10^{-5}—10^{-3} g Cu/g ZnS in Abhängigkeit von bestimmten experimentellen Faktoren, wie Zusammensetzung des Trägergases oder Züchtungstemperatur, Kristalle mit blauer oder seltener mit grüner Elektrolumineszenz beobachtet werden. Von ausschlaggebender Bedeutung für die Bildung der unter UV-Anregung grünleuchtenden oder der gleichzeitig elektrolumineszenten blauen

* Vortrag auf dem Symposion über Lumineszenz, Balatonvilágos, 7—10 Juni 1961.

Zentren war eine durch die Versuchsbedingungen vorgegebene Akzeptorstellenkonzentration des Grundmaterials [3].

Durch nachträgliche Diffusionsversuche in verschiedenen Gasatmosphären (an der Luft sowie unter Chlorwasserstoff und H_2S—HCl-Gasgemischen) konnten Kristalle mit der himmelblauen eigenaktivierten oder der grünen Photolumineszenz in blauleuchtende Beispiele umgewandelt werden. Nur im letzten Falle war dann eine entsprechende Elektrolumineszenz erkennbar. Mitunter verliefen die Aktivatordiffusionen beim Vorliegen höherer Chlorwasserstoff-Anteile auch an vorher nichtlumineszierenden Kristallen positiv. Als günstigste Einwanderungstemperatur für Kupfer erwies sich in allen Experimenten das Gebiet um 400 °C. Der Diffusionsprozess begann bereits bei 300° C. Es entstanden bei diesen relativ niedrigen Temperaturen jedoch nur Beispiele mit intensitätsschwachem Leuchten bei Anregung durch elektrische Felder. ZnS-Kristalle, welche bereits während der Züchtung als elektrolumineszenzfähig entstanden waren, erfuhren durch eine nachträgliche Cu-Dotierung in ihrem Lumineszenzverhalten keine wesentliche Beeinflussung. Bei vorgegebener hoher Aktivatorkonzentration kam es nur zu einem im Vergleich zur Ausgangskonzentration sehr geringen Einbau des Cu. In den meisten Fällen erwies es sich als vorteilhaft, den Kristall nachträglich mit einer heissen verdünnten KCN-Lösung zu behandeln. Auf Grund der Beseitigung der oberflächlich anhaftenden Aktivatorschicht konnte das Lumineszenzverhalten besser beobachtet werden.

Die von ORTMANN [4] an Cu-dotierten Zinksulfid-Pulvern durch entsprechendes Nachtempern gefundenen Effekte der Grün-Blau-Umwandlung der Photolumineszenz konnten auf Grund der durchgeführten Ein- und Auswanderungsexperimente an Einkristallen bestätigt werden. Mit der blauen Fluoreszenz verbunden war, wie erwähnt, jeweils wieder eine blaue Elektrolumineszenz zu beobachten.

Die Anwendung höherer Diffusionstemperaturen ergab bei gleicher vorgegebener Aktivatorkonzentration im Vergleich zum Versuch bei 400 °C einen geringeren Einbau des Kupfers im grünleuchtenden Zustand. Bei Verwendung von Schwefelwasserstoff liessen die aktivierten Kristalle meisten einen Cu-Ausbau erkennen. So konnte ein grünleuchtendes Prisma bei nachträglichem mehrstündigen Tempern um 450° C in einer H_2S-Gasatmosphäre in ein blaulumineszierendes Beispiel umgewandelt werden, welches dann gleichzeitig Elektrolumineszenz zeigte.

Die mikroskopische Beobachtung des Leuchtens bei Anregung durch elektrische Felder zwischen Kupferelektroden (ohne Kontaktierung) ergab eine über das gesamte Kristallvolumen gleichmässig verteilte Lumineszenz. Dabei wurde eine 300-fache Vergrösserung verwendet. Nur an den senkrecht zur optischen Achse verlaufenden Streifen oder an anderen mechanischen Baufehlern kam es zu einem verstärkten Austritt des Lumineszenzlichtes. Die Elektro-

lumineszenz blieb während der Auflösung der Kristalle in Säure erhalten. Reststücke ergaben nach Anlösen mit konzentrierter Salpetersäure in jeder Phase das typische Leuchten des Ausgangskristalls.

Die vorliegende kurze und zusammenfassende Beschreibung der rein qualitativen Ergebnisse sollte zunächst nur einige Hinweise für die Präparation elektrolumineszenter ZnS-Einkristalle durch nachträgliche Diffusionsversuche mit Kupfer geben. Diese ersten grundlegenden Versuche werden zur Zeit weitergeführt und die Ergebnisse zu einem späteren Zeitpunkt an anderer Stelle publiziert.

LITERATUR

1. H. Hartmann, Phys. Stat. Sol., **2**, 585, 1962.
2. H. Hartmann, Phys. Stat. Sol., **2**, 929, 1962.
3. N. Riehl und H. Ortmann, Monographie Nr. 72 zur Angew. Chem. 1957.
4. H. Ortmann, Mber. Dt. Akad. Wiss., **2**, 3, 1960.

О ПОЯВЛЕНИИ ЭЛЕКТРОЛЮМИНЕСЦЕНЦИИ В ЦИНКСУЛЬФИДНОМ МОНОКРИСТАЛЛЕ ЧЕРЕЗ МИГРАЦИЮ МЕДИ

Г. Гартманн и Г. Шульц

Резюме

Светящийся цинксульфидный монокристалл диффузионным приемом дополняется относительно высокой концентрацией меди, вследствие чего одновременно с синей флуоресценцией, вызванной UV-излучением, появляется и синяя электролюминесценция. Качественно описываются результаты миграции меди. При этом при 300-кратном увеличении по всему объёму кристалла наблюдаются равномерно распределённые светящиеся точки, которые усиленно выражаются только при наличии перпендикулярной оптической оси полосы или других дефектов, имеющихся в механической структуре.

PION DECAY AND THE ANOMALOUS INTERACTION OF MUONS

By

CHÉN SHÍ* and G. MARX

INSTITUTE OF THEORETICAL PHYSICS, ROLAND EÖTVÖS UNIVERSITY, BUDAPEST

(Received 19. VI. 1961)

One of the most puzzling problems of elementary particle physics is the origin of the muon mass. It seems that the most convincing explanation for the electron-muon mass difference is to suppose an "anomalous" intermediately strong interaction (beside the weak and electromagnetic interactions) referring to muons only. On the other hand, a definite experimental proof for such an anomalous interaction does not exist as yet. If, however, the coupling constant and the range of the interaction is not too large, one can quite well imagine that the consequences of this interaction remain unobserved for moderate energies of our present experimental possibilities.** As it is known, indirect effects, where the interaction takes place only virtually, and thus the short range does not present any obstacle, produce a much more serious limitation for the existence of an anomalous interaction. One of the most accurately known data of the muon is its anomalous magnetic moment. The good agreement between the experimental and theoretical values represents the most serious argument against such an anomalous interaction [4]. MARSHAK has also drawn attention [5] to the good agreement between theoretical and experimental values of the branching ratios $(\pi \to e) : (\pi \to \mu)$, which may serve as a similar argument [6]. Here we wish to give a semi-quantitative check in order to get some information about the limitations for the anomalous interaction due to the above-mentioned branching ratio.

The relevant experimental and theoretical values are: The magnetic moment of the muon [4]

$$\mu_{\text{exp}} = (1{,}001145 \pm 0{,}000022)\ \mu_0.$$

* Now in Peking, at the Academia Sinica.

** An interaction having a range of the order of a nucleon Compton wave length in the energy range $E < 1$ GeV does not produce any observable effect. Some measurements with cosmic ray energies seem to point to some anomalous interaction [1]. More detailed information can be expected only from high-energy accelerators. Because of technical difficulties such experiments were started only very recently [2]. Muon-nucleus scattering experiments with an accuracy of more than 10^{-30} cm^2 for momentum transfers of several GeV/c would be highly desirable [3, 4].

Quantumelectrodynamics gives

$$\mu_{\text{theor}} = 1{,}001165\ \mu_0\,,$$

thus the supposed anomalous contribution must be less than

$$\delta\mu = \mu_{\text{exp}} - \mu_{\text{theor}} = (-2{,}0 \pm 2{,}2)\cdot 10^{-5}\,\mu_0. \tag{1}$$

The experimental branching ratio $(\pi^+ \to e^+) : (\pi^+ \to \mu^+)$ is [7]

$$R_{\text{exp}} = (1.21 \pm 0.07)\cdot 10^{-4}.$$

The theory of the universal weak $V - A$ interaction gives the result

$$R_{\text{theor}} = 1.28\cdot 10^{-4}\,,$$

which may be modified by an electromagnetic correction [8]

$$R'_{\text{theor}} = 1.23\cdot 10^{-4}.$$

Thus the "anomalous" correction — resulting from the "strange" muon interaction — must be less than

$$\frac{\delta w}{w} = \frac{R_{\text{theor}} - R_{\text{exp}}}{R_{\text{exp}}} = (5 \pm 6)\cdot 10^{-2}, \tag{2}$$

$$\frac{\delta w'}{w} = \frac{R'_{\text{theor}} - R_{\text{exp}}}{R_{\text{exp}}} = (2 \pm 6)\cdot 10^{-2}, \tag{3}$$

respectively.

Let us suppose first that the anomalous interaction is caused by a scalar meson (σ) having the rest mass m coupled to the muons (μ) and nucleons (M) with the same coupling constant g [9]. Restriction (1) gives [5, 10]

$$\frac{g^2}{\hbar c} < 10^{-4}\left(\frac{m}{\mu}\right)^2. \tag{4}$$

If we do not wish to suppose an extremely large σ-mass ($m \gg M$), g has to be small as to its order or smaller than the electric charge. (Pseudoscalar and vector meson give a similar result [10, 11].)

We have calculated the effect of the σ-interaction on the $\pi \to \mu$ decay. From the diagram Fig. 1 in the lowest order of the perturbation theory, with

the cut-off parameter Λ for the K-meson one obtains

$$\frac{\delta w}{w} = \frac{1}{(4\pi)^2}\left(\frac{g^2}{\hbar c}\right)^2\left(\frac{\Lambda}{M}\right)^4 F(\Lambda, \Lambda_\pi, M)\left(\frac{M}{\mu}\right)^2,$$

where F is of the order of unity. (The interference term drops out.) (2) and (3) require

$$\frac{g^2}{\hbar c} \lesssim \left(\frac{\Lambda}{M}\right)^{-2} \cdot \frac{\mu}{M}. \tag{5}$$

Supposing $\Lambda \geqq m$, (4) and (5) give

$$\frac{g^2}{\hbar c} < 10^{-2}.$$

Thus it seems that the σ-interaction proposed by SCHWINGER cannot be strong.

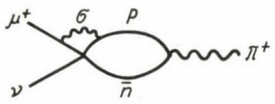

Fig. 1

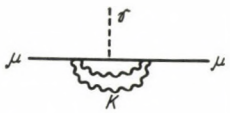

Fig. 2

Another possibility studied here is the intermediately strong K-pair interaction having the interaction Lagrangian

$$L_{\text{int}} = -G\varphi_\alpha^+ (\overleftarrow{\partial_i} - \overrightarrow{\partial_i})\varphi_\alpha (\overline{\psi}_n \gamma_i \psi_n + \overline{\psi}_p \gamma_i \psi_p + \overline{\psi}_\mu \gamma_i \psi_\mu). \tag{6}$$

This coupling was studied repeatedly [4, 13, 14] in connection with the hyperon model of GOLDHABER [12]. Considering (6) as the expression describing the kaonic interactions of strange particles, $G\varkappa^2 \sim 1$ ($\varkappa$ is the kaon mass). Is this assumption in agreement with the properties of the muon?

The anomalous magnetic moment of muons, corresponding to the diagram Fig. 2 was calculated by VÉRTES [15]:

$$\frac{\delta\mu}{\mu_0} \sim \frac{1}{8(2\pi)^4}\frac{m^2}{\Lambda^2}(G\Lambda^2)^2. \tag{7}$$

Here Λ is the cut-off momentum for kaon field. Factors of "2π" of the order 10^{-4}, originated from the double virtual kaon line play an important role. (7) and (1) together give

$$G\Lambda^2 \leq \frac{\Lambda}{m}. \tag{8}$$

The correction to the decay probability $\pi \to \mu$ according to Fig. 3 in the lowest order of perturbation theory is

$$\frac{\delta w}{w} = \frac{1}{2^2 \pi^4} (G\Lambda^2)^2 I + \frac{1}{2^6 \pi^8} (G\Lambda^2)^4 I'. \tag{9}$$

The first is the interference term between 3a and 3b, the second corresponds to 3b. I and I' denote integrals of the order of unity, but containing also $\varkappa$, M, Λ and Λ_π. "2π"-s here are also important. The second term is small compared to the first, thus comparing (9) and (2—3)

$$G\Lambda^2 < 2. \tag{10}$$

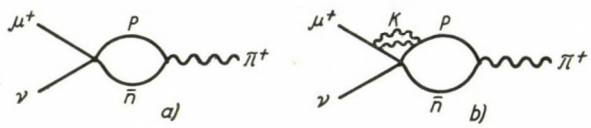

Fig. 3

(8) and (10) give that the effects treated above allow an interaction of the type (6) if

$$G\Lambda^2 \approx 1.$$

(11) can be fulfilled if e. g.

$$G\varkappa^2 \approx 1, \quad \Lambda \approx \varkappa,$$

which was supposed also in [11, 13, 14]. Thus the hypothesis of the "universal" kaon interaction can be maintained considering the anomalous magnetic moment and the branching ratio $(\pi \to e) : (\pi \to \mu)$. (The "reality of the 2π-s" and the applicability of the perturbation theory is in this case, of course, questionable.) Another possibility, leading also to (11) is

$$G\varkappa^2 \ll 1, \quad \Lambda \gg \varkappa,$$

then we may well believe the perturbation theory to be correct, but the effects which are not divergent (i. e. do not contain Λ) turn out to be small, contradicting the basic idea of the GOLDHABER model.

The central problem remains the theoretical determination of the muon-electron mass difference. Perturbational calculations given by COWLAND [11] (for scalar σ-interaction) and by VÉRTES [15] (for K-pair interaction) show the anomalous mass δm to be small:

$$\frac{\delta m}{m} \lesssim 10^{-3}.$$

Unfortunately, it may be decided only by means of other methods than the perturbation theory, whether an anomalous muon interaction which does not contradict the experimental results (1), (2), (3) may explain the anomalous mass of the muon or not. According to our opinion the first possibility is not yet excluded.

Note added in proof: The newest experimental value for $\delta\mu/\mu_0$ in (1) is $3 \pm 5. \ 10^{-6}$, according to the report of G. CHARPAK et al. at he XI. High Energy Conference in Geneva, 1962. This result does not modify the essence of our conclusions given above.

REFERENCES

1. A. W. WOLFENDALE et al., Proc. Phys. Soc., **A70**, 421, 1957;
   W. L. WHITTMORE and R. P.SHUTT, Phys. Rev., **88**, 1312, 1957
2. C. Y. KIM et al., Phys. Rev., in the press.
3. I. R. GATLAND, Nucl. Phys., **9**, 267, 1958.
4. G. MARX and K. L. NAGY, Acta Phys. Hung., **11**, 161, 1960.
5. G. CHARPAK et al., Phys. Rev. Lett., **6**, 52, 1961.
6. R. E. MARSHAK, Conference on High Energy Physics, Kiev, 1959.
7. C. D. ANDERSON et. al., Phys. Rev., **119**, 2050, 1960.
8. R. KINOSHITA, Phys. Rev. Lett., **2**, 477, 1959.
9. J. SCHWINGER, Ann. of Phys., **2**, 407, 1957.
10. S. COWLAND, Nucl. Phys., **8**, 397, 1958.
11. L. B. OKUN, private communication.
12. M. GOLDHABER, Phys. Rev., 101, 431, 1956.
13. G. GYÖRGYI, Nucl. Physics, 10, 197, 1959.
14. G. MARX and K. L. NAGY, Nucl. Phys., **12**, 125, 1958.
15. P. VÉRTES, Acta Phys. Hung., **13**, 341, 1961.

ZUR THEORIE DER ELEKTRONENSTRUKTUR DES Br-ATOMS UND DES Te-ATOMS

Von

R. GÁSPÁR

FORSCHUNGSGRUPPE FÜR THEORETISCHE PHYSIK DER UNGARISCHEN AKADEMIE DER WISSENSCHAFTEN, BUDAPEST

(Eingegangen: 20. X. 1961)

Wir haben die Einelektronenergien und die radialen Eigenfunktionen mehrerer Atome mit Hilfe eines universellen Potentialfeldes bestimmt [1]. Die erste Rechnung, die sich mit einem Halogenatom beschäftigt, ist die hier angegebene, welche die Struktur des Br-Atoms aufklärt. Die Berechnungen über das Te-Atom sollen die Elektronenstruktur einer der schwersten Elemente der VI_b Gruppe im periodischen System der Elemente erklären.

1. Einführung

Die radiale Schrödinger-Gleichung, welche die Wellenfunktionen und die Energieeigenwerte der Elektronenzustände bestimmt, lautet

$$\frac{d^2f}{dx^2} + \left[\varepsilon + \frac{\gamma}{x}\frac{e^{-\lambda_0 x}}{1+A_0 x} + \zeta\frac{e^{-ax}}{1+Ax} - \frac{l(l+1)}{x^2}\right]f = 0\,, \tag{1}$$

wo

$$\varepsilon = 2E\mu^2 e^{-2} a_0^{-1}, \quad \gamma = 2Z\mu a_0^{-1}, \quad \zeta = \frac{8}{3}k_a C\, 0{,}8853^2\, e^{-2} \tag{2}$$

und $x = r\mu^{-1}$, $\mu = 0{,}8853\, a_0 Z^{-1/3}$, $k_a = (3/4)(3/\pi)^{1/3}\ e^2$ ist.

In (2) bezeichnet r den Abstand des Elektrons vom Kern, Z die Ordnungszahl des Atoms, E die Energie und f die radiale Eigenfunktion des Elektrons. Die Werte der Konstanten sind die folgenden:

$$\lambda_0 = 0{,}1837\,, \quad A_0 = 1{,}05, \quad a = 0{,}04, \quad A = 9 \quad \text{und} \quad C = 3{,}1 a_0^{-1}.$$

Mit l wurde die Nebenquantenzahl des Elektrons bezeichnet. Wir lösen die Differentialgleichung (1) mit den Randbedingungen

$$f(0) = f'(0) = \ldots = f^{(l-1)}(0) = 0\,,$$
$$f^{(l)} = \text{const.}\,,$$
$$\lim_{x\to\infty} f(x) = 0\,.$$

Über das Problem der Ableitung und der Lösung der Differentialgleichung (1) gibt eine frühere Arbeit [2] Auskunft.

2. Elektronenstruktur des Br-Atoms

Die Elektronenkonfiguration des Br-Atoms im Grundzustand ist die folgende:

$$(1s)^2\,(2s)^2\,(2p)^6\,(3s)^2\,(3p)^6\,(4s)^2\,(3d)^{10}\,(4p)^5.$$

Die Elektronenstruktur unterscheidet sich von derjenigen der früher behandelten Atome hauptsächlich dadurch, dass hier zuerst eine nicht abgeschlossene $(np)^5$ Schale auftritt.

Die radialen Wellenfunktionen des Br-Atoms geben wir in Tab. I und II an, wo auch die totale radiale Dichte der Elektronen und die Potentialwerte mitgeteilt sind. Die Tab. III enthält die Einelektronenergien, neben diesen haben wir die Mittelwerte der Röntgentermwerte als Experimentalwerte angegeben. Die beste Übereinstimmung zwischen den berechneten und gemessenen Werten besteht unserer Erwartung entsprechend in dem Fall der locker gebundenen Elektronen [3].

Die aus den Versuchen auf indirektem Wege erhaltenen Werte für die diamagnetische Suszeptibilität beziehen sich auf das Br-Ion. Unsere Rechnungen geben die Einelektronwellenfunktionen des Br^--Atoms, und wenn wir eine Pseudodichte des Br^--Ions mit den Besetzungszahlen des Br^--Ions und den Wellenfunktionen des Br-Atoms berechnen, dann befindet sich die so erhaltene Elektronendichte in einer kleineren Umgebung des Atomkerns als im freien Br^--Ion, weil wir die gegenseitige Abstossung zwischen dem letzten *np* Elektron und den Elektronen des neutralen Atoms vernachlässigt haben. So können wir erwarten, dass der Wert der diamagnetischen Suszeptibilität, mit dieser Elektronendichte berechnet, kleiner sein wird als jener im freien Ion. In der Tat ist der berechnete Wert der diamagnetischen Suszeptibilität, $-27{,}72\ 10^{-6}$ cm^3 Mol^{-1}, im Vergleich zu dem empirischen Wert, $-39{,}0\ 10^{-6}$ cm^3 Mol^{-1}, wirklich eine kleinere Grösse.

3. Elektronenstruktur des Te-Atoms

Die Elektronenkonfiguration des Te-Atoms im Grundzustand ist die folgende:

$$(1s)^2\,(2s)^2\,(2p)^6\,(3s)^2\,(3p)^6\,(3d)^{10}\,(4s)^2\,(4p)^6\,(4d)^{10}\,(5s)^2\,(5p)^4.$$

Unter den Elementen in der VI_b-Gruppe des periodischen Systems der Elemente sind Te und Se bekannt als Halbleiter, die sehr ähnliche Eigenschaften haben. Diesen Elementen können wir das Polonium zuordnen, das eine sehr

ähnliche Gitterstruktur aufweist. Die Elektronenstruktur der Atome dieser Elemente unterscheidet sich von derjenigen der früher behandelten Atome der VI_b-Gruppe dadurch, dass hier die Elektronen in den $(ns)^2\,(np)^4$ Schalen in starker Wechselwirkung mit den Elektronen einer inneren $[(n-1)d]^{10}$ Schale stehen.

Die radialen Wellenfunktionen des Te-Atoms geben wir in Tab. IV, V. und VI an. In diesen Tabellen sind auch die totalen radialen Dichten der Elektronen und die Werte des universellen Potentials mitgeteilt. Die Tab. VII

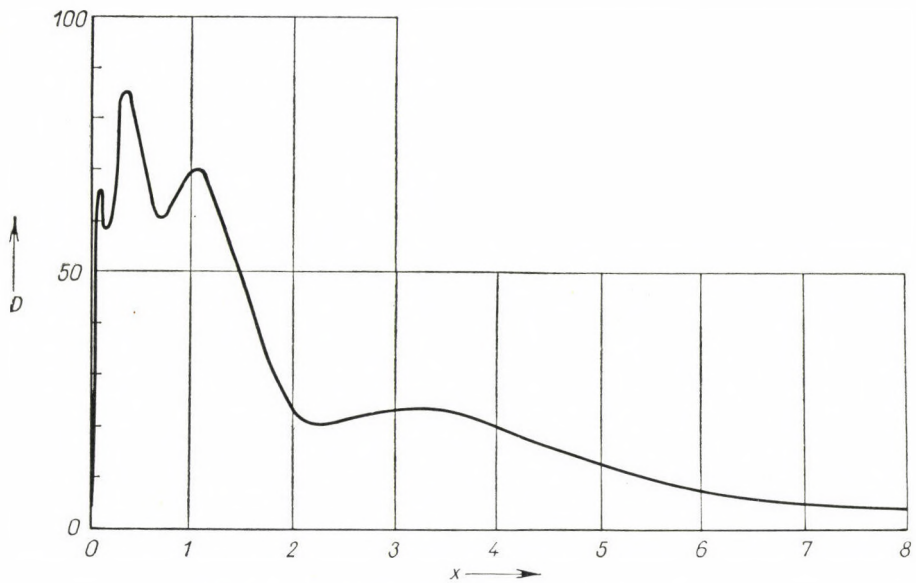

Abb. 1. Die radiale Dichte $D = 4\pi r^2 \varrho$ des Te-Atoms

enthält die Einelektronenergien und die als experimentelle Werte angegebenen Röntgentermmittelwerte. In Abb. 1 haben wir die radiale Dichte $D = 4\pi r^2 \varrho$ des Te-Atoms aufgezeichnet. Abb. 1 zeigt deutlich die räumliche Verteilung der Elektronengruppen im Te-Atom.

Für die Durchführung der numerischen Rechnungen möchte ich Frau I. Kocsis auch an dieser Stelle meinen Dank aussprechen.

LITERATUR

1. Siehe z. B. R. Gáspár, Acta Phys. Hung., **12,** 335, 1960.
2. R. Gáspár, Acta Phys. Hung., **3,** 263, 1954.
3. Landolt—Börnstein, Zahlenwerte und Funktionen, Bd. I. Teil. 1. Atome und Ionen. Springer-Verlag, Berlin, 1950. S. 396.

Tabelle I

Die radialen Eigenfunktionen f der s-Elektronen des Br-Atoms und das Potential V des Br-Atoms
f in atomaren Einheiten von $1/a_0^{1/2}$, V in atomaren Einheiten von e/a_0;
x in dimensionslosen Längeneinheiten

x	f				V
	1s	2s	3s	4s	
0,000	0,000	0,000	0,000	0,000	
0,006	0,629	0,197	0,079	0,028	3138,86
0,012	1,189	0,372	0,148	0,054	1560,02
0,018	1,685	0,526	0,210	0,076	1033,68
0,024	2,123	0,660	0,264	0,095	770,533
0,030	2,507	0,777	0,310	0,112	612,625
0,036	2,842	0,876	0,349	0,126	507,344
0,042	3,133	0,960	0,383	0,138	432,167
0,048	3,384	1,029	0,410	0,148	375,789
0,054	3,597	1,085	0,431	0,155	331,947
0,060	3,776	1,128	0,448	0,161	296,885
0,066	3,925	1,159	0,460	0,166	268,203
0,072	4,046	1,180	0,467	0,168	244,314
0,078	4,142	1,191	0,470	0,169	224,108
0,084	4,215	1,192	0,470	0,169	206,800
0,090	4,268	1,185	0,466	0,168	191,807
0,108	4,323	1,119	0,436	0,157	156,874
0,126	4,257	1,000	0,384	0,138	131,983
0,144	4,108	0,840	0,315	0,113	113,372
0,162	3,903	0,653	0,235	0,084	98,948
0,180	3,663	0,446	0,148	0,052	87,454
0,198	3,405	0,227	0,056	0,018	78,091
0,216	3,139	0,003	−0,037	−0,015	70,325
0,234	2,874	−0,220	−0,129	−0,049	63,785
0,252	2,617	−0,440	−0,219	−0,081	58,209
0,270	2,371	−0,653	−0,304	−0,112	53,404
0,288	2,139	−0,857	−0,385	−0,141	49,222
0,324	1,722	−1,230	−0,528	−0,192	42,315
0,360	1,370	−1,551	−0,643	−0,233	36,858
0,396	1,080	−1,816	−0,728	−0,262	32,452
0,432	0,844	−2,027	−0,784	−0,281	28,830
0,468	0,656	−2,186	−0,813	−0,289	25,808
0,504	0,507	−2,299	−0,815	−0,288	23,255
0,540	0,390	−2,369	−0,795	−0,278	21,074
0,576	0,298	−2,404	−0,754	−0,260	19,194
0,612	0,227	−2,407	−0,696	−0,236	17,559
0,648	0,171	−2,383	−0,623	−0,207	16,129
0,684	0,129	−2,339	−0,539	−0,173	14,867
0,720	0,095	−2,277	−0,444	−0,136	13,750
0,756	0,069	−2,202	−0,343	−0,097	12,754
0,792	0,048	−2,116	−0,236	−0,056	11,862
0,828	0,031	−2,024	−0,127	−0,014	11,060
0,864	0,017	−1,926	−0,015	0,027	10,336
0,900	0,004	−1,825	0,096	0,069	9,681
0,936		−1,724	0,207	0,110	9,085
1,008		−1,522	0,420	0,187	8,044
1,080		−1,329	0,620	0,257	7,168
1,152		−1,150	0,801	0,318	6,425
1,224		−0,988	0,961	0,368	5,788
1,296		−0,843	1,099	0,407	5,239

Tabelle I (Fortsetzung)

x	f				V
	1s	2s	3s	4s	
1,368		−0,715	1,215	0,436	4,761
1,440		−0,603	1,309	0,454	4,344
1,512		−0,507	1,384	0,462	3,976
1,584		−0,424	1,439	0,461	3,652
1,656		−0,354	1,477	0,452	3,363
1,728		−0,294	1,500	0,435	3,106
1,800		−0,244	1,509	0,412	2,875
1,872		−0,202	1,506	0,382	2,668
1,944		−0,166	1,493	0,348	2,482
2,016		−0,136	1,472	0,309	2,312
2,088		−0,111	1,443	0,267	2,159
2,160		−0,090	1,407	0,222	2,020
2,304		−0,058	1,323	0,126	1,776
2,448		−0,035	1,228	0,025	1,571
2,592		−0,018	1,126	−0,076	1,397
2,736		−0,003	1,024	−0,175	1,249
2,880			0,923	−0,270	1,122
3,024			0,827	−0,360	1,011
3,168			0,737	−0,443	0,915
3,312			0,653	−0,519	0,831
3,456			0,577	−0,587	0,757
3,600			0,507	−0,648	0,692
3,744			0,444	−0,702	0,635
3,888			0,388	−0,748	0,583
4,032			0,339	−0,787	0,537
4,176			0,294	−0,819	0,496
4,320			0,255	−0,845	0,459
4,608			0,191	−0,881	0,396
4,896			0,142	−0,898	0,344
5,184			0,105	−0,898	0,300
5,472			0,078	−0,886	0,264
5,760			0,057	−0,864	0,234
6,048			0,041	−0,835	0,208
6,336			0,030	−0,801	0,186
6,624			0,021	−0,763	0,167
6,912			0,014	−0,723	0,151
7,200			0,009	−0,681	0,136
7,488			0,005	−0,639	0,124
7,776			0,002	−0,598	0,113
8,064				−0,557	0,104
8,640				−0,481	0,088
9,216				−0,411	0,075
9,792				−0,349	0,065
10,368				−0,294	0,056
10,944				−0,247	0,050
11,520				−0,207	0,044
12,096				−0,173	0,039
12,672				−0,144	0,035
13,248				−0,119	0,032
13,824				−0,099	0,029
14,400				−0,082	0,026
14,976				−0,067	0,024

Tabelle I (Fortsetzung)

x	f				V
	$1s$	$2s$	$3s$	$4s$	
16,128				−0,046	0,021
17,280				−0,031	0,018
18,432				−0,020	0,015
19,584				−0,013	0,014
20,736				−0,008	0,012
21,888				−0,005	0,011
23,040				−0,002	0,010
24,192					0,009
25,344					0,008
26,496					0,007
27,648					0,006
28,800					0,006
29,952					0,005
31,104					0,005

Tabelle II

Die radialen Eigenfunktionen f der p- und d-Elektronen des Br-Atoms und die radiale Dichte D des Br-Atoms
f in atomaren Einheiten von $1/a_0^{1/2}$, D in atomaren Einheiten von $1/a_0$;
x in dimensionslosen Längeneinheiten

x	f				D
	$2p$	$3p$	$4p$	$3d$	
0,000	0,000	0,000	0,000	0,000	0,000
0,006	0,003	0,001	0,000	0,000	0,883
0,012	0,012	0,005	0,002	0,000	3,154
0,018	0,027	0,011	0,003	0,000	6,335
0,024	0,046	0,018	0,006	0,000	10,054
0,030	0,070	0,028	0,009	0,000	14,027
0,036	0,098	0,039	0,012	0,001	18,038
0,042	0,130	0,052	0,016	0,001	21,928
0,048	0,164	0,066	0,020	0,001	25,587
0,054	0,202	0,081	0,025	0,002	28,937
0,060	0,243	0,097	0,030	0,003	31,935
0,066	0,286	0,114	0,035	0,003	34,554
0,072	0,331	0,132	0,041	0,004	36,791
0,078	0,378	0,151	0,047	0,005	38,652
0,084	0,426	0,170	0,052	0,006	40,152
0,090	0,475	0,189	0,058	0,008	41,319
0,108	0,630	0,250	0,077	0,013	43,093
0,126	0,789	0,312	0,096	0,019	42,952
0,144	0,949	0,374	0,115	0,027	41,708
0,162	1,106	0,433	0,134	0,037	40,021
0,180	1,259	0,490	0,151	0,048	38,370
0,198	1,404	0,543	0,167	0,060	37,061
0,216	1,541	0,591	0,182	0,074	36,261
0,234	1,668	0,634	0,195	0,090	36,025
0,252	1,785	0,672	0,206	0,106	36,335
0,270	1,891	0,704	0,215	0,124	37,123
0,288	1,987	0,730	0,223	0,143	38,045

Tabelle II (Fortsetzung)

x	f				D
	$2p$	$3p$	$4p$	$3d$	
0,324	2,146	0,766	0,233	0,185	41,354
0,360	2,264	0,780	0,236	0,230	44,706
0,396	2,343	0,774	0,233	0,279	47,707
0,432	2,388	0,748	0,223	0,329	49,947
0,468	2,403	0,707	0,209	0,381	51,007
0,504	2,392	0,650	0,190	0,434	51,513
0,540	2,359	0,582	0,167	0,488	50,895
0,576	2,308	0,504	0,141	0,541	49,527
0,612	2,243	0,418	0,113	0,594	47,597
0,648	2,166	0,326	0,082	0,647	45,295
0,684	2,081	0,229	0,051	0,698	42,804
0,720	1,990	0,130	0,019	0,748	40,277
0,756	1,895	0,029	−0,013	0,796	37,843
0,792	1,798	−0,072	−0,045	0,842	35,599
0,828	1,700	−0,173	−0,077	0,886	33,164
0,864	1, 602	−0,272	−0,108	0,928	31,930
0,900	1,506	−0,368	−0,137	0,968	30,569
0,936	1,411	−0,462	−0,166	1,005	29,534
1,008	1,232	−0,639	−0,218	1,074	28,382
1,080	1,067	−0,799	−0,264	1,132	28,275
1,152	0,919	−0,941	−0,303	1,182	28,943
1,224	0,786	−1,064	−0,333	1,223	30,078
1,296	0,669	−1,168	−0,356	1,255	31,436
1,368	0,567	−1,254	−0,372	1,280	32,798
1,440	0,479	−1,323	−0,381	1,297	34,004
1,512	0,403	−1,376	−0,383	1,308	34,944
1,584	0,339	−1,414	−0,380	1,312	35,556
1,656	0,284	−1,439	−0,370	1,311	35,813
1,728	0,237	−1,452	−0,356	1,306	35,718
1,800	0,197	−1,454	−0,338	1,296	35,293
1,872	0,164	−1,448	−0,315	1,282	34,571
1,944	0,136	−1,433	−0,290	1,264	33,597
2,016	0,113	−1,412	−0,261	1,244	32,416
2,088	0,093	−1,385	−0,230	1,222	31,076
2,160	0,077	−1,353	−0,197	1,197	29,618
2,304	0,052	−1,278	−0,127	1,143	26,511
2,448	0,034	−1,194	−0,053	1,085	23,363
2,592	0,022	−1,105	0,022	1,024	20,364
2,736	0,013	−1,015	0,096	0,962	17,632
2,880	0,006	−0,926	0,169	0,900	15,232
3,024		−0,839	0,239	0,839	13,182
3,168		−0,758	0,306	0,780	11,474
3,312		−0,681	0,368	0,723	10,082
3,456		−0,610	0,426	0,669	8,969
3,600		−0,544	0,479	0,618	8,094
3,744		−0,484	0,527	0,570	7,418
3,888		−0,430	0,571	0,524	6,903
4,032		−0,381	0,610	0,482	6,516
4,176		−0,336	0,645	0,442	6,226
4,320		−0,297	0,675	0,405	6,009
4,608		−0,230	0,724	0,340	5,717
4,896		−0,177	0,758	0,284	5,440
5,184		−0,136	0,780	0,236	5,351
5,472		−0,104	0,792	0,197	5,170
5,760		−0,079	0,795	0,163	4,961

Tabelle II (Fortsetzung)

x	f				D
	$2p$	$3p$	$4p$	$3d$	
6,048		−0,060	0,790	0,135	4,722
6,336		−0,046	0,779	0,112	4,457
6,624		−0,034	0,764	0,093	4,237
6,912		−0,026	0,744	0,076	3,877
7,200		−0,020	0,722	0,063	3,577
7,488		−0,015	0,698	0,052	3,280
7,776		−0,011	0,672	0,043	2,992
8,064		−0,008	0,645	0,035	2,716
8,640		−0,004	0,590	0,024	2,210
9,216		−0,002	0,536	0,016	1,774
9,792			0,483	0,011	1,410
10,368			0,433	0,007	1,111
10,944			0,387	0,005	0,870
11,520			0,344	0,003	0,677
12,096			0,305	0,002	0,525
12,672			0,270	0,001	0,406
13,248			0,238	0,001	0,313
13,824			0,210		0,240
14,400			0,185		0,185
14,976			0,163		0,141
16,128			0,125		0,083
17,280			0,096		0,048
18,432			0,073		0,028
19,584			0,056		0,016
20,736			0,043		0,009
21,888			0,032		0,005
23,040			0,024		0,003
24,192			0,018		0,002
25,344			0,014		0,001
26,496			0,010		0,001
27,648			0,007		
28,800			0,005		
29,952			0,003		
31,104			0,002		

Tabelle III

Die mit dem universellen Potential bestimmten Energieterme der Elektronen des Br-Atoms und die Röntgentermwerte nach LANDOLT und BÖRNSTEIN
(Es werden die arithmetischen Mittelwerte der Röntgendublette angegeben)
Die Energiewerte sind in atomaren Einheiten von e^2/a_0 angegeben

	1*s*	2*s*	3*s*	4*s*
Universelles Potential	490,0	62,79	9,227	0,8989
Nach LANDOLT—BÖRNSTEIN	496,3	—	9,740	—
	2*p*	3*p*	4*p*	
Universelles Potential	57,007	7,1086	0,4256	
Nach LANDOLT—BÖRNSTEIN	58,025	6,7025	0,2500	
	3*d*			
Universelles Potential	3,126			
Nach LANDOLT—BÖRNSTEIN	2,600			

Tabelle IV

Die radialen Eigenfunktionen f der s-Elektronen des Te-Atoms
f in atomaren Einheiten von $1/a_0^{1/2}$; x in dimensionslosen Längeneinheiten

x	f				
	1s	2s	3s	4s	5s
0,000	0,000	0,000	0,000	0,000	0,000
0,006	0,278	0.090	0,040	0,017	0,006
0,012	0,516	0,167	0,074	0,032	0,011
0,018	0,719	0,232	0,102	0,044	0,015
0,024	0,891	0,286	0,126	0,054	0,018
0,030	1,034	0,330	0,145	0,063	0,021
0,036	1,152	0,364	0,160	0,069	0,023
0,042	1,249	0,390	0,171	0,074	0,025
0,048	1,326	0,409	0,179	0,077	0,026
0,054	1,385	0,420	0,184	0,079	0,027
0,060	1,431	0,426	0,186	0,080	0,027
0,066	1,461	0,425	0,185	0,079	0,027
0,072	1,480	0,420	0,182	0,078	0,026
0,078	1,490	0,410	0,177	0,076	0,026
0,084	1,490	0,396	0,170	0,073	0,025
0,090	1,483	0,379	0,161	0,069	0,023
0,108	1,427	0,309	0,128	0,054	0,018
0,126	1,335	0,220	0,086	0,036	0,012
0,144	1,223	0,121	0,039	0,016	0,005
0,162	1,104	0,016	−0,009	−0,005	−0,002
0,180	0,984	−0,089	−0,057	−0,026	−0,009
0,198	0,869	−0,192	−0,104	−0,046	−0,016
0,216	0,761	−0,289	−0,146	−0,065	−0,022
0,234	0,662	−0,380	−0,185	−0,081	−0,027
0,252	0,572	−0,463	−0,219	−0,096	−0,032
0,270	0,492	−0,538	−0,248	−0,108	−0,036
0,288	0,422	−0,604	−0,272	−0,117	−0,040
0,324	0,305	−0,710	−0,303	−0,130	−0,044
0,360	0,218	−0,783	−0,315	−0,133	−0,045
0,396	0,153	−0,826	−0,309	−0,128	−0,043
0,432	0,105	−0,845	−0,287	−0,116	−0,039
0,468	0,069	−0,844	−0,253	−0,099	−0,033
0,504	0,042	−0,827	−0,209	−0,077	−0,025
0,540	0,020	−0,798	−0,157	−0,053	−0,017
0,576		−0,761	−0,101	−0,027	−0,008
0,612		−0,717	−0,042	0,000	0,001
0,648		−0,670	0,018	0,028	0,010
0,684		−0,621	0,077	0,054	0,019
0,720		−0,572	0,135	0,079	0,028
0,756		−0,523	0,191	0,103	0,036
0,792		−0,477	0,243	0,124	0,043
0,828		−0,432	0,292	0,143	0,049
0,864		−0,390	0,337	0,159	0,054
0,900		−0,351	0,377	0,173	0,058
0,936		−0,315	0,413	0,184	0,062
1,008		−0,251	0,472	0,198	0,066
1,080		−0,198	0,515	0,203	0,067
1,152		−0,155	0,542	0,198	0,064
1,224		−0,120	0,557	0,185	0,059
1,296		−0,093	0,560	0,166	0,051
1,368		−0,071	0,553	0,141	0,042

Tabelle IV (Fortsetzung)

x	f				
	1s	2s	3s	4s	5s
1,440		−0,054	0,540	0,113	0,031
1,512		−0,041	0,520	0,081	0,020
1,584		−0,031	0,497	0,047	0,008
1,656		−0,023	0,470	0,013	−0,004
1,728		−0,016	0,442	−0,022	−0,017
1,800		−0,011	0,413	−0,056	−0,028
1,872		−0,007	0,383	−0,090	−0,040
1,944		−0,004	0,354	−0,122	−0,050
2,016		−0,001	0,325	−0,153	−0,060
2,088			0,297	−0,181	−0,069
2,160			0,271	−0,208	−0,077
2,304			0,222	−0,254	−0,090
2,448			0,179	−0,292	−0,098
2,592			0,142	−0,321	−0,103
2,736			0,109	−0,342	−0,104
2,880			0,082	−0,355	−0,102
3,024			0,058	−0,362	−0,097
3,168			0,036	−0,364	−0,089
3,312			0,017	−0,361	−0,080
3,456				−0,355	−0,068
3,600				−0,345	−0,056
3,744				−0,333	−0,042
3,888				−0,320	−0,028
4,032				−0,305	−0,013
4,176				−0,289	0,001
4,310				−0,273	0,016
4,608				−0,241	0,045
4,896				−0,210	0,072
5,184				−0,181	0,097
5,472				−0,155	0,119
5,760				−0,132	0,139
6,048				−0,111	0,156
6,336				−0,094	0,170
6,624				−0,078	0,182
6,912				−0,065	0,191
7,200				−0,054	0,198
7,488				−0,045	0,203
7,776				−0,037	0,207
8,064				−0,031	0,209
8,640				−0,021	0,209
9,216				−0,014	0,205
9,792				−0,009	0,198
10,368				−0,006	0,189
10,944				−0,004	0,179
11.520				−0,002	0,168
12,096					0,157
12,672					0,145
13,248					0,134
13,824					0,123
14,400					0,113
14,976					0,104
16,128					0,086
17,280					0,071

Tabelle IV (Fortsetzung)

x	f				
	$1s$	$2s$	$3s$	$4s$	$5s$
18,432					0,058
19,584					0,047
20,736					0,038
21,888					0,031
23,040					0,025
24,192					0,020
25,344					0,016
26,496					0,013
27,648					0,010
28,800					0,008
29,952					0,006
31,104					0,005
32,256					0,004
33,408					0,003
34,560					0,002
36,864					0,001

Tabelle V

Die radialen Eigenfunktionen f der p-Elektronen des Te-Atoms und die radiale Dichte D des Te-Atoms; f in atomaren Einheiten von $1/a_0^{1/2}$, D in atomaren Einheiten von $1/a_0$; x in dimensionslosen Längeneinheiten

x	f				D
	$2p$	$3p$	$4p$	$5p$	
0,000	0,000	0,000	0,000	0,000	0,000
0,006	0,002	0,001	0,000	0,000	2,195
0,012	0,007	0,003	0,001	0,000	7,575
0,018	0,016	0,007	0,003	0,001	14,701
0,024	0,028	0,013	0,005	0,001	22,548
0,030	0,042	0,019	0,008	0,002	30,410
0,036	0,058	0,026	0,011	0,003	37,806
0,042	0,076	0,034	0,014	0,004	44,456
0,048	0,096	0,043	0,018	0,005	50,195
0,054	0,117	0,053	0,022	0,006	54,966
0,060	0,139	0,063	0,026	0,007	58,769
0,066	0,162	0,073	0,030	0,008	61,664
0,072	0,186	0,084	0,035	0,009	63,729
0,078	0,210	0,094	0,039	0,010	65,067
0,084	0,235	0,105	0,044	0,011	65,787
0,090	0,260	0,116	0,048	0,012	65,996
0,108	0,336	0,149	0,062	0,016	64,594
0,126	0,411	0,181	0,075	0,019	61,915
0,144	0,482	0,210	0,086	0,022	59,564
0,162	0,548	0,236	0,097	0,025	58,400
0,180	0,607	0,258	0,106	0,027	58,704
0,198	0,660	0,277	0,113	0,029	60,391
0,216	0,707	0,290	0,118	0,031	63,166
0,234	0,746	0,300	0,121	0,031	66,644
0,252	0,778	0,306	0,123	0,032	70,440

Tabelle V (Fortsetzung)

x	f				D
	$2p$	$3p$	$4p$	$5p$	
0,270	0,804	0,307	0,123	0,032	74,206
0,288	0,824	0,305	0,121	0,031	77,664
0,324	0,847	0,290	0,113	0,029	82,918
0,360	0,849	0,262	0,100	0,026	85,401
0,396	0,836	0,225	0,083	0,021	85,173
0,432	0,811	0,180	0,063	0,016	82,797
0,468	0,776	0,130	0,040	0,010	79,046
0,504	0,735	0,076	0,016	0,004	74,685
0,540	0,690	0,020	−0,008	−0,003	70,368
0,576	0,642	−0,037	−0,032	−0,009	66,569
0,612	0,594	−0,092	−0,055	−0,015	63,583
0,648	0,546	−0,146	−0,077	−0,021	61,538
0,684	0,499	−0,198	−0,098	−0,026	60,442
0,720	0,455	−0,246	−0,116	−0,031	60,210
0,756	0,412	−0,291	−0,133	−0,035	60,693
0,792	0,372	−0,333	−0,147	−0,038	61,715
0,828	0,335	−0,370	−0,160	−0,042	63,087
0,864	0,301	−0,404	−0,170	−0,044	64,629
0,900	0,269	−0,433	−0,177	−0,046	66,180
0,936	0,240	−0,459	−0,183	−0,047	67,602
1,008	0,190	−0,499	−0,188	−0,048	69,655
1,080	0,149	−0,526	−0,185	−0,047	70,251
1,152	0,117	−0,540	−0,175	−0,044	69,235
1,224	0,090	−0,545	−0,160	−0,039	66,727
1,296	0,070	−0,541	−0,139	−0,033	63,009
1,368	0,054	−0,530	−0,115	−0,026	58,456
1,440	0,041	−0,513	−0,089	−0,019	53,423
1,512	0,032	−0,493	−0,060	−0,011	48,248
1,584	0,024	−0,469	−0,030	−0,003	43,205
1,656	0,018	−0,444	0,000	0,005	38,503
1,728	0,014	−0,417	0,031	0,013	34,284
1,800	0,011	−0,390	0,061	0,021	30,630
1,872	0,008	−0,363	0,090	0,029	27,576
1,944	0,006	−0,337	0,118	0,036	25,119
2,016	0,005	−0,311	0,145	0,043	23,226
2,088	0,004	−0,287	0,170	0,049	21,845
2,160	0,004	−0,263	0,193	0,054	20,922
2,304	0,003	−0,220	0,235	0,064	20,133
2,448		−0,182	0,269	0,070	20,328
2,592		−0,150	0,296	0,075	21,059
2,736		−0,122	0,317	0,077	21,962
2,880		−0,099	0,332	0,077	22,793
3,024		−0,080	0,341	0,075	23,404
3,168		−0,065	0,345	0,072	23,722
3,312		−0,052	0,346	0,067	23,730
3,456		−0,042	0,343	0,061	23,445
3,600		−0,033	0,337	0,055	22,898
3,744		−0,026	0,329	0,047	22,132
3,888		−0,021	0,320	0,039	21,200
4,032		−0,017	0,308	0,030	20,152
4,176		−0,013	0,296	0,021	19,032
4,320		−0,010	0,283	0,011	17,878
4,608		−0,006	0,257	−0,007	15,585

Tabelle V (Fortsetzung)

x	f				D
	$2p$	$3p$	$4p$	$5p$	
4,896		—0,003	0,230	—0,026	13,446
5,184		—0,002	0,204	—0,044	11,551
5,472			0,179	—0,061	9,931
5,760			0,156	—0,077	8,581
6,048			0,136	—0,091	7,477
6,336			0,118	—0,104	6,586
6,624			0,101	—0,116	5,871
6,912			0,087	—0,126	5,300
7,200			0,075	—0,135	4,842
7,488			0,064	—0,143	4,473
7,776			0,054	—0,150	4,172
8,064			0,046	—0,155	3,922
8,640			0,033	—0,164	3,527
9,216			0,024	—0,169	3,219
9,792			0,017	—0,172	2,957
10,368			0,012	—0,173	2,719
10,944			0,009	—0,171	2,498
11,520			0,006	—0,169	2,288
12,096			0,004	—0,165	2,088
12,672			0,003	—0,161	1,898
13,248			0,002	—0,156	1,720
13,824			0,002	—0,151	1,553
14,400			0,001	—0,145	1,398
14,976			0,001	—0,139	1,255
16,128				—0,127	1,005
17,280				—0,115	0,799
18,432				—0,104	0,631
19,584				—0,094	0,497
20,736				—0,084	0,389
21,888				—0,075	0,304
23,040				—0,066	0,237
24,192				—0,059	0,184
25,344				—0,052	0,143
26,496				—0,046	0,110
27,648				—0,041	0,085
28,800				—0,036	0,066
29,952				—0,031	0,051
31,104				—0,028	0,039
32,256				—0,024	0,030
33,408				—0,021	0,023
34,560				—0,019	0,017
36,864				—0,014	0,0102
39,168				—0,011	0,0059
41,472				—0,008	0,0034
43,776				—0,006	0,0019
46,080				—0,005	0,0011
48,384				—0,003	0,0006
50,688				—0,002	0,0003
52,992				—0,002	0,0001
55,296				—0,001	0,00005

Tabelle VI

Die radialen Eigenfunktionen f der d-Elektronen des Te-Atoms und das Potential V des Te-Atoms; f in atomaren Einheiten von $1/a_0$, V in atomaren Einheiten von e/a_0, x in dimensionslosen Längeneinheiten

x	f		V
	$3d$	$4d$	
0,000	0,000	0,000	
0,006	0,000	0,000	4085,52
0,012	0,000	0,000	2029,88
0,018	0,000	0,000	1344,67
0,024	0,000	0,000	1002,06
0,030	0,000	0,000	796,516
0,036	0,001	0,000	659,503
0,042	0,001	0,000	561,654
0,048	0,002	0,001	488,284
0,054	0,002	0,001	431,237
0,060	0,003	0,001	385,617
0,066	0,004	0,001	348,307
0,072	0,005	0,002	317,232
0,078	0,006	0,002	290,952
0,084	0,007	0,003	268,441
0,090	0,008	0,003	248,945
0,108	0,014	0,005	203,525
0,126	0,020	0,007	171,173
0,144	0,028	0,010	146,990
0,162	0,037	0,013	128,251
0,180	0,048	0,017	113,322
0,198	0,059	0,021	101,162
0,216	0,072	0,026	91,078
0,234	0,086	0,030	82,590
0,252	0,100	0,035	75,353
0,270	0,115	0,041	69,116
0,288	0,131	0,046	63,692
0,324	0,163	0,057	54,732
0,360	0,197	0,069	47,655
0,396	0,231	0,080	41,942
0,432	0,264	0,091	37,247
0,468	0,296	0,101	33,331
0,504	0,327	0,111	30,023
0,540	0,356	0,119	27,198
0,576	0,383	0,127	24,763
0,612	0,408	0,134	22,646
0,648	0,430	0,139	20,794
0,688	0,450	0,143	19,161
0,720	0,467	0,147	17,715
0,756	0,482	0,149	16,426
0,792	0,495	0,150	15,273
0,828	0,505	0,149	14,235
0,864	0,513	0,148	13,299
0,900	0,519	0,146	12,452
0,936	0,524	0,143	11,681
1,008	0,526	0,134	10,3354
1,080	0,523	0,122	9,2044
1,152	0,514	0,108	8,2444
1,224	0,501	0,091	7,4223

Tabelle VI (Fortsetzung)

x	f		V
	$3d$	$4d$	
1,296	0,485	0,074	6,7130
1,368	0,466	0,054	6,0967
1,440	0,446	0,035	5,5579
1,512	0,424	0,014	5,0842
1,584	0,401	—0,006	4,6655
1,656	0,378	—0,027	4,2938
1,728	0,355	—0,047	3,9624
1,800	0,332	—0,066	3,6657
1,872	0,310	—0,086	3,3991
1,944	0,289	—0,104	3,1587
2,016	0,268	—0,122	2,9413
2,088	0,249	—0,139	2,7441
2,160	0,230	—0,154	2,5647
2,304	0,196	—0,183	2,2515
2,448	0,166	—0,209	1,9885
2,592	0,140	—0,230	1,7658
2,736	0,117	—0,248	1,5757
2,880	0,098	—0,262	1,4124
3,024	0,081	—0,274	1,2713
3,168	0,068	—0,282	1,1486
3,312	0,056	—0,288	1,0413
3,456	0,046	—0,292	0,9471
3,600	0,038	—0,294	0,8640
3,744	0,031	—0,294	0,7904
3,888	0,026	—0,292	0,7250
4,032	0,021	—0,289	0,6666
4,176	0,017	—0,285	0,6143
4,320	0,014	—0,281	0,5674
4,608	0,010	—0,269	0,4870
4,896	0,006	—0,255	0,4211
5,184	0,004	—0,240	0,3666
5,472	0,003	—0,225	0,3211
5,760	0,002	—0,210	0,2828
6,048	0,001	—0,194	0,2505
6,336	0,001	—0,180	0,2229
6,624		—0,165	0,1992
6,912		—0,152	0,1788
7,200		—0,139	0,1612
7,488		—0,128	0,1458
7,776		—0,117	0,1324
8,064		—0,107	0,1206
8,640		—0,088	0,10097
9,216		—0,073	0,08555
9,792		—0,061	0,07325
10,368		—0,050	0,06332
10,944		—0,041	0,05521
11,520		—0,034	0,04854
12,096		—0,028	0,04298
12,672		—0,023	0,03832
13,248		—0,019	0,03438
13,824		—0,015	0,03102
14,400		—0,013	0,02814
14,976		—0,010	0,02565

Tabelle VI (Fortsetzung)

x	f		V
	$3d$	$4d$	
16,128		—0,007	0,02158
17,280		—0,005	0,01844
18,432		—0,003	0,01594
19,584		—0,002	0,01393
20,736		—0,001	0,01229
21,888		—0,001	0,01091
23,040		—0,001	0,00976
24,192			0,00877
25,344			0,00791
26,496			0,00717
27,648			0,00652
28,800			0,00595
29,952			0,00544
31,104			0,00499
32,256			0,00458
33.408			0,00421
34,560			0,00388
36,864			0,00331
39,168			0,00284
41,472			0,00244
43,776			0,00211
46,080			0,00182
48,384			0,00158
50,688			0,00138
52,992			0,00120
55,296			0,00105
57,600			0,00092

Tabelle VII

Die mit dem universellen Potential bestimmten Energieterme der Elektronen des Te-Atoms und die Röntgentermwerte nach LANDOLT und BÖRNSTEIN (Es werden die arithmetischen Mittelwerte der Röntgendublette angegeben). Als Wert des $5p$-Terms steht die erste Ionisationsenergie. (Die Energiewerte sind in atomaren Einheiten von e^2/a_0 angegeben)

	$1s$	$2s$	$3s$	$4s$	$5s$
Universelles Potential	1133,62	167,45	31,38	4,843	0,3816
Nach LANDOLT—BÖRNSTEIN	1171,62	181,90	37,07	6,220	—
	$2p$	$3p$	$4p$	$5p$	
Universelles Potential	158,27	27,32	3,434	0,1320	
Nach LANDOLT—BÖRNSTEIN	164,88	31,10	4,065	0,3290	
	$3d$	$4d$			
Universelles Potential	18,92	1,035			
Nach LANDOLT—BÖRNSTEIN	21,28	1,512			

THERMAL SHOCK INVESTIGATIONS ON GERMANIUM MONOCRYSTALS

By

Z. Bodó, G. Pásztor, M. S. Szilágyi and A. Zawadowski

RESEARCH INSTITUTE FOR TELECOMMUNICATION TECHNIQUE, BUDAPEST

(Received 15. XII. 1961)

In the course of our experiments we examined the time dependence of a thermoelectric transient process taking place under the influence of a pulselike heat liberation within a heater put on a germanium monocrystal. The measuring adjustment can be seen in Fig. 1. The heater W is heated up within 100 μsec by the energy-stored condenser C. The heat is transferred to the germanium crystal by means of a mica plate of a thickness of 5—10 μ, coated with an evaporated gold layer. The evaporated gold layer sets up a contact with the surface of the crystal. Having put a contact also on the opposite (cold) side of the crystal we obtained the time dependence of the arising thermovoltage. The measurements were carried out on various samples. From the four characteristics to be seen in Fig. 2, the *a)* and *b)* ones show the measuring results of homogeneous *n*-, or *p*-type crystals of the same geometric dimensions (their thickness: 0.7 cm, their area: 0.25 cm^2) while the characteristics *c)* and *d)* show the resultant thermovoltages of combined systems made out of slices of opposite types and of a thickness of 0.03 cm. These thin samples were of the same composition as the former crystals (they were sliced from them). In the moments following the discharge of the condenser the total heat-drop takes place close to the surface of the crystal and later spreads over to the more distant parts of it. Consequently, if the thermoelectric coefficient reverses its sign because of the p—n junction near the surface, the thermovoltage put down from the sample also changes its sign in the course of time (see Fig. 3).

We tried to explain the measured results by the following calculation.

It is known that the thermal conductivity of germanium used for the production of rectifiers and transistors is decisively determined by the thermal conductivity of the grating (the thermal conductivity of the electrons and the holes can be neglected) and according to the measurements we obtain a value of $\varkappa = 0.14$ cal/cmsecK°.

Considering the density of germanium near room-temperature ($\varrho = 5.32$ g/cm^3) and its specific heat ($C = 0.074$ cal/gK°) [1] the constant in the diffe-

rential equation of heat propagation holding for the temperature T within germanium

$$\frac{\partial T}{\partial t} - \frac{\varkappa}{\varrho C} \Delta T = 0 \tag{1}$$

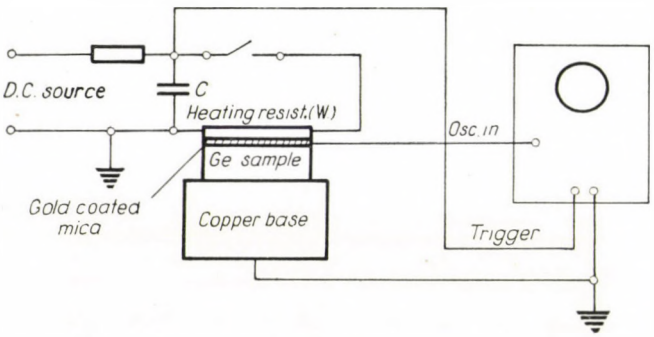

Fig. 1

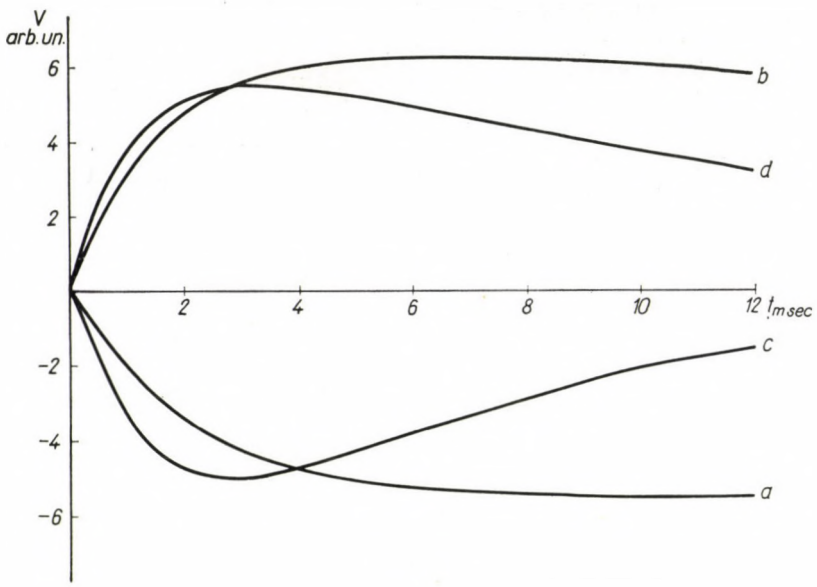

Fig. 2

is known:

$$a^2 = \frac{\varkappa}{\varrho C} = 0{\cdot}356 \text{ cm}^2 \text{ sec}^{-1}. \tag{2}$$

So in the case of one-dimensional problems (of the same temperature at a plane of $x = \text{const.}$) the temperature is given by the solutions $T(x, t)$ of the partial

differential equation

$$\frac{\partial T}{\partial t} = a^2 \frac{\partial^2 T}{\partial x^2}, \tag{3}$$

If germanium occupies the half space of $x > 0$, $T(0, t) = f(t)$ is a given limit and as is known, the solution is given by the integral

$$T(x, t) = \frac{2}{\sqrt{\pi}} \int_{\frac{x}{2a\sqrt{t}}}^{\infty} f\left(t - \frac{x^2}{4a^2 \xi^2}\right) e^{-\xi^2} d\xi \tag{4}$$

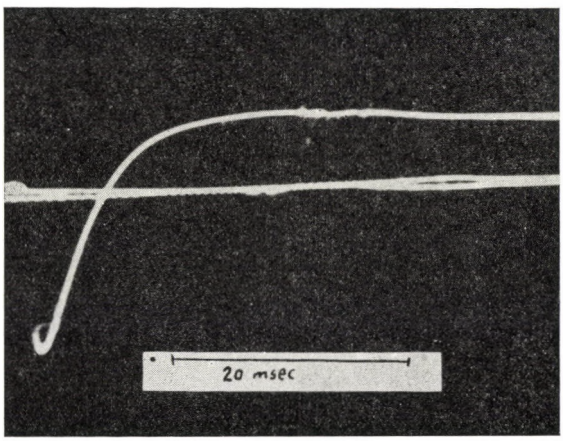

Fig. 3

satisfying the initial condition $T(x, 0) = 0$. This value of $T(x, t)$ means the temperature difference referring to the temperature of the plane $x = \infty$.

Let us take a homogeneous germanium monocrystal, the differential thermovoltage of which (α) should be much higher than that of the metals. Let us place the crystal so that one of its faces falls in the plane $x = 0$, its opposite face in the plane $x = \infty$ (which can be regarded as an infinite one) and according to these planes let us put metallic contacts on the germanium crystal.

The thermovoltage between these two metallic contacts is given by

$$\varphi(t) = \oint \alpha dT \approx \alpha f(t) \tag{5}$$

in such cases, when the thermovoltage of the metals is neglected and when the rise of temperature is not sufficiently high for the temperature dependence of α to be taken into consideration. Equation (5) indicates that by means of the measurements of $\varphi(t)$ and α the values of $f(t)$ can be determined and by the help of equation (4) $T(x, t)$ can be calculated.

Consequently, the curves obtained from the homogeneous samples can be regarded as simple thermocouple temperature-time dependence measurements, in which germanium forms one branch of the thermocouple.

The calculation was considerably simplified by the fact that the measured functions $f(t)$ could be approximated from the instant $t = 0$ on a very large section by the following analytic function:

$$f(t) = A\,(e^{-\lambda t} - e^{-\mu t})\,, \tag{6}$$

where A, λ and μ are approximately chosen constants. Thus from equation (4) we get

$$T(x,t) = Ae^{-\frac{x^2}{4a^2 t}}\left\{ U\left(\sqrt{\lambda t} + i\sqrt{\frac{x^2}{4a^2 t}}\right) - U\left(\sqrt{\mu t} + i\sqrt{\frac{x^2}{4a^2 t}}\right)\right\}, \tag{7}$$

where

$$U(s + ir) = \frac{1}{\pi}\int_{-\infty}^{+\infty} \frac{re^{-\xi^2}}{(s-\xi)^2 + r^2}\, d\xi\,. \tag{8}$$

is a tabular [2] function.

Knowing $T(x, t)$ e.g. in case of a p-type sample of a thickness d (and of a thermovoltage α_p, put on a sample of n-type and of a diff. thermovoltage α_n) the function obtained by measurement can be calculated:

$$\varphi(t) = \oint \alpha dT = \alpha_n T(d,t) + \alpha_p [T(0,t) - T(d,t)]\,, \tag{9}$$

The curves calculated by equation (9) showed a qualitative agreement with the measured results. The measured and calculated curves were of similar shapes, but a quantitative agreement could not be attained. One reason for this is certainly that the heat transfer between the two germanium pieces was neglected in the calculation (the heat transfer coefficients were considered as infinite), but this cannot be the sole reason for the discrepancy.

According to the above, the curve measured on the single sample can be regarded as a measurement in time of the temperature drop on the germanium sample. In the case of measurements effectuated on p-, and n-type materials should be $\dfrac{\varphi_n(t)}{\varphi_p(t)} = \dfrac{\alpha_n}{\alpha_p} = \text{const.}$

According to our measured results this is not the case. Further examinations showed that the form of the curves $\varphi(t)$ depends, also in the case of the same material, considerably on the state of the surface. The surface is highly reactive to various chemical effects (corrosion, boiling in carbon tetrachloride, or in water, etc.) and even physical (rubbing with soft leather) ones. It changes also after fresh attacking, staying in the air for a certain time. The extent of

the observed changes ranges from about 20 to 30% and it is improbable that it could be explained simply by the incidental change of the heat transfer between gold and germanium. It is possible that the surface returns to the state of thermic equilibrium only after a much longer time than does the interior of the material. In any case it seems to be worthwhile to continue the experiments, because this seems to be a new method for the examination of surfaces.

REFERENCES

1. E. M. Conwell, Proc. I. R. E., **40**, 1327, 1952.
2. *В. Н. Фаддеева, Н. М. Терентев:* Таблицы значений интеграла вероятностей от комплексного аргумента. Гос. Изд. Технико-теоретической лит. Москва. 1954.
3. *В. Г. Мельник, И. Г. Мельник, С. С. Гутин.* Доклады А. Н. СССР, **121**, 852, 1958.

RECENSIONES

Lehrbuch der Kernphysik, Band II, Physik der Atomkerne

Herausgegeben von Prof. Dr. G. HERTZ, mit Beiträgen von K. F. ALEXANDER, D. GIESSLER, K. LANIUS, A. LÖSCHE, D. LYONS, G. RICHTER, J. SCHINTLMEISTER, C. F. WEISS, S. WOHLRAB und W. LOHMANN. B. G. Teubner Verlagsgesellschaft, Leipzig, 1960. 915 Seiten mit 328 Abbildungen.

Der zweite Band des Lehrbuchs der Kernphysik enthält die eigentliche Kernphysik, d. h. den Stoff, den die Verfasser dem Ziel des Lehrbuches entsprechend für die Ausbildung des Kernphysikers von Wichtigkeit gehalten haben. Es war eine schwierige Aufgabe, aus der ungeheuren Fülle der Tatsachen diejenigen auszuwählen, welche als gesicherte Grundlagen bzw. Gesetzmässigkeiten dem selbständig arbeitenden Kernphysiker bekannt sein müssen. Die richtige Auswahl ist den Verfassern gut gelungen, das behandelte Material ist einerseits gross und erschöpfend, sodass es als genügende Grundlage für die weitere Entwicklung gelten kann, anderseits enthält der Band keine Betrachtungen über unwesentliche Einzelheiten.

Das Buch gliedert sich in vier Kapitel: *A)* Eigenschaften der stabilen Kerne, *B)* Kernumwandlungen, *C)* Theorie der Atomkerne, *D)* Neutronenphysik; der Anhang enthält zwei ausführliche Kerntafeln.

A) *Eigenschaften der stabilen Kerne*

In diesem Kapitel werden zunächst die Kernbausteine, der Aufbau und die Systematik der Atomkerne, der Massendefekt und die Bindungsenergie und schliesslich der Kernspin und die Kernmomente behandelt. Es wird hauptsächlich das Tatsachenmaterial dargestellt, ohne dass schon eine genauere Kenntnis der erst später behandelten Theorie vorausgesetzt wäre.

B) *Kernumwandlungen*

Dieses Kapitel bildet den Hauptteil des Buches. In den ersten zwei Abschnitten werden der radioaktive Zerfall und die spontanen Kernumwandlungen behandelt. Als Einleitung dient eine historische Darstellung, der Entwicklung der Kernphysik aus der Lehre vom radioaktiven Zerfall entsprechend. Der exponentielle Zerfall, die allgemeine Zerfallstheorie, die natürlichen Zerfallsreihen, die Eigenschaften des Radiums, die spontane Spaltung und die Emission von Alphateilchen bilden die wichtigsten Punkte dieses Abschnittes.

Die folgenden Abschnitte über Kernreaktionen und Kernspaltung bringen eine Zusammenfassende Darstellung des ausserordentlich grossen Beobachtungsmaterials auf dem Gebiete der Kernreaktionen bei niederen Energien, d. h. bei solchen Energien, bei denen noch keine neuen schweren Teilchen wie Mesonen usw. entstehen.

Die experimentellen Anordnungen zur Beobachtung von Kernreaktionen, die Äquivalenz von Masse und Energie, der Zwischenkern, der Wirkungsquerschnitt und seine Energieabhängigkeit, die γ-induzierten Reaktionen, die Kernreaktionen mit Neutronen, mit Protonen, mit a-Teilchen, mit Deuteronen, mit »schweren Ionen«, mit Elektronen und mit Neutrinos sowie die thermonuklearen Reaktionen werden ebenso ausführlich behandelt wie die Tatsachen und die Energetik der Kernspaltung, die Asymmetrie, das Tröpfchenmodell und die Dynamik der Spaltung, die Radioaktivität der Spaltprodukte, die Spaltneutronen und die verzögerten Neutronen.

Da eine Darstellung dieses ungeheuer vielfältigen Gebietes ohne Eingehen auf die Theorie der Kernreaktionen nicht möglich ist, werden in den nächsten Abschnitten die wesent-

lichsten Ergebnisse dieser Theorie in möglichst einfacher und physikalisch verständlicher Weise abgeleitet. Es werden der Compoundkern nach dem Fermigas-Modell, die allgemeinen Eigenschaften des Wirkungsquerschnitts und das Einteilchenmodell ausführlich behandelt.

In einem Schlussabschnitt über Kernprozesse bei extrem hohen Energien wurde der Nachdruck auf die Darstellung der experimentellen Ergebnisse gelegt, da die theoretischen Entwicklungen auf diesem Gebiete noch stark im Flusse sind.

C) *Theorie der Atomkerne*

In diesem Kapitel wird eine einführende Darstellung der Kerntheorie gegeben. Das Material ist in drei Abschnitte eingeteilt: Theorie der leichtesten Kerne, Theorie der leichten bis schweren Kerne und Theorie des Beta-Zerfalls. Im umfangreichsten mittleren Abschnitt finden wir wieder zwei Teile, und zwar: Teil 1. *Kernkräfte* mit Abhandlungen über Ladungsunabhängigkeit der Kernkräfte, Sättigung und Austauschcharakter der Kernkräfte, Kernkräfte und Mesonentheorie, sowie Typen von Potentialen und Teil 2. *Kernmodelle*, mit den folgenden Abschnitten: 1. Schalenmodell, 2. Kollektives Modell, 3. Compoundkern-Modell, 4. Optisches Modell und 5. Bemerkungen über die Grundlagen der Kernmodelle.

Aus dem Gebiete der Kernmodelle wird die durch den Erfolg des Schalenmodells ausgelöste neuere Entwicklung zum kollektiven und optischen Modell in ihren Hauptzügen dargestellt, obwohl hier manche Dinge noch im Flusse sind. Die Verwendung der Quantenmechanik wurde möglichst eingeschränkt, gewisse Vorkenntnisse auf diesem Gebiete sind aber zum Verständnis unerlässlich.

D) *Neutronenphysik*

Das Kapitel enthält anstatt einer vollständigen Behandlung dieses umfangreichen Gebietes nur einzelne, ausführliche Darstellungen charakteristischer und wichtiger Teilgebiete, wie Eigenschaften des freien Neutrons, Erzeugung freier Neutronen, experimentelle Methoden der Neutronenspektroskopie und Bewegung von Neutronen in kompakter Materie. Bei der Beschreibung der experimentellen Methoden werden hauptsächlich diejenigen hervorgehoben, welche sich von den im ersten Band behandelten Verfahren besonders charakteristisch unterscheiden.

Am Schluss des Bandes befinden sich zwei ausführliche und nicht nur für den Lernenden, sondern auch für den auf kernphysikalischem Gebiet schon selbständig arbeitenden Leser sehr nützliche Kerntabellen, welche die wichtigsten Daten für die Anfang 1959 bekannten, etwa 1500 Kerne enthalten. Aus der beigegebenen farbigen Kerntafel kann man einfach die Art der Umwandlung, das Auftreten von metastabilen Zuständen, evt. auftretendem doppeltem β-Zerfall usw. entnehmen.

Das sehr schöne, mit vielen guten Abbildungen und Tabellen ausgestattete Buch, welches als Lehrbuch an den Universitäten und Hochschulen der Deutschen Demokratischen Republik eingeführt wurde, kann allen an Kernphysik interessierten Fachleuten empfohlen werden.

DR. L. BOZÓKY

P. T. LANDSBERG, Thermodynamics with Quantum Statistical Illustrations.

X + 500 pages, Interscience Publishers, New York—London, 1961; Volume 2 of Monographs in Statistical Physics and Thermodynamics, edited by I. Prigogine.

Of the five main chapters of the book, the first three deal with the general theory of the fundamental laws of classical thermodynamics. The basic idea of the author's particular treatment of the subject may be characterized by the statement that it is the latest development of the axiomatic approach inaugurated by C. CARATHÉODORY. It is not only the first systematic, genetic exposition of the laws and statements of classical heat theory, built up on strictly axiomatic grounds, but also presents many new criticisms and generalizations. In this respect, the book fills a wide gap in the literature on thermodynamical principles.

The strict axiomatic treatment involves an abstract style which could be partly modified only by inserting numerous carefully chosen examples. Thus the book will be of interest only to the reader already well acquainted with general thermodynamics.

Chapter I begins with an exposition on the nature and scope of thermodynamics, and proceeds immediately to the exact definition of partitions and enclosures, both adiabatic and diathermic. It is to be welcomed that the author does not avoid but points out explicitly all the conceptual difficulties, an attitude characteristic of the whole work. The derivation of the

concept of empirical temperature, by use of the zeroth law follows. In the remainder of the chapter, the first law is expounded, together with a thorough topological investigation of equilibrium states in the phase space. The use of topology is an essential and novel feature of the treatment throughout the book.

Chapter II begins with the classification of representative sets of points in the phase space. The axiomatic foundation of the second law corresponds in all relevant respects to the treatment of CARATHÉODORY. It may be noted that the author discards the concept of reversibility and makes use of the term quasi-static process for any continuous sequence of equilibrium states. He calls attention to the fact that neither this concept nor that of reversibility are used without ambiguity in current thermodynamical literature.

Chapter III is devoted to the axiomatics of the third law, and in many respects introduces new results. An axiomatic treatment of this law, on the lines inaugurated by CARATHÉODORY, was long due, since its various formulations are of a later date than CARATHÉODORY's work. LANDSBERG points out that one has to go beyond the theorem on Pfaffians as established by CARATHÉODORY, and by making explicit reference to the boundaries of the domain of definition of the Pfaffian equations for quasi-static adiabatic changes, he gives the necessary conceptual and mathematical extension. It is shown that the assertion of the tendency of entropy approaching a finite value at $T \to 0$, and the principle of unattainability of the absolute zero of temperature, are not equivalent statements (the former one going further) and are not deducible from one another. This result may be reassuring to those who think the principle of unattainability comes within the scope of the second law. The last paragraph of the chapter gives a thorough discussion of the problematics of any axiomatic approach, and dispels the common belief that thermodynamics is a discipline particularly suited to this sort of treatment, and presents a possible system of thermodynamic axioms, without pretending to have reached this goal definitively.

Chapter IV deals with basic applications and extensions, such as the empirical determination of entropy and absolute temperature scales, the extension of thermodynamics to open and non-equilibrium systems (simple and compound systems), application to chemical thermodynamics, additional thermodynamic functions and their properties, the classical ideal and quantum gas. These topics, more familiar to those who are acquainted with "ordinary" thermodynamics, are indispensable for a better understanding of the basic principles discussed in the previous chapters. The treatment leads to the threshold of irreversible thermodynamics, but without entering it. The paragraph on thermodynamic cycles is a careful and thought-raising study of the correlations between the various formulations of the second law.

Chapter V is a survey of some combinations of thermodynamics and statistical mechanics, treating basic problems such as the statistical mechanics of the ideal gas, black-body radiation and paramagnetics. The methods of statistical mechanics and the statistical concept of entropy are discussed on a broad basis, including their applications to general information theory (non-thermodynamic entropy). Paragraph 34 of this chapter is perhaps the most enlightening one logically. It compares the fundamental principles of thermodynamics with those of statistical mechanics and clarifies the relations of interdependence and overlapping among them. Everyone who is interested in the basic principles underlying thermodynamics and statistical physics should acquaint himself with these parts of the book.

A better understanding of the text is furthered throughout by many original and instructive "problems" and by appendices which go deeper into some details. The first appendix gives a valuable comment on the mode of treatment adopted.

On the whole, it may be safely stated that LANDSBERG's book is an original and, in view of its crystal-clear logic, an almost unique contribution to thermodynamical literature. The attractive lay-out gives credit to Interscience Publishers. As a welcome innovation, the book has for its frontispiece the portraits of the pioneers in the field of thermodynamics, from ROBERT BOYLE to CONSTANTIN CARATHÉODORY.

G. SCHAY

J. F. NYE: Propriétés physiques des cristaux

Leurs représentation par des tenseurs et des matrices
traduit de l'anglais par D. Blanc et T. Pujbe. — Dunod, Paris, 362 pages
16×25, 87 Figures. 1962.

Solid state physics has during the last few years reached the stage, where the need for, and the possibility of obtaining detailed information on monocrystalline samples is continually increasing. Results from the free electron model having been duly derived and compared with experiments, it has been established that this theory is only capable of interpreting scalar

characteristics of crystals. It had been tacitly assumed that the microcrystalline texture of the solid gives rise to isotropy, which would enable any solid property to be described by means of tensors of zero rank, i.e. scalars. This expectation having naturally failed, the free electron model has had to be discarded, and on the same level of approximation the lattice potential has had to be explicitly taken into consideration.

Crystal properties now appear in tensorial form, crystal symmetry establishing relations between the tensor components. Solid state physicists, and particularly experimentalists, are confronted with a new formalism, which has been little used in the past. This forms the subject matter of the book by J. F. NYE (original English edition in 1957). This book is very helpful and instructive. Starting from fundamental assumptions it introduces tensors and matrices, and makes the distinction between them quite clear. The various physical properties are clearly defined in this context, and the subsequent calculations are always helped by physical reasoning, not being merely some convenient applications of a mathematical theorem chosen from the realm of physics. The layout of the book, together with the numerous well chosen examples, the summaries at the end of chapters, and the very clear type and printing makes enjoyable reading and enables the reader entirely familiarise himself with the subject. It is felt, however, that it is unfortunate that a few topics are neglected. The transport properties of conducting crystals, although of universal interest, are somewhat superficially treated. None of the magnetic effects, even the most common, the Hall effect and magneto-resistivity, are mentioned. In this setting the real significance of the Onsager principle is lost. Nevertheless the book contains much other useful information, is easy to read, and can be highly recommended.

E. NAGY

R. H. DICKE—J. P. WITTKE: **Introduction to Quantum Mechanics**

Addison—Wesley Publishing Company, Inc. Reading, Massachusetts, USA. (10—15. Chitty St. London W. 1) 369 pages, 1960.

The purpose of the book is to introduce the reader into the physical concepts and mathematical formalisms of non-relativistic quantum mechanics, by giving illustrative examples of both theory and methods. It is assumed that the reader is familiar with atomic structure, classical mechanics, electromagnetism, integral and differential calculus and differential equations at the undergraduate level.

The book is intended to serve as a textbook at the graduate level but is also suitable for advanced undergraduates. The most particular part of the book is its last chapter, dealing with quantum statistical mechanics, where the techniques that play an important role in modern physics are developed. The first section, containing three chapters, points out the inability of classical concepts to explain many atomic-scale phenomena and suggests how to alter the basic ideas of classical mechanics to explain experimental observations.

In Chapter 1 the review of several phenomena, e.g. black body radiation, photoelectric effect, atomic line spectra, is given.

Chapter 2 introduces the concept of wave function. Several examples illustrating the uncertainty principle are discussed.

In Chapter 3 the quantum mechanical law of motion, the time-dependent Schrödinger equation, is outlined and its simplest applications corresponding to the motion of a particle in one dimension are given. This chapter also introduces the concept of probability density current.

Chapter 4 begins with a brief discussion of the properties of Fourier integrals and the Dirac delta function. Expectation values of physical quantities are then calculated.

In Section 2 quantum theory is further developed in six chapters by close analogy with the general formulations of classical mechanics. Some elements of classical formalisms: Lagrange's equations, Poisson brackets etc. can be found in Chapter 5.

In Chapter 6 quantum mechanics is established on a formal postulatory basis. The role of the operator algebra in quantum formalisms is investigated.

Chapter 7 is devoted to the problem of measurement. An explanatory example of photon polarization is investigated in detail.

Chapter 8 shows that for classical systems quantum mechanics leads to the same predictions as classical mechanics.

Chapter 9 treats of angular momentum operators. The addition of two angular momenta is also considered here.

The Schrödinger equation with spherically symmetric potential is treated in Chapter 10. The radial equation is solved for the case of the hydrogen atom and the three dimensional harmonic oscillator.

The third Section represents a considerable broadening of the material and of the scope of the problems that can be handled.

In Chapter 11 the matrix representation of wave functions and operators is introduced. This chapter also deals with the Schrödinger, Heisenberg and interaction representations.

In Chapter 12 the matrix formalism for angular momentum operators is first developed; systems with one-half spin are further discussed. The problem of paramagnetic resonance is treated in detail. Some elements of the theory of Hilbert space and transformations between two representations are considered in Chapter 13.

In Chapter 14 the most important approximation methods such as perturbation theories, variational method, WKB method are introduced and applied to various problems.

In Chapter 15 the interaction of a charged particle and a strong electromagnetic field is discussed. Treatment of the Zeeman effect and the resonant transitions between atomic energy levels are also included in this chapter

Chapter 16 is devoted to the problem of scattering. After introducing some important concepts the Born approximation and the method of partial waves are treated.

Chapter 17 discusses the effects of statistics on the behaviour of particle systems. Examples of the helium atom and hydrogen molecule are considered.

The last chapter (Chapter 18) contains some elements of quantum statistical mechanics. The density matrix formalism is introduced for the description of mixed states. The equation of motion of the density matrix is derived. Moreover ordered and disordered ensembles, entropy, various stationary ensembles, Bose—Einstein and Fermi—Dirac statistics are briefly discussed.

P. SZÉPFALUSY

V. HEINE: **Group Theory in Quantum Mechanics**

An Introduction to its Present Usage.
Pergamon Press, London—Oxford—New York—Paris, 1960.

The value of the application of group theory in quantum mechanics was recognized early. Soon after the foundation of quantum mechanics several papers and three books (E. P. WIGNER, 1931; H. WEYL, 1931; B. L. VAN DER WAERDEN, 1932) dealt with this subject. In the following decades the field of application steadily widened and was extended to the theory of polyatomic molecules and solid bodies, nuclear physics and quantum field theory. As there has been a tremendous amount of review literature dealing with this subject, it is all the more surprising that not a single book has appeared until very recently, which has attempted to sum up this field, even in its main outlines. In his book W. HEINE introduces the present usage of group theory in quantum mechanics. As stated in the preface, the book has been written for research students in physics and chemistry, at a level now offered at many universities. This entailed a serious restriction on the selection of the subject matter. The reader is assumed to have completed only a preliminary basic course in quantum mechanics (e.g. L. SCHIFF: Quantum Mechanics) a specialized knowledge of particular branches of physics is not assumed. Therefore, where possible, the simpler applications of basic principles are demonstrated. For the sake of logical sequence the necessary matrix algebra etc. is given in a separate appendix. Within its necessary limitations, the treatment is simple, concise and clear. At the end of most sections there is a brief summary and references are given to enable the reader to obtain a more detailed knowledge of the subject. A series of problems to be solved by the reader is appended to each section. These problems are extremely varied, some being simple drill in the methods described in the section, while others are extensions of the subject matter to problems which have had to be omitted in the text owing to the limited size of the volume. The examples are very useful in promoting a thorough understanding of the material.

In Chapter I the essential mathematical concepts and expressions of symmetry operations and symmetry transformations of the Hamiltonian in general are given, the definition of the group is formulated, group representations are introduced and the grounds for the application of group theory to quantum mechanics are established.

Chapter II illustrates the applications of group theory to the quantum theory of the free atom. First the irreducible representations of the full rotation group and their properties as well as the relationship between infinitesimal rotation operators and angular momentum are shown, then the reduction of the product representtation $D^J \times D^{J'}$ is studied. This is followed

by the transformation properties of the spin, the spin functions and the Pauli principle. Unfortunately, a more detailed description of the representations of the symmetric group (Young symmetrizer) is missing. At the end of this chapter the calculations of matrix elements and selection rules are developed.

Chapter III is devoted to the irreducible representations of finite groups. Here the concept of character is introduced and the projection operators, with which the functions belonging to a given row of a given irreducible representation can be identified, are given. The irreducible representations of product groups and the derivation and representations of crystal point groups are described. Finally, the relationship between group theory and the Dirac method is shown.

In Chapter IV group theory is applied to the disturbance of paramagnetic ions in crystalline fields, the time reversal transformations and Kramer's theorem; a general formula for the calculation of Wigner coefficients is given. In the last section hyperfine structure is discussed.

In Chapter V group theory is applied to the quantum theory of molecules. First the electron wave function is considered with regard to the most frequently used (Valence Bond, Molecular Orbital, Hybrid Orbital) approaches. This section lacks detailed coverage. The classification of the electronic states of the molecule is possible, whatever the approach, only by means of group theory. The remainder of this chapter deals with molecular vibrations.

Chapter VI is devoted to solid state physics. The irreducible representations of space groups, the boundaries of the symmetry of crystals and finally the so-called tensor properties of crystals are considered.

In Chapter VII on nuclear physics, isotopic spin formalism is introduced and it is shown how to build up the correct antisymmetric nuclear wave function. This Chapter also deals with nuclear forces, the shell model and the deuteron. New concepts such as "intrinsic parity" and "strangeness" are touched on. The application of group theory to nuclear reactions is investigated. The fundamental (conservation) theorem is also treated here.

Chapter VIII is devoted to relativistic quantum mechanics. The irreducible representations of the proper and the complete Lorentz group are described, which leads to the Dirac equation. In this connection charge conjugation and the transformation properties of physical quantities in general are treated. The next section deals with beta decay. Finally, the recently discovered parity non-conservation and the symmetries of positronium are dealt with.

The eight chapters are completed by an Appendix of considerable extent. This includes the required matrix algebra and theoretical group theorems with proofs, the tables of Wigner coefficients, the character tables of usual crystal point groups, etc.

The Lagrangian formalism and the transformation properties of fields are not included, apparently because these are beyond the scope of the book.

In conclusion it may be stated that the book is very useful primarily for researchers interested in atomic, molecular and solid state physics. The applications of group theory to quantum mechanics are described in detail. For those who wish to study special problems more thoroughly a list of General References and a bibliography are included at the end of the book.

E. KAPUY

Printed in Hungary

A kiadásért felel az Akadémiai Kiadó igazgatója Műszaki szerkesztő: Farkas Sándor

A kézirat nyomdába érkezett: 1962. XII. 3. — Terjedelem: 7,50 (A/5) ív, 24 ábra

62.56377 Akadémiai Nyomda, Budapest — Felelős vezető: Bernát György

The *Acta Physica* publish papers on physics, in English, German, French and Russian.
The *Acta Physica* appear in parts of varying size, making up volumes.
Manuscripts should be addressed to:

Acta Physica, Budapest 502, Postafiók 24.

Correspondence with the editors and publishers should be sent to the same address.
The rate of subscription to the *Acta Physica* is 110 forints a volume. Orders may be placed with "Kultúra" Foreign Trade Company for Books and Newspapers (Budapest I., Fő u. 32. Account No. 43-790-057-181) or with representatives abroad.

Les *Acta Physica* paraissent en français, allemand, anglais et russe et publient des travaux du domaine de la physique.
Les *Acta Physica* sont publiés sous forme de fascicules qui seront réunis en volumes.
On est prié d'envoyer les manuscrits destinés à la rédaction à l'adresse suivante:

Acta Physica, Budapest 502, Postafiók 24.

Toute correspondance doit être envoyée à cette même adresse.
Le prix de l'abonnement est de 110 forints par volume.
On peut s'abonner à l'Entreprise du Commerce Extérieur de Livres et Journaux «Kultúra» (Budapest I., Fő u. 32. — Compte-courant No. 43-790-057-181) ou à l'étranger chez tous les représentants ou dépositaires.

«*Acta Physica*» публикуют трактаты из области физических наук на русском, немецком, английском и французском языках.
«*Acta Physica*» выходят отдельными выпусками разного объема. Несколько выпусков составляют один том.
Предназначенные для публикации рукописи следует направлять по адресу:

Acta Physica, Budapest 502, Postafiók 24.

По этому же адресу направлять всякую корреспонденцию для редакции и администрации.
Подписная цена «*Acta Physica*» — 110 форинтов за том. Заказы принимает предприятие по внешней торговле книг и газет «*Kultúra*» (Budapest I., Fő u. 32. Текущий счет: № 43-790-057-181) или его заграничные представительства и уполномоченные.

22,— Ft

INDEX

COMMUNICATIONES BREVES

RECENSIONES

Acta Phys. Hung. Tom. XV. Fasc. 3. Budapest, 20. II. 1963

Index: 26.022

ACTA PHYSICA

ACADEMIAE SCIENTIARUM HUNGARICAE

TOMUS XV. FASCICULUS 4.

AKADÉMIAI KIADÓ, BUDAPEST
1963

ACTA PHYS. HUNG.

ACTA PHYSICA

A MAGYAR TUDOMÁNYOS AKADÉMIA FIZIKAI KÖZLEMÉNYEI

SZERKESZTŐSÉG ÉS KIADÓHIVATAL: BUDAPEST V., ALKOTMÁNY UTCA 21.

Az *Acta Physica* német, angol, francia és orosz nyelven közöl értekezéseket a fizika tárgyköréből.

Az *Acta Physica* változó terjedelmű füzetekben jelenik meg: több füzet alkot egy kötetet.

A közlésre szánt kéziratok a következő címre küldendők:

Acta Physica, Budapest 502, Postafiók 24.

Ugyanerre a címre küldendő minden szerkesztőségi és kiadóhivatali levelezés.

Az *Acta Physica* előfizetési ára kötetenként belföldre 80 forint, külföldre 110 forint. Megrendelhető a belföld számára az Akadémiai Kiadónál (Budapest V., Alkotmány utca 21. Bankszámla 05-915-111-46), a külföld számára pedig a „Kultúra" Könyv- és Hírlap Külkereskedelmi Vállalatnál (Budapest I., Fő u. 32. Bankszámla 43-790-057-181 sz.), vagy annak külföldi képviseleteinél és bizományosainál.

Die *Acta Physica* veröffentlichen Abhandlungen aus dem Bereiche der Physik in deutscher, englischer, französischer und russischer Sprache.

Die *Acta Physica* erscheinen in Heften wechselnden Umfanges. Mehrere Hefte bilden einen Band.

Die zur Veröffentlichung bestimmten Manuskripte sind an folgende Adresse zu richten:

Acta Physica, Budapest 502, Postafiók 24.

An die gleiche Anschrift ist auch jede für die Redaktion und den Verlag bestimmte Korrespondenz zu senden.

Abonnementspreis pro Band: 110 forint. Bestellbar bei dem Buch- und Zeitungs-Aussenhandels-Unternehmen »Kultúra« (Budapest I., Fő u. 32. Bankkonto Nr. 43-790-057-181) oder bei seinen Auslandsvertretungen und Kommissionären.

SOME REMARKS ON THE ENERGY BAND STRUCTURE OF PROTEIN

By

J. LADIK

CENTRAL RESEARCH INSTITUTE FOR CHEMISTRY OF THE HUNGARIAN ACADEMY OF SCIENCES, BUDAPEST

(Presented by G. Schay.— Received 2. II. 1962)

The energy bands of protein were calculated by using the chemical model of EVANS and GERGELY devised to demonstrate the way in which the infinite MO-s are originated. The calculation based on the simple LCAO MO theory was performed by the method developed by KOUTECKÝ and ZAHRADNIK [7]. In the first approximation the $2p_z$ orbitals of the C, O and N atoms of the peptide (H—N—C=O) group were used, while in a second four-centre approximation also the empty $2p_z$ orbital of the H atom was taken into consideration. A variation of the values of the integrals α_H, $\beta_{N,H}$ and $\beta_{O,H}$ has shown the results to change only to a slight extent with the values of these parameters.

The first three-centre approximation resulted in 5,11 ev for the width of the forbidden band between the highest filled and the lowest unfilled band, while in the four-centre approximation this value was only 3.95 ev. These findings and the fact that the band widths obtained were larger than those given by EVANS and GERGELY suggest the electronic conductivity of protein, found experimentally, to arise from the mobility of the π electrons on the infinite MO-s of the model considered.

The results of the more realistic four-centre approximation also show in comparison with a free monopeptide group a significant increase in electron affinity and a considerable stabilization energy ($\sim$32 kcal/mole peptide groups) in the protein molecule.

The first theoretical calculation for the energy bands of protein was performed in 1949 by EVANS and GERGELY [1]. These authors used for their calculations the model shown in Fig. 1, according to which the π electrons of the peptide groups of the protein chains are interacting through the H bonds (indicated by dotted lines) and so infinite molecular orbitals, perpendicular to the direction of the protein chains are formed. These MO-s can go through different protein chains or through the different parts of the same folded chain.

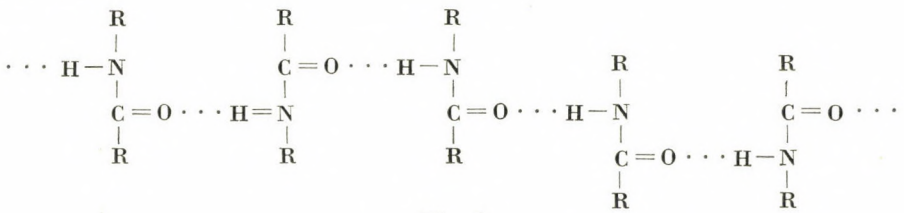

Fig. 1

EVANS and GERGELY have assumed a delocalization of the π electrons in the protein molecule so as to interpret several experimental findings which

suggest a possible energy transfer to take place in this molecule with the aid of electron wandering. Recently ELEY and his coworkers [2], [3], [4] have stated different types of proteins to be semiconductors with a forbidden band width of 2.6—3.1 ev. This semiconductivity is interpreted by ELEY and SPIVEY [4] for various reasons as electronic and not protonic, while TAYLOR [5] does not exclude the possibility of protonic conductivity in proteins. For their calculations, EVANS and GERGELY used the simple LCAO MO method, taking the peptide $\left(\begin{array}{l} O = C \\ \quad\quad | \\ \quad\quad N-H \end{array}\right)$ group as the elementary cell in the "one-dimensional solid" of the model. Assuming the N atom to be in a trigonal sp^2 hybrid state and taking only the C, O and N atoms of the peptide groups as centres, they obtained the band structure shown in Table I.

Table I

The energy bands of protein in ev relative to the lowest filled level

Band 1	0 —0,13	Doubly filled
Band 2	3,17—3,43	Doubly filled
Band 3	6,48—6,60	Unfilled

It is seen from the above Table that according to this calculation the forbidden band width is 3.05 ev, which is in good agreement with the values found experimentally by ELEY and coworkers. It must be noted that in the case of a pyramidal N atom they obtained $\sim$4.2 ev for the forbidden band width. However, the trigonal sp^2 hybrid state of the N atom seems to be the more realistic assumption.

The above calculation would nevertheless appear to be somewhat unsatisfactory, and that for two reasons. When, namely, the calculation was being carried out, the suitable integral values α_i and $\beta_{i,j}$ in the LCAO MO method were not yet known for the compounds containing hetero atoms and the estimated values used by EVANS and GERGELY seem to be somewhat unrealistic. On the other hand, if a π electron interaction through the H bonds is assumed, it would appear necessary to take into account also the empty $2p_z$ orbital of the H atom. The calculation of the energy bands of protein was therefore repeated by the present author, by means of the simple LCAO MO method (HÜCKEL method), on the basis of the model of EVANS and GERGELY, but with the α_i and $\beta_{i,j}$ values which the literature usually records. The calculation was performed both for a peptide group with three-centre π electron MO-s,

$$\Psi_j = \sum_{i=1}^{3} c_{i,j} \varphi_i , \tag{1}$$

and for a peptide group with four-centre π electron MO-s,

$$\Psi_j = \sum_{i=1}^{4} c_{i,j}\,\psi_i\,, \tag{2}$$

as the elementary cell. Here ψ_i stands for the SLATER-type $2p_z$ orbital for the i-th atom and the $c_{i,j}$-s are constant.

It should be noted that shortly after the completion of this calculation the work of SUARD, BERTHIER and PULLMAN [6] was published on the SCF LCAO MO calculation of the energy bands of protein. In the more refined approximation of these authors also the lone electron pair of the O atom was taken into account. They got $\sim$5 ev for the forbidden band width, this value representing in this case the energy necessary to promote an electron from the energy band that arises from the levels of the electron pairs of the O atoms to the unfilled band. On the other hand, the energy necessary to promote a π electron to the conduction band was found by the above authors to be $\sim$6.7 ev (the mean value for the excitation energies into singlet or triplet states). In the calculation of SUARD, BERTHIER and PULLMAN, however, the empty $2p_z$ orbitals of the H atoms were equally disregarded, so that the results of this more simple calculation may also contribute to the solution of the problem.

Method

The energy bands were calculated by the method of KOUTECKÝ and ZAHRADNIK [7]. Accordingly the LCAO MO of an infinite one-dimensional macromolecule (or of a cycle molecule of N cells, where N is a very large number, with the first and the N^{th} cell adjoining) can be written in the form

$$\Psi_{m,p}(\bar{r}) = \sum_{j=1}^{N} \sum_{l=1}^{n} a_{m,p;j,l}\,\varphi_l(\bar{r}_l - j\bar{a})\,. \tag{3}$$

Here n is the number of atoms in the elementary cell, $\bar{a}$ is the primitive translation vector in the direction of the chain, $\bar{r}_l$ the position vector of the electron taken from the l^{th} nucleus, $\varphi_l(\bar{r}_l - j\bar{a})$ denotes the atomic orbital of the l^{th} atom in the j^{th} elementary cell, and $a_{m,p;j,l}$ mean its coefficient in the MO with quantum numbers m and p ($m = 1, \ldots, n$; $p = 1, \ldots, N$). Since the wave function (3) must be invariant with respect to the translation $\bar{a}$ or its multiples

$$\Psi_{m,p}(\bar{r} + j\bar{a}) = \Psi_{m,p}(\bar{r})\,, \tag{4}$$

it follows (see for example [8]) that

$$a_{m,p;j,l} = \exp\left(\frac{i2\pi p_j}{N}\right) a_{m,p;l}\,. \tag{5}$$

Writing

$$\frac{2\pi p}{N} = k \tag{6}$$

for a very large N we may consider k to change continuously from 0 to 2π.

By performing a usual variation procedure with the wave function (3), neglecting the overlap integrals and applying the usual approximations of the HÜCKEL form of the LCAO MO theory, one gets the following secular determinant [7]

$$\begin{vmatrix} \gamma_1-\varepsilon & \gamma_{1,2} & \gamma_{1,3} & \cdots & \gamma_{1,n} \\ \gamma_{2,1} & \gamma_2-\varepsilon & \gamma_{2,3} & \cdots & \gamma_{2,n} \\ \gamma_{3,1} & \gamma_{3,2} & \gamma_3-\varepsilon & \cdots & \gamma_{3,n} \\ \cdots & \cdots & \cdots & \cdots & \cdots \\ \gamma_{n,1} & \gamma_{n,2} & \gamma_{n,3} & \cdots & \gamma_n-\varepsilon \end{vmatrix} = 0. \tag{7}$$

Here $$\gamma_l = \alpha_l + \beta^+_{l,l}\, e^{ik} + \beta^-_{l,l}\, e^{-ik},$$

and $$\gamma_{l,s} = \beta_{l,s} + \beta^+_{l,s}\, e^{ik} + \beta^-_{l,s} \cdot e^{-ik},$$

where α_1 and $\beta_{l,s}$ are the usual integrals α_i and $\beta_{i,j}$ of the HÜCKEL method,[1] $\beta^+_{1,1}$ resp. $\beta^-_{1,1}$ are the resonance integrals between the l^{th} atom of an elementary cell and the l^{th} atom of the next cell on the right, resp. left of it. $\beta^+_{1,s}$, resp. $\beta^-_{1,s}$ stand for the resonance integral between the l^{th} atom of a cell and the s^{th} atom of the next neighbouring cell right, resp. left of it.

In the case of protein, the model shown in Fig. 2 can be taken as a first approximation. According to this model a peptide group (HN—C = O) forms the elementary cell and only the $2p_z$ orbitals of the C, O and the hybridized N atom are taken into account.

$$-\underset{2}{\mathrm{C}}=\underset{3}{\mathrm{O}}\cdots\mathrm{H}-\underset{1}{\mathrm{N}}-\underset{2}{\mathrm{C}}=\underset{3}{\mathrm{O}}\cdots\mathrm{H}-\underset{1}{\mathrm{N}}-\underset{2}{\mathrm{C}}=$$

Fig. 2

The dotted lines indicate the hydrogen bonds through which the π electron interaction takes place. On the basis of this model it is possible to immediately write up the appropriate secular determinant of the protein molecule:

$$\cdots \begin{vmatrix} \alpha_1-\varepsilon & \beta_{1,2} & \beta^-_{1.3}\, e^{-ik} \\ \beta_{2,1} & \alpha_2-\varepsilon & \beta_{2,3} \\ \beta^+_{3.1}\, e^{ik} & \beta_{3,2} & \alpha_3-\varepsilon \end{vmatrix} = 0. \tag{8}$$

[1] The latter are resonance integrals between atoms belonging to the same cell.

(According to the HÜCKEL approximation integrals $\beta_{i,j}$ between the nearest neighbour atoms were considered.)

For the value of $\alpha_1 = \alpha_N$ taking into account that the N atom 1 is in the sp^2 hybrid state and that it takes part in a hydrogen bonding as hydrogen donor with a slight modification of its value as given in the literature [9], [10], the value $\alpha_{N-H} \ldots = \alpha_N - 0{,}20\beta = (0{,}90-0{,}20)\,\beta = 0{,}70\beta$ was used. Here $\alpha_{N-H} \ldots$ denotes the integral value α of an N atom taking part in a hydrogen bond, α_N is the same integral when the H atom attached to the N atom does not take part in a hydrogen bond and β is the resonance integral between two C atoms in benzene. For $\alpha_2 = \alpha_{OC_N}$(a C atom in the neighbourhood of an N and O atom) the value of $0{,}27\beta$ was taken [11], [12], while for $\alpha_3 = \alpha_0$, considering again that the O atom takes part in a hydrogen bond, by slightly modifying the value reported in the literature [9], [10], $\alpha_O \ldots {}_{H-} = \alpha_O + 0.20\beta = (1.30 + 0.20)\,\beta = 1.50\beta$ was used. Here $\alpha_O \ldots {}_H$ stands for the integral α for an O atom taking part in a hydrogen bond and α_O for an O atom which does not. For $\beta_{1,2} = \beta_{2,1} = \beta_{C,N}$ the value $\beta_{C,N} = \beta$, while for $\beta_{2,3} = \beta_{3,2} = \beta_{C,O}$ the value $\beta_{C,O} = 2.00\ \beta$ was employed [9]. For the integral value $\beta^-_{1,3} = \beta^+_{3,1}$ denoting the interaction between the π electrons of the O and N atom through the hydrogen bond, the value 0.20β was used after PULLMAN [10]. It is to be noted that each time when somewhat modified parameter values, as compared with those given in the literature, were used, their application seemed to be reasonable on the basis of calculations performed for other compounds containing hetero atoms.

The numerical parameter values given above allow the eq. (8) to be solved. Substituting the maximum resp. minimum values of e^{ik} and e^{-ik}, i.e. $+1$, resp. -1, the upper and lower limits of the energy bands can be obtained.

As a second approximation the model shown in Fig. 3 was employed. Here the empty $2p_z$ orbital of the H atom being also considered there will

$$\underset{3}{\text{C}}=\underset{4}{\text{O}}\cdots\underset{1}{\text{H}}-\underset{2}{\text{N}}-\underset{3}{\text{C}}=\underset{4}{\text{O}}\cdots\underset{1}{\text{H}}-\underset{2}{\text{N}}-$$

Fig. 3

now be four atoms in the elementary cell. The appropriate secular determinant will be the following:

$$\begin{vmatrix} \alpha_1 - \varepsilon & \beta_{1,2} & 0 & \beta^-_{1.4} - e^{-ik} \\ \beta_{2,1} & \alpha_2 - \varepsilon & \beta_{2,3} & 0 \\ 0 & \beta_{3,2} & \alpha_3 - \varepsilon & \beta_{3,4} \\ \beta^+_{4.1}\, e^{ik} & 0 & \beta_{4,3} & \alpha_4 - \varepsilon \end{vmatrix} = 0 \cdot \qquad (9)$$

Here for $\alpha_1 = \alpha_H = -0.60\beta$ was taken. The negative sign is reasonable, considering that between a π electron on the $2p_z$ orbital of the H atom and the 1s electron a repulsion is taking place (β is negative !). For $\beta_{1,2} = \beta_{2,1} = \beta_{N,H}$ the value 0.80β and for $\beta^-_{1,4} = \beta^+_{4,1} = \beta_{O,H}$ giving the interaction between the π electron of the O atom and the π electron of the otherwise empty $2p_z$ orbital of the H atom, a value of 0.40β was used. The other integrals α_i and $\beta_{i,j}$ are the same as in (8), so that the values given above were used for them. By substituting the parameter values and $+1$, resp. -1 for e^{ik} and e^{-ik} in (9), the upper and lower limits of the resulting four energy bands can be calculated.

For the sake of comparison, the energy levels of a peptide group were also calculated. For this calculation the same α_i and $\beta_{i,j}$ values were used as in equ. (8), only $\beta^-_{1,3} = \beta^+_{3,1} = 0$ (a peptide group which, though bonded by hydrogen bonds to other peptide groups, is not in π interaction with them). In a second case the values $\alpha_N = 0.90\beta$ and $\alpha_O = 1.30\beta$ were employed, taking the other parameters constant (a peptide group being neither in hydrogen bonding, nor in π electron interaction with other groups).

Since the above choice of the integrals α_H, $\beta_{N,H}$ and $\beta_{O,H}$ is rather arbitrary, it seemed useful to investigate the effect of the variation of these parameters. This was performed on the simplified system shown in Fig. 4.

$$\overset{1}{O} \cdots H\overset{2}{-}\overset{3}{N}$$

Fig. 4

Here the parameter values $\alpha_O = 1.50\beta$, $\alpha_N = 0.70\beta$ were kept constant, and for the other three parameters the values shown in Table II were applied.

Table II

The values in β units of α_H, $\beta_{N,H}$ and $\beta_{O,H}$ used for the investigation on the parameter variation of the O ... H—N system

Number	α_H	$\beta_{N,H}$	$\beta_{O,H}$
1	—0,60	0,80	0,40
2	—0,40	0,80	0,40
3	—0,80	0,80	0,40
4	—0,60	0,80	0,30
5	—0,60	0,80	0,50
6	—0,60	0,70	0,40
7	—0,60	0,90	0,40

Results

Using the appropriate parameter values given above equ. (8) results in the energy band system shown in Table III.

Table III

The energy bands of protein in the three-centre approximation

	In β units	In ev	Band width in ev	
Band 1	3.215— 3,066	7,68— 7,33	0,35	Doubly filled
Band 2	0,995— 0,697	2,38— 1,66	0.72	Doubly filled
Band 3	—1.443— —1.587	—3.45— —3.79	0.34	Unfilled

In Table III the energy values are given in relation to $E_C + \alpha_C$, where E_C is the energy of a $2p$ electron in a free carbon atom and α_C is the integral α of a C atom in a carbon chain. The results obtained from equ. (8) in β units are converted to ev-s with the aid of the β value, $\beta = -2.39$ ev, given by PARISER ans PARR [13] on the basis of the electronic spectrum of benzene. Forbidden band widths are as follows: 4.95 ev ($= 2.071\ \beta$) between the two filled bands and 5.11 ev ($= 2.140\ \beta$) between the second filled and the unfilled band.

Results arrived at by the solution of equ. (9) are shown in Table IV.

Table IV

The energy bands of protein in the four-centre approximation

	In β units	In ev	Band width in ev	
Band 1	3.202— 3,133	7.65— 7.49	0.16	Doubly filled
Band 2	1.270— 1.036	3.04— 2.48	0.56	Doubly filled
Band 3	—0.615— —1.001	—1.47— —2.39	0.92	Unfilled
Band 4	—1.520— —1.754	—3.63— —4.19	0.56	Unfilled

Here the zero point of the energy scale is the same as in the preceding case. The forbidden band widths are 4.45 ev ($= 1.863\ \beta$), 3.95 ev ($= 1.651\ \beta$) and 1.24 ev ($= 0.519\ \beta$), respectively.

The results calculated for a peptide group in the two above mentioned cases are condensed in Table V.

By assuming in a rough approximation the density of the levels to be equal in all parts of a band, it will be possible to estimate the stabilization

Table V

The π electron levels of a monopeptide group in β units

Energy level	Peptide group with H bonds	Peptide group without H bonds
ε_1	3.13	3.03
ε_2	0.85	1.00
ε_3	−1.51	−1.55

due to the π electron interaction between the peptide groups of the protein molecule. This is performed with the aid of the equation

$$2\left(\frac{E_{1,1}+E_{1,2}}{2}+\frac{E_{2,1}+E_{2,2}}{2}\right)-2(\varepsilon_1+\varepsilon_2), \tag{10}$$

where $E_{i,1}$ means the lower and $E_{i,2}$ the upper limit of the i^{th} doubly filled energy band ($i = 1, 2$) and ε_1, ε_2 stands for the energies of the filled MO-s of a peptide group. The results are given in kcal/mole peptide group in Table VI.

Table VI

Stabilization energy of the protein molecule in kcal/mole peptide group

	Peptide group with H bonds	Peptide group without H bonds
Protein three-centre approximation	0.7	− 4.8
Protein four-centre approximation	37.1	32.3

The energy levels obtained for the simplified system previously mentioned (see Fig. 4) with the varied parameter values given in Table II, are shown in Table VII.

Table VII

Results of the parameter variation investigation in β units

Number	ε_1	ε_2	ε_3	E	ΔE_1	ΔE_2
1	1.61	1.03	−1.03	4.25	0.58	2.06
2	1.62	1.05	−0.87	4.29	0.57	1.92
3	1.59	1.00	−1,19	4.18	0.59	2.19
4	1.55	1.06	−1.01	4.16	0.49	2.07
5	1.66	1.00	−1.06	4.32	0.66	2.06
6	1.59	0.96	−0.96	4.14	0.63	1.92
7	1.62	1.09	−1.11	4.33	0.53	2.20

Here ε_1, ε_2, ε_3 mean the MO energies of the O . . . H—N system, $E = 2\varepsilon_1 + \varepsilon_2$ is the total π electron energy of this system, $\Delta E_1 = (\varepsilon_2 - \varepsilon_1)$ and $\Delta E_2 = (\varepsilon_3 - \varepsilon_2)$.

Discussion

A comparison of the results obtained for the energy bands of protein in the three-centre approximation (Table III) with those of EVANS and GERGELY (Table I) will show that if more realistic parameter values and the method of KOUTECKÝ and ZAHRADNIK [7] are applied, the value (5.11 ev) obtained for the width of the forbidden band between the highest filled and the unfilled band will significantly exceed the value of 3.05 ev calculated by EVANS and GERGELY. There is a close agreement between the former value and that of $\sim$5 ev, obtained by SUARD, BERTHIER and PULLMAN [6] for the forbidden band width in their SCF LCAO MO calculation of protein. It is essential, however, to point out that according to these authors the highest filled band arises from the levels of the lone σ-type electron pairs of the O atoms and the value of $\sim$5 ev is the midpoint of the excitation energies to a singlet, resp. triplet state, while in the calculation of EVANS and GERGELY as well as in the present calculation, the highest filled band is a π electron band. Since in both the SCF and the above calculation it turned out that the theoretical forbidden band width ($\sim$5 ev) does not agree with the experimental one (2.6—3.1 ev) found by ELEY and his coworkers [4] it would seem probable that the electronic conductivity of protein reported by the latter authors could not arise from the model discussed.

The case with the results of the four-centre approximation is quite different. Here for the forbidden band width under discussion a value of only 3.95 ev was found (see Table IV), and if it is considered that in a real protein molecule there are lattice errors, impurities, other groups of the molecule able to perturb the π electron system of the model, etc., this value does not exclude the possibility of the electronic conductivity observed in protein to arise chiefly from the π electron system of the model discussed. It seems probable that in an SCF calculation the four-centre approximation would also result in the value of $\sim$4 ev for the forbidden band width between the band arising from the levels of the σ-type lone electron pairs of the O atoms and the lowest unfilled π-type band. In this respect particular interest attaches to the results of the calculations of SUARD, BERTHIER and PULLMAN, presently in progress as mentioned in their paper previously referred to.

It appeared equally interesting to make a comparison between the excitation energies obtained in the three-, resp. four-centre approximation and the corresponding values for a monopeptide group (see Table V). It may be seen that in this simple approximation the energy of the first excitation was of 2.55 β for a free monopeptide group, this value decreasing to 2.36 β

for a monopeptide group which is in H bonding with other peptide groups; in the energy band model of protein its value is 2.14 β, if the three-centre approximation is used and finally in the four-centre approximation of the energy band structure its value was found to be as low as 1.65 β.

Coming back to the problem of conduction in proteins, it is interesting to compare the widths of the lowest unfilled band, in the calculation of EVANS and GERGELY, in the three, resp. four-centre approximation of the present calculation and in the SCF calculation. The appropriate values are of 0.12 ev, 0.34 ev, 0.92 ev (see Tables I, III, IV) and 1.30 ev [6]. From these, with the aid of the equation

$$\delta E = \frac{h^2}{8a^2 m^*}, \tag{11}$$

where δE is the band width, h the Planck constant, a the lattice constant and m^* the effective electronic mass, it is possible to estimate the effective electronic masses for the different approximations. ELEY ans SPIVEY [4] give $\delta E = 0.1$ ev, assuming for the lattice constant of the protein macromolecule (an O = C—NH unit) $a = 4$ Å, $m^* = 40\ m$, where m is the mass of a free electron. On this basis we get $m^* = 33\ m$, 12 m, 4 m, 3 m in the cases listed above. These lower m^* values mean higher conductivities ($\varkappa_0 \sim m^{*3/2} e^{-m^{*1/2}}$, see equ. (6) and (9) of [4], where $\varkappa_0$ is the specific conductivity). It must be noted that also the band widths of the filled bands are by far larger according to the results of the present as well as to those of the SCF calculation, than the values given by EVANS and GERGELY (see Table I, III and IV and also Table IV of [9]).

The width of the forbidden band between the two filled bands is 3.04 ev in the case reported by EVANS and GERGELY, while in the present calculation it was found to be 4.95 ev in the three-centre, and 4.45 ev in the four-centre approximation (see Table I, Table III and Table IV). In view of these higher forbidden band widths, as well as of the fact that the band widths of the filled bands are higher than those published by EVANS and GERGELY, the criterion given by MASON for the carcinogenic activity of aromatic hydrocarbons [15] would appear to be untenable in its original form. To allow the problem to be further investigated, some plausible chemical models for the carcinogenic hydrocarbon-protein, resp. carcinogenic hydrocarbon-nucleotide base complexes have to be constructed and the electronic structures of these complexes calculated [16]. Such attempts are in progress.

It is of interest to compare the ionisation potential and electron affinity values of a free monopeptide group with the corresponding values obtained for the band structure model of protein in the three-, resp. four-centre approximation. From Table V one gets for a free monopeptide group the value $I = 1.00\ \beta + E_C + \alpha_C$ for the ionization potential, and $E_a = -1.55\ \beta + E_C + \alpha_C$

for the electronaffinity, where E_C (the energy of a $2p$ electron in a free carbon atom) and α_C (the integral α of a carbon atom in benzene) are negative values. With respect to protein the following values are obtained from Tables III and IV:

$$I = 0.70\,\beta + E_C + \alpha_C\,, \quad E_A = -\,1.44\,\beta + E_C + \alpha_C$$

(three-centre approximation),

$$I = 1.04\,\beta + E_C + \alpha_C\,, \quad E_A = -\,0.62\,\beta + E_C + \alpha_C$$

(four-centre approximation).

This shows that compared with the value of a free peptide group the ionization potential decreases in the case of the three-centre approximation of protein, while in the four-centre approximation it shows a slight increase. The electron affinity of the protein is somewhat increased in the case of the three-centre approximation as compared to the corresponding value of the peptide group, but a significant increase is revealed ($\sim$2.1 ev) in the case of the four-centre approximation. In other words it would seem that if the H atom of the hydrogen bond is also considered as a centre, a strengthening of the electron acceptor property of protein could be theoretically expected, as compared with a free monopeptide group.

In Table VI the estimated stabilization energy of the protein molecule can be seen in its relation to peptide groups which are not in π electron interaction. The values in this Table show that in the case of the three-centre approximation only a 0.7 kcal/mole peptide group stabilization energy is obtained for the protein molecule as compared to peptide groups bonded by H bonds and a system of free monopeptide groups is by $\sim$5 kcal/mole peptide group more stable than the protein molecule. GERGELY gives 0.5—1.0 kcal/mole peptide group for the stabilization energy, which is in good agreement with the first value. In the four-centre approximation, on the other hand, very large stabilization values are obtained for the protein molecule (37.1, resp. 32.3 kcal/mole peptide groups).

From Tables II and VII illustrating the results of the parameter variation investigation of the O . . . H—N system we can see that its energy levels do not appear to change considerably with the variation of the values of the integrals α_H, $\beta_{N,H}$ and $\beta_{O,H}$. No significant variation is seen in the energy differences between these levels (ΔE_1, ΔE_2) and the sum of the energy of the all π electrons (E) shows also only slight changes. The above results suggest the energy band structure of protein obtained by the four-centre approximation not to undergo significant changes with the variation of the parameter values used either. It could be thus concluded that though the present results were obtained by using integrals that were somewhat arbitrarily estimated, they nevertheless appear to be realistic within the framework of the simple LCAO MO theory.

Acknowledgements

The author should like to express his gratitude to J. KOUTECKÝ, Corresponding Member of the Czechoslovakian Academy of Sciences, for calling his attention to the method described in the present paper and to the necessity of performing investigations on parameter variation, to T. A. HOFFMANN, Dr. of Physical Sciences for helpful discussions and to G. BICZÓ, scientific research worker, for having helped with the numerical calculations.

REFERENCES

1. M. G. EVANS and J. GERGELY, Biochim. Biophys. Acta, **3**, 188, 1949.
2. D. D. ELEY, G. D. PARFITT, M. J. PERRY and D. H. TAYSUM, Trans. Far. Soc., **49**, 79, 1953.
3. M. H. CARDEW and D. D. ELEY, Disc. Far. Soc., **27**, 115, 1959.
4. D. D. ELEY and D. I. SPIVEY, Trans. Far. Soc., **56**, 1432, 1960.
5. P. TAYLOR, Disc. Far. Soc., **27**, 236, 1959.
6. M. SUARD, G. BERTHIER and B. PULLMAN, Biochim. Biophys. Acta, **52**, 254, 1961.
7. J. KOUTECKÝ, R. ZAHRADNIK, Coll. Czechoslov. Chem. Comm., **25**, 811, 1960.
8. J. R. REITZ, Solid State Physics, Vol. I, 1. Academic Press, New York, 1955.
9. B. PULLMAN and A. PULLMAN, Rev. Mod. Phys., **32**, 428, 1960.
10. B. PULLMAN and A. PULLMAN, Biochim. Biophys. Acta, **36**, 343, 1959.
11. D. W. DAVIES, Trans. Far. Soc., **51**, 449, 1955.
12. C. A. COULSON and J. HERR, Trans. Far. Soc., **47**, 681, 1951.
13. J. PARISER and J. PARR, J. Chem. Phys., **21**, 466, 1953; ibid. **21**, 767, 1953.
14. W. SHOCKLEY, Electrons and Holes in Semiconductors, Van Nostrand, 1950, p. 398.
15. R. MASON, Nature, **181**, 820. 1958; Disc. Far. Soc., **27**, 129, 1960; Rad. Research Suppl., **2**, Bioenergetics, Ac. Press., New York—London, 1960 p. 452.
16. J. KOUTECKÝ, private communication.

НЕКОТОРЫЕ ЗАМЕЧАНИЯ О СТРУКТУРЕ ЭНЕРГЕТИЧЕСКИХ ПОЛОС ПРОТЕИНОВ

Й. ЛАДИК

Р е з ю м е

Применением химической модели Эванса и Гергеля, сконструированной для демонстрации пути происхождения бесконечных МО, вычисляются энергетические полосы протеинов. Вычисления, в основе которых лежит простая ЛКАО МО-теория, проводились методом, разработанным Коутецким и Заградником [7]. В первом приближении применились $2p_z$-орбиты атомов C, O и N пептидной группы (H—N—C = O), в то время как во втором четырхцентровом приближении принималась во внимание и незаполненная $2p_z$-орбита атома H. Вариация значений интегралов α_H, $\beta_{N,H}$ и $\beta_{O,H}$ показала, что с изменением значений этих параметров результаты изменяются только в незначительной мере.

Вычисления в первом трёхцентровом приближении для ширины запрещенной полосы между наивысшей заполненной и наинизшей незаполненной полосами дают 5,11 eV, в то время как в четырёхцентровом приближении данная величина оказалась равной 3,95 eV. Эти обнаружения и ширины полос, которые своими значениями больше полученных Эвансом и Гергелем величин, внушают, что электрическая проводимость протеинов, найденная экспериментально, обусловливается подвижностью π-электронов в бесконечных МО рассматриваемой модели.

Результаты более реального четырёхцентрового приближения показывают также что сродство к электрону и рассмотренная энергия устойчивости ($\sim$32 kcal/mol пептидная группа) в молекуле протеина по сравнению со свободной монопептидной группой значительно увеличиваются.

THE SPECIFIC HEAT OF THIN FILMS

By

A. CORCIOVEI and C. MOŢOC

INSTITUTE FOR ATOMIC PHYSICS, BUCHAREST, RUMANIA

(Presented by L. Pál. — Received: 1. III. 1962)

The specific heat of thin films is studied theoretically. It is based on the preliminary study of the problem of thermal vibrations in thin films. After obtaining the dispersion relations, the specific heat is calculated by taking into account the contribution of all vibrational modes to the thermal energy of the thin film. Two limiting cases are considered: the high-temperature case, in which the well-known independence of the specific heat of the temperature T is found, and the low-temperature case in which for the specific heat of thin films with few monoatomic layers a T^2 dependence is found. Finally the dependence of the specific heat on the thickness is considered and it is shown that for large thickness, which corresponds to the solid body, the well-known T^3 dependence of the specific heat is obtained.

As it is known, the theoretical study of the specific heat is based on the calculation of vibrational modes of the solid. In the same manner it is possible to calculate the specific heat of thin films if the vibrational spectrum has been obtained.

In the literature it is the custom when dealing with thin films to use the results obtained in the study of solid bodies and make insignificant modifications of some constants, such as Debye temperature, Curie temperature, etc. This method is not very accurate because the thin film has its characteristic particularities, its specific heat directly depending on the lattice type, the substrate and especially the number q of monoatomic layers of the film.

So as to be able to give a theoretical foundation of the specific heat in thin films it is necessary to study previously the thermal vibrations in these. An important work in this field is MONTROLL's paper [1], in which a theoretical study of thermal vibrations in an ideal bidimensional lattice is given. Unfortunately, in this article only the vibrations within the bidimensional lattice are studied, without taking into account the vibrations normal to the lattice, nor the influence of the substrate.

In a previous paper of CORCIOVEI and BERINDE [2], a thermal vibrational model of simple cubic thin films with q monoatomic layers was developed. It has thus become possible to deal with the problem of the specific heat of thin films, and this is the aim of our paper. After giving a general expression for the specific heat of a thin film with q layers, so as to obtain more conclusive results, two limiting cases are treated, i.e. the case of high and that of low temperatures.

1. Thermal vibrations in thin films

We shall consider the thin film to be a simple cubic lattice, one of the cube planes, namely (001), being parallel to the film plane. The film contains q monoatomic layers, each layer being a square having N atoms along one of its sides. The total number of atoms of the film is N^2q. Each atom can be denoted by the number n of the layer to which it belongs and by its position vector within the considered layer:

$$\mathbf{j} = a(j_x \mathbf{i}_x + j_y \mathbf{i}_y), \tag{1}$$

where a is the lattice constant, j_x, j_y integers and $\mathbf{i}_x$, $\mathbf{i}_y$, $\mathbf{i}_z$ the unit vectors of the three directions of the lattice. The position of the nj atom at the time t will be given by*

$$\mathbf{r}_{n\mathbf{j}} = a(j_x \mathbf{i}_x + j_y \mathbf{i}_y + n\mathbf{i}_z) + \mathbf{u}_{n\mathbf{j}}(t), \tag{2}$$

where $\mathbf{u}_{nj}(t)$ is the displacement of the atom with respect to its equilibrium position.

By assuming that the forces are elastic, the equations of motion may be written in the following form:

$$\begin{aligned}
M\mathbf{u}_{1\mathbf{j}} &= \sum_{\mathbf{j}'} A^{11}_{\mathbf{j}\mathbf{j}'} u_{1\mathbf{j}'} + \sum_{\mathbf{j}'} A^{12}_{\mathbf{j}\mathbf{j}'} u_{2\mathbf{j}'}, \\
M\mathbf{u}_{2\mathbf{j}} &= \sum_{\mathbf{j}'} A^{21}_{\mathbf{j}\mathbf{j}'} u_{1\mathbf{j}'} + \sum_{\mathbf{j}'} A^{22}_{\mathbf{j}\mathbf{j}'} u_{2\mathbf{j}'} + \sum_{\mathbf{j}'} A^{23}_{\mathbf{j}\mathbf{j}'} u_{3\mathbf{j}'}, \\
&\cdots\cdots\cdots\cdots\cdots\cdots\cdots\cdots\cdots\cdots \\
M\mathbf{u}_{q-1,\mathbf{j}} &= \sum_{\mathbf{j}'} A^{q-1,q-2}_{\mathbf{j}\mathbf{j}'} u_{q-2,\mathbf{j}'} + \sum_{\mathbf{j}'} A^{q-1,q-1}_{\mathbf{j}\mathbf{j}'} u_{q-1,\mathbf{j}'} + \sum_{\mathbf{j}'} A^{q-1,q}_{\mathbf{j}\mathbf{j}'} u_{q\mathbf{j}'}, \\
M\mathbf{u}_{q\mathbf{j}} &= \sum_{\mathbf{j}'} A^{q,q-1}_{\mathbf{j}\mathbf{j}'} u_{q-1,\mathbf{j}'} + \sum_{\mathbf{j}'} A^{qq}_{\mathbf{j}\mathbf{j}'} u_{q\mathbf{j}'},
\end{aligned} \tag{3}$$

where $\mathrm{A}_{\mathbf{j}\mathbf{j}'}$ generally represents tensors which determine the constants of the interaction forces. We note that we have neglected $\mathrm{A}^{n,n\pm m}_{\mathbf{j}\mathbf{j}'}$ with $m \geqslant 2$. It should be noted that the particularities connected with thin films are included in (3) by the fact that the equations for the atomic vibrations in various layers are different.

Taking into account the bidimensional periodicity of the lattice, a particular solution of eqs. (3) can be written in the form

* The lattice constant a may be a little different in the Oz direction from those in the Ox and Oy directions, and thus the lattice will be no more perfectly cubic. This situation, as will be seen in the following, can modify the force constants in the Oz direction as compared to those in the Ox and Oy direction.

$$\mathbf{u}_{nj} = \mathbf{e}_n \exp\, i\,(\mathbf{fj} - \omega t)\,, \tag{4}$$

where $\mathbf{e}_n$ is a polarization vector associated with the n layer, ω is the frequency and $\mathbf{f}$ is the propagation vector in the plane of the film, which is of the form

$$\mathbf{f} = f_x \mathbf{i}_x + f_y \mathbf{i}_y = \frac{2\pi}{Na}(m_x \mathbf{i}_x + m_y \mathbf{i}_y)\,, \tag{5}$$

where m_x and m_y are integers so that $-N/2 < m_x, m_y < N/2$. By introducing the solution (4) into the eqs. (3), the following equations are obtained:

$$\begin{aligned}
-M\omega^2 \mathbf{e}_1 \cdot e^{i\mathbf{fj}} &= \sum_{\mathbf{j}'} A_{\mathbf{jj}'}^{11} \mathbf{e}_1 \cdot e^{i\mathbf{fj}'} + \sum_{\mathbf{j}'} A_{\mathbf{jj}'}^{12} \mathbf{e}_2 \cdot e^{i\mathbf{fj}'}\,,\\
-M\omega^2 \mathbf{e}_2 \cdot e^{i\mathbf{fj}} &= \sum_{\mathbf{j}'} A_{\mathbf{jj}'}^{21} \mathbf{e}_1 \cdot e^{i\mathbf{fj}'} + \sum_{\mathbf{j}'} A_{\mathbf{jj}'}^{22} \mathbf{e}_2 \cdot e^{i\mathbf{fj}'} + \sum_{\mathbf{j}'} A_{\mathbf{jj}'}^{23} \mathbf{e}_3 \cdot e^{i\mathbf{fj}'}\,,\\
&\cdots\cdots\cdots\cdots\cdots\cdots\cdots\cdots\cdots\\
-M\omega^2 \mathbf{e}_{q-1} \cdot e^{i\mathbf{fj}} &= \sum_{\mathbf{j}'} A_{\mathbf{jj}'}^{q-1,q-2} \mathbf{e}_{q-2}\, e^{i\mathbf{fj}} +\\
&\quad + \sum_{\mathbf{j}'} A_{\mathbf{jj}'}^{q-1,q-1} \mathbf{e}_{q-1}\, e^{i\mathbf{fj}'} + \sum_{\mathbf{j}'} A_{\mathbf{jj}'}^{q-1,q} \mathbf{e}_q \cdot e^{i\mathbf{fj}'}\,,\\
-M\omega^2 \mathbf{e}_q\, e^{i\mathbf{fj}} &= \sum_{\mathbf{j}'} A_{\mathbf{jj}'}^{q,q-1} \mathbf{e}_{q-1}\, e^{i\mathbf{fj}'} + \sum_{\mathbf{j}'} A_{\mathbf{jj}'}^{qq} \mathbf{e}_q \cdot e^{i\mathbf{fj}'}\,.
\end{aligned} \tag{6}$$

We mention that in (6) each $\mathbf{j}$ belongs to the layer specified by the corresponding e_n, and the summation is to be carried out accordingly.

So as to solve (6) one can make some simplifying assumptions. For example one can consider as significant forces only the forces between the nearest neighbouring atoms, and so neglect all $A_{\mathbf{jj}'}^{nn'}$ where $\mathbf{j}'$is not a nearest neighbour of j. In more refined calculations one could take into account also forces between more distant neighbours. For our purposes this is not necessary.

A method for calculating the dispersion relations is to project the system (6) in the directions $\mathbf{i}_x$, $\mathbf{i}_y$ and $\mathbf{i}_z$ and to set the condition that the components of the vectors $\mathbf{e}_n$ are different from zero, whence the vanishing of the determinant of coefficients results. In this way one obtains the secular equation for ω^2, and thus for every $\mathbf{f}$ we obtain $3q$ positive solutions for ω, denoted by $\omega(\mathbf{f}, \nu, s)$, where s takes the values 1, 2, 3, just as in the case of solid bodies with one atom in each unit cell, and ν takes the values 1, 2, . . ., q as we should have a solid with q different atoms in each unit cell.

In this manner in the case of thin films we obtain $3qN^2$ modes of vibration. In some special cases we may have degeneracies with respect to s, i.e. we may have $\omega(\mathbf{f}, \nu, 1) = \omega(\mathbf{f}, \nu, 2) = \omega(\mathbf{f}, \nu, 3)$. In such a case the "transversal" vibrations and the "longitudinal" vibration for a given $\mathbf{f}$ and ν have the same frequency. As it is known this is not the general case. In the following we shall consider that we have no degeneracy with respect to s, and also that we have no pure "longitudinal" and "transversal" vibrations. A full discussion about

such problems can be found in [2]. We note that the general solution $\mathbf{u}_{nj}$ can be written as a sum of expressions (4) for all possible values of $\mathbf{f}$, v and s.

Now, so as to obtain some more practical solutions we shall assume that the tensors $A_{jj'}^{nn'}$ are diagonal, which means that the force exerted by the j′th atom from the n'th layer on the jth atom of the nth layer has the same direction as the displacement of the j′th atom. In connection with the displacement of the j′th atom of the n'th layer along $\mathbf{i}_x$, we shall denote by A_0 the corresponding diagonal element of $A_{j'j'}^{n'n'}$, by A_1 the corresponding diagonal element of $A_{j'\pm a^i x,j'}^{n'n'}$, by A_2 the diagonal element of $A_{j'\pm a^i y,j'}^{n'n'}$, and by A_2' the diagonal element of $A_{j'\pm a^i z,j'}^{n'\pm 1,n'}$. In the case of the displacement of the j′th atom along $\mathbf{i}_y$ the notations will be analogous to the preceding ones if everywhere $\mathbf{i}_y$ is replaced by $\mathbf{i}_x$ and $\mathbf{i}_x$ by $\mathbf{i}_y$. In the case of the displacement of j′ along $\mathbf{i}_z$ we shall denote by B_0 the diagonal element of $A_{j'j'}^{n'n'}$, by B_1 the diagonal element of $A_{j'\pm a^i z,j'}^{n'\pm 1,n'}$, and by B_2 the diagonal element of $A_{j'\pm a^i y,j'}^{n'n'}$ or $A_{j'\pm a^i y,j'}^{n'n'}$.

We observe that A_0 and B_0 belonging to different atoms situated in different layers can be obtained by means of A_1, A_2, A_2', respectively B_1 and B_2, as a consequence of equilibrium conditions. If the atom is situated in the layer in contact with the substrate, in A_0 and B_0 will appear also the contribution of the substrate force, which we denote by A_p, respectively B_p for the directions $\mathbf{i}_x$ and $\mathbf{i}_y$, respectively $\mathbf{i}_z$. A full discussion is given in [2].

Using the preceding notations, it is possible to write the dispersion relations in the following form:

$$\omega(\mathbf{f}, v, s=1) = \frac{1}{\sqrt{M}}\left[2A_1(1-\cos f_x a) + 2A_2(1-\cos f_y a) + A_2' Z_v\right]^{1/2},$$

$$\omega(\mathbf{f}, v, s=2) = \frac{1}{\sqrt{M}}\left[2A_2(1-\cos f_x a) + 2A_1(1-\cos f_y a) + A_2' Z_v\right]^{1/2}, \qquad (7)$$

$$\omega(\mathbf{f}, v, s=3) = \frac{1}{\sqrt{M}}\left[2B_2(2-\cos f_x a - \cos f_y a) + B_1 Z_v\right]^{1/2},$$

where the q values of Z_v can be obtained by solving the equation

$$\begin{vmatrix}
Z-1 & 1 & 0 & 0 & \dots & 0 \\
1 & Z-2 & 1 & 0 & \dots & 0 \\
0 & 1 & Z-2 & 1 & \dots & 0 \\
0 & 0 & 1 & Z-2 & \dots & 0 \\
\cdot & \cdot & \cdot & \cdot & \cdot & \cdot \\
0 & \dots & Z-2 & 1 & 0 & 0 \\
0 & \dots & 1 & Z-2 & 1 & 0 \\
0 & \dots & 0 & 1 & Z-2 & 1 \\
0 & \dots & 0 & 0 & 1 & Z-1-\alpha
\end{vmatrix} = 0, \qquad (8)$$

where $\alpha = A_p/A_2'$ for the case $s = 1, 2$ and $\alpha = B_p/B_1$ for the case $s = 3$. We note that in the case $q = 1$ we obtain the equation $Z - \alpha = 0$. In [2] are given the solutions of (8) in the approximation $\alpha = 0$, from $q = 2$ to $q = 6$. It is also shown that when α is smaller than 1, it is sufficient for practical purposes to introduce a correction α/q to all the values of Z_ν which have been obtained in the approximation $\alpha = 0$. The values of Z_ν in the approximation $\alpha = 0$ for $q = 1$ to $q = 5$ are given in Table 1.

Table 1

q	1	2		3			4				5				
ν	1	1	2	1	2	3	1	2	3	4	1	2	3	4	5
Z_ν	0	0	2	0	1	3	0	$2-\sqrt{2}$	2	$2+\sqrt{2}$	0	$\frac{1}{2}(3-\sqrt{5}$	$\frac{1}{2}(5-\sqrt{5})$	$\frac{1}{2}(3+\sqrt{5})$	$\frac{1}{2}(5+\sqrt{5})$

For high values of q it is possible to obtain the dispersion relations in the form

$$\begin{aligned}
\omega(\mathbf{f}, \nu, s = 1) &= \frac{1}{\sqrt{M}}\left[2A_1(1 - \cos f_x a) + 2A_2(1 - \cos f_y a) + \right. \\
&\qquad \left. + 2A_2'(1 - \cos f_z a)\right]^{1/2}, \\
\omega(\mathbf{f}, \nu, s = 2) &= \frac{1}{\sqrt{M}}\left[2A_2(1 - \cos f_x a) + 2A_2(1 - \cos f_y a) + \right. \\
&\qquad \left. + 2A_2'(1 - \cos f_z a)\right]^{1/2}, \\
\omega(\mathbf{f}, \nu, s = 3) &= \frac{1}{\sqrt{M}}\left[2B_2(2 - \cos f_x a - \cos f_y a) + \right. \\
&\qquad \left. + 2B_1(1 - \cos f_z a)\right]^{1/2},
\end{aligned} \tag{9}$$

where we have introduced $f_z = (2\pi/qa)\, m_z$ and where m_z is an integer between $-q/2$ and $+q/2$. Evidently the correspondence

$$Z_\nu \to 2(1 - \cos f_z a) \tag{10}$$

exists for high values of q. Also, for the solid body evidently there is

$$A_1 = B_1\,; \quad A_2 = A_2' = B_2\,, \tag{10'}$$

so that the dispersion relations (9) take a more symmetric form. In the case of thin films, these relations hold approximately, but we can maintain them so as to simplify the calculation.

2. Specific heats of thin films

In the preceding paragraph a short account of the features of thermal vibrations in thin films was given. It was possible to obtain $3N^2q$ independent oscillators, each characterized by a frequency $\omega = \omega(\mathbf{f}, \nu, s)$. When we calculate the thermal energy of the thin film, we must take into account the contributions of all oscillators. In this way the energy of the thin film is

$$E = \frac{S}{4\pi^2} \sum_{s=1}^{3} \sum_{\nu=1}^{q} \int_{-\pi/a}^{+\pi/a} \int_{-\pi/a}^{+\pi/a} \frac{\hbar\omega}{e^{\frac{\hbar\omega}{kT}} - 1} \, df_x \, df_y , \tag{11}$$

where the ω are given by (7) and $S = N^2a^2$ is the surface of the thin film.

The integrals which appear in (11) are of the same type. We shall treat for example the case $s = 1$. The integral then reads:

$$I_\nu = \int_{-\pi/a}^{+\pi/a} \int_{-\pi/a}^{+\pi/a} \frac{\frac{\hbar}{\sqrt{M}} \left(4A_1 \sin^2 \frac{f_x a}{2} + 4A_2 \sin^2 \frac{f_y a}{2} + A_2' Z_\nu \right)^{1/2}}{\exp\left[\frac{\hbar}{\sqrt{M} kT} \left(4A_1 \sin^2 \frac{f_x a}{2} + 4A_2 \sin^2 \frac{f_y a}{2} + A_2' Z_\nu \right)^{1/2} \right] - 1} \, df_x \, df_y . \tag{12}$$

It is convenient to make the following changes of variables:

$$f_x = \frac{2}{a} \arcsin\left[\frac{1}{\sqrt{4A_1}} \varrho \cos\Theta \right]; \quad f_y = \frac{2}{a} \arcsin\left[\frac{1}{\sqrt{4A_2}} \varrho \sin\Theta \right] \tag{13}$$

and thus

$$df_x \, df_y = \frac{D(f_x, f_y)}{D(\varrho, \Theta)} \, d\varrho \, d\Theta = \frac{1}{a^2 \sqrt{A_1 A_2}} \cdot \frac{\varrho \, d\varrho \, d\Theta}{\sqrt{\left(1 - \frac{\varrho^2}{4A_1} \cos^2\Theta \right) \left(1 - \frac{\varrho^2}{4A_2} \sin^2\Theta \right)}} .$$

In this way we can write

$$I_\nu = \frac{1}{a^2 \sqrt{A_1 A_2}} \iint \frac{\hbar / \sqrt{M} \, (\varrho^2 + A_2' Z_\nu)^{1/2}}{\exp\left[\frac{\hbar}{\sqrt{M} \cdot kT} (\varrho^2 + A_2' Z_\nu)^{1/2} \right] - 1} \cdot \frac{\varrho \, d\varrho \, d\Theta}{\left[\left(1 - \frac{1}{4A_1} \varrho^2 \cos^2\Theta \right) \left(1 - \frac{1}{4A_2} \varrho^2 \sin^2\Theta \right) \right]^{1/2}} \equiv \iint G_\nu(\varrho, \Theta) \, \varrho \, d\varrho \, d\Theta , \tag{14}$$

where the integration limits must be explained more fully. When we integrate firstly over ϱ and then over Θ, the result is*

$$\iint G_\nu(\varrho,\Theta_\varrho)\,d\varrho\,d\Theta = 4\Bigg[\int_0^{\operatorname{arc\,tg}\sqrt{\frac{A_2}{A_1}}} d\Theta \int_0^{\frac{\sqrt{4A_1}}{\cos\Theta}} G_\nu(\varrho,\Theta)\,\varrho\,d\varrho + \int_{\operatorname{arc\,tg}\sqrt{\frac{A_2}{A_1}}}^{\pi/2} d\Theta \int_0^{\frac{\sqrt{4A_2}}{\sin\Theta}} G_\nu(\varrho,\Theta)\,\varrho\,d\varrho\,, \tag{15}$$

and when we integrate firstly over Θ and then over ϱ the result is

$$\iint G_\nu(\varrho,\Theta)\,\varrho\,d\varrho\,d\Theta = 4\Bigg[\int_0^{\sqrt{4A_2}} \varrho\,d\varrho \int_0^{\pi/2} G_\nu(\varrho,\Theta)\,d\Theta + \int_{\sqrt{4A_2}}^{\sqrt{4A_1}} \varrho\,d\varrho \int_0^{\arcsin\frac{\sqrt{4A_2}}{\varrho}} G_\nu(\varrho,\Theta)\,d\Theta + \int_{\sqrt{4A_1}}^{\sqrt{4(A_1+A_2)}} \varrho\,d\varrho \int_{\arccos\frac{\sqrt{4A_1}}{\varrho}}^{\arcsin\frac{\sqrt{4A_2}}{\varrho}} G_\nu(\varrho,\Theta)\,d\Theta. \tag{15'}$$

In the following it will be more convenient to use formula (15) for the high temperatures case and formula (15′) for the low temperatures case.

At high temperatures we make the common approximation

$$\exp\frac{\hbar\,(\varrho^2 + A_2' Z_\nu)^{1/2}}{\sqrt{M\,kT}} = 1 + \frac{\hbar\,(\varrho^2 + A_2' Z_\nu)^{1/2}}{\sqrt{M}\cdot kT}$$

and in this way I_ν is independent of ν and equal to:

$$I = \frac{4kT}{a^2\sqrt{A_1A_2}}\Bigg[\int_0^{\operatorname{arc\,tg}\sqrt{\frac{A_2}{A_1}}} d\Theta \int_0^{\frac{\sqrt{4A_1}}{\cos\Theta}} \frac{\varrho\,d\varrho}{\left[\left(1-\frac{1}{4A_1}\varrho^2\cos^2\Theta\right)\left(1-\frac{1}{4A_2}\varrho^2\sin^2\Theta\right)\right]^{1/2}} + \int_{\operatorname{arc\,tg}\sqrt{\frac{A_2}{A_1}}}^{\pi/2} d\Theta \int_0^{\frac{\sqrt{4A_2}}{\sin\Theta}} \frac{\varrho\,d\varrho}{\left[\left(1-\frac{1}{4A_1}\varrho^2\cos^2\Theta\right)\left(1-\frac{1}{4A_2}\varrho^2\sin^2\Theta\right)\right]^{1/2}}. \tag{16}$$

* We mention that $A_1 > A_2$. In the integration over ϱ and Θ we must take into account the form of the domain of integration, which is a rectangle with the sides $2\sqrt{4A_1}$ and $2\sqrt{4A_2}$.

By making in the first integral the change of variable

$$\frac{1}{4A_1}\varrho^2\cos^2\Theta = x\,, \qquad \varrho\,d\varrho = \frac{1}{2}\frac{4A_1\,dx}{\cos^2\Theta}$$

we obtain

$$\frac{1}{2}\int_0^{\operatorname{arc\,tg}\sqrt{\frac{A_2}{A_1}}} \frac{4A_1\,d\Theta}{\cos^2\Theta}\left[\sqrt{\frac{A_2}{A_1}}\frac{\cos\Theta}{\sin\Theta}\ln\left(\frac{1+\sqrt{\frac{A_1}{A_2}}\frac{\sin\Theta}{\cos\Theta}}{1-\sqrt{\frac{A_1}{A_2}}\frac{\sin\Theta}{\cos\Theta}}\right)\right], \tag{17}$$

where we have used the integral [3]

$$\int_0^1 \frac{dx}{\sqrt{(1-x)(1-px)}} = \frac{1}{p}\ln\frac{1+p}{1-p}\,.$$

Now the integral (17) may be calculated with the aid of the formula [3]

$$\int_0^1 \frac{1}{x}\ln\frac{1+x}{1-x}\,dx = \frac{\pi^2}{4}\,.$$

By making in (17) the change

$$\sqrt{\frac{A_1}{A_2}}\operatorname{tg}\Theta = \varkappa$$

the result is

$$\frac{\sqrt{A_1 A_2}\,\pi^2}{2}\,.$$

The second integral of (16) can be calculated in a similar manner, it is found to be equal to the first. The final result is

$$I = 4\frac{kT}{a^2}\pi^2. \tag{18}$$

In the same manner the integrals corresponding to $s = 2$ and $s = 3$ may be obtained. By performing the summation over s and ν we obtain or the energy of the thin film at high temperatures:

$$E = 3N^2 q\ kT. \tag{19}$$

This result means that the specific heat per unit volume at high temperatures is independent of T and q.

It is interesting to note that at high temperatures the mathematical task can be accomplished also by means of formula (15′) and one obtains the same result. The proof is given in the Appendix.

More interesting is the case of low temperatures. In order to calculate the energy and the specific heat of the thin film for low temperatures it is more convenient, for mathematical purposes, to use the formula (15′). In this way we must calculate three integrals instead of one. If we make in (15′) the change of variable

$$\frac{1}{4A_2}\varrho^2 \sin^2\Theta = x\,, \qquad d\Theta = \frac{1}{2}\,\frac{dx}{\sqrt{\varkappa\left(\frac{\varrho^2}{4A_2} - x\right)}}$$

we obtain the following expressions

$$I_{v2} = \frac{2}{a^2 A_2}\int_0^{\sqrt{4A_2}} \frac{\frac{\hbar}{\sqrt{M}}(\varrho^2 + A_2' Z_v)^{1/2}}{\exp\left[\frac{\hbar}{\sqrt{M}\,kT}(\varrho^2 + A_2' Z_v)^{1/2}\right] - 1}\,\varrho\,d\varrho \times \tag{20}$$

$$\times \int_0^{\varrho^2/\sqrt{4A_2}} \frac{dx}{\sqrt{\varkappa(1-x)(\varrho^2/4A_2 - x)\left(x - \frac{\varrho^2 - 4A_1}{4A_2}\right)}}\,,$$

$$I_{v2} = \frac{2}{a^2 A_2}\int_{\sqrt{4A_2}}^{\sqrt{4A_1}} \frac{\frac{\hbar}{\sqrt{M}}(\varrho^2 + A_2' Z_v)^{1/2}}{\exp\left[\frac{\hbar}{\sqrt{M}\,kT}(\varrho^2 + A_2' Z_v)^{1/2}\right] - 1}\,\varrho\,d\varrho \times \tag{20′}$$

$$\times \int_0^{1} \frac{dx}{\sqrt{x(1-x)(\varrho^2/4A_2 - x)\left(x - \frac{\varrho^2 - 4A_1}{4A_2}\right)}}\,,$$

$$I_{v3} = \frac{2}{a^2 A_2}\int_{\sqrt{4A_1}}^{\sqrt{4(A_1+A_2)}} \frac{\frac{\hbar}{\sqrt{M}}(\varrho^2 + A_2' Z_v)^{1/2}}{\exp\left[\frac{\hbar}{\sqrt{M}\,kT}(\varrho^2 + A_2' Z_v)^{1/2}\right] - 1}\,\varrho\,d\varrho \times \tag{20″}$$

$$\times \int_{\frac{\varrho^2 - 4A_1}{4A_2}}^{1} \frac{dx}{\sqrt{x(1-x)(\varrho^2/4A_2 - x)\left(x - \frac{\varrho^2 - 4A_1}{4A_2}\right)}}\,.$$

The integration over the variable x can be easily performed if we take into account the general formula [3]

$$\int_u^\beta \frac{dx}{\sqrt{(\alpha - x)(\beta - x)(x - \gamma)(x - \delta)}} = \frac{2}{\sqrt{(\alpha - \gamma)(\beta - \delta)}} \times$$
$$\times F\left(\arcsin \sqrt{\frac{(\alpha - \gamma)(\beta - u)}{(\beta - \gamma)(\alpha - u)}}, \sqrt{\frac{(\beta - \gamma)(\alpha - \delta)}{(\alpha - \gamma)(\beta - \delta)}}\right) \quad (21)$$

which is applicable with the conditions

$$\delta < \gamma < \beta < \alpha \quad (22)$$

and

$$\gamma \leq u < \beta, \quad (22')$$

where $F(\varphi, k)$ is the eliptic integral of the first kind, namely

$$F(\varphi, k) = \int_0^\varphi \frac{d\alpha}{\sqrt{1 - k^2 \sin^2 \alpha}} = \int_0^{\sin\varphi} \frac{dx}{\sqrt{(1 - x^2)(1 - k^2 x^2)}}. \quad (23)$$

In the following will appear also the function $K(k)$, which is defined in the following way:

$$K(k) = F\left(\frac{\pi}{2}, k\right) = \int_0^{\pi/2} \frac{dx}{\sqrt{(1 - x^2)(1 - k^2 x^2)}}. \quad (24)$$

It is not difficult to show that

$$I_{\nu 1} = \frac{4}{a^2 \sqrt{A_1 A_2}} \int_0^{\sqrt{4A_2}} \frac{\frac{\hbar}{\sqrt{M}} (\varrho^2 + A_2' Z_\nu)^{1/2}}{\exp\left[\frac{\hbar}{\sqrt{M} \cdot kT} (\varrho^2 + A_2' Z_\nu)^{1/2}\right] - 1} \times$$
$$\times F\left(\frac{\pi}{2}, \sqrt{\frac{4(A_1 + A_2) - \varrho^2}{16 A_1 A_2} \cdot \varrho^2}\right) \varrho \, d\varrho, \quad (25)$$

because in this case we have

$$\frac{\varrho^2 - 4A_1}{4A_2} < 0 < \frac{\varrho^2}{4A_2} < 1.$$

In this manner we can write also

$$I_{\nu 2} = \frac{16}{a^2} \int_{\sqrt{4A_2}}^{\sqrt{4A_1}} \frac{\frac{\hbar}{\sqrt{M}} (\varrho^2 + A_2' Z_\nu)^{1/2}}{\exp\left[\frac{\hbar}{\sqrt{M}\, kT} (\varrho^2 + A_2' Z_\nu)^{1/2}\right] - 1} \times$$
$$\times F\left(\frac{\pi}{2}, \sqrt{\frac{16 A_1 A_2}{\varrho^2 [4 (A_1 + A_2) - \varrho^2]}}\right) \frac{\varrho\, d\varrho}{\sqrt{\varrho^2 [4 (A_1 + A_2) - \varrho^2]}} \tag{25'}$$

since in this case the order of parameters is

$$\frac{\varrho^2 - 4A_1}{4A_2} < 0 < 1 < \frac{\varrho^2}{4A_2}$$

and similarly

$$I_{\nu 3} = \frac{4}{a^2 \sqrt{A_1 A_2}} \int_{\sqrt{4A_1}}^{\sqrt{4(A_1 + A_2)}} \frac{\frac{\hbar}{\sqrt{M}} (\varrho^2 + A_2' Z_\nu)^{1/2}}{\exp\left[\frac{\hbar}{\sqrt{M}\, kT} (\varrho^2 + A_2' Z_\nu)^{1/2}\right] - 1} \times$$
$$\times F\left(\frac{\pi}{2}, \sqrt{\frac{4 (A_1 + A_2) - \varrho^2}{16 A_1 A_2} \cdot \varrho^2}\right) \varrho d\varrho\,, \tag{25''}$$

because

$$0 < \frac{\varrho^2 - 4A_1}{4A_2} < 1 < \frac{\varrho^2}{4A_2}\,.$$

In order to perform the calculation more easily, we shall suppose $A_1 = A_2' = A$. Similarly we shall suppose $B_1 = B_2 = B$. This hypothesis is not too restrictive because the force constants characterized by these quantities are of the same order of magnitude. In this way the integral (25'), which is the most difficult, vanishes. Further it is now possible to write the integrals I_1 and I_3 in a single integral

$$I_\nu = I_{\nu 1} + I_{\nu 2} + I_{\nu 3} = \frac{4}{a^2 A} \int_0^{\sqrt{8A}} \frac{\frac{\hbar}{\sqrt{M}} (\varrho^2 + A Z_\nu)^{1/2}}{\exp\left[\frac{\hbar}{\sqrt{M}\, kT} (\varrho^2 + A Z_\nu)^{1/2}\right] - 1} \times$$
$$\times F\left(\frac{\pi}{2}, \sqrt{\frac{8A - \varrho^2}{16 A^2} \cdot \varrho^2}\right) \varrho d\varrho\,. \tag{26}$$

We note that in (24) the quantity $\frac{8A-\varrho^2}{16\,A^2}\cdot\varrho^2$ is less then unity.* It is possible to carry out the integration over ϱ by expanding firstly the eliptic integral in a series. Considering that

$$K(k)=\frac{\pi}{2}\left[1+\left(\frac{1}{1.2}\right)^2k^2+\left(\frac{1.3}{2.4}\right)^2k^4+\ldots\right] \tag{27}$$

it may be easily seen that such an expansion leads to a series of integrals with different powers of ϱ. We shall consider only the first term, because the others express the contributions to the energy in increasing powers of T, and thus the significant term at low temperatures is only the first term. In this way we can replace $F\left(\frac{\pi}{2},\ k\right)$ by $\frac{\pi}{2}$ and the result is the following:

$$I_\nu=\frac{2\pi}{a^2A}\int_0^{\sqrt{8A}}\frac{\frac{\hbar}{\sqrt{M}}(\varrho^2+AZ_\nu)^{1/2}}{\exp\left[\frac{\hbar}{\sqrt{M}\,kT}(\varrho^2+A'Z_\nu)^{1/2}\right]-1}\,\varrho d\varrho. \tag{28}$$

If we make the change of variable

$$\frac{\hbar\,(\varrho^2+AZ_\nu)^{1/2}}{\sqrt{M}\,kT}=x$$

we obtain

$$I_\nu=\frac{2\pi}{a^2}\,\frac{M\,(kT)^3}{A\hbar^2}\int_{\sqrt{AZ_\nu}\frac{\hbar}{\sqrt{M}kT}}^{\sqrt{8A+AZ_\nu}\frac{\hbar}{\sqrt{M}kT}}\frac{x^2\,dx}{e^x-1}\,. \tag{29}$$

The energy of the thin film is now given by the sum

$$\frac{S}{4\pi^2}\sum\left[2\,I_\nu(A)+I_\nu(B)\right]$$

* In the same manner it can be shown that the quantity $\frac{4\,(A_1+A_2)-\varrho^2}{16\,A_1A_2}\varrho^2$ in (25) and (25″) is less than unity. In (25′) the reversed quantity $\frac{16\,A_1A_2}{\varrho^2\,[4(A_1+A_2)-\varrho^2]}$ in the corresponding interval remains also less than unity.

over all the contributions corresponding to various Z_ν, where ν takes the values $1, 2, \ldots, q$ and $s = 1, 2$ and 3. The expression of the energy is the following

$$E = \frac{S}{4\pi^2} \sum_{\nu=1}^{1} \frac{2\pi M (kT)^3}{a^2 A\hbar^2} \left[2 \int_{\sqrt{AZ_\nu}\frac{\hbar}{\sqrt{M}kT}}^{\sqrt{8A+AZ_\nu}\frac{\hbar}{\sqrt{M}kT}} \frac{x^2\,dx}{e^x - 1} + \int_{\sqrt{BZ_\nu}\frac{\hbar}{\sqrt{M}kT}}^{\sqrt{zB+BZ_\nu}\frac{\hbar}{\sqrt{M}kT}} \frac{x^2\,dx}{e^x - 1} \right]. \quad (30)$$

Now, as it is known

$$\frac{x^2}{e^x - 1} = \frac{x^2\, e^{-x}}{1 - e^{-x}} = x^2\, e^{-x} (1 + e^{-x} + e^{-2x} + \ldots),$$

because at low temperatures x is a large quantity and thus we can expand $1/1 - e^{-x}$ in series. The only significant term in the integral

$$\int_a^\beta (x^2\, e^{-x} + x^2\, e^{-2x} + \ldots)\, dx \quad (31)$$

is the first one. In fact, the value of the integral (31) when the lower limit is zero, and the upper limit is ∞, is*

$$2 \sum_{k=1}^{\infty} \frac{1}{k^3} = 2\zeta(3) = 2{,}404$$

and when one retains only the first term the result is 2. The case is similar for the integral (31). We remark that all our approximations are introduced so as to overcome mathematical difficulties. It is clear that these approximations do not modify the general features of the problem. We have

$$\int x^2\, e^{-x}\, dx = -x^2\, e^{-x} - 2\, xe^{-x} - 2e^{-x}.$$

By performing now the calculation it is possible to write the energy of the thin film at low temperatures in the form:

$$E = \frac{N^2}{2\pi} \frac{M (kT)^3}{\hbar^2} \sum_{\nu=1}^{q} \left\{ \frac{2}{A} \left[\left(\frac{\hbar}{kT} \right)^2 \frac{AZ_\nu}{M} \exp\left(- \frac{\hbar}{kT} \sqrt{\frac{AZ_\nu}{M}} \right) - \right. \right.$$

$$\left. \left. - \left(\frac{\hbar}{kT} \right)^2 \frac{A(8 + Z_\nu)}{M} \exp\left(- \frac{\hbar}{kT} \sqrt{\frac{A(8 + Z_\nu)}{M}} \right) + \right. \right.$$

* $\zeta(z)$ is Riemann's function.

$$+2\frac{\hbar}{kT}\sqrt{\frac{AZ_\nu}{M}}\exp\left(-\frac{\hbar}{kT}\sqrt{\frac{AZ_\nu}{M}}\right)-$$

$$-2\frac{\hbar}{kT}\sqrt{\frac{A(8+Z_\nu)}{M}}\exp\left(-\frac{\hbar}{kT}\sqrt{\frac{A(8+Z_\nu)}{M}}\right)+$$

$$+2\exp\left(-\frac{\hbar}{kT}\sqrt{\frac{AZ_\nu}{M}}\right)-2\exp\left(-\frac{\hbar}{kT}\sqrt{\frac{A(8+Z_\nu)}{M}}\right)\Bigg]+ \tag{32}$$

$$+\frac{1}{B}\left[\left(\frac{\hbar}{kT}\right)^2\frac{BZ_\nu}{M}\exp\left(-\frac{\hbar}{kT}\sqrt{\frac{BZ_\iota}{M}}\right)-\right.$$

$$-\left(\frac{\hbar}{kT}\right)^2\frac{B(8+Z_\iota)}{M}\exp\left(-\frac{\hbar}{kT}\sqrt{\frac{B(8+Z_\nu)}{M}}\right)\Bigg]+2\left(\frac{\hbar}{kT}\sqrt{\frac{BZ_\nu}{M}}\right)-$$

$$-2\frac{\hbar}{kT}\sqrt{\frac{B(8+Z_\nu)}{M}}\exp\left(-\frac{\hbar}{kT}\sqrt{\frac{B(8+Z_\nu)}{M}}\right)+$$

$$\left.+2\exp\left(-\frac{\hbar}{kT}\sqrt{\frac{BZ_\nu}{M}}\right)-2\exp\left(-\frac{\hbar}{kT}\sqrt{\frac{B(8+Z_\nu)}{M}}\right)\right]\Bigg\}.$$

Of course we can further simplify the results by putting $A = B$. The formula (32) is the general result at low temperatures. So as to obtain the values of the energy for thin films with various q it is necessary for every q to introduce in the expression (32) the values of Z_ν corresponding to q. This is in fact possible for small q, when the solutions of the secular equ. (8) are known. The problem can be solved also for a larger q, using the electronic computer. Evidently for large q the formula (32) has to go over into the known formula corresponding to the solid body. We shall briefly discuss the case q very small and q very large.

The case q very small may be illustrated by taking $q = 1$. This case is evidently a mathematical case, but at low temperatures it gives the behaviour of energy, and thus of specific heat in dependence on temperature. So as to study the ideal case, we shall neglect in the expression of Z the contribution of the substrate. It is easy to show that one obtains

$$E = 2{,}404\,\frac{3N^2}{2\pi}\,\frac{M(kT)^3}{A\hbar^2} \tag{33}$$

and thus the specific heat increases with the square of the temperature at low temperatures. This limiting result was to be expected for an ideal square lattice, and evidently it is valid in the case of a thin film with very small q, when the influence of the substrate is insignificant. When the thin film is deposited on a substrate so that the binding force exerted on it is very high, the specific heat of the thin film diminishes because in the formulae for the energy Z_ν

is never zero. As it is known when q is large the influence of the substrate is no longer significant,and the values taken by Z_ν are very near to the one obtained from (8) when $\alpha = 0$.

In the case of high q, as was shown in the first paragraph, instead of z_ν we can introduce (10), namely

$$2\,(1 - \cos f_z a) = 4 \sin^2 \frac{f_z a}{2} .$$

In this manner the summation over Z_ν in (32) may be replaced by an integral, and thus we shall write

$$\sum_{\nu=1}^{q} \int_{\frac{\hbar}{kT}\sqrt{\frac{\bar{A}Z_\nu}{M}}}^{\frac{\hbar}{kT}\sqrt{\frac{\bar{A}(8+Z_\nu)}{M}}} x^2 e^{-x}\,dx \to 2\,(qa)\,\frac{1}{2\pi}\left(\frac{2}{a}\right)\int_0^{\pi/2} dy \int_{\frac{b}{T}\sin y}^{\frac{b}{T}\sqrt{2+\sin^2 y}} x^2 e^{-x}\,dx ,$$

where we have denoted by b the quantity $2\hbar\sqrt{\bar{A}}/k\sqrt{\bar{M}}$ and where

$$y = \frac{f_z a}{2} .$$

Performing the integration in the expression for the energy we can write

$$\int_0^{\pi/2} [x^2 e^{-x} + 2xe^{-z} + 2e^{-x}]_{\frac{b}{T}\sin y}^{\frac{b}{T}\sqrt{2+\sin^2 y}} dy =$$

$$= \int_0^{\pi/2} \left(\frac{b^2}{T^2}\sin^2 y + 2\,\frac{b}{T}\sin y + 2\right) e^{-\frac{b}{T}\sin y} \cdot dy -$$

$$- \int_0^{\pi/2} \left[\frac{b^2}{T^2}\,(2 + \sin^2 y) + 2\,\frac{b}{T}\sqrt{2+\sin^2 y} + 2\right] e^{-\frac{b}{T}\sqrt{2+\sin^2 y}}\,dy$$

and by using convenient substitutions we obtain:

$$\frac{T}{b} = \int_0^{\frac{b}{T}} (u^2 e^{-u} + 2ue^{-u} + 2e^{-u})\,\frac{du}{\sqrt{1 - \frac{T^2}{b^2}u^2}} - \frac{T^2}{b^2}\int_{\frac{b}{T}\sqrt{2}}^{\frac{b}{T}\sqrt{3}} (v^2 e^{-v} + 2ve^{-v} + 2e^{-v}) \times$$

$$\times \frac{dv}{\sqrt{\left(\frac{T^2 v^2}{b^2} - 2\right)\left(3 - \frac{T^2 v^2}{b^2}\right)}} .$$

At low temperatures only the lowest power in T is significant. Such a contribution is furnished by the first term and in this way for low temperatures in the case of very large values of q one obtains

$$E = 9\frac{N^2 q}{\pi^2}\left(\frac{M}{A\hbar^2}\right)^{3/2}(kT)^4. \tag{34}$$

As it can be seen we have obtained the T^4 dependence of the energy and even the numerical constant is practically the same as the constant obtained with the aid of Debye's method in [4] where, of course, the expression for the Debye temperature,* has to be introduced. In (34) q is of the same order as N. In order to obtain the specific heat, we must take the derivative of (34) with respect to T and the well-known dependence in T^3 is obtained.

In this way we have demonstrated that the general expression (32) shows a T^3 dependence for small values of q and a T^4 dependence for high values of q. As we have pointed out the low-temperature dependence is very much influenced by the presence of the substrate.

Unfortunately, up to the present time, even for moderate values of q, there are no experimental determinations of the specific heat of thin films, neither in the high nor in the low temperature range. It may be remarked that the great difficulty in such kinds of experiments is caused by the presence of the substrate, because the specific heat of the substrate alone has to be determined as well as the specific heat of the substrate together with the thin film. Of course these experiments are very difficult because one must employ very sensitive microcalorimeters and a very accurate experimental technique.

The difficulty arising from the fact that the film is very thin may be overcome by enlarging its surface in such a way that its weight allows the measurement of the corresponding specific heat variations. A simple calculation shows that for high temperatures, using the modern technique of microcalorimeters [5] such determinations are possible, even for thin films with q of the order of 100.

Finally we note that at low temperatures, one must take into account also the contribution of the electronic specific heat, just as in the case of the solid body.

Appendix

We shall show that, for the high temperature case, the integration performed with the aid of formula (15′) leads to the same result as when using the formula (15). For simplicity, we shall suppose from the start $A_1 = A_2$, in order to simplify the calculations. In this way we obtain:

* See for example the formulae (6.32) (6.30) and (5.9) in [4].

$$\iint G(\varrho,\Theta)\,\varrho\,d\varrho\,d\Theta = 4\left[\int_0^{\sqrt{4A}} \varrho\,d\varrho \int_0^{\pi/2} G(\varrho,\Theta)\,d\Theta + \int_{\sqrt{4A}}^{\sqrt{8A}} \varrho\,d\varrho \int_{\arccos\sqrt{4A}/\varrho}^{\operatorname{arc\,sin}\sqrt{4A}/\varrho} G(\varrho,\Theta)\,d\Theta\right],$$

where

$$G(\varrho,\Theta) = \frac{kT}{a^2 A}\,\frac{1}{\left[\left(1-\frac{1}{4A}\varrho^2\cos^2\Theta\right)\left(1-\frac{1}{4A}\varrho^2\sin^2\Theta\right)\right]^{1/2}}\,.$$

Let us make the substitution

$$\frac{1}{4A}\varrho^2\sin^2\Theta = x\,, \qquad d\Theta = \frac{1}{2}\,\frac{dx}{\sqrt{x\,(\varrho^2/4A - x)}}\,.$$

In this manner the integral becomes

$$\iint G(\varrho,\Theta)\,\varrho\,d\varrho\,d\Theta = \frac{2kT}{a^2 A}\left[\int_0^{\sqrt{4A}} \varrho\,d\varrho \int_0^{\varrho^2/4A} \times\right.$$

$$\times \frac{dx}{\sqrt{(1-x)\,(\varrho^2/4A - x)\,x\left(x - \dfrac{\varrho^2 - 4A}{4A}\right)}} +$$

$$\left. + \int_{\sqrt{4A}}^{\sqrt{8A}} \varrho\,d\varrho \int_{\frac{\varrho^2-4A}{4A}}^{1} \frac{dx}{\sqrt{\left(\dfrac{\varrho^2}{4A} - x\right)(1-x)\left(x - \dfrac{\varrho^2-4A}{4A}\right)x}}\right].$$

By taking into account the formulae (21), (22), (22′) from the text we obtain

$$\iint G(\varrho,\Theta)\,\varrho\,d\varrho\,d\Theta = \frac{4kT}{a^2 A}\int_0^{\sqrt{8A}} \varrho\,d\varrho\,F\left(\frac{\pi}{2}, \sqrt{\frac{\varrho^2(8A-\varrho^2)}{16\,A^2}}\right) =$$

$$= \frac{4kT}{a^2 A}\int_0^{\sqrt{8A}} \int_0^{\pi/2} \frac{\varrho\,d\varrho\,d\omega}{\sqrt{1 - \dfrac{(8A-\varrho^2)\,\varrho^2}{16\,A^2}\sin^2\omega}}\,.$$

In order to integrate with respect to ϱ, we can make the substitution $\varrho^2 = u$ and the result is

$$\iint G(\varrho, \Theta)\, \varrho\, d\varrho\, d\Theta = \frac{8kT}{a^2} \int_0^{\pi/2} d\omega \int_0^{8A} \frac{du}{\sqrt{u^2 \sin^2\omega - 8Au \sin^2\omega + 16\, A^2}} =$$

$$= \frac{8kT}{a^2} \int_0^{\pi/2} \frac{d\omega}{\sin\omega} \ln\left(2 \sin\omega \sqrt{u^2 \sin^2\omega - 8u\, A \sin^2\omega + 16A^2} + \right.$$

$$\left. + 2 \sin^2\omega \cdot u - 8A \sin^2\omega\right)\Big|_0^{8A} = \frac{8kT}{a^2} \int_0^{\pi/2} \frac{d\omega}{\sin\omega} \ln \frac{1 + \sin\omega}{1 - \sin\omega} .$$

By integrating over ω we obtain [3]

$$\frac{8kT}{a^2} \int_0^{\pi/2} \frac{d\omega}{\sin\omega} \ln \frac{1 + \sin\omega}{1 - \sin\omega} = \frac{8kT}{a^2} \frac{\pi^2}{2} = \frac{4kT \cdot \pi^2}{a^2} .$$

The energy of the thin film, for the high temperature case is now obtained from (11). The result is

$$E = 3N^2 q\, kT$$

as was to be expected, in accordance with (19).

REFERENCES

1. E. W. Montroll, J. Chem. Phys., **15**, 575, 1947.
2. A. Corciovei and A. Berinde, Revue de Physique, **7**, 107, 1961.
3. *И. М. Рыжик, И. С. Градштейн*, Таблицы интегралов, суммы, рядов и произведений, Москва, 1951.
4. Ch. Kittel, Introduction to Solid State Physics, John Wiley, New York, 1957.
5. E. Calvet and H. Prat, Microcalorimetrie, Paris, 1956.

ИССЛЕДОВАНИЕ УДЕЛЬНОЙ ТЕПЛОТЫ ТОНКИХ ПЛЁНОК

А. КОРЧОВЕИ и К. МОЦОК

Р е з ю м е

Было произведено исследование удельной теплоты тонких пленок. Оно основано на предварительном изучении термических колебаний в тонких пленках. По получении дисперсионных соотношений расчет удельной теплоты производился, учитывая вклад всех видов колебаний в термические энергии тонких пленок. Были приняты два предельных случая: для высоких температур была получена известная независимость удельной теплоты от температуры T, а для низких температур зависимость от T^2 для удельной теплоты.

В последствии принята зависимость удельной теплоты от количества моноатомного слоя q и показано, что при больших значениях q, соответствующих твердому телу, для низких температур получается хорошо известная зависимость удельной теплоты от T^3.

X-RAY INVESTIGATIONS OF THE KINETICS OF ORDERING IN THE ALLOY Cu_3Au

By

H. ELKHOLY* and L. ZSOLDOS

INSTITUTE FOR EXPERIMENTAL PHYSICS, ROLAND EÖTVÖS UNIVERSITY, BUDAPEST

(Presented by E. Nagy. — Received 1. III. 1962)

X-ray technique was used in studying the ordering process of the alloy Cu_3Au. The ordering process could be separated into two processes. The first process is characterized by the formation of stable nuclei and their growth into contiguous antiphase domains of equilibrium order, while the second process is connected with the domain growth and obeys a simple exponential law. It was found also that the domain structure can change only in a direction which leads to an increase in the domain size.

1. Introduction

As early as 1936 a careful study of ordering kinetics in the alloy Cu_3Au by SYKES and EVANS [1] showed that the process of formation of order from the disordered state was far more complex than had been originally supposed. It was shown that ordering takes place by a process of nucleation and growth. Furthermore, there are four possible sublattices on which gold can be located preferentially in the long-range order state. This situation gives rise to the formation of such a network of "antiphase domains" that in each domain gold atoms are located preferentially on a sublattice different from that of neighbouring domains. A significant part of the change in properties during ordering seems to take place at the time when these antiphase domains come into contact with one another [2], and therefore part of the property change is connected with a domain growth process, somewhat analogous to grain growth in a recrystallized metal. Later work served to demonstrate more clearly the complexity of the ordering process.

Recently, NAGY and coworkers [3, 4] have tried to separate the various steps in the establishment of order. By a suitable choice of the conditions of experiment, using resistivity and Hall constant as indicators for the ordering process, they succeeded in separating the ordering kinetics of the alloy Cu_3Au into several distinct stages, which were ascribed to various physical processes. They were interested in the last process; namely the process of domain wall motion. They found that it obeys a simple exponential law with an activation energy of 0.80 ev. In their study of the characteristics of the ordering domains,

* On leave of absence from the Physics Dept., Faculty of Science, Cairo University, Cairo, Egypt.

they found that for every temperature below the critical temperature there is an equilibrium domain structure of an average domain size, and that the process of domain growth is a unidirectional process, in the sense that once a structure of an average domain size is formed, the average domain size should either grow or remain unchanged, but never diminish, irrespective of whether the temperature increases or decreases. If the temperature increases, the average domain size grows to its equilibrium value at the new temperature. If the temperature decreases, the average domain size remains unchanged, and only the long-range order parameter S increases.

The present work is mainly concerned with checking, by direct means, the validity of the unidirectional process of domain growth, together with the validity of the exponential time dependence of the domain wall elimination.

In doing this, X-ray technique was used to determine the domain size from the width of the superlattice lines present in the X-ray powder diagram.

2. Experimental work

The samples were prepared from the same batch, which was used for the previous studies [3, 4]. After an appropriate heat treatment X-ray photographs were taken in a de Wolff-type fourfold Guinier camera [5] using Cu Kα radiation. The ordered structure of the alloy Cu_3Au is rich in strong superlattice lines and the size of the domains can be determined from any of these lines using the formula:

$$D = \frac{\lambda K}{\beta \cos \vartheta}, \tag{1}$$

where D is the mean diameter of the particles (domains) perpendicular to the reflecting planes, K is a form factor with a value of approximately 1, λ is the wave length of the radiation used, β is the true angular breadth of the line, and ϑ is the Bragg angle.

In our investigations, we have used only the 100 and 110 reflexions, because they had the smallest instrumental broadening [$(2.6 \pm 0.1) \cdot 10^{-3}$ radians], and at small domain sizes the higher order reflexions were too broad to get sufficient accuracy. The inaccuracy of our measurements for the very broad lines ($\beta \approx 40 \cdot 10^{-3}$ radians) was about 10%, whereas in the most favourable cases it was reduced to 3%. As a result of the uncertainty of the instrumental broadening, the inaccuracy cannot be smaller than $0.2 \cdot 10^{-3}$ radians, and in the case of very large domains this may cause large error.

The apparent domain size obtained from different lines is not the same, in particular the size calculated from the 100 reflexion is appreciably larger than that for the other reflexions. As it was shown by WILSON [6] this is due to the fact that we have at least two different types of domain walls. One

such wall is lying in the $\{100\}$ planes and gold atoms from the domains do not come into contact. The 100 reflexion is quite insensitive to this fault and therefore the apparent domain size from this reflexion is always larger than for other reflexions.

3. Results and discussions

a) Characters of domains

In the first kind of experiments our main object was to check, by direct means, the validity of the proposition made by NAGY [3] and ELKHOLY [4] that the domain growth is a unidirectional process. In this respect, two experiments were performed. First, two specimens were disordered at 420° C for one hour and then annealed at 360° C for 4.5 hours. One of these specimens

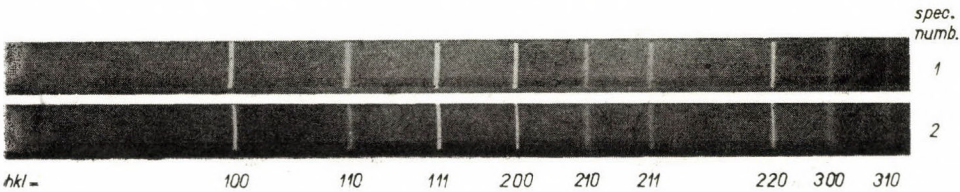

Plate 1. A part of the powder photographs of samples 1 and 2

was directly quenched in water, and the other was transferred to another furnace, having a temperature of 290° C, and annealed there for 7.5 hours and then quenched in water. X-ray photographs were taken of the two specimens (Plate 1) and the domain sizes for the 100 and 110 reflexions were calculated. The results are shown in Table 1. It is clear that the domain sizes are practically the same within the experimental error. This means that the annealing at 290° C did not change the domain size formed at 360° C, which is a direct proof of the validity of the above-mentioned proposition.

Table 1

Specimen number	Heat treatment	$\beta_{100} \cdot 10^3$ rad	$\beta_{110} \cdot 10^3$ rad	D_{100} Å	D_{110} Å
1	disorder → 360° C (4.5 h) → Q	3.10	6.86	505	234
2	disorder → 360° C (4.5 h) → → 290° C (7.5 h) → Q	3.13	7.05	503	228

This property of the domain size can be confirmed still further from the results shown in Table 2. Here six specimens were first disordered at 420° C

for one hour, one of them was transferred to a furnace having a temperature of 360° C and annealed there for 5.5 hours and then quenched in water, the other five specimens were transferred to a furnace having a temperature of 290° C and annealed there for various periods of time, indicated in Table 2, and then transferred to 360° C, annealed there for 5.5 hours and quenched in water. X-ray photographs were taken of the six specimens (Plate 2) and the domain sizes for the 100 and 110 reflexions were calculated. It is clear from Plate 2 and Table 2 that the domain sizes for the six specimens are the same. This fact confirms the supposition that for every temperature there is an equilibrium domain structure of average domain size which cannot further grow except when the temperature increases.

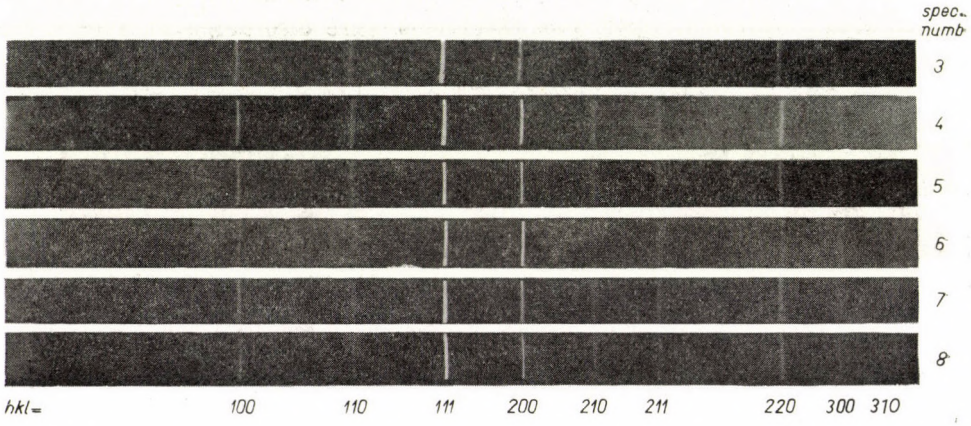

Plate 2. A part of the powder photographs of samples 3—8

Table 2

Specimen number	Heat treatment	$\beta_{100} \cdot 10^3$ rad	$\beta_{110} \cdot 10^3$ rad	D_{100} Å	D_{110} Å
3	disorder → 360° C (5.5 h) → Q	2.38	4.62	661	348
4	disorder → 290° C (2 h) →				
	→ 360° C (5.5 h) → Q	2.08	4.79	756	336
5	disorder → 290° C (6 h) →				
	→ 360° C (5.5 h) → Q	2.07	4.64	760	347
6	disorder → 290° C (11 h) →				
	→ 360° C (5,5 h) → Q	2.21	5.33	712	302
7	disorder → 290° C (13 h) →				
	→ 360° C (5,5 h) → Q	2.21	5.21	712	309
8	disorder → 290° C (15 h) →				
	→ 360° C (5,5 h) → Q	2.10	4.97	749	324

b) Kinetics of the ordering process

In the second kind of experiments, our main object was to study the kinetics of the domain growth process. Fig. 1 shows the relation between the reciprocal line broadening $1/\beta$ (which is proportional to the domain size) and time for the 100 and 110 reflexions of specimens quenched from 345° C to room temperature. A thorough analysis of these curves showed that, disregarding a certain initial portion of the curves, they obeyed a simple exponential law of the form:

$$\frac{1}{\beta} = A - Be^{-at} \quad (\text{for } t > t_0)\,, \tag{2}$$

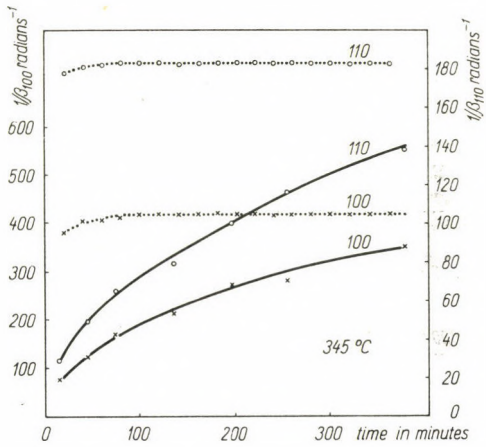

Fig. 1. Relation between time and reciprocal line broadening. The dotted line represents the non-exponential part of the curve

where A, B, a, t_0 are constants depending on temperature. This law can be interpreted by assuming that all the processes except the last one vanish after a time t_0; only the last process, that corresponds to domain wall motion, is still active then. In determining the values of the constants mentioned above, the same procedure as that used by NAGY [3] was followed, namely a semilogarithmic plot of the first differences of $1/\beta$ for constant time differences. Figs. 2 and 3 show this plot of the first differences for time differences $\Delta t = 100$ minutes for both 100 and 110 reflexions. It is clear from Figs. 2 and 3, that the exponential law is obeyed after about 70 minutes, in quite good agreement with the result found by ELKHOLY [4]. If we extrapolate the graphs of Figs. 2 and 3 to zero time, the constants a and B can be determined. Curves b (Figs. 2 and 3) show the exponential law represented by eq. (2). Now if we add the exponential so determined to the points measured, we get

the dotted curves of Fig. 1. It is clear from the horizontal trend of the dotted curves that the kinetics here follow the exponential law. The first part of the dotted curves represents the first process of the kinetics which is characterized by the formation of stable nuclei and their growth into contiguous antiphase domains of equilibrium order. The time constant α for the 100 and 110 reflexions, as determined on the basis of Figs. 2 and 3 are $4.22 \cdot 10^{-3}$ min^{-1} and $3.25 \cdot 10^{-3}\,\mathrm{min}^{-1}$, respectively, the first value being greater, the

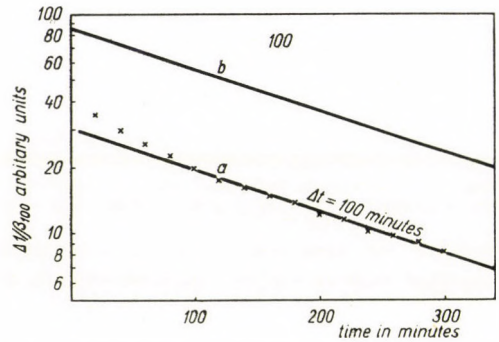

Fig. 2. The first differences of $1/\beta$ with $\Delta t = 100$ min for the reflexion 100

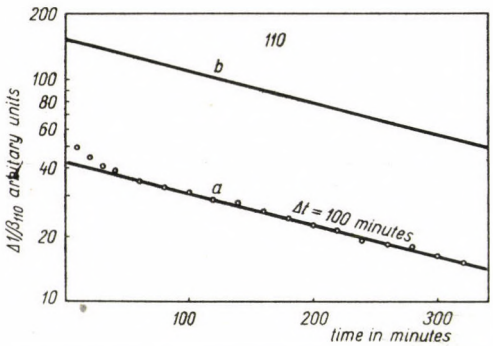

Fig. 3. The first differences of $1/\beta$ with $\Delta t = 100$ min for the reflexion 110

second being less than the value determined by the electrical experiments ($\alpha = 3.9 \cdot 10^{-1}\mathrm{min}^{-1}$) [3, 4]. The average value of α, however, determined from the 100 and 110 reflexions is in good agreement with the value determined in [4].

Acknowledgement

The authors are greatly indebted to Prof. E. NAGY for his helpful advice and discussions and to Mr. I. NAGY for heat-treating the specimens.

REFERENCES

1. C. Sykes and H. Evans, J. Inst. Met., **58**, 255, 1936.
2. C. Sykes and F. W. Jones, Proc. Roy. Soc., *A* **157**, 213, 1936.
3. E. Nagy and I. Nagy, J. Phys. Chem. of Solids, **23**, 1605, 1962.
4. H. Elkholy and E. Nagy, J. Phys. Chem. of Solids, **23**, 1613, 1962.
5. P. M. de Wolff, Acta Cryst., **1**, 207, 1948.
6. A. J. C. Wilson, X-ray Optics, Methuen and Co., London, 1949. p. 81.

ИССЛЕДОВАНИЕ КИНЕТИКИ УПОРЯДОЧЕНИЯ В СПЛАВЕ Cu_3Au РЕНТГЕНОВСКИМ МЕТОДОМ

Г. ЭЛЬКОЛИ и Л. ЖОЛДОШ

Р е з ю м е

При изучении процесса упорядочения сплава Cu_3Au применялся рентгеновский анализ. Процесс упорядочения может быть разделён на два процесса. Первый из них характеризуется формированием устойчивых ядер и ростом в соприкосновенные противофазные домены равновесной упорядоченности, в то время как второй из процессов связан с ростом доменов и подчиняется простому экспоненциальному закону. Показывается далее, что доменная структура может изменяться только в направлении, ведущем к увеличению размера домена.

COMPUTATION OF THE WORKING CYCLE OF AN ADIABATIC MAGNETIC REFRIGERATING PROCESS

By

I. KIRSCHNER

DEPARTMENT OF NUCLEAR PHYSICS, ROLAND EÖTVÖS UNIVERSITY, BUDAPEST

(Presented by L. Jánossy. — Received 26. V. 1962)

Some of the modern experiments in nuclear and solid state physics [1] require extremely low temperatures ($T \ll 1°$ K). Temperatures of this kind can be satisfactorily produced by the process of adiabatic demagnetization. The present paper is discussing the thermodynamical relations on the basis of which the refrigerating process is effected. First the computation is performed for an ideal case and then also for the real refrigerating cycle.

Temperature to be obtained by one demagnetization

To arrive at temperatures $1° \text{ K} \geqslant T \gtrsim 0.01°$ K adiabatic magnetic refrigeration uses the fact that there are some salts [2] which maintain their paramagnetic characteristics up to $10^{-2} - 10^{-3°}$ K, and the entropy of which is large at temperatures around 1° K. The greater part of the entropy of the paramagnetic salt can be taken away by subjecting it to the influence of an intensive magnetic field (15—20 kOersted). The heat which is thereby formed is conducted away from the salt and thus this first stage becomes isotherm. (Fig. 1, $1 \rightarrow 2$.) In the second stage the salt is thermically insulated from its surroundings and the magnetic field is reduced under adiabatic conditions. (Fig. 1, $2 \rightarrow 3$.)

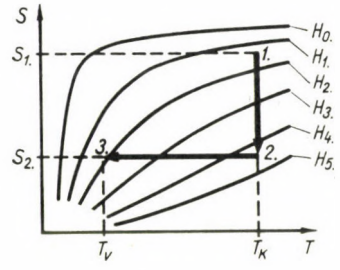

Fig. 1. One demagnetization of a paramagnetic salt. (H is increasing in the direction of increasing index)

Let us characterize the paramagnetic salt by the intensive parameters T and H, respectively by the extensive parameters S and M, where T represents the temperature, H the external magnetic field, S the entropy of salt and M

the molar magnetic moment of the salt. Now [3] the second law of thermodynamics can be expressed in the following form:

$$dU = TdS + HdM, \tag{1}$$

where U stands for the internal energy. The thermodynamical potentials can be expressed in the same way:

$$\begin{aligned} E &= U - HM: && \text{enthalpy,} \\ F &= U - TS: && \text{free energy,} \\ G &= U - TS - HM: && \text{Gibbs potential.} \end{aligned} \tag{2}$$

From these on the basis of (1)

$$\begin{aligned} dE &= T\,dS - M\,dH, \\ dF &= -S\,dT + H\,dM, \\ dG &= -S\,dT - M\,dH. \end{aligned} \tag{3}$$

Applying the Pfaff expressions referring to the total differentials dE, dF and dG we have

$$\begin{aligned} \left(\frac{\partial S}{\partial H}\right)_T &= \left(\frac{\partial M}{\partial T}\right)_H, \\ \left(\frac{\partial T}{\partial H}\right)_S &= -\left(\frac{\partial M}{\partial S}\right)_H, \\ \left(\frac{\partial H}{\partial T}\right)_M &= -\left(\frac{\partial S}{\partial M}\right)_T. \end{aligned} \tag{4}$$

The above expressions are analogous with Maxwell's thermodynamical relations for a gas.

Let us suppose the entropy to be a function of T and H, then

$$TdS = T\left(\frac{\partial S}{\partial T}\right)_H dT + T\left(\frac{\partial S}{\partial H}\right)_T dH, \tag{5}$$

where $T(\partial S/\partial T)_H = C_H$ is the molar heat. Hence the heat to be dissipated from the salt at, the isotherm first stage can be expressed by means of (4):

$$Q = T\int_{H_1}^{H_2}\left(\frac{\partial M}{\partial T}\right)_H dH, \tag{6}$$

where H_1 may be zero as well. From (6) it is to be seen that on switching on the external magnetic field, the amount of heat is obtained which depends

on the value of the original temperature as well as on that of the polarization.

Applying (5) to the adiabatic stage, the reduction of temperature can be obtained from the equation $TdS = 0$:

$$-dT = \frac{T}{C_H}\left(\frac{\partial M}{\partial T}\right)_H dH\,,$$

hence

$$T_k - T_v = \int_{H_k}^{H_v}\left(\frac{\partial M}{\partial S}\right)_H dH. \tag{7}$$

It is obvious from the above that the adiabatic reduction of the magnetic field results in a drop in the temperature of the paramagnetic salt, whereas its increase brings an increase of temperature. If T_k is known, the change in temperature can be calculated from (7).

Let us introduce now an idealization of the paramagnetic salt (as in the case of perfect gases) in the following way:

$$\left(\frac{\partial U}{\partial M}\right)_T \equiv 0. \tag{8}$$

Interpreting the entropy as a function of T and M, we have

$$TdS = T\left(\frac{\partial S}{\partial M}\right)_T dM + T\left(\frac{\partial S}{\partial T}\right)_M dT,$$

where $T(\partial S/\partial T)_M = C_M$ is the molar heat. Hence, taking into consideration also relation (4), the change in the internal energy in a process taking place between two states of equilibrium can be written

$$dU = C_M\,dT - \left[T\left(\frac{\partial H}{\partial T}\right)_M - H\right]dM. \tag{9}$$

Assuming $U = U(T, M)$ and forming the total differential of U, we obtain the relation $U - M$ without any idealization and referring to the general case:

$$\left(\frac{\partial U}{\partial M}\right)_T = -T\left(\frac{\partial H}{\partial T}\right)_M + H.$$

Applying (8) results in:

$$\frac{H}{T} = \left(\frac{\partial H}{\partial T}\right)_M. \tag{10}$$

In other words, if M is constant, the ratio H/T is also constant. From relation (4), however, it is apparent that if M is constant, the value of the entropy remains also unchanged. Thus from the equation referring to an isentropic process, namely

$$S_k(H_k, T_k) = S_v(H_v, T_v), \tag{11}$$

it follows by means of relation (10) that

$$T_v = T_k \cdot \frac{H_v}{H_k}. \tag{12}$$

In case $H_v \to 0$, this formula yields the result $T_v \to 0$, which is not real. Analysing, however, the measurement data of some authors [4] we can safely state that our equation is in good agreement with reality in all the cases where the final demagnetization field is not lower than about a hundred oersted.

Realizing adiabatic demagnetization in practice the initial temperature (T_k) can be secured by placing the paramagnetic salt into a cryostat containing liquid helium.

The approximation of the refrigerating process by the Carnot-cycle

It is obvious that the temperature to be obtained after one magnetization and demagnetization will considerably increase in a comparatively short time depending on the efficiency of the heat insulation. If we are going to perform our experiments under stable temperature conditions for a longer period, then we need a cyclically operating refrigeration equipment capable of continuously conducting heat from a heat reservoir (body to be tested) at the prescribed low temperature ($T \ll 1°$ K). The main parts of an apparatus [5] of this type (Fig. 2) are the following: B: helium bath; C: paramagnetic salt (working substance); R: heat reservoir; K_B and K_R: heat rectifiers (thermal valves), which have to let the heat through in one part of the cycle and to act as heat insulators in the other; M: cooling magnet for magnetization and demagnetization; M_B and M_R: magnets regulating the thermal valves. All of them are built into a vacuum chamber cooled down to helium temperature. It can be seen that test sample C is connected with helium vessel B through the thermal valve K_B and is also in contact with heat reservoir R through K_R. It is just that factor which enables the refrigerating equipment to operate continuously.

The heat rectifying role of the thermal valves is made possible by an anomaly of superconduction, i. e. by the fact that in superconducting condition metals become bad heat conductors:

$$K_{sup}/K_{norm} = (T/T_{tr})^2,$$

where K_{norm} represents the heat conductivity in normal condition, K_{sup} stands for the heat conductivity in superconducting condition, and T_{tr} is the temperature of superconducting transition. The required condition can be obtained by means of an external magnetic field, because at a given temperature a magnetic field of proper intensity is capable of changing the condition of the metal from a superconducting one into a normal one i. e. into the state of "great" heat conductivity.

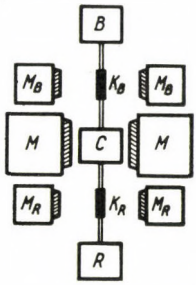

Fig. 2. Main parts of the refrigerating equipment

Investigation of the refrigerating cycle requires knowledge of the entropy-temperature curves of the paramagnetic salts at different values of the magnetic field. In this connection J. R. HULL and R. A. HULL [6] have performed calculations with a statistical thermodynamical method. Partition function Z can be expressed for paramagnetic ions in the following form:

$$Z = \sum_{m=-J}^{J}{}' \exp(-mg\beta H/kT),$$

wherefrom the thermodynamical functions are:

free energy: $$F = RT \cdot \ln Z,$$

entropy: $$S = -\frac{\partial F}{\partial T} = R\left(\ln Z - Z^{-1} \cdot x \cdot \frac{dZ}{dx}\right),$$

magnetization: $$M = \frac{\partial F}{\partial H} = ST\,\frac{\partial \ln Z}{\partial H},$$

where R = universal gas constant, and $x = -g\beta H/kT$. After expressing Z explicitly and performing the required derivations:

$$S = R \ln (2J+1) + \int_0^H \left(\frac{\partial M}{\partial T}\right)_M dH. \tag{13}$$

M is described by the Brillouin function

$$M = \frac{1}{2} Ng\beta \left[(2J+1)\, cth\, (2J+1) \frac{g\beta H}{2kT} - cth \frac{g\beta H}{2kT} \right],$$

where N: Loschmidt number, g: Lande factor, β: Bohr magneton, J: angular-moment quantum number, k: Boltzmann constant. The curves obtained on the basis of the formula for $J = \frac{5}{2}$ are illustrated by Fig. 3.

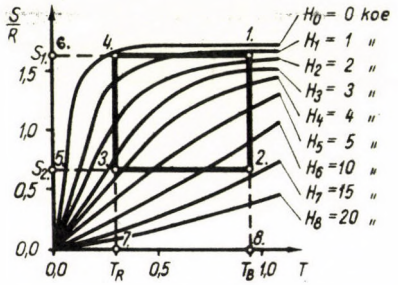

Fig. 3. Curves S—T, and the ideal Carnot cycle

Having obtained $S - T$ curves, let us follow the refrigerating cycle of an ideal paramagnetic salt on hand of the Carnot cycle taking place between helium temperature T_B and reservoir temperature T_R. For the Carnot approximation of the refrigeration process, it is indispensable that the Carnot-type refrigerating equipment should be operating along two isotherms and two isentropies (Fig. 3). An ideal Carnot cycle can be realized along the way 1.2.3.4.1., where paths $\overline{1.2.}$, $\overline{2.3.}$, $\overline{3.4.}$, $\overline{4.1.}$ are at right angles to each other, and where the direction of advancement depends on the unequality $T_R < T_B$. In order to make the Carnot cycle ideal, the following condition* must be met:

a) the contacts between the working substance and the helium bath, respectively between the working substance and the reservoir must be fully isotherm on the sections $\overline{1.2.}$ and $\overline{3.4.}$

b) the heat insulation of the working substance must be fully adiabatic on the sections $\overline{2.3.}$ and $\overline{4.1.}$

* This involves the heat conductivity of the thermal valves to be infinite in normal condition and zero in superconducting state.

If along line $\overline{1.2}$. a magnetic field is applied on C, thermal valve K_B opens and heat of amount Q_1 will flow isothermically from C into B at a temperature T_B.

Along line $\overline{2.3}$ we perform an isentropical demagnetization from temperature T_B to T_R while both thermal valves are closed. From the II-nd law it follows that the change of the internal energy is a result of work, the value of which is denoted by A_1. (This work is performed on the test sample by the external magnetic field.)

Along the line $\overline{3.4}$ heat Q_2 flows isothermically into C from R. This line means a demagnetization and during this K_R is open, K_B is closed.

Line $\overline{4.1}$ as an adiabatic magnetization, returns the cycle into its original state, the temperature of C is increasing again to T_B, while both thermal valves are closed. The change in the internal energy takes place again by work performed by the working substance against the field. Its value is denoted by A_2.

Thus the energy equation of the full ideal cycle is given by

$$Q_1 - Q_2 + A_1 - A_2 = 0\,,$$

that is

$$Q_1 + A_1 = Q_2 + A_2\,.$$

If the whole adiabatic work is $A_2 - A_1 = A$, the equation of the ideal Carno cycle is:

$$Q_2 = Q_1 - A\,.$$

It is obvious that ideal Carnot cycle is the one at which the maximum heat possible is leaving the reservoir. This heat is denoted by Q_R^{ideal}

$$Q_2 = T_R\,(S_{4.} - S_{3.}) = Q_R^{\text{ideal}}\,. \tag{14}$$

The above quantities are illustrated by Fig. 3.

Quantity

$$Q_1 = T_B\,(S_{1.} - S_{2.}) = T_B\,(S_{4.} - S_{3.})$$

is shown by area 1. 2. 5. 6. 1., heat

$$Q_2 = T_R\,(S_{4.} - S_{3.}) = T_R\,(S_{1.} - S_2) = Q_R^{\text{ideal}}$$

is shown by area 4. 3. 5. 6. 4. Work A is illustrated by area 1. 2. 3. 4. 1. A itself is a difference of two members, out of which work

$$A_1 = S_{2.}\,(T_B - T_R) = S_{3.}\,(T_B - T_R)$$

is shown by area 2. 8. 7. 3. 2., work

$$A_2 = S_{1.}\,(T_B - T_R) = S_{4.}\,(T_B - T_R)$$

is represented by area 1. 8. 7. 4. 1.

The calculation of the real refrigerating cycle

In reality no ideal Carnot cycle exists partly because of the undesired heat and imperfect heat insulation of the various parts of the refrigerating equipment and partly on account of the imperfect heat contacts.

The strong dependence of the heat conductivity of the thermal valves and of the heat capacity of the paramagnetic working substance on temperature excludes isotherm conditions. The main reason for the deviation from the adiabatic line must be sought for in the heat leakage, heat seeping through the closed thermal valves.

From the sources generating heat in the apparatus the eddy current is the most important one. This comes from the regulated alteration of the

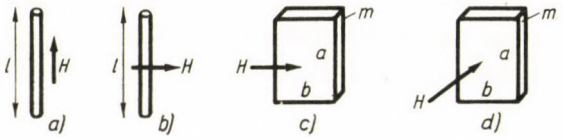

Fig. 4. The direction of the magnetic field relative to the copper details

magnetic field and from its vibration and is apparent on the copper components. The amount of heat being formed during time dt is given by

$$dQ = \frac{1}{\Omega} \Phi^2 dt,$$

where Ω: electric resistance, Φ: voltage. This latter is given by

$$\Phi = -\mu \frac{d}{dt} \int_0^f H_n \, df.$$

With this dQ becomes:

$$dQ = \frac{\mu^2}{\Omega} \left(\frac{d}{dt} \int_0^f H_n df \right)^2 dt. \tag{15}$$

Here df is the surface element of the component, μ is its permeability, ϱ is its specific resistance. Performing the required calculations, we obtain formulas (16)—(19) for the heat formed in the various positions numbered according to Fig. 4.

a) The field H is parallel to the wire:

$$dQ = \frac{r^4 l\pi}{8\varrho} \mu^2 \left(\frac{dH}{dt}\right)^2 dt\,; \tag{16}$$

b) The field H is perpendicular to the wire:

$$dQ = \frac{4r^4 l\pi}{\varrho} \mu^2 \left(\frac{dH}{dt}\right)^2 dt\,; \tag{17}$$

c) The field H is parallel to the foil:

$$dQ = \frac{abm^3}{\varrho} \mu^2 \left(\frac{dH}{dt}\right)^2 dt\,; \tag{18}$$

d) The field H is perpendicular to the plate:

$$dQ = \frac{a^2 b^2 m}{\varrho} \mu^2 \left(\frac{dH}{dt}\right)^2 dt. \tag{19}$$

In the case of the approximation by the Carnot cycle [7] we assumed that under normal conditions the thermal valves have zero heat resistance (on the parts $\overline{1.2.}$ and $\overline{3.4.}$ of the cycle) and possess an infinite heat resistance in the superconducting state, on the sections $\overline{2.3.}$ and $\overline{4.1.}$ of the cycle. In fact, however, thermal valves have a considerable heat conductance in the closed condition too and possess a significant thermal resistance also if open. That is the reason why the refrigerating cycle is taking place between temperatures T_1 and T_2, instead of T_B and T_R; the magnetization increases the temperature of the salt to $T_1 > T_B$, whereas demagnetization results in a temperature $T_2 < T_R$. In a real refrigerating equipment it is just this factor which ensures a continuous flow of heat. The finite thermal conductivity of the thermal valves (respectively their heat resistance) manifests itself in losses of the heat flow. Along line $\overline{1.2.}$ heat flows not only from C into B, but through the "closed" K_R also into R, thus

$$Q_1 = Q_B^{\overline{1.2.}} + Q_R^{1.2.}. \tag{20}$$

Similarly along line $\overline{3.4.}$ heat flows not only from R into C, but also from B through the "closed" K_B:

$$Q_2 = Q_R^{\overline{3.4.}} + Q_B^{\overline{3.4.}}. \tag{21}$$

The quantities included in expressions (20) and (21) have the following meaning: $Q_B^{\overline{1.2.}}$ is the heat flowing from C into B along line $\overline{1.2.}$; $Q_R^{\overline{1.2.}}$ is the heat current

from C into R along line $\overline{1.2.}$; $Q_R^{\overline{3.4.}}$ is flowing from R into C along the section $\overline{3.4.}$; and finally $Q_B^{\overline{3.4.}}$ represents the quantity of heat flowing back along the section $\overline{3.4.}$ from B into C. In the case of the ideal cycle we have

$$Q_R^{\overline{1.2.}} = 0 \qquad \text{and} \qquad Q_B^{\overline{3.4.}} = 0.$$

In fact, these quantities are determined by the heat conductivity of the thermal valves in superconducting condition. The heat conductivity of the thermal valves is expressed by

$$K = k \cdot T^n, \tag{22}$$

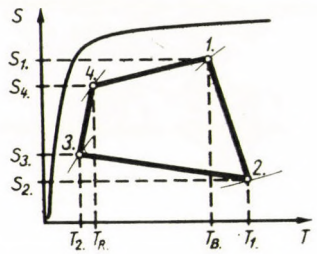

Fig. 5. The real refrigerating cycle

where k = constant. Generalization of the experimental results [8] applied to superconducting metals resulted in

$$\begin{aligned} K_{\text{norm}} &= a \cdot T, \\ K_{\text{sup}} &= b \cdot T^3, \end{aligned} \tag{23}$$

where a and b are experimental constants, for which $a \gg b$. Thus in the real refrigerating cycle (Fig. 5) the energy equation (14) looses its validity and is replaced by the following equation:

$$Q_R^{1.2.3.4.1.} = Q_R^{\overline{3.4.}} - Q_R^{\overline{1.2.}} < Q_R^{\text{ideal}}, \tag{24}$$

which means that in the course of the real cycle the value of the heat to be conducted from the reservoir is far below the ideal one. Thus the equalities characterizing the ideal Carnot cycle namely

$$S_{1.} = S_{4.} \qquad \text{and} \qquad S_{2.} = S_{3.}$$

disappear and in their stead equation

$$S_{4.} - S_{3.} = \alpha \cdot (S_{1.} - S_{2.}) \tag{25}$$

comes into force, where $\alpha < 1$.

The entropy changes of the test sample during magnetization, respectively demagnetization, can be expressed by heat flows in the following way:

$$(S_{2.} - S_{1.}) \int_{T_B}^{T_1} dT = Q_B^{\overline{1.2.}} + Q_R^{\overline{1.2.}},$$

$$(S_{4.} - S_{3.}) \int_{T_2}^{T_R} dT = Q_R^{\overline{3.4.}} + Q_B^{\overline{3.4.}}.$$

The quantities in equ. (20) and (21) can be expressed by the heat transport equation referring to the thermal valves:

$$\dot{Q} = \frac{q}{l} \frac{k}{n+1} (T_x^{n+1} - T_y^{n+1}).$$

This equ. results when using (22). From this formula we can compute by means of (23) the heat energy flowing through the thermal valves:

$$\begin{aligned} Q_B^{\overline{1.2.}} &= (q_B/l_B) \frac{a}{2} (T_1^2 - T_B^2)\, t_{\overline{1.2.}}, \\ Q_R^{\overline{3.4.}} &= (q_R/l_R) \frac{a}{2} (T_R^2 - T_2^2)\, t_{\overline{3.4.}}, \\ Q_B^{\overline{3.4.}} &= (q_B/l_B) \frac{b}{4} (T_B^4 - T_2^4)\, t_{\overline{3.4.}}, \\ Q_R^{\overline{1.2.}} &= (q_R/l_R) \frac{b}{4} (T_1^4 - T_R^4)\, t_{\overline{1.2.}}, \end{aligned} \tag{26}$$

where $t_{\overline{1.2.}}$, respectively $t_{\overline{3.4.}}$ stand for the time required for part $\overline{1.2.}$, respectively $\overline{3.4.}$ of the cycle, q means the cros-section and l the length of the thermal valves. The efficiency of the cycle taking place in this way is determined by these inequalities:

$$\begin{aligned} Q_B^{\overline{1.2.}} &\geqslant Q_B^{\overline{3.4.}}, \\ Q_R^{\overline{3.4.}} &> Q_R^{\overline{1.2.}}, \\ Q_B^{\overline{1.2.}} &\geqslant Q_R^{\overline{1.2.}}. \end{aligned} \tag{27}$$

REFERENCES

1. M. E. Rose, Nucleonics, **3,** 23, 1948.
2. E. Ambler and R. P. Hudson, Rep. Progr. Phys., **18,** 255, 1955.
3. I. Kirschner, Magy. Fiz. Folyóirat, **8,** 117, 1960.

4. C. E. Wiersma and W. J. de Haas, Physica, **3,** 491, 1936.
H. B. G. Casimir, Physica, **7,** 70, 1940.
C. V. Heer, C. B. Barnes and J. G. Daunt, Phys. Rev., **76,** 985, 1949.
5. C. V. Heer, C. B. Barnes and J. G. Daunt, Rev. Sci. Instr., **25,** 1088, 1954.
R. A. Erickson and C. V. Heer, Phys. Rev., **108,** 896, 1957.
6. J. R. Hull and R. A. Hull, Journ. Chem. Phys., **9,** 465, 1941.
7. I. Kirschner, Magy. Fiz. Folyóirat, **8,** 487, 1960.
8. C. A. Renton and K. Mendelssohn, Proc. Roy. Soc., **230,** 157, 1955.
H. B. Montgomery, Proc. Roy. Soc., **244,** 85, 1958.

СЧЁТ ДЕЙСТВУЮЩЕГО ЦИКЛА АДИАБАТИЧЕСКОГО МАГНИТНОГО ОХЛАЖДАЮЩЕГО ПРОЦЕССА

И. КИРШНЕР

Р е з ю м е

Часть исследований ядерной физики и физики твёрдых тел требует сверхнизкитемпературы ($T \ll 1°$ К). Можно создать такие низкие температуры процессом адиабатиа ческого размагничивания. В этой работе рассмотрим термодинамические соотношения, но основе котоых происходит охлаждающий процесс. Расчёт произведен для идеальног и также для действительного цикла.

ON THE ANOMALOUS SPLITTING OF THE MULTIPLET Σ STATES IN DIATOMIC MOLECULES II.

By

I. Kovács

DEPARTMENT OF ATOMIC PHYSICS, POLYTECHNICAL UNIVERSITY, BUDAPEST

(Received 25. X. 1962)

This paper supplements a previous paper on a similar subject [1]. The theory developed there to interpret the anomalous splitting of multiplet Σ terms is applied to terms as yet missing, namely the $^4\Sigma$, $^5\Sigma$, and $^6\Sigma$ terms.

It has been shown in two previous papers [1], [2] that the "anomalous multiplet splitting" of the $X^2\Sigma^+$ term of the HgH molecule, the $B^2\Sigma$ term of the YO molecule, the $A^3\Sigma_u^+$ and $B'^3\Sigma_u^-$ terms of the N_2 molecule, as well as the $^7\Sigma$ term of the MnH molecule can be very satisfactorily interpreted theoretically as the perturbations of not too far lying Π terms. The experimental examples mentioned above show that such anomalous splittings may occur quite often, however, when they were first found they could not be interpreted as the theory was then lacking. With assumptions similar to the previous ones the present paper aims at extending the theory to the anomalous splittings that may be expected in the case of the Σ terms as yet missing — namely the $^4\Sigma$, $^5\Sigma$, $^6\Sigma$ terms — the author hoping thus to draw the attention of the experimental research worker to these possibilities.

As is well known, for the dependence on the rotational quantum number of the components of multiplet Σ terms relatively simple formulae are valid that can be arrived at after solving the separated wave equation and taking into account the mutual perturbations of the components belonging to Hund's case a), completed with the perturbation terms of the spin-spin interaction, as well as the interaction between rotation and spin [3]. Deviations from the formulae thus gained are called "anomalous splittings".

Considering the terms neglected at the separation of the wave equation and those of the spin-orbit interaction, and taking the perturbations of the Σ and Π states of the same and different multiplicity into account these perturbations will — if the states mentioned are lying far enough — not change the structure of the Σ term formulae referred to above, i.e. their dependence on the rotational quantum numbers will remain the same and apart from a small constant displacement only the values of the constants in the original formulae will be modified [4], [2].

However, if the perturbing terms are lying nearer to the Σ terms at issue so that the change in their distance with the rotational quantum number cannot be neglected, then, beside the changes in the value of the constants, also such correction terms will occur as to bring about changes in the structure of the formulae; in other words, the dependence on the rotational quantum number in the original formulae will also change. These new additional terms excellently describe the anomalous multiplet splittings in each of the cases observed so far with the exception of one (see later).

A detailed derivation of the calculations can be found in earlier works [1], [2]; here only the final results are given for the missing cases, as well as a slightly more exact form of the formula derived earlier for the case of the $^7\Sigma$ term.

Denote by $\overline{F_i(N)}$ the terms observed by the experimental research worker as unperturbed (i.e. such terms where the values of the original constants have changed, but where the structure of the formulae remained the same); $F_i'(N)$ be the actually observed, that is perturbed terms. Then

$$\Delta F_i(N) = F_i'(N) - \overline{F_i(N)}$$

denoted the measured deviation from the original formulae. For these we have the following expressions:

In case of $^4\Sigma$ *terms*:

$$\begin{aligned}
\Delta F_1(N) &= -\left[3\sigma(N+1) - \tau\right] N^2, \\
\Delta F_2(N) &= -\left[\sigma(N-3)(N+1) + \tau(N+3)\right] N, \\
\Delta F_3(N) &= +\left[\sigma N(N+4) - \tau(N-2)\right](N+1), \\
\Delta F_4(N) &= +\left[3\sigma N + \tau\right](N+1)^2,
\end{aligned} \tag{1}$$

where

$$\sigma = 4\,\frac{\xi\eta\,(B_\Pi - B_\Sigma)}{(h\nu)^2}\,; \quad \tau = \frac{\xi^2\,(B_\Pi - B_\Sigma)}{(h\nu)^2} \tag{2}$$

and ξ is the constant occurring in the matrix elements of the spin-orbit interaction, η is that of the interaction coming from the terms neglected at the separation of the wave equation, B_Σ and B_Π are the unperturbed values of the rotational constants of the perturbed and perturbing terms, occurring in the original multiplet formulae (that is, not those occurring in the $\overline{F_i(N)}$) and finally $h\nu$ is the difference between the corresponding vibrational states of the perturbed and perturbing terms.

In case of $^5\Sigma$ *terms*:

$$\begin{aligned}
\Delta F_1(N) &= -\left[\sigma(2N+3)(N+1) - 2\tau(2N+1)\right]N\,,\\
\Delta F_2(N) &= -\left[\sigma(N+1)^2 - \tau(N-4)\right]N,\\
\Delta F_3(N) &= 0\,,\\
\Delta F_4(N) &= +\left[\sigma N^2 + \tau(N+5)\right](N+1)\,,\\
\Delta F_5(N) &= +\left[\sigma(2N-1)N + 2\tau(2N+1)\right](N+1),
\end{aligned} \tag{3}$$

where

$$\sigma = 8\,\frac{\xi\eta\,(B_\Pi - B_\Sigma)}{(h\nu)^2}\,;\quad \tau = \frac{\xi^2\,(B_\Pi - B_\Sigma)}{(h\nu)^2}\,. \tag{4}$$

In case of $^6\Sigma$ *terms*:

$$\begin{aligned}
\Delta F_1(N) &= -5\left[\sigma(N+1) - \tau\right]N^2,\\
\Delta F_2(N) &= -\left[\sigma(3N-5)(N+1) + \tau(N+15)\right]N,\\
\Delta F_3(N) &= -\left[\sigma N(N+1)(N-8) + 2\tau(2N-3)(N+4)\right],\\
\Delta F_4(N) &= +\left[\sigma N(N+1)(N+9) - 2\tau(2N+5)(N-3)\right],\\
\Delta F_5(N) &= +\left[\sigma(3N+8)N - \tau(N-14)\right](N+1)\,,\\
\Delta F_6(N) &= +5\left[\sigma N + \tau\right](N+1)^2,
\end{aligned} \tag{5}$$

where

$$\sigma = 4\,\frac{\xi\eta\,(B_\Pi - B_\Sigma)}{(h\nu)^2}\,;\quad \tau = \frac{2}{3}\,\frac{\xi^2\,(B_\Pi - B_\Sigma)}{(h\nu)^2}\,. \tag{6}$$

In case of $^7\Sigma$ *terms*:

$$\begin{aligned}
\Delta F_1(N) &= -\left[3\sigma(N+1)(N+2) - \tau(9N+4)\right]N\,,\\
\Delta F_2(N) &= -\left[\sigma(N+1)(2N+3) - \tau(4N-11)\right]N\,,\\
\Delta F_3(N) &= -\left[\sigma N(N+1)^2 - \frac{1}{2}\tau(N-5)(2N-9)\right],\\
\Delta F_4(N) &= 0\,,\\
\Delta F_5(N) &= +\left[\sigma N^2(N+1) + \frac{1}{2}\tau(N+6)(2N+11)\right],\\
\Delta F_6(N) &= +\left[\sigma N(2N-1) + \tau(4N+15)\right](N+1)\,,\\
\Delta F_7(N) &= +\left[3\sigma(N-1)N + \tau(9N+5)\right](N+1)\,,
\end{aligned} \tag{7}$$

where the value of σ and τ is identical with (4).

Comparison with the experiment. Up to the present time the rotational fine structure of three $^4\Sigma$ terms has been studied. NEVIN [5] has investigated a $^4\Sigma^-$ state in the O_2^+ molecule, but here there was no observable deviation from the unperturbed formulae. KLEMAN and WERHAGEN [6] have studied the rotational fine structure of a $^4\Sigma$ term in the GeH molecule. Although in this case some deviation from the unperturbed formulae really occurred,

unfortunately so few branches were published that it was impossible to establish on the ground of the available experimental data whether the observed deviations could be interpreted by means of the above theory. Finally, VERMA [7] has analysed a $^4\Sigma$ state in the SiF molecule, where some deviations appeared again from the unperturbed formulae. These deviations, however, are of a type different from those treated in the present work, so they cannot be interpreted by the theory outlined above. HOUGEN [8] worked out a theory to explain this case (which may be considered a development of the older one given by BUDÓ and the author [4]), however, only moderate agreement was found between his theory and the experimental data. Thus the theoretical interpretation of the deviations experienced in connection with the $^4\Sigma$ term of SiF is still missing.

At present $^5\Sigma$ and $^6\Sigma$ terms the fine structure of which has been analysed are not known.

The $^7\Sigma$ term of the MnH molecule was studied by NEVIN [9]. Deviation from the older formulae was found for the first time in this case and it was exactly to explain this that the author elaborated the theory given above. In this case as well as in others the theory is again in excellent agreement with the experimental data [2].

REFERENCES

1. I. KOVÁCS, Act. Phys., Hung., **15**, 1, 1962.
2. I. KOVÁCS, Proc. Roy. Ir. Acad., **60A**, 15, 1959.
3. H. A. KRAMERS, Zs. f. Phys., **33**, 422; **53**, 429, 1929.
4. A. BUDÓ and I. KOVÁCS, Hung. Act. Phys., **1**, No 3, 1948.
5. T. E. NEVIN, Phil. Trans. Roy. Soc. (London) A, **237**, 471, 1938, Proc. Roy. Soc. (London) A, **174**, 371, 1940.
6. B. KLEMAN and E. WERHAGEN, Ark. f. Fys., **6**, 399, 1953.
7. R. D. VERMA, Can. J. Phys., **40**, 586, 1962.
8. J. T. HOUGEN, Can. J. Phys., **40**, 598, 1962.
9. T. E. NEVIN, Proc. Roy. Ir. Acad., **48**, 1, 1942.

ОБ АНОМАЛЬНОМ РАСЩЕПЛЕНИИ МУЛЬТИПЛЕТНЫХ Σ СОСТОЯНИЙ В ДВУХАТОМНЫХ МОЛЕКУЛАХ II

И. КОВАЧ

Р е з ю м е

В данной работе в качестве дополения к предыдущей, занимающейся подобными же вопросами статье, распостраняется теория, разработанная для интерпретации аномального расщепления мультиплетных Σ-термов, для случая пока отсутствующих мультиплетных Σ-термов, а именно для термов $^4\Sigma$, $^5\Sigma$ и $^6\Sigma$.

ON THE CORRELATION PROBLEM IN THE THEORY OF ATOMS AND MOLECULES

By

E. KAPUY

RESEARCH GROUP FOR THEORETICAL PHYSICS OF THE HUNGARIAN ACADEMY OF SCIENCES, BUDAPEST

(Presented by A. Kónya. — Received 14. XI. 1962)

Two methods which avoid infinite summations in taking into account the electronic correlations are discussed and compared. It can be seen that further calculations are necessary before a decision is reached as to their value. It depends, too, on the development of computational techniques in the future. Both methods allow for the maximum localization of groups and for giving an exact measure for the localizability of those groups in a real system. Neither of them verifies at present the transferability of some (chemically invariant) groups. It can be shown that before applying the generalized bond energy concept the total energy should be corrected by the dispersion interaction.

Introduction

In order to treat the physical and chemical properties of atoms and molecules properly we must reach a very high accuracy in the wave function. Among other things it is necessary for this to take into account the electronic correlation effects in full detail. To study the correlation effects two methods can be found in the literature in addition to the well-known method of superposition of configurations, to which both are to some extent related.

The method of superposition of configurations

We assume that there exists a denumerable complete orthonormal set of one-electron spin-orbitals $u_\varkappa$ (which will be specified more exactly later) and the general solution Ψ to the equation

$$H\Psi = E\Psi\,,$$

$$H = H(0) + \sum_{i=1}^{N} H(i) + \sum_{j>i=1}^{N} H(ij)\,,$$

can be expanded as

$$\Psi = \sum_{\mu=0}^{\infty} C_\mu \Phi_\mu\,,$$

where

$$\Phi_\mu = \mathcal{A}_N \left[u_{1\mu}\, u_{2\mu} \ldots u_{N\mu}\right].$$

Here $\mathscr{A}_N$ means the antisymmetrizer

$$\mathscr{A}_N = (N!)^{-\frac{1}{2}} \sum_p (-1)^p P .$$

Φ_μ and Φ_ν are different when they differ at least in one spin-orbital. The totality of the functions Φ_μ which can be constructed from the complete set $u_\varkappa$ also forms a complete set in the N-electron space. The coefficients C_μ are the components of the eigenvector of the secular equation corresponding to the eigenvalue E

$$\sum_\nu (\mu|H|\nu) C_\nu - EC_\mu = 0 .$$

We denote the first N spin-orbitals with the indices $i, j, k \leqslant N$ and all the other orbitals with the indices $a, b, c > N$. Φ_0 is constructed from the first N spin-orbitals.

Let Φ_i^a, Φ_{ij}^{ab}, Φ_{ijk}^{abc}, ... etc. be functions in which the spin-orbitals denoted with i, j, k are replaced by spin-orbitals denoted with a, b, c.

With these notations (and setting C_0 equal to unity) we have

$$\Psi = \Phi_0 + \sum_{a=N+1}^{\infty} \sum_{i=1}^{N} C_i^a \Phi_i^a + \sum_{a<b}^{\infty} \sum_{i<j}^{N} C_{ij}^{ab} \Phi_{ij}^{ab} + \ldots . \tag{1}$$

Assuming that the first N spin-orbitals are solutions to the Hartree-Fock equations, then

$$(0 \mid H \mid {}_i^a) = 0, \text{ for every } i \text{ and } a,$$

and we get the generalized Brillouin's theorem [1, 2] for the energy expression

$$E = (0|H|0) + \sum_{a<b}^{\infty} \sum_{i<j}^{N} (0|H|_{ij}^{ab}) C_{ij}^{ab} .$$

Owing to the infinite summations which cannot be given in closed form this method is unsuitable for practical calculations. There are two methods in which the wave function involves (at least partial) infinite summations implicitly.

Method I. Cluster expansion of the wave function

We define the following functions

$$\begin{aligned} S_i(1) &= \sum_{a=N+1}^{\infty} C_i^a \, u_a(1) , \\ S_{ij}(12) &= \mathscr{A}_2 \sum_{a<b}^{\infty} C_{ij}^{ab} \, u_a(1) \, u_b(2) , \\ S_{ijk}(123) &= \mathscr{A}_3 \sum_{a<b<c}^{\infty} C_{ijk}^{abc} \, u_a(1) \, u_b(2) \, u_c(3) , \\ &\cdots\cdots\cdots\cdots\cdots\cdots\cdots\cdots \\ S_{12\ldots N}(12\ldots_N) &= \mathscr{A}_N \sum_{a<b<c\ldots<h}^{\infty} C_{12\ldots N}^{ab\ldots h} \, u_a(1) \, u_b(2) \ldots u_h(N) . \end{aligned} \tag{2}$$

It can be seen from this definition that the functions S are antisymmetric in their arguments and orthogonal to the first N spin-orbitals

$$\int u_i^*(1) \, S_{ijk\ldots}(123\ldots) \, d\tau_1 = 0 . \tag{3}$$

Substituting these in the wave function (1) we have

$$\Phi = \mathscr{A}_N \left\{ u_1(1) \, u_2(2) \ldots u_N(N) \left[1 + \sum_{i=1}^{N} \frac{S_i(i)}{u_i(i)} + \frac{1}{\sqrt{2!}} \sum_{i<j}^{N} \frac{S_{ij}(ij)}{u_i(i) \, u_j(j)} + \right. \right.$$
$$\left. \left. + \frac{1}{\sqrt{3!}} \sum_{i<j<k}^{N} \frac{S_{ijk}(ijk)}{u_i(i) \, u_j(j) \, u_k(k)} \cdots + \frac{1}{\sqrt{N!}} \frac{S_{12\ldots N}(12\ldots N)}{u_1(1) \, u_2(2) \ldots u_N(N)} \right] \right\} .$$

Independently of the definition (2) the functions u_i and S can be derived from a set of coupled integrodifferential equations entirely equivalent to the original Schrödinger equation. At this stage we shall specify the spin-orbitals u more closely. There are two usual methods for their choice in the literature [1, 3].

1. *Brueckner condition*

The spin-orbitals are chosen so that the functions S_i $(i = 1, 2, \ldots N)$ vanish. This choice is often used in nuclear physics [1, 4, 5]. It is identically satisfied in the theory of infinite uniform nuclear matter for plane-wave orbitals.

2. *Hartree-Fock condition*

The spin-orbitals are chosen so that they satisfy the Hartree-Fock equations

$$\mathscr{H}(1) \, u_i(1) = \varepsilon_i \, u_i(1) , \quad i = 1, 2, \ldots N .$$

In this case the functions S_i are not exactly zero nevertheless they can generally be neglected [6]. This choice is of great importance in the theory of atoms and molecules because the cluster expansion appears to converge in this case and even for small molecules, analytical Hartree-Fock solutions will be available in the near future.

For both choices only the pair functions S_{ij} (12) occur in the energy expression

$$E = (0|H|0) + \sum_{i<j}^{N} (\mathscr{A}_2\, u_i(1)\, u_j(2)\, |H(12)|S_{ij}(12)). \tag{4}$$

Unfortunately in the exact equations determining the pair functions higher cluster functions also appear. Some of the higher cluster functions can be expressed by the lower ones, i.e. they consist of unlinked clusters. Neglecting the functions S_i, e.g., S_{ijkl} can be represented as [5]

$$S_{ijkl} = S_{ij}\, S_{kl} + S_{ik}\, S_{jl} + S_{il}\, S_{jk} + S'_{ijkl}.$$

It means that some of the four-electron collisions are comprised of two simultaneous two-electron collisions. Taking into account only the two-electron collisions we have the wave function

$$\Psi_P = \left\{ \mathscr{A}_N\, u_1(1)\, u_2(2) \ldots u_N(N) \left[1 + \frac{1}{\sqrt{2}} \sum_{i<j}^{N} \frac{S_{ij}(ij)}{u_i(i)\, u_j(j)} + \right. \right. \\ \left. \left. + \frac{1}{4} \sum_{\substack{i<j \\ ij \neq kl}}^{N} \sum_{k<l}^{N} \frac{S_{ij}(ij)\, S_{kl}(kl)}{u_i(i)\, u_j(j)\, u_k(k)\, u_l(l)} \ldots \right. \right. . \tag{5}$$

This may be a good approximation if the cluster expansion converges rapidly. Regarding the Hartree-Fock ground state as the zero-th approximation the remaining perturbation is the following [7]

$$H - \sum_{i=1}^{N} \mathscr{H}(i) + \sum_{i<j}^{N} I_{ij} = \sum_{i<j} \left\{ \frac{1}{r_{ij}} - \varrho_i(j) - \varrho_j(i) + I_{ij} \right\} \equiv \sum_{i<j}^{N} g_{ij},$$

where

$$\varrho_i(j) = \int \frac{d\tau_i}{r_{ij}} [1 - P_{ij}]\, u_i^*(i')\, u_i(i),$$

$$I_{ij} = \int \frac{d\tau_i\, d\tau_j}{r_{ij}} [1 - P_{ij}]\, u_i^*(i')\, u_i(i)\, u_j^*(j')\, u_j(j).$$

The perturbing potential g_{ij} between electrons on different localized orbitals is of short range. Configuration interaction calculation on the Be and the LiH verify this showing that the greater number of the four-electron collisions

are two simultaneous two-electron collisions and the intershell correlation energy is much less than that within the shells [6, 7, 8]. Thus, at least in these cases, the wave function (5) can be considered to be a good approximation.

There are two possibilities for determining the pair functions: the second order perturbation theory or the variational method [7, 9]. Only the latter is suitable for practical purposes. Calculating the energy expression with the wave function (4) (or with a part of it only)

$$E_P = \frac{(\Psi_P|H|\Psi_P)}{(\Psi_P|\Psi_P)}$$

we can deduce equations to determine the pair functions S_{ij}. It can be shown, neglecting terms which seem to be unimportant, that they satisfy equations like those of He or H_2 apart from the Hartree-Fock potentials and the orthogonality conditions (which depend on orbitals other than u_i, u_j, too). The number of different pair functions is less than N in general [10].

As is well-known the Hartree-Fock ground state function Φ_0 is unaffected by the unitary transformation of the orbitals $u_i (i = 1, 2, \ldots N)$. These can be transformed into localized orbitals such as the "equivalent" [11] or the "exclusive" orbitals [12]. It can be easily shown [13] that when the new localized orbitals v_i are related to the old ones by the unitary transformation $\mathbf{T}$

$$v_i = \sum_{k=1}^{N} T_{ik} u_k ,$$

then the pair functions transform as follows

$$\mathscr{S}_{ij} = \sum_{k,l}^{N} \tilde{T}_{ik} \cdot \tilde{T}_{jl} S_{kl} .$$

Here $\tilde{\mathbf{T}}$ means the transposed matrix of $\mathbf{T}$. The energy expression (4) remains invariant. This gives a new possibility for defining localized orbitals or groups seeking that unitary transformation for which the intergroup correlation energy is as small as possible. The correlation energy

$$E_c = \sum_{i<j}^{N} (\mathscr{A}_2 v_i(1) v_j(2)|H(12)|\mathscr{S}_{ij}(12)) = E_c^{\text{intra}} + E_c^{\text{inter}}$$

can be divided into two parts (intra- and intergroup correlation) for each partitioning of the orbitals into groups of a given number of electrons. The best possible ratio between the intragroup and the total correlation energy gives an exact measure for the localizability of those groups. Of course, it applies not only to the exact pair functions but also to their fairly close approximations.

Method II. Many-electron group functions

For a long time it has been proposed that two-electron functions should be used as building units in constructing the antisymmetric total wave function [14]. The handling of such wave functions, however, is very cumbersome [15, 16] unless we impose on the building units the strong orthogonality conditions [17]

$$\int \psi_J^*(12\ldots N_J)\,\psi_I(12'\ldots N_I')\,d\tau_1 = 0\,, \qquad J \neq I\,.$$

These conditions make the formal treatment as simple as that of the Hartree-Fock scheme. For an N-electron system consisting of M groups of N_1, N_2, ... N_M electrons the antisymmetric total wave function can be written as

$$\Psi_0 = \sqrt{\frac{N_1!\,N_2!\ldots N_M!}{N!}} \sum_{P'} (-1)^p\, P'\psi_1(12\ldots N_1)\,\psi_2(N_1+1)\ldots\psi_M(\ldots N).$$

Here P' means those permutations which interchange the electrons between group functions. The energy expression has the following descriptive form [17, 18, 19, 20]

$$\begin{aligned} E_0 = H(0) + \sum_{I=1}^{M} \int \psi_I^*(12\ldots N) \Bigg[& N_I\,H(1) + \\ & + \binom{N_I}{2} \frac{1}{r_{12}} \Bigg] \psi_I(12\ldots N_I)\,d\tau_1\,d\tau_2\ldots d\tau_{N_I} + \\ & + \sum_{\substack{I,J \\ J\neq I}} \frac{N_I\,N_J}{2} \int d\tau_1\,d\tau_2\ldots d\tau_{N_I}\,d\tau_\varkappa\,d\tau_\lambda\ldots d\tau_\omega \times \\ & \times \left[\frac{1-P_{1\varkappa}}{r_{1\varkappa}}\right] \psi_J^*(\varkappa'\lambda'\ldots\omega')\,\psi_J(\varkappa\lambda\ldots\omega)\,\psi_I^*(1'2'\ldots N_I')\,\psi_I(12\ldots N_I). \end{aligned}$$

Recently it has been proved [21, 22] that for M antisymmetric strongly orthogonal many-electron group functions there exists a complete set of orthonormal spin-orbitals $\bar{u}_\varkappa$ which can be partitioned into subsets

$$\bar{u}_{11}, \bar{u}_{12}, \bar{u}_{13}, \ldots\,;\ \bar{u}_{I1}, \bar{u}_{I2}, \bar{u}_{I3}, \ldots\,;\ \bar{u}_{M1}, \bar{u}_{M2}, \bar{u}_{M3}, \ldots$$

such that each ψ_I can be expanded in terms of $\bar{u}_{I1}$, $\bar{u}_{I2}$, $\bar{u}_{I3}$, ... only

$$\psi_I = \sum_{i_1<i_2<\ldots<i_{N_I}} a^I_{i_1<i_2<\ldots<i_{N_I}}\,\mathscr{A}_{N_I}\left[\bar{u}_{I1}\,\bar{u}_{I2}\ldots\bar{u}_{IN_I}\right].$$

Thus the functions ψ_I are localized to different perpendicular subspaces. It means in the configuration interaction picture that the spin-orbitals $\bar{u}_i$ ($i \leqslant N$) and $\bar{u}_a$ ($a > N$) are partitioned into M subsets so that each of the $\bar{u}_i$ must be replaced by such $\bar{u}_a$ as belong to the corresponding subset. In this case the infinite configuration interaction calculation gives the best group functions only for particular (best) complete sets. This theorem makes it impossible to determine the group functions practically without a finite one-electron scheme [23, 24, 25, 26, 27]. It seems suitable to start with the exclusive and oscillator orbitals w_{Ii} ($I = 1, 2, \ldots u$; $i = 1, 2, \ldots u_I$) of the system which are based on an analytical Hartree-Fock calculation [12, 25, 26, 27]. This can be regarded as the first approximation. In most cases the result is likely to be close to the best one for the given basis set used to construct the exclusive and oscillator orbitals. If it were not so we subject the basis w_{Ii} to an arbitrary unitary transformation

$$\bar{w}_{Ii} = \sum_{J_j} V_{Ii,Jj} w_{Jj},$$

which has to be determined so as to give the best ground state energy for the system. In this way we get the best partition of the basis into M subsets of given dimension [25, 26, 27]. To improve convergence the approximate group functions constructed from one-electron orbitals have to be completed with antisymmetric functions which are

1. flexible enough to account for the intragroup correlation (containing the interelectronic coordinates r_{ij} explicitly)

2. orthogonal to all basis orbitals of all the other group functions and to its own group function.

The violation of the strong orthogonality by these "almost" orthogonal group functions is appreciable only if the electron groups of the system are delocalized and the basis is insufficient. (Suitably increasing the basis the non-orthogonality terms can be made as small as desired).

The group functions obtained by this approach are automatically more localized than the equivalent or the exclusive orbitals. This is because not only the zero-th order group functions but also the correlation corrections to them have to be strongly orthogonal in contrast to the pair functions. The ratio between the correlation energy given by this model and the empirical one is an exact measure of the localizability of the electron groups in the system.

The approximate and the exact group functions are antisymmetric solutions to the following M equations

$$Q^I H^I \psi_{Ik}(12 \ldots N_I) = E^{I\varkappa} \psi_{I\varkappa}(12 \ldots N_I), \qquad (6)$$
$$I = 1, 2, \ldots M; \quad \varkappa = 0, 1, 2, \ldots .$$

Here Q^I is an N_I-electron projection operator projecting on the subspace I and H^I is an N_I-electron operator depending on the other $(J \neq I)$ group functions corresponding to the ground state [25, 26, 27]. In addition an N-electron model operator $\mathscr{H}$ can be defined whose eigenfunctions are the antisymmetrized products containing one solution of each of the equations (6). Taking $H - \mathscr{H}$ as perturbation with the eigenfunctions of $\mathscr{H}$ we can carry out a Rayleigh-Schrödinger perturbation calculation. The first order term vanishes, whereas the second order term is the dispersion energy which gives, apart from the Fermi correlation, the intergroup correlation energy of the model. Taking a small external electric or magnetic field as perturbation the first and the second order corrections are strictly additive, i.e., they are the sums of the contributions from the separated groups. For practical purposes, of course, it is more suitable to calculate the dispersion energy and the susceptibilities by the variation method [25, 26, 27].

Comparison of the two methods

Method I seems to be the more systematic one which, including the higher order cluster functions step by step, approaches to the exact solutions to the Schrödinger equation. A complete calculation is out of the question, of course, because it would be equivalent to the exact solution and the rapidity of the convergence cannot generally be estimated. If only the pair correlations are taken into account we have to carry out at least as much computational work as required for N complex two-electron problems. Then we must try to find the localized orbitals or groups, together with the corresponding pair correlations separately.

Method II appears to be closer to the conception of the chemist. Even for the choice of the model (for the partition of the N electrons into M groups) we must be supported by experience. Unfortunately, due to the strong orthogonality conditions the determination of the exact model wave function needs very nearly as much labour as the exact solution of the problem. For this reason it is suitable to restrict ourselves to the approximate (or "almost" orthogonal) group functions. The strict additivity predicted by this approach holds only approximately in a real system. Thus it would be unnecessary to require far more accuracy than that of the model. In spite of the fact that all simultaneous many-electron collisions allowed by the partitioning into M subspaces are taken into account, it is remarkable how much this approach formally simplifies the treatment.

By the interaction of two molecules each of which consists of strongly orthogonal groups we must take into account that each group of the first molecule can overlap each group of the second molecule [28]. It is very probable

that the group functions are localized and chemically invariant as much as possible.

Up to the present neither of the two methods has been able to verify from basic principles the transferability of groups from one system to another.

Various calculations on simpler systems are needed to make a decision about the value of the two methods.

How to treat a filled L shell, a double or triple bond with Method II is still questionable. Constructing the wave function from separated two-electron functions we certainly obtain only a rough approximation. For reasonable approximation we have to treat such a group as a whole. A group of nearly free electrons (π-electron system) must be taken as a whole in both methods.

For systems consisting of groups strongly localized in different regions of space both probably give nearly the same result. Configuration interaction calculation on the Be [6] shows that more than 95% of the obtained correlation energy (37 configurations give about 85% of the observed value) comes of configurations which correspond to two strongly orthogonal two-electron functions. Using two such functions an overlap of 0.99989 can be obtained with the best 37-term wave function of the Be [29]. It seems very likely that for the LiH this separability is also valid [8]. The intershell correlation energy is small, but is not negligible. The generalized bond energy concept [29] can be regarded as a first approximation. Even for molecules consisting of localized groups the London energy must be subtracted from the total energy and the remainder can be identified with the sum of the kinetic energies of the individual groups. In the case of the normal paraffins two nearest neighbour and three next-nearest neighbour London energy (referred to the two-electron functions of the bonds and not to the atoms) fall to one bond energy. This may give an appreciable correction.

It would be necessary to elaborate a suitable procedure to treat the dispersion interaction between groups close to one another (without an expansion in terms of the $\frac{1}{R}$ powers). The methods used for this purpose up to the present [30] give results which can be regarded as agreeing with the observed values only in their order of magnitude.

REFERENCES

1. R. K. Nesbet, Phys. Rev., **109**, 1632, 1958.
2. P.-O. Löwdin, Advances in Chem. Phys., II. 284, 1959.
3. R. K. Nesbet, Rev. Mod. Phys., **33**, 28, 1960.
4. W. Brenig, Nuclear Physics, **4**, 363, 1957.
5. P. Coester and H. Kümmel, Nuclear Physics, **17**, 477, 1960.
6. R. E. Watson, Phys. Rev., **119**, 170, 1960.
7. O. Sinanoğlu, J. Chem. Phys., **36**, 706, 1962.

8. D. D. EBBING, J. Chem. Phys., **36**, 1361, 1962.
9. O. SINANOĞLU, Proc. Roy. Soc., A **260**, 379, 1961.
10. O. SINANOĞLU, J. Chem. Phys., **36**, 3198, 1962.
11. J. E. LENNARD-JONES, Proc. Roy. Soc., A **198**, 1, 14, 1949.
12. J. M. FOSTER and S. F. BOYS, Rev. Mod. Phys., **32**, 300, 1960.
13. O. SINANOĞLU, J. Chem. Phys., **37**, 191, 1962.
14. F. A. FOCK, Doklady Akad. Nauk U. S. S. R., **73**, 735, 1950.
15. F. BOPP, Z. Physik, **156**, 348, 1959.
16. E. KRŐNER, Z. Naturforsch., **15a**, 260, 1960.
17. A. C. HURLEY, J. E. LENNARD-JONES and J. A. POPLE, Proc. Roy. Soc., A **220**, 496, 1953.
18. R. G. PARR, F. O. ELLISON and P. G. LYKOS, J. Chem. Phys., **24**, 1106, 1956.
19. E. KAPUY, Acta Phys. Hung., **9**, 237, 1958.
20. R. MC WEENY, Proc. Roy. Soc. A **253**, 242, 1959; Rev. Mod. Phys., **32**, 335, 1960.
21. R. ARAI, J. Chem. Phys., **33**, 95, 1960.
22. P.-O. LÖWDIN, J. Chem. Phys., **35**, 78, 1961.
23. E. KAPUY, Acta Phys. Hung., **12**, 185, 351, 1960.
24. E. KAPUY, Acta Phys. Hung., **13**, 345, 1961.
25. E. KAPUY, Acta Phys. Hung., **13**, 461, 1961.
26. E. KAPUY, Physics Letters, **1**, 205, 1962.
27. E. KAPUY, Acta Phys. Hung., **15**, 177, 1962.
28. R. MC WEENY, Preprint No. 59, Quant. Chem. Group Uppsala University, Uppsala, Sweden, 1961.
29. T. L. ALLEN and H. SHULL, J. Chem. Phys., **35**, 1644, 1961.
30. K. S. PITZER, Advances in Chem. Phys., II, 59, 1959.
K. S. PITZER and E. J. CATALANO, J. Am. Chem. Soc., **78**, 4844, 1956.

ПРОБЛЕМА КОРРЕЛЯЦИИ В ТЕОРИИ АТОМОВ И МОЛЕКУЛ

Э. КАПУИ

Резюме

Обсуждаются и сравниваются два метода, которыми избегается бесконечное суммирование при учёте корреляций электронов. Показывается, что для суждения о ценности этих методов необходимы дальнейшие вычисления. Это зависит также и от развития вычислительной техники в будущем. Оба метода допускают получения столько локализованных групп, сколько возможно и дают точную меру локализуемости этих групп в реальных системах. Ни одним из них до настоящего времени не доказалась переместимость нескольких (химически инвариантных) групп. Можно показать, что перед применением понятия обобщённой энергии связи полная энергия должна быть исправлена дисперсионным взаимодействием.

COMMUNICATIONES BREVES

A FURTHER APPLICATION OF THE METHOD OF SPIN OPERATORS

By

F. BERENCZ

DEPARTMENT OF THEORETICAL PHYSICS, UNIVERSITY OF SZEGED, SZEGED

(Received: 22. III. 1962)

In a previous paper [1] it was proved that the van der Waerden's formula of spin (angular momentum) summation gives the eigenfunctions of S^2, just as does a general spin operator. A function of the so-called step-up and step-down operators was suggested which, when operating on the eigenfunctions of the total S_z operator related to maximal, minimal and zero projections of the total spin, creates all eigenfunctions of the total S^2 corresponding to the different eigenvalues of the latter. Further it was also shown how the two preceding results can be applied to reduce the order of the secular determinant when using the general method of configuration interaction. In this paper a further application of our results will be given in the case of the determination of the eigenfunctions of atomic states.

It is well known that according to the Pauli principle the eigenfunction referring to the state of a many-electron system must be antisymmetric with regard to electron interchange. Neglecting spin interaction the eigenfunction can be written down in the following product form:

$$\psi = \psi_b(q_1, q_2, \ldots, q_f)\, u_\lambda v_\mu, \ldots, w_\nu, \tag{1}$$

where ψ_b means the space eigenfunction and u_λ, v_μ, . . ., w_ν mean the spin eigenfunctions of the electrons. The antisymmetrical character of the eigenfunction of a many-electron system depends on the behaviour of the space function and the spin function by the electron interchange.

The set of functions (1) belonging to the same energy level constitutes the basic element of the representation of the group of four commutable transformations. These transformations are as follows:

a) the rotation of the q space,

b) the rotation of the spin space,

c) the permutation of $q_1, q_2, \ldots, q_f$,

d) the permutations of $u, v, \ldots, w$.

The eigenfunctions satisfying the Pauli exclusion principle can be obtained by totally reducing at first the two groups of the commutable linear

transformations with respect to the space functions and then with respect to the spin functions. Among the product functions obtained by the previous procedure we must look for those functions, which satisfy the Pauli exclusion principle, that is, which are antisymmetric with regard to electron interchange.

Total reducing of the groups of the commutable linear transformations can be performed on the basis of the theorem, that if the two commutable and reducible systems $\mathfrak{G}$ and $\mathfrak{H}$ are obtained from the linear transformations of the vector space $\mathfrak{R}$, then the basic vectors can be arranged in squares in such a way, that in all squares all rows irreducibly transform themselves in the same way through $\mathfrak{G}$ and all columns through $\mathfrak{H}$.

According to what has been mentioned above, the eigenfunctions satisfying the Pauli exclusion principle can be obtained in the following steps:

a) One constructs the squares of space functions, the columns of which transform themselves according to the irreducible representation D_L of the rotation group and the rows of which transform themselves according to the irreducible representation Δ of the permutation group. Let us denote the rows by the numbers

$$m_L (= L, L-1, \ldots, -L).$$

b) One constructs the squares of spin functions, the columns of which transform themselves according to the irreducible representation D_S of the rotation group and the rows of which transform themselves according to the irreducible representation Δ' of the permutation group. Let us denote the rows by the number

$$m_S (= S, S-1, \ldots, -S).$$

c) One constructs the product functions of the space and spinfunctions, which belong naturally to the product representation $\Delta \times \Delta'$. If the product representation contains the antisymmetric representation, one can construct an antisymmetric spin-orbital function from all rows of the squares of the space functions and spin functions. This can be repeated for all rows and so m_L takes up all values $L, L-1, \ldots, -L$ and m_S takes up all values $S, S-1, \ldots, -S$; one obtains therefore a multiplet term transforming itself according to $D_L \times D_S$ and satisfying the Pauli exclusion principle.

The eigenfunctions of the operator L_z, respectively L^2, and S_z, respectively S^2, constitute the basic vectors of the irreducible representation of the rotation group D_L and D_S and thus the use of our method means great simplification when determining the atomic terms.

REFERENCE

1. F. Berencz, Proc. Phys. Soc., **71**, 152, 1958.

REMARK ON THE THEORY OF THE BULK PHOTOEFFECT IN INHOMOGENEOUS SEMICONDUCTORS

By

G. PATAKI

RESEARCH INSTITUTE FOR TECHNICAL PHYSICS OF THE HUNGARIAN ACADEMY OF SCIENCES, BUDAPEST

(Received 14. IV. 1962)

In inhomogeneous semiconductors, as is well known, under the influence of illumination a so-called bulk photovoltaic effect arises. Several authors have dealt with the theory and application of this phenomenon [1—4]. The most comprehensive review of this problem was given by J. TAUC [5]. Recently,

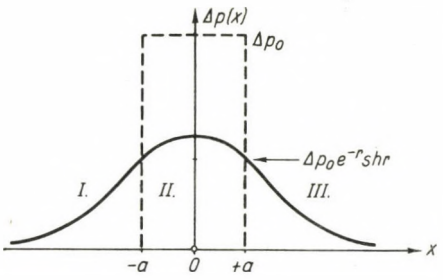

Fig. 1

a treatment different from the one above was presented by C. D. Cox [6]. When investigating the bulk photoeffect, among others it used to be supposed that the concentration of the generated carriers differs from zero only under the illuminated part of the sample. (Fig. 1, dotted line.) This assumption holds in the case discussed in [5], where the width of the illuminated part has been assumed to be larger than the diffusion length. In the following the bulk photo-electromotive force will be determined omitting this assumption. This is all the more of interest, because C. D. Cox, in his experiments did not find saturation of the bulk photo-e. m. f. with increasing illumination in case of the monotonous distribution of impurity and therefore he concluded that the above assumption is insufficient.

In the present paper the influence of the diffusion of the excess carriers from the illuminated part on the bulk photoeffect will be examined. Furtheron we shall assume:

a) the material in question is of n-type and the impurities fully ionized, its resistivity showing an exponential distribution:

$$\varrho = \varrho_0 e^{\gamma x} \quad (n_0(x) = n_0 e^{-\gamma x}); \tag{1}$$

b) the generated carriers fulfil the condition of electrical neutrality, namely $\Delta n(x) = \Delta p(x)$: in the determination of $\Delta p(x)$ the inhomogeneity need not be taken into consideration;*

c) $\Delta p(x)$ fulfils a linear equation and the solution is considered to be valid also at strong illumination.

On the basis of what has been said above the equation to be solved is the following:

$$\frac{d^2 \Delta p(x)}{dx^2} - \frac{\Delta p(x)}{L_p^2} = -\frac{g_0}{D_p}, \tag{2}$$

where g_0 means the number of the carriers generated in unit volume and unit time. Determining $\Delta p(x)$ one has to fit the solutions valid in the different regions at the boundaries of these regions. Together with the condition of normalisation we thus have

$$\begin{aligned} &\Delta p_{\mathrm{I}}(-a) = \Delta p_{\mathrm{II}}(-a), \\ &\Delta p_{\mathrm{II}}(+a) = \Delta p_{\mathrm{III}}(+a), \\ &\int_{-\infty}^{+\infty} div\, i_p\, dx = 0. \end{aligned} \tag{3}$$

On the basis of equs. (3), the solution has a very simple form (Fig. 1):

$$\begin{aligned} \Delta p_{\mathrm{I}}(x) &= \Delta p_0 \,\mathrm{sh}\, r e^{\frac{x}{L_p}} && (x \leqq -a), \\ \Delta p_{\mathrm{II}}(x) &= \Delta p_0 \left(1 - e^{-r} \,\mathrm{ch}\, \frac{x}{L_p}\right) && (-a \leqq x \leqq +a), \\ \Delta p_{\mathrm{III}}(x) &= \Delta p_0 \,\mathrm{sh}\, r e^{-\frac{x}{L_p}} && (x \geqq +a), \end{aligned} \tag{4}$$

where $r \equiv \dfrac{a}{L_p}$ and $\Delta p_0 \equiv \tau_p g_0$ is the value of the steady generation. We shall be in need of the value of $\Delta p_{\mathrm{II}}(x)$ in case of a narrow illumination. In this case $r^2 \ll 1$, so we get:

$$\Delta p_{\mathrm{II}}(x) \approx r \Delta p_0 = \mathrm{const}. \tag{5}$$

The quantity $r\Delta p_0 = \Delta p_r$ may be called a reduced generation. Owing to the diffusion of the carriers one has to reckon with this concentration in region II.

* In the determination of $\Delta p(x)$ the calculations were carried out also by taking the inhomogeneity into account. This does not lead, however, to essential differences compared with the above simple model in case of inhomogeneities occurring in practice.

On the basis of equs. (4) we can determine the bulk photo-e. m. f. According to the formulae of [5] $U = U_c + U_d$, where

$$U_c = \frac{kT}{e}(b+1)\oint \frac{\Delta p(x)}{bn_0(x)+(b+1)\Delta p(x)}\,\frac{1}{n_0(x)}\,\frac{dn_0(x)}{dx}\,dx,$$
$$U_d = -\frac{kT}{e}(b-1)\oint \frac{1}{bn_0(x)+(b+1)\Delta p(x)}\,\frac{d\Delta p(x)}{dx}\,dx. \tag{6}$$

In regions I and III the integration can be carried out quite simply. For this purpose it is sufficient to assume that $\xi \equiv \frac{1}{2}L_p < 1$. If $l \gg L_p$ is assumed too, where l is the length of the sample, then as a result of integration

$$U_{c\mathrm{I}} = -\frac{kT}{e}\,\frac{\xi}{1+\xi}\ln F_b, \qquad U_{c\mathrm{III}} = -\frac{kT}{e}\,\frac{\xi}{1-\xi}\ln F_c,$$
$$U_{d\mathrm{I}} = -\frac{kT}{e}\,\frac{b-1}{b+1}\,\frac{1}{1+\xi}\ln F_b, \quad U_{d\mathrm{III}} = +\frac{kT}{e}\,\frac{b-1}{b+1}\,\frac{1}{1-\xi}\ln F_c, \tag{7}$$
$$F_b \equiv 1 + \frac{\Delta\sigma(b)}{\sigma_{0b}}; \quad F_c \equiv 1 + \frac{\Delta\sigma(c)}{\sigma_{0c}},$$

where σ_{0b}, $\Delta\sigma(b)$ resp. σ_{0c}, $\Delta\sigma(c)$ are the values of conductivities and their changes at the points $-a$, resp. $+a$. In region II the integration can be carried out only numerically. After some transformations $U_{c\mathrm{II}}$ and $U_{d\mathrm{II}}$ can be written as follows:

$$U_{c\mathrm{II}} = -r\xi\,\frac{\Delta\sigma_0}{\sigma_0}\,\frac{kT}{e}\int_{-1}^{+1}\frac{1-e^{-r}\operatorname{ch} ru}{e^{-r\xi u}+\frac{\Delta\sigma_0}{\sigma_0}(1-e^{-r}\operatorname{ch} ru)}\,du; \tag{8}$$

$$U_{d\mathrm{II}} = +\frac{kT}{e}\,\frac{b-1}{b+1}\,re^{-r}\,\frac{\Delta\sigma_0}{\sigma_0}\int_{-1}^{+1}\frac{\operatorname{sh} ru}{e^{-r\xi u}+\frac{\Delta\sigma_0}{\sigma_0}(1-e^{-r}\operatorname{ch} ru)}\,du. \tag{9}$$

Summing up the above electromotive forces, we obtain for the total one:

$$U = U_{\mathrm{II}} - \frac{kT}{e}\,\frac{2}{b+1}\,\frac{\xi}{1-\xi^2}\ln F_b F_c + \frac{kT}{e}\,\frac{b-1}{b+1}\ln\frac{F_c}{F_b} - \frac{2}{b+1}\,\frac{kT}{e}\,\frac{\xi^2}{1-\xi^2}\ln\frac{F_c}{F_b}. \tag{10}$$

The expression (10) can be given a physically meaningful and simple form in case of narrow illumination ($r^2 \ll 1$) and weak inhomogeneity ($\xi^2 \ll 1$). Because of (5) $U_{c\mathrm{II}}$ can then simply be determined, $U_{d\mathrm{II}} \approx 0$ and we get after some transformations

$$U \approx -\frac{kT}{e}\frac{2}{b+1}\ln\frac{1+\dfrac{\Delta\sigma_r}{\sigma_{0c}}}{1+\dfrac{\Delta\sigma_r}{\sigma_{0b}}} - \frac{kT}{e}\frac{2}{b+1}\xi\ln F_b F_c. \qquad (11)$$

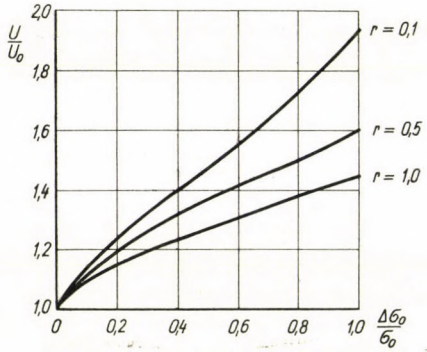

Fig. 2

As it can be seen the first term of (11) is identical with the corresponding formula of [5]:

$$U_0 = -\frac{kT}{e}\frac{2}{b+1}\ln\frac{1+\dfrac{\Delta\sigma_0}{\sigma_{0c}}}{1+\dfrac{\Delta\sigma_0}{\sigma_{0b}}}, \qquad (12)$$

except that $\Delta\sigma_0$ must be substituted by the proper reduced quantity. This term will be saturated by an increasing illumination. The second term is proportional to ξ and does not show saturation.

In order to illustrate what has been said above, in Fig. 2 the quotient U/U_0 is plotted for $\xi = 0, 1$ and at different values of r. U and U_0 are determined on the basis of equs. (10) and (12).

As it can be seen, in case of a narrow illumination the discrepancy may be significant.

The author wishes to thank Dr. Z. Bodó for his valuable advice and critical remarks.

REFERENCES

1. J. Tauc, Czechosl. J. Phys., **5**, 178, 1955.
2. H. Frank, Czechosl. J. Phys., **6**, 433, 1956.
3. Z. Trousil, Czechosl. J. Phys., **6**, 96, 1956.
4. V. E. Lashkarev, E. I. Rashba, V. A. Romanov and Z. A. Demidenko, Journ. Techn. Phys., **28**, 1853, 1958.
5. J. Tauc, Rev. of Mod. Phys., **29**, 308, 1957.
6. C. D. Cox, Can. Journ. Phys., **38**, 1328, 1960.

TRANSMISSION OF 100—472 keV MONOENERGETIC ELECTRONS THROUGH Al ABSORBERS

By

D. BERÉNYI and M. OSVAY

INSTITUTE FOR NUCLEAR RESEARCH OF THE HUNGARIAN ACADEMY OF SCIENCES, DEBRECEN

(Received 11. VII. 1962)

In the course of studies in nuclear physics frequently it is not only the range of electrons in some material that is important but also their absorption or transmission curve. These curves indicate the percentage of electrons passing through a foil relative to the number of electrons originally present in the beam. In this case the energy distribution after traversing the foil is disregarded.

Table I

Measurements for taking series of transmission (absorbtion) curves in Al

Authors	Energy region	Particular energy values in the region
R. O. LANE et al. [1]	0—50 keV	A detailed study from 0 to 50 keV for particular absorbers
I. CARLVIK [2]	75—200 keV	By 25 keV from 75 to 200 keV
H. H. SELIGER [3]	159—960 keV	Transmission curves for electrons and positrons at 159, 250, 336 and 960 keV
B. N. C. AGU et al. [4]	300—700 keV	Curves by 100 keV
J. MARSHALL et al. [5]	429—1696 keV	Transmission curves for 421, 727, 1011, 1370 and 1696 keV electrons

Table I shows the measurements performed and published in this field. It can be seen that in the region of lower energy, measurements are available rather closely, but e.g. in the energy region between 200 and 421 keV transmission curves were published only for some energy values and we lack comprehensive measurements for the region between 100 and 500 keV at the same measurement conditions.

The necessity for completing these measurements arose in our Institute. Thus, we have taken the absorption curves for 100, 150, 200, 219, 252, 281, 308, 334, 391, 417, 445 and 472 keV monoenergetic electrons in the case of Al absorbers. The limit of error for the energy value in our measurements is about ± 2 keV at the higher energies and decreasing toward the lower energies, being about half that amount at the lowest energies.

The source of the electrons was a Cs^{137} sample (cca 100 μC) on a mylar foil. The source was placed in a beta-ray spectrometer of toroid-sector type [6] which provided the monoenergetic electron beams at the suitable setting of the magnetic field in the toroid coil. A scintillation counter with a plastic phosphor was applied as a detector. The Al absorbers were put 2 mm before the surface of the scintillator. The counter was protected from background and scattered radiation by an Al-covered Pb shield.

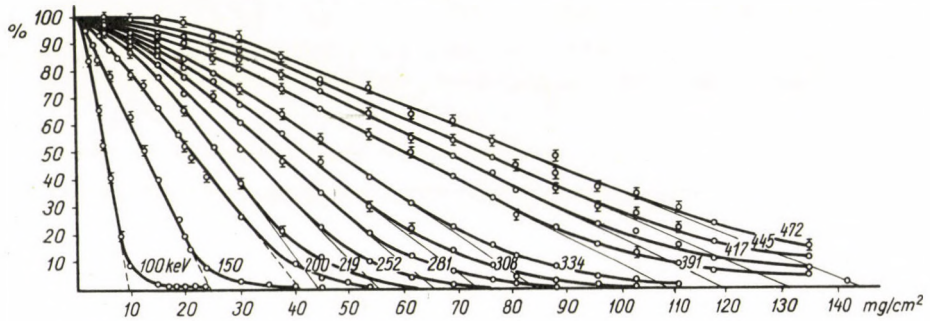

Fig. 1

The transmission curves measured by us can be seen in Fig. 1. To the values indicated on the abscissa one must add about 2 mg/cm^2 absorber thickness because of the effective window thickness of the scintillation counter. This correction can be estimated on the basis of signal-to-noise ratio curves [7].

The extrapolated ranges determined from the curves are generally in close agreement with the values of other authors [8], if we take into consideration the window correction.

At electron energies at which transmission curves were published by other authors too (for 100, 150 and 252, 217 keV) our curves were subjected to a detailed comparison. That was also necessary because in this measurement the electron beam impinged on the face of the absorbers at an angle of cca $40 \pm 5°$ which possibly could lead to deviations. According to the comparison the agreement with CARLVIK's curves [2] is very close (100, 150 keV), while comparing our results with SELIGER's and MARSHALL's curves [3, 5] some deviation is observable. Our curves remain below the corresponding ones of SELIGER and MARSHALL. It must be noted, therefore, that the extrapolated ranges from the

curves of SELIGER are higher than the values accepted in the literature [8] and in the article of MARSHALL et al. the measuring points are not indicated in the diagram [5].

On the basis of our measurements and the results of other authors one can state the rough rules in the energy region of 100—1700 keV for the transmission (absorption) of monoenergetic electrons, as follows. An absorber corresponding to an extrapolated range for an electron energy lets through 80% of a monoenergetic electron beam with an energy double that of the earlier one and for a beam, with about four, or five times higher energy than that of the original beam there being no effect of the absorber in question. Another practical rule: the maximum range is roughly double the extrapolated range.

We are indebted to Professor A. SZALAY for the excellent working conditions at this Institute.

REFERENCES

1. R. O. LANE and D. J. ZAFFARANO, AEC Report, ISC—439, Ames, 1953.
2. I. CARLVIK, Ark. för Fys., **6,** 1, 1953.
3. H. H. SELIGER, Phys. Rev., **100,** 1029, 1955.
4. B. N. C. AGU, T. A. BURDETT and E. MATSUKAWA, Proc. Phys. Soc., **71,** 201, 1958.
5. J. S. MARSHALL and A. G. WARD, Canad. Journ. of Res., **15,** A 39, 1937.
6. A. SZALAY and D. BERÉNYI, Acta Phys. Hung. **10,** 57, 1959.
7. D. BERÉNYI and GY. MÁTHÉ, Nuclear Instruments, **13,** 161, 1961.
8. K. SIEGBAHN, Beta- and Gamma-Ray Spectroscopy. North-Holland Publ. Co., Amsterdam 1955, p. 19.

RECENSIO

DAVID J. ROSE and MELVILLE CLARK. JR.

Plasmas and Controlled Fusion

Published jointly by: The M. I. T. Press, Massachusetts Institute of Technology and John Wiley and Sons, Inc. New York, London

Since 1955 more and more people have been engaged in attempting the solution of the problems of controlling the process of thermonuclear energy. Interest regarding this question has grown particularly at the time of, and since the II. Geneva Conference, and nothing demonstrates better the increasing spread of research activities, than the International Conference at Salzburg in the autumn of 1961, where countries participating in thermo-nuclear research, such as USSR and the USA, have given many lectures. In spite of intensive research unfortunately no decisive progress towards a practical implementation has been achieved. A large amount of experimental and theoretical material has been collected, the survey of which is almost impossible.

This book, containing the most up-to-date results of thermo-nuclear research and plasma physics is of great value to interested researchers. Although Rose and Clark's book was intended as a text book, it is, in my opinion, an outstanding summary of the research in plasma physics and thermonuclear energy. The book includes the material given in a series of lectures over two terms and its primary purpose is to accelerate the increase in the depth of knowledge of students already well trained in plasma and thermo-nuclear physics.

The book consists of 16 chapters. Chapter I deals with the classical energy sources of the world and the estimated development of energy demand. Chapter II very briefly summarizes the essential facts regarding impact phenomena. Chapter III gives those details of impact phenomena, which are primarily important in plasma physics. Chapter IV outlines fundamental kinetic gas theory, but, whilst dealing with these basic ideas the Authors carefully explain their connection with plasma physics. Chapter V reviews the essentials of electro-dynamics, so that in Chapter VI the Authors can establish the basic equation of magneto-hydrodynamics. Chapter VII deals with the macroscopic movement of plasma, on a magnetohydrodynamical basis, whilst Chapter VIII discusses the plasmaphysical results of the Coulomb interaction. Chapter IX deals with the properties of waves of small amplitude formed in the plasma and treats of both magnetohydrodynamic and electro-acoustic waves. Chapter X introduces the equations of motion of the plasma particles and the theory of magnetic mirrors. Chapter XI discusses radiation losses occurring in the plasma. Apart from thermodynamic radiation losses, bremsstrahlung and the consequences of cyclotrone radiation as well as the effect of reflectors are discussed.

The investigation of conditions for stabilizing plasma is one of the main problems of thermo-nuclear research. Rose and Clark devote Chapter XII to the stability of plasma. They examine conditions for stability in the case of minor perturbations, then, employing the energy principle, they explore more general conditions.

Chapter XIII deals with problems concerning the balance of thermonuclear reactor energy and with material technological problems.

In Chapter XIV the Authors examine the pinch-effect used to heat the plasma, and carefully analyse the resulting instabilities. Some diagrams of experimental apparatus are given.

Chapter XV is concerned with apparatus which work on the mirror principle. In this Chapter the Authors turn to mirrors operated both by fast and slow pulsation and also deal with apparatus employing reflection on the stationary principle. In this connection they mention the OGRA built in the USSR, and XDC—1 constructed in the USA, both of which are thermo-nuclear units working on the reflection principle. They describe briefly the principle of thermo-nuclear apparatus known as ASTRON.

An introduction to STELLARATORS is given in the last Chapter. The Authors discuss a number of practical problems and present information about the data of several existing constructions.

This volume is primarily intended for use as a text book; the problems at the end of some of the Chapters are of considerable assistance in achieving this purpose. We wish to note that the book, apart from its use as a text book, can be of great use to those who wish to intensify their study of thermonuclear and plasma research.

L. PÁL

Printed in Hungary

A kiadásért felel az Akadémiai Kiadó igazgatója Műszaki szerkesztő: Farkas Sándor

A kézirat nyomdába érkezett: 1963. I. 4. — Terjedelem: 6,50 (A/5) ív, 17 ábra

63.56468 — Akadémiai Nyomda, Budapest — Felelős vezető: Bernát György

The *Acta Physica* publish papers on physics, in English, German, French and Russian.
The *Acta Physica* appear in parts of varying size, making up volumes.
Manuscripts should be addressed to:

Acta Physica, Budapest 502, Postafiók 24.

Correspondence with the editors and publishers should be sent to the same address.
The rate of subscription to the *Acta Physica* is 110 forints a volume. Orders may be placed with "Kultúra" Foreign Trade Company for Books and Newspapers (Budapest I., Fő u. 32. Account No. 43-790-057-181) or with representatives abroad.

Les *Acta Physica* paraissent en français, allemand, anglais et russe et publient des travaux du domaine de la physique.
Les *Acta Physica* sont publiés sous forme de fascicules qui seront réunis en volumes.
On est prié d'envoyer les manuscrits destinés à la rédaction à l'adresse suivante:

Acta Physica, Budapest 502, Postafiók 24.

Toute correspondance doit être envoyée à cette même adresse.
Le prix de l'abonnement est de 110 forints par volume.
On peut s'abonner à l'Entreprise du Commerce Extérieur de Livres et Journaux «Kultúra» (Budapest I., Fő u. 32. — Compte-courant No. 43-790-057-181) ou à l'étranger chez tous les représentants ou dépositaires.

«*Acta Physica*» публикуют трактаты из области физических наук на русском, немецком, английском и французском языках.
«*Acta Physica*» выходят отдельными выпусками разного объема. Несколько выпусков составляют один том.
Предназначенные для публикации рукописи следует направлять по адресу:

Acta Physica, Budapest 502, Postafiók 24.

По этому же адресу направлять всякую корреспонденцию для редакции и администрации.
Подписная цена «*Acta Physica*» — 110 форинтов за том. Заказы принимает предприятие по внешней торговле книг и газет «*Kultúra*» (Budapest I., Fő u. 32. Текущий счет: № 43-790-057-181) или его заграничные представительства и уполномоченные.

20,— Ft

INDEX

COMMUNICATIONES BREVES

RECENSIO

Acta Phys. Hung. Tom. XV. Fasc. 4. Budapest, 30. III. 1963.

Index: 26.022